

**UNIVERSIDADE FEDERAL DE MINAS GERAIS**  
**Exact Sciences Institute – Chemistry Department**  
**Chemistry Graduation Program**

Renato Lúcio de Carvalho

**RUTHENIUM-CATALYZED DOUBLE ANNULATION OF QUINONES: exploring a  
new frontier towards polycyclic compounds *via* C–H activation**

Belo Horizonte

2022

UFMG/ICEX/DQ. 1.506

T. 688

Renato Lúcio de Carvalho

**RUTHENIUM-CATALYZED DOUBLE ANNULATION OF QUINONES: exploring a new frontier towards polycyclic compounds *via* C–H activation**

Thesis presented to the Chemistry Department of the Exact Sciences Institute of the Universidade Federal de Minas Gerais as a partial requirement for the obtention of Doctor of Science degree – Chemistry.

Advisor: Prof. Dr. Eufrânio Nunes da Silva Júnior

Belo Horizonte

2022

Ficha Catalográfica

C331r Carvalho, Renato Lúcio de.  
2022 Ruthenium-catalyzed double annulation of quinones  
T [manuscrito] : exploring a new frontier towards  
polycyclic compounds via C-H activation / Renato Lúcio  
de Carvalho. 2022.  
396 f. : il., gráfs., tabs.

Orientador: Eufrânio Nunes da Silva Júnior.

Tese (doutorado) - Universidade Federal de Minas  
Gerais - Departamento de Química.

Bibliografia: f.197-219.

Anexos: f. 220-396.

1. Química orgânica - Teses. 2. Quinona - Teses. 3.  
Compostos policíclicos - Teses. 4. Compostos de  
rutênio - Teses. 5. Rutênio - Teses. 6. Catálise -  
Teses. 7. Agentes antineoplásicos - Teses. 8. Raios X  
- Difração - Teses. 9. Catalisadores de metais de  
transição - Teses. 10. Testes biológicos - Teses. 11.  
Ressonância magnética nuclear - Teses. 12. Espectro  
infravermelho - Teses. 13. Espectrometria de massa -  
Teses. 14. Cristalografia - Teses. I. Silva Júnior,  
Eufrânio Nunes da, Orientador. II. Título.

CDU 043



UNIVERSIDADE FEDERAL DE MINAS GERAIS

**"Ruthenium-Catalyzed Double Annulation of Quinones: Exploring a New Frontier Towards Polycyclic Compounds via C-H Activation"**

**Renato Lúcio de Carvalho**

Tese aprovada pela banca examinadora constituída pelos Professores:

Prof. Eufrânio Nunes da Silva Júnior - Orientador  
UFMG

Prof. Antônio Luiz Braga  
UFSC

Prof. Hugo Alejandro Gallardo Olmedo  
UFSC

Prof. Luiz Cláudio de Almeida Barbosa  
UFMG

Prof. Eduardo Eliezer Alberto  
UFMG

Belo Horizonte, 04 de agosto de 2022.



Documento assinado eletronicamente por **Luiz Claudio de Almeida Barbosa, Membro**, em 04/08/2022, às 17:11, conforme horário oficial de Brasília, com fundamento no art. 5º do [Decreto nº 10.543, de 13 de novembro de 2020](#).



Documento assinado eletronicamente por **Eduardo Eliezer Alberto, Professor do Magistério Superior**, em 04/08/2022, às 17:12, conforme horário oficial de Brasília, com fundamento no art. 5º do [Decreto nº 10.543, de 13 de novembro de 2020](#).



Documento assinado eletronicamente por **Eufranio Nunes da Silva Junior, Professor do Magistério Superior**, em 04/08/2022, às 17:12, conforme horário oficial de Brasília, com fundamento no art. 5º do [Decreto nº 10.543, de 13 de novembro de 2020](#).



Documento assinado eletronicamente por **Hugo Alejandro Gallardo Olmedo, Usuário Externo**, em 04/08/2022, às 17:58, conforme horário oficial de Brasília, com fundamento no art. 5º do [Decreto nº 10.543, de 13 de novembro de 2020](#).



Documento assinado eletronicamente por **Antonio Luiz Braga, Usuário Externo**, em 08/08/2022, às 17:26, conforme horário oficial de Brasília, com fundamento no art. 5º do [Decreto nº 10.543, de 13 de novembro de 2020](#).



A autenticidade deste documento pode ser conferida no site [https://sei.ufmg.br/sei/controlador\\_externo.php?acao=documento\\_conferir&id\\_orgao\\_acesso\\_externo=0](https://sei.ufmg.br/sei/controlador_externo.php?acao=documento_conferir&id_orgao_acesso_externo=0), informando o código verificador **1648224** e o código CRC **EE5F42AA**.

I dedicate this thesis to my parents, Carlos and Miraci, who supported me all the way here and gave me enough courage to keep moving forward. My siblings, Geisiane, Gleissiane and Carlos Júnior, my nephews and other relatives, my beloved boyfriend Carlos Henrique, and my beloved friends. I will be always thankful to my God, the one who gave me this opportunity, *my brightest morning star*.

## **ACKNOWLEDGEMENTS**

To God.

To my advisor, and now a close friend, Professor Eufrânio Nunes da Silva Júnior, who has been supportive all along my doctorate, and even before that. Who taught me to look beyond the usual reactions, their challenges and the day-by-day routine and find a way to extract from it an important way to do something great, something useful, something meaningful. The one who made me realize that it is strictly important to give your knowledge back to the society as a gift for the trust that was previously given to us.

To Professor Claus Jacob, of Universität des Saarlandes, Saarbrücken, Germany, for the opportunity of our visit in Germany, which made possible to develop the research here presented.

To Professor Lutz Ackermann, of Georg-August-Universität, Göttingen, Germany, for the great contribution to my knowledge in C–H activation provided during the amazing time that I had the opportunity to be in his phenomenal research group.

To Doctor Rubem Menna-Barreto, of Instituto Oswaldo Cruz, Rio de Janeiro, for the contribution with the trypanocidal assays.

To Professor Claudia Pessoa, of Universidade Federal do Ceará, Fortaleza, for the contribution with the anti-cancer assays.

To Doctor Felipe Fantuzzi, of Julius-Maximilians-Universität, Würzburg, Germany, for the contribution with the computational mechanism studies.

To Doctor Christopher Golz, of Georg-August-Universität, Göttingen, Germany, for the contribution in the X-ray crystallography field.

To my beloved friend and eternal brother Augusto Carvalho, someone that I care a lot and make me so proud. You are my inspiration.

To my friends Renata Gomes, Gleiston Dias, Guilherme Jardim, Luana Alves, Emilay Baessa, Ícaro Bozzi, Mateus Pena, Joyce Cristina, Esther Paz, Hugo Silva, Víctor Soares, Carlos Henrique, Gabriela Graça, Kimberly Chayene, Luísa Guerra, among many others who shared with me the enchantments of the environment in the former lab 200, now lab 503/505. Beyond that, I hereby also would like to cite my eternal friends without borders Nate Ang, Alexej Scheremetjew, Leonardo Massignan, Talita Gontijo and others who gave me an amazing experience during the time I worked in Göttingen, Germany. Our friendship will never be forgotten.

To all professors of the Chemistry Department – ICEX, UFMG, that I had contact along my doctorate. Your individual contributions expanded my knowledges not only about chemistry, but about science in general and the beauty in it.

To the analytical department and all employees of both Chemistry Department of UFMG and Georg-August-Universität, for their individual contribution to the good functionality of both universities.

To the committee who accepted the invitation to contribute to this work.

To CNPq, CAPES, FAPEMIG, INCT-Catálise/CNPq/FAPESC and PRPq-UFMG for the scholarship and fundings deposited to the research here presented.



*“Intelligence is the ability to adapt to change.”*

Stephen Hawking (\*1942 – †2018)

## ABSTRACT

This work presents the construction and development of a new methodology for the obtention of modified naphthoquinoidal compounds *via* a C(sp<sup>2</sup>)-H activation process. In this context, the intrinsic direction capability of the carbonyls, present in naphthoquinones, was explored towards arylation and annulation reactions mediated by ruthenium catalysis. After a sequence of failed results, we expanded this study to the use of directing groups added to the quinoidal structure. The optimization of this method led to the formation of polycyclic quinones, in moderate to optimum yields, from their respective substrates, using a ruthenium-catalyzed double-annulation reaction *via* a C(sp<sup>2</sup>)-H activation process, in the presence of an internal alkyne, copper-II acetate and sodium pivalate. Two scope sets were developed, and for the first one, several alkynes were obtained through a Sonogashira-type reaction, and subsequently applied to the optimized methods, from which eleven double-annulated products were achieved and properly characterized. A second scope was developed using quinoidal compounds previously synthesized after sequential methods of structural modifications, from which seven products were successfully obtained. A complementary study was performed, in which non-symmetrical alkynes, alkenes and alkyl-substituted alkynes were explored, leading to a mixture of regioisomers. From this method, a total of twenty new compounds were successfully obtained, from which fourteen had their structures corroborated *via* X-ray diffraction studies. A mechanism was proposed using literature studies and computational data based on relative energies. After obtaining the final products, biological assays were performed to evaluate the antitumoral activity of each derivative against HL-60 cancer cell lines, amongst six other cancer cell lines, however, presenting low activities. The results presented here were published in the *Chemistry – A European Journal*, furthermore, several review articles were produced using the general knowledge gathered along the development of this presented thesis.

**Keywords:** Quinones. Polycyclic Compounds. Double-Annulation Reaction. C-H Activation. Ruthenium Catalysis.

## RESUMO

Este trabalho apresenta a construção e desenvolvimento de uma nova metodologia para obtenção de compostos naftoquinoidais modificados *via* processos de ativação de ligação C(sp<sup>2</sup>)-H. Nesse contexto, foi explorada a capacidade de direção intrínseca das carbonilas, presentes nas naftoquinonas, em reações de arilação e anelação catalisadas por rutênio. Após sequenciais resultados negativos, expandiu-se para o uso de grupos diretores adicionados à estrutura quinoidal. A otimização do método levou à formação de quinonas policíclicas, com rendimentos moderados a ótimos, a partir de seus respectivos substratos, utilizando uma reação de anelação dupla catalisada por rutênio *via* um processo de ativação de ligação C(sp<sup>2</sup>)-H, na presença de um alcino interno, acetato de cobre-II e pivalato de sódio. Dois escopos foram desenvolvidos, e para o primeiro deles, diversos alcinos foram obtidos através de uma reação tipo Sonogashira, e subsequencialmente aplicados aos métodos otimizados, de onde onze produtos duplamente anelados foram obtidos e devidamente caracterizados. Um segundo escopo foi desenvolvido utilizando-se compostos quinoidais previamente sintetizados após sequenciais métodos de modificação estrutural, de onde sete produtos foram obtidos com sucesso. Um estudo complementar foi feito, onde foram explorados alcinos não-simétricos, alcenos e alcinos alquílicos, levando à formação de uma mistura de dois regioisômeros. A partir deste novo método, um total de vinte novos compostos foram obtidos com sucesso, dentre os quais quatorze tiveram suas estruturas corroboradas *via* difração de raios-X. Um mecanismo pôde ser proposto com base em estudos da literatura e cálculos computacionais de energias relativas. Após a obtenção dos produtos finais, testes biológicos foram feitos para avaliar a atividade antitumoral de cada derivado contra a linhagem de célula cancerígena HL-60, dentre outras seis linhagens, porém com baixa atividade. Os resultados aqui apresentados foram publicados na *Chemistry – A European Journal*, além disso, vários artigos de revisão foram também produzidos a partir do conhecimento geral adquirido ao longo do desenvolvimento desta tese.

**Palavras-chave:** Quinonas. Compostos Policíclicos. Reação de Anelação Dupla. Ativação de ligação C-H. Catálise com Rutênio.

## FIGURES LIST

<b>Figure 1.</b> Atovaquone ( <b>1</b> ) and Buparvaquone ( <b>2</b> ): two important commercially available naphthoquinoidal compounds currently used as drugs for treatment of malaria and bovine theileriosis, respectively. ....	34
<b>Figure 2.</b> Lapachol ( <b>3</b> ) and Vitamin K <sub>1</sub> ( <b>4</b> ): two important naturally available naphthoquinoidal compounds.....	35
<b>Figure 3.</b> Example of the wide range of possible transformations starting from simple naphthoquinones.....	36
<b>Figure 4.</b> Publications in the last three decades about “C–H activation” ( <i>Web of Science</i> , August 5 <sup>th</sup> , 2022). ....	39
<b>Figure 5.</b> C–H modifications provided by transition-metal catalysis, examples of half-sandwich catalysts and their respective general approach.....	41
<b>Figure 6.</b> Achieved yield over time of reaction. ....	67
<b>Figure 7.</b> <sup>1</sup> H-NMR (400 MHz, CDCl <sub>3</sub> ) spectrum analysis of the compound <b>67b</b> .....	79
<b>Figure 8.</b> <sup>13</sup> C-NMR and APT (100 MHz, CDCl <sub>3</sub> ) spectra analysis of the compound <b>67b</b> .....	80
<b>Figure 9.</b> Expansion of the COSY (400 MHz, CDCl <sub>3</sub> ) spectrum of the compound <b>67b</b> . ....	81
<b>Figure 10.</b> Expansion of the HSQC (400 MHz, CDCl <sub>3</sub> ) spectrum of the compound <b>67b</b> . ....	82
<b>Figure 11.</b> Expansion of the HMBC (400 MHz, CDCl <sub>3</sub> ) spectrum of the compound <b>67b</b> . ....	83
<b>Figure 12.</b> Crystal structures of compounds <b>67a-g,k</b> . ....	85
<b>Figure 13.</b> <sup>1</sup> H-NMR (400 MHz, CDCl <sub>3</sub> ) spectrum analysis of the compound <b>58f</b> .....	96
<b>Figure 14.</b> <sup>13</sup> C-NMR and APT (100 MHz, CDCl <sub>3</sub> ) spectra analysis of the compound <b>58f</b> .....	97
<b>Figure 15.</b> <sup>1</sup> H-NMR (400 MHz, CDCl <sub>3</sub> ) spectrum analysis of the compound <b>59f</b> .....	100
<b>Figure 16.</b> <sup>13</sup> C-NMR and APT (100 MHz, CDCl <sub>3</sub> ) spectra analysis of the compound <b>59f</b> ...	101
<b>Figure 17.</b> HSQC (400 MHz, CDCl <sub>3</sub> ) spectrum of the compound <b>59f</b> .....	102
<b>Figure 18.</b> Expansion of the HSQC (400 MHz, CDCl <sub>3</sub> ) spectrum of the compound <b>59f</b> . ....	102
<b>Figure 19.</b> Expansion of the HMBC (400 MHz, CDCl <sub>3</sub> ) spectrum of the compound <b>59f</b> . ...	103
<b>Figure 20.</b> Deeper expansion of the HMBC (400 MHz, CDCl <sub>3</sub> ) spectrum of the compound <b>59f</b> focusing on the carbonyl region. ....	104

<b>Figure 21.</b> Crystal structures of compounds <b>68b-d,g</b> .....	107
<b>Figure 22.</b> Crystal structures of compounds <b>69a</b> and <b>69b</b> .....	109
<b>Figure 23.</b> Relative Gibbs free energy profile for the double-annulation reaction of <b>17a</b> with <b>18a</b> at the $\omega$ B97XD/def2TZVPP+SMD(DCE) and M06-D3/def2TZVPP+SMD(DCE) levels of theory. ....	113
<b>Figure 24.</b> Crystal structure of compound <b>59b</b> .....	154
<b>Figure 25.</b> Crystal structure of compound <b>59c</b> . ....	155
<b>Figure 26.</b> Crystal structure of compound <b>59d</b> .....	156
<b>Figure 27.</b> Crystal structure of compound <b>59g</b> .....	159
<b>Figure 28.</b> Crystal structure of compound <b>67a</b> .....	166
<b>Figure 29.</b> Crystal structure of compound <b>67b</b> .....	167
<b>Figure 30.</b> Crystal structure of compound <b>67c</b> .....	169
<b>Figure 31.</b> Crystal structure of compound <b>67d</b> .....	170
<b>Figure 32.</b> Crystal structure of compound <b>67e</b> .....	172
<b>Figure 33.</b> Crystal structure of compound <b>67f</b> .....	173
<b>Figure 34.</b> Crystal structure of compound <b>67g</b> .....	175
<b>Figure 35.</b> Crystal structure of compound <b>67k</b> .....	180
<b>Figure 36.</b> Crystal structure of compound <b>68d</b> .....	182
<b>Figure 37.</b> Crystal structure of compound <b>68c</b> .....	184
<b>Figure 38.</b> Crystal structure of compound <b>68d</b> .....	185
<b>Figure 39.</b> Crystal structure of compound <b>68g</b> .....	189
<b>Figure 40.</b> Crystal structure of compound <b>69a</b> .....	190
<b>Figure 41.</b> Crystal structure of compound <b>69b</b> .....	191
<b>Figure 42.</b> 3D images of the key intermediates <b>59a-[Ru]</b> and <b>67a'-[Ru]</b> .....	194
<b>Figure 43.</b> 3D images of the transition states <b>TS1-4</b> associated with the C–C and C–N coupling steps. ....	194
<b>Figure A1.</b> <sup>1</sup> H-NMR spectrum of compound <b>49</b> (DMSO- <i>d</i> <sub>6</sub> , 300 MHz). ....	235

<b>Figure A2.</b> $^{13}\text{C}$ -NMR spectrum of compound <b>49</b> (DMSO- $d_6$ , 75 MHz).....	235
<b>Figure A3.</b> $^1\text{H}$ -NMR spectrum of compound <b>51a</b> (CDCl $_3$ , 300 MHz).....	236
<b>Figure A4.</b> $^{13}\text{C}$ -NMR spectrum of compound <b>51a</b> (CDCl $_3$ , 75 MHz).....	236
<b>Figure A5.</b> $^1\text{H}$ -NMR spectrum of compound <b>51b</b> (CDCl $_3$ , 300 MHz).....	237
<b>Figure A6.</b> $^{13}\text{C}$ -NMR spectrum of compound <b>51b</b> (CDCl $_3$ , 75 MHz). ....	237
<b>Figure A7.</b> $^1\text{H}$ -NMR spectrum of compound <b>51c</b> (CDCl $_3$ , 300 MHz).....	238
<b>Figure A8.</b> $^{13}\text{C}$ -NMR spectrum of compound <b>51c</b> (CDCl $_3$ , 75 MHz).....	238
<b>Figure A9.</b> $^1\text{H}$ -NMR spectrum of compound <b>52</b> (CDCl $_3$ , 300 MHz).....	239
<b>Figure A10.</b> $^{13}\text{C}$ -NMR spectrum of compound <b>52</b> (CDCl $_3$ , 75 MHz).....	239
<b>Figure A11.</b> $^1\text{H}$ -NMR spectrum of compound <b>55</b> (CDCl $_3$ , 300 MHz).....	240
<b>Figure A12.</b> $^{13}\text{C}$ -NMR spectrum of compound <b>55</b> (CDCl $_3$ , 75 MHz).....	240
<b>Figure A13.</b> $^1\text{H}$ -NMR spectrum of compound <b>56b</b> (CDCl $_3$ , 400 MHz).....	241
<b>Figure A14.</b> $^{13}\text{C}$ -NMR spectrum of compound <b>56b</b> (CDCl $_3$ , 100 MHz). ....	241
<b>Figure A15.</b> $^1\text{H}$ -NMR spectrum of compound <b>56c</b> (CDCl $_3$ , 400 MHz).....	242
<b>Figure A16.</b> $^{13}\text{C}$ -NMR spectrum of compound <b>56c</b> (CDCl $_3$ , 100 MHz).....	242
<b>Figure A17.</b> $^1\text{H}$ -NMR spectrum of compound <b>56d</b> (CDCl $_3$ , 400 MHz).....	243
<b>Figure A18.</b> $^{13}\text{C}$ -NMR spectrum of compound <b>56d</b> (CDCl $_3$ , 100 MHz). ....	243
<b>Figure A19.</b> $^1\text{H}$ -NMR spectrum of compound <b>56e</b> (CDCl $_3$ , 400 MHz).....	244
<b>Figure A20.</b> $^{13}\text{C}$ -NMR spectrum of compound <b>56e</b> (CDCl $_3$ , 100 MHz).....	244
<b>Figure A21.</b> $^1\text{H}$ -NMR spectrum of compound <b>56f</b> (CDCl $_3$ , 400 MHz).....	245
<b>Figure A22.</b> $^{13}\text{C}$ -NMR spectrum of compound <b>56f</b> (CDCl $_3$ , 100 MHz). ....	245
<b>Figure A23.</b> $^1\text{H}$ -NMR spectrum of compound <b>56g</b> (CDCl $_3$ , 400 MHz).....	246
<b>Figure A24.</b> $^{13}\text{C}$ -NMR spectrum of compound <b>56g</b> (CDCl $_3$ , 100 MHz).....	246
<b>Figure A25.</b> $^1\text{H}$ -NMR spectrum of compound <b>56h</b> (CDCl $_3$ , 400 MHz).....	247
<b>Figure A26.</b> $^{13}\text{C}$ -NMR spectrum of compound <b>56h</b> (CDCl $_3$ , 100 MHz). ....	247
<b>Figure A27.</b> $^1\text{H}$ -NMR spectrum of compound <b>56i</b> (CDCl $_3$ , 400 MHz).....	248
<b>Figure A28.</b> $^{13}\text{C}$ -NMR spectrum of compound <b>56i</b> (CDCl $_3$ , 100 MHz).....	248

<b>Figure A29.</b> $^1\text{H}$ -NMR spectrum of compound <b>56j</b> ( $\text{CDCl}_3$ , 400 MHz).....	249
<b>Figure A30.</b> $^{13}\text{C}$ -NMR spectrum of compound <b>56j</b> ( $\text{CDCl}_3$ , 100 MHz). .....	249
<b>Figure A31.</b> $^1\text{H}$ -NMR spectrum of compound <b>56k</b> ( $\text{CDCl}_3$ , 400 MHz).....	250
<b>Figure A32.</b> $^{13}\text{C}$ -NMR spectrum of compound <b>56k</b> ( $\text{CDCl}_3$ , 100 MHz). .....	250
<b>Figure A33.</b> $^1\text{H}$ -NMR spectrum of compound <b>56l</b> ( $\text{CDCl}_3$ , 400 MHz).....	251
<b>Figure A34.</b> $^{13}\text{C}$ -NMR spectrum of compound <b>56l</b> ( $\text{CDCl}_3$ , 100 MHz).....	251
<b>Figure A35.</b> $^1\text{H}$ -NMR spectrum of compound <b>56m</b> ( $\text{CDCl}_3$ , 400 MHz).....	252
<b>Figure A36.</b> $^{13}\text{C}$ -NMR spectrum of compound <b>56m</b> ( $\text{CDCl}_3$ , 100 MHz). .....	252
<b>Figure A37.</b> $^1\text{H}$ -NMR spectrum of compound <b>56n</b> ( $\text{CDCl}_3$ , 400 MHz).....	253
<b>Figure A38.</b> $^{13}\text{C}$ -NMR spectrum of compound <b>56n</b> ( $\text{CDCl}_3$ , 100 MHz). .....	253
<b>Figure A39.</b> $^1\text{H}$ -NMR spectrum of compound <b>56o</b> ( $\text{CDCl}_3$ , 400 MHz).....	254
<b>Figure A40.</b> $^{13}\text{C}$ -NMR spectrum of compound <b>56o</b> ( $\text{CDCl}_3$ , 100 MHz).....	254
<b>Figure A41.</b> $^1\text{H}$ -NMR spectrum of compound <b>56p</b> ( $\text{CDCl}_3$ , 400 MHz).....	255
<b>Figure A42.</b> $^{13}\text{C}$ -NMR spectrum of compound <b>56p</b> ( $\text{CDCl}_3$ , 100 MHz). .....	255
<b>Figure A43.</b> $^1\text{H}$ -NMR spectrum of compound <b>56q</b> ( $\text{CDCl}_3$ , 400 MHz).....	256
<b>Figure A44.</b> $^{13}\text{C}$ -NMR spectrum of compound <b>56q</b> ( $\text{CDCl}_3$ , 100 MHz). .....	256
<b>Figure A45.</b> $^1\text{H}$ -NMR spectrum of compound <b>56r</b> ( $\text{CDCl}_3$ , 400 MHz). .....	257
<b>Figure A46.</b> $^{13}\text{C}$ -NMR spectrum of compound <b>56r</b> ( $\text{CDCl}_3$ , 100 MHz).....	257
<b>Figure A47.</b> $^1\text{H}$ -NMR spectrum of compound <b>56s</b> ( $\text{CDCl}_3$ , 400 MHz). .....	258
<b>Figure A48.</b> $^{13}\text{C}$ -NMR spectrum of compound <b>56s</b> ( $\text{CDCl}_3$ , 100 MHz).....	258
<b>Figure A49.</b> $^1\text{H}$ -NMR spectrum of compound <b>57a</b> ( $\text{CDCl}_3$ , 400 MHz).....	259
<b>Figure A50.</b> $^{13}\text{C}$ -NMR spectrum of compound <b>57a</b> ( $\text{CDCl}_3$ , 100 MHz).....	259
<b>Figure A51.</b> $^1\text{H}$ -NMR spectrum of compound <b>57b</b> ( $\text{CDCl}_3$ , 400 MHz).....	260
<b>Figure A52.</b> $^{13}\text{C}$ -NMR spectrum of compound <b>57b</b> ( $\text{CDCl}_3$ , 100 MHz). .....	260
<b>Figure A53.</b> $^1\text{H}$ -NMR spectrum of compound <b>57c</b> ( $\text{CDCl}_3$ , 400 MHz). .....	261
<b>Figure A54.</b> $^{13}\text{C}$ -NMR spectrum of compound <b>57c</b> ( $\text{CDCl}_3$ , 100 MHz).....	261
<b>Figure A55.</b> $^1\text{H}$ -NMR spectrum of compound <b>57d</b> ( $\text{CDCl}_3$ , 400 MHz).....	262

<b>Figure A56.</b> $^{13}\text{C}$ -NMR spectrum of compound <b>57d</b> ( $\text{CDCl}_3$ , 100 MHz). .....	262
<b>Figure A57.</b> $^1\text{H}$ -NMR spectrum of compound <b>57e</b> ( $\text{CDCl}_3$ , 400 MHz). .....	263
<b>Figure A58.</b> $^{13}\text{C}$ -NMR spectrum of compound <b>57e</b> ( $\text{CDCl}_3$ , 100 MHz). .....	263
<b>Figure A59.</b> $^1\text{H}$ -NMR spectrum of compound <b>57f</b> ( $\text{CDCl}_3$ , 300 MHz). .....	264
<b>Figure A60.</b> $^{13}\text{C}$ -NMR spectrum of compound <b>57f</b> ( $\text{CDCl}_3$ , 75 MHz). .....	264
<b>Figure A61.</b> $^1\text{H}$ -NMR spectrum of compound <b>57g</b> ( $\text{CDCl}_3$ , 400 MHz). .....	265
<b>Figure A62.</b> $^{13}\text{C}$ -NMR spectrum of compound <b>57g</b> ( $\text{CDCl}_3$ , 100 MHz). .....	265
<b>Figure A63.</b> $^1\text{H}$ -NMR spectrum of compound <b>57i</b> ( $\text{CDCl}_3$ , 400 MHz). .....	266
<b>Figure A64.</b> $^{13}\text{C}$ -NMR spectrum of compound <b>57i</b> ( $\text{CDCl}_3$ , 100 MHz). .....	266
<b>Figure A65.</b> $^1\text{H}$ -NMR spectrum of compound <b>57j</b> ( $\text{CDCl}_3$ , 400 MHz). .....	267
<b>Figure A66.</b> $^{13}\text{C}$ -NMR spectrum of compound <b>57j</b> ( $\text{CDCl}_3$ , 100 MHz). .....	267
<b>Figure A67.</b> $^1\text{H}$ -NMR spectrum of compound <b>57l</b> ( $\text{CDCl}_3$ , 400 MHz). .....	268
<b>Figure A68.</b> $^{13}\text{C}$ -NMR spectrum of compound <b>57l</b> ( $\text{CDCl}_3$ , 100 MHz). .....	268
<b>Figure A69.</b> $^1\text{H}$ -NMR spectrum of compound <b>57m</b> ( $\text{CDCl}_3$ , 400 MHz). .....	269
<b>Figure A70.</b> $^{13}\text{C}$ -NMR spectrum of compound <b>57m</b> ( $\text{CDCl}_3$ , 100 MHz). .....	269
<b>Figure A71.</b> $^1\text{H}$ -NMR spectrum of compound <b>57n</b> ( $\text{CDCl}_3$ , 400 MHz). .....	270
<b>Figure A72.</b> $^{13}\text{C}$ -NMR spectrum of compound <b>57n</b> ( $\text{CDCl}_3$ , 100 MHz). .....	270
<b>Figure A73.</b> $^1\text{H}$ -NMR spectrum of compound <b>57o</b> ( $\text{CDCl}_3$ , 400 MHz). .....	271
<b>Figure A74.</b> $^{13}\text{C}$ -NMR spectrum of compound <b>57o</b> ( $\text{CDCl}_3$ , 100 MHz). .....	271
<b>Figure A75.</b> $^1\text{H}$ -NMR spectrum of compound <b>58a</b> ( $\text{CDCl}_3$ , 400 MHz). .....	272
<b>Figure A76.</b> $^{13}\text{C}$ -NMR spectrum of compound <b>58a</b> ( $\text{CDCl}_3$ , 100 MHz). .....	272
<b>Figure A77.</b> $^1\text{H}$ -NMR spectrum of compound <b>58b</b> ( $\text{DMSO-}d_6$ , 300 MHz). .....	273
<b>Figure A78.</b> $^{13}\text{C}$ -NMR spectrum of compound <b>58b</b> ( $\text{DMSO-}d_6$ , 75 MHz). .....	273
<b>Figure A79.</b> $^1\text{H}$ -NMR spectrum of compound <b>58c</b> ( $\text{DMSO-}d_6$ , 400 MHz). .....	274
<b>Figure A80.</b> $^{13}\text{C}$ -NMR spectrum of compound <b>58c</b> ( $\text{DMSO-}d_6$ , 100 MHz). .....	274
<b>Figure A81.</b> $^1\text{H}$ -NMR spectrum of compound <b>58d</b> ( $\text{CDCl}_3$ , 400 MHz). .....	275
<b>Figure A82.</b> $^{13}\text{C}$ -NMR spectrum of compound <b>58d</b> ( $\text{CDCl}_3$ , 100 MHz). .....	275



<b>Figure A83.</b> $^1\text{H}$ -NMR spectrum of compound <b>58e</b> (DMSO- $d_6$ , 400 MHz). .....	276
<b>Figure A84.</b> $^{13}\text{C}$ -NMR spectrum of compound <b>58e</b> (DMSO- $d_6$ , 100 MHz). .....	276
<b>Figure A85.</b> $^1\text{H}$ -NMR spectrum of compound <b>58f</b> ( $\text{CDCl}_3$ , 400 MHz).....	277
<b>Figure A86.</b> $^{13}\text{C}$ -NMR spectrum of compound <b>58f</b> ( $\text{CDCl}_3$ , 100 MHz). .....	277
<b>Figure A87.</b> $^1\text{H}$ -NMR spectrum of compound <b>58g</b> (DMSO- $d_6$ , 400 MHz). .....	278
<b>Figure A88.</b> $^{13}\text{C}$ -NMR spectrum of compound <b>58g</b> (DMSO- $d_6$ , 100 MHz). .....	278
<b>Figure A89.</b> $^1\text{H}$ -NMR spectrum of compound <b>59a</b> ( $\text{CDCl}_3$ , 400 MHz).....	279
<b>Figure A90.</b> $^{13}\text{C}$ -NMR spectrum of compound <b>59a</b> ( $\text{CDCl}_3$ , 100 MHz).....	279
<b>Figure A91.</b> $^1\text{H}$ -NMR spectrum of compound <b>59b</b> ( $\text{CDCl}_3$ , 400 MHz).....	280
<b>Figure A92.</b> $^{13}\text{C}$ -NMR spectrum of compound <b>59b</b> ( $\text{CDCl}_3$ , 100 MHz). .....	280
<b>Figure A93.</b> $^1\text{H}$ -NMR spectrum of compound <b>59c</b> ( $\text{CDCl}_3$ , 600 MHz). .....	281
<b>Figure A94.</b> $^{13}\text{C}$ -NMR spectrum of compound <b>59c</b> ( $\text{CDCl}_3$ , 150 MHz).....	281
<b>Figure A95.</b> $^1\text{H}$ -NMR spectrum of compound <b>59d</b> ( $\text{CDCl}_3$ , 600 MHz).....	282
<b>Figure A96.</b> $^{13}\text{C}$ -NMR spectrum of compound <b>59d</b> ( $\text{CDCl}_3$ , 150 MHz). .....	282
<b>Figure A97.</b> $^1\text{H}$ -NMR spectrum of compound <b>59e</b> ( $\text{CDCl}_3$ , 400 MHz). .....	283
<b>Figure A98.</b> $^{13}\text{C}$ -NMR spectrum of compound <b>59e</b> ( $\text{CDCl}_3$ , 100 MHz).....	283
<b>Figure A99.</b> $^1\text{H}$ -NMR spectrum of compound <b>59f</b> ( $\text{CDCl}_3$ , 400 MHz).....	284
<b>Figure A100.</b> $^{13}\text{C}$ -NMR spectrum of compound <b>59f</b> ( $\text{CDCl}_3$ , 100 MHz). .....	284
<b>Figure A101.</b> $^1\text{H}$ -NMR spectrum of compound <b>59g</b> (DMSO- $d_6$ , 400 MHz). .....	285
<b>Figure A102.</b> $^{13}\text{C}$ -NMR spectrum of compound <b>59g</b> (DMSO- $d_6$ , 100 MHz).....	285
<b>Figure A103.</b> $^1\text{H}$ -NMR spectrum of compound <b>60</b> (DMSO- $d_6$ , 400 MHz). .....	286
<b>Figure A104.</b> $^{13}\text{C}$ -NMR spectrum of compound <b>60</b> (DMSO- $d_6$ , 100 MHz). .....	286
<b>Figure A105.</b> $^1\text{H}$ -NMR spectrum of compound <b>61</b> (DMSO- $d_6$ , 400 MHz). .....	287
<b>Figure A106.</b> $^{13}\text{C}$ -NMR spectrum of compound <b>61</b> (DMSO- $d_6$ , 100 MHz).....	287
<b>Figure A107.</b> $^1\text{H}$ -NMR spectrum of compound <b>62</b> ( $\text{CDCl}_3$ , 400 MHz).....	288
<b>Figure A108.</b> $^{13}\text{C}$ -NMR spectrum of compound <b>62</b> ( $\text{CDCl}_3$ , 100 MHz).....	288
<b>Figure A109.</b> $^1\text{H}$ -NMR spectrum of compound <b>64</b> ( $\text{CDCl}_3$ , 400 MHz).....	289

<b>Figure A110.</b> <sup>13</sup> C-NMR spectrum of compound <b>64</b> (CDCl <sub>3</sub> , 100 MHz).....	289
<b>Figure A111.</b> <sup>1</sup> H-NMR spectrum of compound <b>65</b> (CDCl <sub>3</sub> , 400 MHz).....	290
<b>Figure A112.</b> <sup>13</sup> C-NMR spectrum of compound <b>65</b> (CDCl <sub>3</sub> , 100 MHz).....	290
<b>Figure A113.</b> <sup>1</sup> H-NMR spectrum of compound <b>67a</b> (CDCl <sub>3</sub> , 400 MHz).....	291
<b>Figure A114.</b> <sup>13</sup> C-NMR spectrum of compound <b>67a</b> (CDCl <sub>3</sub> , 100 MHz).....	291
<b>Figure A115.</b> <sup>1</sup> H-NMR spectrum of compound <b>67b</b> (CDCl <sub>3</sub> , 400 MHz).....	292
<b>Figure A116.</b> <sup>13</sup> C-NMR spectrum of compound <b>67b</b> (CDCl <sub>3</sub> , 100 MHz). ....	292
<b>Figure A117.</b> <sup>1</sup> H-NMR spectrum of compound <b>67c</b> (CDCl <sub>3</sub> , 400 MHz). ....	293
<b>Figure A118.</b> <sup>13</sup> C-NMR spectrum of compound <b>67c</b> (CDCl <sub>3</sub> , 100 MHz).....	293
<b>Figure A119.</b> <sup>1</sup> H-NMR spectrum of compound <b>67d</b> (CDCl <sub>3</sub> , 400 MHz).....	294
<b>Figure A120.</b> <sup>13</sup> C-NMR spectrum of compound <b>67d</b> (CDCl <sub>3</sub> , 100 MHz). ....	294
<b>Figure A121.</b> <sup>1</sup> H-NMR spectrum of compound <b>67e</b> (CDCl <sub>3</sub> , 400 MHz). ....	295
<b>Figure A122.</b> <sup>13</sup> C-NMR spectrum of compound <b>67e</b> (CDCl <sub>3</sub> , 100 MHz).....	295
<b>Figure A123.</b> <sup>1</sup> H-NMR spectrum of compound <b>67f</b> (CDCl <sub>3</sub> , 400 MHz).....	296
<b>Figure A124.</b> <sup>13</sup> C-NMR spectrum of compound <b>67f</b> (CDCl <sub>3</sub> , 100 MHz). ....	296
<b>Figure A125.</b> <sup>1</sup> H-NMR spectrum of compound <b>67g</b> (CDCl <sub>3</sub> , 400 MHz).....	297
<b>Figure A126.</b> <sup>13</sup> C-NMR spectrum of compound <b>67g</b> (CDCl <sub>3</sub> , 100 MHz).....	297
<b>Figure A127.</b> <sup>1</sup> H-NMR spectrum of compound <b>67h</b> (CDCl <sub>3</sub> , 400 MHz).....	298
<b>Figure A128.</b> <sup>13</sup> C-NMR spectrum of compound <b>67h</b> (CDCl <sub>3</sub> , 100 MHz). ....	298
<b>Figure A129.</b> <sup>1</sup> H-NMR spectrum of compound <b>67i</b> (CDCl <sub>3</sub> , 400 MHz).....	299
<b>Figure A130.</b> <sup>13</sup> C-NMR spectrum of compound <b>67i</b> (CDCl <sub>3</sub> , 100 MHz).....	299
<b>Figure A131.</b> <sup>1</sup> H-NMR spectrum of compound <b>67j</b> (CDCl <sub>3</sub> , 400 MHz).....	300
<b>Figure A132.</b> <sup>13</sup> C-NMR spectrum of compound <b>67j</b> (CDCl <sub>3</sub> , 100 MHz). ....	300
<b>Figure A133.</b> <sup>1</sup> H-NMR spectrum of compound <b>67k</b> (CDCl <sub>3</sub> , 400 MHz).....	301
<b>Figure A134.</b> <sup>13</sup> C-NMR spectrum of compound <b>67k</b> (CDCl <sub>3</sub> , 100 MHz). ....	301
<b>Figure A135.</b> <sup>1</sup> H-NMR spectrum of compound <b>68a</b> (CDCl <sub>3</sub> , 400 MHz).....	302
<b>Figure A136.</b> <sup>13</sup> C-NMR spectrum of compound <b>68a</b> (CDCl <sub>3</sub> , 100 MHz).....	302

<b>Figure A137.</b> <sup>1</sup> H-NMR spectrum of compound <b>68b</b> (CDCl <sub>3</sub> , 400 MHz).....	303
<b>Figure A138.</b> <sup>13</sup> C-NMR spectrum of compound <b>68b</b> (CDCl <sub>3</sub> , 100 MHz). .....	303
<b>Figure A139.</b> <sup>1</sup> H-NMR spectrum of compound <b>68c</b> (CDCl <sub>3</sub> , 400 MHz). .....	304
<b>Figure A140.</b> <sup>13</sup> C-NMR spectrum of compound <b>68c</b> (CDCl <sub>3</sub> , 100 MHz).....	304
<b>Figure A141.</b> <sup>1</sup> H-NMR spectrum of compound <b>68d</b> (CDCl <sub>3</sub> , 400 MHz).....	305
<b>Figure A142.</b> <sup>13</sup> C-NMR spectrum of compound <b>68d</b> (CDCl <sub>3</sub> , 100 MHz). .....	305
<b>Figure A143.</b> <sup>1</sup> H-NMR spectrum of compound <b>68e</b> (CDCl <sub>3</sub> , 400 MHz). .....	306
<b>Figure A144.</b> <sup>13</sup> C-NMR spectrum of compound <b>68e</b> (CDCl <sub>3</sub> , 100 MHz).....	306
<b>Figure A145.</b> <sup>1</sup> H-NMR spectrum of compound <b>68f</b> (CDCl <sub>3</sub> , 400 MHz).....	307
<b>Figure A146.</b> <sup>13</sup> C-NMR spectrum of compound <b>68f</b> (CDCl <sub>3</sub> , 100 MHz). .....	307
<b>Figure A147.</b> <sup>1</sup> H-NMR spectrum of compound <b>68g</b> (CDCl <sub>3</sub> , 400 MHz).....	308
<b>Figure A148.</b> <sup>13</sup> C-NMR spectrum of compound <b>68g</b> (CDCl <sub>3</sub> , 100 MHz).....	308
<b>Figure A149.</b> <sup>1</sup> H-NMR spectrum of compound <b>69a</b> (CDCl <sub>3</sub> , 400 MHz).....	309
<b>Figure A150.</b> <sup>13</sup> C-NMR spectrum of compound <b>69a</b> (CDCl <sub>3</sub> , 100 MHz).....	309
<b>Figure A151.</b> <sup>1</sup> H-NMR spectrum of compound <b>69b</b> (CDCl <sub>3</sub> , 400 MHz).....	310
<b>Figure A152.</b> <sup>13</sup> C-NMR spectrum of compound <b>69b</b> (CDCl <sub>3</sub> , 100 MHz). .....	310
<b>Figure B1.</b> Infrared spectrum (IR-KBr) of the compound <b>51a</b> .....	311
<b>Figure B2.</b> Infrared spectrum (IR-KBr) of the compound <b>51b</b> . .....	311
<b>Figure B3.</b> Infrared spectrum (IR-ATR) of the compound <b>52</b> . .....	312
<b>Figure B4.</b> Infrared spectrum (IR-KBr) of the compound <b>55</b> .....	312
<b>Figure B5.</b> Infrared spectrum (IR-ATR) of the compound <b>56b</b> . .....	313
<b>Figure B6.</b> Infrared spectrum (IR-ATR) of the compound <b>56c</b> .....	313
<b>Figure B7.</b> Infrared spectrum (IR-ATR) of the compound <b>56d</b> . .....	314
<b>Figure B8.</b> Infrared spectrum (IR-ATR) of the compound <b>56e</b> .....	314
<b>Figure B9.</b> Infrared spectrum (IR-ATR) of the compound <b>56f</b> . .....	315
<b>Figure B10.</b> Infrared spectrum (IR-ATR) of the compound <b>56g</b> .....	315
<b>Figure B11.</b> Infrared spectrum (IR-ATR) of the compound <b>56h</b> . .....	316

<b>Figure B12.</b> Infrared spectrum (IR-ATR) of the compound <b>56i</b> . .....	316
<b>Figure B13.</b> Infrared spectrum (IR-ATR) of the compound <b>56j</b> . .....	317
<b>Figure B14.</b> Infrared spectrum (IR-ATR) of the compound <b>56k</b> . .....	317
<b>Figure B15.</b> Infrared spectrum (IR-ATR) of the compound <b>56l</b> . .....	318
<b>Figure B16.</b> Infrared spectrum (IR-ATR) of the compound <b>56m</b> . .....	318
<b>Figure B17.</b> Infrared spectrum (IR-ATR) of the compound <b>56n</b> . .....	319
<b>Figure B18.</b> Infrared spectrum (IR-ATR) of the compound <b>56o</b> . .....	319
<b>Figure B19.</b> Infrared spectrum (IR-ATR) of the compound <b>56p</b> . .....	320
<b>Figure B20.</b> Infrared spectrum (IR-ATR) of the compound <b>56q</b> . .....	320
<b>Figure B21.</b> Infrared spectrum (IR-ATR) of the compound <b>56r</b> . .....	321
<b>Figure B22.</b> Infrared spectrum (IR-ATR) of the compound <b>56s</b> . .....	321
<b>Figure B23.</b> Infrared spectrum (IR-ATR) of the compound <b>57a</b> . .....	322
<b>Figure B24.</b> Infrared spectrum (IR-KBr) of the compound <b>57b</b> . .....	322
<b>Figure B25.</b> Infrared spectrum (IR-KBr) of the compound <b>57c</b> . .....	323
<b>Figure B26.</b> Infrared spectrum (IR-ATR) of the compound <b>57d</b> . .....	323
<b>Figure B27.</b> Infrared spectrum (IR-KBr) of the compound <b>57e</b> . .....	324
<b>Figure B28.</b> Infrared spectrum (IR-KBr) of the compound <b>57f</b> . .....	324
<b>Figure B29.</b> Infrared spectrum (IR-ATR) of the compound <b>57g</b> . .....	325
<b>Figure B30.</b> Infrared spectrum (IR-ATR) of the compound <b>57i</b> . .....	325
<b>Figure B31.</b> Infrared spectrum (IR-ATR) of the compound <b>57j</b> . .....	326
<b>Figure B32.</b> Infrared spectrum (IR-ATR) of the compound <b>57l</b> . .....	326
<b>Figure B33.</b> Infrared spectrum (IR-ATR) of the compound <b>57m</b> . .....	327
<b>Figure B34.</b> Infrared spectrum (IR-ATR) of the compound <b>57n</b> . .....	327
<b>Figure B35.</b> Infrared spectrum (IR-ATR) of the compound <b>57o</b> . .....	328
<b>Figure B36.</b> Infrared spectrum (IR-ATR) of the compound <b>58a</b> . .....	328
<b>Figure B37.</b> Infrared spectrum (IR-ATR) of the compound <b>58b</b> . .....	329
<b>Figure B38.</b> Infrared spectrum (IR-ATR) of the compound <b>58c</b> . .....	329

<b>Figure B39.</b> Infrared spectrum (IR-KBr) of the compound <b>58d</b> .	330
<b>Figure B40.</b> Infrared spectrum (IR-KBr) of the compound <b>58e</b> .	330
<b>Figure B41.</b> Infrared spectrum (IR-ATR) of the compound <b>58f</b> .	331
<b>Figure B42.</b> Infrared spectrum (IR-ATR) of the compound <b>58g</b> .	331
<b>Figure B43.</b> Infrared spectrum (IR-ATR) of the compound <b>59a</b> .	332
<b>Figure B44.</b> Infrared spectrum (IR-ATR) of the compound <b>59b</b> .	332
<b>Figure B45.</b> Infrared spectrum (IR-ATR) of the compound <b>59c</b> .	333
<b>Figure B46.</b> Infrared spectrum (IR-ATR) of the compound <b>59d</b> .	333
<b>Figure B47.</b> Infrared spectrum (IR-ATR) of the compound <b>59e</b> .	334
<b>Figure B48.</b> Infrared spectrum (IR-ATR) of the compound <b>59f</b> .	334
<b>Figure B49.</b> Infrared spectrum (IR-ATR) of the compound <b>59g</b> .	335
<b>Figure B50.</b> Infrared spectrum (IR-KBr) of the compound <b>60</b> .	335
<b>Figure B51.</b> Infrared spectrum (IR-KBr) of the compound <b>61</b> .	336
<b>Figure B52.</b> Infrared spectrum (IR-KBr) of the compound <b>62</b> .	336
<b>Figure B53.</b> Infrared spectrum (IR-KBr) of the compound <b>64</b> .	337
<b>Figure B54.</b> Infrared spectrum (IR-KBr) of the compound <b>65</b> .	337
<b>Figure B55.</b> Infrared spectrum (IR-ATR) of the compound <b>67a</b> .	338
<b>Figure B56.</b> Infrared spectrum (IR-ATR) of the compound <b>67b</b> .	338
<b>Figure B57.</b> Infrared spectrum (IR-ATR) of the compound <b>67c</b> .	339
<b>Figure B58.</b> Infrared spectrum (IR-ATR) of the compound <b>67d</b> .	339
<b>Figure B59.</b> Infrared spectrum (IR-ATR) of the compound <b>67e</b> .	340
<b>Figure B60.</b> Infrared spectrum (IR-ATR) of the compound <b>67f</b> .	340
<b>Figure B61.</b> Infrared spectrum (IR-ATR) of the compound <b>67g</b> .	341
<b>Figure B62.</b> Infrared spectrum (IR-ATR) of the compound <b>67h</b> .	341
<b>Figure B63.</b> Infrared spectrum (IR-ATR) of the compound <b>67i</b> .	342
<b>Figure B64.</b> Infrared spectrum (IR-ATR) of the compound <b>67j</b> .	342
<b>Figure B65.</b> Infrared spectrum (IR-ATR) of the compound <b>67k</b> .	343

<b>Figure B66.</b> Infrared spectrum (IR-ATR) of the compound <b>68a</b> .....	343
<b>Figure B67.</b> Infrared spectrum (IR-ATR) of the compound <b>68b</b> . .....	344
<b>Figure B68.</b> Infrared spectrum (IR-ATR) of the compound <b>68c</b> .....	344
<b>Figure B69.</b> Infrared spectrum (IR-ATR) of the compound <b>68d</b> . .....	345
<b>Figure B70.</b> Infrared spectrum (IR-ATR) of the compound <b>68e</b> .....	345
<b>Figure B71.</b> Infrared spectrum (IR-ATR) of the compound <b>68f</b> . .....	346
<b>Figure B72.</b> Infrared spectrum (IR-ATR) of the compound <b>68g</b> .....	346
<b>Figure B73.</b> Infrared spectrum (IR-ATR) of the compound <b>69a</b> .....	347
<b>Figure B74.</b> Infrared spectrum (IR-ATR) of the compound <b>69b</b> . .....	347
<b>Figure C1.</b> HRMS-ESI (+) of compound <b>52</b> . .....	348
<b>Figure C2.</b> MS-EI (+) of compound <b>56b</b> .....	348
<b>Figure C3.</b> HRMS-EI (+) of compound <b>56c</b> .....	349
<b>Figure C4.</b> HRMS-EI (+) of compound <b>56d</b> . .....	349
<b>Figure C5.</b> HRMS-EI (+) of compound <b>56e</b> .....	350
<b>Figure C6.</b> HRMS-EI (+) of compound <b>56f</b> . .....	351
<b>Figure C7.</b> HRMS-ESI (+) of compound <b>56h</b> .....	351
<b>Figure C8.</b> HRMS-EI (+) of compound <b>56i</b> . .....	352
<b>Figure C9.</b> HRMS-ESI (+) of compound <b>56j</b> .....	352
<b>Figure C10.</b> HRMS-EI (+) of compound <b>56k</b> . .....	353
<b>Figure C11.</b> HRMS-EI (+) of compound <b>56i</b> . .....	353
<b>Figure C12.</b> HRMS-EI (+) of compound <b>56m</b> . .....	354
<b>Figure C13.</b> HRMS-ESI (+) of compound <b>56n</b> .....	354
<b>Figure C14.</b> HRMS-EI (+) of compound <b>56o</b> . .....	355
<b>Figure C15.</b> HRMS-EI (+) of compound <b>56p</b> . .....	355
<b>Figure C16.</b> HRMS-EI (+) of compound <b>56q</b> . .....	356
<b>Figure C17.</b> HRMS-ESI (+) of compound <b>56r</b> . .....	356
<b>Figure C18.</b> HRMS-EI (+) of compound <b>56s</b> .....	357

<b>Figure C19.</b> HRMS-ESI (+) of compound <b>57a</b> .	357
<b>Figure C20.</b> HRMS-ESI (+) of compound <b>57e</b> .	358
<b>Figure C21.</b> HRMS-EI (+) of compound <b>57g</b> .	358
<b>Figure C22.</b> HRMS-ESI (+) of compound <b>57i</b> .	359
<b>Figure C23.</b> HRMS-ESI (+) of compound <b>57j</b> .	359
<b>Figure C24.</b> HRMS-ESI (+) of compound <b>57l</b> .	360
<b>Figure C25.</b> HRMS-ESI (+) of compound <b>57m</b> .	360
<b>Figure C26.</b> HRMS-ESI (+) of compound <b>57n</b> .	361
<b>Figure C27.</b> HRMS-ESI (+) of compound <b>57o</b> .	361
<b>Figure C28.</b> HRMS-ESI (+) of compound <b>58a</b> .	362
<b>Figure C29.</b> HRMS-ESI (+) of compound <b>58b</b> .	362
<b>Figure C30.</b> HRMS-ESI (+) of compound <b>58c</b> .	363
<b>Figure C31.</b> HRMS-ESI (+) of compound <b>58d</b> .	363
<b>Figure C32.</b> HRMS-ESI (+) of compound <b>58e</b> .	364
<b>Figure C33.</b> HRMS-ESI (+) of compound <b>58f</b> .	364
<b>Figure C34.</b> HRMS-ESI (+) of compound <b>58g</b> .	365
<b>Figure C35.</b> HRMS-ESI (+) of compound <b>59a</b> .	365
<b>Figure C36.</b> HRMS-ESI (+) of compound <b>59b</b> .	366
<b>Figure C37.</b> HRMS-ESI (+) of compound <b>59c</b> .	366
<b>Figure C38.</b> HRMS-ESI (+) of compound <b>59d</b> .	367
<b>Figure C39.</b> HRMS-ESI (+) of compound <b>59e</b> .	367
<b>Figure C40.</b> HRMS-ESI (+) of compound <b>59f</b> .	368
<b>Figure C41.</b> HRMS-ESI (+) of compound <b>59g</b> .	368
<b>Figure C42.</b> HRMS-ESI (+) of compound <b>67a</b> .	369
<b>Figure C43.</b> HRMS-ESI (+) of compound <b>67b</b> .	369
<b>Figure C44.</b> HRMS-ESI (+) of compound <b>67c</b> .	370
<b>Figure C45.</b> HRMS-ESI (+) of compound <b>67d</b> .	370

<b>Figure C46.</b> HRMS-ESI (+) of compound <b>67e</b> . .....	371
<b>Figure C47.</b> HRMS-ESI (+) of compound <b>67f</b> . .....	371
<b>Figure C48.</b> HRMS-ESI (+) of compound <b>67g</b> . .....	372
<b>Figure C49.</b> HRMS-ESI (+) of compound <b>67h</b> . .....	372
<b>Figure C50.</b> HRMS-ESI (+) of compound <b>67i</b> . .....	373
<b>Figure C51.</b> HRMS-ESI (+) of compound <b>67j</b> . .....	373
<b>Figure C52.</b> HRMS-ESI (+) of compound <b>67k</b> . .....	374
<b>Figure C53.</b> HRMS-ESI (+) of compound <b>68a</b> . .....	374
<b>Figure C54.</b> HRMS-ESI (+) of compound <b>68b</b> . .....	375
<b>Figure C55.</b> HRMS-ESI (+) of compound <b>68c</b> . .....	375
<b>Figure C56.</b> HRMS-ESI (+) of compound <b>68d</b> . .....	376
<b>Figure C57.</b> HRMS-ESI (+) of compound <b>68e</b> . .....	376
<b>Figure C58.</b> HRMS-ESI (+) of compound <b>68f</b> . .....	377
<b>Figure C59.</b> HRMS-ESI (+) of compound <b>68g</b> . .....	377
<b>Figure C60.</b> HRMS-ESI (+) of compound <b>69a</b> . .....	378
<b>Figure C61.</b> HRMS-ESI (+) of compound <b>69b</b> . .....	378



## SCHEMES LIST

<b>Scheme 1.</b> A brief view on the C–H activation history.....	38
<b>Scheme 2.</b> Examples of currently known polycyclic quinones synthesis.....	45
<b>Scheme 3.</b> Previous knowledge and purpose for C–H arylation on naphthoquinones. ....	47
<b>Scheme 4.</b> Previously reported Ruthenium-catalyzed annulation and possible extrapolation of the method to a quinone without any additional DG. ....	48
<b>Scheme 5.</b> Previously reported Ruthenium-catalyzed annulation and possible extrapolation of the method to a quinone bearing a C-2 acetamide DG. ....	49
<b>Scheme 6.</b> C–H activation at the C-5 position of 1,4-naphthoquinone ( <b>5</b> ). ....	51
<b>Scheme 7.</b> Ruthenium-catalyzed C–H arylation trial.....	51
<b>Scheme 8.</b> Modified substrates used to force the C–H activation at the C-5 position.....	53
<b>Scheme 9.</b> C–H annulation trial using substrate <b>5</b> and sulfoxonium ylide <b>55</b> . ....	54
<b>Scheme 10.</b> Aryl-amination process towards compounds <b>60</b> and <b>61</b> , and proposed mechanism.....	57
<b>Scheme 11.</b> Amination process towards compound <b>58a</b> and proposed simplified mechanism.....	58
<b>Scheme 12.</b> Acetylation process towards compound <b>59a</b> and proposed mechanism. ....	59
<b>Scheme 13.</b> Acetylation process towards compound <b>62</b> .....	60
<b>Scheme 14.</b> Acetylation process towards compound <b>63</b> .....	60
<b>Scheme 15.</b> Acylation process towards compound <b>64</b> and proposed mechanism. ....	61
<b>Scheme 16.</b> C–H annulation trial using substrates with synthesizable DG and sulfoxonium ylide <b>55</b> . ....	62
<b>Scheme 17.</b> First C–H double annulation trials on substrates with synthesizable DG and alkyne <b>56a</b> . ....	63
<b>Scheme 18.</b> Ruthenium catalysts used in the first double-annulation trials and their respective usual synthesis.....	65
<b>Scheme 19.</b> Synthesis of symmetrical internal alkynes, obtained scope and substrates that failed the procedure. ....	75

<b>Scheme 20.</b> Simplified mechanism of the Sonogashira-type reaction.....	76
<b>Scheme 21.</b> First scope: double annulation reaction between compound <b>59a</b> and symmetrical internal alkynes <b>56a-k</b> . .....	77
<b>Scheme 22.</b> Spatial representation of the four possible rotamers of the compound <b>67j</b> .....	84
<b>Scheme 23.</b> Comparison of A-ring and B-ring modifications, using hydroxylation as an example.....	86
<b>Scheme 24.</b> Synthetic procedure of compound <b>57a</b> and its proposed mechanism. ....	87
<b>Scheme 25.</b> Reduction of nitro-group towards formation of the amino group in compound <b>57b</b> and its respective mechanism. ....	88
<b>Scheme 26.</b> Acetylation process towards the compound <b>57c</b> . ....	89
<b>Scheme 27.</b> Synthetic procedure of compounds <b>57d</b> and <b>57e</b> and its proposed C–C coupling mechanism. ....	90
<b>Scheme 28.</b> Synthetic route for obtention of compound <b>57f</b> and its proposed mechanism. ....	90
<b>Scheme 29.</b> Synthesis used to achieve compound <b>57g</b> and its respective proposed mechanism, and failed synthesis of compound <b>57h</b> .....	91
<b>Scheme 30.</b> Synthetic procedure of compound <b>57i</b> and its proposed mechanism. ....	92
<b>Scheme 31.</b> Acetylation process towards compound <b>57j</b> .....	92
<b>Scheme 32.</b> Failed acylation process towards compound <b>57k</b> .....	93
<b>Scheme 33.</b> Synthetic procedure of compound <b>57l</b> .....	93
<b>Scheme 34.</b> Oxidative synthesis of compounds <b>57m</b> and <b>57n</b> .....	94
<b>Scheme 35.</b> Oxidative synthesis of compound <b>57o</b> . ....	94
<b>Scheme 36.</b> Amination process towards compounds <b>58b-g</b> , obtained scope and failed substrates. ....	95
<b>Scheme 37.</b> Synthetic procedure of compound <b>58f</b> and the observed by-product <b>58f-2</b> . ....	97
<b>Scheme 38.</b> Plausible explanation for the observed regioselectivity on the synthesis of compound <b>58b</b> . ....	98
<b>Scheme 39.</b> Acetylation process towards compounds <b>59b-g</b> .....	99

<b>Scheme 40.</b> Second scope: double annulation reaction between compounds <b>59b-g</b> and symmetrical internal alkyne <b>56b</b> . .....	106
<b>Scheme 41.</b> Complementary study: double annulation reaction between compound <b>59a</b> and non-symmetrical internal alkyne <b>43</b> . .....	108
<b>Scheme 42.</b> Failed C–H annulation reaction using the substrate <b>57c</b> bearing the acetamide DG at the C-5 position.....	110
<b>Scheme 43.</b> Proposed mechanism for the double-annulation reaction <i>via</i> C(sp <sup>2</sup> ) <sub>Ar</sub> –H activation using compound <b>67a</b> as example. ....	111

## TABLES LIST

<b>Table 1.</b> Modifications of the standard conditions to force the activation at the C-5 position of the 1,4-naphthoquinone ( <b>5</b> ). .....	52
<b>Table 2.</b> Modifications of the standard conditions aiming to force the annulation reaction using sulfoxonium ylide ( <b>55</b> ).....	55
<b>Table 3.</b> Catalyst optimization for the double-annulation of the compound <b>59a</b> . .....	64
<b>Table 4.</b> Catalyst loading optimization for the double-annulation of the compound <b>59a</b> . .....	66
<b>Table 5.</b> Temperature optimization for the double-annulation of the compound <b>59a</b> . .....	67
<b>Table 6.</b> Optimization of the time of reaction for the double-annulation of compound <b>59a</b> ... ..	68
<b>Table 7.</b> Solvent optimization for the double-annulation of the compound <b>59a</b> . .....	69
<b>Table 8.</b> Optimization of the applied solvent volume.....	69
<b>Table 9.</b> Optimization process for the applied amount of alkyne.....	70
<b>Table 10.</b> Oxidant optimization for the double-annulation of the compound <b>59a</b> .....	71
<b>Table 11.</b> Additive optimization for the double-annulation of the compound <b>59a</b> . .....	72
<b>Table 12.</b> Optimization process for the applied amount of additive.....	72
<b>Table 13.</b> Validation tests for the double-annulation reaction of compound <b>59a</b> .....	73
<b>Table 14.</b> Activity of some double-annulated products against HL-60 cancer cell lines. ....	114
<b>Table 15.</b> Activity of products <b>67a-k</b> , <b>68a-b</b> , <b>69a</b> and <b>69b</b> against seven cancer cell lines..	196
<b>Table D1.</b> Crystallographic data of compound <b>59b</b> .....	379
<b>Table D2.</b> Crystallographic data of compound <b>59c</b> . .....	380
<b>Table D3.</b> Crystallographic data of compound <b>59d</b> .....	381
<b>Table D4.</b> Crystallographic data of compound <b>59g</b> . .....	382
<b>Table D5.</b> Crystallographic data of compound <b>67a</b> . .....	383
<b>Table D6.</b> Crystallographic data of compound <b>67b</b> .....	384
<b>Table D7.</b> Crystallographic data of compound <b>67c</b> . .....	385
<b>Table D8.</b> Crystallographic data of compound <b>67d</b> .....	386
<b>Table D9.</b> Crystallographic data of compound <b>67e</b> . .....	387

<b>Table D10.</b> Crystallographic data of compound <b>67f</b> .....	388
<b>Table D11.</b> Crystallographic data of compound <b>67g</b> .....	389
<b>Table D12.</b> Crystallographic data of compound <b>67k</b> .....	390
<b>Table D13.</b> Crystallographic data of compound <b>68b</b> .....	391
<b>Table D14.</b> Crystallographic data of compound <b>68c</b> .....	392
<b>Table D15.</b> Crystallographic data of compound <b>68d</b> .....	393
<b>Table D16.</b> Crystallographic data of compound <b>68g</b> .....	394
<b>Table D17.</b> Crystallographic data of compound <b>69a</b> .....	395
<b>Table D18.</b> Crystallographic data of compound <b>69b</b> .....	396

## ABBREVIATIONS

APT	attached proton test
ATR	attenuated total reflection
CAPES	Coordination for the Improvement of Higher Education Personnel ( <i>Coordenação de Aperfeiçoamento de Pessoal de Nível Superior</i> )
CCDC	Cambridge Crystallographic Data Centre
CNPq	National Council for Scientific and Technological Development ( <i>Conselho Nacional de Desenvolvimento Científico e Tecnológico</i> )
COSY	homonuclear correlation spectroscopy
Cp	cyclopentadienyl
DBU	1,8-Diazabicyclo(5.4.0)undec-7-ene
DCE	1,2-dichloroethane
DCM	dichloromethane
DEPT	distortionless enhancement by polarization transfer
DG	directing group
DMA	<i>N,N</i> -dimethylacetamide
DMF	<i>N,N</i> -dimethylformamide
DMSO	dimethyl sulfoxide
DMSO- <i>d</i> <sub>6</sub>	deuterated dimethyl sulfoxide
DQ	Chemistry Department ( <i>Departamento de Química</i> )
EI-MS	electronic ionization mass spectrometry
ESI-MS	electrospray ionization mass spectrometry
FAPEMIG	Research Support Foundation of Minas Gerais ( <i>Fundação de Amparo à Pesquisa do Estado de Minas Gerais</i> )
FAPESC	Research Support Foundation of Santa Catarina ( <i>Fundação de Amparo à Pesquisa do Estado de Santa Catarina</i> )
FT-IR	Fourier-transform infrared spectroscopy
GC-MS	gas chromatography mass spectrometry
HCT-116	human colon cancer cell line
HL-60	human leukemia cell line
HMBC	heteronuclear multiple bond correlation
HRMS	high resolution mass spectrometry
HSQC	heteronuclear single quantum correlation

IBX	2-iodobenzoic acid
IC <sub>50</sub>	inhibitory concentration of 50% of the parasitary population
ICE <sub>x</sub>	Exact Sciences Institute ( <i>Instituto de Ciências Exatas</i> )
INCT	Science and Technology National Institutes ( <i>Institutos Nacionais de Ciência e Tecnologia</i> )
IR	infrared spectroscopy
IUPAC	International Union of Pure and Applied Chemistry
<i>J</i>	coupling constant
L929	mouse fibroblast cell line
MCF-7	human breast cancer cell line
<i>m</i> -CPBA	<i>meta</i> -chloroperbenzoic acid
MD	Maryland
Mes	mesitylene
MS	mass spectrometry
MTT	3-(4,5-dimethylthiazol-2-yl)-2,5-diphenyltetrazolium bromide
NCI-H460	human lung cancer cell line
NIS	<i>N</i> -iodosuccinimide
NMR	nuclear magnetic resonance
NMP	<i>N</i> -methylpyrrolidone
N.R.	no reaction
PC3	human prostatic cell line
PIFA	phenyliodine bis(trifluoroacetate)
PRPq	Research Pro-Rectory ( <i>Pró-Reitoria de Pesquisa</i> )
ROS	reactive oxygen species
RPMI	Roswell Park Memorial Institute
r.t.	room temperature
SET	single electron transfer
SNB-19	human glioblastoma cell line
Tc	thiophene-2-carboxylate
TEAB	tetraethylammonium bromide
Tf	triflate
TFA	trifluoroacetic acid

TFAA	trifluoroacetic anhydride
TLC	thin layer chromatography
TOF	time of flight
THF	tetrahydrofuran
TS	transition state
UFMG	Federal University of Minas Gerais <i>(Universidade Federal de Minas Gerais)</i>



## TABLE OF CONTENTS

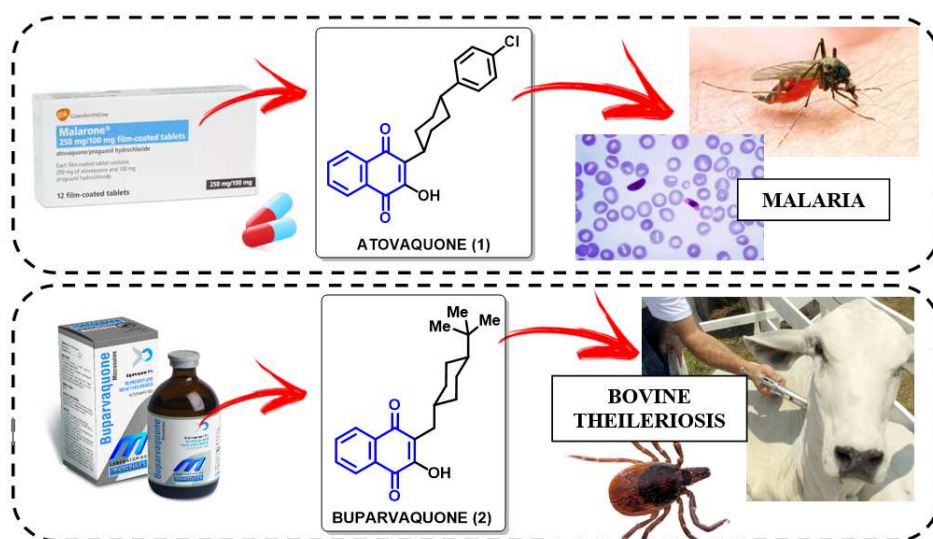
<b>1.</b>	<b>INTRODUCTION</b>	<b>34</b>
1.1.	Quinones: definition, sources, applications, and biological activity	34
1.2.	C–H activation reactions	37
1.3.	Important aspects surrounding C–H activation reactions	39
1.3.1.	Transition-metal-based catalyst	39
1.3.2.	Directing groups	42
1.3.3.	Coupling partners	43
1.4.	Polycyclic quinones	44
<b>2.</b>	<b>RESEARCH PROPOSAL</b>	<b>46</b>
2.1	General research proposal	46
2.2.	Evaluation of the intrinsic directing behaviour of quinoidal compounds towards a ruthenium catalyzed C(sp <sup>2</sup> )–H arylation reaction	46
2.3.	Evaluation of the intrinsic directing behaviour of quinoidal compounds towards a ruthenium catalyzed C(sp <sup>2</sup> )–H annulation reaction	47
2.4.	Evaluation of additional directing groups on quinoidal substrates towards a ruthenium catalyzed C(sp <sup>2</sup> )–H annulation reaction	48
<b>3.</b>	<b>RESULTS AND DISCUSSION</b>	<b>50</b>
3.1.	C–H arylation trials on 1,4-naphthoquinone (5)	50
3.2.	C–H annulation trials on 1,4-naphthoquinone (5)	54
3.3.	Synthesis of substrates containing additional DG	56
3.3.1.	Synthesis of compounds 60 and 61	56
3.3.2.	Synthesis of the substrates 58a and 59a	57
3.3.3.	Other acylation procedures	59
3.4.	C–H annulation trials on naphthoquinones bearing an additional DG at the C-2 position	61
3.5.	Optimization of the method	64
3.6.	Scope analysis	74
3.6.1.	Synthesis of substituted symmetrical internal alkynes (65b-s)	74
3.6.2.	Symmetrical internal alkyne scope analysis	76
3.6.3.	Synthesis of A-ring modified naphthoquinoidal molecules	86
3.6.4.	Amination at the C-2/C-3 position	94
3.6.5.	Acetylation of the amino group	98

3.6.6.	A-ring-substituted quinones scope analysis.....	105
3.6.7.	Complementary studies.....	107
<b>3.7.</b>	<b>Mechanistic proposal.....</b>	<b>110</b>
<b>3.8.</b>	<b>Biological assays.....</b>	<b>114</b>
<b>4.</b>	<b>CONCLUSION AND PERSPECTIVES.....</b>	<b>115</b>
<b>5.</b>	<b>EXPERIMENTAL.....</b>	<b>116</b>
<b>5.1.</b>	<b>Materials and equipment.....</b>	<b>116</b>
<b>5.2.</b>	<b>C–H arylation trials.....</b>	<b>119</b>
5.2.1.	Synthesis of arylating agent <b>49</b> .....	119
5.2.2.	Synthesis of modified substrates ( <b>51a-c</b> ).....	120
5.2.3.	General C–H arylation procedure.....	123
<b>5.3.</b>	<b>C–H annulation trials.....</b>	<b>124</b>
5.3.1.	Synthesis of sulfoxonium ylide ( <b>55</b> ).....	124
5.3.2.	Synthesis of symmetrical internal alkynes ( <b>56b-s</b> ).....	125
5.3.3.	Synthesis of A-ring modified quinones ( <b>57a-o</b> ).....	136
5.3.4.	Amination at the C-2 or C-3 positions of the A-ring modified quinones ( <b>58a-g</b> ).....	147
5.3.5.	Acetylation at the amino group of 5-amino-1,4-naphthoquinones ( <b>59a-g</b> ).....	153
5.3.6.	Synthesis of naphthoquinones with different DG located at the C-2 position.....	159
5.3.7.	General C–H annulation procedure using sulfoxonium ylide <b>55</b> .....	163
5.3.8.	General C–H annulation procedures using alkynes ( <b>67a-69b</b> ).....	164
<b>5.4.</b>	<b>Computational data.....</b>	<b>192</b>
<b>5.5.</b>	<b>Antitumor assays.....</b>	<b>195</b>
<b>REFERENCES</b> .....		<b>197</b>
<b>APPENDICES</b> .....		<b>220</b>
<i>Appendices: List of Compounds</i> .....		221
<i>Appendices A: NMR Spectra</i> .....		235
<i>Appendices B: IR Spectra</i> .....		311
<i>Appendices C: Mass Spectra</i> .....		348
<i>Appendices D: Crystallographic Data</i> .....		379

## 1. INTRODUCTION

### 1.1. Quinones: definition, sources, applications, and biological activity

Quinones, in their simplest form, are classified as six-membered carbocyclic compounds containing two carbonyl groups, either separated by vinyl groups within a ring (*para*-quinones) or adjacent to each other (*ortho*-quinones), as defined by Weaver and Pettus.<sup>1</sup> Amongst infinite possibilities, naphthoquinones are one of the most versatile quinones with a wide range of applications, due to their pharmacological activities (**Figure 1**),<sup>2</sup> and their peculiar contribution on catalytical<sup>3</sup> and electrochemical synthesis.<sup>4</sup>



**Figure 1.** Atovaquone (1) and Buparvaquone (2): two important commercially available naphthoquinoidal compounds currently used as drugs for treatment of malaria<sup>2a</sup> and bovine theileriosis,<sup>2b</sup> respectively.

Naphthoquinoidal compounds are planar structures, derived from naphthalene, containing an aryl group (defined here as A-ring) fused on a quinoidal unit (defined here as B-ring), with different substitution patterns.<sup>5</sup> Naphthoquinones derivatives are easily found in nature<sup>6</sup> and at least two eminent examples can be cited here: lapachol\* (3) and vitamin K<sub>1</sub>\* (4). Lapachol (3) is one of the organic compounds found on *Tabebuia* trees, known in Latin America

<sup>1</sup> Weaver, M. G.; Pettus, T. R. R. *Comprehensive Organic Synthesis*, 2014, 2<sup>nd</sup> ed., 7, 373-410.

<sup>2</sup> (a) Ke, F.; Yu, J.; Chen, W.; Si, X.; Li, X.; Yang, F.; Liao, Y.; Zuo, Z. *Biochem. Biophys. Res. Commun.*, 2018, 504, 374-379; (b) Devadevi, N.; Rajkumar, K.; Vijaylakshmi, P. *Int. J. Chem. Stud.*, 2018, 6, 1-3.

<sup>3</sup> Jardim, G. A. M.; Bozzi, I. A. O.; Oliveira, W. X. C.; Mesquita-Rodrigues, C.; Menna-Barreto, R. F. S.; Kumar, R. A.; Gravel, E.; Doris, E.; Braga, A. L.; Silva Júnior, E. N. *New J. Chem.*, 2019, 43, 13751-13763.

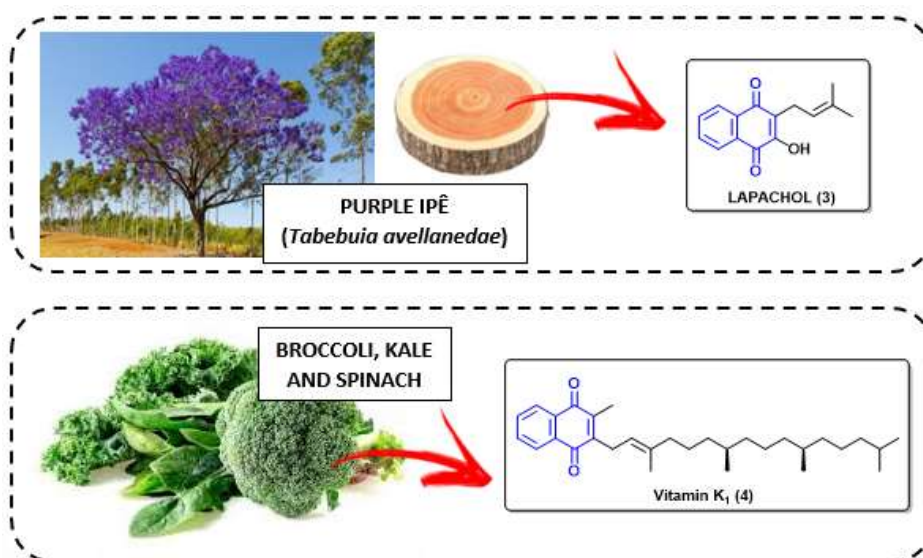
<sup>4</sup> Kharm, A.; Jacob, C.; Bozzi, I. A. O.; Jardim, G. A. M.; Braga, A. L.; Salomão, K.; Gatto, C. C.; Silva, M. F. S.; Pessoa, C.; Stangier, M.; Ackermann, L.; Silva Júnior, E. N. *Eur. J. Org. Chem.*, 2020, 2020, 4474-4486.

<sup>5</sup> Gaultier, J.; Hauw, C. *Acta Cryst.*, 1965, 18, 179-183.

<sup>6</sup> Tikkanen, L.; Matsushima, T.; Natori, S.; Yoshihira, K. *Mut. Res.*, 1983, 124, 25-34.

by their common name “Ipê” (**Figure 2**).<sup>7</sup> Lapachol was isolated for the first time by M. Arnaudon in 1858,<sup>8</sup> and its first complete synthesis was performed in 1927, by Louis Fieser.<sup>9</sup> This compound is known to have antitumoral,<sup>10</sup> trypanocidal<sup>11</sup> and antimalarial<sup>12</sup> activities.

Vitamin K<sub>1</sub> (**4**), also known as phylloquinone, belongs to the family of vitamins K, which are all naphthoquinoidal molecules.<sup>13</sup> Phylloquinone is considered as major dietary source of vitamin K for humans, and, unlike vitamin D, it cannot be synthesized in human organisms. Therefore, it must be obtained with a diet based on green vegetables such as green salads, broccoli, kale, and spinach (**Figure 2**), and in some oils and fats, as well.<sup>14</sup> They are crucial for the metabolism of the proteins responsible for coagulation processes, meaning that the lack of this vitamin can cause spontaneous haemorrhages and several other circulating health complications.<sup>15</sup>



**Figure 2.** Lapachol (**3**) and Vitamin K<sub>1</sub> (**4**): two important naturally available naphthoquinoidal compounds.

\* A complete list of the enumerated compounds of this thesis can be found at the Appendices, page S2.

<sup>7</sup> Hussain, H.; Krohn, K.; Ahmad, V. U.; Miana, G. A.; Green, I. R. *Arkivoc*, **2007**, 2, 145-171.

<sup>8</sup> Arnaudon, M. C. R. *Acad. Sci. (Paris)*, **1858**, 46, 1152-1156.

<sup>9</sup> Fieser, L. F. *J. Am. Chem. Soc.*, **1927**, 49, 857-864.

<sup>10</sup> Oliveira, L. G.; Silva, M. M.; Paula, F. C. S.; Pereira-Maia, E. C.; Donnici, C. L.; Simone, C. A.; Frézard, F.; da Silva Júnior, E. N.; Demicheli, C. *Molecules*, **2011**, 16, 10314-10323.

<sup>11</sup> Moura, K. G. C.; Emery, F. S.; Pinto, C. N.; Pinto, M. C. F. R.; Dantas, A. P.; Salomão, K.; Castro, S. L.; Pinto, A. V. *J. Braz. Chem. Soc.*, **2001**, 12, 325-338.

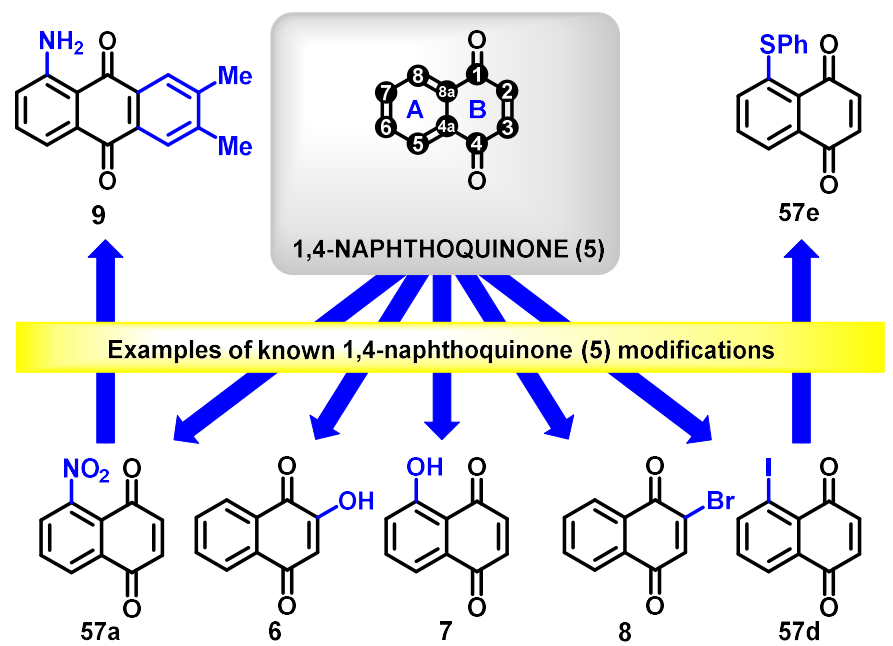
<sup>12</sup> Andrade-Neto, V. F.; Goulart, M. O. F.; Filho, J. F. S.; Silva, M. J.; Pinto, M. C. F. R.; Pinto, A. V.; Zalis, M. G.; Carvalho, L. H.; Krettli, A. U. *Bioorg. Med. Chem. Lett.*, **2004**, 14, 1145-1149.

<sup>13</sup> Hirota, Y. *Vitamins (Japan)*, **2017**, 92, 63-72.

<sup>14</sup> Garber, A. K.; Binkley, N. C.; Krueger, D. C.; Suttie, J. W. *J. Nutr.*, **1999**, 129, 1201-1203.

<sup>15</sup> Schurgers, L. J.; Vermeer, C. *Haemostasis*, **2000**, 30, 298-307.

Naphthoquinoidal structures are considerably reactive and of extreme importance giving their synthetic versatility. In a few steps, it is possible to obtain more complex naphthoquinoidal molecules, starting from the simplest 1,4-naphthoquinone (**5**), applying modifications on both A- and B-rings (**Figure 3**).<sup>16</sup>



**Figure 3.** Example of the wide range of possible transformations starting from simple naphthoquinones.

Quinones in general, including naphthoquinones, are known for their notable and valuable biological activities, such as anticancer,<sup>17</sup> trypanocidal,<sup>18</sup> anti-malarial,<sup>19</sup> antibiotic,<sup>20</sup>

<sup>16</sup> (a) Jardim, G. A. M.; Silva, T. L.; Goulart, M. O. F.; Carlos A. de Simone, C. A.; Barbosa, J. M. C.; Salomão, K.; Solange L. de Castro, S. L.; Bower, J. F.; da Silva Júnior, E. N. *Eur. J. Med. Chem.*, **2017**, *136*, 406-419; (b) Dumanska, Y.; Shakh, Y.; Kudrinetska, A.; Bolibrukh, K.; Karkhut, A.; Lytvyn, B.; Kovalchuk, O.; Marshalok, O.; Platonov, M.; Polovkovych, S.; Novikov, V. *Res. J. Pharm. Biol. Chem. Sci.*, **2013**, *4*, 1471-1479; (c) Nasiri, H. R.; Madej, G.; Panish, R.; Lafontaine, M.; Bats, J. W.; Lancaster, C. R. D.; Schwalbe, H. *J. Med. Chem.*, **2013**, *56*, 9530-9541; (d) Dias, G. G.; Rogge, T.; Kuniyil, R.; Jacob, C.; Menna-Barreto, R. F. S.; da Silva Junior, E. N.; Ackermann, L. *Chem. Commun.*, **2018**, *54*, 12840-12843; (e) Su, J.; Zhang, Y.; Chen, M.; Li, W.; Qin, X.; Xie, Y.; Qin, L.; Huang, S.; Zhang, M. *Synlett*, **2019**, *30*, 630-634.

<sup>17</sup> (a) Perchellet, E. M.; Sperflage, B. J.; Wang, Y.; Huang, X.; Tamura, M.; Hua, D. H.; Perchellet, J.-P. *Anti-Cancer Drugs*, **2002**, *13*, 567-581; (b) Perchellet, E. M.; Wang, Y.; Weber, R. L.; Lou, K.; Hua, D. H.; Perchellet, J.-P. *Anti-Cancer Drugs*, **2004**, *15*, 929-946; (c) Dolfi, S. C.; Yang, Z.; Lee, M.-J.; Guan, F.; Hong, J.; Yang, C. S. *J. Agric. Food Chem.*, **2013**, *61*, 8533-8540.

<sup>18</sup> (a) Ramírez-Macías, I.; Marín, C.; Es-Samti, H.; Fernández, A.; Guardia, J. J.; Zentar, H.; Agil, A.; Chahboun, R.; Alvarez-Manzaneda, E.; Sánchez-Moreno, M. *Parasitol. Intern.*, **2012**, *61*, 405-413; (b) Sarkhosh, M.; Khorshidi, N.; Niazi, A.; Leardi, R. *Chemomet. Intell. Lab. Sys.*, **2014**, *139*, 168-174.

<sup>19</sup> (a) Caro, D.; Florez, M.; Gaitan, R.; Martinez, E.; Baldiris, R.; Vivas-Reyes, R. *Afinidad*, **2017**, *74*, 185-193; (b) Ahenkorah, S.; Coertzen, D.; Tong, J. X.; Fridianto, K.; Wittlin, S.; Birkholtz, L.-M.; Tan, K. S. W.; Lam, Y.; Go, M.-L.; Haynes, R. K. *ACS Med. Chem. Lett.*, **2020**, *11*, 49-55.

\* *Web of Science*, August 5<sup>th</sup> 2022.

antioxidant,<sup>21</sup> and even anti-HIV<sup>22</sup>. Their antitumor activity, specifically, is associated to the ability of generating reactive oxygen species (ROS),<sup>23</sup> and possible inhibition of the enzyme topoisomerase-II, resulting on tearing DNA molecules.<sup>24</sup>

## 1.2. C–H activation reactions

Synthetic chemistry has been developed significantly since the ascension of C–H activation methods. In the last few decades, there has been a notable increase on the number of publications citing this subject, counting 2607 publications in the last year, and 1296 already in this year.\* Molecules that were previously difficult to be synthesized, can now be obtained mostly in a single step.<sup>25</sup> This revolutionary method may bring an important and desired development in pharmaceuticals and fine chemistry in general, leading to a more reachable access to several added-value molecules.<sup>26</sup>

The first application of a C–H activation method is often attributed to Otto Dimroth (**Scheme 1**), a German chemist that, in 1902, performed a single-step substitution from C(sp<sup>2</sup>)–H to C(sp<sup>2</sup>)–Hg<sup>II</sup> using benzene (**10**) as substrate.<sup>27</sup> Fifty-three years later, Shunsuke Murahashi published a notable work covering a cobalt-catalyzed C(sp<sup>2</sup>)–H annulation to generate 2-phenylisoindolin-1-one (**13**) from (*E*)-*N*,1-diphenylmethanimine (**12**).<sup>28a</sup> In 1988, Zanobini and co-workers published a very important contribution for the studies of rhodium-mediated C–H activation reactions, now applied on terminal alkynes. From this study it was possible to understand that also C(sp)–H bonds are possible to get activated in the presence of an electronic

<sup>20</sup> (a) Wolfbeis, O. S.; Furlinger, E. *Microchim. Acta*, **1983**, *81*, 385-398; (b) Krohn, K. *Eur. J. Org. Chem.*, **2002**, *2002*, 1351-1362.

<sup>21</sup> (a) Muronetz, V. I.; Asryants, R. A.; Semenyuk, P. I.; Mishchenko, N. P.; Vasilieva, E. A.; Fedoreyev, S. A.; Schmalhausen, E. V. *Curr. Org. Chem.*, **2017**, *21*, 2125-2133; (b) Maringer, L.; Roiser, L.; Wallner, G.; Nitsche, D.; Buchberger, W. *Polym. Degrad. Stab.*, **2016**, *131*, 91-97.

<sup>22</sup> Stagliano, K. W.; Emadi, A.; Lu, Z.; Malinakova, H. C.; Twenter, B.; Yu, M.; Holland, L. E.; Rom, A. M.; Harwood, J. S.; Amin, R.; Johnson, A. A.; Pommier, Y. *Bioorg. Med. Chem.*, **2006**, *14*, 5651-5665.

<sup>23</sup> Shukla, H.; Chitrakar, R.; Bibi, H. A.; Gaje, G.; Koucheqi, A.; Trush, M. A.; Zhu, H.; Li, R.; Jia, Z. *Toxicol. Lett.*, **2020**, *322*, 120-130.

<sup>24</sup> (a) Waugh, T. M.; Masters, J.; Aliev, A. E.; Marson, C. M. *ChemMedChem*, **2002**, *15*, 114-124; (b) Zhou, D.-C.; Lu, Y.-T.; Mai, Y.-W.; Zhang, C.; Xia, J.; Yao, P.-F.; Wang, H.-G.; Huang, S.-L.; Huang, Z.-S. *Bioorg. Chem.*, **2019**, *91*, 103131.

<sup>25</sup> (a) Hanchate, V.; Devarajappa, R.; Prabhu, K. R. *Org. Lett.*, **2020**, *8*, 2878-2882; (b) Ma, X.; Zhao, X.; Zhu, R.; Zhang, D. *J. Org. Chem.*, **2020**, *85*, 5995-6007; (c) Sagadevan, A.; Charitou, A.; Wang, F.; Ivanona, M.; Vuagnat, M.; Greaney, M. F. *Chem. Sci.*, **2020**, *11*, 4439-4443; (d) Thombal, R. S.; Lee, Y. R. *Org. Lett.*, **2020**, *22*, 3397-3401.

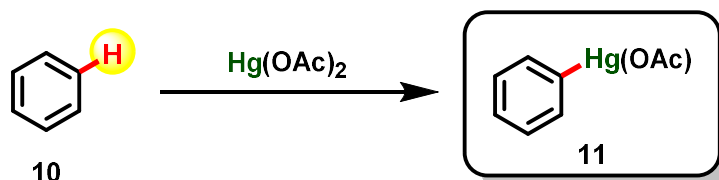
<sup>26</sup> (a) Yuan, S.; Chang, J.; Yu, B. *Top. Curr. Chem.*, **2020**, *378*, 23; (b) Zhang, X.; Bai, R.; Xiong, H.; Xu, H.; Hou, W. *Bioorg. Med. Chem. Lett.*, **2020**, *30*, 126916.

<sup>27</sup> Dimroth, O. *Berichte Deut. Chem. Gesell.*, **1902**, *35*, 2032-2045.

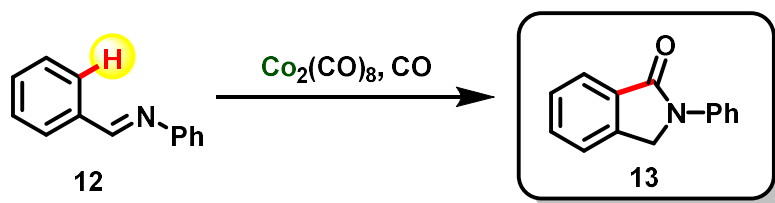
<sup>28</sup> (a) Murahashi, S. *J. Am. Chem. Soc.*, **1955**, *77*, 6403-6404; (b) Bianchini, C.; Mealli, C.; Peruzzini, M.; Vizza, F.; Zanobini, F. *J. Organometal. Chem.*, **1988**, *346*, C53-C57.

unsaturated active rhodium species  $[\text{Rh}(\text{N}(\text{CH}_2\text{CH}_2\text{PPh}_2)_3)]^+$ .<sup>28b</sup> A breakthrough in this field happened when Robert G. Bergman reported, in 1982, an iridium catalyzed  $\text{C}(\text{sp}^3)\text{-H}$  activation that caught the attention of the whole chemical community to the versatile use of transition metals for intermolecular  $\text{C-H}$  activation reactions, also on  $\text{sp}^3$  hybridized carbons.<sup>29</sup>

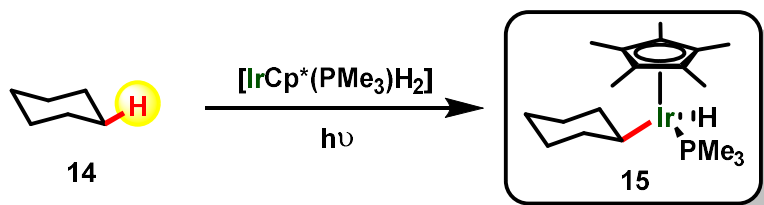
Otto Dimroth (1902)



Shunsuke Murahashi (1955)



Robert Bergman (1982)



**Scheme 1.** A brief view on the  $\text{C-H}$  activation history.

After Bergman's distinguish work from 1982, the number of publications covering the theme " $\text{C-H}$  activation" increased exponentially, indicating the importance of Bergman's contribution to this field (**Figure 4**). Nowadays there are several brilliant scientific minds in this subject. Names, like Debabrata Maiti,<sup>30</sup> Lutz Ackermann,<sup>31</sup> Frank Glorius<sup>32</sup> and Nicolai Cramer,<sup>33</sup> represent a new worldwide era in Chemistry Research.

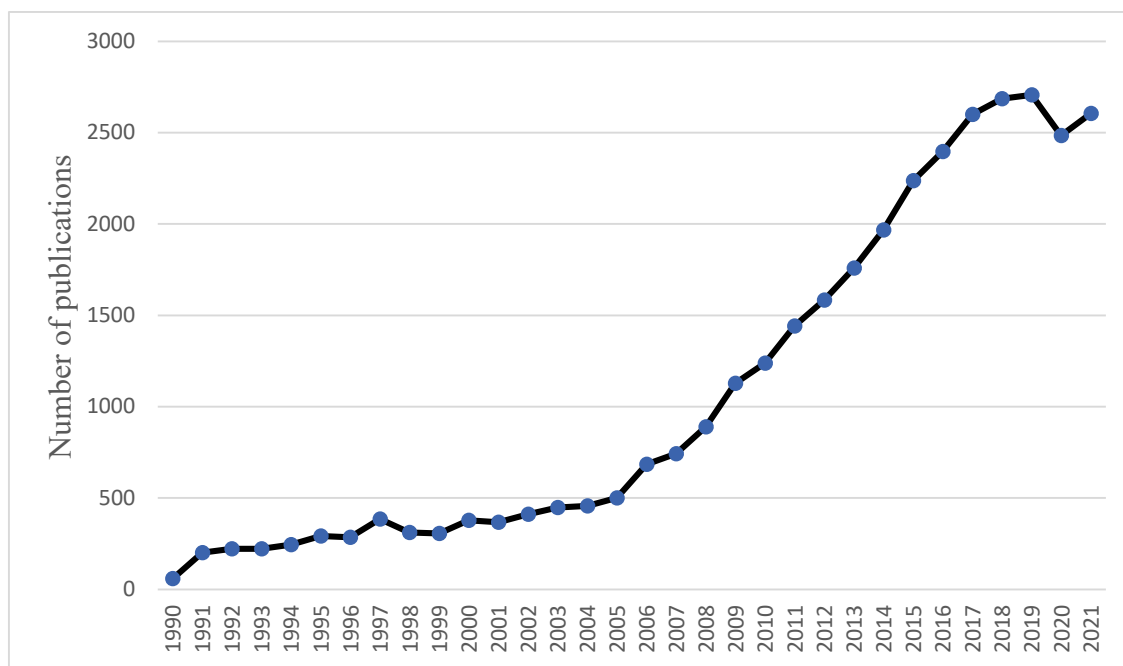
<sup>29</sup> Janowicz, A. H.; Bergman, R. G. *J. Am. Chem. Soc.*, **1982**, *104*, 352-354.

<sup>30</sup> Agasti, S.; Pal, T.; Achar, T. K.; Maiti, S.; Pal, D.; Mandal, S.; Daud, K.; Lahiri, G. K.; Maiti, D. *Angew. Chem. Int. Ed.*, **2019**, *58*, 11039-11043.

<sup>31</sup> Zhu, C.; Kuniyil, R.; Jei, B. B.; Ackermann, L. *ACS Catal.*, **2020**, *10*, 4444-4450.

<sup>32</sup> Lu, Q.; Mondal, S.; Cembellín, S.; Greßies, S.; Glorius, F. *Chem. Sci.*, **2019**, *10*, 6560-6564.

<sup>33</sup> Wang, S.-G.; Liu, Y.; Cramer, N. *Angew. Chem. Int. Ed.*, **2019**, *58*, 18136-18140.



**Figure 4.** Publications in the last three decades about “C–H activation”  
(*Web of Science*, August 5<sup>th</sup>, 2022).

### 1.3. Important aspects surrounding C–H activation reactions

Throughout the years, it has been observed that some specific aspects about C–H activation reactions must be taken into consideration while developing the methodology to increase its performance.<sup>34</sup> These aspects vary mostly according to which C–H activation pathway the reaction takes place. In summary, it is plausible to say that a well-developed C–H activation process is a result of the right combination between the transition-metal-based catalyst, type of directing group, coupling partner and additive (when necessary), not to mention the rest of the required conditions, such as base, oxidants, solvent, temperature, etc. Therefore, these aspects must be well explored basing not only on the characteristics of the desired reaction but also on the state-of-art related to what is being developed.

#### 1.3.1. Transition-metal-based catalyst

A C–H activation is a specific field of a C–H transformation in which a transition-metal-based catalyst must be required, due to the possible interaction between their *d* orbitals and the

<sup>34</sup> Carvalho, R. L.; Dias, G. G.; Pereira, C. L. M.; Ghosh, P.; Maiti, D.; da Silva Júnior, E. N. *J. Braz. Chem. Soc.*, **2021**, 32, 917-952.



$\sigma$ (C–H) bond. In this process, the interaction between the C–H bond itself and the metallic centre of the catalyst weaken the  $\sigma$  bond and leads to its breakage. From this moment, different transition states and intermediates may be generated *in situ*, according to the mechanistic pathway the reaction may occur, but in all of them the hydrogen gets substituted by a transient metal–C bond.<sup>35</sup>

For this purpose, several transition metals have been studied so far, however, four of them have been proven to be the most versatile and active ones: ruthenium,<sup>36</sup> rhodium,<sup>37</sup> palladium,<sup>38</sup> and iridium.<sup>39</sup> Their applications lay within a large range including C–H annulation,<sup>40</sup> allylation,<sup>41</sup> alkenylation,<sup>42</sup> alkynylation,<sup>43</sup> arylation,<sup>44</sup> borylation,<sup>45</sup> carbonylation,<sup>46</sup> etc (**Figure 5**). Among the possible catalyst templates, the half-sandwich dimers are the ones that represent most of the studies developed so far, not only due to the versatility intrinsic to this type of catalyst, but as well to their relatively easy approach.<sup>47</sup>

<sup>35</sup> Ess, D. H.; Goddard III, W. A.; Periana, R. A. *Organometallics*, **2010**, *29*, 6459-6472.

<sup>36</sup> (a) Arockiam, P. B.; Bruneau, C.; Dixneuf, P. H. *Chem. Rev.*, **2012**, *112*, 5879-5918; (b) Duarah, G.; Kaishap, P. P.; Begum, T.; Gogoi, S. *Adv. Synth. Catal.*, **2019**, *361*, 654-672.

<sup>37</sup> (a) Colby, D. A.; Bergman, R. G.; Ellman, J. A. *Chem. Rev.*, **2010**, *110*, 624-655; (b) Song, L.; Tian, G.; Van der Eycken, E. V. *Mol. Catal.*, **2018**, *459*, 129-134; (c) Wang, Z.; Xu, H. *Tetrahedron Lett.*, **2019**, *60*, 664-667.

<sup>38</sup> (a) Li, B.-J.; Yang, S.-D.; Shi, Z.-J. *Synlett*, **2008**, *7*, 949-957; (b) Chen, X.; Engle, K. M.; Wang, D.-H.; Yu, J.-Q. *Angew. Chem. Int. Ed.*, **2009**, *48*, 5094-5115; (c) Engelin, C. J.; Fristrup, P. *Molecules*, **2011**, *16*, 951-969.

<sup>39</sup> (a) Slugovc, C.; Padilla-Martínez, I.; Sirol, S.; Carmona, E. *Coord. Chem. Rev.*, **2001**, *213*, 129-157; (b) Tenn, W. J.; Young, K. J. H.; Bhalla, G.; Oxgaard, J.; Goddard, W. A.; Periana, R. A. *J. Am. Chem. Soc.*, **2005**, *127*, 14172-14173; (c) Wu, X.; Sun, S.; Yu, J.-T.; Cheng, J. *Synlett*, **2019**, *30*, 21-29.

<sup>40</sup> (a) Zhang, J. J.; Zhang, M.; Lu, M.; He, Y.; Li, S.; Fan, L.; Zhang, X.; Wu, J.-K.; Yang, X. *Chem. Commun.*, **2022**, *58*, 5144-5147; (b) Li, X.; Li, D.; Zhang, X. *Org. Biomol. Chem.*, **2022**, *20*, 1475-1479; (c) Singh, A.; Shukla, R. K.; Volla, C. M. R. *Chem. Sci.*, **2022**, *13*, 2043-2049; (d) Li, J.; Xu, X.; Luo, Z.; Yao, Z.; Yang, J.; Zhang, X.; Xu, L.; Wang, P.; Shi, Q. *Adv. Synth. Catal.*, **2022**, *364*, 1264-1270.

<sup>41</sup> (a) Zhang, S.-S.; Liu, Y.-Z.; Zheng, Y.-C.; Xie, H.; Chen, S.-Y.; Song, J.-L.; Shu, B. *Adv. Synth. Catal.*, **2022**, *364*, 64-70; (b) Wu, M.-S.; Ruan, X.-Y.; Han, Z.-Y.; Gong, L.-Z. *Chem. Eur. J.*, **2022**, *28*, e202104218; (c) Xiong, Q.; Xiao, L.; Dong, X.-Q.; Wang, C.-J. *Org. Lett.*, **2022**, *24*, 2579-2584.

<sup>42</sup> (a) Bakthadoss, M.; Reddy, T. T.; Agarwal, V.; Sharada, D. S. *Chem. Commun.*, **2022**, *58*, 1406-1409; (b) Zhao, H.; Luo, Z.; Yang, J.; Li, B.; Han, J.; Xu, L.; Lai, W.; Walsh, P. J. *Chem. Eur. J.*, **2022**, *in press*, DOI: 10.1002/chem.202200441; (c) Xiong, P.; Hemming, M.; Ivlev, S. I.; Meggers, E. *J. Am. Chem. Soc.*, **2022**, *144*, 6964-6971.

<sup>43</sup> (a) Deng, K.-Z. Jia, W.-L.; Fernández-Ibáñez, M. A. *Chem. Eur. J.*, **2022**, *28*, e202104107; (b) Ma, L.; Zhang, X.; Tuo, Y.; Zheng, Q.-Z. *J. Org. Chem.*, **2022**, *87*, 3691-3700; (c) Tan, E.; Nannini, J.; Stoica, O.; Echavarren, A. M. *Org. Lett.*, **2021**, *23*, 1263-1268.

<sup>44</sup> (a) Gao, T.-H.; Xiong, Y.; Guo, P.; Liu, F.-S.; Zhao, L. *Inorg. Chem. Commun.*, **2022**, *140*, 109403; (b) Xu, Y.-X.; Liang, Y.-Q.; Cai, Z.-J.; Ji, S.-J. *Org. Lett.*, **2022**, *24*, 2601-2606; (c) Li, H.-L.; Yang, D.-F.; Jing, H.-Q.; Antilla, J. C.; Kuninobu, Y. *Org. Lett.*, **2022**, *24*, 1286-1291.

<sup>45</sup> (a) Shi, Y.; Yang, Y.; Xu, S. *Angew. Chem. Int. Ed.*, **2022**, *61*, e202201463; (b) Wang, T.-C.; Wang, P.-S.; Chen, D.-F.; Gong, L.-Z. *Sci. China Chem.*, **2022**, *65*, 298-303; (c) Lu, S.; Zheng, T.; Ma, J.; Deng, Z.; Qin, S.; Chen, Y.; Liang, Y. *Angew. Chem. Int. Ed.*, **2022**, *61*, e202201285.

<sup>46</sup> (a) Li, D.-K.; Zhang, B.; Ye, Q.; Deng, W.; Xu, Z.-Y. *Organometallics*, **2022**, *41*, 441-449; (b) Cheng, M.; Huang, X.-Y.; Yang, F.; Zhao, D.-M.; Ji, K.; Chen, Z.-S. *Org. Lett.*, **2022**, *24*, 1237-1242; (c) Yang, Y.-Z.; He, D.-L.; Li, J.-H. *Org. Lett.*, **2022**, *23*, 5039-5043.

<sup>47</sup> Jardim, G. A. M.; de Carvalho, R. L.; Nunes, M. P.; Machado, L. A.; Almeida, L. D.; Bahou, K. A.; Bower, J. B.; da Silva Júnior, E. N. *Chem. Commun.*, **2022**, *58*, 3101-3121.

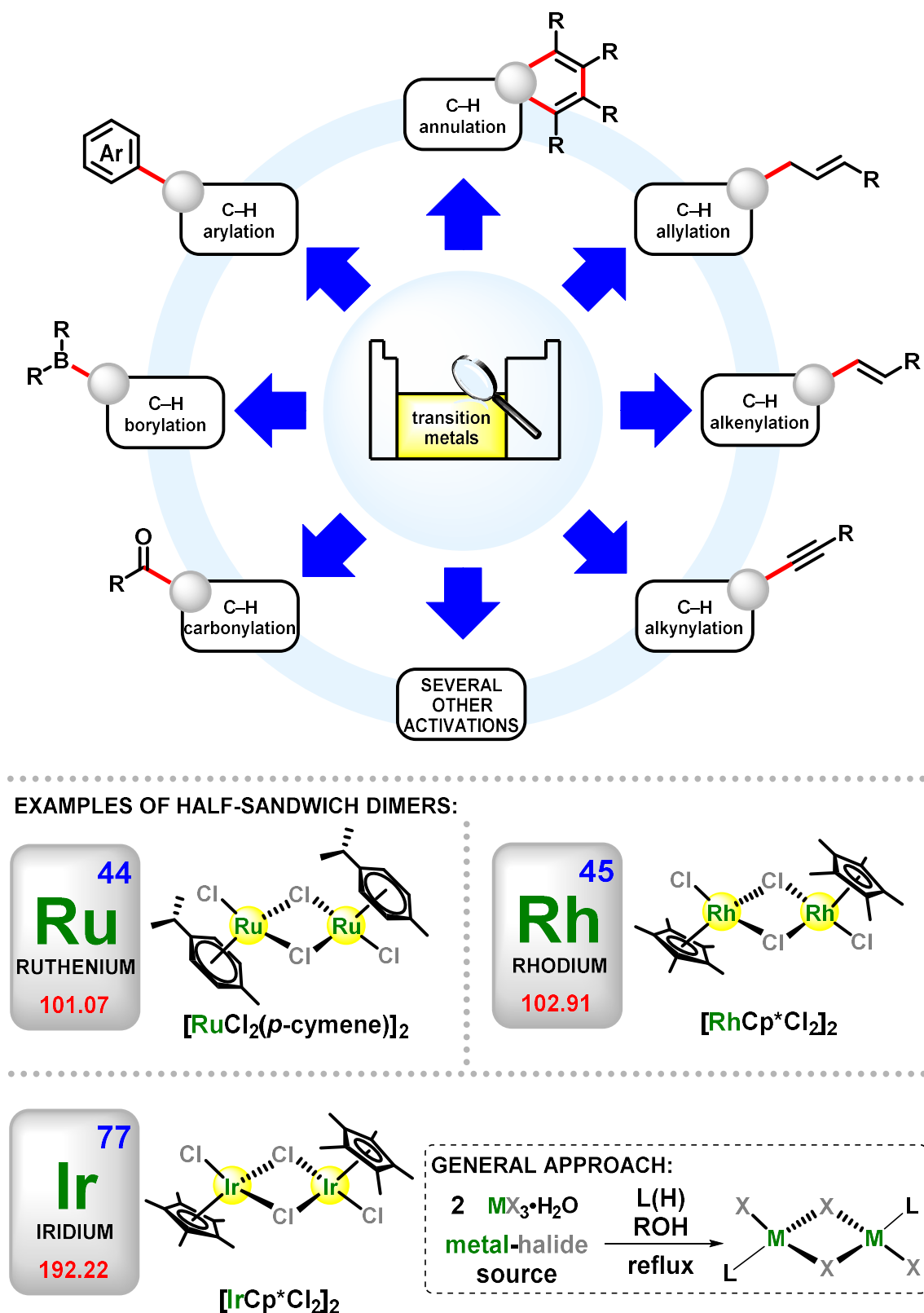


Figure 5. C–H modifications provided by transition-metal catalysis, examples of half-sandwich catalysts and their respective general approach.

Although the already mentioned relevance of these four metals, it is important to state they are not widely accessible, due to their usual higher prices when compared to other metals, including other transition metals. Because of that, it is possible to observe a rising demand for the development of cheaper and more accessible catalytic systems, using, for example, transition metals of the *3d* family.<sup>48</sup> Members of this family are usually more abundant, therefore cheaper, and easier to be accessed. Some of them, such as cobalt,<sup>49</sup> nickel<sup>50</sup> and iron,<sup>51</sup> has already proven to be promising and robust catalysts to be used on several C–H activation methods.

### 1.3.2. Directing groups

Directing group (DG) is a portion of the molecule that usually bears non-bonding electron pairs, responsible for coordinating with the metallic centre of the catalyst and leading it to the site of the molecule in which the C–H activation is desired to happen.<sup>52</sup> It can be composed of simpler structures, such as alcohol, amine, amide, thiol,<sup>53</sup> or even more complex structures, including extended pyrimidines,<sup>54</sup> quinolines, or any other organic function that makes this metal-DG interaction possible.<sup>55</sup> It is important to mention that they are not always required, since some C–H activation reactions may proceed in a non-directed fashion.<sup>56</sup> However, when they are required, they become one of the most crucial tools.

Nowadays there are several examples of valuable directing groups well known and explored. The size and construction of the DG may lead to different activations on distinct sites

---

<sup>48</sup> de Carvalho, R. L.; de Miranda, A. S.; Nunes, M. P.; Gomes, R. S.; Jardim, G. A. M.; da Silva Júnior, E. N. *Beilstein J. Org. Chem.*, **2021**, *17*, 1849-1938.

<sup>49</sup> (a) Zhang, H.; Sun, M.-C.; Yang, D.; Li, T.; Song, M.-P.; Niu, J.-L. *ACS Catal.*, **2022**, *12*, 1650-1656; (b) Ghosh, P.; Schoch, R.; Bauer, M. *Angew. Chem. Int. Ed.*, **2022**, *134*, e202110821; (c) Yao, Q.-J.; Chen, J.-H.; Song, H.; Huang, F.-R.; Shi, B.-F. *Angew. Chem. Int. Ed.*, **2022**, *61*, e202202892.

<sup>50</sup> (a) Yao, C.; Zhang, T.; Gonçalves, T. P.; Huang, K.-W. *Chem. Commun.*, **2022**, *58*, 1593-1596; (b) Campbell, M. W.; Yuan, M.; Polites, V. C.; Gutierrez, O.; Molander, G. A. *J. Am. Chem. Soc.*, **2021**, *143*, 3901-3910; (c) Murugesan, V.; Ganguly, A.; Karthika, A.; Rasappan, R. *Org. Lett.*, **2021**, *23*, 5389-5393.

<sup>51</sup> (a) Sahoo, K.; Panda, N. *Adv. Synth. Catal.*, **2022**, *364*, 1023-1030; (b) Yu, Z.; Li, G.; Zhang, J.; Liu, L. *Org. Chem. Front.*, **2021**, *8*, 3770-3775; (c) Dey, D.; Patra, M.; Al-Hunaiti, A.; Yadav, H. R.; Al-mherat, A.; Arar, S.; Maji, M.; Choudhury, A. R.; Biswas, B. *J. Mol. Struct.*, **2019**, *1180*, 220-226.

<sup>52</sup> Murali, K.; Machado, L. A.; de Carvalho, R. L.; Pedrosa, L. F.; Mukherjee, R.; da Silva Júnior, E. N.; Maiti, D. *Chem. Eur. J.*, **2021**, *27*, 12453-12508.

<sup>53</sup> Kumar, S.; Kumar, A.; Sharma, D.; Das, P. *Chem. Rec.*, **2022**, *22*, e202100171.

<sup>54</sup> Achar, T. K.; Zhang, X.; Mondal, R.; Shanavas, M. S.; Maiti, S.; Maity, S.; Pal, N.; Paton, R. S.; Maiti, D. *Angew. Chem. Int. Ed.*, **2019**, *58*, 10353-10360.

<sup>55</sup> Ahmad, M. S.; Meguellati, K. *ChemistrySelect*, **2022**, *7*, e202103716.

<sup>56</sup> (a) Ramadoss, B.; Jin, Y.; Asako, S.; Iliès, L. *Science*, **2022**, *375*, 658-663; (b) Bellina, F.; La Manna, M.; Rosadoni, E. *Curr. Org. Chem.*, **2021**, *25*, 2116-2141.

of the same template, making it possible to achieve *ortho*-,<sup>57</sup> *meta*-,<sup>58</sup> and even *para*-activations<sup>59</sup>. It is also important to mention that there is an increasing demand on removal methodologies of these directing groups,<sup>60</sup> making it possible to use activated molecules as substrates on important late-stage modifications towards even more complex molecules.

### 1.3.3. Coupling partners

C–H activation reactions usually happen between the substrate (the compound that bears the directing group) and the coupling partner (the portion to be added into the structure of the substrate). Although most of the coupling partners are separate entities, there are some cases in which the coupling partner is a member within the structure of the substrate itself, these cases can be characterized as an intramolecular C–H activation.<sup>61</sup>

The choice of coupling partner varies according to the type of C–H activation that is being desired. Some examples can be found here, such as *N*-halosuccinimides<sup>57b</sup> and copper(II) halides<sup>62</sup> as C–H halogenating agents; internal alkynes<sup>63</sup> and sulfoxonium ylides<sup>64</sup> as C–H annulating agents, terminal alkynes,<sup>65</sup> bromoalkynes<sup>66</sup> or hypervalent iodine species<sup>67</sup> as alkynylating agents, etc. There is not a clear aspect for the choice of the coupling partner, however, some of them may be more active than others in different conditions. To gather a greater knowledge on the reaction under development, different coupling partners can be studied and attempted for the same reaction, starting from what is known in that specific field and projecting that knowledge forward, expanding it to new frontiers and even more challenging studies and research.

---

<sup>57</sup> (a) Hammarback, A.; Bishop, A. L.; Jordan, C.; Athavan, G.; Eastwood, J. B.; Burden, T. J.; Bray, J. T. W.; Clarke, F.; Robinson, A.; Krieger, J.-P.; Whitwood, A.; Clark, I. P.; Towrie, M.; Lynam, J. M.; Fairlamb, I. J. S. *ACS Catal.*, **2022**, *12*, 1532-1544; (b) Wang, Y.; Wang, H.; Yang, Q.; Xie, S.; Zhu, H. *Eur. J. Org. Chem.*, **2022**, DOI: 10.1002/ejoc.202200316.

<sup>58</sup> (a) Dutta, U.; Maiti, D. *Acc. Chem. Res.*, **2022**, *55*, 354-372; (b) Luan, Y.-Y.; Gou, X.-Y.; Shi, W.-Y.; Liu, H.-C.; Chen, X.; Liang, Y.-M. *Org. Lett.*, **2022**, *24*, 1136-1140.

<sup>59</sup> Dutta, U.; Maiti, S.; Pimparkar, S.; Maiti, S.; Gahan, L. R.; Krenske, E. H.; Lupton, D. W.; Maiti, D. *Chem. Sci.*, **2019**, *10*, 7426-7432.

<sup>60</sup> de Carvalho, R. L.; Almeida, R. G.; Murali, K.; Machado, L. A.; Pedrosa, L. F.; Dolui, P.; Maiti, D.; da Silva Júnior, E. N. *Org. Biomol. Chem.*, **2021**, *19*, 525-547.

<sup>61</sup> (a) Chen, Y.; Lyu, H.; Quan, Y.; Xie, Z. *Org. Lett.*, **2021**, *23*, 4163-4167; (b) Liao, Y.; Zhou, Y.; Zhang, Z.; Fan, J.; Liu, F.; Shi, Z. *Org. Lett.*, **2021**, *23*, 1251-1257.

<sup>62</sup> Singh, A.; Dey, A.; Pal, K.; Dash, O. P.; Volla, C. M. R. *Org. Lett.*, **2022**, *24*, 1941-1946.

<sup>63</sup> Wang, Q.; Nie, Y.-H.; Liu, C.-X.; Zhang, W.-W.; Wu, Z.-J.; Gu, Q.; Zheng, C.; You, S.-L. *ACS Catal.*, **2022**, *12*, 3083-3093.

<sup>64</sup> Yin, C.; Li, L.; Yu, C. *Org. Biomol. Chem.*, **2022**, *20*, 1112-1116.

<sup>65</sup> Zeng, Z.; Yan, F.; Dai, M.; Yu, Z.; Liu, F.; Zhao, Z.; Bai, R.; Lan, Y. *Organometallics*, **2022**, *41*, 270-277.

<sup>66</sup> Guo, L.-Y.; Li, Q.; Liu, Y.-T.; Li, L.; Ni, Y.-Q.; Li, Y.; Pan, F. *Adv. Synth. Catal.*, **2022**, *364*, 1109-1116.

<sup>67</sup> Han, C.; Tian, X.; Zhang, H.; Rominger, F.; Hashmi, S. K. *Org. Lett.*, **2021**, *23*, 4764-4768.

## 1.4. Polycyclic quinones

Polycyclic quinones are an important sub-class of quinones with desirable biological activities<sup>68</sup> and, consequentially, there is a considerable demand for innovative and effective methods to achieve these compounds in a more accessible way.<sup>69</sup> Metal-catalyzed C–H annulation reactions are a compelling approach to achieve such compounds.<sup>70</sup> Grubbs catalysts were previously used to perform ring-closing metathesis to afford polycyclic compounds.<sup>71</sup> Nitrogenated quinones were also prepared by tricomponent reactions *via* C–H functionalization of naphthoquinones (**Scheme 2**).<sup>72</sup>

Polycyclic quinones prepared *via* palladium catalysis presented desirable antitumor activity, specifically, antileukemic activity, as described by Koketsu and co-workers.<sup>73</sup> Several attempts of modification on the quinoidal structure in order to achieve more active anticancer molecules were performed, including C–H iodination,<sup>74</sup> oxygenation,<sup>16d</sup> alkenylation,<sup>75</sup> sequential C–H iodination/thiolation<sup>76</sup> and selenation.<sup>3</sup> Most of these methods functionalize the compound at the C-5 position, as addressed in **Figure 3** (Page 3), while the construction of polycyclic quinoidal motifs remains a challenge. Thus, based on previous reported C–H annulation reactions for the construction of heterocyclic rings,<sup>77</sup> it is understandable that new

<sup>68</sup> (a) Rodrigues, T.; Werner, M.; Roth, J.; da Cruz, E. H. G.; Marques, M. C.; Akkapeddi, P.; Lobo, S. A.; Koeberle, A.; Corzana, F.; da Silva Júnior, E. N.; Werz, O.; Bernardes, G. J. L. *Chem. Sci.*, **2018**, *9*, 6899-6903; (b) de Castro, S. L.; Emery, F. S.; da Silva Júnior, E. N. *Eur. J. Med. Chem.*, **2013**, *69*, 678-700; (c) Kallifidas, D.; Kang, H.-S.; Brady, S. F. *J. Am. Chem. Soc.*, **2012**, *134*, 19552-19555; (d) Powis, G. *Pharmacol. Ther.*, **1987**, *35*, 57; (e) O'Brien, P. J. *Chem. Biol. Interact.*, **1991**, *80*, 1. (f) Hillard, E. A.; Abreu, F. C.; Ferreira, D. C.; Jaouen, G.; Goulart, M. O. F.; Amatore, C. *Chem. Commun.*, **2008**, *23*, 2612.

<sup>69</sup> Wood, J. M.; da Silva Júnior, E. N.; Bower, J. F. *Org. Lett.*, **2020**, *22*, 265-269.

<sup>70</sup> (a) Ambler, B. R.; Turnbull, B. W. H.; Suravarapu, S. R.; Uteuliyev, M. M.; Huynh, N. O.; Krische, M. J. *J. Am. Chem. Soc.*, **2018**, *140*, 9091-9094; (b) Bender, M.; Turnbull, B. W. H.; Ambler, B. R.; Krische, M. J. *Science*, **2017**, *357*, 779-781.

<sup>71</sup> (a) Arisawa, M.; Fujii, Y.; Kato, H.; Fukuda, H.; Matsumoto, T.; Ito, M.; Abe, H.; Ito, Y.; Shuto, S. *Angew. Chem. Int. Ed.*, **2013**, *52*, 1003-1007; (b) Fujii, Y.; Takehara, T.; Suzuki, T.; Fujioka, H.; Shuto, S.; Arisawa, M. *Adv. Synth. Catal.*, **2015**, *357*, 4055-4062.

<sup>72</sup> Liu, Y.; Sun, J.-W. *J. Org. Chem.*, **2012**, *77*, 1191-1197.

<sup>73</sup> Suematsu, N.; Ninomiya, M.; Sugiyama, H.; Udagawa, T.; Tanaka, K.; Koketsu, M. *Bioorg. Med. Chem. Lett.*, **2019**, *29*, 2243-2247.

<sup>74</sup> Jardim, G. A. M.; da Silva Júnior, E. N.; Bower, J. F. *Chem. Sci.*, **2016**, *7*, 3780-3784.

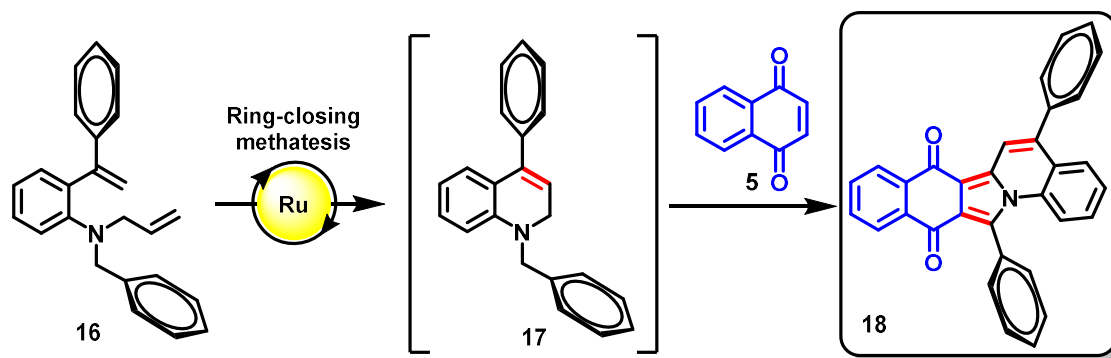
<sup>75</sup> Dias, G. G.; do Nascimento, T. A.; de Almeida, A. K. A.; Bombaça, A. C. S.; Menna-Barreto, R. F. S.; Jacob, C.; Warratz, S.; da Silva Júnior, E. N.; Ackermann, L. *Eur. J. Org. Chem.*, **2019**, *2019*, 2344-2353.

<sup>76</sup> Jardim, G. A. M.; Oliveira, W. X. C.; de Freitas, R. P.; Menna-Barreto, R. F. S.; Silva, T. L.; Goulart, M. O. F.; da Silva Júnior, E. N. *Org. Biomol. Chem.*, **2018**, *16*, 1686-1691.

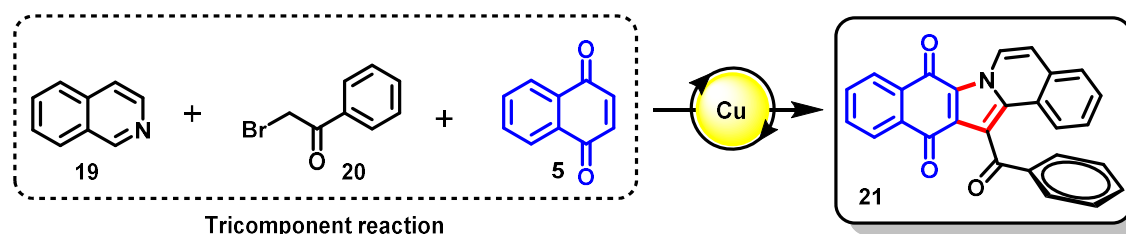
<sup>77</sup> (a) Ackermann, L. *Acc. Chem. Res.*, **2014**, *47*, 281-295; (b) Rouquet, G.; Chatani, N. *Angew. Chem. Int. Ed.*, **2013**, *52*, 11726-11743; (c) Peng, S.; Liu, S.; Zhang, S.; Cao, S.; Sun, J. *Org. Lett.*, **2015**, *17*, 5032-5035; (d) Jayakumar, J.; Parthasarathy, K.; Chen, Y.-H.; Lee, T.-H.; Chuang, S.-C.; Cheng, C.-H. *Angew. Chem. Int. Ed.*, **2014**, *53*, 9889-9892; (e) Rakshit, S.; Patureau, F. W.; Glorius, F. *J. Am. Chem. Soc.*, **2010**, *132*, 9585-9587; (f) Song, G.; Chen, D.; Pan, C.-L.; Crabtree, R. H.; Li, X. *J. Org. Chem.*, **2010**, *75*, 7487-7490; (g) Satoshi, M.; Nobuyoshi, U.; Koji, H.; Tetsuya, S.; Masahiro, M. *Chem. Lett.*, **2010**, *39*, 744-746; (h) Kong, W.-J.; Finger, L. H.; Messinis, A. M.; Kuniyil, R.; Oliveira, J. C. A.; Ackermann, L. *J. Am. Chem. Soc.*, **2019**, *141*, 17198-17206; (i) Zhu, C.; Kuniyil, R.; Ackermann, L. *Angew. Chem. Int. Ed.*, **2019**, *58*, 5338-5342; (j) Tian, C.; Dhawa, U.;

C–H activation/annulation could be developed as a complementary method for the construction of these desired cyclic systems.

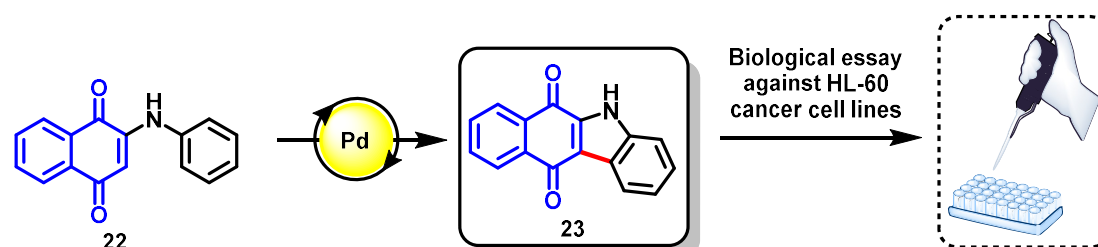
Arisawa and Shuto (2013 and 2015):



Liu (2012):



Koketsu (2019):



**Scheme 2.** Examples of currently known polycyclic quinones synthesis.

Scheremetjew, A.; Ackermann, L. *ACS Catal.*, **2019**, *9*, 7690-7696; (k) Mei, R.; Koeller, J.; Ackermann, L. *Chem. Commun.*, **2018**, *54*, 12879-12882; (l) Mei, R.; Wang, H.; Warratz, S.; Macgregor, S. A.; Ackermann, L. *Chem. Eur. J.*, **2016**, *22*, 6759-6763; (m) Ma, W.; Ackermann, L. *Synthesis*, **2014**, *46*, 2297-2304; (n) Li, J.; Ackermann, L. *Tetrahedron*, **2014**, *70*, 3342-3348; (o) Song, W.; Ackermann, L. *Chem. Commun.*, **2013**, *49*, 6638-6640; (p) Kornhaas, C.; Li, J.; Ackermann, L. *J. Org. Chem.*, **2012**, *77*, 9190-9198.

## 2. RESEARCH PROPOSAL

### 2.1. General research proposal

As already mentioned, the synthetic methods applied on the construction of polycyclic quinones are still a challenging subject, considering the lack of examples in the literature. The purpose of this research work is to develop a new and accessible method to synthesize new modified quinones, in a single C–H activation step, exploring both intrinsic and synthesizable directing groups. In each of these cases, once reaching success, a plausible optimization shall be developed and scopes including a large variety of substrates must be accounted as well, in order to properly explore the range of applicability of the developed methods. All obtained products will be evaluated against several cancer cell lines, including HL-60, a human leukemia cell line, through a collaboration with our partner, Dr. Cláudia Pessoa (Fortaleza-CE, Brazil).

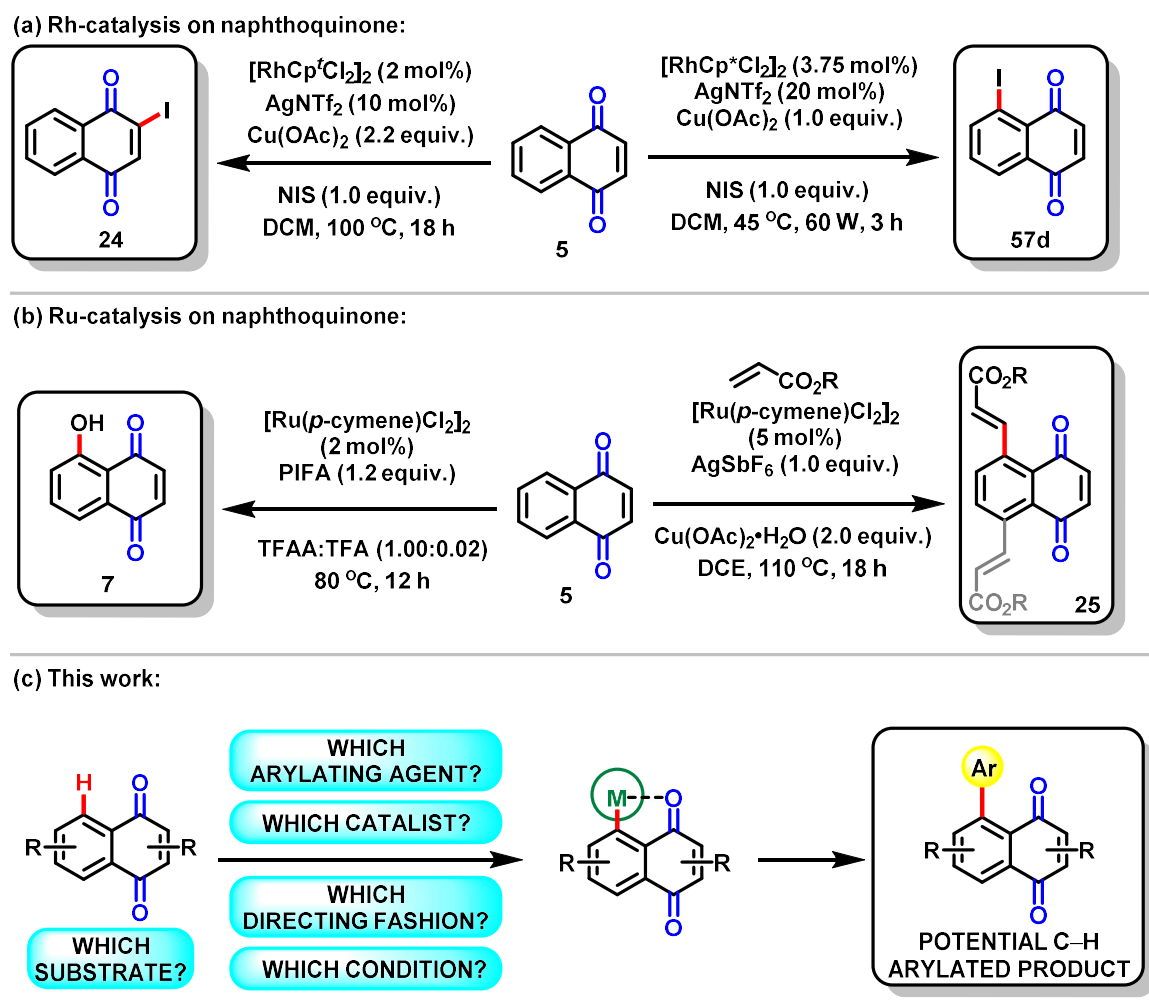
### 2.2. Evaluation of the intrinsic directing behaviour of quinoidal compounds towards a ruthenium catalyzed C(sp<sup>2</sup>)–H arylation reaction

The starting point of the research described in this thesis is aimed at the construction of a plausible C(sp<sup>2</sup>)–H arylation methodology involving naphthoquinoidal structures as substrates. This proposal was developed exploring the intrinsic directing behaviour offered by their carbonyl groups, considering that these groups have the ability to coordinate with the metalcentre of the catalyst, which may lead to the desired C(sp<sup>2</sup>)–H arylation at the C-5 position of the quinone. This quinoidal characteristic has been already explored by our research group, from which valuable C(sp<sup>2</sup>)–H activations were achieved and previously published (Scheme 3a,b).<sup>16a,16d,76</sup> Keeping in mind that specific adaptations are necessary for specific C–H modifications, the pathway this research must take place shall include a complete evaluation of each important aspect from both elements: **QUINONES** and **C–H ACTIVATION (Scheme 3c)**. This study may lead to the successful obtention of several new molecules with potential bioactive properties.

---

<sup>16</sup> (a) Jardim, G. A. M.; Silva, T. L.; Goulart, M. O. F.; Carlos A. de Simone, C. A.; Barbosa, J. M. C.; Salomão, K.; Solange L. de Castro, S. L.; Bower, J. F.; da Silva Júnior, E. N. *Eur. J. Med. Chem.*, **2017**, *136*, 406-419; (d) Dias, G. G.; Rogge, T.; Kuniyil, R.; Jacob, C.; Menna-Barreto, R. F. S.; da Silva Junior, E. N.; Ackermann, L. *Chem. Commun.*, **2018**, *54*, 12840-12843.

<sup>76</sup> Jardim, G. A. M.; Oliveira, W. X. C.; de Freitas, R. P.; Menna-Barreto, R. F. S.; Silva, T. L.; Goulart, M. O. F.; da Silva Júnior, E. N. *Org. Biomol. Chem.*, **2018**, *16*, 1686-1691.



**Scheme 3.** Previous knowledge and purpose for C–H arylation on naphthoquinones.

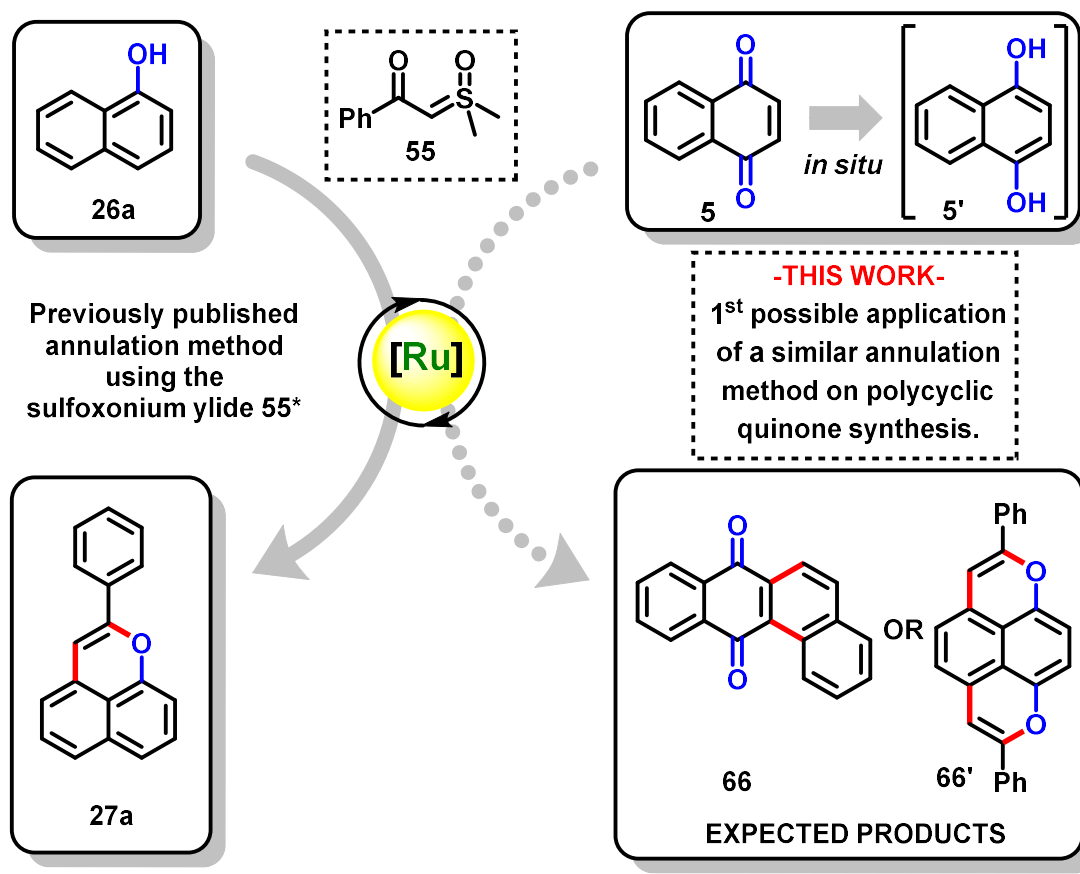
### 2.3. Evaluation of the intrinsic directing behaviour of quinoidal compounds towards a ruthenium catalyzed C(sp<sup>2</sup>)–H annulation reaction

In the second part of this project, a ruthenium-catalyzed C(sp<sup>2</sup>)–H annulation was designed towards the obtention of cyclic quinones, still exploring the intrinsic directing behaviour of the carbonyl groups, with no additional directing group added to the structure. Based on a procedure discussed in literature,<sup>80</sup> we are focusing on using the sulfoxonium ylide **55** as annulation agent, and this reaction is expected to take place involving the hydrogen atoms positioned at the C-2 and C-3 positions, since they are more labile, leading to the polycyclic quinone **66**. However, we must not exclude the possibility for this reaction to happen at the C-

<sup>80</sup> Ma, W.; Tan, Y.; Wang, Y.; Li, Z.; Li, Z.; Gu, L.; Mei, R.; Cheng, A. *Org. Lett.*, **2021**, *23*, 6200-6205.



5 and/or the C-8 positions, leading to a possible hydroquinone derivative polycyclic product **66'**, considering the possible *in situ* generation of the 1,4-hydroquinone intermediate **5'**.



\*Conditions: **26a** (0.2 mmol), **55** (1.5 equiv.),  $[\text{RuCl}_2(p\text{-cymene})]_2$  (5 mol%),  $\text{Cu}(\text{OAc})_2 \cdot \text{H}_2\text{O}$  (20 mol%), KOAc (2.0 equiv.), DCM (0.1 M), 100 °C, 16 h, Ar; then  $\text{Tf}_2\text{O}$  (0.5 equiv.), r.t., 2 h.

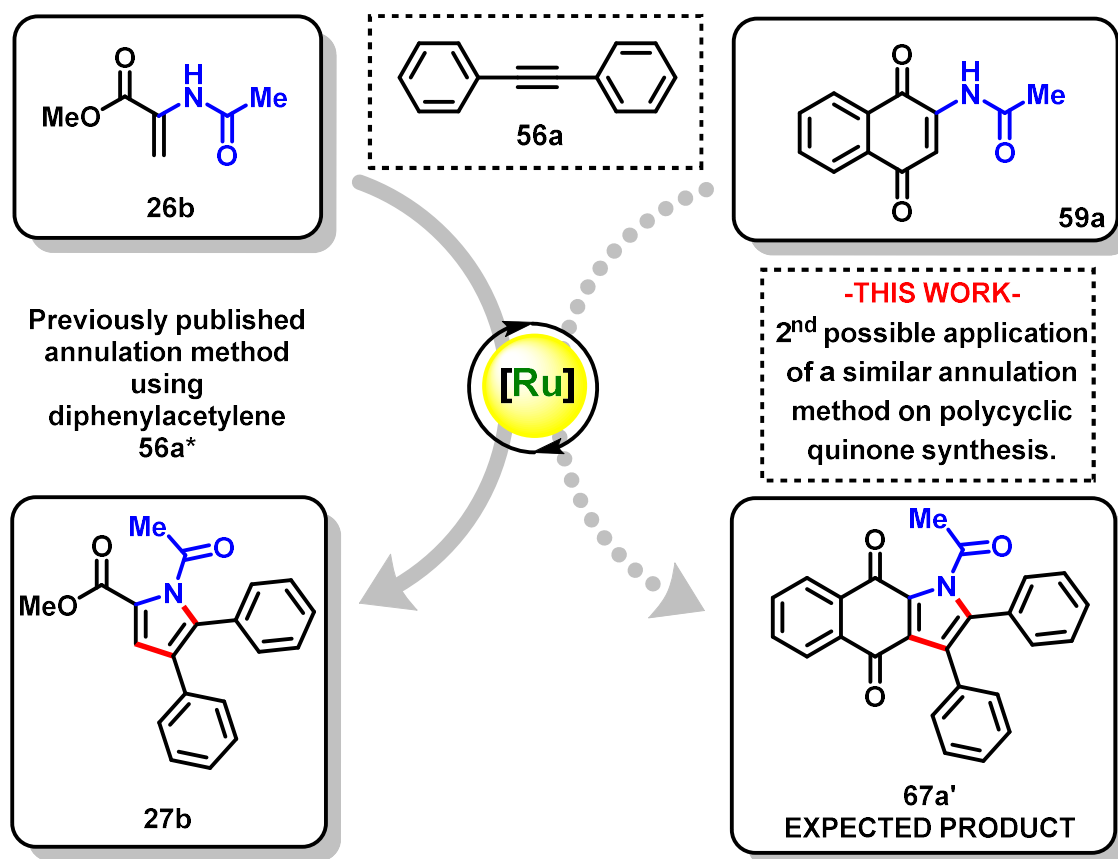
**Scheme 4.** Previously reported Ruthenium-catalyzed annulation<sup>80</sup> and possible extrapolation of the method to a quinone without any additional DG.

#### 2.4. Evaluation of additional directing groups on quinoidal substrates towards a ruthenium catalyzed C(sp<sup>2</sup>)-H annulation reaction

Subsequently, the next step is aimed at the construction of a plausible C(sp<sup>2</sup>)-H annulation methodology involving naphthoquinoidal structures bearing synthesizable directing groups as substrates. Based on previous works, in which polycyclic compounds were achieved using ruthenium catalysis on the compound **26b** in the presence of internal alkynes,<sup>78</sup> a new similar method was applied to quinones with a similar directing group. For this purpose, a

<sup>78</sup> (a) Wang, L.; Ackermann, L. *Org. Lett.*, **2013**, *15*, 176-179; (b) Gońka, E.; Yang, L.; Steinbock, R.; Pescioioli, F.; Kuniyil, R.; Ackermann, L. *Chem. Eur. J.*, **2019**, *25*, 16246-16250.

quinone containing an acetamide at the C-2 position (**Compound 59a**) was developed and submitted to several attempts with adaptable modifications to the original published annulation method (**Scheme 5**).



\*Conditions: 26 (0.5 mmol), 56a (2.0 equiv.), [RuCl<sub>2</sub>(*p*-cymene)]<sub>2</sub> (5 mol%), Cu(OAc)<sub>2</sub>·H<sub>2</sub>O (1.0 equiv.), <sup>t</sup>AmOH (0.25 M), 120 °C, 22 h.

**Scheme 5.** Previously reported Ruthenium catalyzed annulation<sup>78a</sup> and possible extrapolation of the method to a quinone bearing a C-2 acetamide DG.

All the observed results achieved during the construction of this work will be fully discussed in the following sessions, including the challenges faced over the syntheses, possible modifications and adaptations that were necessary in order to lead to the desired compounds and the complete characterization and biological assays performed with each achieved final molecules.

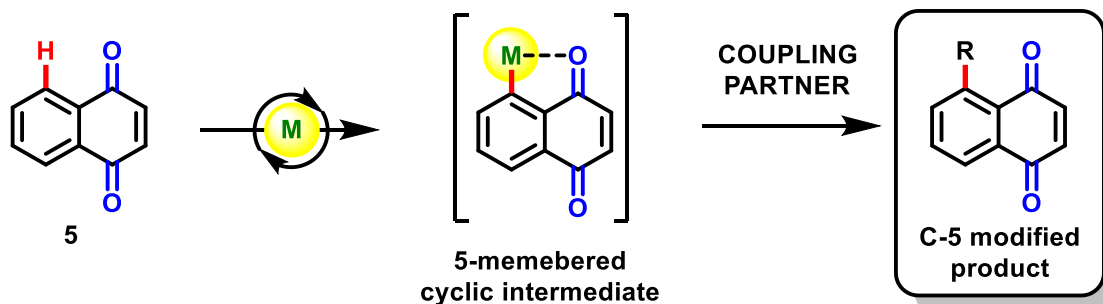
### 3. RESULTS AND DISCUSSION

The obtained results will be discussed in a sequence of eight sections, according to the development of the strategy, leading to the actual C–H activation project that is the key to this thesis work. The first and second sections will present discussions about the intrinsic directing behaviour within the naphthoquinoidal structure, from the first C–H arylation trial on the A-ring (section 3.1.) until the exploring of different conditions used towards the C–H annulation on the 1,4-naphthoquinone (**5**), aiming the construction of new rings (section 3.2.). In the third and fourth sections, the structural inclusion (section 3.3.) and use of different directing groups applied on two different C–H annulation reactions (section 3.4.) will be discussed. In the latter, it will be also discussed the development of the strategy towards the main subject of this thesis, the double annulation of quinones bearing synthesizable DG. In the fifth section, it will be presented the logical process used to optimize the annulation method (section 3.5.). The sixth section will discuss about the range of application of the optimized method on different scopes (section 3.6.). The seventh section will discuss about the mechanistic insights and the computational studies correlated to the proposed mechanism (section 3.7.). The eighth and final section will present the observed biological activities for the compounds obtained in this work (section 3.8.).

The obtained compounds were characterized by  $^1\text{H}$  and  $^{13}\text{C}$  Nuclear Magnetic Resonance Spectroscopy, Infrared Spectroscopy, Mass Spectrometry and, in several cases, Crystallographic Analysis. The collected spectra are presented at the Appendices section of this work.

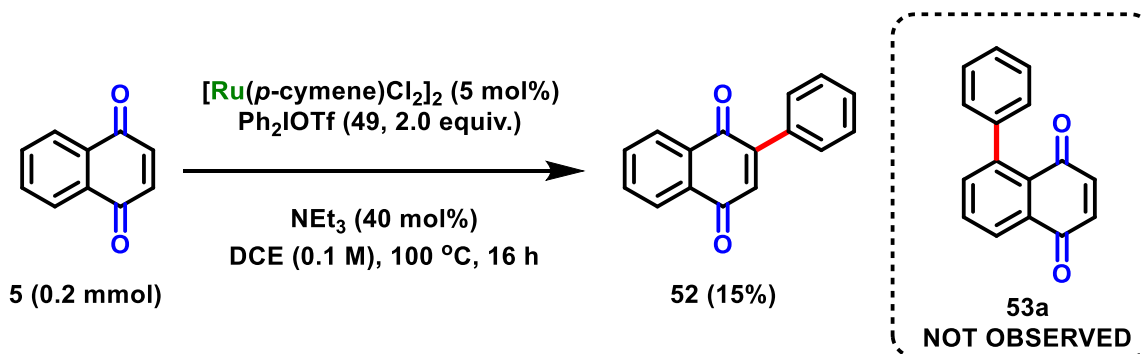
#### 3.1. C–H arylation trials on 1,4-naphthoquinone (**5**)

As previously discussed here, naphthoquinoidal molecules present two carbonyl groups that can behave as intrinsic DG in certain occasions. From this aspect, the C-5 position (A-ring) can be directly activated, passing through a 5-membered metalacyclic intermediate (**Scheme 6**). Our research group has already extensively explored that fact, from which plausible C(5)–H iodination,<sup>76</sup> hydroxylation<sup>16d</sup> and alkenylation<sup>75</sup> reactions were successfully achieved.



**Scheme 6.** C–H activation at the C-5 position of 1,4-naphthoquinone (5).

Led by this previous knowledge, in order to further explore the intrinsic directing behaviour presented by naphthoquinoidal substrates, a first ruthenium-catalyzed C–H arylation was essayed, using diphenyliodonium trifluoromethanesulfonate (compound **49**) as coupling partner, a known arylating agent on C–H activation processes (**Scheme 7**). In this occasion, a surprisingly different regioselectivity was observed, the 2-aryl-1,4-naphthoquinone (compound **52**) was achieved instead of the desired 5-aryl-1,4-naphthoquinone (compound **53a**).



**Scheme 7.** Ruthenium-catalyzed C–H arylation trial.

This observation can still represent a promising outcome, however, the catalytic behaviour of the method must be confirmed. Therefore, the same system was repeated, but in absence of the ruthenium-catalyst. In this study, a similar yield was achieved, confirming that this reaction does not follow a classic metallic catalysis. Beyond that, this reaction has been already published in 2014 by Wang and Ding,<sup>79</sup> using 1,4-naphthoquinone (compound **5**) as substrate and diphenyliodonium trifluoromethanesulfonate (compound **49**) as arylating agent with some minor variations.

<sup>79</sup> Wang, D.; Ge, B.; Li, L.; Shan, J.; Ding, Y. *J. Org. Chem.*, **2014**, *79*, 8607-8613.

From that perspective, several experiments varying crucial aspects of the condition were tried, aiming to force an C–H activation at the C-5 position (**Table 1**), including the use of different additives (**Table 1**, entries 1-8), diphenyliodonium hexafluorophosphate as coupling partner (**Table 1**, entry 11), or even a rhodium-catalyst (**Table 1**, entry 18). But in all cases, the undesired 2-aryl-1,4-naphthoquinone (compound **52**) was obtained instead of the aimed 5-aryl-1,4-naphthoquinone (compound **53a**).

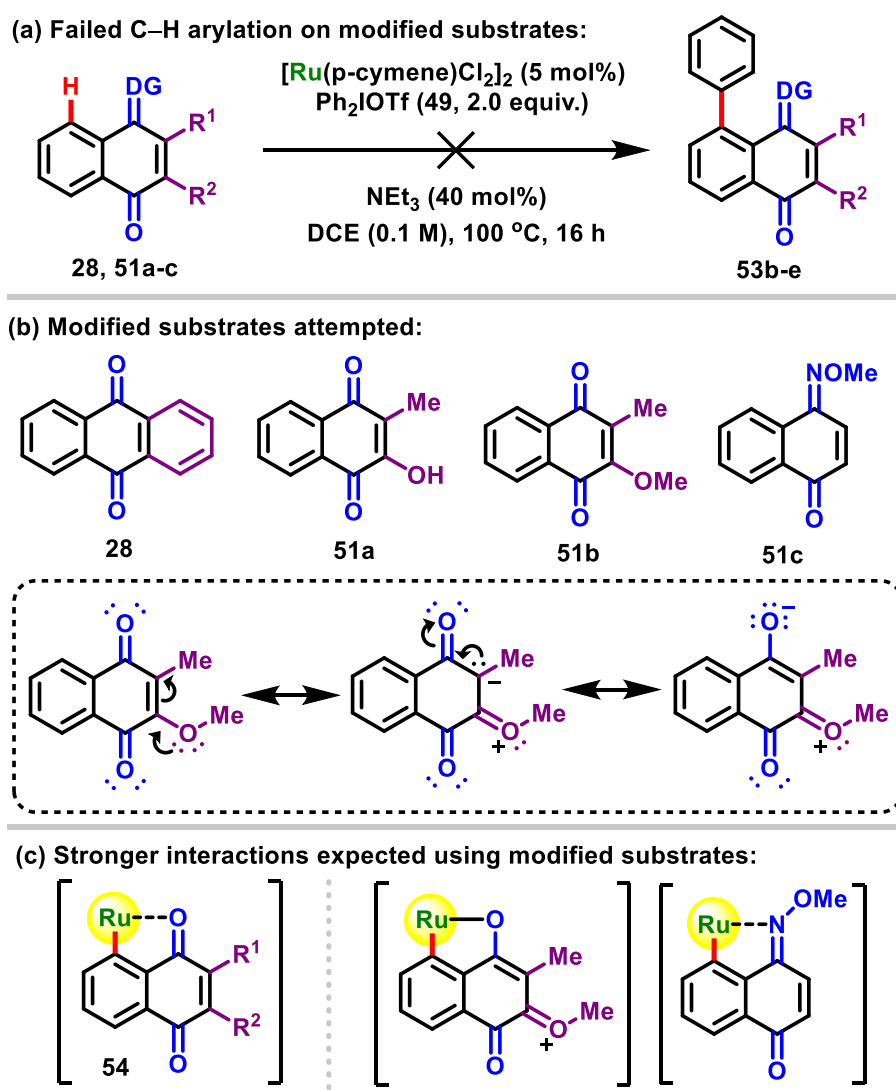
**Table 1.** Modifications of the standard conditions to force the activation at the C-5 position of the 1,4-naphthoquinone (**5**).

Entry	Modification from standard procedure	Yield ( <b>52</b> )	Yield ( <b>53a</b> )
1	KOAc (20 mol %) as additive	0	0
2	K <sub>2</sub> CO <sub>3</sub> (20 mol %) as additive	0	0
3	MesCO <sub>2</sub> H (20 mol %) as additive	42	0
4	MesCO <sub>2</sub> H/K <sub>2</sub> CO <sub>3</sub> (20 mol %) as additive	50	0
5	KPF <sub>6</sub> (20 mol %) as additive	0	0
6	AgSbF <sub>6</sub> (20 mol %) as additive	0	0
7	PPh <sub>3</sub> (20 mol %) as additive	6	0
8	KNO <sub>3</sub> (20 mol %) as additive	0	0
9	2-methoxy-1,4-naphthoquinone (0.2 mmol) instead of 1,4-naphthoquinone ( <b>5</b> )	12	0
10	2-bromo-1,4-naphthoquinone (0.2 mmol) instead of 1,4-naphthoquinone ( <b>5</b> )	5	0
11	Ph <sub>2</sub> IPF <sub>6</sub> ( <b>50</b> , 2.0 equiv.) instead of Ph <sub>2</sub> IOTf ( <b>49</b> )	6	0
12	80 °C	6	0
13	120 °C	12	0
14	1,4-dioxane as solvent, at 80 °C	6	0
15	1,4-dioxane as solvent, at 100 °C	5	0
16	1,4-dioxane as solvent, at 120 °C	6	0
17	CuCl (10 mol %) as co-catalyst	0	0
18	[RhCp*Cl <sub>2</sub> ] <sub>2</sub> (5 mol %) as catalyst	0	0

**Standard conditions:** 1,4-naphthoquinone (**5**, 0.2 mmol), [Ru(*p*-cymene)Cl<sub>2</sub>]<sub>2</sub> (5 mol %), Ph<sub>2</sub>IOTf (**49**, 2.0 equiv.), NEt<sub>3</sub> (40 mol %), DCE (0.1 M), 100 °C, 16 h.

The next step to force the C–H activation at the C-5 position is to occupy the C-2 and C-3 positions, leaving the C-5 position as the only site available for reaction. In this case, compounds **28**, **51a**, **51b** were designed to be used. A special attention shall be given to the compounds **51a** and **51b**, since they present important resonance contributors that can interact strongly with the metalcentre of the catalysts. Sadly, all these three trials failed to lead to any product (**Scheme 8**).

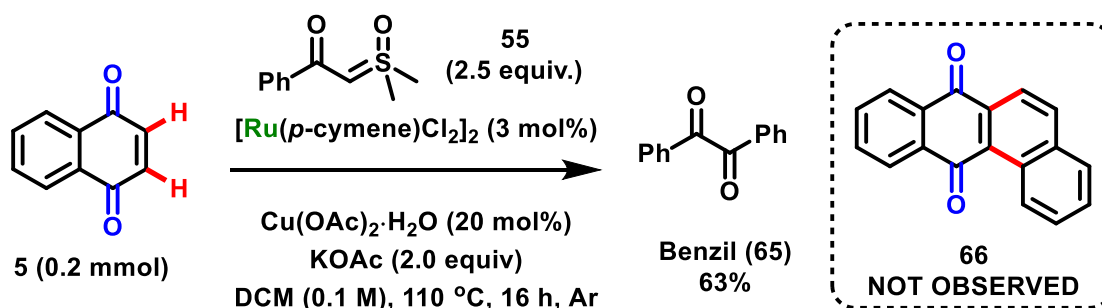
Based on the Lewis acid-base theory, we considered the fact that  $sp^2$ -hybridized nitrogen atoms may interact stronger with  $d$ -orbitals of transition metals than  $sp^2$ -hybridized oxygen atoms. Therefore, compound **51c** was designed to fulfil this purpose. However, despite the efforts towards the success of this study, this procedure culminated on failure (**Scheme 8**).



**Scheme 8.** Modified substrates used to force the C–H activation at the C-5 position.

### 3.2. C–H annulation trials on 1,4-naphthoquinone (5)

After facing the unsuccessful results previously described, we decided to move forward with the studies regarding the intrinsic directing-behaviour of the 1,4-naphthoquinone (compound **5**). With that purpose, a ruthenium-catalyzed C–H annulation reaction was tried using the sulfoxonium ylide **55** as annulation agent (**Scheme 9**). This procedure was based on a work previously published by Ma, Gu, and co-workers, from which the ylide presented a peculiar and notable reactivity leading to open and/or cyclic products according to the procedure that was applied.<sup>80</sup> A promising pale-yellow product was successfully obtained, however, after careful characterization, it was concluded that the achieved compound was benzil (compound **65**). Although no product was observed in the absence of catalyst, characterizing this as a catalytic method, benzil (**65**) can be easily achieved using only benzoyl chloride and lithium under ultrasound irradiation.<sup>81</sup> Therefore, a methodology applying ruthenium-(*p*-cymene) chloride dimer – a considerably expensive catalyst – is not a promising and applicable project for this matter.



**Scheme 9.** C–H annulation trial using substrate **5** and sulfoxonium ylide **55**.

To further explore this reaction, several other experiments were tried aiming to force the interaction between the possible *in situ* generated ruthenium-ylide intermediate and the naphthoquinoidal substrate (**Table 2**). This study included several variations on the oxidant amount (**Table 2**, entries 1-5) and solvent (**Table 2**, entries 6-21). In all cases, only benzil was obtained.

<sup>80</sup> Ma, W.; Tan, Y.; Wang, Y.; Li, Z.; Li, Z.; Gu, L.; Mei, R.; Cheng, A. *Org. Lett.*, **2021**, *23*, 6200-6205.

<sup>81</sup> Han, B. H.; Boudjouk, P. Organic sonochemistry. *Tetrahedron Lett.*, **1981**, *22*, 2757-2758.

**Table 2.** Modifications of the standard conditions aiming to force the annulation reaction using sulfoxonium ylide (**55**).

Entry	Modification from standard procedure	Yield ( <b>65</b> )	Yield ( <b>66</b> )
1	Cu(OAc) <sub>2</sub> ·H <sub>2</sub> O (10 mol %)	27	0
2	Cu(OAc) <sub>2</sub> ·H <sub>2</sub> O (30 mol %)	31	0
3	Cu(OAc) <sub>2</sub> ·H <sub>2</sub> O (40 mol %)	31	0
4	Cu(OAc) <sub>2</sub> ·H <sub>2</sub> O (50 mol %)	19	0
5	Cu(OAc) <sub>2</sub> ·H <sub>2</sub> O (1.0 equiv.)	0	0
6	DCE (0.1 M) as solvent	64	0
7	chloroform (0.1 M) as solvent	77	0
8	toluene (0.1 M) as solvent	54	0
9	hexane (0.1 M) as solvent	0	0
10	heptane (0.1 M) as solvent	0	0
11	ethyl acetate (0.1 M) as solvent	38	0
12	water (0.1 M) as solvent	0	0
13	2-methyl-2-butanol (0.1 M) as solvent	42	0
14	methanol (0.1 M) as solvent	10	0
15	ethanol (0.1 M) as solvent	13	0
16	NMP (0.1 M) as solvent	0	0
17	DMA (0.1 M) as solvent	0	0
18	DMF (0.1 M) as solvent	0	0
19	1,4-dioxane (0.1 M) as solvent	12	0
20	xylene (0.1 M) as solvent	23	0
21	DMSO (0.1 M) as solvent	9	0
22	5-hydroxy-1,4-naphthoquinone (0.2 mmol) instead of 1,4-naphthoquinone ( <b>5</b> )	12	0
23	1,4-benzoquinone ( <b>34</b> , 0.2 mmol) instead of 1,4-naphthoquinone ( <b>5</b> )	9	0

**Standard conditions:** 1,4-naphthoquinone (**5**, 0.2 mmol), **55** (2.5 equiv.), [Ru(*p*-cymene)Cl<sub>2</sub>]<sub>2</sub> (3 mol %), Cu(OAc)<sub>2</sub>·H<sub>2</sub>O (20 mol %), KOAc (2.0 equiv.), DCM (0.1 M), 110 °C, 16 h.

These studies included even the use of naphthoquinoidal substances bearing different substituents at the A-ring, to force the interaction of the C=C bond present in the B-ring with



the metallic-center of the catalyst. This trial was still unsuccessful, leading to the formation of benzil (**65**) exclusively (**Table 2**, entries 22 and 23).

### 3.3. Synthesis of substrates containing additional DG

Since the intrinsic-direction group ability of the carbonyl groups of the 1,4-naphthoquinone (**5**) did not work as expected, we decided to move forward using synthesizable directing-groups placed at the C-2 position of the B-ring of 1,4-naphthoquinone. From this strategy, a C–H activation at the C-3 position is expected to happen. The idea here is to explore the coordinating chemistry offered by different directing groups already known in literature, which syntheses were previously described, including the hydroxy group present in lawsone (compound **6**), *N*-pyridylamino group (compound **60**), *N*-pyrimidylamino group (compound **61**), the simplest amino group (compound **58a**), the simplest acetamido group (compound **59a**), acetate group (compound **62**) and benzamido group (compound **64**).

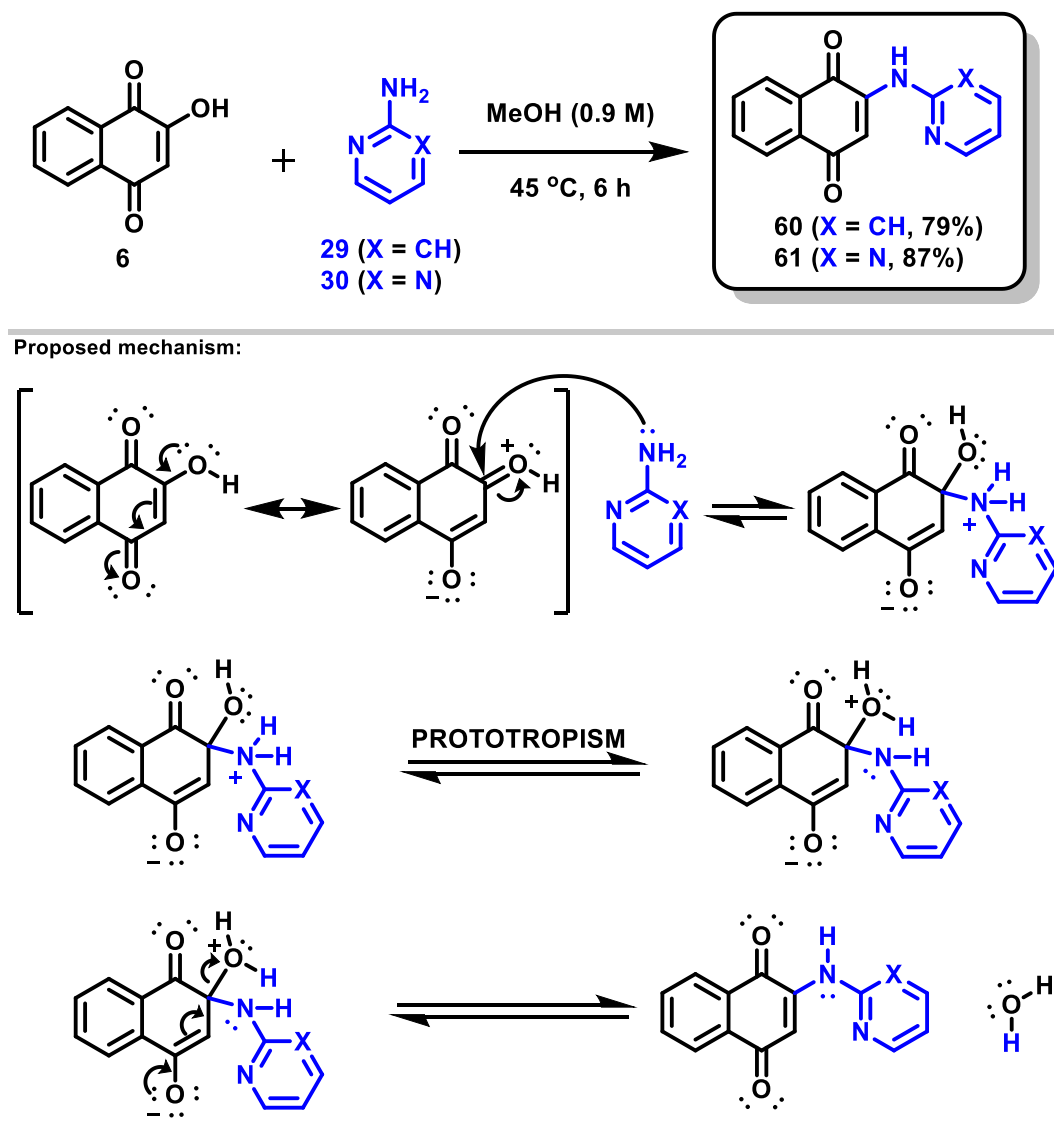
These substrates were obtained according to a respective previously published procedure, with exception of the substrates 1,4-naphthoquinone (**5**) and lawsone (**6**), which are commercially available. The pyridinic and pyrimidinic products were obtained separately, using a different strategy.

#### 3.3.1. Synthesis of compounds **60** and **61**

The compounds **60** and **61** were obtained according to a procedure already published in the literature.<sup>82</sup> This synthesis starts from lawsone (**6**) in methanol. For this reaction to happen, it is not necessary any base or acid auxiliary, since the lone pair of electrons from the amino group present in compounds **30** and **29** directly attacks the carbon bearing the most positive partial charge. It is basically a nucleophilic substitution in which the hydroxy portion gets substituted by the amine portion, mediated by a prototropism step. A subsequent elimination of water leads to the obtention of the desired product. The desired compound **60** was achieved in 79% while compound **61** was obtained in 87% yield (**Scheme 10**).

---

<sup>82</sup> Chioma, F.; Ekennia, A. C.; Ibeji, C. U.; Okafor, S. N.; Onwudiwe, D. C.; Osowole, A. A.; Ujam, O. T. *J. Mol. Struct.*, **2018**, *1163*, 455-464.



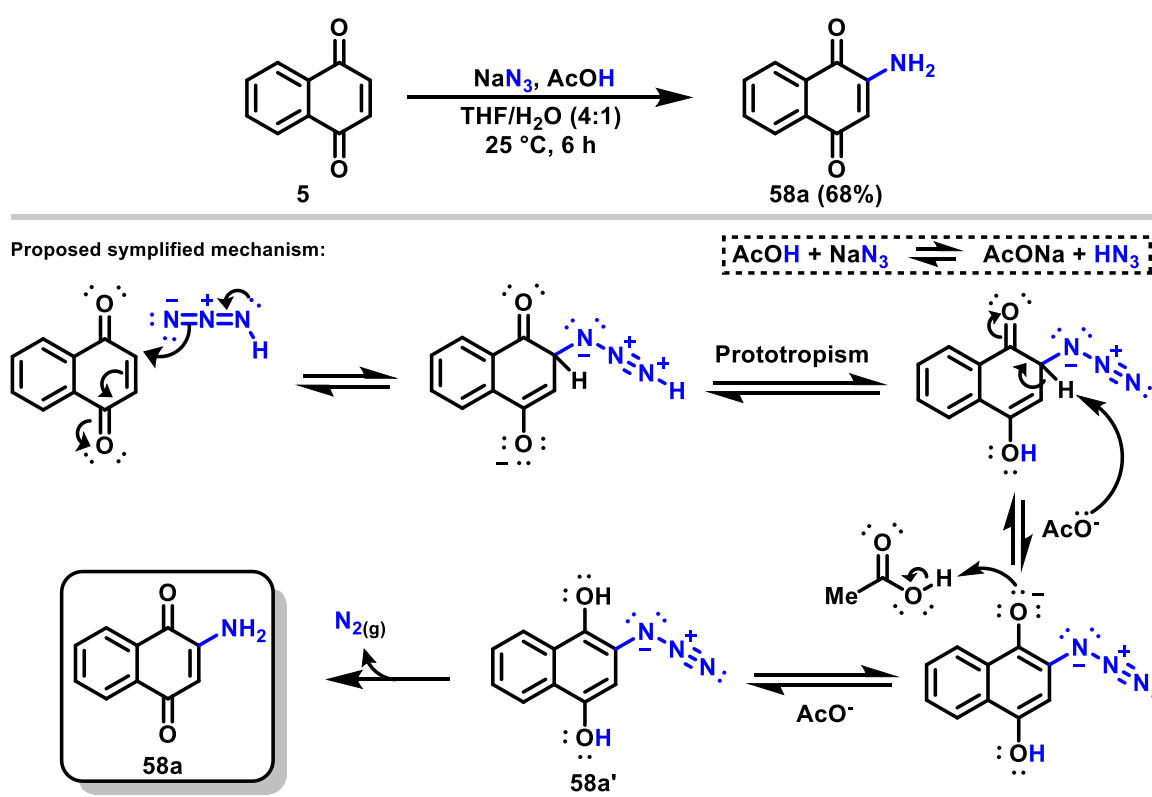
**Scheme 10.** Aryl-amination process towards compounds **60** and **61**, and proposed mechanism.

### 3.3.2. Synthesis of the substrates **58a** and **59a**

The amination reaction was performed based on a previous work published by Xuejun Wen and James Chou.<sup>83</sup> It occurs on the C-2 position of the 1,4-naphthoquinone (**5**) in the presence of sodium azide and acetic acid. The proposed mechanism involved in this reaction (**Scheme 11**) does not start directly with the sodium azide, but the hydrazoic acid (HN<sub>3</sub>) instead, which can be previously obtained with the reaction between sodium azide and acetic acid. Once the hydrazoic acid is obtained, it can then be added to the C-2 position of the substrate,

<sup>83</sup> Josey, B. J.; Inks, E. S.; Wen, X.; Chou, C. J. *J. Med. Chem.*, **2013**, *56*, 1007-1022.

generating the intermediate azidohydronaphthoquinone (**58a'**). The latter can then suffer either intra or intermolecular reduction-oxidation, generating the desired amine **58a**, and nitrogen gas, the main force pushing the equilibrium towards the product formation. The residual acid may protonate the amine on the product, so a treatment with NaOH 1 M is necessary to both destroy the excess of acetic acid (keeping it on the aqueous phase) and deprotonate any protonated amine (keeping it on the organic phase). After a complete work-up of the reaction, involving a column chromatography (in hexane 1:1 ethyl acetate), the desired product **58a** was achieved as an orange solid in 68% yield (**Scheme 11**).

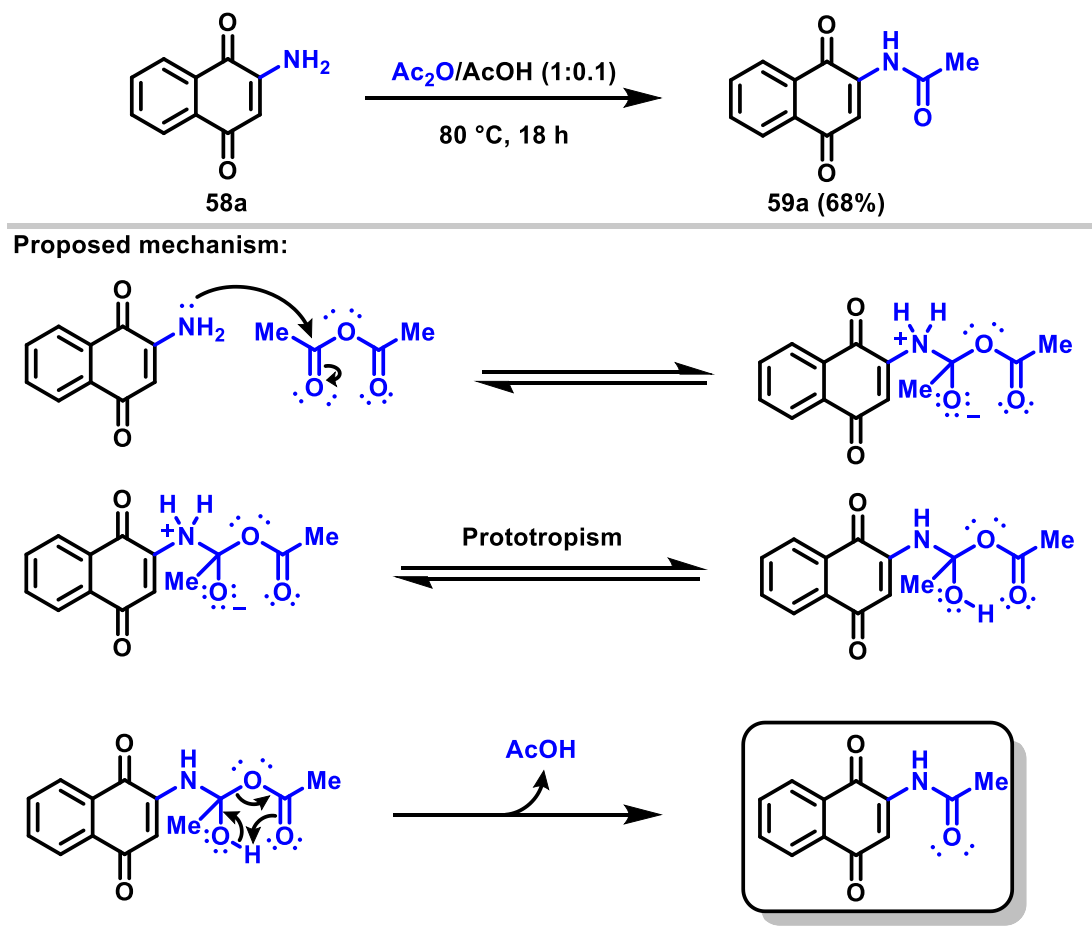


**Scheme 11.** Amination process towards compound **58a** and proposed simplified mechanism.

The subsequential acetylation is a classic reaction using acetic anhydride under heat, catalyzed by acetic acid, as described in the proposed mechanism (**Scheme 12**). Based on a previous work,<sup>84</sup> the acetylated product (**59a**) was obtained as a crystalline yellow solid in 68% yield. The work-up of this reaction is very simple, since the product precipitates after the reaction is completed. This precipitation process can be performed under room temperature, but

<sup>84</sup> Fieser, L. F.; Hartwell, J. L. *J. Am. Chem. Soc.*, **1935**, *57*, 1482-1484.

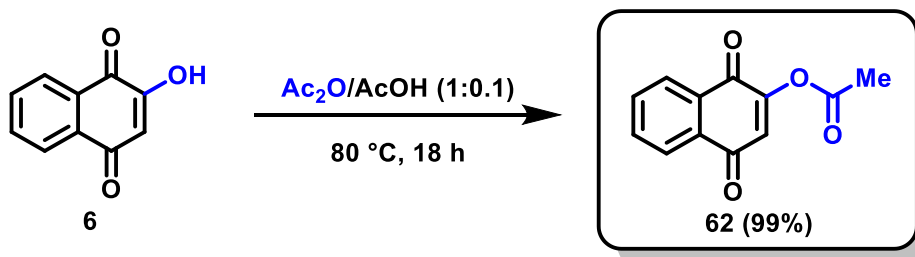
after several trials, it was observed that decreasing the temperature until around  $-22\text{ }^{\circ}\text{C}$ , delivers more crystalline products in better yields.



**Scheme 12.** Acetylation process towards compound **59a** and proposed mechanism.

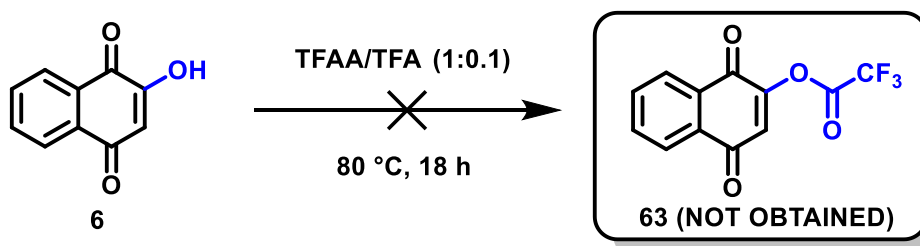
### 3.3.3. Other acylation procedures

The compound **62** was obtained by using the same acetylation procedure previously described for the obtention of compound **59a**, starting from compound **6**. The only observed difference was that the final product did not simply precipitate after the completion of the reaction. Therefore, a continuous flow of air inside the fume hood was applied to remove the excess of solvent. This process led to the successful obtention of compound **62** as a pure and crystalline yellow solid in 99% yield (**Scheme 13**).



**Scheme 13.** Acetylation process towards compound **62**.

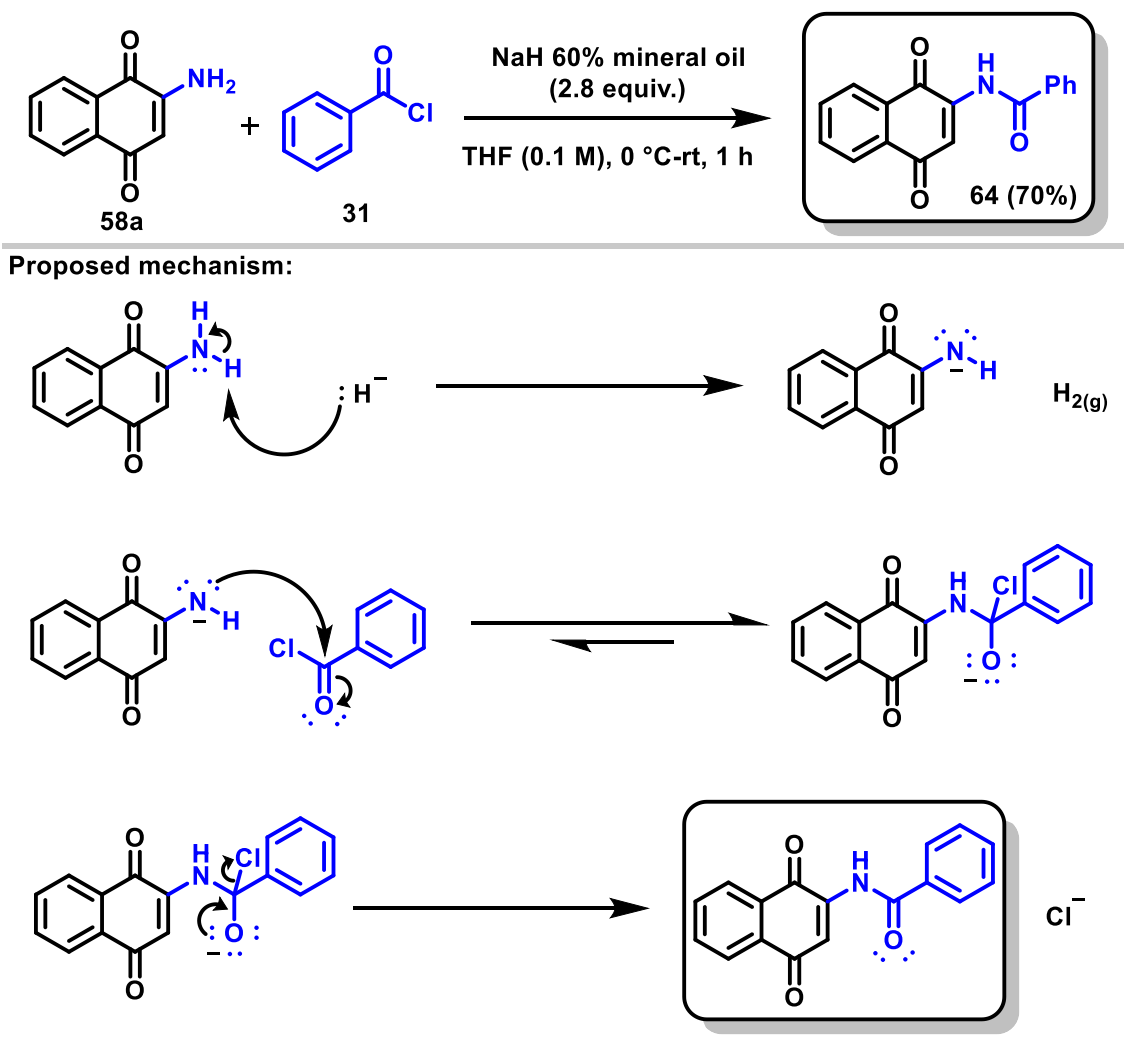
Following this same idea, the substitution of acetic acid and acetic anhydride to trifluoroacetic acid (TFA) and trifluoroacetic anhydride (TFAA) was tried aiming at the formation of the compound **63** (**Scheme 14**). However, it did not work as expected, from which procedure, only the substrate was observed even after an overnight reaction.



**Scheme 14.** Acetylation process towards compound **63**.

An acylation reaction was performed to the obtention of the compound **64**, adapted from a procedure already described in literature.<sup>85</sup> In this case, a first step requires a slow addition of sodium hydride to a solution of the amine **58a**. This step must be done slowly, due to the large releasing of hydrogen gas, originated from the reaction between the hydride and the hydrogen atom of the amino group, generating a dark blue amide solution. A second step is a nucleophilic substitution using benzoyl chloride. This step is usually quick and considerably exothermic; therefore, an iced bath is required to keep control over the reaction course. The desired product was obtained as an orange solid, in 70% yield (**Scheme 15**).

<sup>85</sup> Yin, J.; Rainier, J. D. *Tetrahedron Lett.*, **2020**, *61*, 151800.



**Scheme 15.** Acylation process towards compound **64** and proposed mechanism.

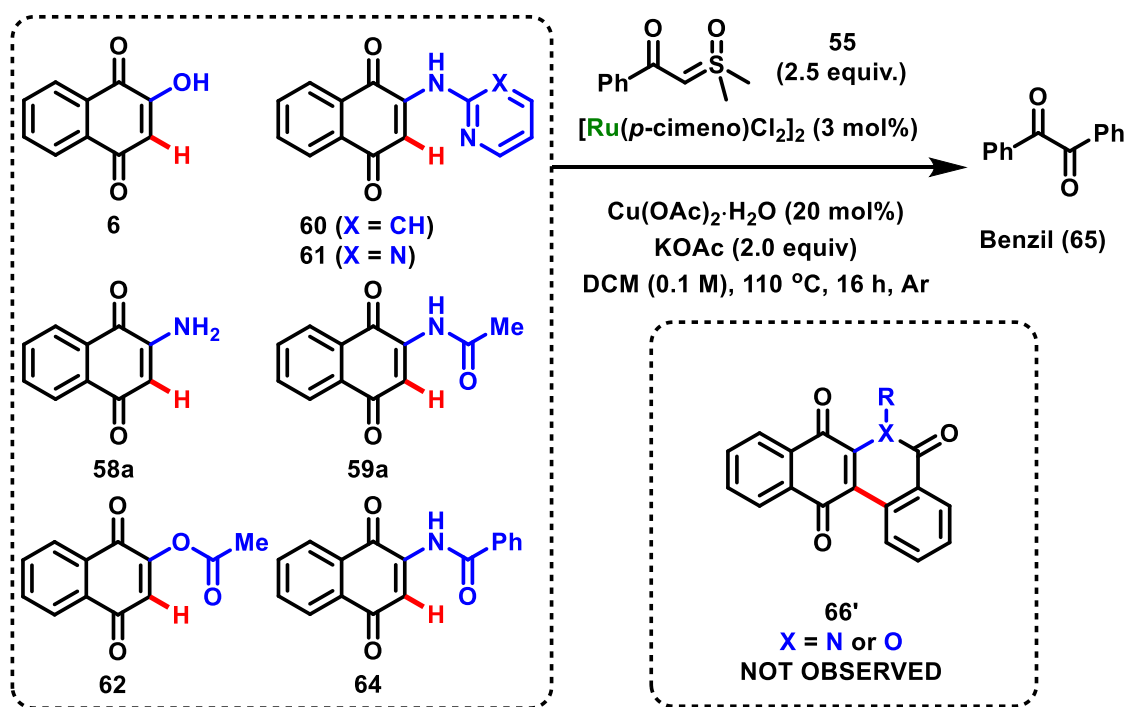
### 3.4. C–H annulation trials on naphthoquinones bearing an additional DG at the C-2 position

Once all substrates were obtained and completely characterized, the C–H annulation chemistry previously described using sulfoxonium ylide (**55**) was used as standard (**Scheme 16**). In every single case, the only observed product was still benzil (compound **65**).

At this point, the best strategy would be to change the coupling partner. Based on what has been observed in the literature, another very promising annulating agent would be diphenylacetylene (**56a**), a symmetrical internal diphenyl alkyne with an extended  $\pi$  system strong enough to interact with the metalcentre of the ruthenium-catalyst.<sup>86</sup> The first C–H

<sup>86</sup> Duarah, G.; Kaishap, P. P.; Begum, T.; Gogoi, S. *Adv. Synth. Catal.*, **2019**, *361*, 645-672.

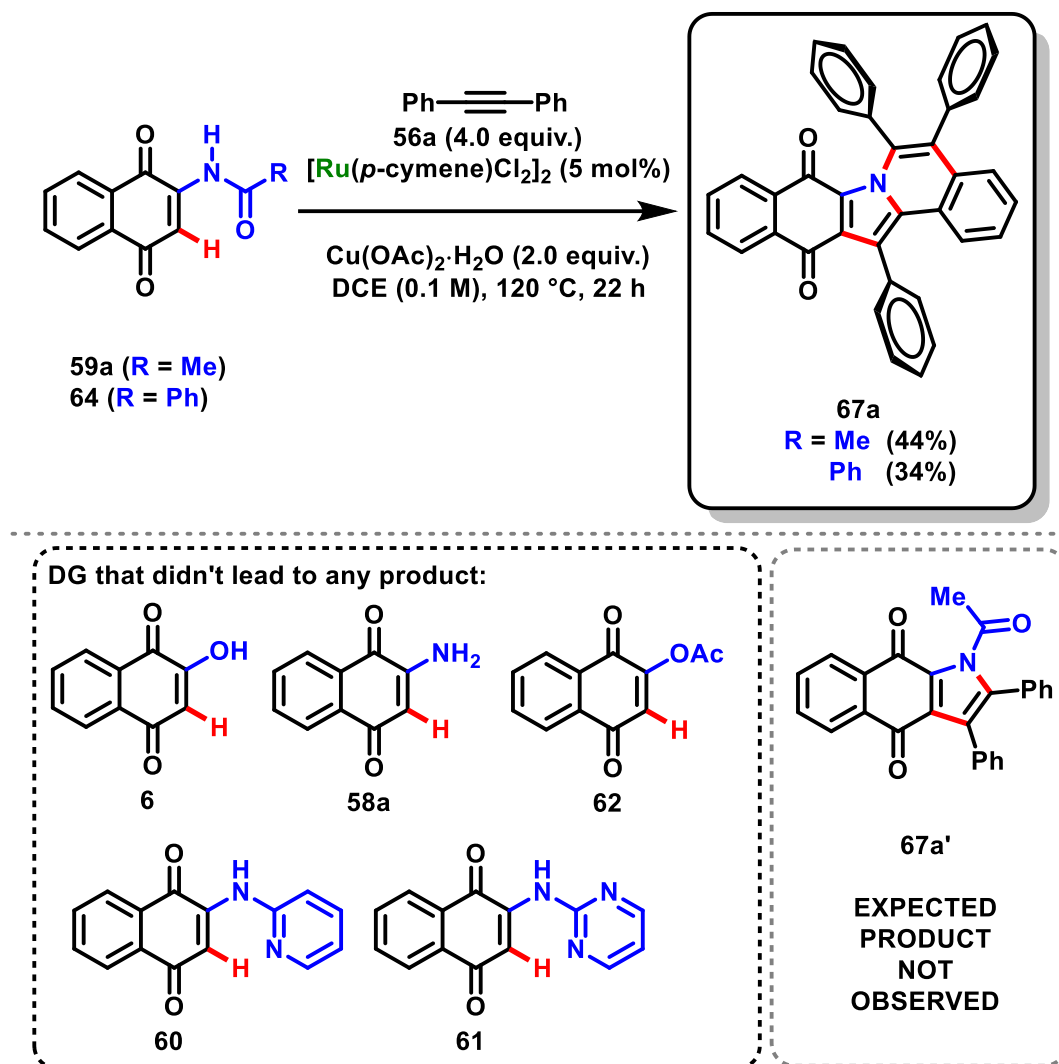
annulation experiment was adapted from a procedure published by Ackermann and co-workers,<sup>78a</sup> using the same C-2 substituted substrates previously described (from **Scheme 16**) and the simplest internal alkyne (diphenylacetylene, compound **56a**), in the presence of 5.0 mol %  $[\text{Ru}(p\text{-cymene})\text{Cl}_2]_2$  as catalyst, 2.0 equivalents of  $\text{Cu}(\text{OAc})_2 \cdot \text{H}_2\text{O}$  as oxidant, and using 1,2-dichloroethane as solvent, at 120 °C for 22 h, under nitrogen atmosphere.



**Scheme 16.** C–H annulation trial using substrates with synthesizable DG and sulfoxonium ylide **55**.

Based on the observed products described by Ackermann and co-workers,<sup>78a</sup> a single C–H annulation reaction was expected to happen, leading to the idealized compound **67a'**. However, after careful analysis, a surprisingly distinct product was obtained. From the first trials, an intriguing double-annulated compound (**67a**) could be successfully achieved, in which four new bonds were made in a single step: two C–N bonds and two C–C bonds (**Scheme 17**). Thus, further experiments were conducted *via* modifications of parameters such as solvent, temperature and catalyst load, aiming at the optimization of the procedure and preparation of the compound in better yields.

<sup>78</sup> (a) Wang, L.; Ackermann, L. *Org. Lett.*, **2013**, *15*, 176-179



**Scheme 17.** First C–H double annulation trials on substrates with synthesizable DG and alkyne **56a**.

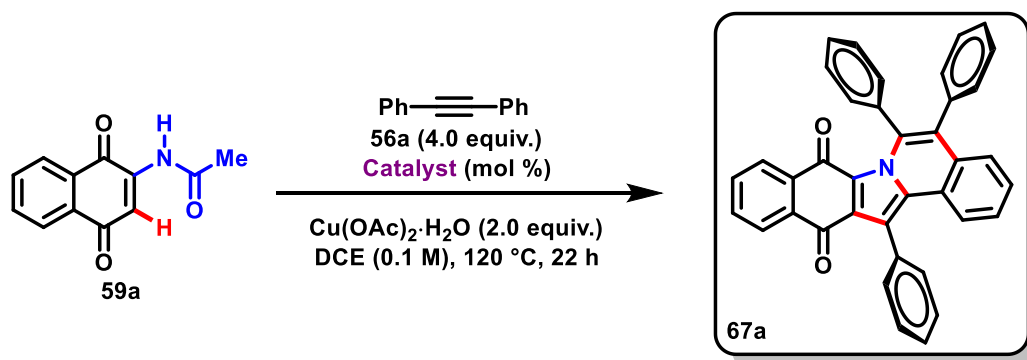
This observed amazing result turned this reaction into the main project of this research, which are further explored and described in the following sections. Therefore, all efforts were concentrated to develop these results into a plausible scientific production.



### 3.5. Optimization of the method

The first optimization parameter to be tested is the catalyst itself, since different catalysts can either improve the reaction or deliver distinct products.<sup>87</sup> Therefore, several commercially available or pre-synthesized<sup>88</sup> ruthenium catalysts (**Scheme 18**), with various ligands (**Table 3**, entries 1-9), as well as different metals (**Table 3**, entries 10-12) were tried. This study led us to conclude that  $[\text{Ru}(p\text{-cymene})\text{Cl}_2]_2$  is indeed the best catalyst to be used in this double-annulation procedure.

**Table 3.** Catalyst optimization for the double-annulation of the compound **59a**.



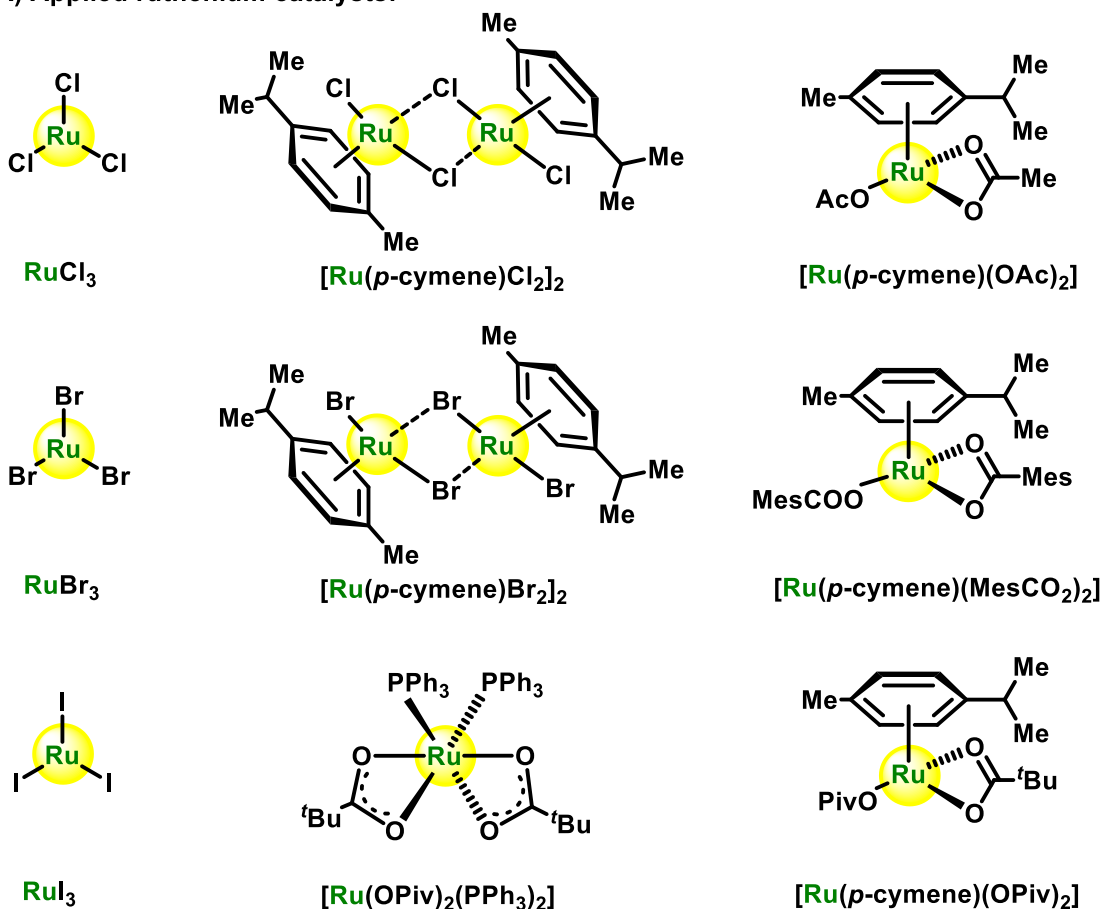
Entry	Ruthenium source	mol %	Yield (%)
1	$\text{RuCl}_3$	10.0	N.R.
2	$\text{RuBr}_3$	10.0	N.R.
3	$\text{RuI}_3$	10.0	N.R.
4	$[\text{Ru}(p\text{-cymene})\text{Cl}_2]_2$	5.0	44
5	$[\text{Ru}(p\text{-cymene})\text{Br}_2]_2$	5.0	19
6	$[\text{Ru}(p\text{-cymene})(\text{AcO})_2]$	10.0	13
7	$[\text{Ru}(p\text{-cymene})(\text{MesCO}_2)_2]$	10.0	16
8	$[\text{Ru}(p\text{-cymene})(\text{PivO})_2]$	10.0	15
9	$[\text{Ru}(\text{PivO})_2(\text{PPh}_3)_2]$	10.0	N.R.
10	$[\text{RhCp}^*\text{Cl}_2]_2$	5.0	25
11	$[\text{IrCp}^*\text{Cl}_2]_2$	5.0	N.R.
12	$[\text{CoCp}^*(\text{CO})\text{I}_2]_2$	5.0	N.R.

N.R. = No Reaction.

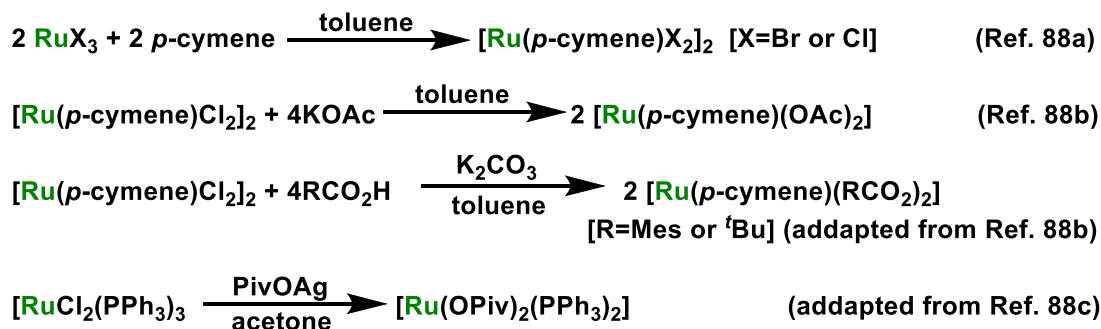
<sup>87</sup> Wang, Y.; Zhu, S.; Zou, L.-H. *Eur. J. Org. Chem.*, **2019**, 2019, 2179–2201.

<sup>88</sup> (a) Bennet, M. A.; Huang, T.-N.; Matheson, T. W.; Smith, A. K. *Inorg. Synth.*, **2007**, 16, 74-78; (b) Lorion, M. M.; Ackermann, L. *Encycl. Reag. Org. Synth.*, **2017**, 1-3. DOI: 10.1002/047084289x.rn02097; (c) Hey, D. A.; Fischer, P. J.; Baratta, W.; Kühn, F. E. *Dalton Trans.*, **2019**, 48, 4625-4635.

A) Applied ruthenium catalysts:



B) Usual procedures for ruthenium catalysts synthesis:

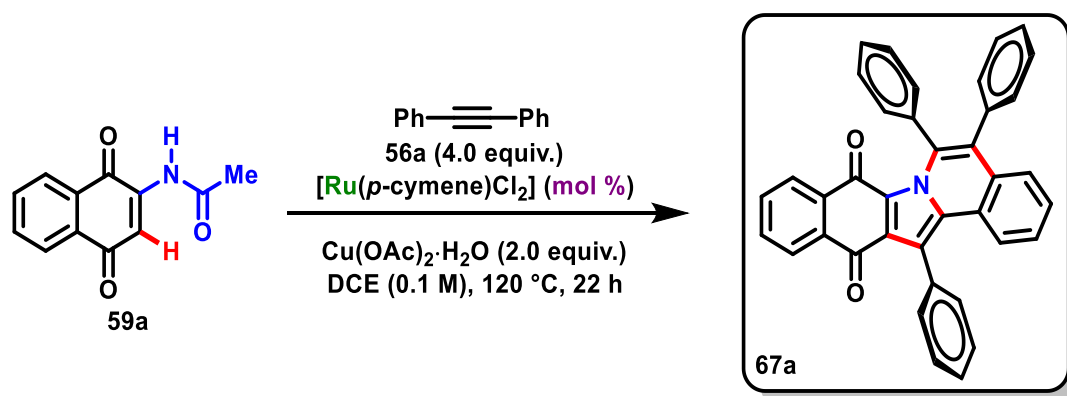


**Scheme 18.** Ruthenium catalysts used in the first double-annulation trials and their respective usual synthesis.<sup>88</sup>

The next step is to determine the best amount of catalyst to be applied. In the first scan, it was observed that a lower amount of catalyst (2.5 mol %) and a higher amount as well (10.0 mol %) delivered no good results (Table 4, entries 1 and 3 respectively). From these data, it can be inferred that the stability of the catalyst in the reactive environment might be questionable. To clarify it, a second scan took place, in which the same amount of catalyst was added in different portions to ensure that the catalyst reacts promptly before decomposing

(**Table 4**, entries 4 and 5). From this scan, it was observed that a second loading of 5.0 mol % of catalyst in 12 hours after the beginning of the reaction (1<sup>st</sup> load of 5.0 mol % at the beginning of the reaction and 2<sup>nd</sup> load of 5.0 mol % after 12 h of reaction) is the procedure that delivers the best results, with a yield of 66%. Additionally, this procedure means that a higher amount of catalyst must be used, and to avoid it for now, the remaining part of the optimization studies was developed in a single 5.0 mol % load.

**Table 4.** Catalyst loading optimization for the double-annulation of the compound **59a**.



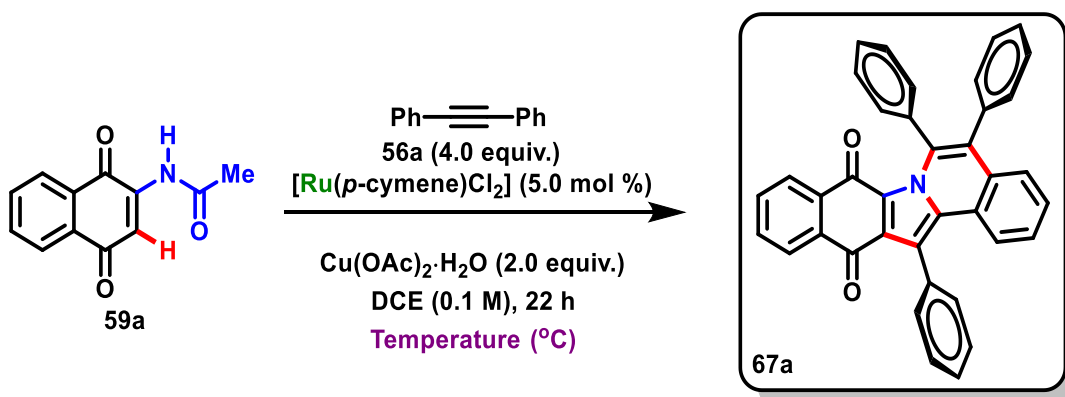
Entry	$[\text{Ru}(p\text{-cymene})\text{Cl}_2]_2$ (mol %)	Yield (%)
1	2.5	7
2	5.0	44
3	10.0	11
4	2 x 2.5*	15
5	2 x 5.0*	66

\*2<sup>nd</sup> load proceeded 12 h after the beginning of the reaction.

The next parameter to be studied was the temperature. Catalytic reactions are usually extremely sensible to the temperature,<sup>89</sup> and the same fact was observed in this work (**Table 5**). Surprisingly, 100 °C is already too low for this reaction, and at this point, no product was observed. A slight increase in the yield was observed in a higher temperature (48% at 140 °C), but this is not a safe condition to work with 1,2-dichloroethane, regarding the equipment that was available at this point of the research. Because of it, we decided to keep the 120 °C as standard temperature, which, by the way, is already higher than the boiling temperature of the solvent (83.5 °C), therefore the setting up of the reaction requires strong glassware, such as a Schlenk tube that supports higher internal pressure.

<sup>89</sup> (a) Chen, R.; Cui, S. *Org. Lett.*, **2017**, *19*, 4002-4005; (b) Zheng, L.; Hua, R. *J. Org. Chem.*, **2014**, *79*, 3930-3936.

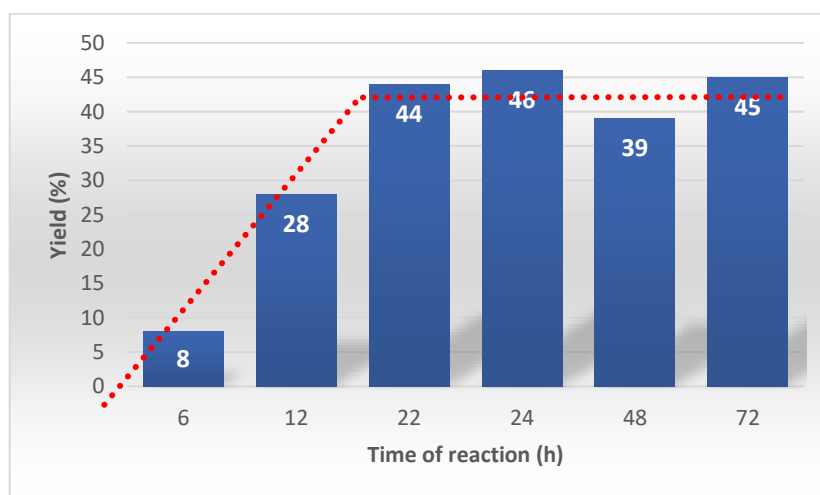
**Table 5.** Temperature optimization for the double-annulation of the compound **59a**.



Entry	Temperature ( $^{\circ}\text{C}$ )	Yield (%)
1	140	48
2	<b>120</b>	<b>44</b>
3	100	N.R.
4	60	N.R.

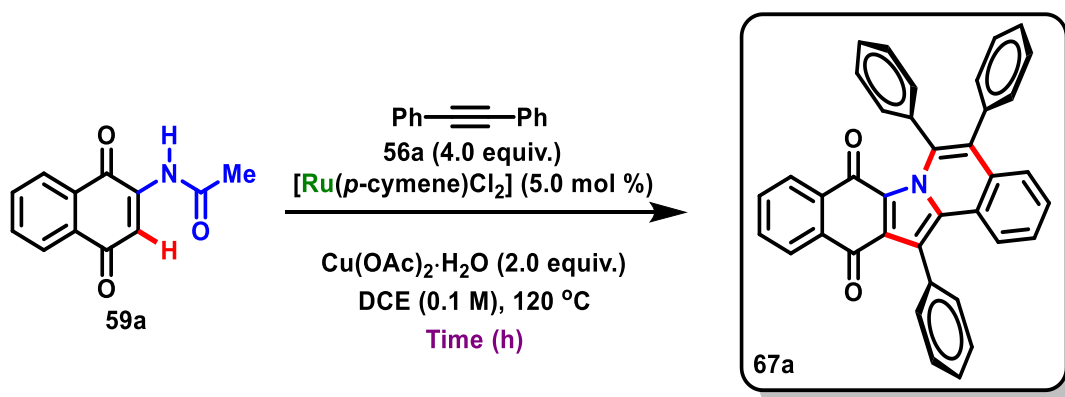
N.R. = No Reaction.

Another important studied parameter was the time of the reaction (**Table 6**). It was observed that after 24 h there is no increase in the yield (**Figure 6**), which basically means that, at around 22 to 24 h, the reaction system either reaches the maximum yield or the catalyst gets totally decomposed into a non-active species.



**Figure 6.** Achieved yield over time of reaction.

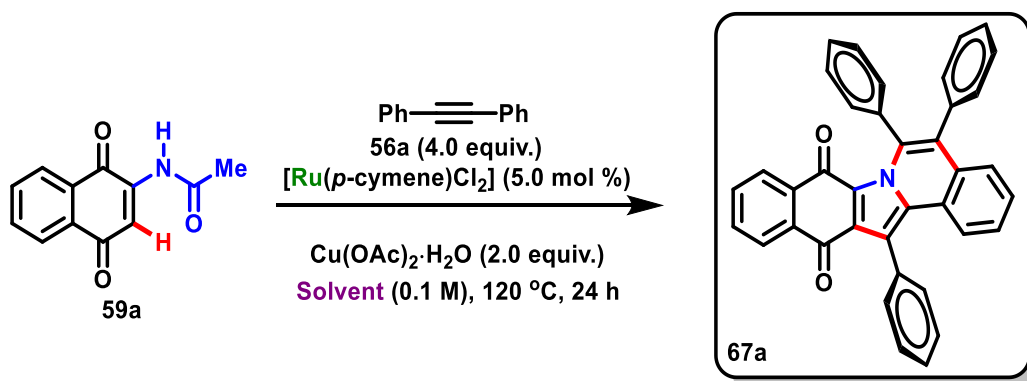
**Table 6.** Optimization of the time of reaction for the double-annulation of compound **59a**.



Entry	Time (h)	Yield (%)
1	6	8
2	12	28
3	22	44
4	24	46
5	48	39
6	72	45

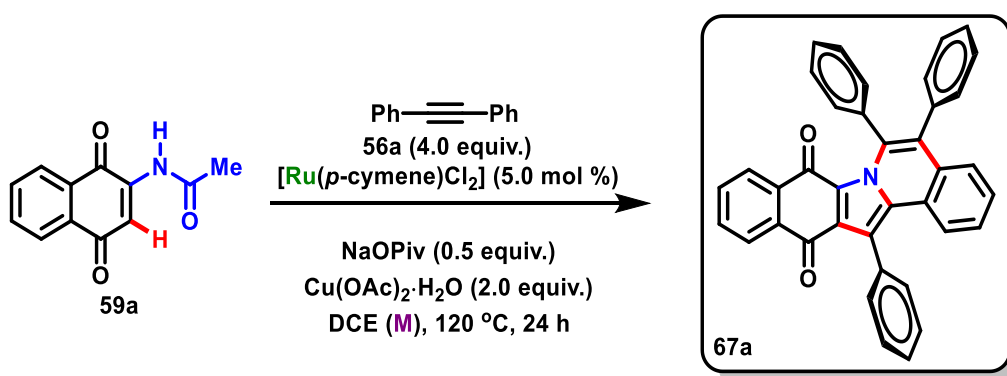
This leads to another very important parameter: the solvent (**Table 7**). Solvents with different chemical properties were tried (polar protic, polar aprotic and nonpolar) and the best observed results were obtained using 1,2-dichloroethane (46%, without additive). Considering the outcome, it is important to verify what would be the best volume of solvent to be used (**Table 8**). This study was completed later in the research process, but from this data, we could clearly observe that 2.0 mL of 1,2-dichloroethane for a 0.2 mmol scale of substrate (100 mM) resulted in the maximum yield (63%, using NaOPiv as additive, which will be discussed later).

**Table 7.** Solvent optimization for the double-annulation of the compound **59a**.



Entry	Solvent (2.0 mL)	Yield (%)
<b>1</b>	<b>1,2-Dichloroethane (DCE)</b>	<b>46</b>
2	2-Methyl-2-butanol	16
3	<i>N,N</i> -Dimethylacetylene (DMA)	6
4	<i>N,N</i> -Dimethylformamide (DMF)	16
5	<i>N</i> -methylpyrrolidone (NMP)	27
6	Toluene	12
7	Water	3
8	Dichloromethane (DCM)	9
9	Chloroform	12
10	1,4-Dioxane	8
11	Xylene	16

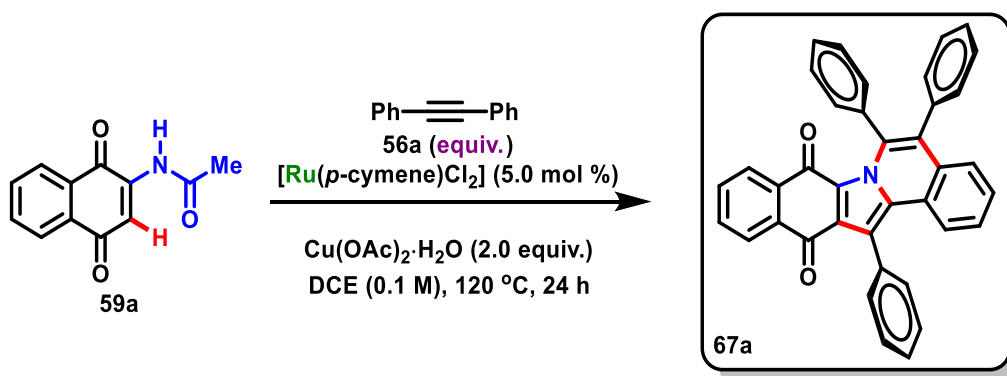
**Table 8.** Optimization of the applied solvent volume.



Entry	DCE volume (mL)	Yield (%)
1	1.0	28
2	1.5	53
<b>3</b>	<b>2.0</b>	<b>63</b>
4	2.5	52
5	3.0	48

The logical sequence now is to verify the right combination between the reactants to find the best equivalency. For that, different equivalents of diphenylacetylene were tried (**Table 9**). The best yield was obtained when 6.0 equivalents of diphenylacetylene was used (49%), but this condition represents a low economy of reactants, and since only one test was performed, there is not enough statistic data to indicate that this difference significates an actual increase of the yield. Therefore, 4.0 equivalents of diphenylacetylene were kept as the standard amount.

**Table 9.** Optimization process for the applied amount of alkyne.

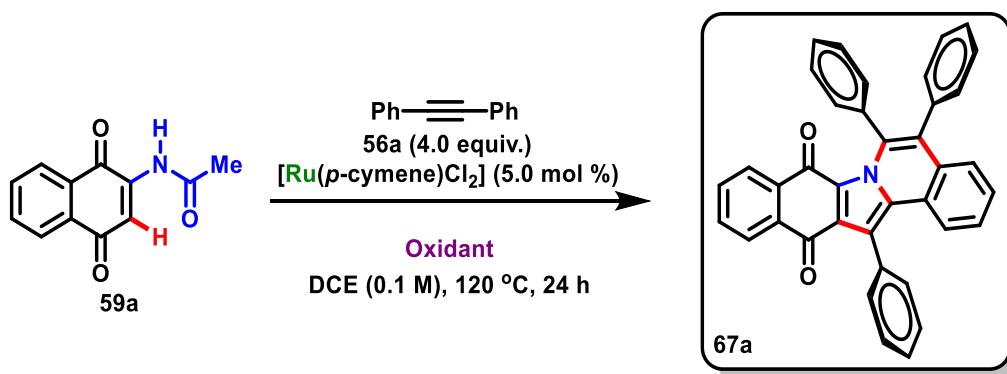


Entry	Diphenylacetylene 18a (equiv.)	Yield (%)
1	2.0	29
2	3.0	33
3	4.0	46
4	5.0	42
5	6.0	49

The amount and chemical nature of the oxidant can be the key to avoid a quick decomposition of the catalyst.<sup>90</sup> For this study, three different Cu<sup>II</sup> sources were tried as oxidants: Cu(OAc)<sub>2</sub>·H<sub>2</sub>O, Cu(CO<sub>2</sub>CF<sub>3</sub>)<sub>2</sub> and CuCl<sub>2</sub> (**Table 10**, entries 1, 2 and 3, respectively), all of them used in 2.0 equivalents. Amongst those, only Cu(OAc)<sub>2</sub>·H<sub>2</sub>O led to the formation of the desired product (46%). A higher amount of oxidant (4.0 equiv.) did not result in a better yield (27%, using NaOPiv as additive, which will be discussed later) as much as the outcome achieved using 2.0 equivalents (**Table 10**, entries 4 and 5), which indicates that the same necessary oxidant to perform the reaction might be the cause of the observed catalyst decomposition.

<sup>90</sup> (a) Wu, B.; Gao, X.; Yan, Z.; Chen, M.-W.; Zhou, Y.-G. *Org. Lett.*, **2015**, *17*, 6134-6137; (b) Ma, W.; Weng, Z.; Fang, X.; Gu, L.; Song, Y.; Ackermann, L. *Eur. J. Org. Chem.*, **2019**, *2019*, 41-45.

**Table 10.** Oxidant optimization for the double-annulation of the compound **59a**.



Entry	Oxidant	equiv.	Additive (equiv.)	Yield (%)
1	Cu(OAc) <sub>2</sub> ·H <sub>2</sub> O	2.0	-	46
2	Cu(CF <sub>3</sub> CO <sub>2</sub> ) <sub>2</sub>	2.0	-	N.R.
3	CuCl <sub>2</sub>	2.0	-	N.R.
4	<b>Cu(OAc)<sub>2</sub>·H<sub>2</sub>O</b>	<b>2.0</b>	<b>NaOPiv (0.5)</b>	<b>63</b>
5	Cu(OAc) <sub>2</sub> ·H <sub>2</sub> O	4.0	NaOPiv (0.5)	27

N.R. = No Reaction.

As mentioned before, the use of an additive can be a good strategy to improve the performance of the catalyst, since it helps the proximation between the catalyst and the substrates, making it easier for the C–H activation to happen.<sup>91</sup> For this study six potential additives, already known to be useful for ruthenium catalysis,<sup>92</sup> were scanned on 0.2 equivalents (**Table 11**), and the best result was observed when using sodium pivalate, in a yield of 55%. With the best additive in hand, a quick study about the right amount of it was performed (**Table 12**), and it was observed that 0.5 equivalents of NaOPiv delivered the best possible yield of 63%. Beyond that point, the yield started to decrease, and it was no longer possible to recover the not-reacted starting material, indicating that a high excess of additive can damage the substrate.<sup>93</sup>

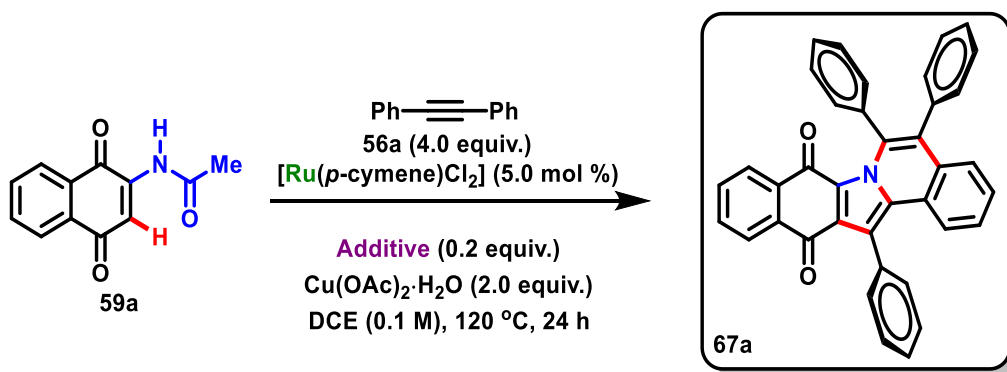
<sup>91</sup> Mukherjee, K.; Shankar, M.; Ghosh, K.; Sahoo, A. K. *Org. Lett.*, **2018**, *20*, 1914-1918.

<sup>92</sup> (a) Gandeepan, P.; Koeller, J.; Korvorapun, K.; Mohr, J.; Ackermann, L. *Angew. Chem. Int. Ed.*, **2019**, *58*, 9820-9825; (b) Yetra, S. R.; Rogge, T.; Warratz, S.; Struwe, J.; Peng, W.; Vana, P.; Ackermann, L. *Angew. Chem. Int. Ed.*, **2019**, *58*, 7490-7494; (c) Qiu Y.; Tian, C.; Massignan, L.; Rogge, T.; Ackermann, L. *Angew. Chem. Int. Ed.*, **2018**, *57*, 5818-5822; (d) Ma, W. Weng, Z.; Rogge, T.; Gu, L.; Lin, J.; Peng, A.; Luo, X.; Gou, X.; Ackermann, L. *Adv. Synth. Catal.*, **2018**, *360*, 704-710.

<sup>93</sup> (a) Rota, P.; Allevi, P.; Colombo, R.; Costa, M. L.; Anastasia, M. *Angew. Chem. Int. Ed.*, **2010**, *49*, 1850-1853; (b) Zhang, G.; Liu, C.; Yi, H.; Meng, Q.; Bian, C.; Chen, H.; Jian, J.-X.; Wu, L.-Z.; Lei, A. *J. Am. Chem. Soc.*, **2015**, *137*, 9273-9280; (c) Guilarte, V.; Castroviejo, M. P.; García-García, P.; Fernández-Rodríguez, M. A.; Sanz, R. *J. Org. Chem.*, **2011**, *76*, 3416-3437.

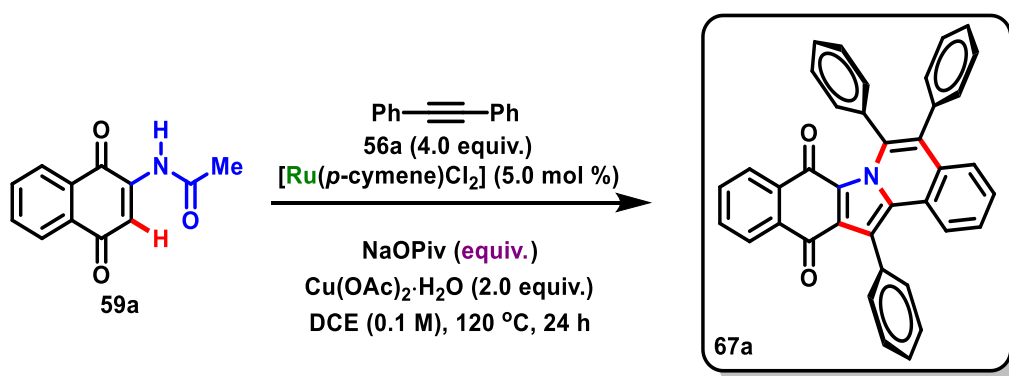


**Table 11.** Additive optimization for the double-annulation of the compound **59a**.



Entry	Additive (0.2 equiv.)	Yield (%)
1	Potassium hexafluorophosphate ( $\text{KPF}_6$ )	27
2	Cesium acetate ( $\text{CsOAc}$ )	24
3	Potassium acetate ( $\text{KOAc}$ )	50
4	Sodium acetate ( $\text{NaOAc}$ )	48
5	2,4,6-Trimethylbenzoic acid ( $\text{MesCO}_2\text{H}$ )	19
6	<b>Sodium pivalate (<math>\text{NaOPiv}</math>)</b>	<b>55</b>

**Table 12.** Optimization process for the applied amount of additive.

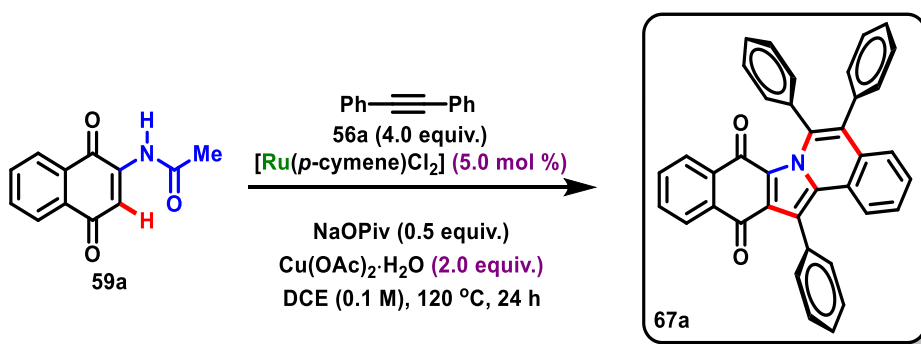


Entry	Sodium pivalate (equiv.)	Yield (%)
1	0.2	55
2	0.4	52
3	<b>0.5</b>	<b>63</b>
4	1.0	47
5	2.0	47
6	3.0	48

In the last step, this optimized method was applied, with the double load of catalyst, in which an 80% yield was observed (**Table 13**, entry 2). After this optimization, it was possible to conclude the standard conditions to be applied in the scope studies: 0.2 mmol of compound **59a**, 4.0 equivalents of compound **56a**, 2.0 equivalents of Cu(OAc)<sub>2</sub>·H<sub>2</sub>O, 0.5 equivalents of NaOPiv, single or double loading of 5.0 mol % of [Ru(*p*-cymene)Cl<sub>2</sub>]<sub>2</sub>, 2.0 mL of 1,2-dichloroethane, 120 °C for 24 h under nitrogen.

Three validation tests were also performed to evaluate the catalytical behaviour of the method: without any catalyst, without any oxidant, and under air, and no reaction was observed in any of them (**Table 13**, entries 3-5). At this point, it was possible to almost double the achieved yield from the initial 44% to 80%. That represents, beyond the numbers, a significant approach on a new double-annulation method, from which four new bonds are generated in a single-step reaction, *via* C–H activation, in a good yield.

**Table 13.** Validation tests for the double-annulation reaction of compound **59a**.



Entry	Deviation from standard procedures	[Ru( <i>p</i> -cymene)Cl <sub>2</sub> ] (mol %)	Yield (%)
1	None	5.0	63
2	None	2 x 5.0*	80
3	No catalyst	-	N.R.
4	No oxidant	5.0	N.R.
5	Under air	5.0	N.R.

N.R. = No Reaction. \*2<sup>nd</sup> load 12 h after the beginning of the reaction.

### 3.6. Scope analysis

After the optimization was completed, two methods were obtained: single and double load of the catalyst (General Procedure A and General Procedure B, respectively). The next logical step is to apply these methods on different substrates to confirm its range of applicability.

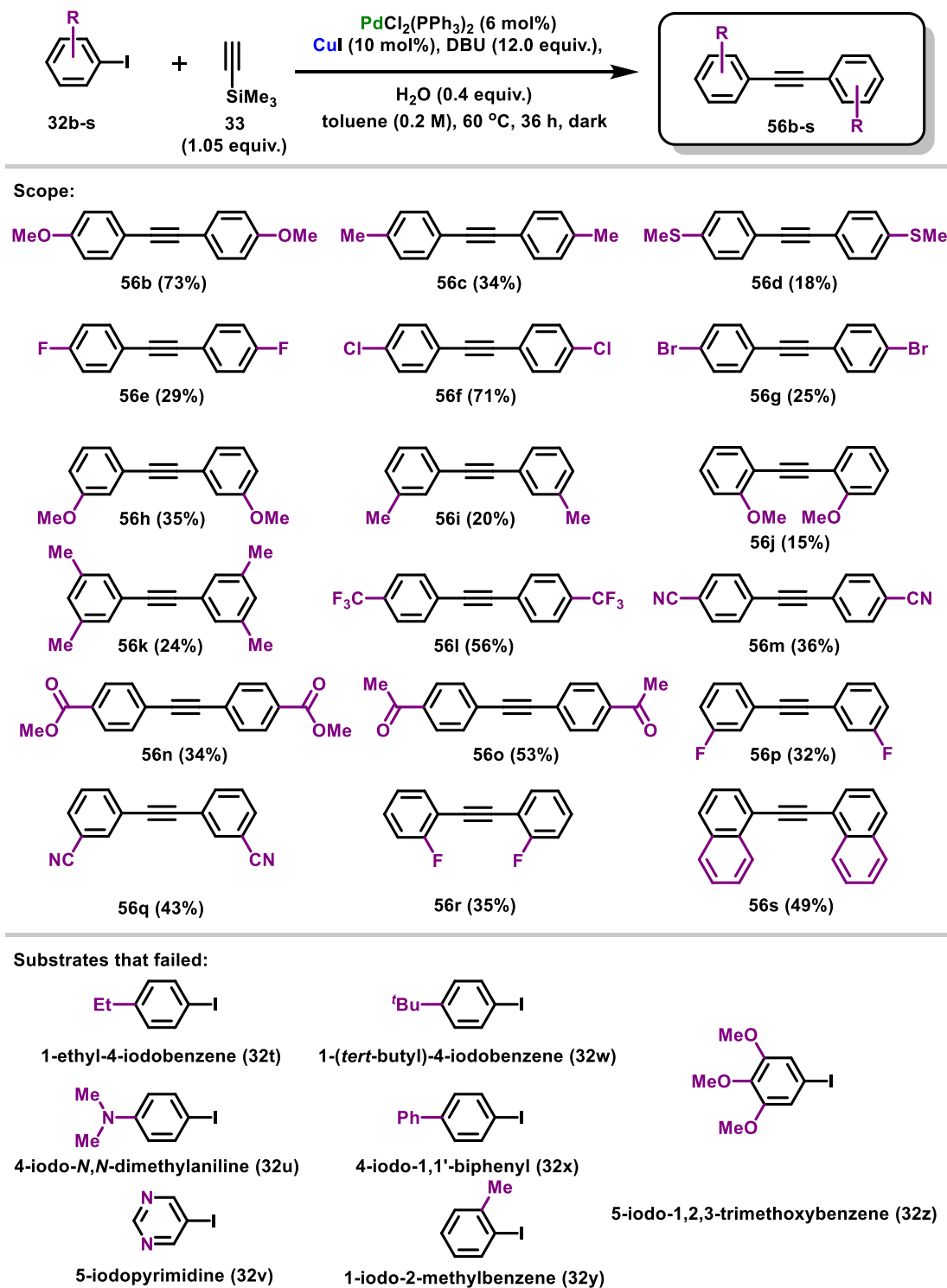
#### 3.6.1. Synthesis of substituted symmetrical internal alkynes (65b-s)

With exception of the diphenylacetylene (**56a**), a known commercially available alkyne, all the other modified symmetrical alkynes used to build the first scope were synthesized. This procedure followed a palladium/copper catalyzed Sonogashira-type reaction described by Brisbois and Grieco (2002) in the presence of iodoarenes (**32b-s**) and trimethylsilylacetylene (**33**).<sup>94</sup> From this method, eighteen internal alkynes (**56b-s**) were successfully achieved, with yields varying from 15% to 73% (**Scheme 19**); however, seven specific iodoarenes did not lead to their respective desired internal alkynes. In most of the cases, a complex mixture of products was achieved, from which it was not possible to successfully isolate the alkyne using the usual purification processes.

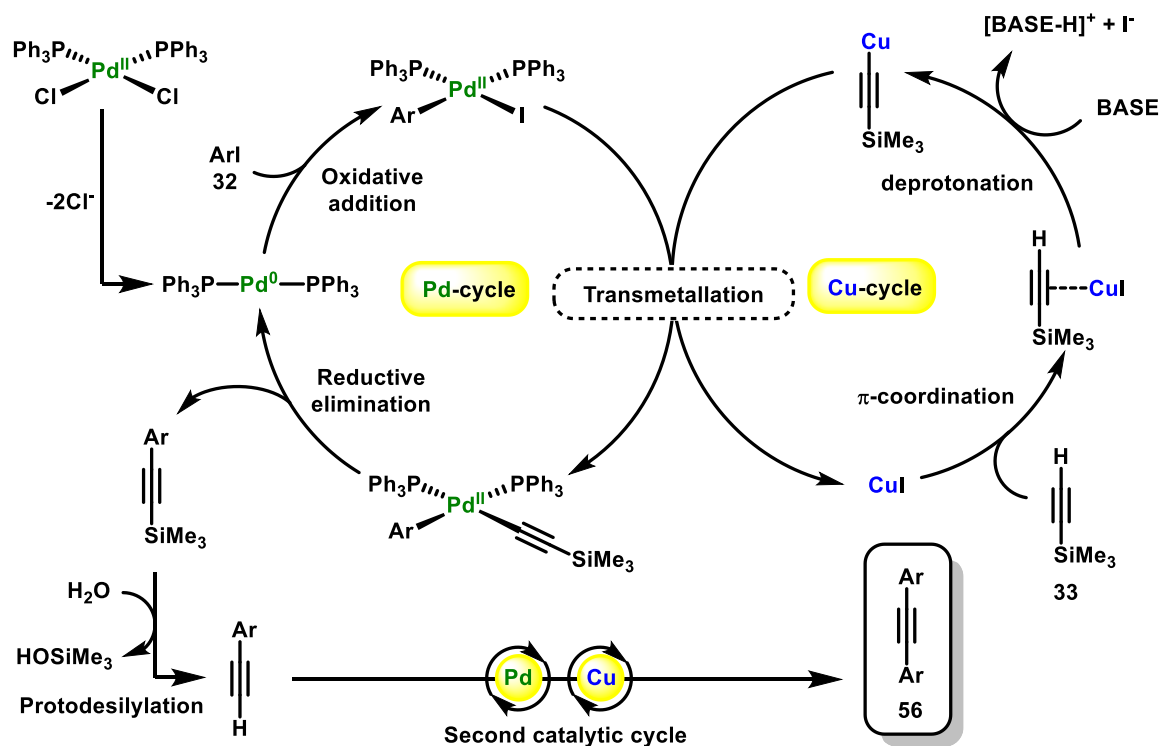
This reaction requires darkness to produce a better result, since the intermediates are photo sensible, therefore aluminum foil was applied all over the system before activating the heating source. Its mechanism can be divided by two main parts: the first catalytic cycle in which the first C–C bond is generated, and the second catalytic cycle, when the second C–C bond is achieved (**Scheme 20**). In the first catalytic cycle, a cooperative catalysis between palladium-II and copper-I leads to the intermediate, in which the protecting group TMS remains. A protodesilylation mediated by the intentionally added water and DBU leads to the formation of a new terminal alkyne. Once the new C(sp)–H bond is made, it can then undergo a second catalytic cycle, from which the final internal alkyne **56** was obtained.

---

<sup>94</sup> Mio, M. J.; Kopel, L.C.; Braun, J. B.; Gadzikwa, T. L.; Hull, K. L.; Brisbois, R. G.; Markworth, C. J.; Grieco, P. A. *Org. Lett.* **2002**, *4*, 3199-3202.



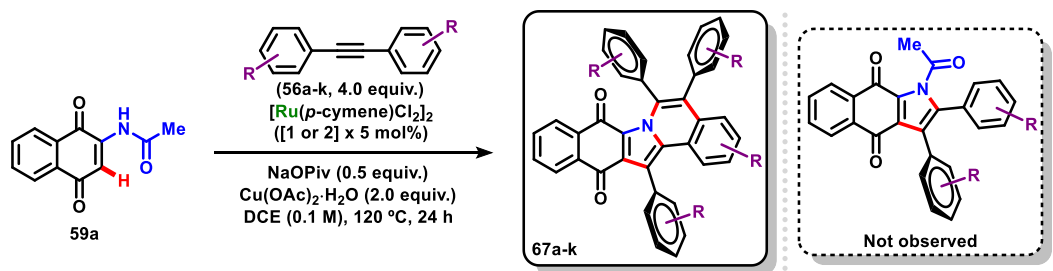
**Scheme 19.** Synthesis of symmetrical internal alkynes, obtained scope and substrates that failed the procedure.



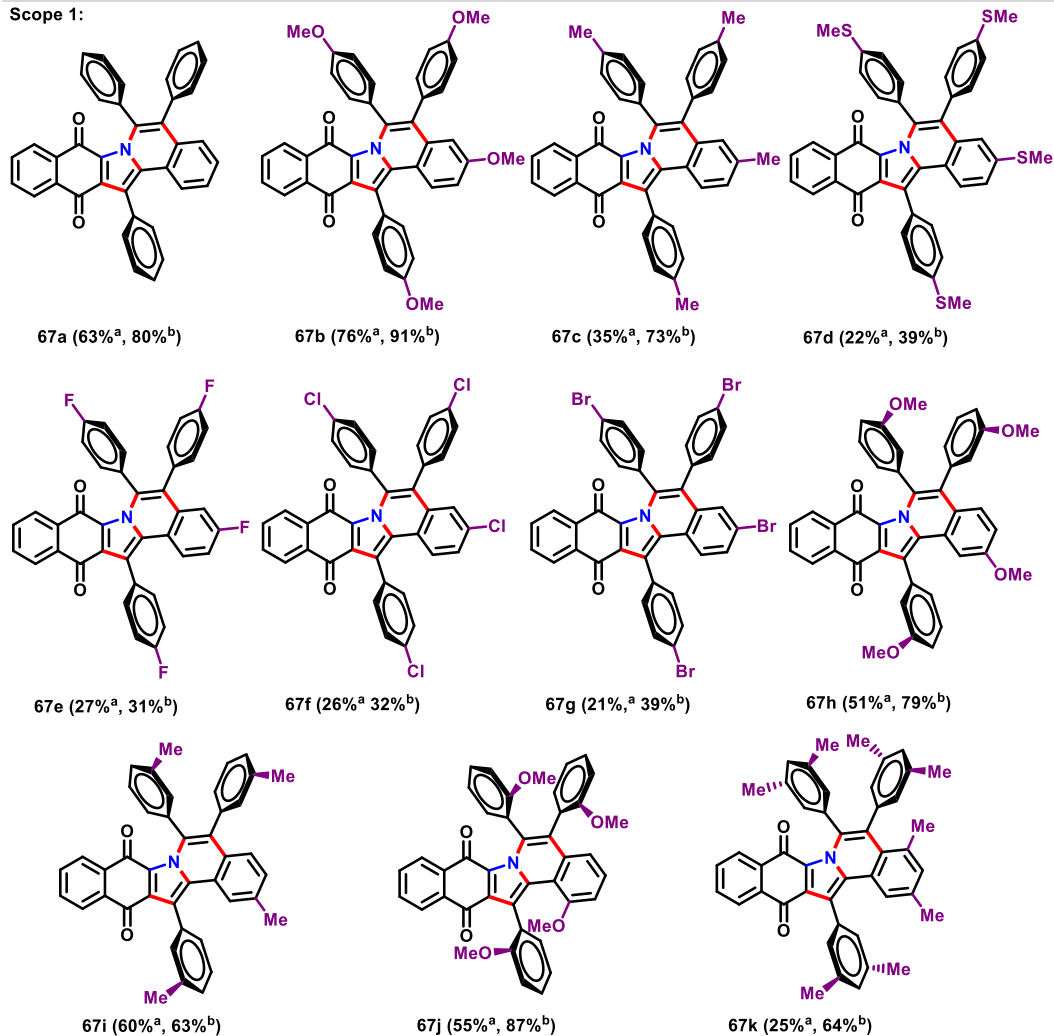
**Scheme 20.** Simplified mechanism of the Sonogashira-type reaction.

### 3.6.2. Symmetrical internal alkyne scope analysis

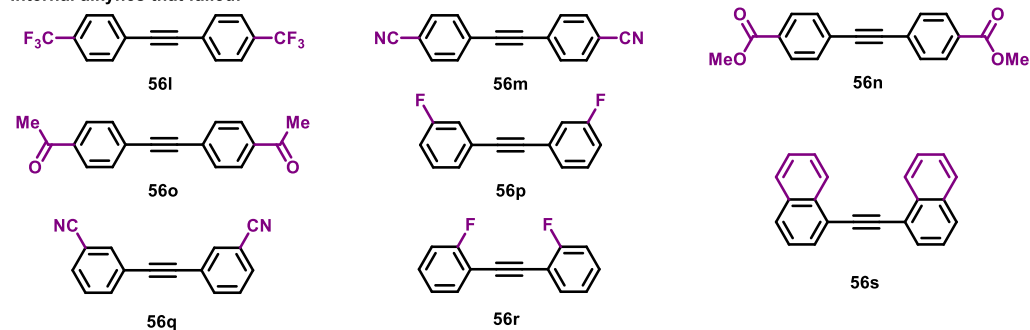
In the first scope study, the previously described symmetrical alkynes (compounds **56b-s**) containing a large variety of substituent groups, along with the commercially available alkyne **56a**, were submitted to both General Procedures A and B, using the simplest modified quinone **67a** as substrate, from which the compounds **67a-k** were successfully obtained (**Scheme 21**). In some cases, there was no considerable yield improvement between the single and double loading of catalyst (**67e-g**). On the other hand, there were some cases when an expressive difference was observed. The synthesis of compound **67c** and **67k** can be cited here as examples. In the case of the obtention of compound **67c**, the yield increased from 35% to 73%; and in the synthesis of compound **67k**, the yield increased from 25% to 64%. Some symmetrical internal alkynes containing nitrile, carbonylated groups, strongly deactivating or highly bulky substituents were tried as well but no products were observed.



Scope 1:



Internal alkynes that failed:



<sup>a</sup>General Procedure A: 1 x 5 mol% of [Ru(*p*-cymene)Cl<sub>2</sub>]<sub>2</sub>.

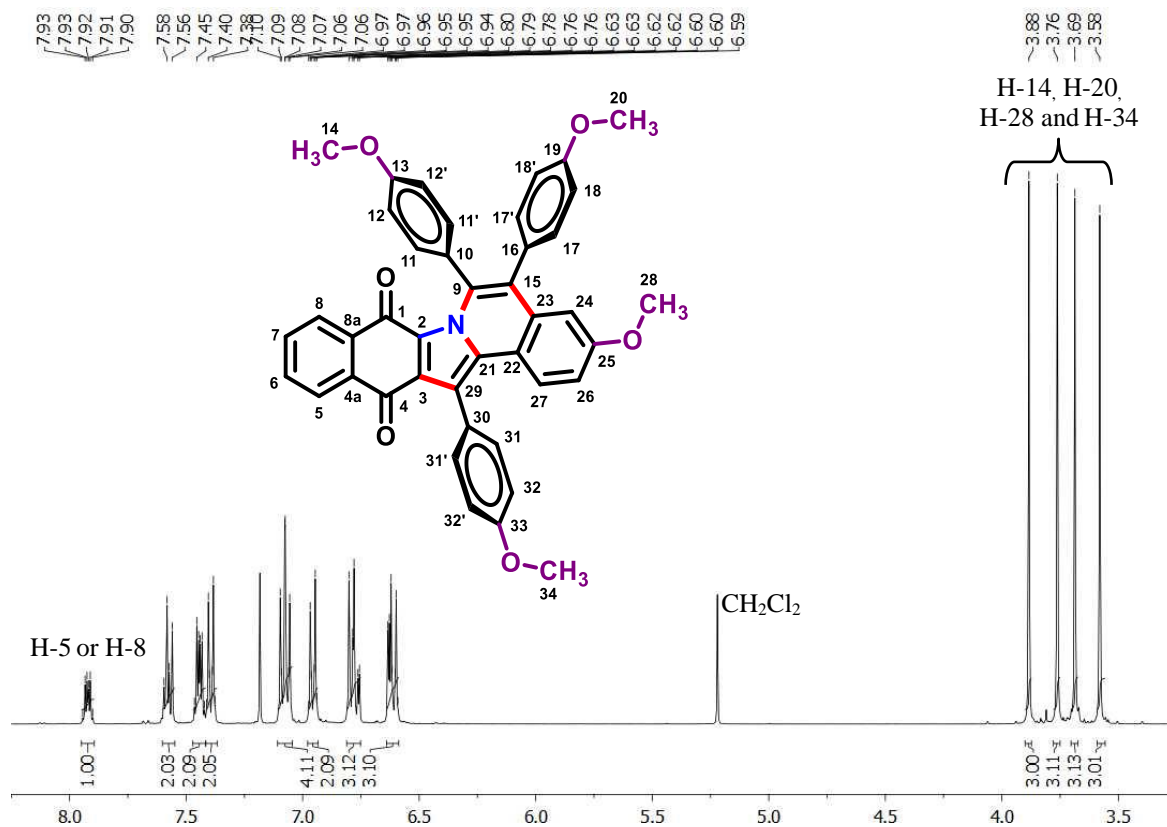
<sup>b</sup>General Procedure B: 2 x 5 mol% of [Ru(*p*-cymene)Cl<sub>2</sub>]<sub>2</sub>, 2<sup>nd</sup> load proceeded 12 h after the beginning of the reaction.

**Scheme 21.** First scope: double annulation reaction between compound **59a** and symmetrical internal alkynes **56a-k**.

After the synthesis of each double-annulated compound, a complete characterization was performed to fully identify the chemical structure of all of them, which includes  $^1\text{H}$ -NMR and  $^{13}\text{C}$ -NMR spectroscopies, COSY, HSQC, HMBC, infrared spectroscopy, high- and low-resolution mass spectrometry, melting point and, in most cases, even crystallographic data studies. The compound **67b** will be used as example for the discussion about NMR characterization due for three important aspects:

- It presented cleaner spectra due for the *para*-positioned methoxy groups, which will facilitate not only the discussion, but also the understanding of the characterization.
- When compared to the other products, it was the one achieved in the best yield (76% by General Procedure A and 91% by General Procedure B).
- Due for this good yield, the *para*-methoxy alkyne **56b** was used as standard internal alkyne in the second scope. Therefore, the compound **67b** is the link between the first and the second scope.

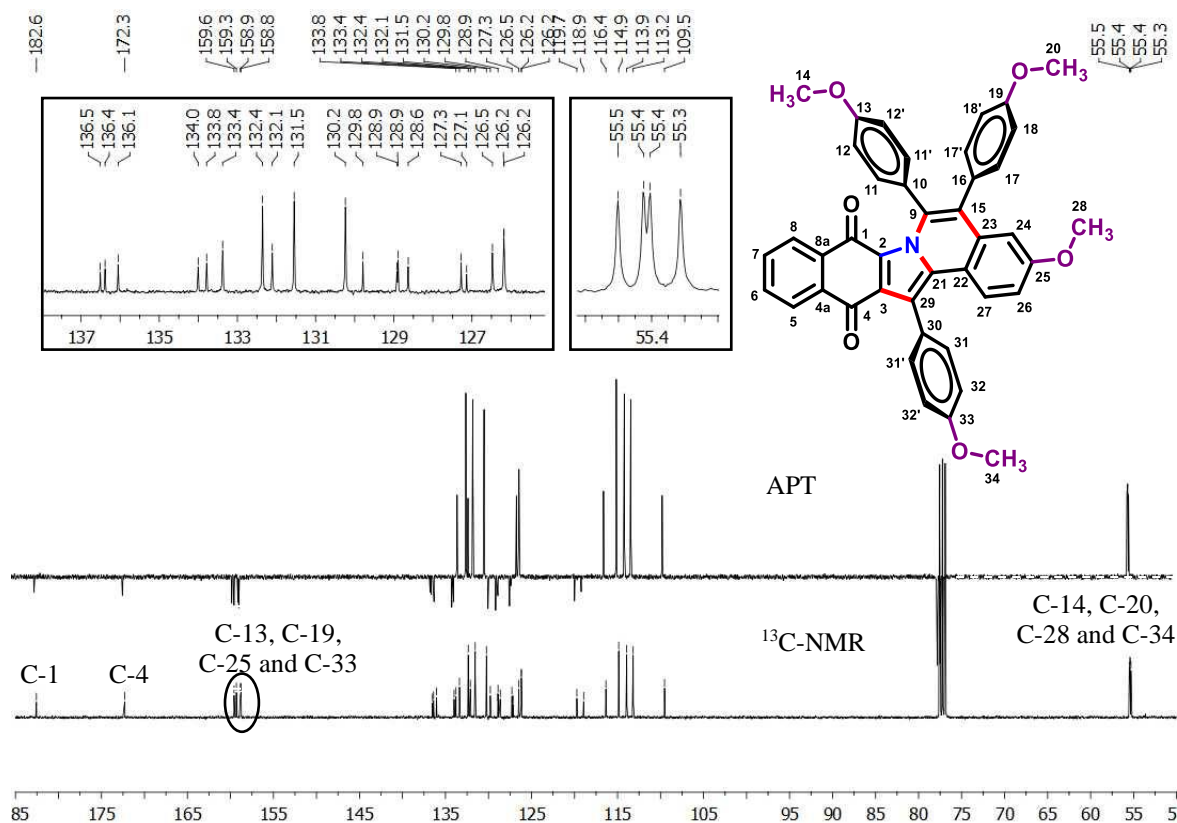
In the  $^1\text{H}$ -NMR spectrum analysis (**Figure 7**), it is possible to see all the expected four singlets, at 3.88, 3.76, 3.69 and 3.58 ppm, each one integrated to 3H, attributed to the four methoxy groups located at the positions H-14, H-20, H-28 and H-34, but it is not possible to identify which one is specifically correlated to which signal, since they are all in a similar chemical environment. All the 19 aromatic hydrogen atoms can be seen in the aromatic region of the spectrum. One aromatic signal that can be highlighted is the multiplet located at 7.93-7.90, integrated to 1H. It is the most deshielded aromatic hydrogen, which can be attributed to H-5 or H-8, the ones closer to the carbonyl groups that will strongly suffer their electronic-withdrawal inductive and resonance effects and even their diamagnetic anisotropic deshielding effect.



**Figure 7.** <sup>1</sup>H-NMR (400 MHz, CDCl<sub>3</sub>) spectrum analysis of the compound **67b**.

In the analysis of the <sup>13</sup>C-NMR and APT spectra (**Figure 8**), it is easy to identify the signals corresponding to the four methoxy carbon atoms C-14, C-20, C-28 and C-34, located at 55.5, 55.4, 55.4 and 55.3 ppm. However, it is also not possible to attribute each one of them to its specific signal. The same aspect happens to the four aromatic carbons directly attached to these methoxy groups (C-13, C-19, C-25 and C-33). They are not hydrogenated and are considerably deshielded *via* inductive effects. These facts led their attribution to the signals at 159.6, 159.3, 158.9, 158.8 ppm. Other two very important carbon atoms to be discussed are the ones from the carbonyl groups located at C-1 and C-4. The position of the nitrogen atom makes the electronic density over the carbon C-4 get slightly higher than the C-1 due to resonance and inductive effects, making it more shielded. Therefore, it is possible to assume that the signal from 182.6 ppm can be attributed to the carbon at the C-1 position, while the one at 172.3 is related to the carbon located at the C-4 position.

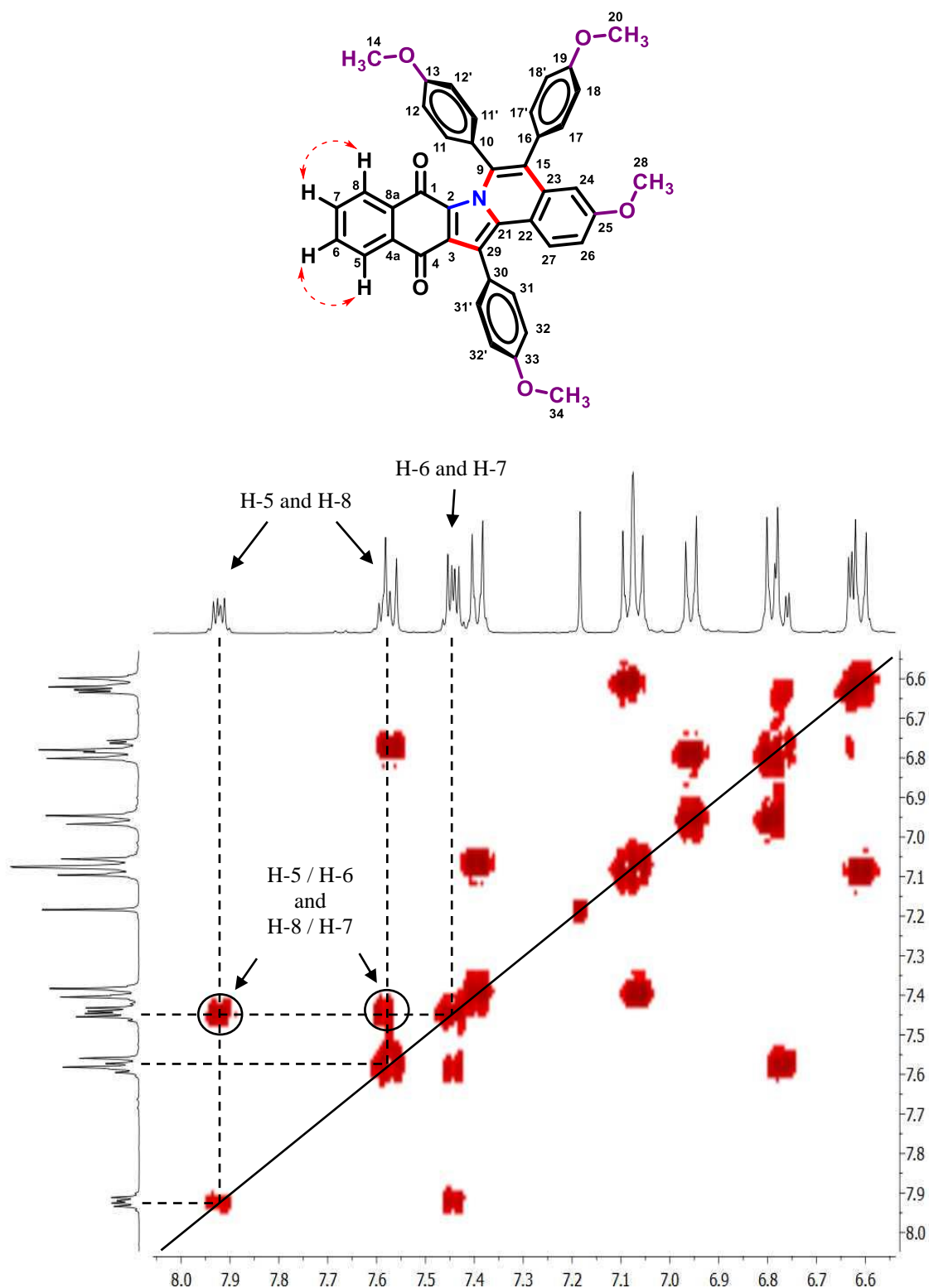




**Figure 8.**  $^{13}\text{C}$ -NMR and APT (100 MHz,  $\text{CDCl}_3$ ) spectra analysis of the compound **67b**.

Unfortunately, because it is not possible to specifically attribute any of the aromatic signals on the  $^1\text{H}$ -NMR spectrum, there is not enough information that can be achieved with the analysis over the COSY spectrum of the compound **67b** (Figure 9). The methoxy groups are spatially isolated, so they do not interact with any other signals from the molecule, and for that reason they are not even displayed on the panel of the COSY spectrum. However, it is possible to see a correlation between the multiplet at 7.94-7.90 (H-5 or H-8, 1H) and the multiplet at 7.46-7.42 (2H). There are only two possible vicinal  $^1\text{H}$  interactions that may result in this signal: H-7 / H-8 or H-5 / H-6. Since the multiplet at 7.46-7.42 (2H) shows only two interactions in the COSY panel: the one mentioned above and the multiplet located at 7.60-7.56 (2H), it is possible to conclude that:

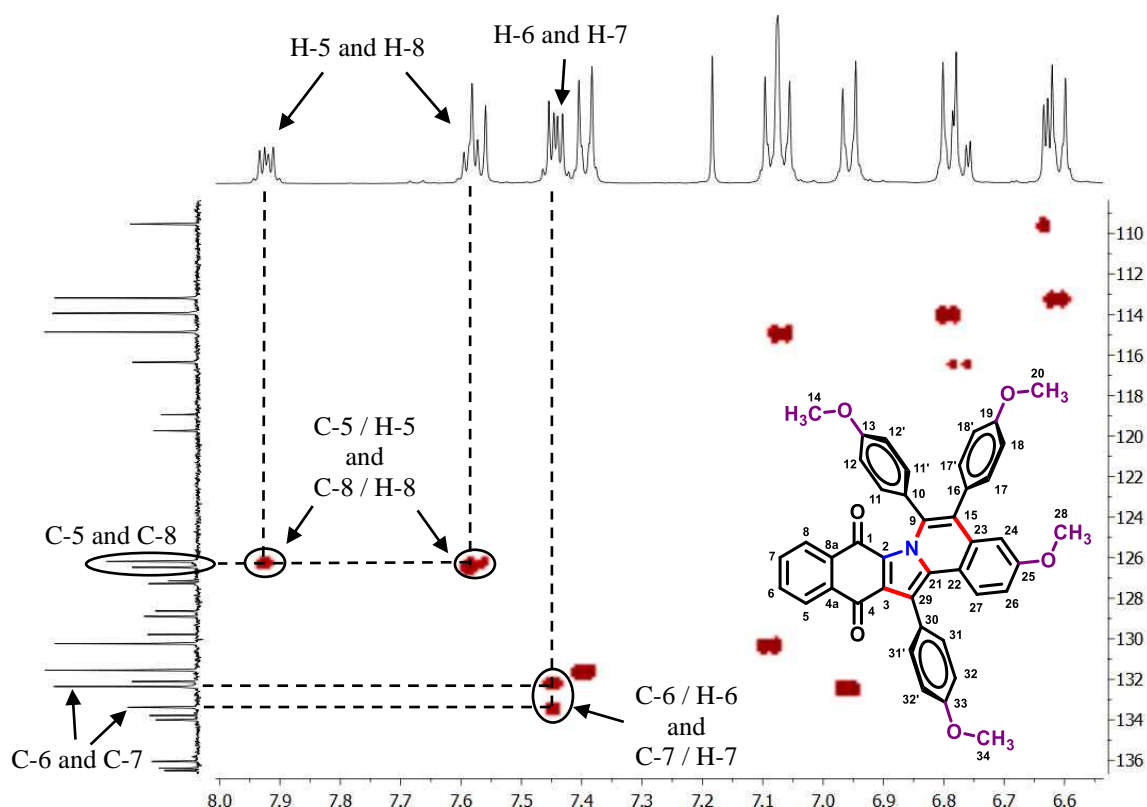
- The signals corresponding to the hydrogen atoms located at H-5 and H-8 can be either the multiplet located at 7.60-7.56 (2H) or the 7.94-7.90 (1H).
- The multiplet at 7.46-7.42 (2H) can be attributed to the hydrogen atoms located at H-6 and H-7 positions, and only.



**Figure 9.** Expansion of the COSY (400 MHz, CDCl<sub>3</sub>) spectrum of the compound **67b**.

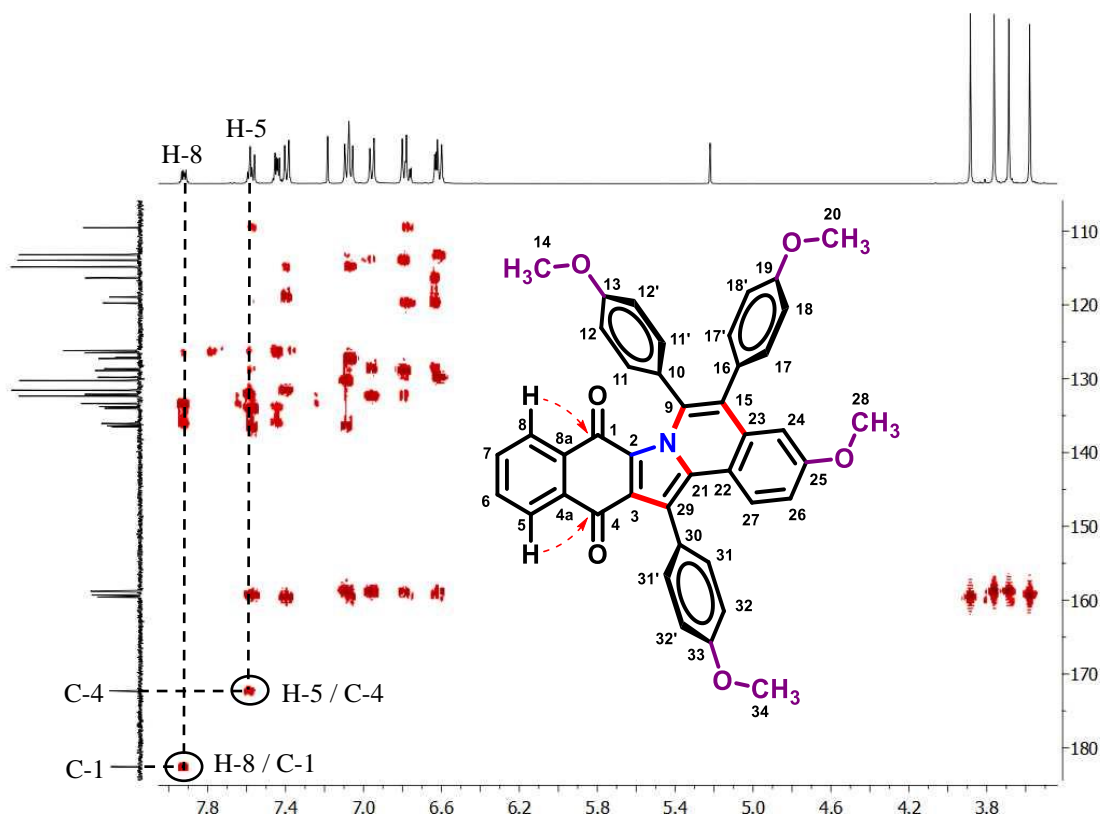
To correctly assign the hydrogen atoms and the carbon atoms using a HSQC analysis, either the assignment on the <sup>1</sup>H-NMR or on the <sup>13</sup>C-NMR must be previously known. As previously discussed here (**Figure 7** and **Figure 8**), the complete attribution on the aromatic

system was not possible on both spectra, and for this reason it was not possible, here, to correctly assign each one of them as well. But a correlation between the COSY and the HSQC analysis (**Figure 10**) made it possible to recognize that two of the carbon signals at 126.2 and 126.5 ppm can be attributed to C-5 and C-8, and that the carbon signals at 132.4 and 133.4 ppm must be attributed to C-6 and C-7. The complexity of these double-annulated molecules, according to their size and extended conjugation, made it harder to perform a more clear and precise attribution of the signals.



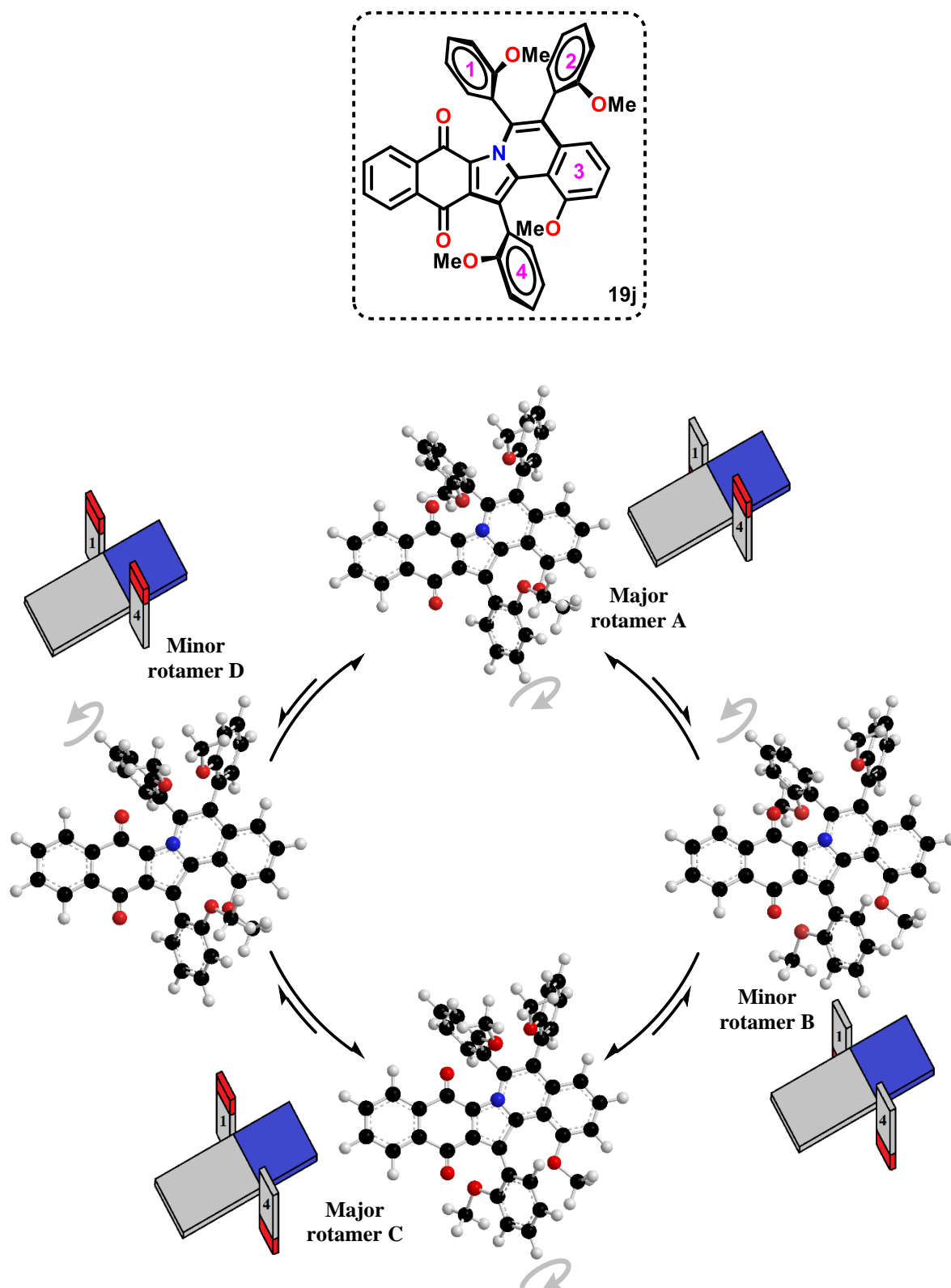
**Figure 10.** Expansion of the HSQC (400 MHz,  $\text{CDCl}_3$ ) spectrum of the compound **67b**.

From the HMBC analysis it was possible to collect valuable information about the right attribution of some of the signals discussed here so far. It was possible to see two interesting  $^3J_{\text{CH}}$  interactions between the carbonyls at 182.6 (C-1) and 172.3 ppm (C-4) and the hydrogen atoms from the multiplet at 7.94-7.90 ppm (1H) and the multiplet at 7.60-7.56 ppm (2H), respectively. It was a clear indication that the multiplet at 7.94-7.90 ppm must be attributed to the hydrogen located at the H-8 position, and also that one of the two hydrogen atoms under the integration of the multiplet at 7.60-7.56 ppm must be the hydrogen located at the H-5 position (**Figure 11**).



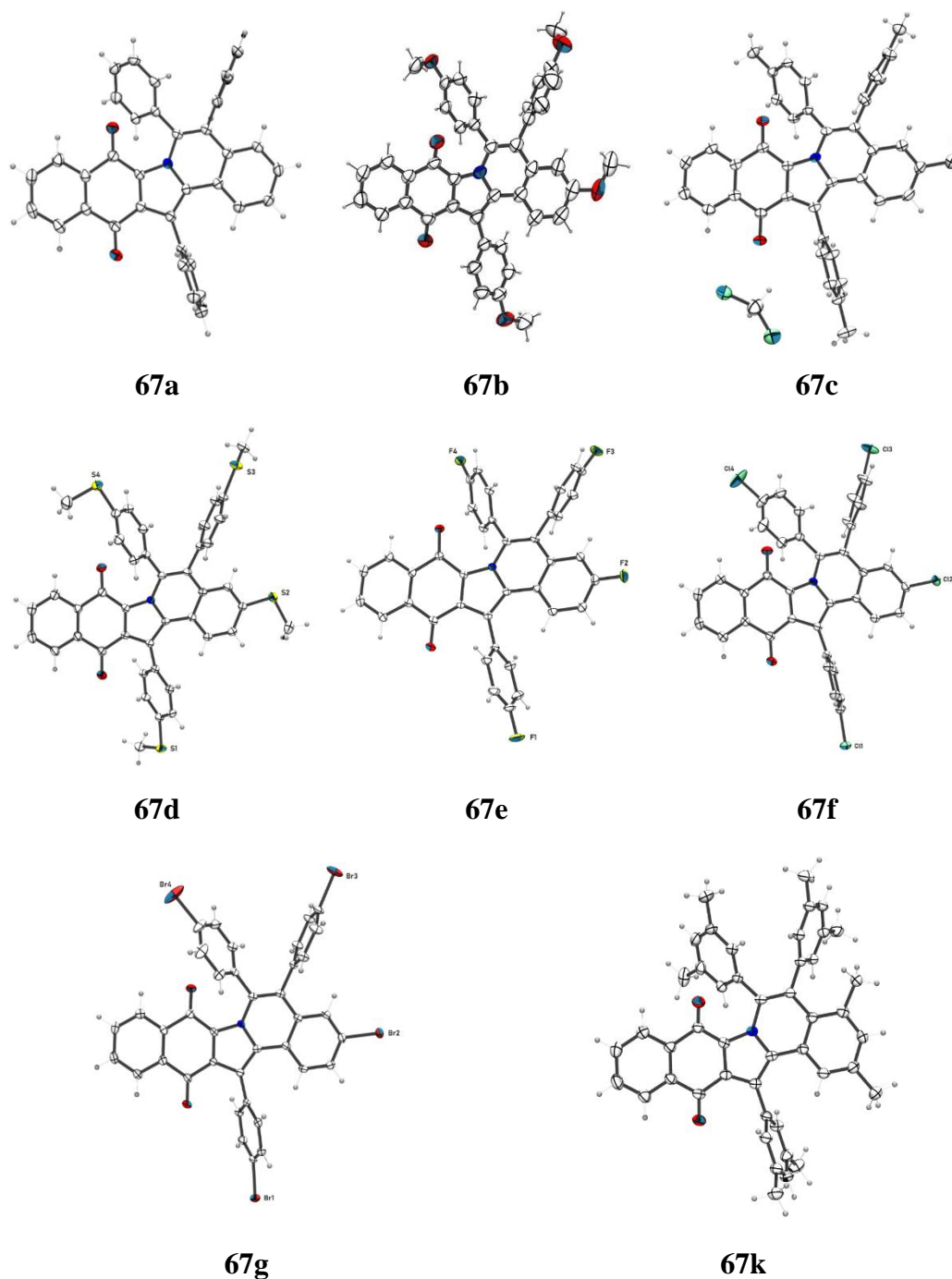
**Figure 11.** Expansion of the HMBC (400 MHz,  $\text{CDCl}_3$ ) spectrum of the compound **67b**.

A different behaviour was observed when an *ortho*-substituted symmetrical internal alkyne (compound **56j**) was applied for the synthesis of compound **67j**. In this specific case there is a steric effect between the *ortho*-methoxy group and the carbonyls, making it difficult for the  $\text{C}_{\text{Ar}}\text{-C}$  rotation at the rings **1** and **4**. This phenomenon generates four possible rotamers (**Scheme 22**) that cannot be separated by usual chromatographic techniques, in a ratio of 38:33:17:12 determined by  $^1\text{H-NMR}$  analysis, meaning that there are two preferred configurations, probably the ones presenting the methoxy groups of the rings **1** and **4** on opposite sides of the molecule (rotamers **A** and **C**). To fully understand this behaviour, an attempt to isolate a pure sample was performed, in which this substance was submitted to a partial recrystallization process on a dichloromethane/pentane system at  $-75\text{ }^\circ\text{C}$  and a single crystal was obtained. This crystal was then directly submitted to a  $^1\text{H-NMR}$  at  $-75\text{ }^\circ\text{C}$  in a 400 MHz machine and it revealed that even at this temperature there was a conversion happening between the isomers. For this reason, it was observed four times more NMR signals than expected.



**Scheme 22.** Spatial representation of the four possible rotamers of the compound **67j**.

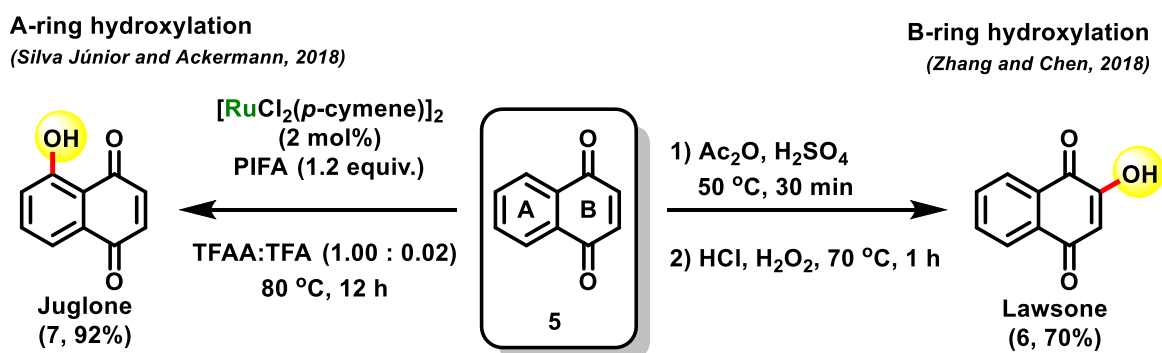
The structure of several products was confirmed by crystallographic data analysis, not only for the compound **67b**, which characterization was previously discussed here, but for a total of eight compounds of the first scope (**Figure 12**).



**Figure 12.** Crystal structures of compounds **67a-g,k**.

### 3.6.3. Synthesis of A-Ring modified naphthoquinoidal molecules

For the construction of the second scope, A-ring modified quinones were designed. However, modifications on the A-ring<sup>16d</sup> of the naphthoquinone **5** are not so trivial as the ones on the B-ring<sup>95</sup> since the A-ring is less active and more stable than the B-ring (**Scheme 23**). This fact represents a challenge in this present work, since the developed C–H double annulation happens at the C-3 position of the substrate and the acetamido DG located at the C-2 position. Therefore, the substrates that were used in the second scope of this work were designed in such a way that the B-ring must stay untouched during their obtention.



**Scheme 23.** Comparison of A-ring and B-ring modifications, using hydroxylation as an example.

Based on previous known procedures used in our research group, a range of fifteen different A-ring modified species were designed, with substituents of different chemical behaviours (electron-donating groups, electron-withdrawing groups, bulky groups, etc.) to study their contribution and/or effect on the final annulation reaction.

An aromatic nitration can be performed in several different ways,<sup>96</sup> but just like any other aromatic substitution, they need an activated species to disrupt the aromatic system and, therefore, perform the substitution. In this case, it is important to generate nitronium ion *in situ*. Nitration reactions, as exemplified by Brocklehurst,<sup>97</sup> usually apply fuming nitric acid as

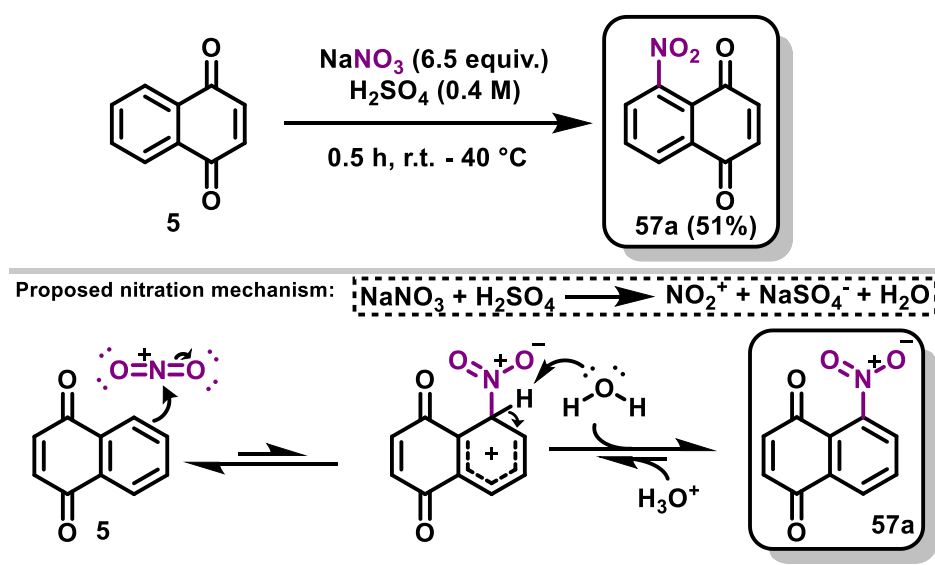
<sup>16</sup> (d) Dias, G. G.; Rogge, T.; Kuniyil, R.; Jacob, C.; Menna-Barreto, R. F. S.; da Silva Junior, E. N.; Ackermann, L. *Chem. Commun.*, **2018**, 54, 12840-12843.

<sup>95</sup> Zhou, Q.; Peng, C.; Du, F.; Zhou, L.; Shi, Y.; Du, Y.; Liu, D.; Sun, W.; Zhang, M.; Chen, G. *Eur. J. Med. Chem.*, **2018**, 151, 39-50.

<sup>96</sup> (a) Calvo, R.; Zhang, K.; Passera, A.; Katayev, D. *Nature Commun.*, **2019**, 10, 3410; (b) Huang, B.; Fan, C.; Yu, H.; Ma, J.; Pan, C.; Zhang, D.; Zheng, A.; Li, Y.; Sun, Y. *Mol. Catal.*, **2018**, 446, 140-151; (c) Hiller, M.; Sittel, T.; Wadepohl, H.; Enders, M. *Chem. Eur. J.*, **2019**, 25, 10668-10677; (d) Meng, G.; Zheng, M.-L.; Zheng, A.-Q.; Wang, M.; Shi, J. *Chin. Chem. Lett.*, **2014**, 25, 87-89; (e) Ma, X. M.; Li, B. D.; Chen, L.; Lu, M.; Lv, C. X. *Chin. Chem. Lett.*, **2012**, 23, 809-812.

<sup>97</sup> Brocklehurst, C. E.; Lehmann, H.; La Vecchia, L. *Org. Process Res. Dev.*, **2011**, 15, 1447-1453.

nitration agent. This compound is highly corrosive, and extremely dangerous. Therefore, it is important to try another less aggressive but still effective system. Based on a previous published method,<sup>16a</sup> in this current work it was used a mixture of sodium nitrate and concentrated sulfuric acid. This system is less aggressive (even though it is still corrosive) and it successfully generates the crucial nitronium ion (**Scheme 24**). Therefore, the compound **57a** was obtained in 51% yield as yellow crystals. This compound plays an important role in the scope, since the nitro group is a strong electron withdrawal group, and its presence on the A-ring can possibly show what is the effect of the A-ring substituents on the B-ring annulation reactions.



**Scheme 24.** Synthetic procedure of compound **57a** and its proposed mechanism.

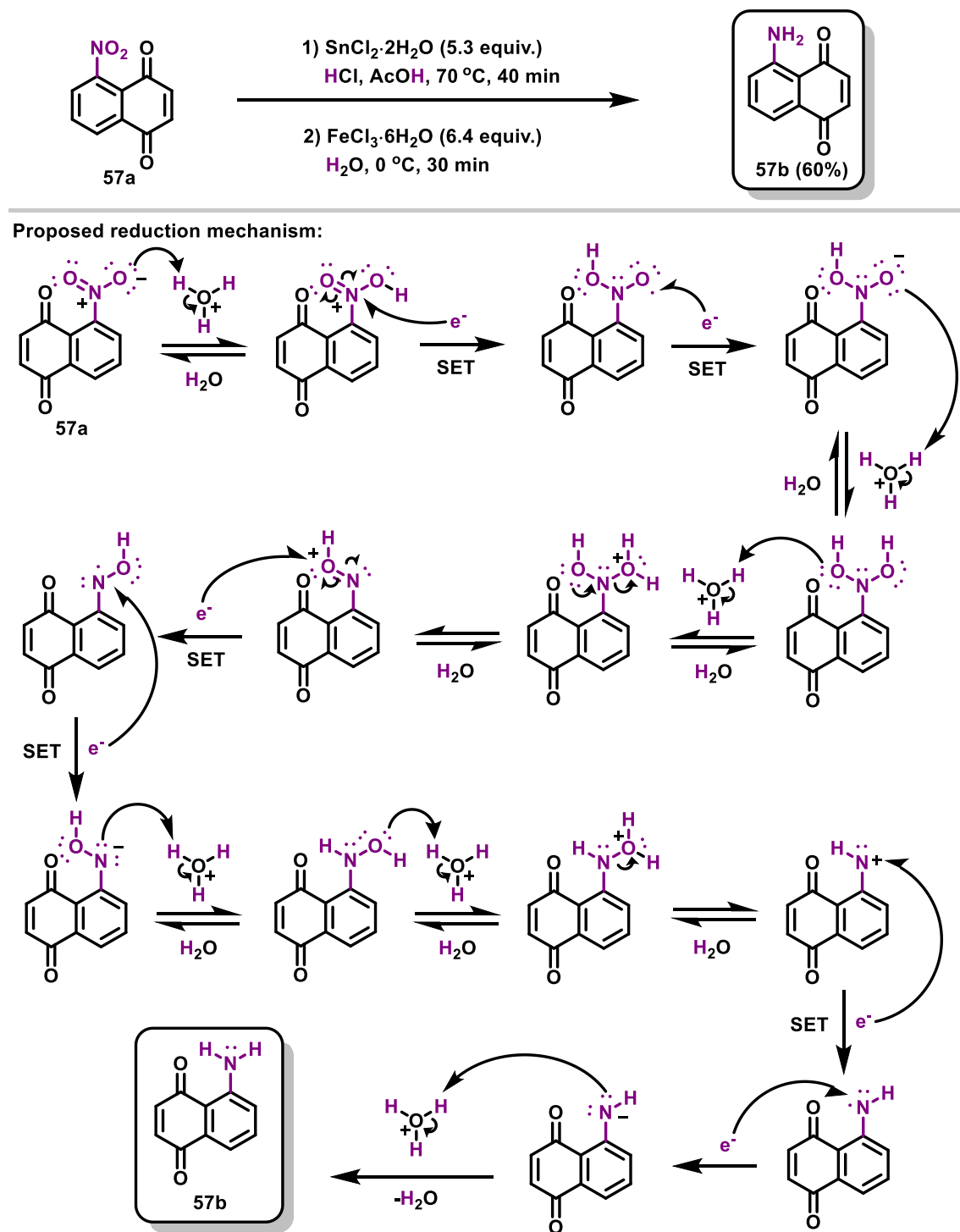
A reduction of the nitro group present in the compound **57a** led to the successful achievement of the amine **57b**, based on a process already explored by our research group.<sup>74</sup> From this perspective it was possible to reverse the electronic effect of the substituent in the overall reaction, considering that an electron withdrawing group is reversed into an electron donating group (**Scheme 25**).

This reaction occurred in the presence of tin chloride and iron chloride, where enough electrons were transferred into the new amino group *via* several sequential single electron transfer (SET) processes. Along the reductive salts, hydrochloric acid was used as proton source. The desired product was obtained as a dark purple solid, in 60% yield (**Scheme 25**).

<sup>16</sup> (a) Jardim, G. A. M.; Silva, T. L.; Goulart, M. O. F.; Carlos A. de Simone, C. A.; Barbosa, J. M. C.; Salomão, K.; Solange L. de Castro, S. L.; Bower, J. F.; da Silva Júnior, E. N. *Eur. J. Med. Chem.*, **2017**, *136*, 406-419.

<sup>74</sup> Jardim, G. A. M.; da Silva Júnior, E. N.; Bower, J. F. *Chem. Sci.*, **2016**, *7*, 3780-3784.

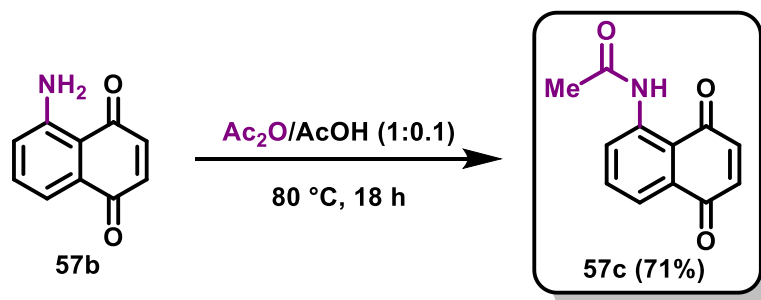




**Scheme 25.** Reduction of nitro-group towards formation of the amino group in compound **57b** and its respective mechanism.

From amine **57b**, another distinguish product was achieved. Using the usual acetylation applied here so far, an acetamide substituent was successfully achieved, present in compound **57c**, in 71% yield (**Scheme 26**). This substituent can also act as directing group, and this fact can lead to very important conclusions about the main annulation reaction, from which it may

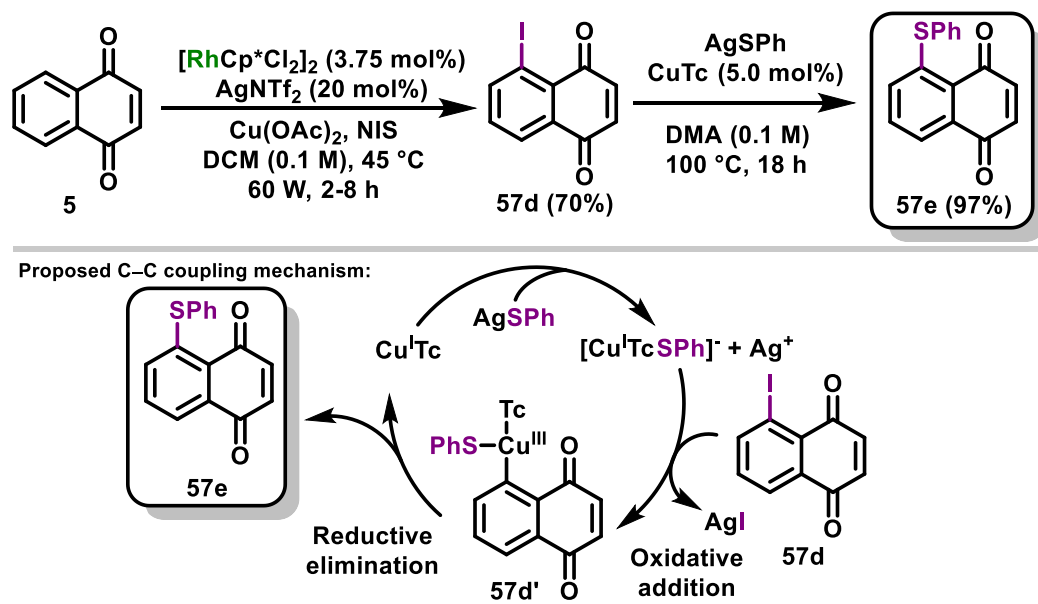
be possible to study the regioselectivity of the method, since this acetamido group may lead to a side annulation at the C-6 position. If this side activation works, a new research frontier could be reached. In the other hand, if it doesn't work, it still proves the high regioselectivity of the developed reaction, attesting its wide applicability.



**Scheme 26.** Acetylation process towards the compound **57c**.

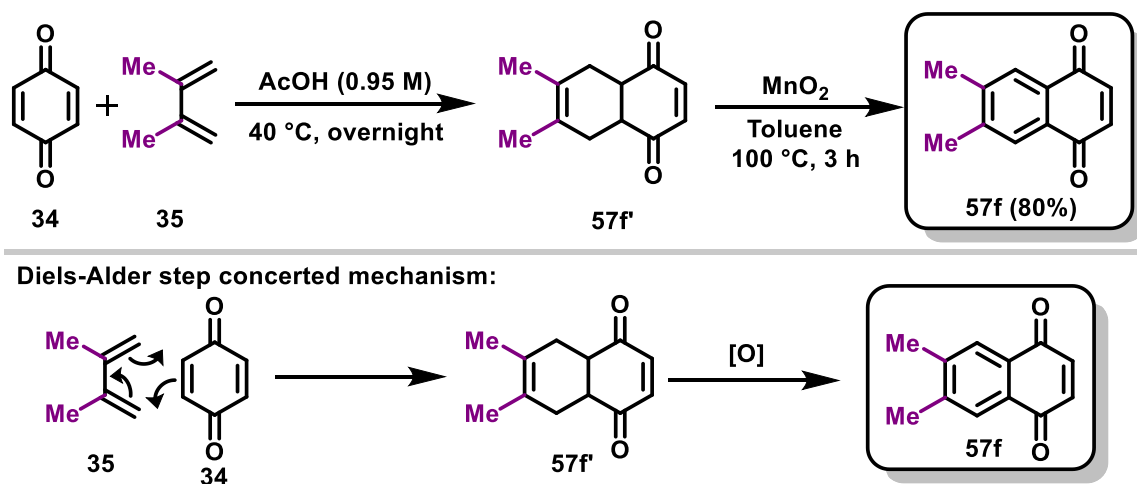
Another important point to observe is the substituent steric effect on the annulation reaction. For that purpose, iodinated products, such as **57d**, and arylated substituents, like the thiophenol present in compound **57e**, may offer a different behaviour. As previously discussed on other publications from our research group,<sup>76</sup> or the compound **57e** to be obtained, its previous iodine compound (**57d**) is necessary. We have successfully performed a reaction to obtain the compound **57d** (**Scheme 27**). It is a rhodium catalyzed C–H iodination in the presence of a silver-I salt. This reaction can be performed without microwave irradiation, but there is a considerable loss of yield. The necessary iodinated naphthoquinone **57d** was obtained in 70% yield as red crystals. Once obtained, treated, and fully characterized, it was sequentially used on the synthesis process of **57e** via a copper-silver catalyzed phenylthiolation. This mechanism resembles the Liebeskind–Srogl coupling reaction.<sup>98</sup> It starts with a transferring reaction between the silver-thiophenyl salt and copper(I) thiophene-2-carboxylate generating the active reactant [Cu<sup>I</sup>TcSPh]<sup>-</sup> and Ag<sup>+</sup>. Silver-I salts usually react promptly with iodine generating solid silver-I iodide, which is basically the sequential reaction with compound **57d**, generating the complex intermediate **57d'** via an oxidative addition of the copper-I reactant. Then, a reductive elimination generates the product **57e** and the original form of the catalyst, Cu<sup>I</sup>Tc. This synthesis was almost quantitative (97% yield), and the compound **57e** was obtained as a red solid (**Scheme 27**).

<sup>98</sup> Prokopcová, H.; Kappe, C. O. *Angew. Chem. Int. Ed.*, **2009**, *48*, 2276-2286.



**Scheme 27.** Synthetic procedure of compounds **57d** and **57e** and its proposed C–C coupling mechanism.

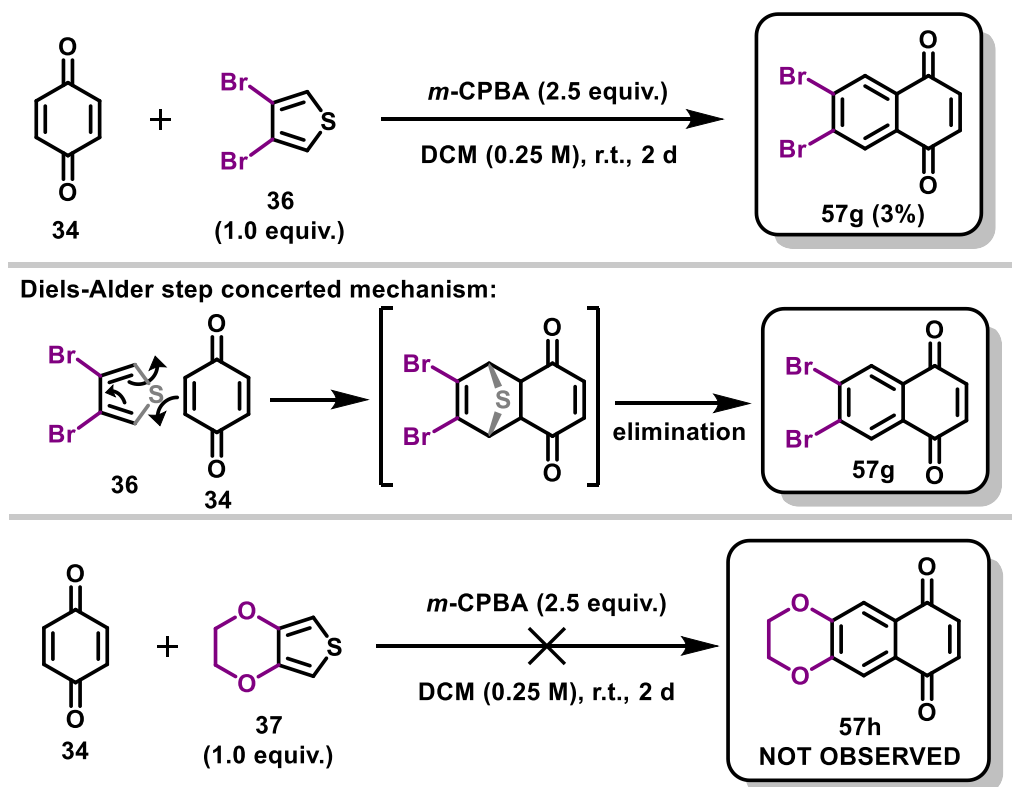
The compound **57f** was obtained based on a previously reported method used by our research group.<sup>16d</sup> It is essentially a Diels-Alder type reaction, under acid catalysis, leading to the formation of the intermediate **57f'**, followed by an oxidation with manganese oxide to establish the aromatic system (**Scheme 28**). The product **57f** was obtained in 80% yield as yellow crystals.



**Scheme 28.** Synthetic route for obtention of compound **57f** and its proposed mechanism.

Still following a Diels-Alder reaction, compounds **57g** and **57h** were also designed, based on a previously reported procedure using thiophenes as dienes and 1,4-benzoquinone (**34**)

as dienophiles.<sup>99</sup> Although very promising, a very low yield was observed in the formation of compound **57g**, obtained as a green solid in only 3% yield. Furthermore, the compound **57h** was not even observed (**Scheme 29**). These results made it unreasonable to use these compounds as substrates, especially considering the necessary subsequential two steps (amination and acetylation).

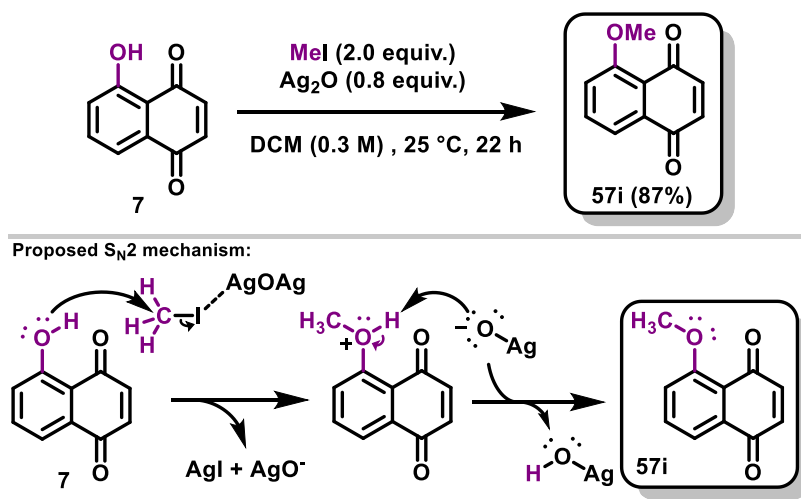


**Scheme 29.** Synthesis used to achieve compound **57g** and its respective proposed mechanism, and failed synthesis of compound **57h**.

One of the simplest electron-donating groups that can be achieved is the methoxy group. Compound **57i** is a simple result of a protection on the hydroxyl group of Juglone (**7**),<sup>100</sup> a commercially available compound that was directly used without previous purification. Using iodomethane, in the presence of silver-I oxide, it is easy to perform this S<sub>N</sub>2 reaction (**Scheme 30**). In fact, the product was successfully obtained in 87% yield as orange crystals, even without the need of further purification *via* column chromatography.

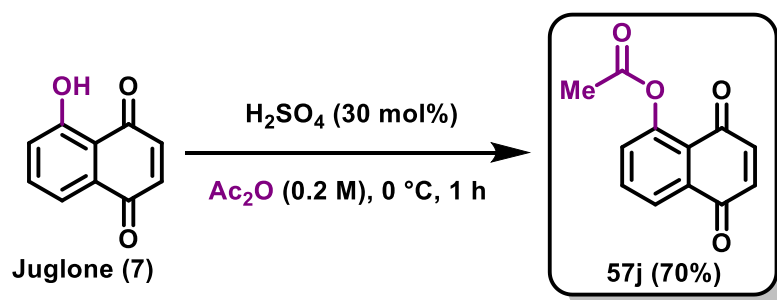
<sup>99</sup> Torssell, K. *Acta Chem. Scand. B*, **1976**, *30*, 353-357.

<sup>100</sup> Contant, P.; Haess, M.; Riegl, J.; Scalone, M.; Visnick, M. *Synthesis*, **1999**, *5*, 821-828.



**Scheme 30.** Synthetic procedure of compound **57i** and its proposed mechanism.

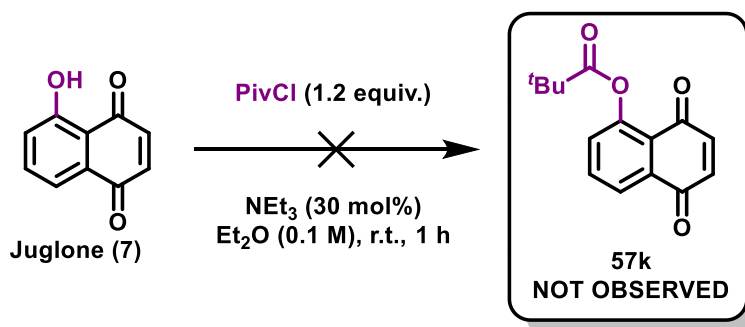
Another possible simple protection of the hydroxy group of the Juglone (**7**) is the acetylation reaction. This process can easily be achieved using acetic anhydride, under acidic catalysis with sulfuric acid.<sup>101</sup> This reaction follows the familiar mechanism known for usual acetylation processes, and the desired product **57j** could be obtained as a yellow solid in 70% yield (**Scheme 31**).



**Scheme 31.** Acetylation process towards compound **57j**.

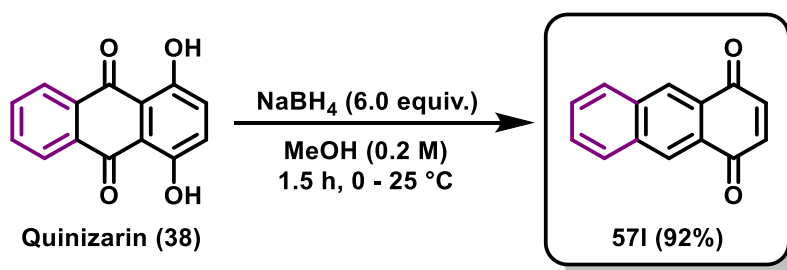
Another protection of the hydroxy group of the Juglone (**7**) using pivaloyl chloride was attempted, from which compound **57k** was expected. However, this reaction did not lead to a successful result, even under acid or basic catalysis (**Scheme 32**).

<sup>101</sup> Fieser, L. F.; Dunn, J. T. *J. Am. Chem. Soc.*, **1937**, *59*, 1016-1021.



**Scheme 32.** Failed acylation process towards compound **57k**.

Compound **57i** (1,4-anthraquinone) is a peculiar A-ring modified naphthoquinone. Its synthesis was based on a simple previously reported method.<sup>102</sup> The large aromatic system gives this class of compounds an unique chemical behaviour and, as a result, it may present a different and interesting outcome for the annulation reaction. Starting from Quinizarin (**38**), a dye used to color gasoline<sup>103</sup> or heating oils,<sup>104</sup> compound **57i** was obtained *via* a simple reduction reaction, in the presence of sodium borohydride, in 92% yield, as a brown solid (**Scheme 33**). Since the starting material is a very colorful orange powder, it is easy to follow the development of the reaction as a brown color starts to take place in the system.



**Scheme 33.** Synthetic procedure of compound **57i**.

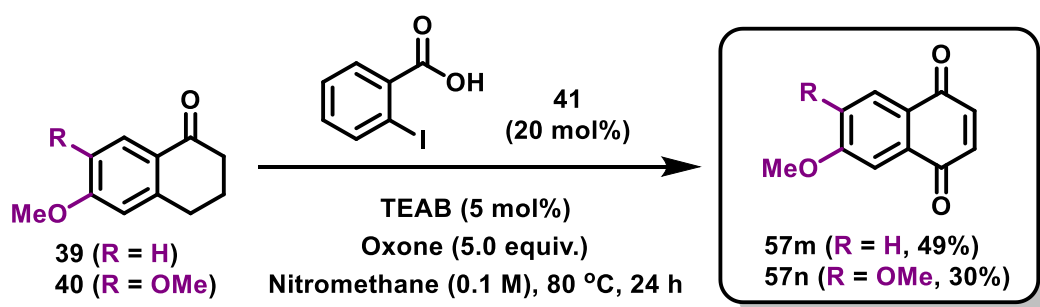
An additional procedure also explored by our research group was the one towards the compound **57m** and **57n**, adapted from previous reported work.<sup>16a</sup> This process makes it possible to directly obtain a naphthoquinoidal structure with a substituent at the C-6 and/or C-7 position, and it is important to clarify that direct substitutions at these positions are difficult to achieve directly from unactive substrates, such as the 1,4-naphthoquinone (**5**) itself. In this

<sup>102</sup> Yamakado, T.; Takahashi, S.; Watanabe, K.; Matsumoto, Y.; Osuka, A.; Saito, S. *Angew. Chem. Int. Ed.*, **2018**, *130*, 5536-5541.

<sup>103</sup> Haloulos, I.; Theodorou, D.; Zannikou, Y.; Zannikos, F. *Accred. Qual. Assur.*, **2016**, *21*, 203-210.

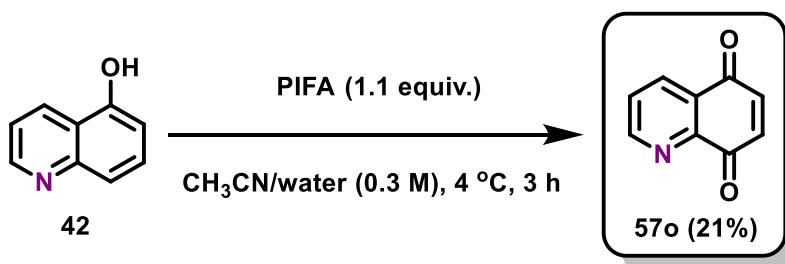
<sup>104</sup> Tucker, K. B. E.; Sawyer, R.; Stockwell, P. B. *Analyst*, **1970**, *95*, 730-737.

procedure, aryl-substituted tetralones **39** and **40** can be oxidized to naphthoquinoidal products in a simple manner. For this purpose, oxone and 2-iodobenzoic acid (**41**) were used as pre-oxidizing agents, in the presence of TEAB, in which a hypervalent iodine structure (IBX) is formed *in situ* and act directly as an oxidizing agent. The desired quinone **57m** was achieved as a yellow solid in 49% yield, while the quinone **57n** was achieved as an orange solid in 30% yield (Scheme 34).



Scheme 34. Oxidative synthesis of compounds **57m** and **57n**.

The last designed substrate, compound **57o**, was originated from 5-hydroxy-quinoline (**42**), *via* an oxidative procedure using PIFA previously discussed in literature.<sup>105</sup> This process led to the successful formation of the desired quinone **57o** as a brown solid, in 21% yield (Scheme 35).



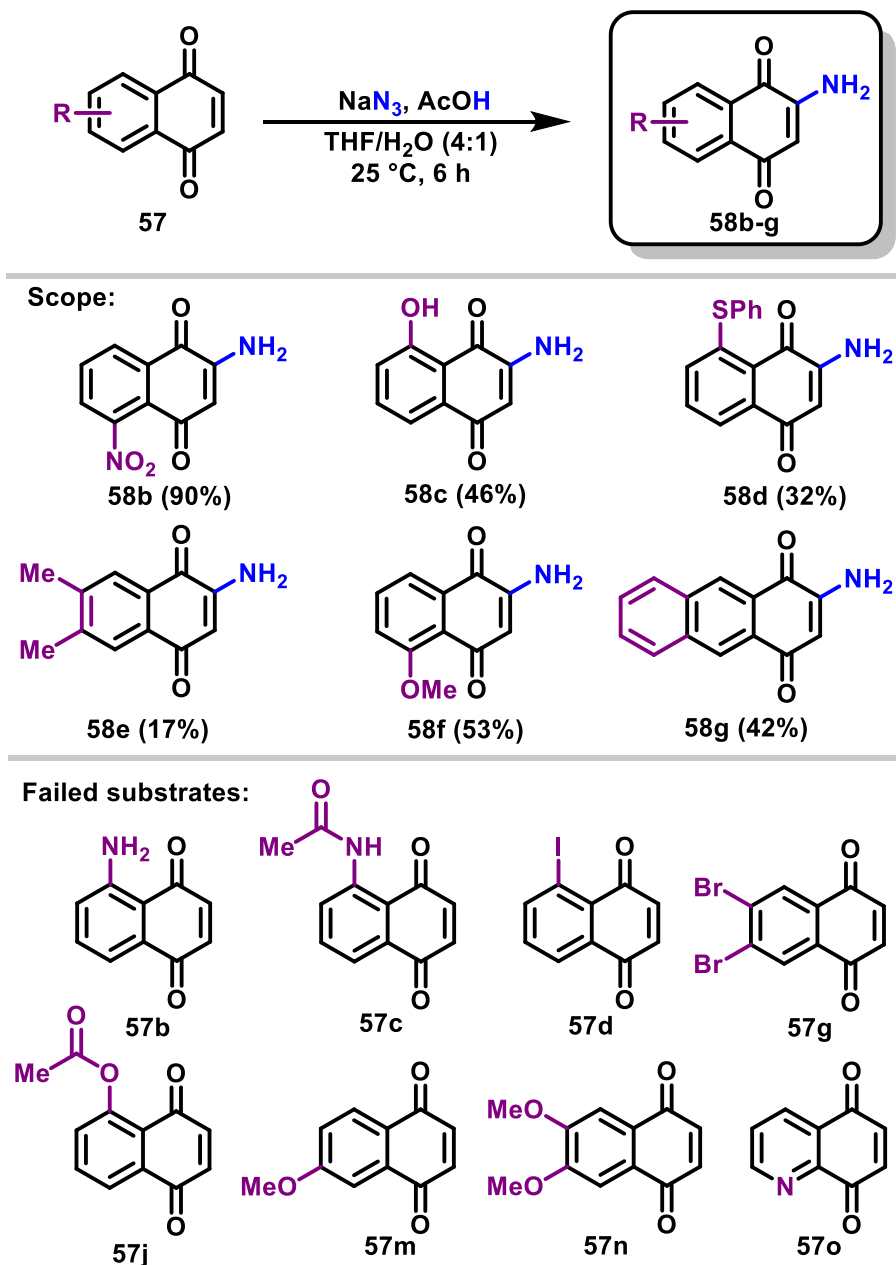
Scheme 35. Oxidative synthesis of compound **57o**.

### 3.6.4. Amination at the C-2/C-3 position

The amination reaction was performed on the A-ring modified substrates previously described using the same procedure applied on the 1,4-naphthoquinone **5** towards the obtention of the amine **58a**.<sup>83</sup> Using the thirteen achieved substrates (**57a**, **57b**, **57c**, **57d**, **57e**, **57f**, **57g**,

<sup>105</sup> Barret, R.; Daudon, M. *Tetrahedron Lett.*, **1990**, *31*, 4871-4872.

57i, 57j, 57l, 57m, 57n and 57o) and the commercially available Juglone (7), six aminated products (58b-g) were successfully obtained (Scheme 36).

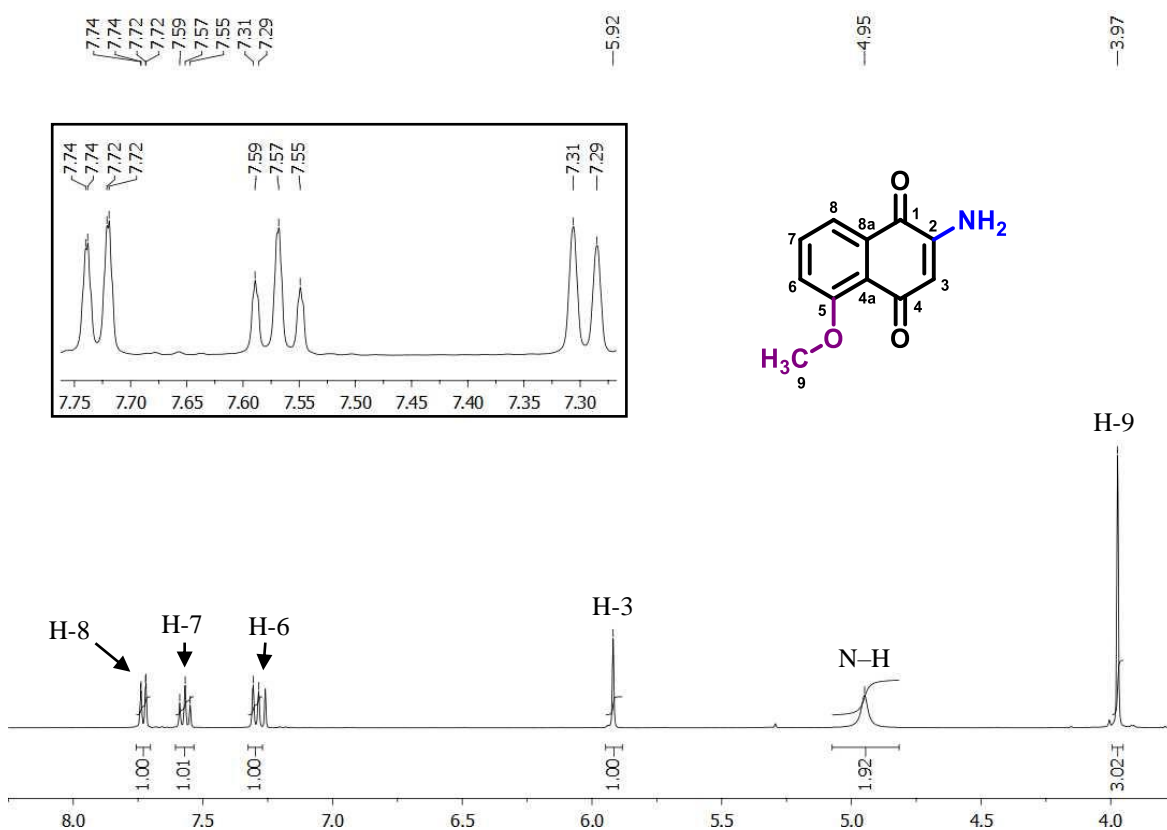


**Scheme 36.** Amination process towards compounds **58b-g**, obtained scope and failed substrates.

The  $^1\text{H-NMR}$  spectrum analysis of the compound **58f**, for example, shows an explicit singlet integrated to 3H at 3.97 ppm, clearly attributed to the methoxy group (H-9), and another singlet integrated to 1H at 5.92 ppm that can be attributed to the remaining hydrogen of the B-ring (H-3). There is also a broad singlet integrated to 2H at 4.95 ppm, which can be attributed to the two hydrogen atoms present on the amino group. In the aromatic section, all the expected

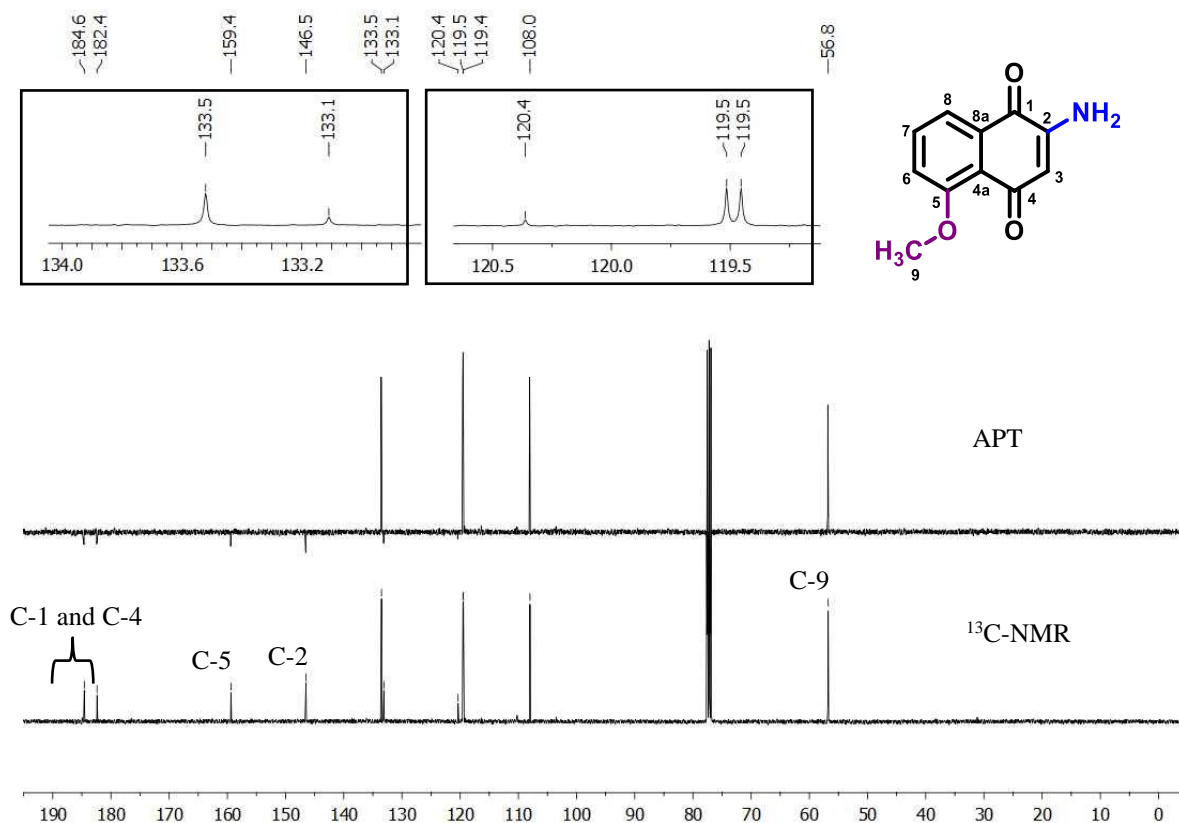


signals related to the aromatic hydrogen atoms from A-ring can be observed. The first signal is a doublet of doublets at 7.73 ppm ( $J = 8.0, 0.7$  Hz, 1H), related to the most deshielded hydrogen H-8. The remaining doublet at 7.29 ppm ( $J = 8.0$  Hz, 1H) can be attributed to the hydrogen located at H-6. This analysis leads to the last signal, a triplet at 7.57 ppm ( $J = 8.0$  Hz, 1H), which must be attributed to the H-7 atom, the only aromatic one adjacent to two other hydrogen atoms (**Figure 13**).



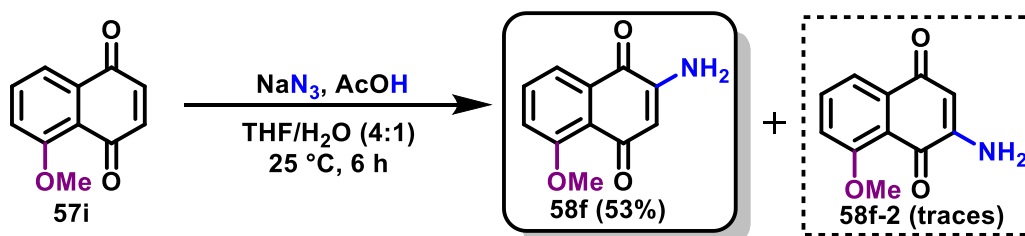
**Figure 13.**  $^1\text{H-NMR}$  (400 MHz,  $\text{CDCl}_3$ ) spectrum analysis of the compound **58f**.

Analyzing the  $^{13}\text{C-NMR}$  and APT spectra (**Figure 14**), the first signals to be pointed out are the ones located at 184.6 and 182.4 ppm, non-hydrogenated and extremely deshielded, which can be attributed to the carbonyls located at C-1 and C-4. The next signals are the second-most deshielded non-hydrogenated carbons, after the carbonyls, located at 159.4 and 146.5 ppm, that can be attributed to C-5 and C-2 respectively, since they are directly bonded to very electronegative atoms (oxygen and nitrogen), and they are also not hydrogenated. Another important signal to be considered is located at 56.8 ppm, which can be clearly attributed to the methoxy group, C-9.



**Figure 14.**  $^{13}\text{C}$ -NMR and APT (100 MHz,  $\text{CDCl}_3$ ) spectra analysis of the compound **58f**.

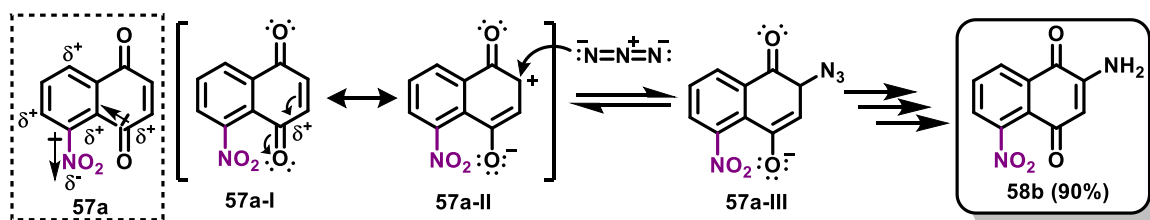
Most of these quinones led to two different products each, isomeric between themselves, if the amination happens at the C-2 or C-3 position, such as **58b**, **58c**, **58d** and **58f**. The product **58f** is a good example, since this reaction could generate a by-product, the nominated compound **58f-2** (Scheme 37). These by-products were in fact observed in all the processes where this phenomenon could happen, but in very low amount, sometimes even just traces.



**Scheme 37.** Synthetic procedure of compound **58f** and the observed by-product **58f-2**.

The reasons that led to this observed regioselectivity are not clear for all cases. More specifically, electron-donating groups, such as thiophenyl (**58d**) and methoxy groups (compound **58f**) led each to their respective amines on different positions (C-3 and C-2,

respectively). But, in the other hand, the nitro group, present on the compound **58b**, delivered specifically on the C-2 position, which can be explained by the strong positive partial-charge this group generates on the *ortho* and *para* position of the A-ring, deactivating it. Consequently, it is easy to recognize, as described in **Scheme 38**, that the C-2 position gets a significant increase on its electrophilicity *via* inductive and resonance effects, facilitating the approach of the azide anion.

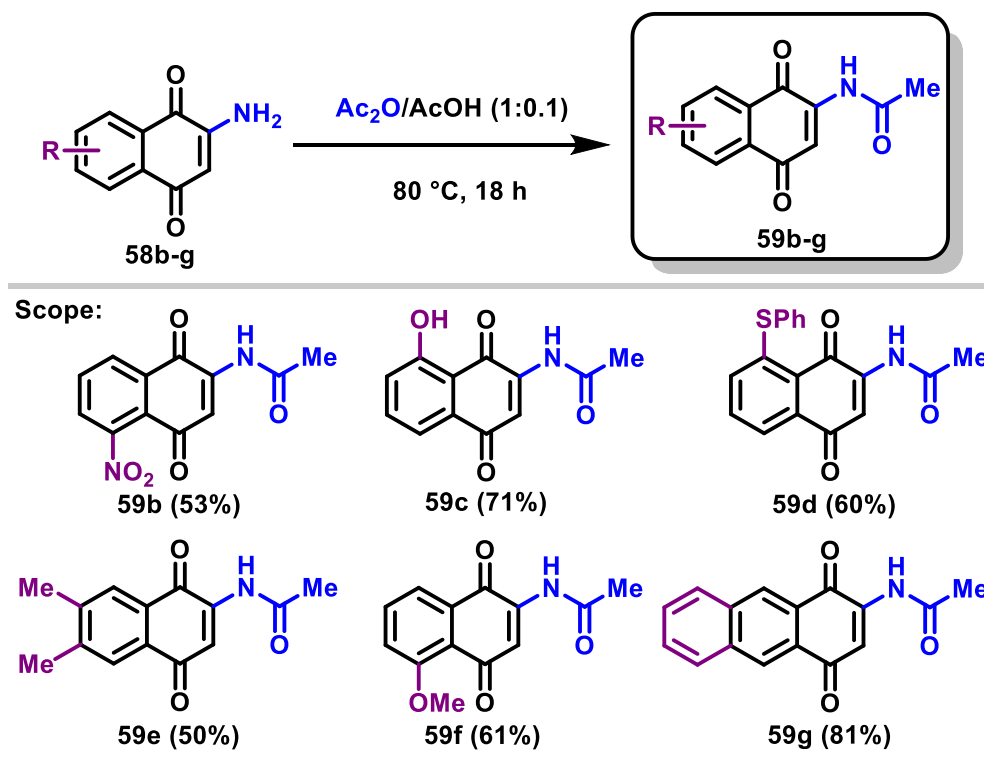


**Scheme 38.** Plausible explanation for the observed regioselectivity on the synthesis of compound **58b**.

To determine where this amination is happening, a careful spectra analysis must be done, since the visual and chemical properties of both products are very similar. Bidimensional NMR and crystallographic analyses are powerful tools to help with this determination, and a larger spatial interaction may be observed on the acetylated products than with the amine, resulting on a better and more precise analysis. Therefore, these extra characterizations were all performed after the following acetylation reaction.

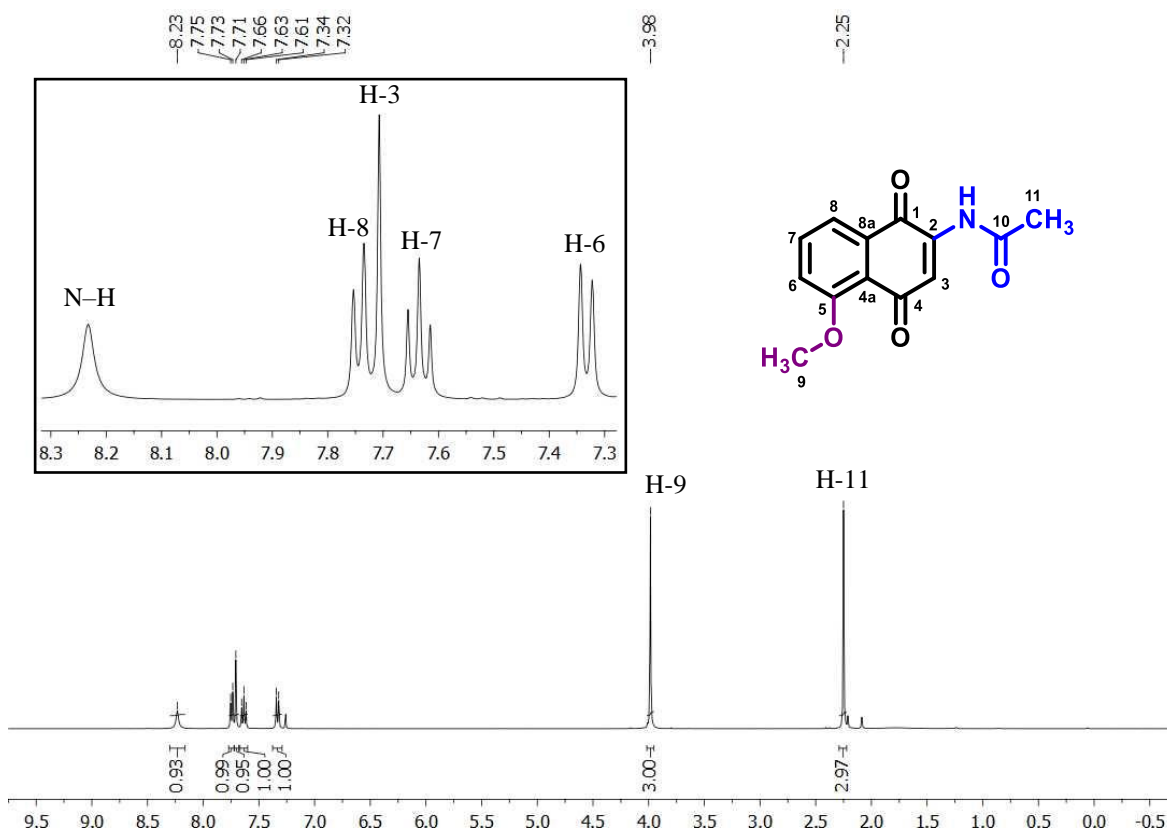
### 3.6.5. Acetylation of the amino group

The six previously described 2-amine-1,4-naphthoquinones (**58b-g**) were submitted to the same acetylation procedure described for the obtention of compound **59a**.<sup>84</sup> In this step, six acetylated products (**59b-g**) were successfully achieved in medium to good yields (**Scheme 39**). At this point, all attempted substrates led to their respective acetylated product, with no failures.



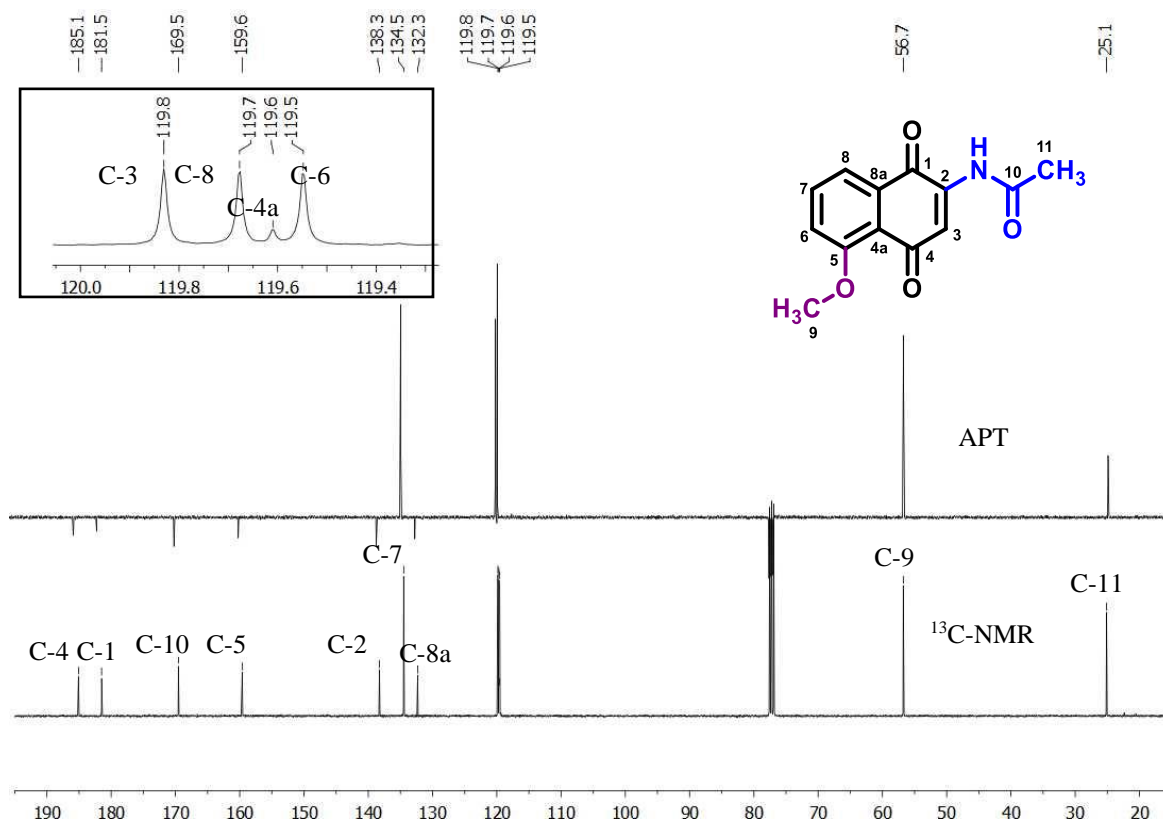
**Scheme 39.** Acetylation process towards compounds **59b-g**.

The compound **59f** will be used as example to discuss the NMR characterization data. Through a careful analysis on its  $^1\text{H-NMR}$  spectrum (**Figure 15**), it was possible to see the signal attributed to the methoxy group H-9 as a singlet integrated to 3H at 3.98 ppm. Another singlet integrated to 3H can be seen at 2.25 ppm, attributed to the methyl group of the acetyl portion. There is also a broad singlet integrated to 1H at 8.23 ppm, related to the remaining hydrogen atom present on the amide portion. The acetylation causes a huge difference in the electronic density on this hydrogen, since the non-bonding electrons from the nitrogen are now shared not only with the carbonyls of the quinone but also even more effectively with the carbonyl of the acetyl group. That leads to a strong deshielding effect on the hydrogen, shifting its signal towards the left side of the spectrum. In the aromatic section, all the expected signals attributed to the aromatic hydrogen atoms from A-ring can be observed. The first signal is a doublet at 7.75 ppm ( $J = 8.0$  Hz, 1H) that can be attributed to the most deshielded hydrogen H-8. The following signal is a singlet at 7.71 ppm, integrated to 1H, related to the remaining hydrogen of the B-ring H-3. Afterwards, there is a triplet at 7.63 ppm ( $J = 8.2$  Hz, 1H) that can be attributed to the hydrogen at H-7, the only hydrogen atom vicinal to other two hydrogen atoms. And the last one is a doublet at 7.33 ppm ( $J = 8.4$  Hz, 1H) related to the hydrogen at H-6 position.



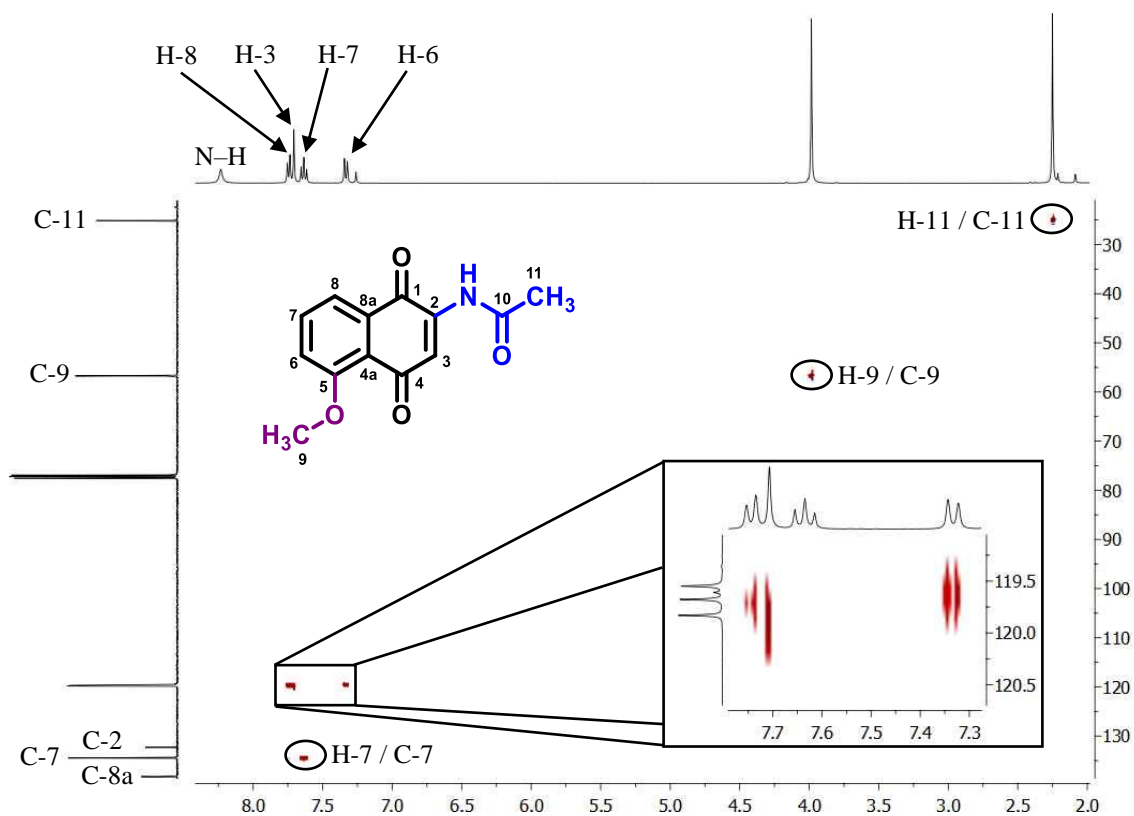
**Figure 15.** <sup>1</sup>H-NMR (400 MHz, CDCl<sub>3</sub>) spectrum analysis of the compound **59f**.

In the analysis of the <sup>13</sup>C-NMR and APT spectra (**Figure 16**), the first signals pointed out are the ones located at 185.1 and 181.5 ppm, corresponding to non-hydrogenated and extremely deshielded carbon atoms, which can be attributed to the carbonyls located at C-4 and C-1, respectively. Another important signal located at 169.5 ppm can be related to the carbonyl of the acetyl group, at C-10 position. Methyl signals are also easy and important to be pointed out. In this case, because the methoxy group has a carbon directly attached to oxygen, its signal should be shifted towards a higher shielded region than the methyl group from the acetyl group. With this information, it becomes easy to correlate the signal at 56.7 ppm to the methoxy group (C-9 position) and the signal at 25.1 ppm to the methyl from the acetyl group (C-11 position).

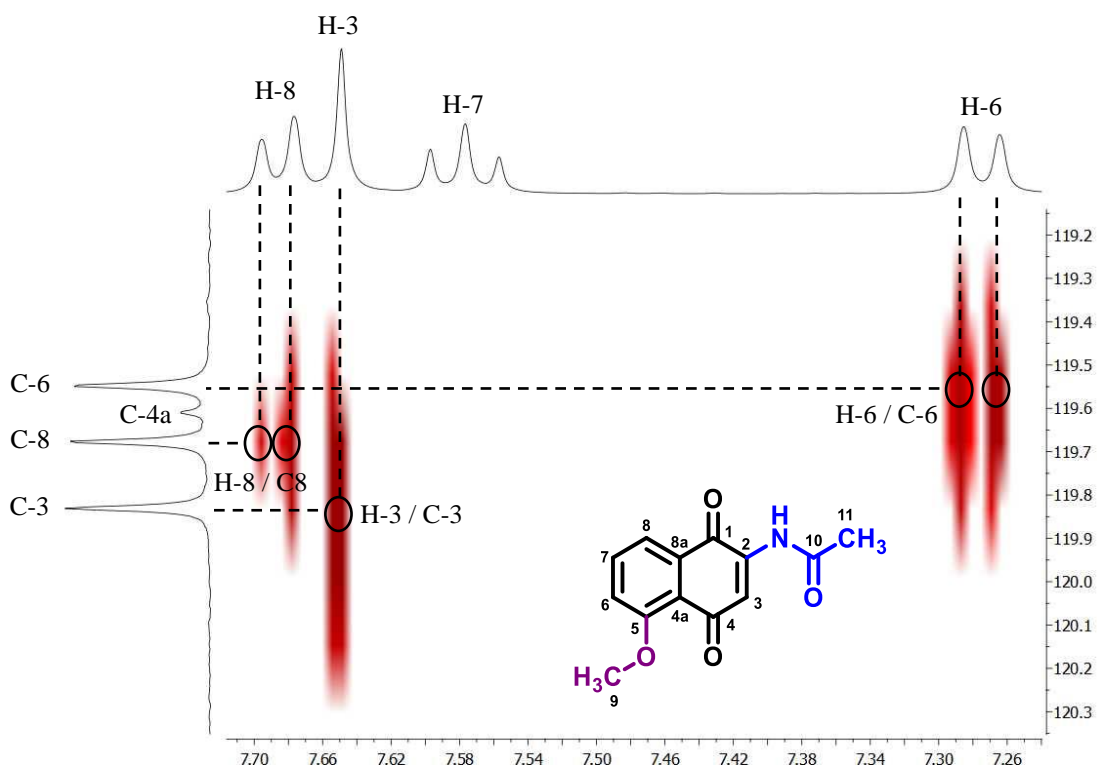


**Figure 16.**  $^{13}\text{C}$ -NMR and APT (100 MHz,  $\text{CDCl}_3$ ) spectra analysis of the compound **59f**.

Since all hydrogen atoms were already assigned, it is possible to determine the hydrogenated carbons using a HSQC analysis (**Figure 17**). Naturally, it was observed the signal correlated to the interaction between the hydrogen atoms from the methyl group located at H-11 with the carbon C-11, the hydrogens from the methoxy group located at H-9 with their corresponding carbon C-9 and the hydrogen at the H-7 position with the carbon C-7. These observations corroborated the assignment of the methyl group at the C-11 position, according not only to the expected chemical shift but also to what is observed here. However, to correctly assign the hydrogen atoms H-3, H-6 and H-8 to their respective carbon atoms, a deeper analysis was necessary. Using an expanded image of this specific region (**Figure 18**), it is possible to locate the center of the signals that can be attributed to the hydrogen atoms at H-3, H-6 and H-8 positions, assigned at the horizontal axis. It is possible to project each one of these centered signals to their respective carbon atoms from the vertical axis, from which the correct assignment of the carbon atoms at C-3, C-6 and C-8 positions was made.

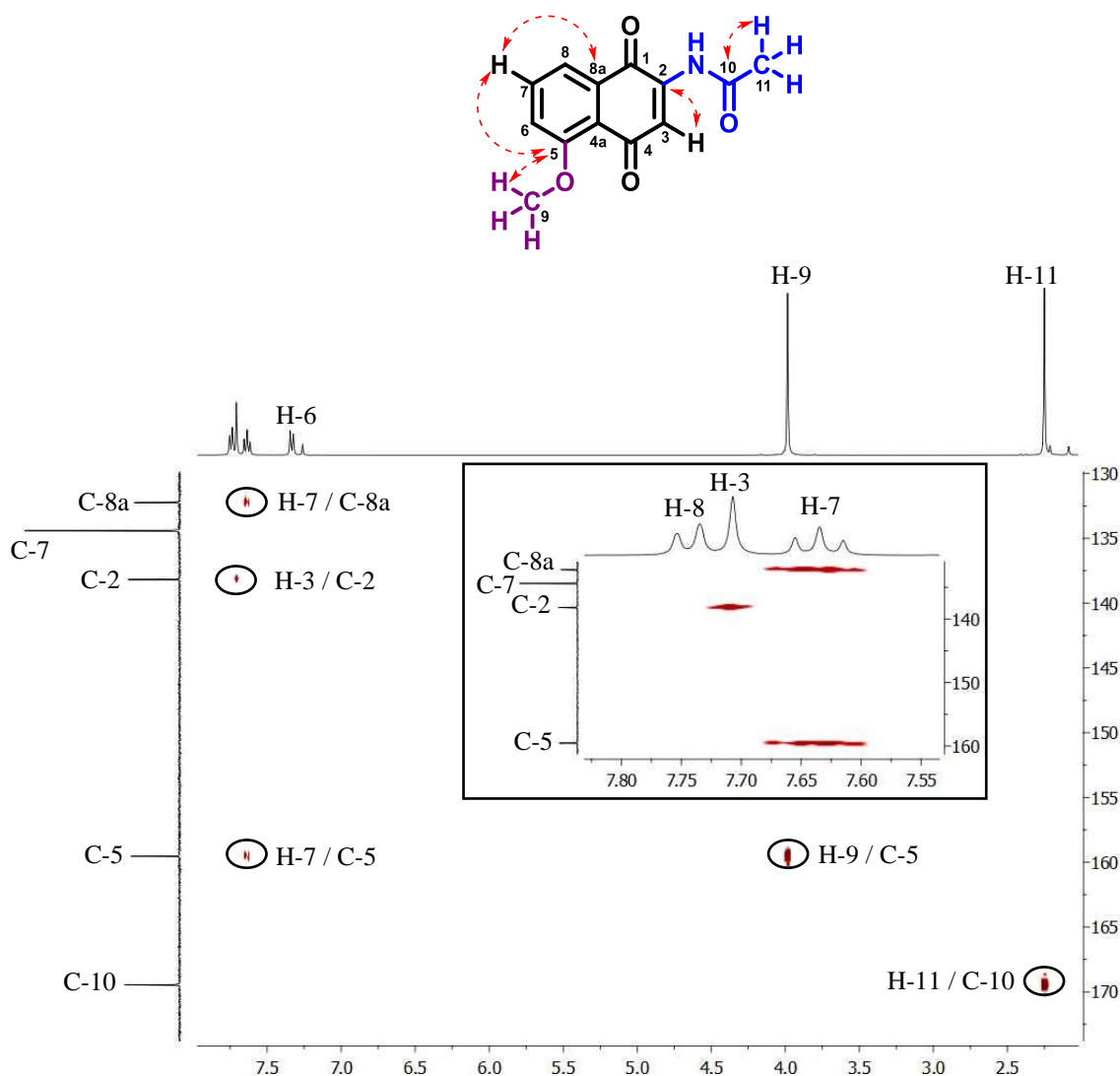


**Figure 17.** HSQC (400 MHz, CDCl<sub>3</sub>) spectrum of the compound **59f**.



**Figure 18.** Expansion of the HSQC (400 MHz, CDCl<sub>3</sub>) spectrum of the compound **59f**.

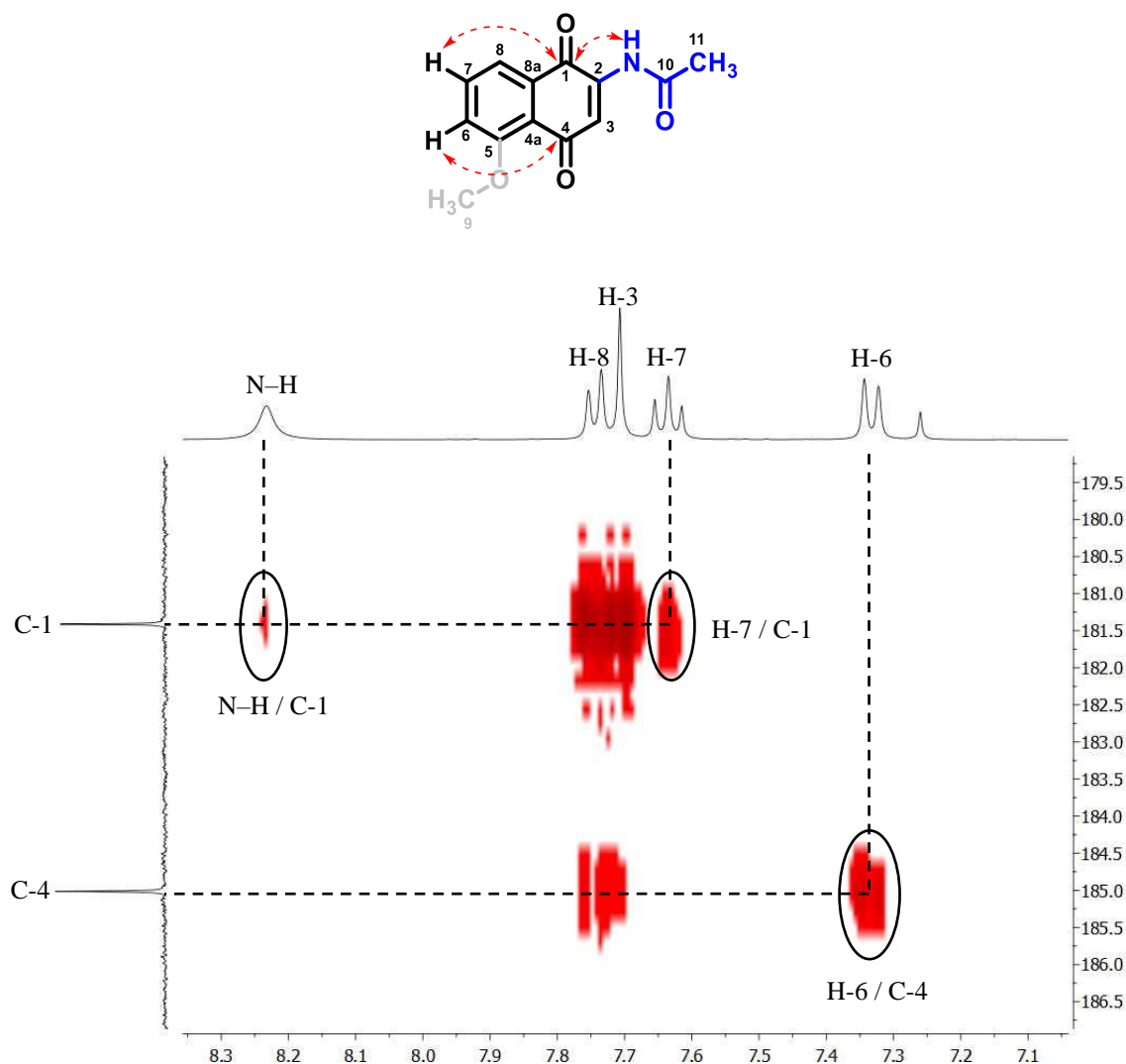
Another strictly important analysis to correctly assign the right position of the acetamido group as well as the non-hydrogenated carbons is the HMBC analysis, since this type of spectrum shows distal interactions. In this spectrum (**Figure 19**) it is possible to see a clear  $^2J_{CH}$  interaction between the hydrogen H-11 and the carbon from the carbonyl C-10, and it is also easy to recognize the signal correlated to the spin-spin coupling  $^3J_{CH}$  between the hydrogen from the methoxy group H-9 and the aryl carbon directly bonded the methoxy group C-5. This same carbon also shows a  $^3J_{CH}$  with the hydrogen H-7. Following the sequence, the hydrogen H-7 also presents another  $^3J_{CH}$  interaction with the non-hydrogenated carbon C-8a. Another important non-hydrogenated carbon in this matter is the naphthoquinoidal carbon directly bonded to the amido group, C-2, which presents a  $^2J_{CH}$  interaction with the hydrogen H-3.



**Figure 19.** Expansion of the HMBC (400 MHz,  $CDCl_3$ ) spectrum of the compound **59f**.



The previous mentioned interactions observed in the HMBC spectrum already indicates the right relative position of the methoxy (at C-5) and the acetamido (at C-2) groups. However, in order to corroborate this proposal, a deeper analysis at the same HMBC spectrum can be done. A further expansion was made, focusing on the region of the carbonyls C-1 and C-4 (**Figure 20**), from which it is possible to observe an  $^3J_{CH}$  interaction between the hydrogen from the amide portion and the carbonyl C-1. This same carbonyl also presents a  $^4J_{CH}$  interaction with the hydrogen C-7. To complement this analysis, it is also possible to recognize a  $^4J_{CH}$  interaction between the hydrogen C-6 and the other carbonyl C-4. From these observations, it is possible to conclude that the acetamido group and the methoxy group are located on opposite sides of the naphthoquinoidal structure.



**Figure 20.** Deeper expansion of the HMBC (400 MHz, CDCl<sub>3</sub>) spectrum of the compound **59f** focusing on the carbonyl region.

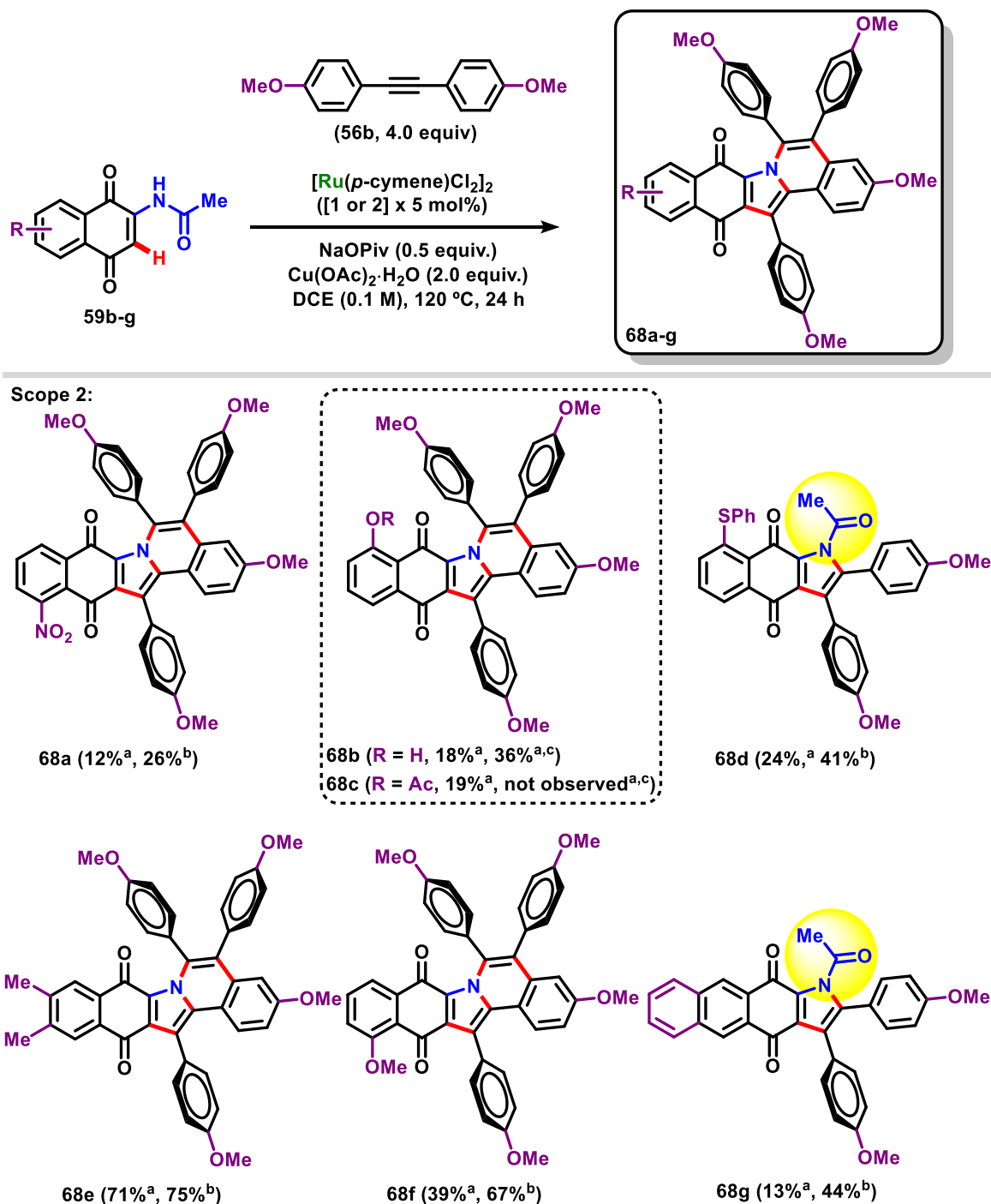
### 3.6.6. A-ring-substituted quinones scope analysis

In the second scope of the study, the A-ring modified quinones previously synthesized (compounds **59b-g**) were applied on both double annulation General Methods A and B (except compound **59c**, applied only on General Procedure A, due to lack of enough amount of substrate) using the symmetrical internal alkyne that presented the best performance from the first scope, compound **56b**, containing a *para*-positioned methoxy group, from which compounds **68a-g** were successfully obtained (**Scheme 40**).

Special attention shall be given to the compound **68c**, previously designed to be obtained from its respective substrate, bearing an acetyl group at the C-5 position, however this substrate was never obtained. Surprisingly, the product **68c** was obtained in 19% yield, not from the acetylated substrate, but as a by-product from its hydroxy correlated substrate **59c**.

The best yields are the ones achieved in the synthesis of compounds **68e** and **68f** (75 and 67% respectively, applying General Procedure B). From this perception, based not only on this scope but also on the previous one, it is possible to infer that effective electron-donating groups improve the reaction performance. Probably, it was caused by a stronger and easier  $\pi$ -interaction between the ruthenium core of the catalyst and the conjugated system of both substrates.

In the process of double-annulation reaction, it is expected a single-annulation to happen first, then a second alkyne to be added afterwards to the molecule *via* C–H activation (as it will be discussed later with the proposed mechanism). In this matter, the single-annulated intermediate is expected to be detected, but in most of the cases, it was not. Only the final double-annulated products were observed. Surprisingly, two specific substrates generated only the single-annulated intermediates, compounds **68d** and **68g**. In these cases, the double-annulated final products were not observed even after a longer time (48 h) of reaction or in the presence of a higher amount of the alkyne **56b** (6.0 equiv.). It is not clear the specific reason for this observed behaviour.



<sup>a</sup>General Procedure A: 1 x 5 mol% of  $[\text{Ru}(p\text{-cymene})\text{Cl}_2]_2$ .

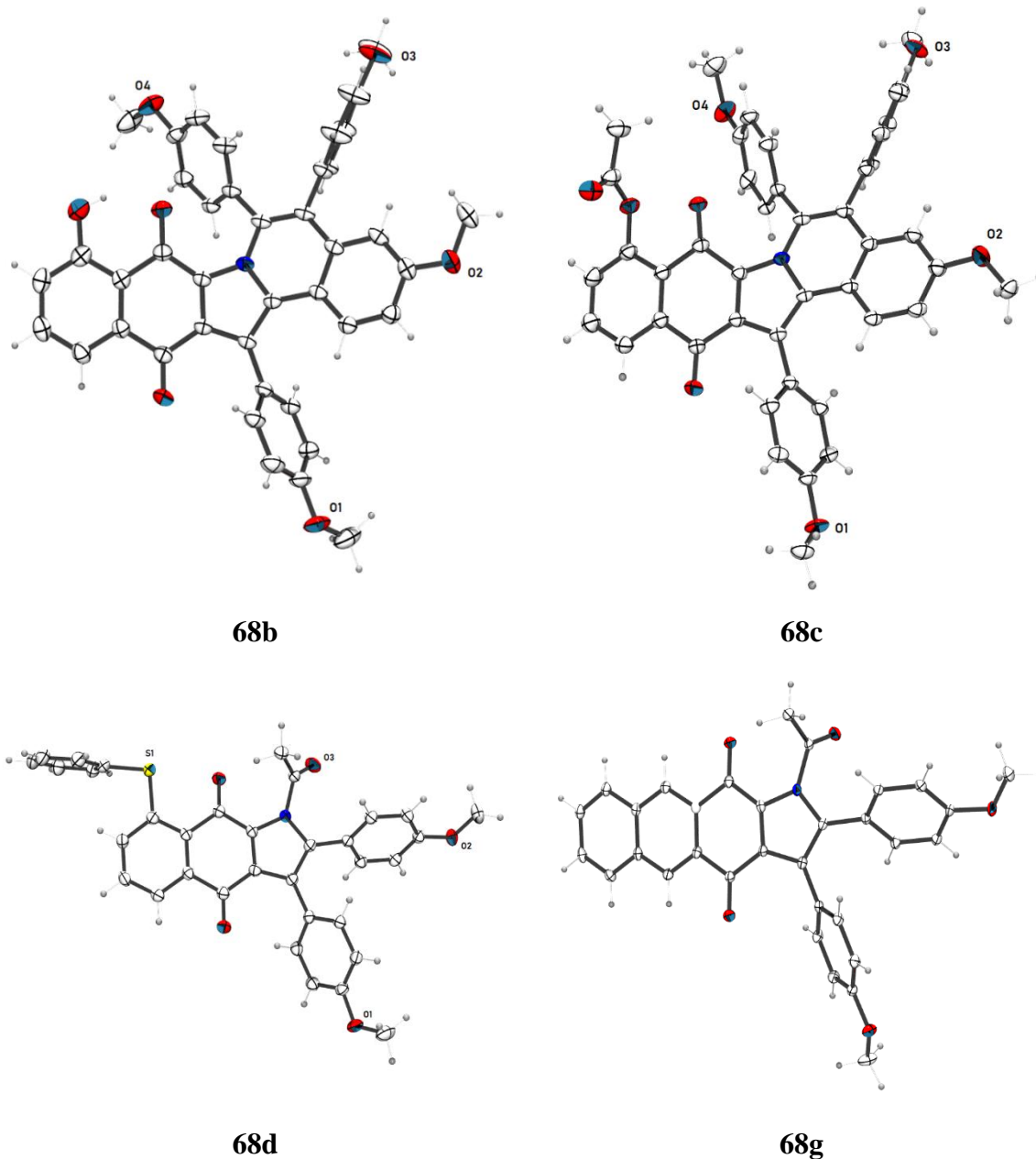
<sup>b</sup>General Procedure B: 2 x 5 mol% of  $[\text{Ru}(p\text{-cymene})\text{Cl}_2]_2$ , 2<sup>nd</sup> load proceeded 12 h after the beginning of the reaction.

<sup>c</sup>Without NaOPiv.

**Scheme 40.** Second scope: double annulation reaction between compounds **59b-g** and symmetrical internal alkyne **56b**.

After the synthesis of each annulated compound of the second scope, a complete characterization was also performed, including <sup>1</sup>H-NMR and <sup>13</sup>C-NMR spectroscopies, COSY, HSQC, HMBC, infrared spectroscopy, high- and low-resolution mass spectrometry, and

melting point. Beyond these methods, four products could have their structures confirmed by crystallographic data analysis (**Figure 21**).

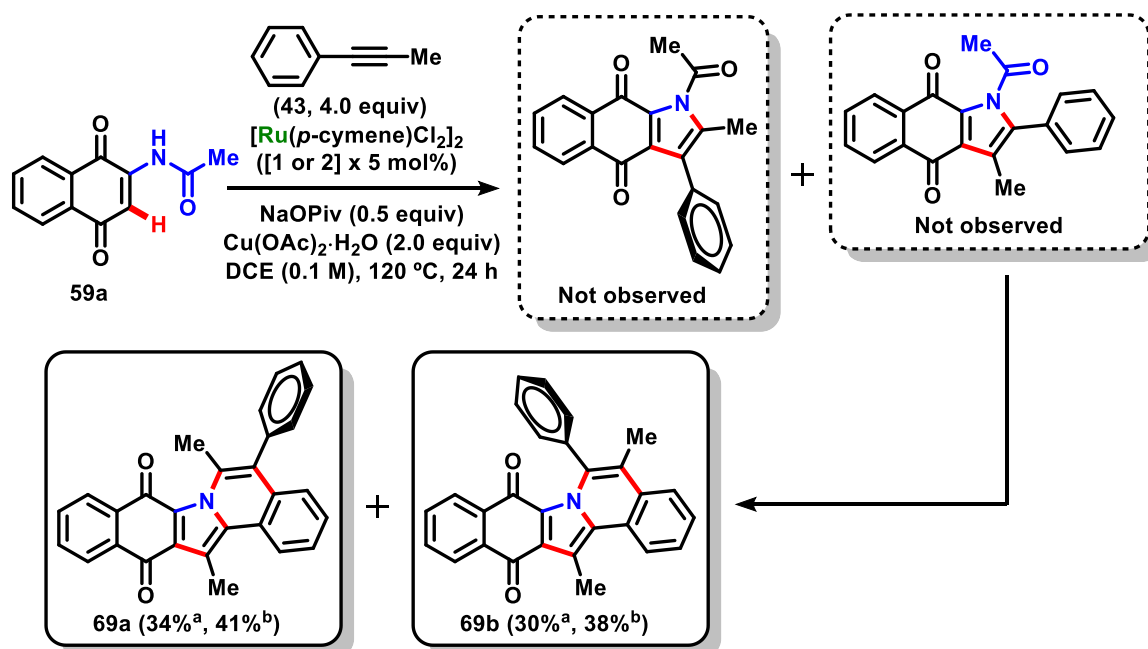


**Figure 21.** Crystal structures of compounds **68b-d,g**.

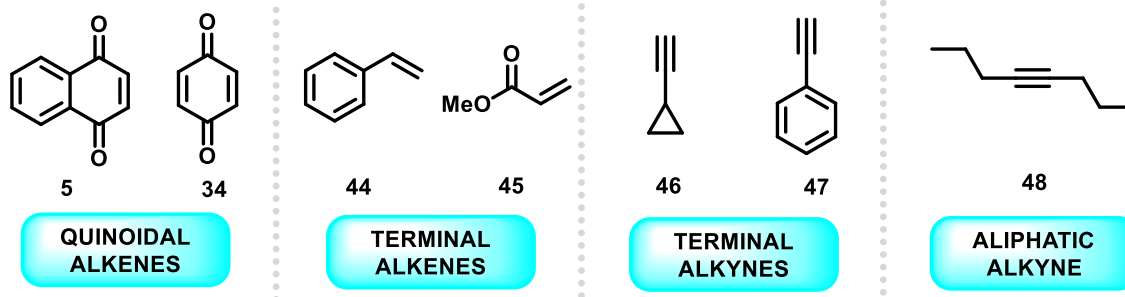
### 3.6.7. Complementary studies

After a complete analysis on the effect of the substituents on both the A-ring modified quinone and the symmetrical internal alkyne, another distinguish study was performed involving the use of non-symmetrical internal alkynes and/or aliphatic alkynes, also some

selected alkenes. For this purpose, the simplest quinone (compound **59a**) was submitted to both General Procedures A and B of double-annulation, in the presence of compounds **5**, **34**, **43-48**. However, only methyl-phenylacetylene (compound **43**) successfully reacted in the standard conditions, generating the products **69a** and **69b** in a 1:1 ratio (Scheme 41). A careful analysis on the structure of the alkyne makes it possible to realize that there is only one possible site for a  $C(sp^2)_{Ar}-H$  activation for this case, since this specific developed method is not adapted to a  $C(sp^3)-H$  activation. From this fact, only one intermediate could lead to the final double-annulated product, and the other intermediate would not go forward and should stop on the single-annulated product. In fact, in this synthesis, none of the single-annulated intermediates were observed.



Unsuccessful alkynes and alkenes tried in the complementary study



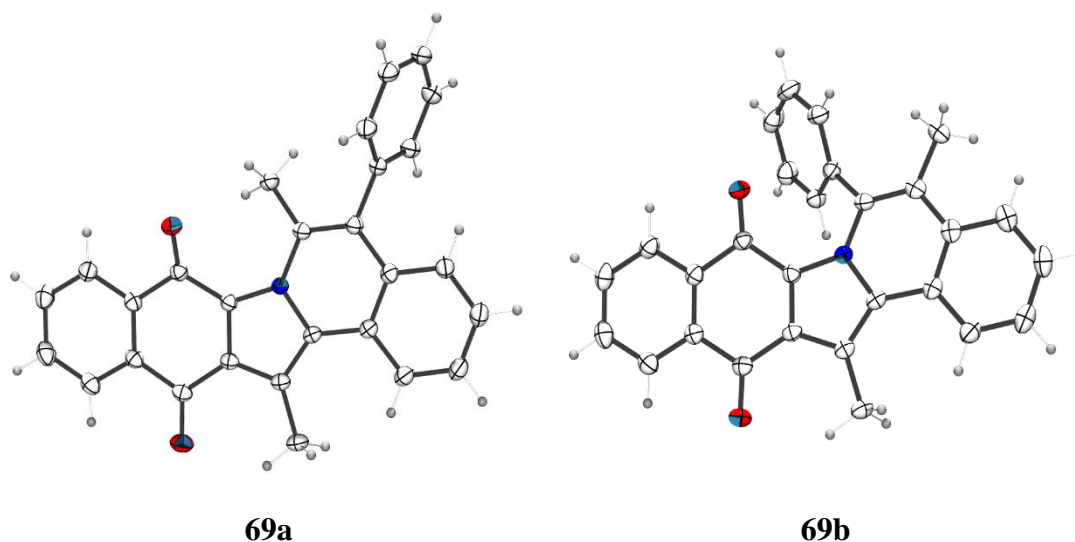
<sup>a</sup>General Procedure A: 1 x 5 mol% of  $[Ru(p\text{-cymene})Cl_2]_2$ .

<sup>b</sup>General Procedure B: 2 x 5 mol% of  $[Ru(p\text{-cymene})Cl_2]_2$ , 2<sup>nd</sup> load proceeded 12 h after the beginning of the reaction.

**Scheme 41.** Complementary study: double annulation reaction between compound **59a** and non-symmetrical internal alkyne **43**.

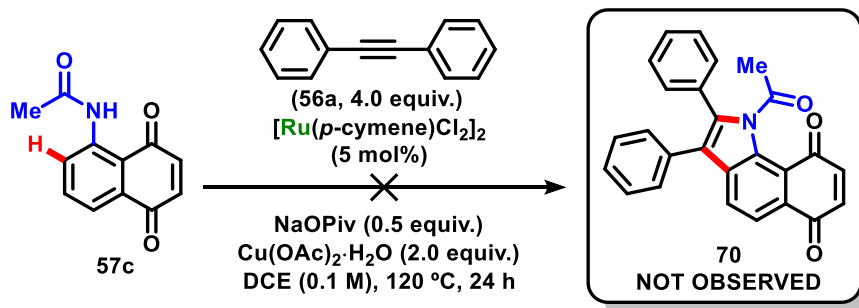
Further analysis on these results made it reasonable to conclude that the presence of a triple bond on the structure of the coupling partner is strictly important, since no cyclization was observed when only alkenes were applied. In the cases of the terminal alkynes, the acidity of the C(sp)–H group may interfere directly on the activity of the catalyst; however, it still does not explain the lack of reactivity of the internal aliphatic alkynes. Although it is not yet clear, this observed result may indicate that the internal alkyne must present at least one aryl group for the overall reaction to happen. This unexpected behaviour is still under analysis.

Both double-annulated products **69a** and **69b** were completely characterized *via*  $^1\text{H}$ -NMR and  $^{13}\text{C}$ -NMR spectroscopy, COSY, HSQC, HMBC, infrared spectroscopy, high- and low-resolution mass spectrometry, melting point and crystallographic data analysis (**Figure 22**).



**Figure 22.** Crystal structures of compounds **69a** and **69b**.

After these observations, a final complementary study was performed to explore the specific requirements of this developed reaction to successfully happen. For that purpose, compound **57c** was submitted to the optimized procedure A, from which the formation of product **70** was expected *via* a single activation at the C-7 position of the substrate, however, no product was observed (**Scheme 42**). This result testifies the fact that modifications at the A-ring of naphthoquinoidal molecules often requires specific systems, sometimes more energy and efforts than a usual C–H activation can offer, explaining the initial issues on the C-5 arylation of the 1,4-naphthoquinone (**5**).

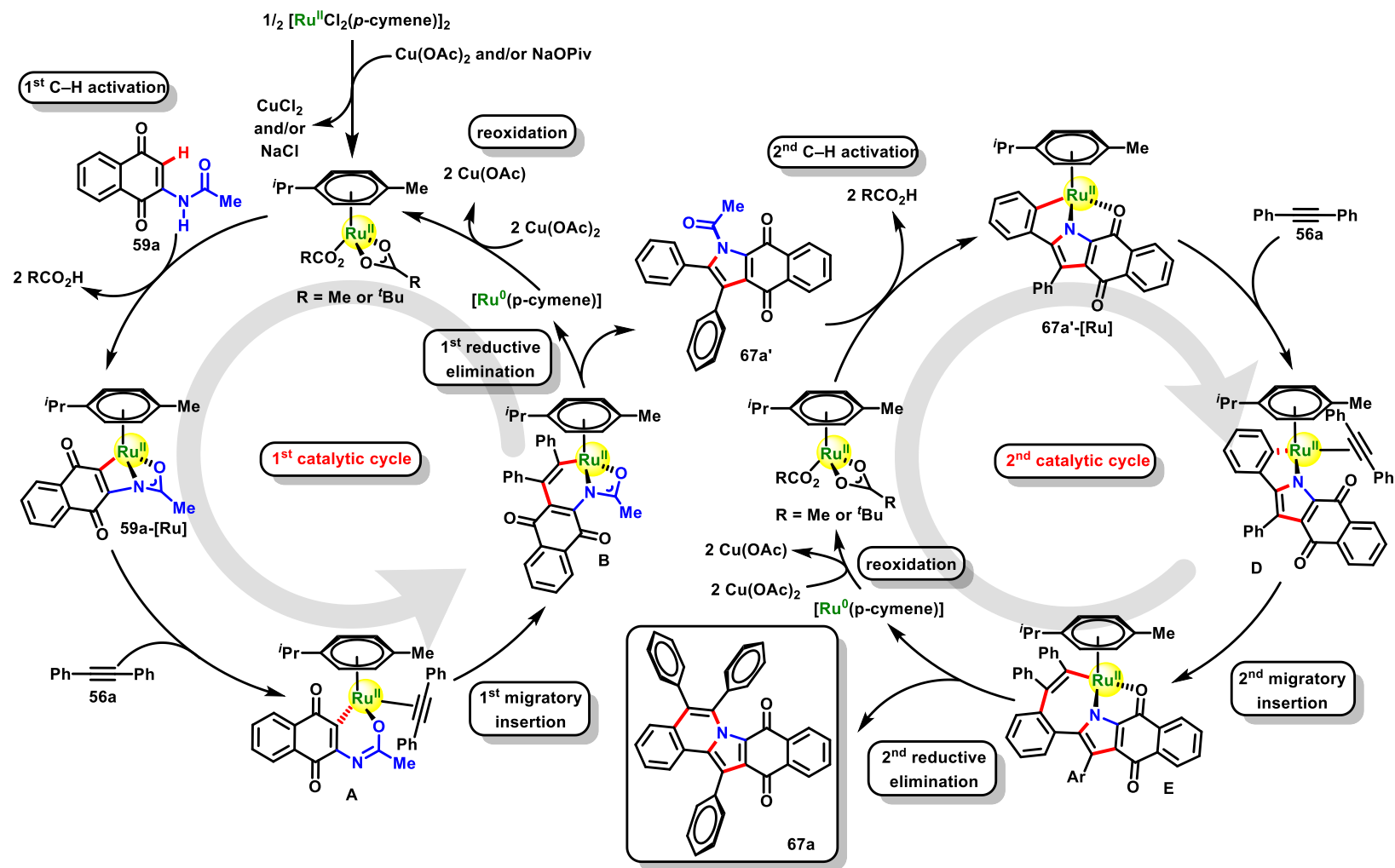


**Scheme 42.** Failed C–H annulation reaction using the substrate **57c** bearing the acetamide DG at the C-5 position.

### 3.7. Mechanistic proposal

A careful analysis on previous published works<sup>77a,i,l,o</sup> led us to propose a possible mechanism adapted to this reaction (**Scheme 43**). It starts with an activation of the catalyst, when the original dimer is dismembered, and the chlorides are exchanged with acetates or pivalates, generating the active ruthenium-II species. After that, a C–H activation step led to the intermediate **59a**-[Ru]. A subsequent interaction with the triple bond of the alkyne causes a reorganization of the ligands, generating the intermediate **A**, which *via* a first migratory insertion leads to the intermediate **B**, with the first formed C–C bond. Now, the first reductive elimination leads to the intermediate **67a'** (the one expected to be observed through the synthesis) and an inactive ruthenium-0 species. A reduction from copper-II acetate to copper-I acetate causes a reoxidation and “re-acetylation” on the ruthenium-0 onto the active ruthenium-II species. In the cases of the synthesis of compounds **68d** and **68g**, the mechanism somehow stops on their respective intermediate, but in all other cases, it moves towards the second cycle.

The second catalytic cycle starts with a second C–H activation between the intermediate **67a'** and the active ruthenium-II species, leading to the intermediate **67a'**-[Ru]. A subsequent interaction with the triple bond of a second alkyne causes a reorganization of the ligands, generating the intermediate **D**. It is followed by a second migratory insertion leading to the intermediate **E**, with the formation of the second C–C bond. Here, the second reductive elimination takes place and leads to the final product **67a** and an inactive ruthenium-0 species. Another reduction from copper-II acetate to copper-I acetate causes a re-oxidation and “re-acetylation” on the ruthenium-0 generating the active ruthenium-II species, recharging the catalytic cycle.



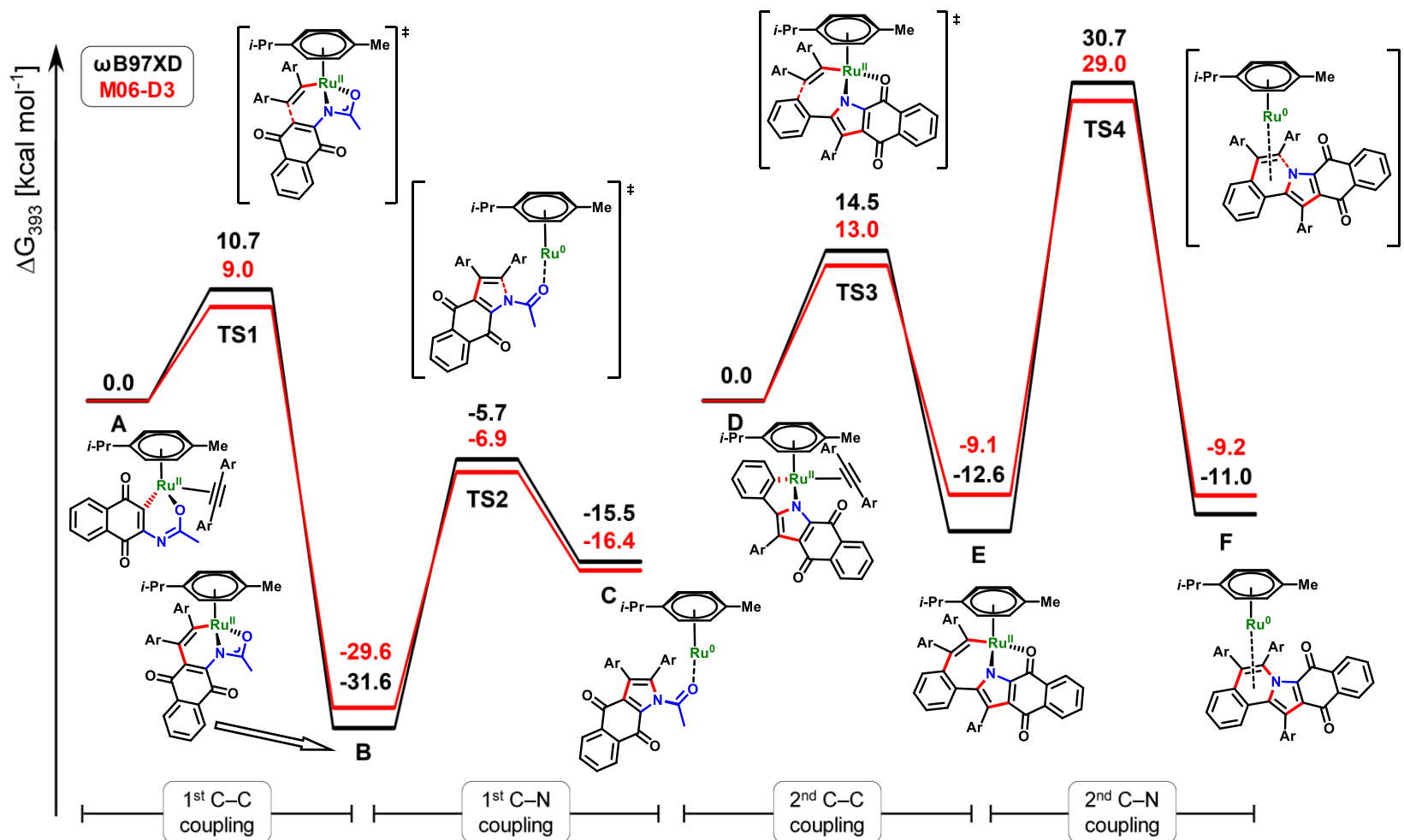
**Scheme 43.** Proposed mechanism for the double-annulation reaction via C(sp<sup>2</sup>)<sub>Ar</sub>-H activation using compound **67a** as example.



To confirm this proposed mechanism, computational data was obtained for each intermediate and the relative theoretical free Gibbs energy-level was calculated and analyzed, using two different levels of theory ( $\omega$ B97XD and M06-D3), fixing intermediates **A** and **D** as points of correlation (0.0 kcal mol<sup>-1</sup>) for the 1<sup>st</sup> and 2<sup>nd</sup> catalytic cycles, respectively (**Figure 23**).

The energy barrier for the first migratory insertion from the intermediate **A** to the transition state **TS1** is only 10.7 kcal mol<sup>-1</sup>, while intermediate **B** is stabilized by 31.6 kcal mol<sup>-1</sup> in comparison to **A**, making this first C–C bond formation the quicker one to happen. The first C–N coupling, from intermediate **B** to **C**, is achieved afterwards through a transition state **TS2** with an energy barrier of 25.9 kcal mol<sup>-1</sup>, and the intermediate **C** has an energy level 16.1 kcal mol<sup>-1</sup> higher than its original intermediate **B**, making this a considerably endothermic step.

In the second catalytic cycle, the energy barrier of the migratory insertion step from the intermediate **D** to its transition state **TS3** is 14.5 kcal mol<sup>-1</sup>, and the following intermediate **E** is favorable by 12.6 kcal mol<sup>-1</sup> in comparison to **D**. However, the second C–N coupling from intermediate **E** to **F**, through the transition state **TS4**, has an extremely high energy barrier of 43.3 kcal mol<sup>-1</sup>, with intermediate **F** almost on the same energetic level of intermediate **E**, only 1.6 kcal mol<sup>-1</sup> higher. This high energy barrier explains the high temperature needed to perform this reaction (120 °C).



**Figure 23.** Relative Gibbs free energy profile for the double-annulation reaction of **59a** with **56a** at the  $\omega\text{B97XD}/\text{def2TZVPP}+\text{SMD}(\text{DCE})$  and  $\text{M06-D3}/\text{def2TZVPP}+\text{SMD}(\text{DCE})$  levels of theory.

### 3.8. Biological assays

Once achieved and fully characterized, all twenty final products (**67a-k**, **68a-g** and **69a,b**) were tested for cytotoxic activity in cell culture *in vitro* using seven cancer cell lines (**HCT-116**: human colon cancer cell line, **L929**: mouse fibroblast cell line, **MCF-7**: human breast cancer cell line, **HL-60**: human leukemia cell line, **SNB-19**: human glioblastoma cell line, **NCI-H460**: human lung cancer cell line, **PC3**: human prostatic cell line) employing the MTT method. Despite the unmeasurable efforts spent here to achieve several new molecules, unfortunately, none of the products prepared in this study showed a desirable antitumor activity against any of the above-mentioned cancer cell lines. In all cases, the compounds presented values of  $IC_{50} > 15 \mu M$ , except against HL-60, for the derivatives presented in **Table 14**, a considerable high value when compared to Doxorubicin, the positive control adopted in this assay.

**Table 14.** Activity of some double-annulated products against HL-60 cancer cell lines.

Compounds	$IC_{50}$ ( $\mu M$ )
<b>67d</b>	2.92 (2.38-3.60)
<b>67j</b>	13.19 (11.69-14.88)
<b>68a</b>	8.45 (6.98-10.23)
<b>68g</b>	3.17 (2.66-3.77)
<b>Doxorubicin</b>	0.02 (0.01-0.02)

#### 4. CONCLUSIONS AND PERSPECTIVES

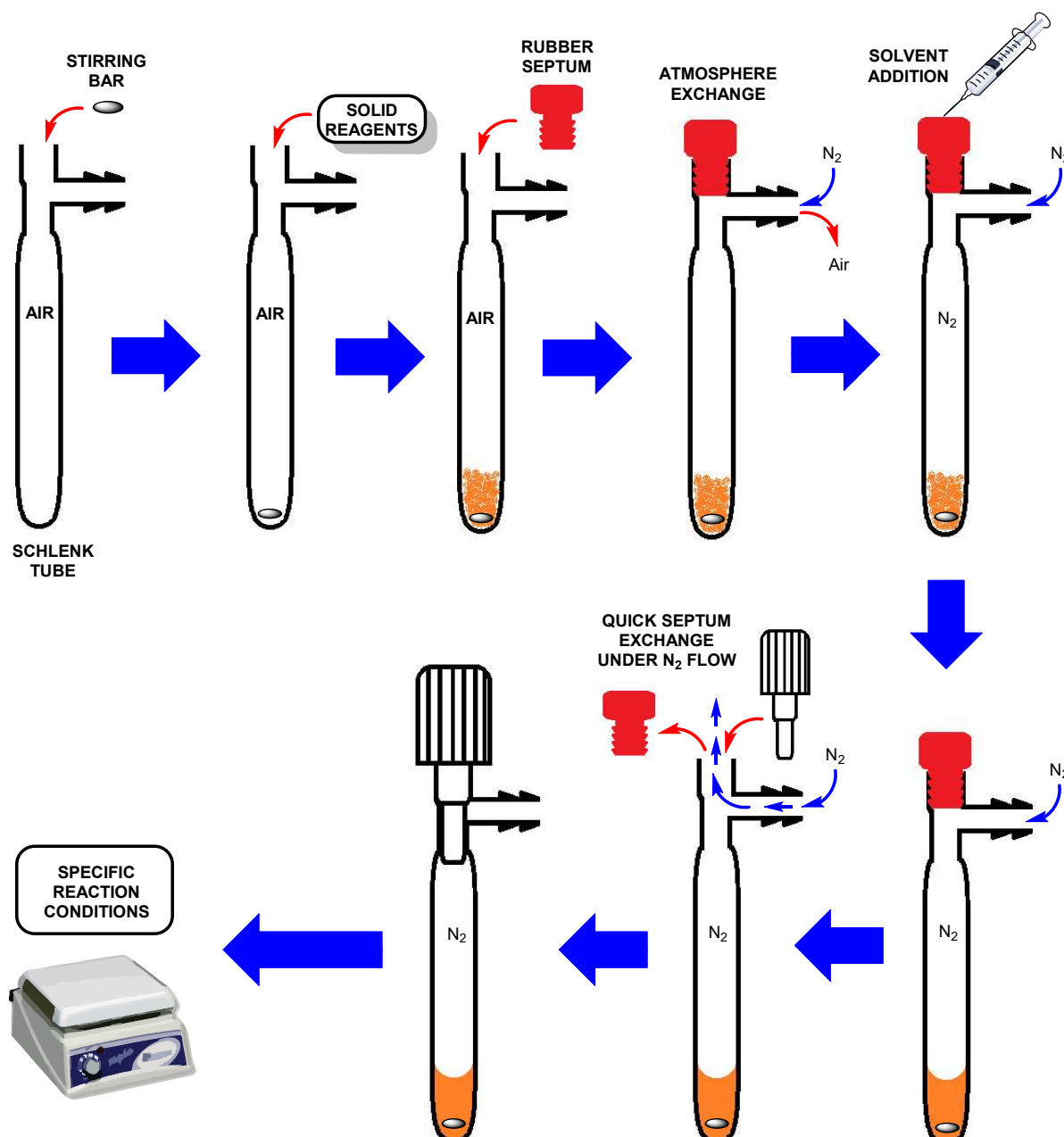
In a general point of view, this work presents the complete analysis of the intrinsic directing behaviour of the carbonyl groups of naphthoquinoidal compounds, from which none of the expected positive results were achieved. However, once the pathway of the research shifted into the analysis of the directing behaviour of synthesizable DG, placed at the C-2 position of the 1,4-naphthoquinone, some extremely interesting results were observed. This project led to the obtention of twenty new polycyclic quinones *via* a ruthenium-catalyzed double annulation reaction, and the synthesis method applied for the obtention of their respective starting materials were completely described. A total of eighteen compounds had their structure confirmed by crystallographic data analysis (four substrates, eight products from the first scope, four from the second scope and two from the complementary studies).

This developed method is characterized as a new procedure that can generate four new bonds (two C–C bonds and two C–N bonds) in a single step *via* a current spotlight process known as C(sp<sup>2</sup>)–H activation reaction. It presented moderate to good yields on both general methods A and B (12% to 91%). Computational studies and literature studies made it possible to propose a plausible and interesting mechanism for this reaction. All achieved products were evaluated against seven cancer cell lines, including HL-60, a human leukemia cell line. Unfortunately, none of them presented a promising antitumor activity. The results achieved in this project and hereby described were published in 2020 in *Chemistry – A European Journal* and served as a primary source of knowledge to the production of several other important review articles regarding specific aspects of C–H activation procedures. This innovative method can offer to the scientific society a quicker and easier way to achieve complex polycyclic molecules applying a single-step reaction and can contribute to the development of new compounds yet to be discovered.

## 5. EXPERIMENTAL

### 5.1. Materials and equipment

All metal-catalyzed reactions were carried out under a nitrogen atmosphere in a 10 mL Schlenk or pressure tubes, according to the general procedure described in the scheme below.

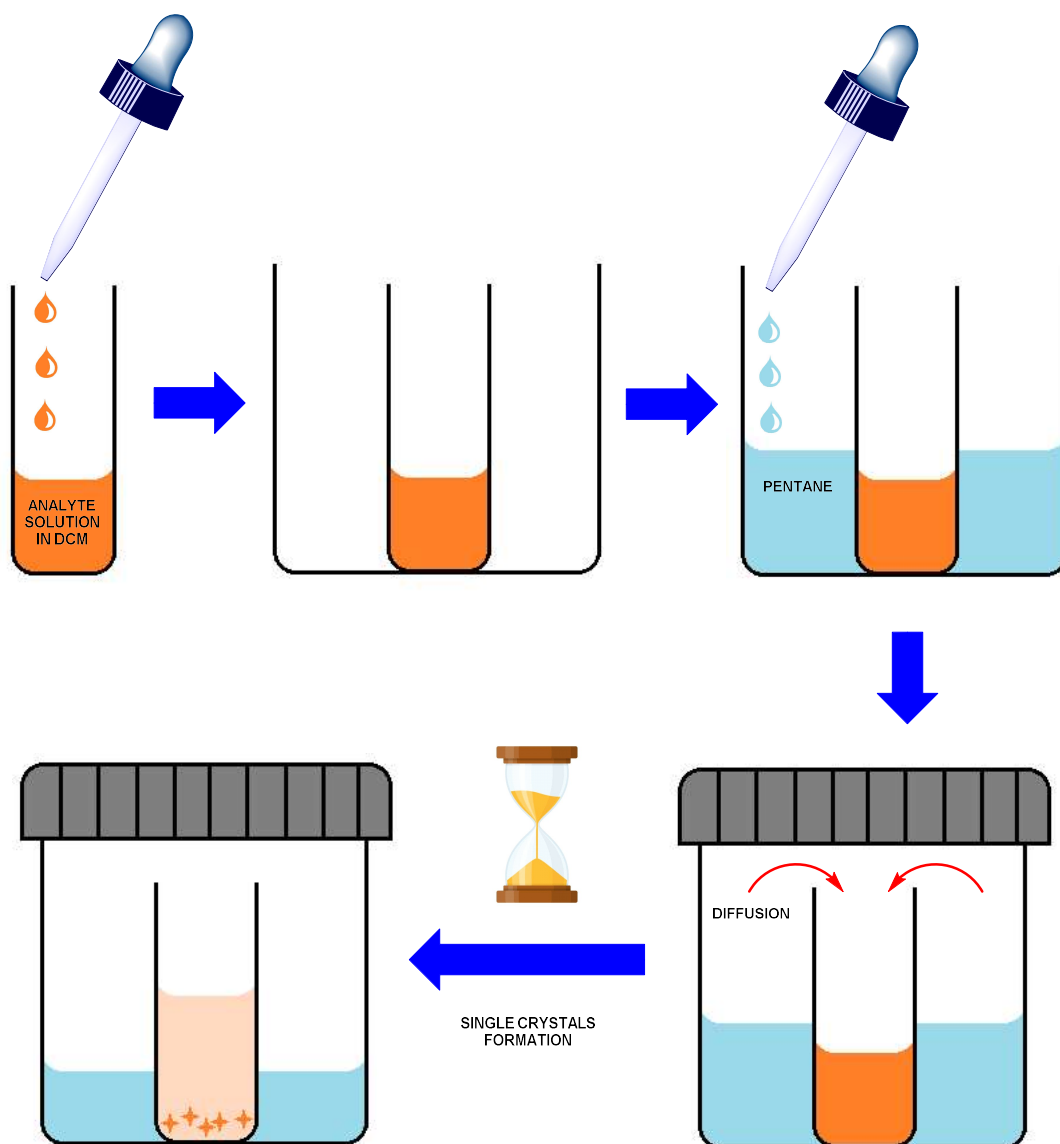


The solvents were dried using the following methods: 1,2-dichloroethane (DCE), *N,N*-dimethylformamide (DMF), *N,N*-dimethylacetamide (DMA) and *N*-methylpyrrolidone (NMP) were dried with CaH<sub>2</sub> and distilled under an atmosphere of N<sub>2</sub>; 2-methyl-2-butanol, toluene and *o*-xylene were dried using Na and distilled under an atmosphere of N<sub>2</sub>. 1,4-Naphthoquinone (**5**) and 1,4-benzoquinone (**34**) were purified *via* reduced pressure sublimation using a cold finger sublimation apparatus (50 °C, 0.9 mbar). Alkenes **44** and **45**, and alkynes **56a**, **43**, **46**, **47** and **48** were used as purchased, without further purification. Other chemicals were obtained from commercial sources and used without further purification.

The reaction concentration is expressed in molar (M), this concentration was calculated by the ratio of the amount of the main reactant (limiting agent) in mmol and the volume of solvent applied, in mL. Yields refer to isolated compounds, estimated to be >95% pure as determined by <sup>1</sup>H-NMR. TLC: Merck, TLC Silica gel 60 F<sub>254</sub>, detection at 254 nm. Infrared spectra were recorded on a Bruker ATR FT-IR Alpha device and IR Prestige-21 Shimadzu using KBr plates. Mass-spectra: EI-MS: Jeol AccuTOF at 70 eV; ESI-MS: Bruker maXis and MicroTOF. High resolution mass spectrometry (HRMS): Bruker maXis, Bruker MicroTOF and Jeol AccuTOF. Melting points: Büchi 540 capillary melting point apparatus, values are uncorrected. NMR spectra were recorded on Varian Mercury VX 300, Inova-500, Inova-600 and Bruker Avance 300, Avance III 300, Avance III HD 400, Avance III 400, Avance III HD 500 and Avance NEO 600 instruments, if not otherwise specified, chemical shifts ( $\delta$ ) are provided in ppm. <sup>13</sup>C-NMR shifts are classified as: C<sub>q</sub> (non-hydrogenated carbon), CH, CH<sub>2</sub>, CH<sub>3</sub>, indicating the nature of the carbon assigned, according to what observed by DEPT or ATP analysis. All structure names were given under IUPAC rules by CS ChemDraw Ultra program.

Single crystals were recrystallised from a mixture of dichloromethane and pentane using a system of vapor diffusion. In this case, the analyte was dissolved in the lowest amount of dichloromethane possible and placed in a small flask which was then placed inside a larger flask, according to the general scheme below. Pentane was poured inside the larger flask, but outside the smaller flask, until the limit of pentane exceeded the limit of dichloromethane. The larger flask was tightly capped, and the system was placed on a motionless surface. This system must stay untouched and completely steady until the formation of the single crystals. After the slow diffusion of pentane into the dichloromethane (it usually takes within three to five days), the crystals were obtained and analysed on a Bruker D8 Venture AgMo Dual Source

diffractometer. Using Olex2,<sup>106</sup> the structures were solved with the XT<sup>107</sup> structure solution program using Intrinsic Phasing and refined with the XL<sup>108</sup> refinement package using Least Squares minimisation.



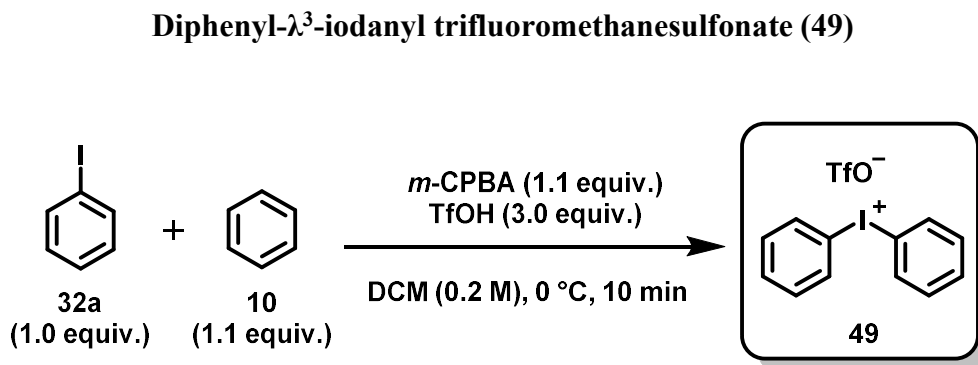
<sup>106</sup> Dolomanov, O. V.; Bourhis, L. J.; Gildea, R. J.; Howard, J. A. K.; Puschmann, H. *J. Appl. Cryst.*, **2009**, *42*, 339-341.

<sup>107</sup> Sheldrick, G. M. *Acta Cryst.*, **2015**, *A71*, 3-8.

<sup>108</sup> Sheldrick, G. M. *Acta Cryst.*, **2008**, *A64*, 112-122.

## 5.2. C–H arylation trials

### 5.2.1. Synthesis of arylating agent 49



In a 100 mL round bottom flask, *m*-CPBA (2.46 g, 11 mmol) and iodobenzene (**32a**, 1.14 mL, 10 mmol) were dissolved in 44 mL of DCM (0.2 M) and the solution was stirred at room temperature for 10 min. Benzene (**10**, 980  $\mu$ L, 11 mmol) was then added to the solution, and the mixture was cooled down to 0  $^\circ$ C. Triflic acid (2.7 mL, 30 mmol) was carefully added dropwise to the mixture. The solution was kept under stirring for additional 10 minutes, while it naturally reached room temperature. The solvent was removed under reduced pressure, then 100 mL of diethyl ether was added. After stirring for 30 minutes at room temperature and sitting in freezer at -22  $^\circ$ C for 1 h, a precipitate was formed. The solid was filtrated under vacuum and washed with diethyl ether (3 x 50 mL), leading to the obtention of compound **49** (3.8 g, 90%) as an off-white solid.

**Melting point:** 175-178  $^\circ$ C.

**$^1\text{H}$  NMR (300 MHz, DMSO- $d_6$ )  $\delta$ :** 8.26 (d,  $J$  = 7.5 Hz, 4H), 7.66 (t,  $J$  = 7.5 Hz, 2H), 7.53 (t,  $J$  = 7.5 Hz, 4H).

**$^{13}\text{C}$  NMR (75 MHz, DMSO- $d_6$ )  $\delta$ :** 135.2 (CH), 132.1 (CH), 131.8 (CH), 116.5 (C<sub>q</sub>).

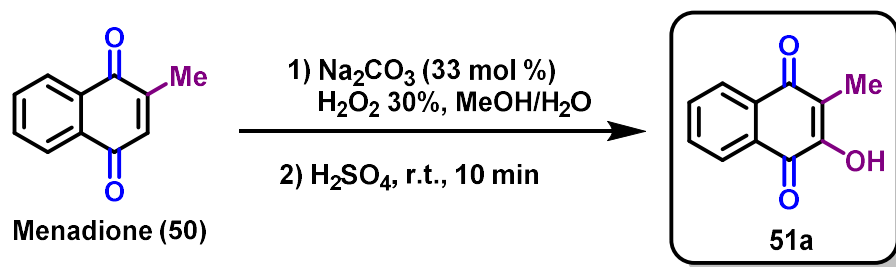
*The analytical data are in accordance with those reported in the literature.*<sup>109</sup>

<sup>109</sup> Osuský, P.; Nociarová, J.; Smolíček, M.; Gyepes, R.; Georgiou, D.; Polyzos, I.; Fakis, M.; Hrobárik, P. *Org. Lett.*, **2021**, *23*, 5512-5517.



### 5.2.2. Synthesis of modified substrates (51a-c)

#### 2-hydroxy-3-methylnaphthalene-1,4-dione (51a)



Menadione (**50**, 1 g, 5.8 mmol) was dissolved in 10 mL of methanol (0.6 M) at 0 °C under continuous stirring. A solution of sodium carbonate (200 mg, 1.9 mmol) in 6 mL of a mixture H<sub>2</sub>O<sub>2</sub> 30% 1:5 water was carefully added to the reaction at 0 °C. Once the reaction is complete, 100 mL of distilled water was added, from which a white precipitate was formed. The solid was filtered off and redissolved in 5 mL of concentrated sulfuric acid. The solution was stirred for 10 min at room temperature. Afterwards, 20 mL of distilled water was added, from which a yellow precipitate was formed. After filtration, the product was purified by column chromatography (Hexane/EtOAc 4:1), leading to the formation of the desired product **51a** (781 mg, 72%) as a yellow solid.

**Melting point:** 173-175 °C.

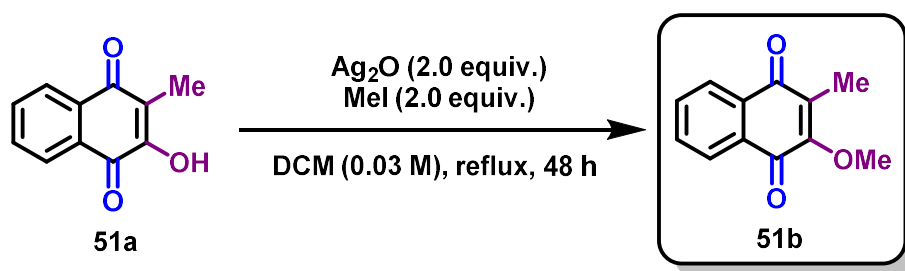
**<sup>1</sup>H NMR (300 MHz, CDCl<sub>3</sub>)**  $\delta$ : 8.11 (dd,  $J = 7.8, 1.2$  Hz, 1H), 8.07 (dd,  $J = 7.5, 1.2$  Hz, 1H), 7.74 (td,  $J = 7.5, 1.2$  Hz, 1H), 7.67 (td,  $J = 7.8, 1.2$  Hz, 1H), 7.33 (s, 1H), 2.10 (s, 3H).

**<sup>13</sup>C NMR (75 MHz, CDCl<sub>3</sub>)**  $\delta$ : 185.2 (C<sub>q</sub>), 181.3 (C<sub>q</sub>), 153.3 (C<sub>q</sub>), 135.0 (CH), 133.0 (CH + C<sub>q</sub>), 129.6 (C<sub>q</sub>), 126.9 (CH), 126.3 (CH), 120.7 (C<sub>q</sub>), 8.8 (CH<sub>3</sub>).

**IR (KBr):** 3371 (s, O–H), 1660 (s, C=O), 1646 (s, C=O), 1590 (s, CH<sub>3</sub>), 1275 (s, C–O), 1071 (s, C–O), 723 (s, C–H<sub>Ar</sub>) cm<sup>-1</sup>.

*The analytical data are in accordance with those reported in the literature.<sup>16d</sup>*

### 2-methoxy-3-methylnaphthalene-1,4-dione (**51b**)



Compound **51a** (188 mg, 1.0 mmol) was dissolved in 30 mL of DCM (0.03 M) in a 100 mL rounded-bottom flask. Silver-I oxide (464 mg, 2.0 mmol) and iodomethane (125  $\mu\text{L}$ , 2.0 mmol) was added to the solution. The mixture was kept under reflux for 48 h. Once the reaction was complete, the mixture was filtered in a celite pad, washed with DCM and purified by column chromatography (*n*-Hexane/EtOAc 5:1). Product **51b** (313 mg, 75%) was obtained as a yellow solid.

**Melting point:** 100-104 °C.

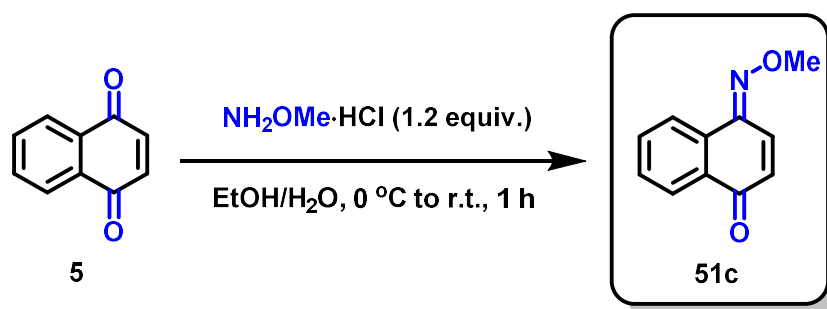
**$^1\text{H}$  NMR (300 MHz,  $\text{CDCl}_3$ )  $\delta$ :** 8.08-8.03 (m, 2H), 7.72-7.66 (m, 2H), 4.12 (s, 3H), 2.10 (s, 3H).

**$^{13}\text{C}$  NMR (75 MHz,  $\text{CDCl}_3$ )  $\delta$ :** 185.9 ( $\text{C}_q$ ), 181.4 ( $\text{C}_q$ ), 158.0 ( $\text{C}_q$ ), 133.9 (CH), 133.4 (CH), 132.1 ( $\text{C}_q$ ), 131.9 ( $\text{C}_q$ ), 131.6 ( $\text{C}_q$ ), 126.3 (CH), 126.3 (CH), 61.2 ( $\text{CH}_3$ ), 9.5 ( $\text{CH}_3$ ).

**IR (KBr):** 1674 (s, C=O), 1651 (s, C=O), 1614 (s,  $\text{CH}_3$ ), 1592 (s,  $\text{CH}_3$ ), 1267 (s, C–O), 1086 (s, C–O), 721 (s, C–H<sub>Ar</sub>)  $\text{cm}^{-1}$ .

*The analytical data are in accordance with those reported in the literature.<sup>16d</sup>*

**(E)-4-(methoxyimino)naphthalen-1(4H)-one (51c)**



1,4-Naphthoquinone (**5**, 680 mg, 4.3 mmol) was dissolved in 25 mL of ethanol (0.17 M). The solution was then cooled down to  $0\text{ }^\circ\text{C}$ . A solution of methoxyamine hydrochloride (420 mg, 5.0 mmol) in 10 mL of distilled water was carefully added. The mixture was kept under vigorous stirring for additional 1h while naturally reaching room temperature. Column chromatography ("Hexane/EtOAc 4:1) on silica gel led to the successful obtention of compound 51c (626 mg, 78%) as a yellow solid.

**Melting point:** 80-85  $^\circ\text{C}$ .

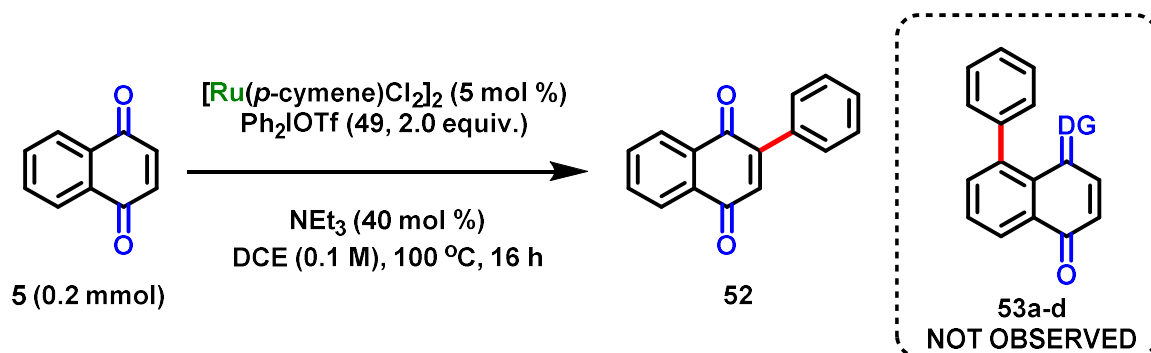
**$^1\text{H}$  NMR (300 MHz,  $\text{CDCl}_3$ )  $\delta$ :** 8.22 (dd,  $J = 7.2, 1.5$  Hz, 1H), 8.13 (dd,  $J = 7.8, 1.5$  Hz, 1H), 7.87 (d,  $J = 10.5$  Hz, 1H), 7.61 (td,  $J = 7.2, 1.5$  Hz, 1H), 7.54 (td,  $J = 7.8, 1.5$  Hz, 1H), 6.61 (d,  $J = 10.5$  Hz, 1H), 4.20 (s, 3H).

**$^{13}\text{C}$  NMR (75 MHz,  $\text{CDCl}_3$ )  $\delta$ :** 185.4 ( $\text{C}_q$ ), 145.8 ( $\text{C}_q$ ), 133.0 ( $\text{C}_q$ ), 132.9 (CH), 132.0 (CH), 130.5 ( $\text{C}_q$ ), 129.8 (CH), 126.7 (CH), 126.5 (CH), 123.0 (CH), 64.0 ( $\text{CH}_3$ ).

*The analytical data are in accordance with those reported in the literature.*<sup>110</sup>

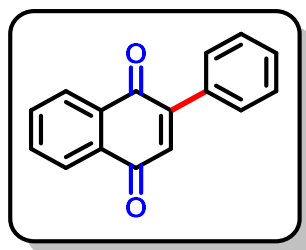
<sup>110</sup> Fischer, A.; Golding, R. M.; Tennant, W. C. *J. Chem. Soc.*, **1965**, 1127, 6032-6035.

### 5.2.3. General C–H arylation procedure



Under an atmosphere of  $\text{N}_2$ , a 10 mL Schlenk tube was charged with the corresponding naphthoquinone (0.20 mmol),  $[\text{RuCl}_2(p\text{-cymene})]_2$  (6 mg, 5 mol %) and  $\text{Ph}_2\text{IOTf}$  (**49**, 172 mg, 0.4 mmol). Then, a solution of  $\text{NEt}_3$  (11  $\mu\text{L}$ , 0.08 mmol) in DCE (2 mL, 0.1 M) was added *via* a syringe. The reaction mixture was heated to 100 °C for 16 h. The mixture was then cooled to room temperature, filtered through a pad of celite and the solvent was removed under reduced pressure. The crude product was purified by column chromatography on silica gel ( $^n\text{Hexane/EtOAc}$  4:1).

#### 2-phenylnaphthalene-1,4-dione (**52**)



The general procedure for C–H arylation was followed by using **5** (32 mg, 0.20 mmol) as starting material. Purification by column chromatography on silica gel ( $^n\text{Hexane/EtOAc}$  4:1) yielded **52** (7 mg, 15%) as an orange solid. Product **53a** was not observed.

**Melting point:** 95-98 °C.

$^1\text{H NMR}$  (300 MHz,  $\text{CDCl}_3$ )  $\delta$ : 8.22-8.17 (m, 1H), 8.15-8.10 (m, 1H), 7.81-7.75 (m, 2H), 7.62-7.56 (m, 2H), 7.51-7.47 (m, 3H), 7.09 (s, 1H).

$^{13}\text{C}$  NMR (75 MHz,  $\text{CDCl}_3$ )  $\delta$ : 185.3 ( $\text{C}_q$ ), 184.5 ( $\text{C}_q$ ), 148.3 ( $\text{C}_q$ ), 135.4 (CH), 134.0 (CH), 134.0 (CH), 133.5 ( $\text{C}_q$ ), 132.6 ( $\text{C}_q$ ), 132.2 ( $\text{C}_q$ ), 130.2 (CH), 129.6 (CH), 128.6 (CH), 127.2 (CH), 126.1 (CH).

IR (KBr): 1651 (*s*, C=O), 1588 (*m*, C=O), 757 (*s*, C–H<sub>Ar</sub>)  $\text{cm}^{-1}$ .

HRMS-ESI (+): 235.0751  $[\text{M}+\text{H}]^+$ . Calc. for  $(\text{C}_{16}\text{H}_{11}\text{O}_2)^+$ : 235.0754.

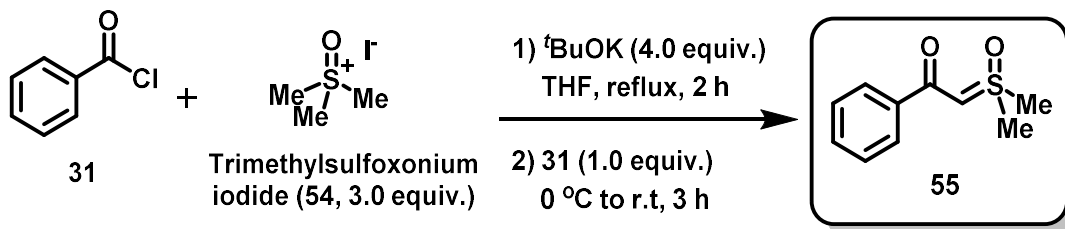
The analytical data are in accordance with those reported in the literature.<sup>111</sup>

Compounds **28**, **51a**, **51b**, **51c** were submitted to the same general procedure described above for the ruthenium-catalyzed C–H arylation aiming the obtention of their respective products analogues **53b-e**, however, in all cases, only the respective starting material was observed after 16 h of reaction.

### 5.3. C–H annulation trials

#### 5.3.1. Synthesis of sulfoxonium ylide (**55**)

##### 2-(dimethyl(oxo)- $\lambda^6$ -sulfanylidene)-1-phenylethan-1-one (**55**)



Potassium *tert*-butoxide (1.50 g, 13.6 mmol) was dissolved in 15 mL of dry THF. Trimethylsulfoxonium iodide (**54**, 2.24 g, 10.2 mmol) was then added to the solution. The mixture was kept under reflux (around 66 °C) for 2 h. Once complete, the reaction was cooled to 0 °C, and benzoyl chloride (**31**, 395  $\mu\text{L}$ , 3.4 mmol) was carefully added dropwise. The final mixture was stirred at room temperature for additional 3 h. Afterwards, the solvent was removed under reduced pressure, and 40 mL of distilled water was added. The aqueous solution was extracted with ethyl acetate (8 x 20 mL). The organic phase was dried over  $\text{Na}_2\text{SO}_4$  and purified by column chromatography (*n*-Hexane/EtOAc 4:1) on silica gel. Product **55** (222 mg, 81%) was achieved as an off-white solid.

<sup>111</sup> Gontijo, T. B.; de Carvalho, R. L.; Dantas-Pereira, L.; Menna-Barreto, R. F. S.; Rogge, T.; Ackermann, L. da Silva Júnior, E. N. *Bioorg. Med. Chem.*, **2021**, *40*, 116164.

**Melting point:** 114-116 °C.

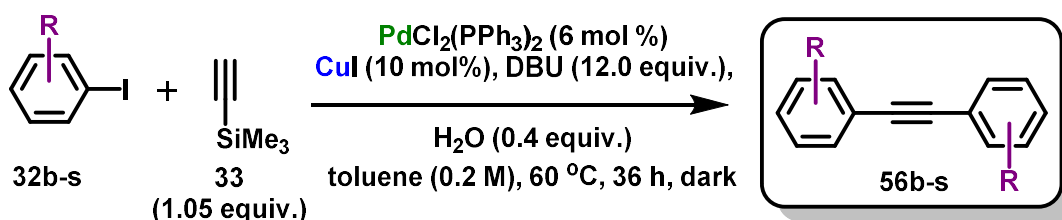
**<sup>1</sup>H NMR (300 MHz, CDCl<sub>3</sub>) δ:** 7.79-7.76 (m, 2H), 7.44-7.34 (m, 3H), 5.00 (s, 1H), 3.49 (s, 6H).

**<sup>13</sup>C NMR (75 MHz, CDCl<sub>3</sub>) δ:** 182.5 (C<sub>q</sub>), 138.9 (C<sub>q</sub>), 130.9 (CH), 128.3 (CH), 126.6 (CH), 68.7 (CH), 42.4 (CH<sub>3</sub>).

**IR (KBr):** 3435 (w, O–H<sub>residual water</sub>), 3011 (m, C–H<sub>Alkene</sub>), 1587 (m, CH<sub>3</sub>), 1532 (s, C=O), 1389 (s, S=O), 1177 (s, S=O), 705 (s, C–H<sub>Ar</sub>) cm<sup>-1</sup>.

The analytical data are in accordance with those reported in the literature.<sup>112</sup>

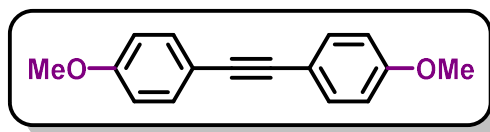
### 5.3.2. Synthesis of symmetrical internal alkynes (56b-s)



Under an atmosphere of N<sub>2</sub>, a 100 mL Schlenk flask was charged with the corresponding iodoarene (**32**, 9.6 mmol), PdCl<sub>2</sub>(PPh<sub>3</sub>)<sub>2</sub> (101 mg, 6 mol %) and copper-I iodide (91 mg, 10 mol %). Then, a solution of trimethylsilylacetylene (**33**, 714 μL, 5.04 mmol), DBU (9 mL, 58.0 mmol) and water (35 μL, 1.92 mmol) in toluene (24 mL, 0.2 M) was added *via* a syringe. The flask was covered in aluminium foil to avoid any incidental light, and the reaction mixture was heated to 60 °C for 36 h. The mixture was then cooled to room temperature and portioned into ethyl acetate (50 mL) and water (50 mL). The organic phase was washed with HCl 1M (3 x 75 mL) and saturated NaCl solution (1 x 75 mL). The organic residue was dried over Na<sub>2</sub>SO<sub>4</sub>, filtered, and purified by column chromatography on silica gel (<sup>n</sup>Hexane/EtOAc 9:1).

<sup>112</sup> Rahman, M.; Szostak, M. *Org. Lett.*, **2021**, 23, 4818-4822.

### 1,2-bis(4-methoxyphenyl)ethyne (**56b**)



The general procedure for synthesis of symmetrical internal alkynes was followed by using *p*-iodoanisole (**32b**, 2.25 g, 9.6 mmol) as starting material. Purification by column chromatography on silica gel (Hexane/EtOAc 9:1) yielded **56b** (835 mg, 73%) as white crystals.

**Melting point:** 137-140 °C.

**<sup>1</sup>H NMR (400 MHz, CDCl<sub>3</sub>)**  $\delta$ : 7.39-7.35 (m, 4H), 6.81-6.77 (m, 4H), 3.75 (s, 6H).

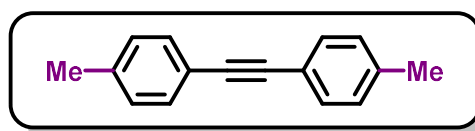
**<sup>13</sup>C NMR (100 MHz, CDCl<sub>3</sub>)**  $\delta$ : 159.6 (C<sub>q</sub>), 133.1 (CH), 115.9 (C<sub>q</sub>), 114.2 (CH), 88.2 (C<sub>q</sub>), 55.5 (CH<sub>3</sub>).

**IR (ATR):** 1456 (m, CH<sub>3</sub>), 1243 (s, C–O), 1024 (s, C–O) cm<sup>-1</sup>.

**MS-EI (+):** 238.1 [M]<sup>+</sup>. **Calc. for (C<sub>16</sub>H<sub>14</sub>O<sub>2</sub>)<sup>+</sup>:** 238.1.

*The analytical data are in accordance with those reported in the literature.*<sup>94</sup>

### 1,2-di-*p*-tolylethyne (**56c**)



The general procedure for synthesis of symmetrical internal alkynes was followed by using 1-iodo-4-methylbenzene (**32c**, 2.10 g, 9.6 mmol) as starting material. Purification by column chromatography on silica gel (Hexane/EtOAc 9:1) yielded **56c** (337 mg, 34%) as white crystals.

**Melting point:** 131-133 °C.

**<sup>1</sup>H NMR (400 MHz, CDCl<sub>3</sub>)**  $\delta$ : 7.44 (d, *J* = 8.0 Hz, 4H), 7.17 (d, *J* = 8.0 Hz, 4H), 2.38 (s, 6H).

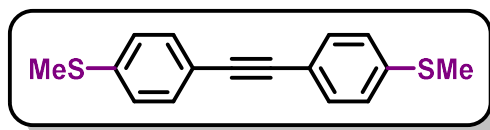
**<sup>13</sup>C NMR (100 MHz, CDCl<sub>3</sub>)**  $\delta$ : 138.4 (C<sub>q</sub>), 131.6 (CH), 129.3 (CH), 120.6 (C<sub>q</sub>), 89.1 (C<sub>q</sub>), 21.7 (CH<sub>3</sub>).

**IR (ATR):** 1513 (m, CH<sub>3</sub>), 812 (s, C–H<sub>Ar</sub>) cm<sup>-1</sup>.

**HRMS-EI (+):** 206.1089 [M]<sup>+</sup>. **Calc. for (C<sub>16</sub>H<sub>14</sub>)<sup>+</sup>:** 206.1096.

*The analytical data are in accordance with those reported in the literature.*<sup>94</sup>

### 1,2-bis(4-(methylthio)phenyl)ethyne (56d)



The general procedure for synthesis of symmetrical internal alkynes was followed by using (4-iodophenyl)(methyl)sulfane (**32d**, 2.40 g, 9.6 mmol) as starting material. Purification by column chromatography on silica gel (*n*-Hexane/EtOAc 9:1) yielded **56d** (237 mg, 18%) as yellow crystals.

**Melting point:** 161-165 °C.

**<sup>1</sup>H NMR (400 MHz, CDCl<sub>3</sub>)**  $\delta$ : 7.43 (d, *J* = 8.0 Hz, 4H), 7.20 (d, *J* = 8.0 Hz, 4H), 2.50 (s, 6H).

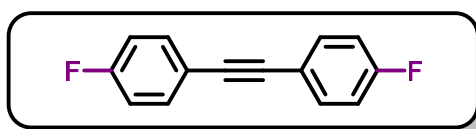
**<sup>13</sup>C NMR (100 MHz, CDCl<sub>3</sub>)**  $\delta$ : 139.4 (C<sub>q</sub>), 132.0 (CH), 126.1 (CH), 119.8 (C<sub>q</sub>), 89.5 (C<sub>q</sub>), 15.6 (CH<sub>3</sub>).

**IR (ATR):** 814 (s, C–H<sub>Ar</sub>) cm<sup>-1</sup>.

**HRMS-EI (+):** 270.0534 [M]<sup>+</sup>. **Calc. for (C<sub>16</sub>H<sub>14</sub>S<sub>2</sub>)<sup>+</sup>:** 270.0537.

*The analytical data are in accordance with those reported in the literature.*<sup>113</sup>

### 1,2-bis(4-fluorophenyl)ethyne (56e)



The general procedure for synthesis of symmetrical internal alkynes was followed by using 1-fluoro-4-iodobenzene (**32e**, 2.13 g, 9.6 mmol) as starting material. Purification by column chromatography on silica gel (*n*-Hexane/EtOAc 9:1) yielded **56e** (298 mg, 29%) as white crystals.

**Melting point:** 95-99 °C.

**<sup>1</sup>H NMR (400 MHz, CDCl<sub>3</sub>)**  $\delta$ : 7.53-7.48 (m, 4H), 7.07-7.02 (m, 4H).

**<sup>13</sup>C NMR (100 MHz, CDCl<sub>3</sub>)**  $\delta$ : 162.8 (d, <sup>1</sup>*J*<sub>C-F</sub> = 248.1 Hz, C<sub>q</sub>), 133.7 (d, <sup>3</sup>*J*<sub>C-F</sub> = 8.3 Hz, CH), 119.4 (d, <sup>4</sup>*J*<sub>C-F</sub> = 3.5 Hz, C<sub>q</sub>), 115.9 (d, <sup>2</sup>*J*<sub>C-F</sub> = 22.0 Hz, CH), 88.2 (d, <sup>5</sup>*J*<sub>C-F</sub> = 0.6 Hz, C<sub>q</sub>).

**IR (ATR):** 1230 (s, C–F), 842 (s, C–H<sub>Ar</sub>) cm<sup>-1</sup>.

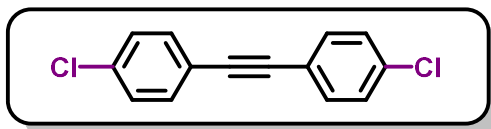
<sup>113</sup> Melzig, L.; Metzger, A.; Knochel, P. *Chem. Eur. J.*, **2011**, *17*, 2948-2956.



**HRMS-EI (+):** 214.0594 [M]<sup>+</sup>. **Calc. for (C<sub>14</sub>H<sub>8</sub>F<sub>2</sub>)<sup>+</sup>:** 214.0594.

*The analytical data are in accordance with those reported in the literature.*<sup>94</sup>

### 1,2-bis(4-chlorophenyl)ethyne (56f)



The general procedure for synthesis of symmetrical internal alkynes was followed by using 1-chloro-4-iodobenzene (**32f**, 2.29 g, 9.6 mmol) as starting material. Purification by column chromatography on silica gel (<sup>n</sup>Hexane/EtOAc 9:1) yielded **56f** (842 mg, 71%) as off-white crystals.

**Melting point:** 176-178 °C.

**<sup>1</sup>H NMR (400 MHz, CDCl<sub>3</sub>)** δ: 7.45 (d, *J* = 8.4 Hz, 4H), 7.33 (d, *J* = 8.4 Hz, 4H).

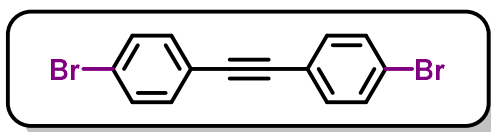
**<sup>13</sup>C NMR (100 MHz, CDCl<sub>3</sub>)** δ: 134.7 (C<sub>q</sub>), 133.0 (CH), 129.0 (CH), 121.6 (C<sub>q</sub>), 89.4 (C<sub>q</sub>).

**IR (ATR):** 831 (*s*, C–H<sub>Ar</sub>), 824 (*s*, C–Cl) cm<sup>-1</sup>.

**HRMS-EI (+):** 245.9994 [<sup>35</sup>Cl, M]<sup>+</sup>. **Calc. for (C<sub>14</sub>H<sub>8</sub>Cl<sub>2</sub>)<sup>+</sup>:** 245.9998.

*The analytical data are in accordance with those reported in the literature.*<sup>94</sup>

### 1,2-bis(4-bromophenyl)ethyne (56g)



The general procedure for synthesis of symmetrical internal alkynes was followed by using 1-bromo-4-iodobenzene (**32g**, 2.72 g, 9.6 mmol) as starting material. Purification by column chromatography on silica gel (<sup>n</sup>Hexane/EtOAc 9:1) yielded **56g** (403 mg, 25%) as white crystals.

**Melting point:** 185-190 °C.

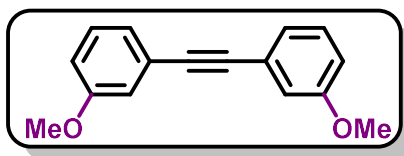
**<sup>1</sup>H NMR (400 MHz, CDCl<sub>3</sub>)** δ: 7.49 (dt, *J* = 8.4, 2.4 Hz, 4H), 7.38 (dt, *J* = 8.4, 2.4 Hz, 4H).

**<sup>13</sup>C NMR (100 MHz, CDCl<sub>3</sub>)** δ: 133.2 (CH), 131.9 (CH), 123.0 (C<sub>q</sub>), 122.1 (C<sub>q</sub>), 89.6 (C<sub>q</sub>).

**IR (ATR):** 818 (*s*, C–H<sub>Ar</sub>), 507 (*s*, C–Br) cm<sup>-1</sup>.

The analytical data are in accordance with those reported in the literature.<sup>94</sup>

### 1,2-bis(3-methoxyphenyl)ethyne (56h)



The general procedure for synthesis of symmetrical internal alkynes was followed by using *m*-iodoanisole (**32h**, 2.25 g, 9.6 mmol) as starting material. Purification by column chromatography on silica gel (<sup>n</sup>Hexane/EtOAc 9:1) yielded **56h** (400 mg, 35%) as light yellow crystals.

**Melting point:** 63-66 °C.

**<sup>1</sup>H NMR (400 MHz, CDCl<sub>3</sub>) δ:** 7.27 (t, *J* = 8.0 Hz, 2H), 7.15 (dt, *J* = 8.0, 1.2 Hz, 2H), 7.08 (dd, *J* = 2.4, 1.2 Hz, 2H), 6.91 (ddd, *J* = 8.0, 2.4, 1.2 Hz, 2H), 3.83 (s, 6H).

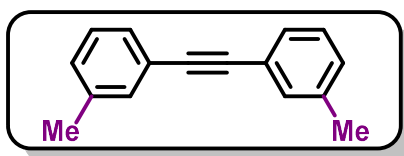
**<sup>13</sup>C NMR (100 MHz, CDCl<sub>3</sub>) δ:** 159.5 (C<sub>q</sub>), 129.6 (CH), 124.4 (CH), 124.4 (C<sub>q</sub>), 116.5 (CH), 115.2 (CH), 89.3 (C<sub>q</sub>), 55.5 (CH<sub>3</sub>).

**IR (ATR):** 1426 (*m*, CH<sub>3</sub>), 1205 (*s*, C–O), 1046 (*s*, C–O) cm<sup>-1</sup>.

**HRMS-ESI (+):** 239.1066 [M+H]<sup>+</sup>. **Calc. for (C<sub>16</sub>H<sub>15</sub>O<sub>2</sub>)<sup>+</sup>:** 239.1067.

The analytical data are in accordance with those reported in the literature.<sup>114</sup>

### 1,2-di-*m*-tolylethyne (56i)



The general procedure for synthesis of symmetrical internal alkynes was followed by using 1-iodo-3-methylbenzene (**32i**, 2.09 mg, 9.6 mmol) as starting material. Purification by column chromatography on silica gel (<sup>n</sup>Hexane/EtOAc 9:1) yielded **56i** (198 mg, 20%) as white crystals.

**Melting point:** 78-80 °C.

<sup>114</sup> Gauthier, R.; Mamone, M.; Paquin, J.-F. *Org. Lett.*, **2019**, *21*, 9024-9027.

**<sup>1</sup>H NMR (400 MHz, CDCl<sub>3</sub>) δ:** 7.38 (br s, 2H), 7.35 (br d, *J* = 7.6 Hz, 4H), 7.25 (t, *J* = 7.6 Hz, 2H), 7.16 (br d, *J* = 7.6 Hz, 2H), 2.37 (s, 6H)

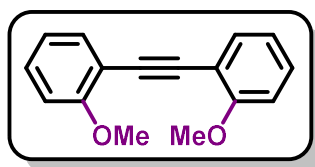
**<sup>13</sup>C NMR (100 MHz, CDCl<sub>3</sub>) δ:** 138.2 (C<sub>q</sub>), 132.4 (CH), 129.3 (CH), 128.9 (CH), 128.4 (CH), 123.4 (C<sub>q</sub>), 89.4 (C<sub>q</sub>), 21.5 (CH<sub>3</sub>).

**IR (ATR):** 1488 (*m*, CH<sub>3</sub>), 784 (*s*, C–H<sub>Ar</sub>) cm<sup>-1</sup>.

**HRMS-EI (+):** 206.1091 [M]<sup>+</sup>. **Calc. for (C<sub>16</sub>H<sub>14</sub>)<sup>+</sup>:** 206.1096.

*The analytical data are in accordance with those reported in the literature.*<sup>94</sup>

### 1,2-bis(2-methoxyphenyl)ethyne (56j)



The general procedure for synthesis of symmetrical internal alkynes was followed by using *o*-iodoanisole (**32j**, 2.25 g, 9.6 mmol) as starting material. Purification by column chromatography on silica gel (<sup>n</sup>Hexane/EtOAc 9:1) yielded **56j** (172 mg, 15%) as off-white crystals.

**Melting point:** 112-116 °C.

**<sup>1</sup>H NMR (400 MHz, CDCl<sub>3</sub>) δ:** 7.53 (dd, *J* = 7.6, 2.0 Hz, 2H), 7.29 (ddd, *J* = 8.4, 7.6, 1.6 Hz, 2H), 6.93 (td, *J* = 7.6, 0.8 Hz, 2H), 6.90 (br d, *J* = 8.4 Hz, 2H), 3.93 (s, 6H).

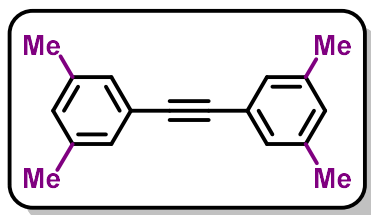
**<sup>13</sup>C NMR (100 MHz, CDCl<sub>3</sub>) δ:** 160.1 (C<sub>q</sub>), 133.8 (CH), 129.8 (CH), 120.6 (CH), 113.0 (C<sub>q</sub>), 110.9 (CH), 90.0 (C<sub>q</sub>), 56.1 (CH<sub>3</sub>).

**IR (ATR):** 1465 (*m*, CH<sub>3</sub>), 1242 (*s*, C–O), 1021 (*s*, C–O) cm<sup>-1</sup>.

**HRMS-ESI (+):** 239.1067 [M+H]<sup>+</sup>. **Calc. for (C<sub>16</sub>H<sub>15</sub>O<sub>2</sub>)<sup>+</sup>:** 239.1067.

*The analytical data are in accordance with those reported in the literature.*<sup>114</sup>

### 1,2-bis(3,5-dimethylphenyl)ethyne (**56k**)



The general procedure for synthesis of symmetrical internal alkynes was followed by using 1-iodo-3,5-dimethylbenzene (**32k**, 2.23 g, 9.6 mmol) as starting material. Purification by column chromatography on silica gel (Hexane/EtOAc 9:1) yielded **56k** (270 mg, 24%) as white crystals.

**Melting point:** 121-125 °C.

**<sup>1</sup>H NMR (400 MHz, CDCl<sub>3</sub>)**  $\delta$ : 7.17 (s, 4H), 6.97 (s, 2H), 2.32 (s, 12H).

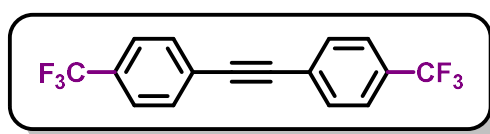
**<sup>13</sup>C NMR (100 MHz, CDCl<sub>3</sub>)**  $\delta$ : 138.1 (C<sub>q</sub>), 130.2 (CH), 129.5 (CH), 123.3 (C<sub>q</sub>), 89.3 (C<sub>q</sub>), 21.3 (CH<sub>3</sub>).

**IR (ATR):** 1596 (m, CH<sub>3</sub>), 843 (s, C-H<sub>Ar</sub>) cm<sup>-1</sup>.

**HRMS-EI (+):** 234.1405 [M]<sup>+</sup>. **Calc. for (C<sub>18</sub>H<sub>18</sub>)<sup>+</sup>:** 234.1409.

*The analytical data are in accordance with those reported in the literature.*<sup>115</sup>

### 1,2-bis(4-(trifluoromethyl)phenyl)ethyne (**56l**)



The general procedure for synthesis of symmetrical internal alkynes was followed by using 1-iodo-4-(trifluoromethyl)benzene (**32l**, 2.61 g, 9.6 mmol) as starting material. Purification by column chromatography on silica gel (Hexane/EtOAc 9:1) yielded **56l** (845 mg, 56%) as white crystals.

**Melting point:** 105-108 °C.

**<sup>1</sup>H NMR (400 MHz, CDCl<sub>3</sub>)**  $\delta$ : 7.64 (dd, *J* = 10.6, 8.8 Hz, 8H).

**<sup>13</sup>C NMR (100 MHz, CDCl<sub>3</sub>)**  $\delta$ : 132.2 (t, <sup>3</sup>*J*<sub>C-F</sub> = 28.7 Hz, CH), 130.7 (q, <sup>2</sup>*J*<sub>C-F</sub> = 32.5 Hz, C<sub>q</sub>), 126.6 (C<sub>q</sub>), 125.6 (q, <sup>4</sup>*J*<sub>C-F</sub> = 3.8 Hz, CH), 124.1 (q, <sup>1</sup>*J*<sub>C-F</sub> = 270.5 Hz, C<sub>q</sub>), 90.4 (C<sub>q</sub>).

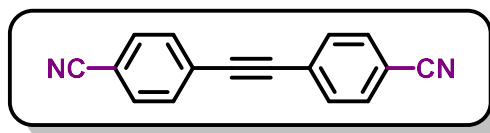
<sup>115</sup> Li, W.; Tang, J.; Li, S.; Zheng, X.; Yuan, M.; Xu, B.; Jiang, W.; Fu, H.; Li, R.; Chen, H. *Org. Lett.*, **2020**, *22*, 7814-7819.

**IR (ATR):** 1135 (s, C–F), 838 (s, C–H<sub>Ar</sub>) cm<sup>-1</sup>.

**HRMS-EI (+):** 314.0523 [M]<sup>+</sup>. **Calc. for (C<sub>16</sub>H<sub>8</sub>F<sub>6</sub>)<sup>+</sup>:** 314.0525.

*The analytical data are in accordance with those reported in the literature.*<sup>94</sup>

#### 4,4'-(ethyne-1,2-diyl)dibenzonitrile (**56m**)



The general procedure for synthesis of symmetrical internal alkynes was followed by using 4-iodobenzonitrile (**32m**, 2.20 g, 9.6 mmol) as starting material. Purification by column chromatography on silica gel (Hexane/EtOAc 9:1) yielded **56m** (394 mg, 36%) as an off-white solid.

**Melting point:** 255-260 °C.

**<sup>1</sup>H NMR (400 MHz, CDCl<sub>3</sub>)**  $\delta$ : 7.67 (d, *J* = 7.8 Hz, 4H), 7.63 (d, *J* = 7.8 Hz, 4H).

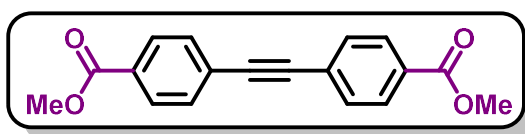
**<sup>13</sup>C NMR (100 MHz, CDCl<sub>3</sub>)**  $\delta$ : 132.5 (CH), 132.4 (CH), 127.3 (C<sub>q</sub>), 118.4 (C<sub>q</sub>), 112.6 (C<sub>q</sub>), 91.8 (C<sub>q</sub>).

**IR (ATR):** 2226 (s, C≡N), 829 (m, CH<sub>Ar</sub>) cm<sup>-1</sup>.

**HRMS-EI (+):** 228.0683 [M]<sup>+</sup>. **Calc. for (C<sub>16</sub>H<sub>8</sub>N<sub>2</sub>)<sup>+</sup>:** 228.0687.

*The analytical data are in accordance with those reported in the literature.*<sup>113</sup>

#### dimethyl 4,4'-(ethyne-1,2-diyl)dibenzoate (**56n**)



The general procedure for synthesis of symmetrical internal alkynes was followed by using methyl 4-iodobenzoate (**32n**, 2.52 g, 9.6 mmol) as starting material. Purification by column chromatography on silica gel (Hexane/EtOAc 9:1) yielded **56n** (480 mg, 34%) as white crystals.

**Melting point:** 221-224 °C.

**<sup>1</sup>H NMR (400 MHz, CDCl<sub>3</sub>)**  $\delta$ : 8.03 (br s, 4H), 7.61 (br s, 4H), 3.93 (s, 6H).

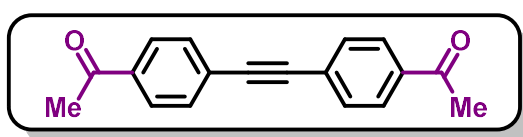
$^{13}\text{C}$  NMR (100 MHz,  $\text{CDCl}_3$ )  $\delta$ : 166.7 ( $\text{C}_q$ ), 131.8 (CH), 130.1 ( $\text{C}_q$ ), 129.8 (CH), 127.6 ( $\text{C}_q$ ), 91.6 ( $\text{C}_q$ ), 52.5 ( $\text{CH}_3$ ).

IR (ATR): 1714 (s, C=O), 1431 (m,  $\text{CH}_3$ ), 1404 (m,  $\text{CH}_3$ ), 1274 (s, C–O), 1097 (s, C–O) 767 (s, C–H<sub>Ar</sub>)  $\text{cm}^{-1}$

HRMS-ESI (+): 295.0967  $[\text{M}+\text{H}]^+$ . Calc. for  $(\text{C}_{18}\text{H}_{15}\text{O}_4)^+$ : 295.0965.

The analytical data are in accordance with those reported in the literature.<sup>94</sup>

### 1,1'-(ethyne-1,2-diylbis(4,1-phenylene))bis(ethan-1-one) (56o)



The general procedure for synthesis of symmetrical internal alkynes was followed by using 1-(4-iodophenyl)ethan-1-one (**32o**, 2.36 g, 9.6 mmol) as starting material. Purification by column chromatography on silica gel (<sup>n</sup>Hexane/EtOAc 9:1) yielded **56o** (667 mg, 53%) as an off-white solid.

**Melting point:** 200-202 °C.

$^1\text{H}$  NMR (400 MHz,  $\text{CDCl}_3$ )  $\delta$ : 7.94 (d,  $J$  = 8.2 Hz, 4H), 7.61 (d,  $J$  = 8.2 Hz, 4H), 2.60 (s, 6H).

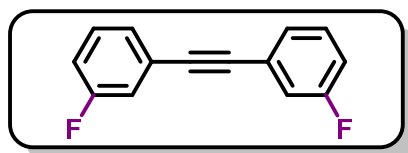
$^{13}\text{C}$  NMR (100 MHz,  $\text{CDCl}_3$ )  $\delta$ : 197.4 ( $\text{C}_q$ ), 136.8 ( $\text{C}_q$ ), 132.0 (CH), 128.5 (CH), 127.6 ( $\text{C}_q$ ), 91.8 ( $\text{C}_q$ ), 26.8 ( $\text{CH}_3$ ).

IR (ATR): 1673 (s, C=O), 1402 (m,  $\text{CH}_3$ ), 833 (s, C–H<sub>Ar</sub>)  $\text{cm}^{-1}$

HRMS-EI (+): 262.0990  $[\text{M}]^+$ . Calc. for  $(\text{C}_{18}\text{H}_{14}\text{O}_2)^+$ : 262.0994.

The analytical data are in accordance with those reported in the literature.<sup>94</sup>

### 1,2-bis(3-fluorophenyl)ethyne (56p)



The general procedure for synthesis of symmetrical internal alkynes was followed by using 1-fluoro-3-iodobenzene (**32p**, 2.13 g, 9.6 mmol) as starting material. Purification by column

chromatography on silica gel (Hexane/EtOAc 9:1) yielded **56p** (329 mg, 32%) as white crystals.

**Melting point:** 55-59 °C.

**<sup>1</sup>H NMR (400 MHz, CDCl<sub>3</sub>) δ:** 7.35-7.31 (m, 4H), 7.25-7.21 (m, 2H), 7.09-7.03 (m, 2H).

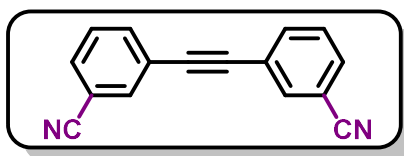
**<sup>13</sup>C NMR (100 MHz, CDCl<sub>3</sub>) δ:** 162.6 (d, <sup>1</sup>J<sub>C-F</sub> = 245.2 Hz, C<sub>q</sub>), 130.2 (d, <sup>3</sup>J<sub>C-F</sub> = 8.6 Hz, CH), 127.8 (d, <sup>4</sup>J<sub>C-F</sub> = 3.1 Hz, CH), 124.9 (d, <sup>3</sup>J<sub>C-F</sub> = 9.4 Hz, C<sub>q</sub>), 118.7 (d, <sup>2</sup>J<sub>C-F</sub> = 22.7 Hz, CH), 116.2 (d, <sup>2</sup>J<sub>C-F</sub> = 21.1 Hz, CH), 89.1 (d, <sup>4</sup>J<sub>C-F</sub> = 3.4 Hz, C<sub>q</sub>).

**IR (ATR):** 1152 (s, C–F), 780 (s, C–H<sub>Ar</sub>) cm<sup>-1</sup>.

**HRMS-EI (+):** 214.0592 [M]<sup>+</sup>. **Calc. for (C<sub>14</sub>H<sub>8</sub>F<sub>2</sub>)<sup>+</sup>:** 214.0594.

*The analytical data are in accordance with those reported in the literature.<sup>94</sup>*

### 3,3'-(ethyne-1,2-diyl)dibenzonitrile (**56q**)



The general procedure for synthesis of symmetrical internal alkynes was followed by using 3-iodobenzonitrile (**32q**, 2.20 g, 9.6 mmol) as starting material. Purification by column chromatography on silica gel (Hexane/EtOAc 9:1) yielded **56q** (471 mg, 43%) as white crystals.

**Melting point:** 123-125 °C.

**<sup>1</sup>H NMR (400 MHz, CDCl<sub>3</sub>) δ:** 7.81 (s, 2H), 7.75 (d, *J* = 7.8 Hz, 2H), 7.65 (d, *J* = 7.8 Hz, 2H), 7.50 (t, *J* = 7.8 Hz, 2H).

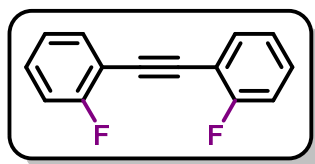
**<sup>13</sup>C NMR (100 MHz, CDCl<sub>3</sub>) δ:** 135.9 (CH), 135.2 (CH), 132.3 (CH), 129.7 (CH), 124.1 (C<sub>q</sub>), 118.1 (C<sub>q</sub>), 113.3 (C<sub>q</sub>), 89.3 (C<sub>q</sub>).

**IR (ATR):** 2226 (m, C≡N), 793 (s, CH<sub>Ar</sub>) cm<sup>-1</sup>.

**HRMS-EI (+):** 228.0688 [M]<sup>+</sup>. **Calc. for (C<sub>16</sub>H<sub>8</sub>N<sub>2</sub>)<sup>+</sup>:** 228.0687.

*The analytical data are in accordance with those reported in the literature.<sup>94</sup>*

### 1,2-bis(2-fluorophenyl)ethyne (56r)



The general procedure for synthesis of symmetrical internal alkynes was followed by using 1-fluoro-2-iodobenzene (**32r**, 2.13 g, 9.6 mmol) as starting material. Purification by column chromatography on silica gel (*n*-Hexane/EtOAc 9:1) yielded **56r** (360 mg, 35%) as white crystals.

**Melting point:** 45-46 °C.

**<sup>1</sup>H NMR (400 MHz, CDCl<sub>3</sub>) δ:** 7.58-7.54 (m, 2H), 7.37-7.31 (m, 2H), 7.17-7.10 (m, 4H).

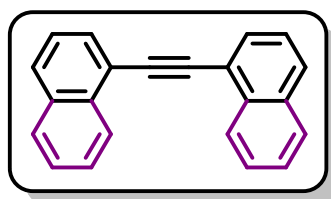
**<sup>13</sup>C NMR (100 MHz, CDCl<sub>3</sub>) δ:** 162.8 (d, <sup>1</sup>J<sub>C-F</sub> = 250.6 Hz, C<sub>q</sub>), 133.7 (d, <sup>5</sup>J<sub>C-F</sub> = 0.7 Hz, CH), 130.6 (d, <sup>3</sup>J<sub>C-F</sub> = 8.0 Hz, CH), 124.2 (d, <sup>4</sup>J<sub>C-F</sub> = 3.8 Hz, CH), 115.7 (d, <sup>2</sup>J<sub>C-F</sub> = 20.7 Hz, CH), 111.8 (d, <sup>2</sup>J<sub>C-F</sub> = 15.5 Hz, C<sub>q</sub>), 87.9 (d, <sup>4</sup>J<sub>C-F</sub> = 3.6 Hz, C<sub>q</sub>).

**IR (ATR):** 1217 (s, C–F), 755 (s, C–H<sub>Ar</sub>) cm<sup>-1</sup>.

**HRMS-ESI (+):** 237.0490 [M+Na]<sup>+</sup>. **Calc. for (C<sub>14</sub>H<sub>8</sub>F<sub>2</sub>Na)<sup>+</sup>:** 237.0486.

*The analytical data are in accordance with those reported in the literature.*<sup>94</sup>

### 1,2-di(naphthalen-1-yl)ethyne (56s)



The general procedure for synthesis of symmetrical internal alkynes was followed by using 1-iodonaphthalene (**32s**, 2.44 g, 9.6 mmol) as starting material. Purification by column chromatography on silica gel (*n*-Hexane/EtOAc 9:1) yielded **56s** (655 mg, 49%) as an off-white solid.

**Melting point:** 124-126 °C.

**<sup>1</sup>H NMR (400 MHz, CDCl<sub>3</sub>) δ:** 8.60 (d, *J* = 8.3 Hz, 2H), 7.92-7.89 (m, 6H), 7.68-7.64 (m, 2H), 7.60-7.51 (m, 4H).



$^{13}\text{C}$  NMR (100 MHz,  $\text{CDCl}_3$ )  $\delta$ : 133.5 (2 x  $\text{C}_q$ ), 130.8 (CH), 129.1 (CH), 128.6 (CH), 127.1 (CH), 126.7 (CH), 126.5 (CH), 125.6 (CH), 121.3 ( $\text{C}_q$ ), 92.6 ( $\text{C}_q$ ).

IR (ATR): 769 (s, C–H<sub>Ar</sub>)  $\text{cm}^{-1}$ .

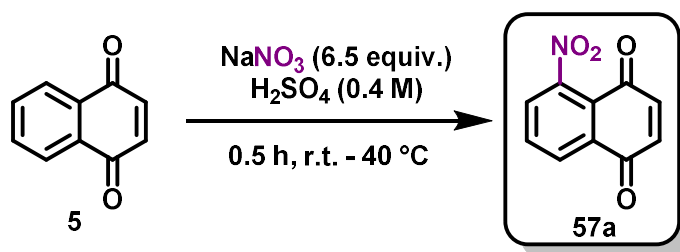
HRMS-EI (+): 278.1095 [ $\text{M}$ ]<sup>+</sup>. Calc. for ( $\text{C}_{22}\text{H}_{14}$ )<sup>+</sup>: 278.1096.

The analytical data are in accordance with those reported in the literature.<sup>94</sup>

Compounds **32t-z** were submitted to the same general procedure described above for the synthesis of symmetrical internal alkynes, aiming the obtention of their respective products **56t-z**, however, in all cases, only the respective starting materials were observed after 36 h of reaction.

### 5.3.3. Synthesis of A-ring modified quinones (57a-o)

#### 5-Nitro-1,4-naphthoquinone (57a)



1,4-Naphthoquinone (**5**, 2.00 g, 12.6 mmol) was dissolved in concentrated sulfuric acid (25 mL) at 5 °C. A solution of sodium nitrate (7.00 g, 82.4 mmol) in concentrated sulfuric acid (5 mL) was carefully added in 3 portions. The solution was kept under stirring at room temperature for 25 min and at 40 °C for an additional 5 min. The solution was cooled down to room temperature and poured on crushed ice. The precipitate was filtered, washed with water and purified by column chromatography (dichloromethane) to provide **57a** (1.32 g, 51%) as yellow crystals.

**Melting point:** 163-165 °C.

$^1\text{H}$  NMR (400 MHz,  $\text{CDCl}_3$ )  $\delta$ : 8.29 (d,  $J$  = 7.8 Hz, 1H), 7.90 (t,  $J$  = 7.8 Hz, 1H), 7.74 (d,  $J$  = 7.8 Hz, 1H), 7.07-7.01 (m, 2H).

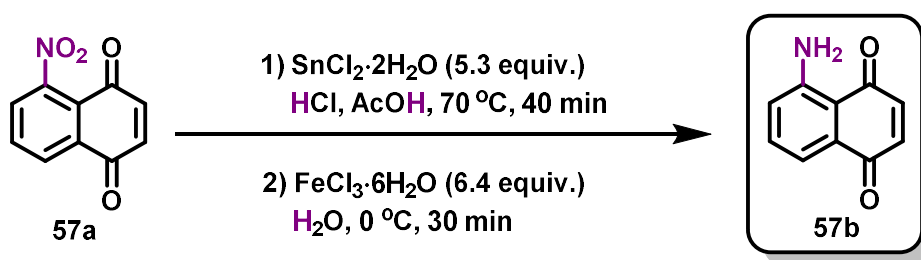
$^{13}\text{C}$  NMR (100 MHz,  $\text{CDCl}_3$ )  $\delta$ : 182.8 ( $\text{C}_q$ ), 181.4 ( $\text{C}_q$ ), 148.5 ( $\text{C}_q$ ), 139.3 (CH), 138.3 (CH), 134.9 (CH), 132.9 ( $\text{C}_q$ ), 129.2 (CH), 127.7 (CH), 123.1 ( $\text{C}_q$ ).

**IR (ATR):** 1670 (*s*, C=O), 1591 (*m*, C=O), 1530 (*s*, NO<sub>2</sub>), 1324 (*s*, C–N), 1297 (*s*, NO<sub>2</sub>), 786 (*s*, C–H<sub>Ar</sub>) cm<sup>-1</sup>.

**HRMS-ESI (+):** 204.0290 [M+H]<sup>+</sup>. **Calc. for (C<sub>10</sub>H<sub>6</sub>NO<sub>4</sub>)<sup>+</sup>:** 204.0291.

*The analytical data are in accordance with those reported in the literature.*<sup>116</sup>

### 5-Amino-1,4-naphthoquinone (**57b**)



Compound **57a** (1.02 g, 5.0 mmol) was dissolved in glacial acetic acid (35 mL, 0.14 M) under continuous stirring at 50 °C. A solution of SnCl<sub>2</sub>·2H<sub>2</sub>O (6.00 g, 26.5 mmol) in hydrochloric acid 1M (10 mL) was carefully added. The solution was kept under stirring at 70 °C for 40 min. The solution was cooled down to 25 °C. A solution of FeCl<sub>3</sub>·6H<sub>2</sub>O (8.70 g, 32.0 mmol) in distilled cold water (10 mL) was added, and the final mixture was stirred for additional 30 min at room temperature. Once the reaction was complete, the mixture was dropwise poured on crushed ice. After filtration, compound **57b** (856 mg, 99%) was obtained as purple crystals.

**Melting point:** 180-183 °C.

**<sup>1</sup>H NMR (400 MHz, CDCl<sub>3</sub>) δ:** 7.44-7.40 (m, 2H), 6.97-6.92 (m, 1H), 6.87 (d, *J* = 10.2 Hz, 1H), 6.84 (d, *J* = 10.2 Hz, 1H), 6.69 (br s, 2H).

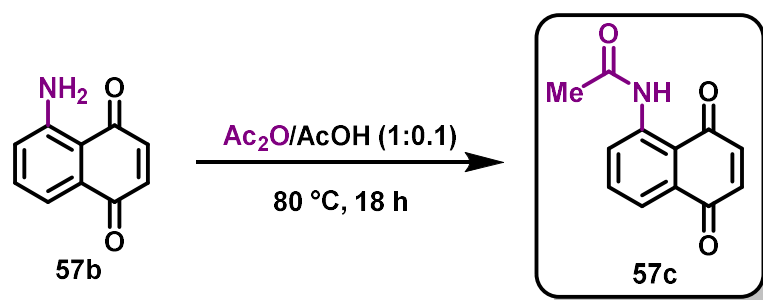
**<sup>13</sup>C NMR (100 MHz, CDCl<sub>3</sub>) δ:** 187.3 (C<sub>q</sub>), 185.6 (C<sub>q</sub>), 150.2 (C<sub>q</sub>), 140.7 (CH), 137.4 (CH), 134.7 (CH), 133.0 (C<sub>q</sub>), 123.4 (CH), 117.2 (CH), 112.4 (C<sub>q</sub>).

**IR (KBr):** 3400 (*m*, NH<sub>2</sub>), 3289 (*m*, NH<sub>2</sub>), 1634 (*s*, C=O), 1603 (*s*, C=O), 1543 (*m*, NH<sub>2</sub>), 1299 (*s*, C–N), 785 (*s*, C–H<sub>Ar</sub>) cm<sup>-1</sup>.

*The analytical data are in accordance with those reported in the literature.*<sup>16a</sup>

<sup>116</sup> Mangel, N.; Snider, B. B. *Org. Lett.*, **2009**, *11*, 4926-4929.

### 5-Acetamide-1,4-naphthoquinone (57c)



The compound **57b** (150 mg, 0.9 mmol) was dissolved in a mixture of acetic anhydride (2.0 mL, 0.4 M) and glacial acetic acid (200  $\mu$ L) in a sealed tube. The mixture was heated to 80 °C for 18 h. The mixture was then cooled to room temperature and the solvent was removed under constant air flow. The final product was washed with *n*-hexane and dried out to provide compound **57c** (134 mg, 71%) as a yellow solid.

**Melting point:** 175-177 °C.

**<sup>1</sup>H NMR (400 MHz, CDCl<sub>3</sub>)  $\delta$ :** 11.84 (s, 1H), 9.05 (dd,  $J$  = 8.0, 1.2 Hz, 1H), 7.80 (dd,  $J$  = 8.0, 1.2 Hz, 1H), 7.70 (t,  $J$  = 8.0 Hz, 1H), 6.95-6.88 (m, 2H), 2.29 (s, 3H).

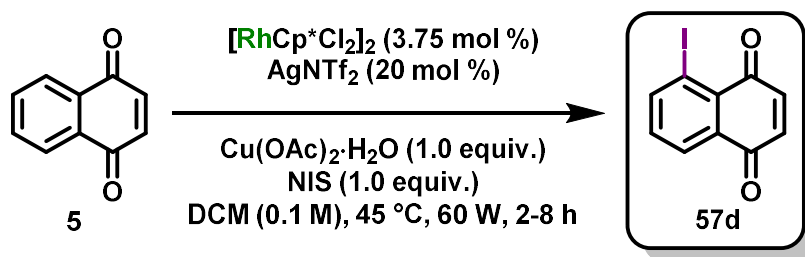
**<sup>13</sup>C NMR (100 MHz, CDCl<sub>3</sub>)  $\delta$ :** 189.2 (C<sub>q</sub>), 184.6 (C<sub>q</sub>), 170.1 (C<sub>q</sub>), 141.4 (C<sub>q</sub>), 140.0 (CH), 138.1 (CH), 135.8 (CH), 132.3 (C<sub>q</sub>), 126.1 (CH), 122.0 (CH), 116.0 (C<sub>q</sub>), 25.8 (CH<sub>3</sub>).

**IR (KBr):** 3212 (w, N-H), 1706 (s, C=O), 1665 (s, C=O), 1643 (s, C=O), 1582 (m, N-H), 1406 (m, CH<sub>3</sub>), 1296 (s, C-N), 1261 (s, C-N), 762 (s, C-H<sub>Ar</sub>) cm<sup>-1</sup>.

*The analytical data are in accordance with those reported in the literature.*<sup>117</sup>

<sup>117</sup> Suchard, O.; Kane, R.; Roe, B. J.; Zimmermann, E.; Jung, C.; Waske, P. A.; Mattay, J.; Oelgemöller, M. *Tetrahedron*, **2006**, 62, 1467-1473.

### 5-Iodo-1,4-naphthoquinone (57d)



1,4-Naphthoquinone (**5**, 158 mg, 1.00 mmol), [RhCp\*Cl<sub>2</sub>]<sub>2</sub> (23 mg, 37.5 μmol, 3.75 mol %), silver bis(trifluoromethanesulfonyl)imide (78 mg, 0.20 mmol), *N*-iodosuccinimide (225 mg, 1.00 mmol) and copper acetate (182 mg, 1.00 mmol) were placed in a reaction tube under an inert N<sub>2</sub> atmosphere of a glovebox. Dichloromethane (10.0 mL, 0.1 M) was added, and the mixture was irradiated in a CEM Discover microwave apparatus (60 W) at 45 °C. After cooling, the reaction mixture was filtered through a pad of celite and concentrated under reduced pressure. The residue was purified by column chromatography (toluene) to provide **57d** (200 mg, 70%) as red crystals.

**Melting point:** 171-174 °C.

**<sup>1</sup>H NMR (400 MHz, CDCl<sub>3</sub>) δ:** 8.36 (d, *J* = 7.8 Hz, 1H), 8.15 (d, *J* = 7.8 Hz, 1H), 7.35 (t, *J* = 7.8 Hz, 1H), 7.02 (d, *J* = 10.3 Hz, 1H), 6.94 (d, *J* = 10.3 Hz, 1H).

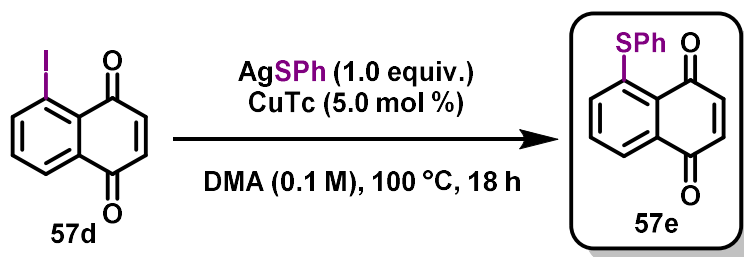
**<sup>13</sup>C NMR (100 MHz, CDCl<sub>3</sub>) δ:** 183.7 (C<sub>q</sub>), 183.3 (C<sub>q</sub>), 148.3 (CH), 139.9 (CH), 137.2 (CH), 134.4 (C<sub>q</sub>), 133.8 (CH), 130.8 (C<sub>q</sub>), 127.7 (CH), 92.9 (C<sub>q</sub>).

**IR (ATR):** 1665 (*s*, C=O), 1613 (*w*, C=O), 782 (*m*, C–H<sub>Ar</sub>), 563 (*m*, C–I) cm<sup>-1</sup>.

*The analytical data are in accordance with those reported in the literature.*<sup>118</sup>

<sup>118</sup> Carvalho, R. L.; Jardim, G. A. M.; Santos, A. C. C.; Araujo, M. H.; Oliveira, W. X. C.; Bombaça, A. C. S.; Menna-Barreto, R. F. S.; Gopi, E.; Gravel, E.; Doris, E.; Silva Júnior, E. N. *Chem. Eur. J.*, **2018**, *57*, 15227-15235.

### 5-Thiophenyl-1,4-naphthoquinone (57e)



Compound **57d** (142 mg, 0.50 mmol), AgSPh (108 mg, 0.50 mmol) and CuTc (4.0 mg, 25  $\mu$ mol, 5.0 mol %) were dissolved in DMA (5.0 mL, 0.1 M). The mixture was heated to 100 °C for 18 h. After cooling to 25 °C, the solvent was removed under reduced pressure. The residue was purified by column chromatography (toluene) to provide **57e** (103 mg, 97%) as a red solid.

**Melting point:** 157-158 °C.

**$^1\text{H}$  NMR (400 MHz,  $\text{CDCl}_3$ )  $\delta$ :** 7.84 (d,  $J = 7.9$  Hz, 1H), 7.61-7.59 (m, 2H), 7.49-7.48 (m, 3H), 7.39 (t,  $J = 7.9$  Hz, 1H), 7.06-7.02 (m, 2H), 6.94 (d,  $J = 10.3$  Hz, 1H).

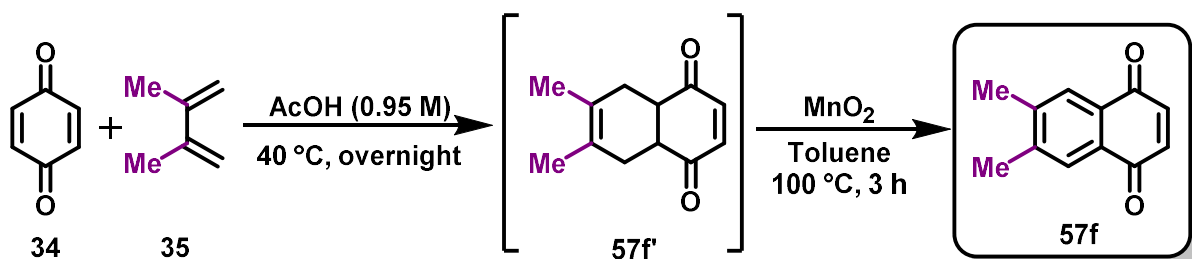
**$^{13}\text{C}$  NMR (100 MHz,  $\text{CDCl}_3$ )  $\delta$ :** 185.5 ( $\text{C}_q$ ), 185.0 ( $\text{C}_q$ ), 146.0 ( $\text{C}_q$ ), 139.9 (CH), 137.3 (CH), 136.3 (CH), 133.7 ( $\text{C}_q$ ), 132.9 (CH), 131.9 (CH), 131.5 ( $\text{C}_q$ ), 130.3 (CH), 130.1 (CH), 126.7 ( $\text{C}_q$ ), 123.7 (CH).

**IR (KBr):** 1662 (s, C=O), 1641 (s, C=O), 749 (s, C-H<sub>Ar</sub>), 690 (m, S-Ph)  $\text{cm}^{-1}$ .

**HRMS-ESI (+):** 267.0470  $[\text{M}+\text{H}]^+$ . **Calc. for  $(\text{C}_{16}\text{H}_{11}\text{SO}_2)^+$ :** 267.0480.

*The analytical data are in accordance with those reported in the literature.*<sup>76</sup>

### 6,7-Dimethyl-1,4-naphthoquinone (57f)



1,4-Benzoquinone (**34**, 1.03 g, 9.50 mmol) and 2,3-dimethyl-1,3-butadiene (**35**, 1.2 mL, 10.2 mmol) were dissolved in glacial acetic acid (10 mL, 0.95 M) and the solution was heated to 55 °C for 4 h. After cooling to 25 °C, acetic acid was evaporated under reduced pressure and

ethanol (20 mL) was added. The solid was filtered off and washed with water (100 mL), ethanol (50 mL) and diethyl ether (50 mL) to provide the intermediate **57f** as a white solid, which was used in the sequence without further purification. The intermediate was dissolved in toluene (100 mL) and heated to 100 °C. MnO<sub>2</sub> (13.0 g, 87.0 mmol) was carefully added, and the solution was heated to 100 °C for 3 h. The solution was filtered through a pad of celite and the filtrate was evaporated under reduced pressure. The crude product was recrystallized from ethanol to provide **57f** (2.00 g, 80%) as a yellow solid.

**Melting point:** 115-117 °C.

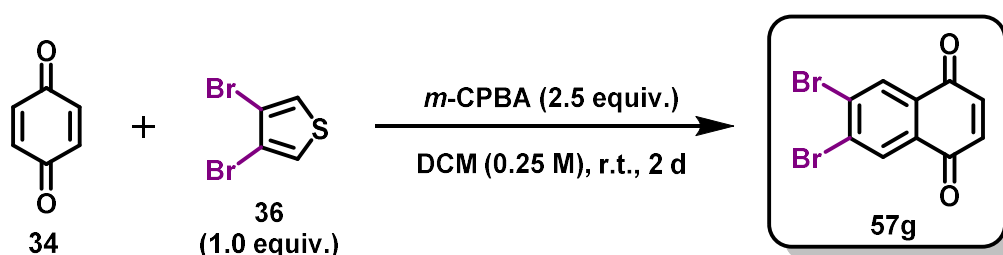
**<sup>1</sup>H NMR (300 MHz, CDCl<sub>3</sub>)** δ: 7.80 (s, 2H), 6.89 (s, 2H), 2.39 (s, 6H).

**<sup>13</sup>C NMR (75 MHz, CDCl<sub>3</sub>)** δ: 185.3 (C<sub>q</sub>), 143.9 (C<sub>q</sub>), 138.6 (CH), 130.0 (C<sub>q</sub>), 127.5 (CH), 20.5 (CH<sub>3</sub>).

**IR (KBr):** 1668 (s, C=O), 1598 (s, C=O), 1328 (s, CH<sub>3</sub>), 1310 (s, CH<sub>3</sub>), 837 (s, C-H<sub>Ar</sub>) cm<sup>-1</sup>.

The analytical data are in accordance with those reported in the literature.<sup>119</sup>

#### 6,7-Dibromo-1,4-naphthoquinone (**57g**)



1,4-Benzoquinone (**34**, 1.1 g, 10.0 mmol), **36** (1.1 mL, 10.0 mmol) and *m*-CPBA (4.6 g, 25.0 mmol) were dissolved in DCM (40 mL, 0.25 M) in a 100 mL rounded bottom flask. The solution was stirred at room temperature for 48 h and additional 6 h under reflux. The mixture was filtrated to separate the remaining *m*-CPBA. The organic phase was washed with a solution of NaHCO<sub>3</sub> (1M, 50 mL) and dried over Na<sub>2</sub>CO<sub>3</sub>. The solvent was removed under reduced pressure. Ethanol (5 mL) was added to the residue and the mixture was kept under reduced temperature (-22 °C) in the freezer for precipitation. The desired compound **57g** (88 mg, 3%) was obtained as a green solid.

**Melting point:** 169-172 °C.

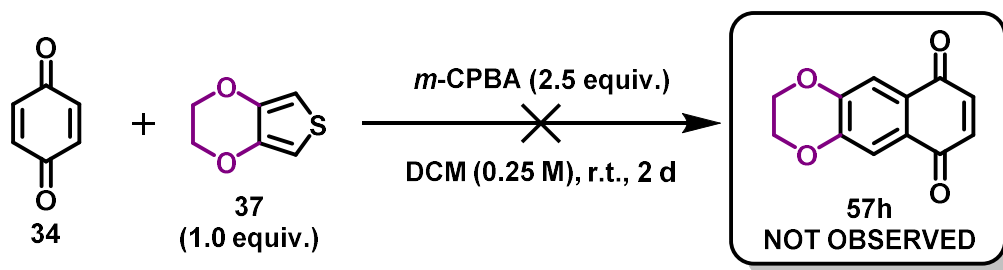
**<sup>1</sup>H NMR (400 MHz, CDCl<sub>3</sub>)** δ: 8.28 (s, 2H), 6.99 (s, 2H).

<sup>119</sup> Zhang, L.-L.; Da, B.-C.; Xiang, S.-H.; Zhu, S.; Yuan, Z.-Y.; Guo, Z.; Tan., B. *Tetrahedron*, **2019**, 75, 1689-1696.

$^{13}\text{C}$  NMR (100 MHz,  $\text{CDCl}_3$ )  $\delta$ : 183.4 ( $\text{C}_q$ ), 138.8 (CH), 132.2 ( $\text{C}_q$ ), 131.9 (CH), 131.2 ( $\text{C}_q$ ).  
IR (ATR): 1659 (*s*, C=O), 1572 (*s*, C=O), 1308 (*s*,  $\text{CH}_3$ ), 839 (*s*, C–H<sub>Ar</sub>), 702 (*m*, C–Br)  $\text{cm}^{-1}$ .  
HRMS-EI (+): 313.8578 [ $^{79}\text{Br}$ , M+H] $^+$ . Calc. for  $(\text{C}_{10}\text{H}_4\text{Br}_2\text{O}_2)^+$ : 313.8578.

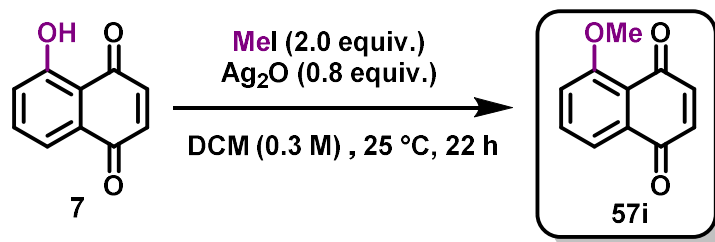
The analytical data are in accordance with those reported in the literature.<sup>120</sup>

### 2,3-dihydronaphtho[2,3-*b*][1,4]dioxine-6,9-dione (57h)



The same procedure described above for the synthesis of compound 57g was also applied for the obtention of 57h, using 37 (1.06 mL, 10.0 mmol) as substrate. After the procedure was completed, no product was observed.

### 5-Methoxy-1,4-naphthoquinone (57i)



Juglone (7, 500 mg, 2.87 mmol), iodomethane (351  $\mu\text{L}$ , 800 mg, 5.63 mmol) and  $\text{Ag}_2\text{O}$  (550 mg, 2.37 mmol) were dissolved in dichloromethane (9 mL, 0.3 M). The solution was kept under vigorous stirring at 25 °C and under a nitrogen atmosphere for 22 h. Afterwards, additional iodomethane (149  $\mu\text{L}$ , 340 mg, 2.39 mmol) and  $\text{Ag}_2\text{O}$  (550 mg, 2.37 mmol) were added, and the mixture was stirred for a further 3 h. The solution was filtered through a pad of celite and washed with dichloromethane. The solution was then concentrated under reduced pressure to provide 57i (469 mg, 87%) as orange crystals.

**Melting point:** 180-182 °C.

<sup>120</sup> Bailey, D.; Williams, V. E. *Tetrahedron Lett.*, **2004**, 45, 2511-2513.

**<sup>1</sup>H NMR (400 MHz, CDCl<sub>3</sub>) δ:** 7.72-7.65 (m, 2H), 7.30 (dd, *J* = 8.1, 1.3 Hz, 1H), 6.87-6.82 (m, 2H), 3.99 (s, 3H).

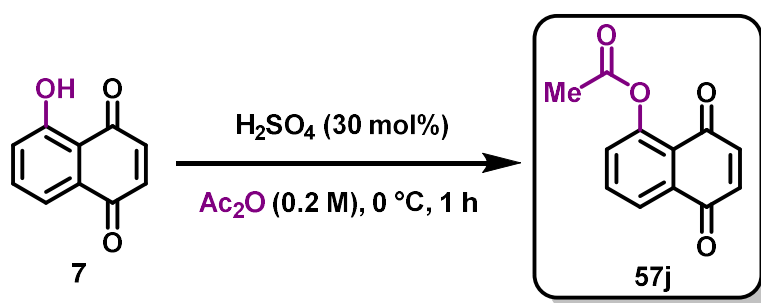
**<sup>13</sup>C NMR (100 MHz, CDCl<sub>3</sub>) δ:** 185.4 (C<sub>q</sub>), 184.5 (C<sub>q</sub>), 159.8 (C<sub>q</sub>), 141.0 (CH), 136.4 (CH), 135.2 (CH), 134.2 (C<sub>q</sub>), 119.9 (C<sub>q</sub>), 119.3 (CH), 118.1 (CH), 56.7 (CH<sub>3</sub>).

**IR (ATR):** 1651 (*s*, C=O), 1613 (*s*, C=O), 1469 (*m*, CH<sub>3</sub>), 1273 (*m*, C–O) cm<sup>-1</sup>.

**HRMS-ESI (+):** 189.0546 [M+H]<sup>+</sup>. **Calc. for (C<sub>11</sub>H<sub>9</sub>O<sub>3</sub>)<sup>+</sup>:** 189.0546.

*The analytical data are in accordance with those reported in the literature.*<sup>121</sup>

### 5-Acetoxy-1,4-naphthoquinone (57j)



Juglone (7, 870 mg, 5.0 mmol) and sulfuric acid (75 μL, 1.4 mmol) were dissolved in acetic anhydride (7 mL, 0.2 M) in a 25 mL rounded bottom flask. The solution was kept under stirring at 0 °C for 1 h. The solvent was removed under continuous flow of air. Afterwards, column chromatography (<sup>n</sup>Hexane/EtOAc 1:1) led to the obtention of compound **57j** (757 mg, 70%) as an yellow solid.

**Melting point:** 146-149 °C.

**<sup>1</sup>H NMR (400 MHz, CDCl<sub>3</sub>) δ:** 8.04 (d, *J* = 8.0 Hz, 1H), 7.76 (t, *J* = 8.0 Hz, 1H), 7.38 (d, *J* = 8.0 Hz, 1H), 6.93 (d, *J* = 10.3 Hz, 1H), 6.84 (d, *J* = 10.3 Hz, 1H), 2.44 (s, 3H).

**<sup>13</sup>C NMR (100 MHz, CDCl<sub>3</sub>) δ:** 184.4 (C<sub>q</sub>), 183.8 (C<sub>q</sub>), 169.6 (C<sub>q</sub>), 149.7 (C<sub>q</sub>), 140.1 (CH), 137.5 (CH), 135.0 (CH), 133.7 (C<sub>q</sub>), 129.9 (CH), 125.2 (CH), 123.4 (C<sub>q</sub>), 21.3 (CH<sub>3</sub>).

**IR (ATR):** 1755 (*s*, C=O), 1660 (*s*, C=O), 1592 (*s*, C=O), 1192 (*s*, C–O), 785 (*s*, C–H<sub>Ar</sub>) cm<sup>-1</sup>.

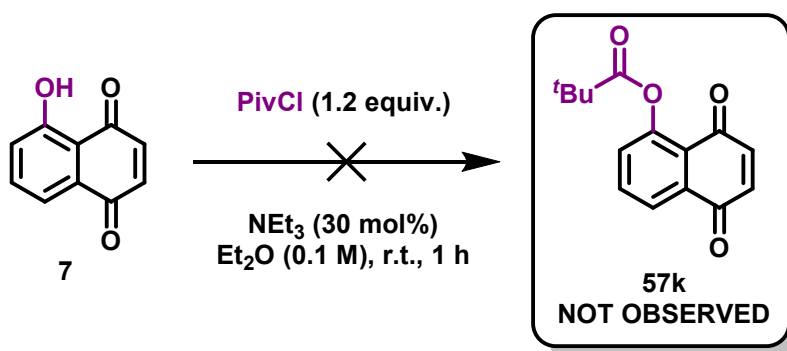
**HRMS-ESI (+):** 239.0316 [M+Na]<sup>+</sup>. **Calc. for (C<sub>12</sub>H<sub>8</sub>O<sub>4</sub>Na)<sup>+</sup>:** 239.0315.

*The analytical data are in accordance with those reported in the literature.*<sup>121</sup>

<sup>121</sup> Montenegro, R. C.; Araújo, A. J.; Molina, M. T.; Filho, J. D. B. M.; Rocha, D. D.; López-Montero, E.; Goulart, M. O. F.; Bento, E. S.; Alves, A. P. N. N.; Pessoa, C.; Moraes, M. O.; Costa-Lotufu, L. V. *Chem.-Biol. Int.*, **2010**, *184*, 439-448.

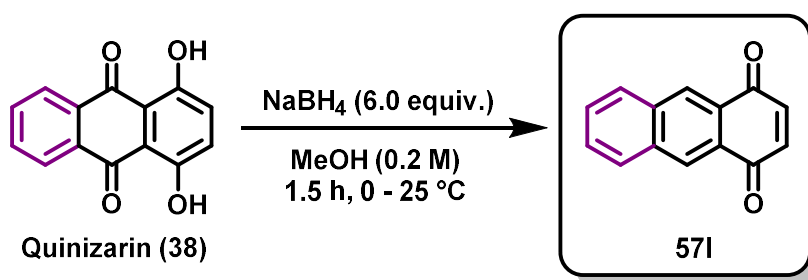


### 5,8-dioxo-5,8-dihydronaphthalen-1-yl pivalate (57k)



Juglone (**7**, 500 mg, 2.9 mmol) and triethylamine (500  $\mu$ L, 0.9 mmol) were dissolved in diethyl ether (30 mL, 0.1 M) in a 100 mL rounded bottom flask. The solution was kept under stirring at room temperature for 30 min. A solution of pivaloyl chloride (430  $\mu$ L, 3.5 mmol) in diethyl ether (20 mL) was carefully added dropwise, and the final mixture was kept under stirring at room temperature for additional 1 h. After this time, through an analysis on TLC (<sup>n</sup>Hexane/EtOAc 4:1) it was possible to observe that no product was obtained.

### 1,4-Anthraquinone (57l)



Quinizarin (**38**, 989 mg, 4.12 mmol) was dissolved in methanol (19 mL, 0.2 M) at 0 °C. Sodium borohydride (945 mg, 25.0 mmol) was added carefully. The reaction was stirred for 90 min at 0 °C. An aq. solution of hydrochloric acid (6 M, 18 mL) was added and the precipitate was filtered off and washed with water to afford **57l** (791 mg, 92%) as a brown solid.

**Melting point:** 212-216 °C.

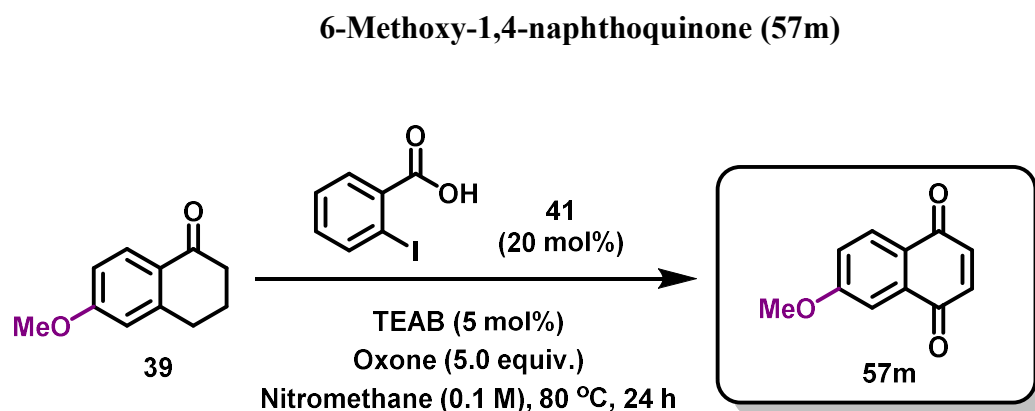
**<sup>1</sup>H NMR (400 MHz, CDCl<sub>3</sub>)  $\delta$ :** 8.55 (s, 2H), 8.01 (s, 2H), 7.66 (s, 2H), 7.03 (s, 2H).

**<sup>13</sup>C NMR (100 MHz, CDCl<sub>3</sub>)  $\delta$ :** 184.8 (C<sub>q</sub>), 140.2 (CH), 134.9 (C<sub>q</sub>), 130.4 (CH), 129.8 (CH), 129.0 (CH), 128.5 (C<sub>q</sub>).

**IR (ATR):** 1665 (*s*, C=O), 1614 (*m*, C=O), 763 (*s*, C–H<sub>Ar</sub>) cm<sup>-1</sup>.

**HRMS-ESI (+):** 209.0604 [M+H]<sup>+</sup>. **Calc. for (C<sub>14</sub>H<sub>9</sub>O<sub>2</sub>)<sup>+</sup>:** 209.0597.

*The analytical data are in accordance with those reported in the literature.*<sup>122</sup>



Under an atmosphere of N<sub>2</sub>, a 100 mL Schlenk flask was charged with the compound **39** (705 mg, 4.0 mmol), 2-iodobenzoic acid (**41**, 198 mg, 0.8 mmol), TEAB (42 mg, 0.2 mmol), oxone (6.0 g, 20.0 mmol) and dry nitromethane (40 mL, 0.1 M) was added *via* a syringe. The reaction mixture was heated to 80 °C for 24 h. The mixture was then cooled to room temperature and filtered on a celite pad. The solvent was removed under reduced pressure. Column chromatography on silica gel (Hexane/EtOAc 5:1) led to the obtention of compound **57m** (367 mg, 49%) as a yellow solid.

**Melting point:** 125-129 °C.

**<sup>1</sup>H NMR (400 MHz, CDCl<sub>3</sub>)** δ: 8.01 (d, *J* = 8.6 Hz, 1H), 7.49 (d, *J* = 2.5 Hz, 1H), 7.20 (dd, *J* = 8.6, 2.5 Hz, 1H), 6.94-6.88 (m, 2H), 3.94 (s, 3H).

**<sup>13</sup>C NMR (100 MHz, CDCl<sub>3</sub>)** δ: 185.4 (C<sub>q</sub>), 184.3 (C<sub>q</sub>), 164.3 (C<sub>q</sub>), 139.2 (CH), 138.4 (CH), 134.1 (C<sub>q</sub>), 129.1 (CH), 125.7 (C<sub>q</sub>), 120.7 (CH), 109.8 (CH), 56.1 (CH<sub>3</sub>).

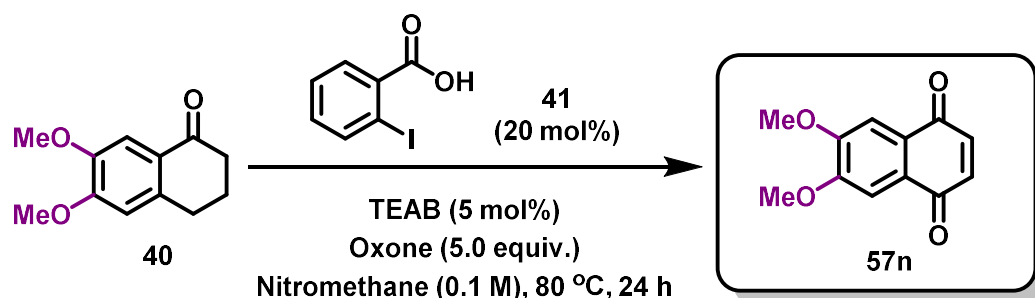
**IR (ATR):** 1662 (*s*, C=O), 1587 (*s*, C=O), 1456 (*m*, CH<sub>3</sub>), 1312 (*s*, C–O), 832 (*s*, C–H<sub>Ar</sub>) cm<sup>-1</sup>.

**HRMS-ESI (+):** 189.0548 [M+H]<sup>+</sup>. **Calc. for (C<sub>11</sub>H<sub>9</sub>O<sub>3</sub>)<sup>+</sup>:** 189.0546.

*The analytical data are in accordance with those reported in the literature.*<sup>16a</sup>

<sup>122</sup> Nor, S. M. M.; Sukari, M. A. H. M.; Azziz, S. S. S. A.; Fah, W. C.; Alimon, H.; Juhan, S. F. *Molecules*, **2013**, *18*, 8046-8062.

### 6,7-Dimethoxy-1,4-naphthoquinone (57n)



The same procedure described above for the obtention of compound **57m** was also applied for the obtention of compound **57n**, using the tetralone derivative **40** (824 mg, 4.0 mmol) as substrate. Once the reaction was complete, compound **57n** (262 mg, 30%) as an orange solid.

**Melting point:** 235-237 °C.

**<sup>1</sup>H NMR (400 MHz, CDCl<sub>3</sub>)**  $\delta$ : 7.46 (s, 2H), 6.85 (2H), 4.00 (s, 6H).

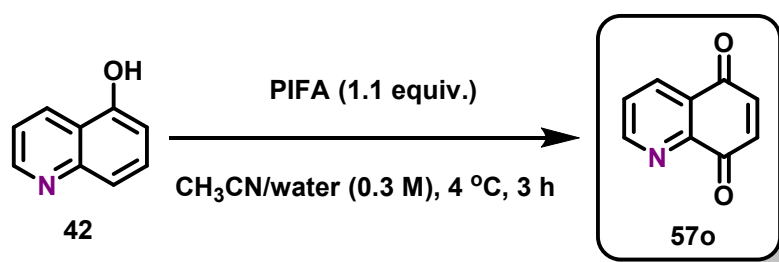
**<sup>13</sup>C NMR (100 MHz, CDCl<sub>3</sub>)**  $\delta$ : 184.7 (C<sub>q</sub>), 153.7 (C<sub>q</sub>), 138.5 (CH), 126.8 (C<sub>q</sub>), 108.0 (CH), 56.7 (CH<sub>3</sub>).

**IR (ATR):** 1661 (s, C=O), 1578 (s, C=O), 1454 (s, CH<sub>3</sub>), 1316 (s, C–O), 836 (s, C–H<sub>Ar</sub>) cm<sup>-1</sup>.

**HRMS-ESI (+):** 219.0652 [M+H]<sup>+</sup>. **Calc. for (C<sub>12</sub>H<sub>11</sub>O<sub>4</sub>)<sup>+</sup>:** 219.0652.

*The analytical data are in accordance with those reported in the literature.<sup>16a</sup>*

### Quinoline-5,8-dione (57o)



Compound **42** (290 mg, 2.0 mmol) was dissolved in distilled water (2.0 mL). A solution of PIFA (2.5 g, 2.2 mmol) in acetonitrile (4.0 mL) was carefully added dropwise to the mixture at 4 °C. The reaction was kept under vigorous stirring for 3 h while naturally reaching room temperature, from which a dark brown precipitate was generated. After the reaction was

complete, a filtration under reduced pressure led to the obtention of compound **57o** (133.3 mg, 21%) as a brown solid.

**Melting point:** 127-129 °C (decomposition).

**<sup>1</sup>H NMR (300 MHz, CDCl<sub>3</sub>) δ:** 9.05 (dd, *J* = 4.5, 1.7 Hz, 1H), 8.42 (dd, *J* = 7.9, 1.7 Hz, 1H), 7.70 (dd, *J* = 7.9, 4.5 Hz, 1H), 7.15 (d, *J* = 10.4 Hz, 1H), 7.06 (d, 10.4 Hz, 1H).

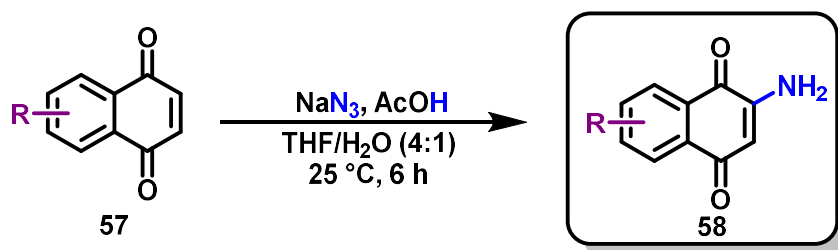
**<sup>13</sup>C NMR (75 MHz, CDCl<sub>3</sub>) δ:** 184.7 (C<sub>q</sub>), 183.3 (C<sub>q</sub>), 155.0 (CH), 147.6 (C<sub>q</sub>), 139.3 (CH), 138.2 (CH), 134.8 (CH), 129.3 (C<sub>q</sub>), 128.0 (CH).

**IR (ATR):** 1668 (*s*, C=O), 1578 (*m*, C=O), 1077 (*m*, C–N), 798 (*s*, C–H<sub>Ar</sub>) cm<sup>-1</sup>.

**HRMS-ESI (+):** 160.0395 [M+H]<sup>+</sup>. **Calc. for (C<sub>9</sub>H<sub>6</sub>NO<sub>2</sub>)<sup>+</sup>:** 160.0393.

*The analytical data are in accordance with those reported in the literature.*<sup>123</sup>

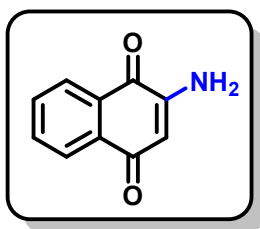
#### 5.3.4. Amination at the C-2 or C-3 positions of the A-ring modified quinones (58a-g)



The corresponding A-ring modified quinone **57** (1.0 equiv.) was dissolved in a mixture of THF and water (4:1, 0.315 M). A solution of sodium azide (3.3 equiv.) in a mixture of water and glacial acetic acid (3:1, 4.81 M) was slowly added. The solution was kept under vigorous stirring at 25 °C for 6 h. The solution was concentrated under vacuum, dissolved in ethyl acetate and extracted with an aq. NaOH solution (1 M) and a saturated aq. NaCl solution. The organic phase was dried over NaSO<sub>4</sub>, filtered and purified by column chromatography ("Hexane/EtOAc 1:1).

<sup>123</sup> Wellauer, J.; Miladinov, D.; Buchholz, T.; Schütz, J.; Stemmler, R. T.; Medlock, J. A.; Bonrath, W.; Sparr, C. *Chem. Eur. J.*, **2021**, *27*, 9748-9752.

### 2-Amino-1,4-naphthoquinone (58a)



The General Procedure for Amination of Quinones was followed using 1,4-naphthoquinone (**5**, 1.00 g, 5.80 mmol) and  $\text{NaN}_3$  (1.25 g, 19.2 mmol). Purification by column chromatography on silica gel (*n*-Hexane/EtOAc 1:1) yielded **58a** (685 mg, 68%) as an orange solid.

**Melting point:** 199-204 °C.

**$^1\text{H}$  NMR (400 MHz,  $\text{CDCl}_3$ )  $\delta$ :** 8.08-8.04 (m, 2H), 7.72 (td,  $J = 7.6, 1.2$  Hz, 1H), 7.63 (td,  $J = 7.6, 1.2$  Hz, 1H), 6.00 (s, 1H), 5.18 (s, 2H).

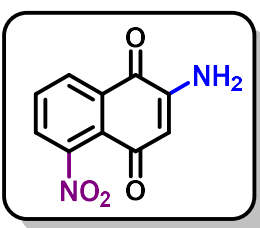
**$^{13}\text{C}$  NMR (100 MHz,  $\text{CDCl}_3$ )  $\delta$ :** 184.0 ( $\text{C}_q$ ), 182.0 ( $\text{C}_q$ ), 148.5 ( $\text{C}_q$ ), 134.8 (CH), 133.5 ( $\text{C}_q$ ), 132.5 (CH), 130.7 ( $\text{C}_q$ ), 126.4 (CH), 126.3 (CH), 105.3 (CH).

**IR (ATR):** 3182 (w,  $\text{NH}_2$ ), 1612 (m, C=O), 1558 (m, C=O), 1269 (m, C–N), 723 (s, C–H<sub>Ar</sub>)  $\text{cm}^{-1}$ .

**HRMS-ESI (+):** 174.0546  $[\text{M}+\text{H}]^+$ . **Calc. for  $(\text{C}_{10}\text{H}_8\text{NO}_2)^+$ :** 174.0550.

*The analytical data are in accordance with those reported in the literature.*<sup>124</sup>

### 2-Amino-5-nitro-1,4-naphthoquinone (58b)



The General Procedure for Amination of Quinones was followed using **57a** (1.20 g, 5.80 mmol) and  $\text{NaN}_3$  (1.25 g, 19.23 mmol). Purification by column chromatography on silica gel (*n*-Hexane/EtOAc 1:1) yielded **58b** (1.10 g, 90%) as an orange solid.

**Melting point:** 238-242 °C.

<sup>124</sup> Zhang, J.; Chang, C.-W. *T. J. Org. Chem.*, **2009**, *74*, 4414-4417.

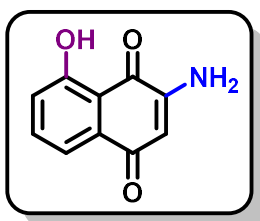
**<sup>1</sup>H NMR (300 MHz, DMSO-*d*<sub>6</sub>)**  $\delta$ : 8.16-8.11 (m, 1H), 8.02-7.97 (m, 2H), 7.41 (br s, 2H), 5.86 (s, 1H).

**<sup>13</sup>C NMR (75 MHz, DMSO-*d*<sub>6</sub>)**  $\delta$ : 179.5 (C<sub>q</sub>), 179.1 (C<sub>q</sub>), 150.6 (CH), 147.6 (C<sub>q</sub>), 136.0 (C<sub>q</sub>), 134.1 (C<sub>q</sub>), 127.7 (CH), 125.8 (CH), 120.8 (C<sub>q</sub>), 102.0 (CH).

**IR (ATR):** 3391 (*m*, OH<sub>water residue</sub>), 3285 (*m*, NH<sub>2</sub>), 1697 (*m*, C=O), 1603 (*m*, C=O), 1538 (*s*, NO<sub>2</sub>), 1356 (*s*, NO<sub>2</sub>), 1251 (*s*, C–N) cm<sup>-1</sup>.

**HRMS-ESI (+):** 219.0406 [M+H]<sup>+</sup>. **Calc. for (C<sub>10</sub>H<sub>7</sub>N<sub>2</sub>O<sub>4</sub>)<sup>+</sup>:** 219.0400.

### 3-Amino-5-hydroxy-1,4-naphthoquinone (58c)



The General Procedure for Amination of Quinones was followed using Juglone (**7**, 1.10 g, 5.8 mmol) and NaN<sub>3</sub> (1.25 g, 19.2 mmol). In this specific case, water was employed for the extraction procedure. Purification by column chromatography on silica gel ("Hexane/EtOAc 1:1) yielded **58c** (504 mg, 46%) as an orange solid.

**Melting point:** 250-253 °C.

**<sup>1</sup>H NMR (400 MHz, DMSO-*d*<sub>6</sub>)**  $\delta$ : 11.49 (s, 1H), 7.69-7.65 (m, 1H), 7.41-7.15 (m, 4H), 5.77 (s, 1H).

**<sup>13</sup>C NMR (100 MHz, DMSO-*d*<sub>6</sub>)**  $\delta$ : 186.2 (C<sub>q</sub>), 181.1 (C<sub>q</sub>), 160.3 (C<sub>q</sub>), 150.2 (C<sub>q</sub>), 137.4 (CH), 133.5 (C<sub>q</sub>), 121.7 (CH), 117.5 (CH), 114.2 (C<sub>q</sub>), 102.6 (CH).

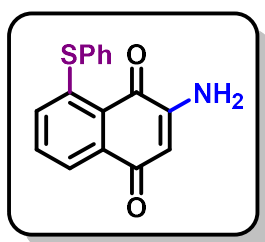
**IR (ATR):** 3391 (*m*, OH), 3160 (*m*, NH<sub>2</sub>), 1583 (*s*, C=O), 1551 (*s*, C=O), 1373 (*m*, O-H<sub>Ar</sub>) 1322 (*m*, C–O), 1261 (*s*, C–N), 824 (*s*, CH<sub>Ar</sub>) cm<sup>-1</sup>.

**HRMS-ESI (+):** 190.0497 [M+H]<sup>+</sup>. **Calc. for (C<sub>10</sub>H<sub>8</sub>NO<sub>3</sub>)<sup>+</sup>:** 190.0499.

*The analytical data are in accordance with those reported in the literature.*<sup>125</sup>

<sup>125</sup> Bao, N.; Ou, J.; Shi, W.; Li, N.; Chen, L.; J. Sun. *Eur. J. Org. Chem.*, **2018**, 2018, 2254-2258.

### 3-Amino-5-triophenyl-1,4-naphthoquinone (58d)



The General Procedure for Amination of Quinones was followed using **57e** (130 mg, 0.50 mmol) and  $\text{NaN}_3$  (108 mg, 1.65 mmol). Purification by column chromatography on silica gel (*n*-Hexane/EtOAc 1:1) yielded **58d** (46 mg, 32%) as an orange solid.

**Melting point:** 162-165 °C.

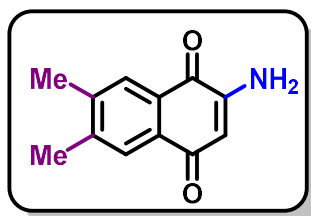
**$^1\text{H}$  NMR (400 MHz,  $\text{CDCl}_3$ )  $\delta$ :** 7.86 (dd,  $J = 7.8, 1.0$  Hz, 1H), 7.62-7.60 (m, 2H), 7.51-7.49 (m, 3H), 7.37 (t,  $J = 7.8$  Hz, 1H), 6.92 (dd,  $J = 7.8, 1.0$  Hz, 1H), 6.01 (s, 1H), 5.32 (s, 2H).

**$^{13}\text{C}$  NMR (100 MHz,  $\text{CDCl}_3$ )  $\delta$ :** 183.3 ( $\text{C}_q$ ), 181.6 ( $\text{C}_q$ ), 149.1 ( $\text{C}_q$ ), 146.1 ( $\text{C}_q$ ), 136.3 (CH), 135.3 ( $\text{C}_q$ ), 133.6 (CH), 131.3 ( $\text{C}_q$ ), 130.3 (CH), 130.2 (CH), 130.1 (CH), 125.3 (CH), 123.3 ( $\text{C}_q$ ), 104.1 (CH).

**IR (KBr):** 3382 (*m*,  $\text{NH}_2$ ), 1602 (*s*,  $\text{C}=\text{O}$ ), 1556 (*s*,  $\text{C}=\text{O}$ ), 1240 (*m*,  $\text{C}-\text{N}$ ), 746 (*w*,  $\text{C}-\text{H}_{\text{Ar}}$ ), 702 (*w*, S-Ph)  $\text{cm}^{-1}$ .

**HRMS-ESI (+):** 282.0589  $[\text{M}+\text{H}]^+$ . **Calc. for  $(\text{C}_{16}\text{H}_{12}\text{SNO}_2)^+$ :** 282.0583.

### 2-Amino-6,7-dimethyl-1,4-naphthoquinone (58e)



The General Procedure for Amination of Quinones was followed using **57f** (70 mg, 0.38 mmol) and  $\text{NaN}_3$  (82 mg, 1.26 mmol). Purification by column chromatography on silica gel (*n*-Hexane/EtOAc 1:1) yielded **58e** (21 mg, 27%) as an orange solid.

**Melting point:** 208-210 °C.

**<sup>1</sup>H NMR (400 MHz, DMSO-*d*<sub>6</sub>)**  $\delta$ : 7.66 (s, 1H), 7.62 (s, 1H), 7.03 (br s, 2H), 5.74 (s, 1H), 2.32 (s, 3H), 2.31 (s, 3H).

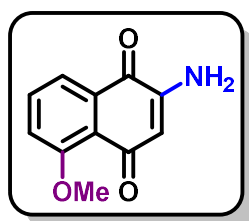
**<sup>13</sup>C NMR (100 MHz, DMSO-*d*<sub>6</sub>)**  $\delta$ : 182.1 (C<sub>q</sub>), 181.8 (C<sub>q</sub>), 150.2 (C<sub>q</sub>), 144.1 (C<sub>q</sub>), 140.9 (C<sub>q</sub>), 131.1 (C<sub>q</sub>), 128.2 (C<sub>q</sub>), 126.5 (CH), 126.2 (CH), 102.0 (CH), 19.8 (CH<sub>3</sub>), 19.3 (CH<sub>3</sub>).

**IR (KBr)**: 3408 (*m*, OH<sub>water</sub> residue), 3119 (*m*, NH<sub>2</sub>), 1615 (*s*, C=O), 1585 (*s*, C=O), 1548 (*s*, CH<sub>3</sub>), 1346 (*s*, CH<sub>3</sub>), 1281 (*s*, CH<sub>3</sub>), 848 (*s*, C–H<sub>Ar</sub>) cm<sup>-1</sup>.

**HRMS-ESI (+)**: 202.0866 [M+H]<sup>+</sup>. **Calc. for (C<sub>12</sub>H<sub>12</sub>NO<sub>2</sub>)<sup>+</sup>**: 202.0863.

*The analytical data are in accordance with those reported in the literature.*<sup>126</sup>

### 2-Amino-5-methoxy-1,4-naphthoquinone (58f)



The General Procedure for Amination of Quinones was followed using **57i** (400 mg, 2.10 mmol) and NaN<sub>3</sub> (452 mg, 6.97 mmol). Purification by column chromatography on silica gel (*n*Hexane/EtOAc 1:1) **58f** (227 mg, 53%) as an orange solid.

**Melting point**: 158-161 °C.

**<sup>1</sup>H NMR (400 MHz, CDCl<sub>3</sub>)**  $\delta$ : 7.73 (dd, *J* = 8.0, 0.7 Hz, 1H), 7.57 (t, *J* = 8.0 Hz, 1H), 7.29 (d, *J* = 8.0 Hz, 1H), 5.92 (s, 1H), 4.95 (s, 2H), 3.97 (s, 3H).

**<sup>13</sup>C NMR (100 MHz, CDCl<sub>3</sub>)**  $\delta$ : 184.6 (C<sub>q</sub>), 182.4 (C<sub>q</sub>), 159.4 (C<sub>q</sub>), 146.5 (C<sub>q</sub>), 133.5 (CH), 133.1 (C<sub>q</sub>), 120.4 (C<sub>q</sub>), 119.5 (CH), 119.4 (CH), 108.0 (CH), 56.8 (CH<sub>3</sub>).

**IR (ATR)**: 3374 (*m*, NH<sub>2</sub>), 1633 (*s*, C=O), 1564 (*s*, C=O), 1259 (*m*, CH<sub>3</sub>), 1218 (*s*, C–O), 974 (*s*, C–O), 742 (*m*, C–H<sub>Ar</sub>) cm<sup>-1</sup>.

**HRMS-ESI (+)**: 204.0660 [M+H]<sup>+</sup>. **Calc. for (C<sub>11</sub>H<sub>10</sub>NO<sub>3</sub>)<sup>+</sup>**: 204.0655.

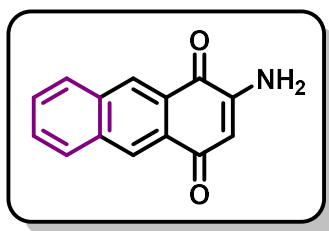
*The analytical data are in accordance with those reported in the literature.*<sup>127</sup>

<sup>126</sup> Guo, J.; Kiran, I. N. C.; Reddy, R. S.; Gao, J.; Tang, M.; Liu, Y.; He, Y. *Org. Lett.*, **2016**, *18*, 2499-2502.

<sup>127</sup> Arnone, A.; Merlini, L.; Nasini, G.; Pava, O. V. *Synth. Comm.*, **2007**, *37*, 2569-2577.



### 2-Amino-1,4-anthraquinone (58g)



The general procedure for amination was followed by using **57i** (604 mg, 2.90 mmol) and NaN<sub>3</sub> (625 mg, 8.70 mmol) as starting material. Purification by column chromatography on silica gel (Hexane/EtOAc 1:1) yielded **58g** (273 mg, 42%) as a brown solid.

**Melting point:** 282-285 °C.

**<sup>1</sup>H NMR (400 MHz, DMSO-*d*<sub>6</sub>)**  $\delta$ : 8.61 (s, 1H), 8.47 (s, 1H), 8.25-8.18 (m, 2H), 7.75–7.68 (2H), 7.25 (br s, 2H), 5.96 (s, 1H).

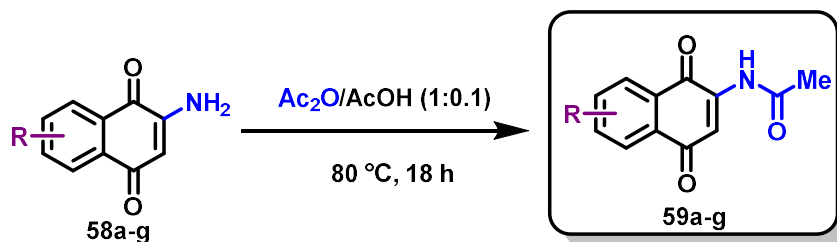
**<sup>13</sup>C NMR (100 MHz, DMSO-*d*<sub>6</sub>)**  $\delta$ : 181.4 (C<sub>q</sub>), 181.3 (C<sub>q</sub>), 151.4 (C<sub>q</sub>), 135.0 (C<sub>q</sub>), 133.5 (C<sub>q</sub>), 130.1 (CH), 129.7 (CH), 129.6 (CH), 128.7 (CH), 128.2 (CH), 127.6 (2 × C<sub>q</sub>), 126.4 (CH), 104.3 (CH).

**IR (ATR):** 3392 (*w*, OH<sub>water residue</sub>), 3273 (*w*, NH<sub>2</sub>), 1686 (*m*, C=O), 1619 (*m*, C=O), 1263 (*s*, C–N), 751 (*s*, CH<sub>Ar</sub>) cm<sup>-1</sup>.

**HRMS-ESI (+):** 224.0708 [M+H]<sup>+</sup>. **Calc. for (C<sub>14</sub>H<sub>10</sub>NO<sub>2</sub>)<sup>+</sup>:** 224.0706.

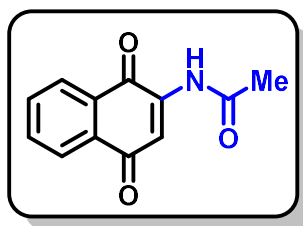
Compounds **57b**, **57c**, **57d**, **57g**, **57h**, **57j**, **57k**, **57m**, **57n** and **57o** were submitted to the same general procedure described above for the amination of A-ring modified quinones, aiming the obtention of their respective products **58**, however, in all cases, only the respective starting materials were observed.

### 5.3.5. Acetylation at the amino group of 5-amino-1,4-naphthoquinones (59a-g).



The corresponding 5-amino-1,4-naphthoquinone **58** was dissolved in a mixture of acetic anhydride and glacial acetic acid (1.0:0.1, 0.32 M) in a sealed tube. The mixture was heated to 120 °C for 18 h. The mixture was then cooled to room temperature, and -22 °C afterwards to generate the precipitate. The precipitate was filtered off and washed with water to provide the corresponding product.

#### *N*-(1,4-Dioxo-1,4-dihydronaphthalen-2-yl)acetamide (**59a**)



The general procedure for acetylation of 5-amino-1,4-naphthoquinones was followed using **58a** (300 mg, 1.40 mmol). Precipitation and filtration yielded **59a** (260 mg, 68%) as a yellow solid. **Melting point:** 205-209 °C.

**<sup>1</sup>H NMR (400 MHz, CDCl<sub>3</sub>) δ:** 8.36 (br s, 1H), 8.10 (dt, *J* = 10.0, 1.8 Hz, 2H), 7.85 (s, 1H), 7.78 (td, *J* = 10.0, 1.8 Hz, 1H), 7.72 (td, *J* = 10.0, 1.8 Hz, 1H), 2.29 (s, 3H).

**<sup>13</sup>C NMR (100 MHz, CDCl<sub>3</sub>) δ:** 185.5 (C<sub>q</sub>), 181.2 (C<sub>q</sub>), 169.6 (C<sub>q</sub>), 140.1 (C<sub>q</sub>), 135.2 (CH), 133.5 (CH), 132.4 (C<sub>q</sub>), 130.1 (C<sub>q</sub>), 126.9 (CH), 126.6 (CH), 117.4 (CH), 25.2 (CH<sub>3</sub>).

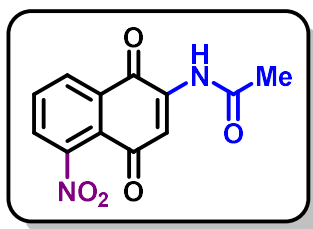
**IR (ATR):** 3292 (*w*, N-H), 1701 (*m*, C=O), 1670 (*m*, C=O), 1636 (*m*, C=O), 1592 (*w*, CH<sub>3</sub>), 722 (*s*, C-H<sub>Ar</sub>) cm<sup>-1</sup>.

**HRMS-ESI (+):** 216.0655 [M+H]<sup>+</sup>. **Calc. for (C<sub>12</sub>H<sub>10</sub>NO<sub>3</sub>)<sup>+</sup>:** 216.0655.

*The analytical data are in accordance with those reported in the literature.*<sup>128</sup>

<sup>128</sup> Dinda, B. K.; Basak, S.; Ghosh, B.; Mal, D. *Synthesis*, **2016**, *48*, 1235-1245.

***N*-(5-Nitro-1,4-dioxo-1,4-dihydronaphthalen-2-yl)acetamide (59b)**



The general procedure for acetylation of 5-amino-1,4-naphthoquinones was followed using **58b** (384 mg, 1.76 mmol). Precipitation and filtration yielded **59b** (243 mg, 53%) as a green solid.

**Melting point:** 290-294 °C.

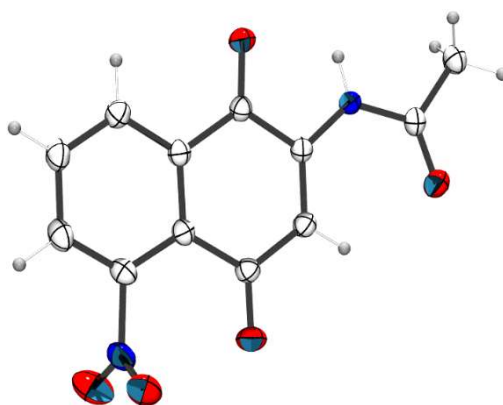
**<sup>1</sup>H NMR (400 MHz, CDCl<sub>3</sub>) δ:** 8.32-8.29 (m, 2H), 7.88 (s, 1H), 7.85 (t, *J* = 8.0 Hz, 1H), 7.73 (dd, *J* = 8.0, 1.1 Hz, 1H), 2.30 (s, 3H).

**<sup>13</sup>C NMR (100 MHz, CDCl<sub>3</sub>) δ:** 181.5 (C<sub>q</sub>), 179.5 (C<sub>q</sub>), 172.0 (C<sub>q</sub>), 169.5 (C<sub>q</sub>), 139.8 (C<sub>q</sub>), 134.2 (CH), 131.1 (C<sub>q</sub>), 129.2 (CH), 128.7 (CH), 123.4 (C<sub>q</sub>), 117.8 (CH), 25.2 (CH<sub>3</sub>).

**IR (ATR):** 3308 (*m*, N-H), 1719 (*m*, C=O), 1676 (*m*, C=O), 1638 (*m*, C=O), 1542 (*s*, NO<sub>2</sub>), 1495 (*s*, CH<sub>3</sub>), 1335 (*s*, NO<sub>2</sub>), 1209 (*s*, C-N), 739 (*m*, C-H<sub>Ar</sub>) cm<sup>-1</sup>.

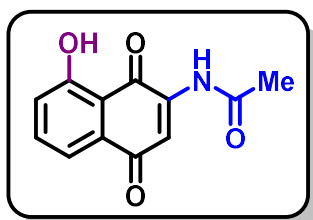
**HRMS-ESI (+):** 261.0513 [M+H]<sup>+</sup>. **Calc. for (C<sub>12</sub>H<sub>9</sub>N<sub>2</sub>O<sub>5</sub>)<sup>+</sup>:** 219.0400.

*The structure of the product was also confirmed by X-ray diffraction (CCDC number = 1984912) as shown below.*



**Figure 24.** Crystal structure of compound **59b**.

***N*-(8-Hydroxy-1,4-dioxo-1,4-dihydronaphthalen-2-yl)acetamide (59c)**



The general procedure for acetylation of 5-amino-1,4-naphthoquinones was followed using **58c** (333 mg, 1.76 mmol). Precipitation and filtration yielded **59c** (289 mg, 71%) as an orange solid.

**Melting point:** 214-217 °C.

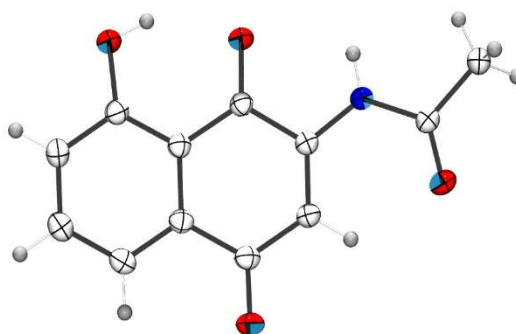
**<sup>1</sup>H NMR (600 MHz, CDCl<sub>3</sub>) δ:** 11.40 (s, 1H), 8.31 (br s, 1H), 7.83 (s, 1H), 7.67 (t, *J* = 7.4 Hz, 1H), 7.64 (dd, *J* = 7.4, 1.4 Hz, 1H), 7.24 (dd, *J* = 8.2, 1.4 Hz, 1H), 2.30 (s, 3H).

**<sup>13</sup>C NMR (150 MHz, CDCl<sub>3</sub>) δ:** 185.3 (C<sub>q</sub>), 184.6 (C<sub>q</sub>), 169.4 (C<sub>q</sub>), 161.9 (C<sub>q</sub>), 140.0 (C<sub>q</sub>), 138.1 (CH), 132.2 (C<sub>q</sub>), 123.9 (CH), 119.5 (CH), 118.2 (CH), 113.7 (C<sub>q</sub>), 25.3 (CH<sub>3</sub>).

**IR (ATR):** 3266 (*m*, N-H and O-H), 1715 (*m*, C=O), 1634 (*m*, C=O), 1604 (*m*, C=O), 1489 (*m*, CH<sub>3</sub>), 1367 (*m*, O-H<sub>Ar</sub>), 1021 (*m*, C–N), 729 (*s*, C–H<sub>Ar</sub>) cm<sup>-1</sup>.

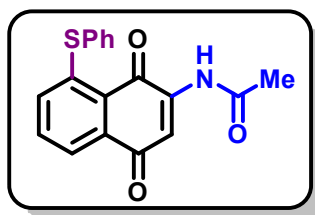
**HRMS-ESI (+):** 232.0607 [M+H]<sup>+</sup>. **Calc. for (C<sub>12</sub>H<sub>10</sub>NO<sub>4</sub>)<sup>+</sup>:** 232.0604.

*The structure of the product was also confirmed by X-ray diffraction (CCDC number = 1984913) as shown below.*



**Figure 25.** Crystal structure of compound **59c**.

***N*-[1,4-Dioxo-8-(phenylthio)-1,4-dihydronaphthalen-2-yl]acetamide (59d)**



The general procedure for acetylation of 5-amino-1,4-naphthoquinones was followed using **578** (280 mg, 1.00 mmol). Precipitation and filtration yielded **59d** (194 mg, 60%) as an orange solid.

**Melting point:** 238-240 °C.

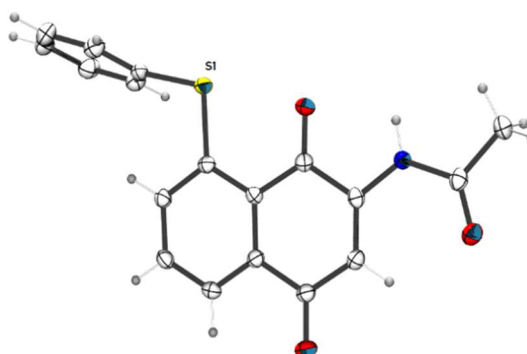
**<sup>1</sup>H NMR (600 MHz, CDCl<sub>3</sub>) δ:** 8.53 (s, 1H), 7.88 (dd, *J* = 8.0, 0.9 Hz, 1H), 7.83 (s, 1H), 7.62-7.60 (m, 2H), 7.53-7.50 (m, 3H), 7.42 (t, *J* = 8.0 Hz, 1H), 7.00 (dd, *J* = 8.0, 0.9 Hz, 1H), 2.30 (s, 3H).

**<sup>13</sup>C NMR (150 MHz, CDCl<sub>3</sub>) δ:** 185.1 (C<sub>q</sub>), 180.7 (C<sub>q</sub>), 169.6 (C<sub>q</sub>), 147.0 (C<sub>q</sub>), 140.6 (C<sub>q</sub>), 136.3 (CH), 134.0 (CH), 134.0 (CH), 131.2 (CH), 130.9 (C<sub>q</sub>), 130.4 (C<sub>q</sub>), 130.4 (CH), 124.8 (C<sub>q</sub>), 123.6 (CH), 116.3 (CH), 25.3 (CH<sub>3</sub>).

**IR (KBr):** 3295 (*m*, N-H), 1698 (*s*, C=O), 1641 (*s*, C=O), 1620 (*s*, C=O), 1489 (*s*, CH<sub>3</sub>), 740 (*s*, C-H<sub>Ar</sub>), 690 (*m*, S-Ph) cm<sup>-1</sup>.

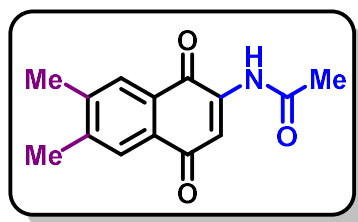
**HRMS-ESI (+):** 324.0688 [M+H]<sup>+</sup>. **Calc. for (C<sub>18</sub>H<sub>14</sub>SNO<sub>3</sub>)<sup>+</sup>:** 324.0689.

The structure of the product was also confirmed by X-ray diffraction (CCDC number = 1984914) as shown below.



**Figure 26.** Crystal structure of compound **59d**.

***N*-(6,7-Dimethyl-1,4-dioxo-1,4-dihydronaphthalen-2-yl)acetamide (59e)**



The general procedure for acetylation of 5-amino-1,4-naphthoquinones was followed using **59e** (21 mg, 0.10 mmol). Precipitation and filtration yielded **59e** (12 mg, 50%) as a yellow solid.

**Melting point:** 120-122 °C.

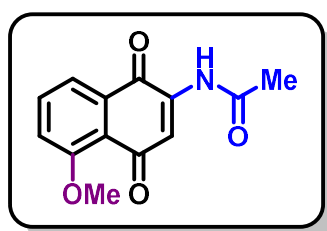
**<sup>1</sup>H NMR (400 MHz, CDCl<sub>3</sub>) δ:** 8.34 (br s, 1H), 7.81 (s, 2H), 7.74 (s, 1H), 2.39 (s, 3H), 2.38 (s, 3H), 2.27 (s, 3H).

**<sup>13</sup>C NMR (100 MHz, CDCl<sub>3</sub>) δ:** 185.8 (C<sub>q</sub>), 181.2 (C<sub>q</sub>), 169.6 (C<sub>q</sub>), 145.4 (C<sub>q</sub>), 143.1 (C<sub>q</sub>), 140.0 (C<sub>q</sub>), 130.4 (C<sub>q</sub>), 128.0 (C<sub>q</sub>), 127.9 (CH), 127.7 (CH), 117.1 (CH), 25.2 (CH<sub>3</sub>), 20.5 (CH<sub>3</sub>), 20.2 (CH<sub>3</sub>).

**IR (ATR):** 3299 (*m*, N-H), 1706 (*m*, C=O), 1668 (*m*, C=O), 1641 (*m*, C=O), 1595 (*s*, CH<sub>3</sub>), 1498 (*s*, CH<sub>3</sub>), 1213 (*s*, C-N), 740 (*m*, C-H<sub>Ar</sub>) cm<sup>-1</sup>.

**HRMS-ESI (+):** 244.0971 [M+H]<sup>+</sup>. **Calc. for (C<sub>14</sub>H<sub>14</sub>NO<sub>3</sub>)<sup>+</sup>:** 244.0968.

***N*-(5-Methoxy-1,4-dioxo-1,4-dihydronaphthalen-2-yl)acetamide (59f)**



The general procedure for acetylation of 5-amino-1,4-naphthoquinones was followed using **58f** (203 mg, 1.00 mmol). Precipitation and filtration yielded **59f** (110 mg, 61%) as a brown solid.

**Melting point:** 223-226 °C.

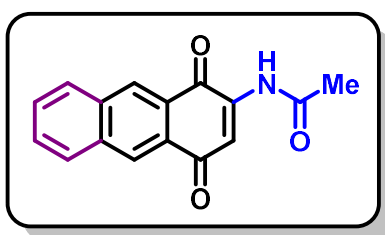
**<sup>1</sup>H NMR (400 MHz, CDCl<sub>3</sub>) δ:** 8.23 (br s, 1H), 7.74 (d, *J* = 8.0 Hz, 1H), 7.71 (s, 1H), 7.63 (t, *J* = 8.0 Hz, 1H), 7.33 (d, *J* = 8.0 Hz, 1H), 3.98 (s, 3H), 2.25 (s, 3H).

$^{13}\text{C}$  NMR (100 MHz,  $\text{CDCl}_3$ )  $\delta$ : 185.1 ( $\text{C}_q$ ), 181.5 ( $\text{C}_q$ ), 169.5 ( $\text{C}_q$ ), 159.6 ( $\text{C}_q$ ), 138.2 ( $\text{C}_q$ ), 134.5 (CH), 132.3 ( $\text{C}_q$ ), 119.8 (CH), 119.7 (CH), 119.6 ( $\text{C}_q$ ), 119.5 (CH), 56.7 ( $\text{CH}_3$ ), 25.1 ( $\text{CH}_3$ ).

IR (ATR): 3274 (*m*, N-H), 1633 (*s*, C=O), 1619 (*s*, C=O), 1563 (*m*,  $\text{CH}_3$ ), 1242 (*s*, C–N), 1000 (*s*, C–O), 761 (*m*, C–H<sub>Ar</sub>)  $\text{cm}^{-1}$ .

HRMS-ESI (+): 246.0757  $[\text{M}+\text{H}]^+$ . Calc. for ( $\text{C}_{13}\text{H}_{12}\text{NO}_4$ )<sup>+</sup>: 246.0761.

***N*-(1,4-Dioxo-1,4-dihydroanthracen-2-yl)acetamide (59g)**



The general procedure for acetylation of 5-amino-1,4-naphthoquinones was followed using **58g** (240 mg, 1.07 mmol). Precipitation and filtration yielded **59g** (232 mg, 81%) as a green solid.

**Melting point:** 300-303 °C.

$^1\text{H}$  NMR (400 MHz,  $\text{DMSO}-d_6$ )  $\delta$ : 9.97 (*s*, 1H), 8.72 (*s*, 1H), 8.58 (*s*, 1H), 8.31-8.25 (*m*, 2H), 7.81-7.74 (*m*, 3H), 2.27 (*s*, 3H).

$^{13}\text{C}$  NMR (100 MHz,  $\text{DMSO}-d_6$ )  $\delta$ : 184.7 ( $\text{C}_q$ ), 179.9 ( $\text{C}_q$ ), 171.4 ( $\text{C}_q$ ), 142.7 ( $\text{C}_q$ ), 134.7 ( $\text{C}_q$ ), 134.1 ( $\text{C}_q$ ), 130.3 (CH), 130.1 (CH), 130.0 (CH), 129.5 (CH), 129.0 (CH), 127.9 ( $\text{C}_q$ ), 127.3 (CH), 127.1 ( $\text{C}_q$ ), 117.8 (CH), 24.6 ( $\text{CH}_3$ ).

IR (ATR): 3290 (*m*, N-H), 1702 (*s*, C=O), 1667 (*s*, C=O), 1637 (*s*, C=O), 1494 (*s*,  $\text{CH}_3$ ), 756 (*s*, C–H<sub>Ar</sub>)  $\text{cm}^{-1}$ .

HRMS-ESI (+): 266.0812  $[\text{M}+\text{H}]^+$ . Calc. for ( $\text{C}_{16}\text{H}_{12}\text{NO}_3$ )<sup>+</sup>: 266.0812.

The structure of the product was also confirmed by X-ray diffraction (CCDC number = 1984915) as shown below.

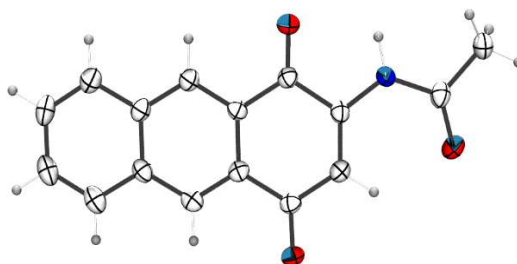
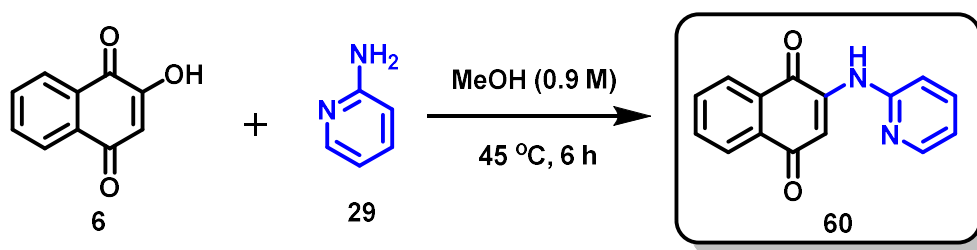


Figure 27. Crystal structure of compound 59g.

### 5.3.6. Synthesis of naphthoquinones with different DG located at the C-2 position

#### 2-(pyridin-2-ylamino)naphthalene-1,4-dione (60)



Lawsonsone (**6**, 1.5 g, 8.6 mmol) was dissolved in methanol (10 mL, 0.9 M) in a 50 mL rounded bottom flask. 2-aminopyridine (**29**, 811 mg, 8.6 mmol) was added to the mixture and it was left under reflux at 45 °C for 6 h. Once the reaction was complete, an orange precipitate was formed after reaching room temperature. A filtration led to the obtention of compound **60** (1.7 g, 79%) as an orange solid.

**Melting point:** 195-198 °C.

**<sup>1</sup>H NMR (400 MHz, DMSO-*d*<sub>6</sub>)**  $\delta$ : 9.39 (br s, 1H), 8.21 (d, *J* = 4.8 Hz, 1H), 8.01 (t, *J* = 6.9 Hz, 1H), 7.91 (t, *J* = 7.5 Hz, 4H), 7.85 (t, *J* = 7.5 Hz, 1H), 7.42 (s, 1H), 5.92 (s, 1H).

**<sup>13</sup>C NMR (100 MHz, DMSO-*d*<sub>6</sub>)**  $\delta$ : 182.2 (C<sub>q</sub>), 179.0 (C<sub>q</sub>), 163.6 (C<sub>q</sub>), 158.1 (CH), 153.5 (C<sub>q</sub>), 152.5 (C<sub>q</sub>), 134.8 (CH), 134.2 (CH), 134.0 (CH), 132.3 (CH), 131.1 (C<sub>q</sub>), 126.1 (CH), 125.9 (CH), 125.7 (CH), 125.3 (CH).

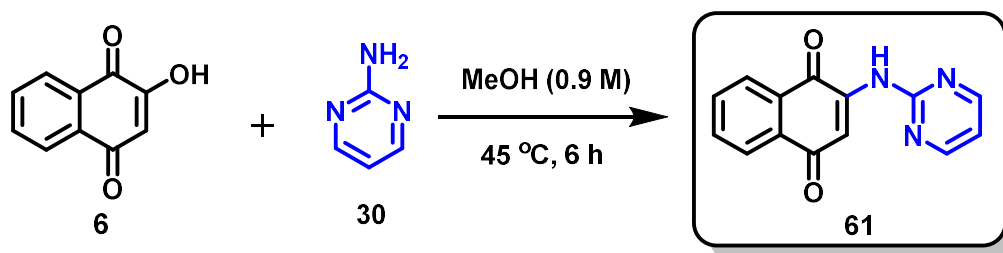
**IR (KBr):** 3495 (*m*, N–H), 3387 (*m*, N–H), 1670 (*s*, C=N), 1653 (*s*, C=O), 1628 (*s*, C=O), 1592 (*m*, N–H), 1491 (*m*, C–H<sub>Alkene</sub>), 1263 (*s*, C–N), 781 (*s*, C–H<sub>Ar</sub>) cm<sup>-1</sup>.

*The analytical data are in accordance with those reported in the literature.*<sup>129</sup>

<sup>129</sup> Dong, Y.; Jiang, H.; Chen, X.-L.; Ye, J.-X.; Zhou, Q.; Gao, L.-S.; Luo, Q.-Q.; Shi, Z.-C.; Li, Z.-H.; He, B. *Synthesis*, **2022**, *54*, 2242-2250.



### 2-(pyrimidin-2-ylamino)naphthalene-1,4-dione (61)



The same procedure described above for the synthesis of compound **59** was also applied on the obtention of compound **61**, using 2-aminopyrimidine (**30**, 818 mg, 8.6 mmol) as substrate. Precipitation and filtration yielded **61** (1.9 g, 87%) as an orange solid.

**Melting point:** 240-245 °C.

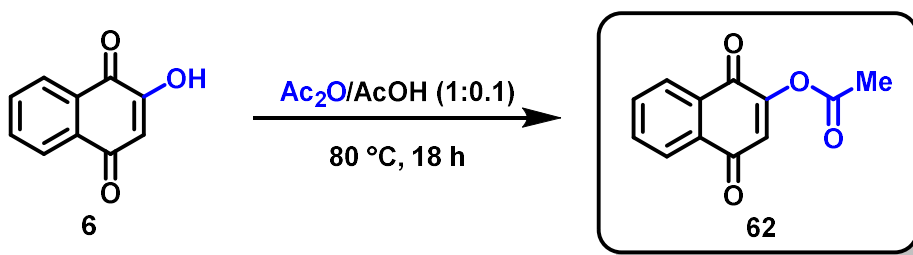
**<sup>1</sup>H NMR (400 MHz, DMSO-*d*<sub>6</sub>)**  $\delta$ : 7.96 (d, *J* = 7.5 Hz, 1H), 7.91 (d, *J* = 7.5 Hz, 1H), 7.81 (t, *J* = 7.5 Hz, 1H), 7.75 (t, *J* = 7.5 Hz, 1H), 6.08 (s, 1H), 4.93-4.82 (br m, 4H).

**<sup>13</sup>C NMR (100 MHz, DMSO-*d*<sub>6</sub>)**  $\delta$ : 184.2 (C<sub>q</sub>), 182.0 (C<sub>q</sub>), 161.3 (C<sub>q</sub>), 153.5 (C<sub>q</sub>), 134.3 (2 x CH), 132.9 (2 x CH), 132.3 (C<sub>q</sub>), 130.8 (C<sub>q</sub>), 125.9 (CH), 125.4 (CH), 110.5 (CH).

**IR (KBr):** 3168 (*s*, N–H), 1675 (*s*, C=N), 1642 (*s*, C=O), 1592 (*m*, N–H), 1579 (*m*, N–H), 1384 (*m*, C–H<sub>Alkene</sub>), 1286 (*s*, C–N), 1258 (*s*, C–N), 1224 (*s*, C–N) cm<sup>-1</sup>.

*The analytical data are in accordance with those reported in the literature.*<sup>82</sup>

### 2-Acetoxy-1,4-naphthoquinone (62)



Lawson's acid (306 mg, 1.8 mmol) was dissolved in a mixture of acetic anhydride (4.0 mL) and glacial acetic acid (400  $\mu$ L) in a sealed tube. The mixture was heated to 80 °C for 18 h. The mixture was then cooled to room temperature and the solvent was removed under constant air flow. The final product was washed with <sup>n</sup>hexane and dried out to provide compound **62** (375 mg, 99%) as a yellow solid.

**Melting point:** 128-131 °C.

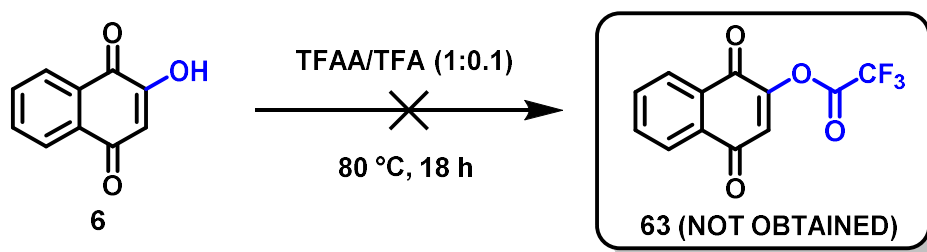
**<sup>1</sup>H NMR (400 MHz, CDCl<sub>3</sub>) δ:** 8.13-8.09 (m, 2H), 7.80-7.75 (m, 2H), 6.77 (s, 1H), 2,40 (s, 3H).

**<sup>13</sup>C NMR (100 MHz, CDCl<sub>3</sub>) δ:** 184.6 (C<sub>q</sub>), 178.7 (C<sub>q</sub>), 167.8 (C<sub>q</sub>), 154.4 (C<sub>q</sub>), 134.5 (CH), 134.1 (CH), 132.0 (C<sub>q</sub>), 131.1 (C<sub>q</sub>), 127.1 (CH), 126.6 (CH), 126.1 (CH), 20.7 (CH<sub>3</sub>).

**IR (KBr):** 1761 (s, C=O), 1678 (s, C=O), 1664 (s, C=O), 1592 (s, CH<sub>3</sub>), 1198 (s, C–O), 1171 (s, C–O), 970 (s, C–O), 743 (s, C–H<sub>Ar</sub>) cm<sup>-1</sup>.

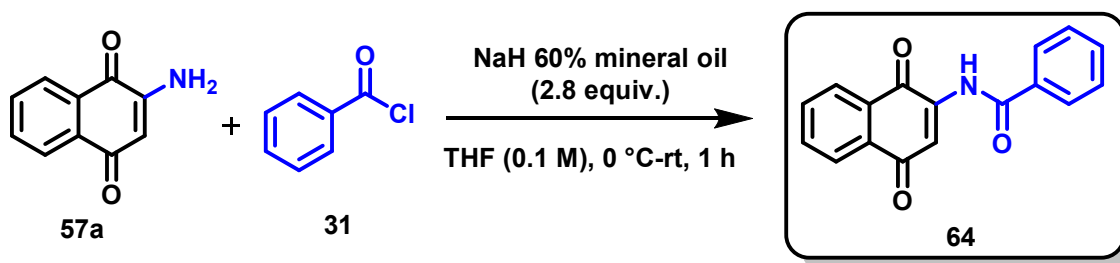
The analytical data are in accordance with those reported in the literature.<sup>130</sup>

### 2-Trifluoroacetoxy-1,4-naphthoquinone (63)



Lawsonsone (153 mg, 0.9 mmol) was dissolved in a mixture of trifluoroacetic anhydride (2.0 mL) and trifluoroacetic acid (200 μL) in a sealed tube. The mixture was heated to 80 °C for 18 h. The mixture was then cooled to room temperature and the solvent was removed under constant air flow. No product was formed, only lawsonsone (6) was obtained back.

### 2-Benzamide-1,4-naphthoquinone (64)



Compound **57a** (300 mg, 1.8 mmol) was dissolved in THF (20 mL, 0.1 M) in a 50 mL rounded bottom flask. Sodium hydride 60% dispersion on mineral oil (200 mg, 5.0 mmol) was

<sup>130</sup> Smith, R. B.; Canton, C.; Lawrence, N. S.; Livingstone, C.; Davis, J. *New J. Chem.*, **2006**, *30*, 1718-1724.

carefully and portion wise added to the solution. Once the evolution of gas stopped, the reaction was cooled down to 0 °C, then benzoyl chloride (**31**, 301  $\mu$ L, 2.7 mmol) was added dropwise to the mixture. The reaction was stirred for 1 h while naturally reaching room temperature. Water (20 mL) was then added to the reaction and the mixture was washed with DCM (3 x 50 mL). The organic phase was washed with a solution of NaOH 1M (1 x 40 mL), hydrochloric acid 1M (1 x 40 mL) and saturated solution of NaCl (1 x 40 mL). Purification by column chromatography (*n*Hexane/EtOAc 7:3) led to the obtention of compound **64** (349 mg, 70%) as an orange solid.

**Melting point:** 133-137 °C.

**<sup>1</sup>H NMR (400 MHz, CDCl<sub>3</sub>)  $\delta$ :** 9.02 (s, 1H), 7.94 (t, *J* = 7.4 Hz, 2H), 7.81 (s, 1H), 7.77 (d, *J* = 7.4 Hz, 2H), 7.65-7.61 (m, 1H), 7.59-7.55 (m, 1H), 7.46 (t, *J* = 7.4 Hz, 1H), 7.38 (t, *J* = 7.4 Hz, 2H).

**<sup>13</sup>C NMR (100 MHz, CDCl<sub>3</sub>)  $\delta$ :** 185.0 (C<sub>q</sub>), 181.0 (C<sub>q</sub>), 165.7 (C<sub>q</sub>), 140.0 (C<sub>q</sub>), 135.0 (CH), 133.3 (CH), 133.1 (C<sub>q</sub>), 132.9 (CH), 132.1 (C<sub>q</sub>), 129.8 (C<sub>q</sub>), 129.0 (CH), 127.3 (CH), 126.7 (CH), 126.3 (CH), 117.1 (CH).

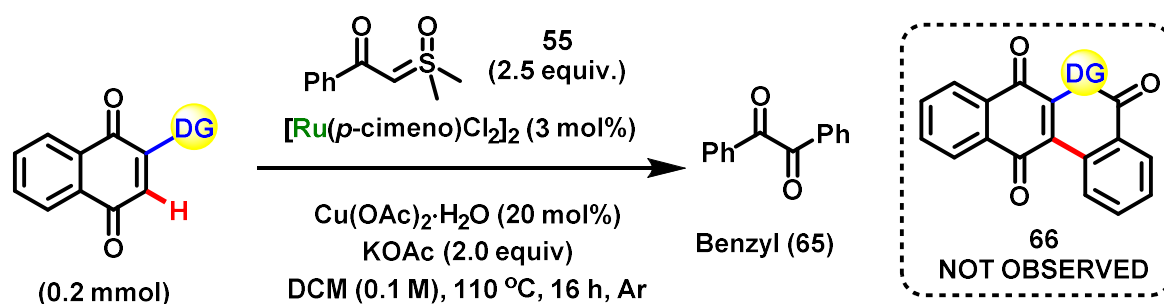
**IR (KBr):** 3365 (*m*, N–H), 1694 (*m*, C=O), 1667 (*m*, C=O), 1642 (*m*, C=O), 1487 (*s*, C–N), 701 (*s*, C–H<sub>Ar</sub>) cm<sup>-1</sup>.

*The analytical data are in accordance with those reported in the literature.*<sup>131</sup>

---

<sup>131</sup> Zhang, C.; Chou, C. J. *Org. Lett.*, **2016**, *18*, 5512-5515.

### 5.3.7. General C–H annulation procedure using sulfoxonium ylide **55**



Under an atmosphere of  $\text{N}_2$ , a 10 mL Schlenk tube was charged with the corresponding naphthoquinone (0.20 mmol), sulfoxonium ylide (**55**, 98 mg, 0.5 mmol),  $[\text{RuCl}_2(p\text{-cymene})]_2$  (3 mg, 3 mol %), copper-II acetate (8 mg, 20 mol%) and potassium acetate (39mg, 0.4 mmol). Then, DCM (2 mL, 0.1 M) was added *via* a syringe. The reaction mixture was heated to 110 °C for 16 h. The mixture was then cooled to room temperature, filtered through a pad of celite and the solvent was removed under reduced pressure. The crude product was purified by column chromatography on silica gel (*n*-Hexane/EtOAc 4:1), leading to the obtention of benzyl (**65**, 23mg, 63%, when 1,4-naphthoquinone **5** was used as substrate) as a bright yellow solid, instead of the desired product **66**.

**Melting point:** 92-95 °C.

**$^1\text{H}$  NMR (600 MHz,  $\text{CDCl}_3$ )  $\delta$ :** 8.13 (dd,  $J = 8.0, 1.1$  Hz, 4H), 7.64-7.61 (m, 2H), 7.49 (t,  $J = 8.0$  Hz, 4H).

**$^{13}\text{C}$  NMR (150 MHz,  $\text{CDCl}_3$ )  $\delta$ :** 171.9 ( $\text{C}_q$ ), 133.9 (CH), 130.4 (CH), 129.4 ( $\text{C}_q$ ), 128.6 (CH).

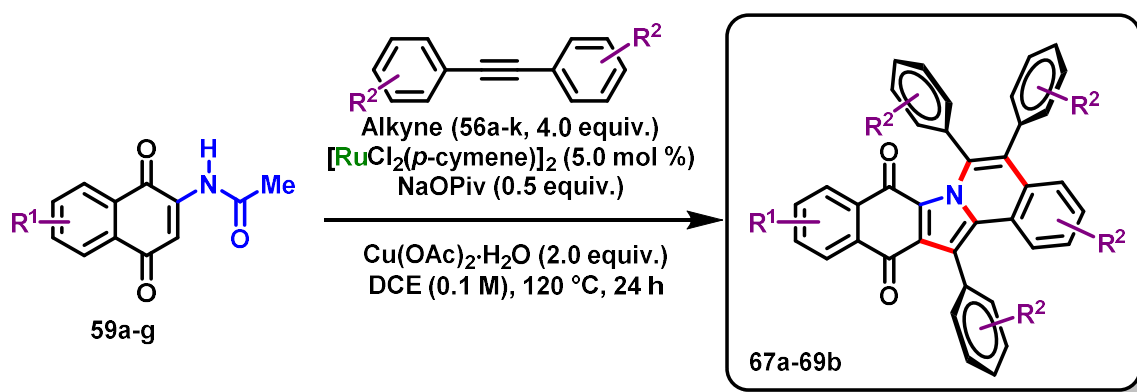
**IR (ATR):** 1705 (*s*,  $\text{C}=\text{O}$ ), 689 (*s*,  $\text{C}-\text{H}_{\text{Ar}}$ )  $\text{cm}^{-1}$ .

*The analytical data are in accordance with those reported in the literature.*<sup>132</sup>

Compounds **5**, **6**, **58a**, **59a**, **60**, **61**, **62** and **64** were submitted to the same general procedure described above for the ruthenium-catalyzed C–H annulation using sulfoxonium ylide **55** aiming the obtention of their respective analogue of product **66**, however, in all cases, only benzyl (**65**) was observed.

<sup>132</sup> Dai, W.; Wang, L.; Shang, S.; Chen, B.; Li, G.; Gao, S. *Chem. Commun.*, **2015**, 51, 11268-11271.

### 5.3.8. General C–H annulation procedure using alkynes (67a-69b)



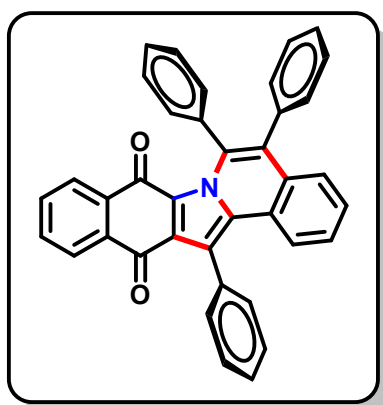
#### General Procedure A:

Under an atmosphere of  $\text{N}_2$ , a 10 mL Schlenk tube was charged with the corresponding naphthoquinone (0.20 mmol),  $\text{Cu}(\text{OAc})_2 \cdot \text{H}_2\text{O}$  (80 mg, 0.40 mmol), the corresponding alkyne (0.80 mmol) and  $[\text{RuCl}_2(p\text{-cymene})]_2$  (6 mg, 5 mol %). Then, DCE (2 mL, 0.1 M) was added *via* a syringe. The reaction mixture was heated to 120 °C for 24 h. The mixture was then cooled to room temperature, filtered through a pad of celite and the solvent was removed under reduced pressure. The crude product was purified by column chromatography on silica gel ( $n\text{-Hexane}/\text{EtOAc}$  4:1).

#### General Procedure B:

Follows the same as described in the general procedure A, except that after 12 h of reaction time, the Schlenk tube was removed from the hot oil bath and cooled to room temperature. A portion of catalyst (6 mg, 5 mol %) was added to the solution under a constant flow of  $\text{N}_2$ . The tube was then sealed once again, and the reaction mixture heated to 120 °C for another 12 h. The mixture was cooled to room temperature, filtered through a pad of celite and the solvent was removed under reduced pressure. The crude product was purified by column chromatography on silica gel ( $n\text{-Hexane}/\text{EtOAc}$  4:1).

**5,6,14-Triphenylbenzo[5,6]indolo[2,1-a]isoquinoline-8,13-dione (67a)**



The general procedure A was followed by using **59a** (43 mg, 0.20 mmol) and diphenylacetylene (**56a**) (142 mg, 0.80 mmol) as starting material. Purification by column chromatography on silica gel (*n*-Hexane/EtOAc 4:1) yielded **67a** (procedure A: 66 mg, 63%; procedure B: 84 mg, 80%) as an orange solid.

**Melting point:** 320-323 °C.

**<sup>1</sup>H NMR (400 MHz, CDCl<sub>3</sub>) δ:** 7.95-7.90 (m, 1H), 7.58-7.48 (m, 7H), 7.46-7.40 (m, 2H), 7.25-7.21 (m, 4H), 7.18-7.10 (m, 4H), 7.09-7.04 (m, 5H).

**<sup>13</sup>C NMR (100 MHz, CDCl<sub>3</sub>) δ:** 182.2 (C<sub>q</sub>), 172.9 (C<sub>q</sub>), 136.9 (C<sub>q</sub>), 136.6 (C<sub>q</sub>), 135.8 (C<sub>q</sub>), 135.7 (C<sub>q</sub>), 135.6 (C<sub>q</sub>), 135.3 (C<sub>q</sub>), 133.7 (C<sub>q</sub>), 133.4 (CH), 132.4 (CH), 131.4 (C<sub>q</sub>), 131.4 (CH), 130.3 (CH), 129.5 (C<sub>q</sub>), 129.4 (CH), 129.0 (CH), 128.6 (C<sub>q</sub>), 128.4 (CH), 128.3 (CH), 128.2 (CH), 128.0 (CH), 127.8 (CH), 127.7 (CH), 127.6 (CH), 127.2 (CH), 126.5 (CH), 126.3 (CH), 125.7 (C<sub>q</sub>), 124.5 (CH), 120.7 (C<sub>q</sub>).

**IR (ATR):** 1662 (*m*, C=O), 1271 (*m*, C–N), 764 (*m*, C–H<sub>Ar</sub>) cm<sup>-1</sup>.

**HRMS-ESI (+):** 526.1803 [M+H]<sup>+</sup>. **Calc. for (C<sub>38</sub>H<sub>24</sub>NO<sub>2</sub>)<sup>+</sup>:** 526.1802.

*The structure of the product was also confirmed by X-ray diffraction (CCDC number = 1984922) as shown below.*

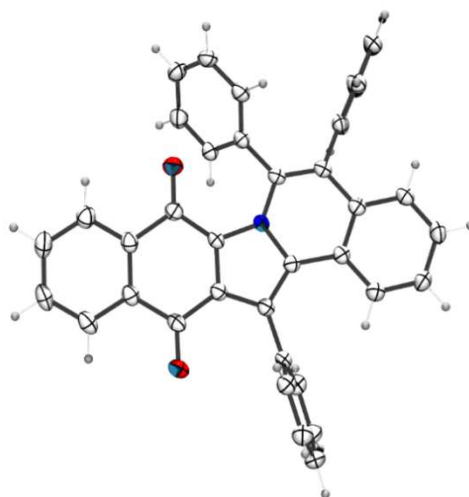
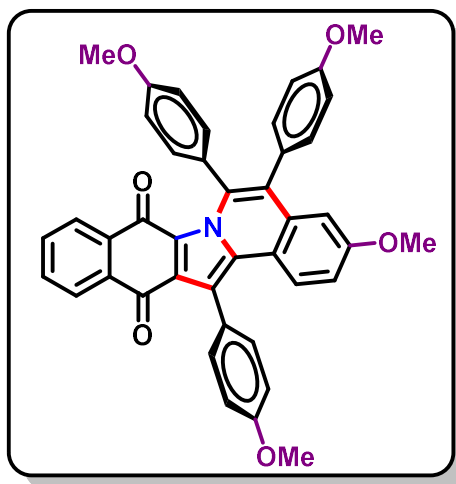


Figure 28. Crystal structure of compound **67a**.

**3-Methoxy-5,6,14-tris(4-methoxyphenyl)benzo[5,6]indolo[2,1-*a*]isoquinoline-8,13-dione**  
**(67b)**



The general procedure A was followed by using **59a** (43 mg, 0.20 mmol) and **56b** (191 mg, 0.80 mmol) as starting material. Purification by column chromatography on silica gel (*n*-Hexane/EtOAc 4:1) yielded **67b** (procedure A: 98 mg, 76%; procedure B: 118 mg, 91%) as a red solid.

**Melting point:** 281-284 °C.

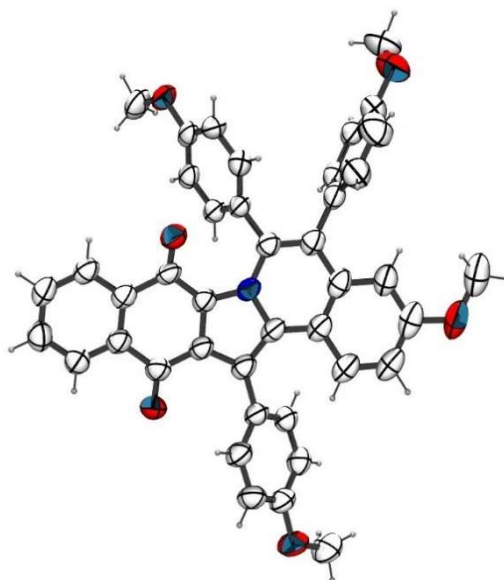
**<sup>1</sup>H NMR (400 MHz, CDCl<sub>3</sub>)**  $\delta$ : 7.94-7.90 (m, 1H), 7.60-7.56 (m, 2H), 7.46-7.42 (m, 2H), 7.41-7.38 (m, 2H), 7.10-7.06 (m, 4H), 6.97-6.94 (m, 2H), 6.80-6.76 (m, 3H), 6.63-6.59 (m, 3H), 3.88 (s, 3H), 3.76 (s, 3H), 3.69 (s, 3H), 3.58 (s, 3H).

**$^{13}\text{C}$  NMR (100 MHz,  $\text{CDCl}_3$ )  $\delta$ :** 182.6 ( $\text{C}_q$ ), 172.3 ( $\text{C}_q$ ), 159.6 ( $\text{C}_q$ ), 159.3 ( $\text{C}_q$ ), 158.9 ( $\text{C}_q$ ), 158.8 ( $\text{C}_q$ ), 136.5 ( $\text{C}_q$ ), 136.4 ( $\text{C}_q$ ), 136.1 ( $\text{C}_q$ ), 134.0 ( $\text{C}_q$ ), 133.8 ( $\text{C}_q$ ), 133.4 (CH), 132.4 (CH), 132.1 (CH), 131.5 (CH), 130.2 (CH), 129.8 ( $\text{C}_q$ ), 128.9 ( $\text{C}_q$ ), 128.9 (CH), 128.6 ( $\text{C}_q$ ), 127.3 ( $\text{C}_q$ ), 127.1 ( $\text{C}_q$ ), 126.5 (CH), 126.2 (CH), 126.2 ( $\text{C}_q$ ), 119.7 ( $\text{C}_q$ ), 118.9 ( $\text{C}_q$ ), 116.4 (CH), 114.9 (CH), 113.9 (CH), 113.2 (CH), 109.5 (CH), 55.5 ( $\text{CH}_3$ ), 55.4 ( $\text{CH}_3$ ), 55.4 ( $\text{CH}_3$ ), 55.3 ( $\text{CH}_3$ ).

**IR (ATR):** 1661 (*m*, C=O), 1606 (*m*, C=O), 1458 (*m*,  $\text{CH}_3$ ), 1243 (*s*, C–N), 1022 (*s*, C–O), 793 (*s*, C–H<sub>Ar</sub>)  $\text{cm}^{-1}$ .

**HRMS-ESI (+):** 646.2218  $[\text{M}+\text{H}]^+$ . **Calc. for  $(\text{C}_{42}\text{H}_{32}\text{NO}_6)^+$ :** 646.2224.

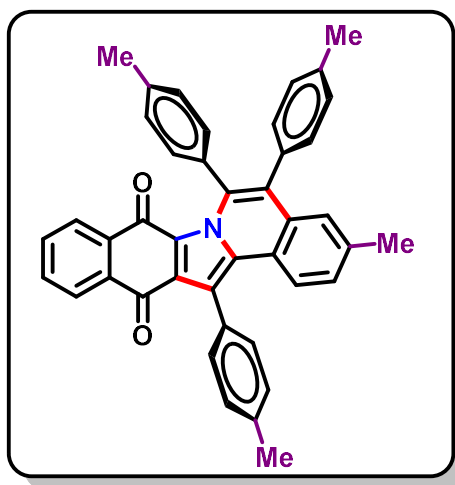
The structure of the product was also confirmed by X-ray diffraction (CCDC number = 1984923) as shown below.



**Figure 29.** Crystal structure of compound **67b**.



### 3-Methyl-5,6,14-tri-*p*-tolylbenzo[5,6]indolo[2,1-*a*]isoquinoline-8,13-dione (67c)



The general procedure A was followed by using **59a** (43 mg, 0.20 mmol) and **56c** (165 mg, 0.80 mmol) as starting material. Purification by column chromatography on silica gel (*n*-Hexane/EtOAc 4:1) yielded **67c** (procedure A: 41 mg, 35%; procedure B: 85 mg, 73%) as an orange solid.

**Melting point:** 322-325 °C.

**<sup>1</sup>H NMR (400 MHz, CDCl<sub>3</sub>)**  $\delta$ : 8.02-7.98 (m, 1H), 7.64-7.62 (m, 1H), 7.59 (d, *J* = 8.9 Hz, 1H), 7.54-7.49 (m, 2H), 7.44 (d, *J* = 8.0 Hz, 2H), 7.40 (d, *J* = 8.0 Hz, 2H), 7.12 (t, *J* = 8.0 Hz, 4H), 7.06-7.05 (m, 2H), 7.00 (d, *J* = 8.0 Hz, 2H), 6.94 (d, *J* = 8.0 Hz, 2H), 2.53 (s, 3H), 2.39 (s, 3H), 2.27 (s, 6H).

**<sup>13</sup>C NMR (100 MHz, CDCl<sub>3</sub>)**  $\delta$ : 182.4 (C<sub>q</sub>), 172.6 (C<sub>q</sub>), 138.3 (C<sub>q</sub>), 137.9 (C<sub>q</sub>), 137.2 (C<sub>q</sub>), 137.0 (C<sub>q</sub>), 136.1 (C<sub>q</sub>), 136.0 (C<sub>q</sub>), 135.8 (C<sub>q</sub>), 134.3 (C<sub>q</sub>), 133.8 (C<sub>q</sub>), 133.7 (C<sub>q</sub>), 133.3 (CH), 132.3 (C<sub>q</sub>), 132.2 (CH), 131.9 (C<sub>q</sub>), 131.2 (CH), 130.1 (2 × CH), 129.4 (CH), 129.2 (C<sub>q</sub>), 129.0 (CH), 128.8 (CH), 128.6 (C<sub>q</sub>), 128.4 (CH), 127.4 (C<sub>q</sub>), 126.9 (CH), 126.4 (CH), 126.2 (CH), 124.4 (CH), 123.2 (C<sub>q</sub>), 120.1 (C<sub>q</sub>), 21.9 (CH<sub>3</sub>), 21.8 (CH<sub>3</sub>), 21.6 (2 × CH<sub>3</sub>).

**IR (ATR):** 1660 (*s*, C=O), 1454 (*m*, CH<sub>3</sub>), 1199 (*s*, C–N), 1143 (*s*, C–N), 799 (*m*, C–H<sub>Ar</sub>) cm<sup>-1</sup>.

**HRMS-ESI (+):** 582.2421 [M+H]<sup>+</sup>. **Calc. for (C<sub>42</sub>H<sub>32</sub>NO<sub>2</sub>)<sup>+</sup>:** 582.2428.

The structure of the product was also confirmed by X-ray diffraction (CCDC number = 1984924) as shown below.

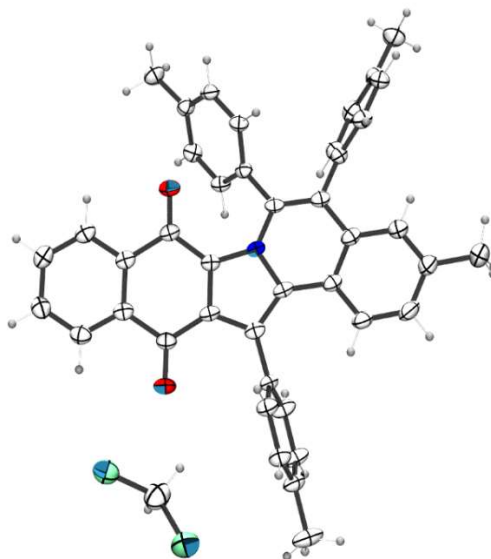
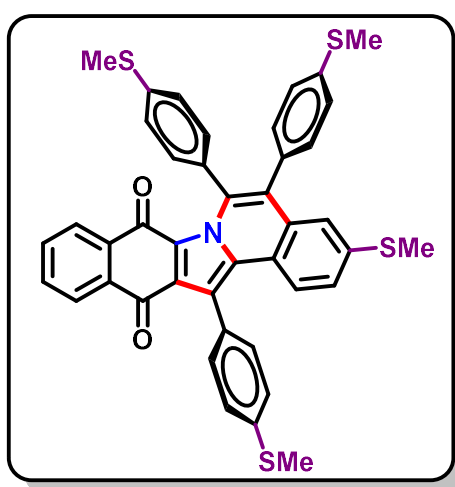


Figure 30. Crystal structure of compound 67c.

**3-(Methylthio)-5,6,14-tris[4-(methylthio)phenyl]benzo[5,6]indolo[2,1-*a*]iso-quinoline-8,13-dione (67d)**



The general procedure A was followed by using **59a** (43 mg, 0.20 mmol) and **56d** (216 mg, 0.80 mmol) as starting material. Purification by column chromatography on silica gel (*n*-Hexane/EtOAc 4:1) yielded **67d** (procedure A: 31 mg, 22%; procedure B: 55 mg, 39%) as a dark red solid.

**Melting point:** 248-252 °C.

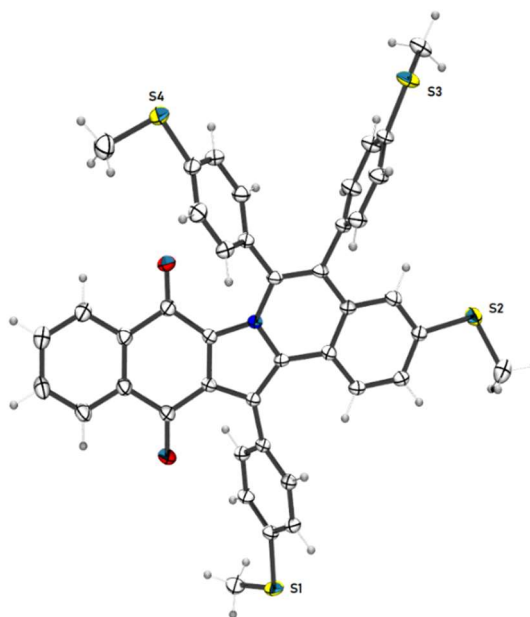
**<sup>1</sup>H NMR (400 MHz, CDCl<sub>3</sub>)**  $\delta$ : 8.02-7.99 (m, 1H), 7.68-7.64 (m, 1H), 7.61 (d, *J* = 8.0 Hz, 1H), 7.57-7.53 (m, 2H), 7.47 (s, 4H), 7.21 (d, *J* = 8.0 Hz, 2H), 7.14-7.11 (m, 3H), 7.06-7.01 (m, 5H), 2.62 (s, 3H), 2.52 (s, 3H), 2.44 (s, 3H), 2.32 (s, 3H).

$^{13}\text{C}$  NMR (100 MHz,  $\text{CDCl}_3$ )  $\delta$ : 182.3 ( $\text{C}_q$ ), 172.6 ( $\text{C}_q$ ), 140.0 ( $\text{C}_q$ ), 138.8 ( $\text{C}_q$ ), 138.3 ( $\text{C}_q$ ), 138.3 ( $\text{C}_q$ ), 136.0 ( $\text{C}_q$ ), 135.9 ( $\text{C}_q$ ), 135.8 ( $\text{C}_q$ ), 133.7 ( $\text{C}_q$ ), 133.6 (CH), 133.4 ( $\text{C}_q$ ), 132.6 ( $\text{C}_q$ ), 132.4 (CH), 132.0 ( $\text{C}_q$ ), 131.7 (CH), 131.4 ( $\text{C}_q$ ), 130.8 (CH), 129.2 (CH), 128.8 ( $\text{C}_q$ ), 128.2 ( $\text{C}_q$ ), 127.6 ( $\text{C}_q$ ), 127.0 (CH), 126.6 (CH), 126.3 (CH), 126.2 (CH), 126.1 (CH), 125.4 (CH), 124.7 (CH), 123.2 (CH), 122.6 ( $\text{C}_q$ ), 119.5 ( $\text{C}_q$ ), 15.7 ( $\text{CH}_3$ ), 15.7 ( $\text{CH}_3$ ), 15.5 ( $\text{CH}_3$ ), 15.4 ( $\text{CH}_3$ ).

**IR (ATR):** 1719 (*m*, C=O), 1666 (*m*, C=O), 1434 (*m*,  $\text{CH}_3$ ), 1273 (*s*, C–N), 733 (*m*, C– $\text{H}_{\text{Ar}}$ ), 694 (*m*, C–S)  $\text{cm}^{-1}$ .

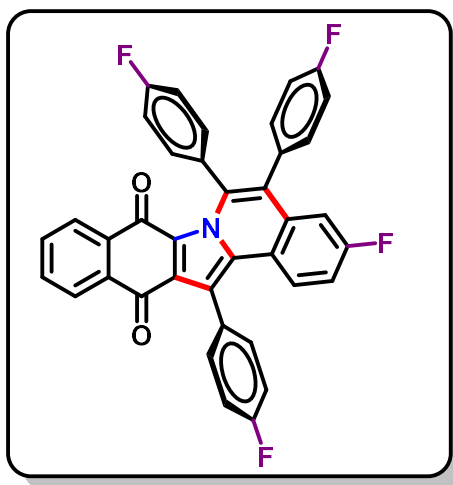
**HRMS-ESI (+):** 710.1301  $[\text{M}+\text{H}]^+$ . **Calc. for  $(\text{C}_{42}\text{H}_{32}\text{NO}_2\text{S}_4)^+$ :** 710.1310.

The structure of the product was also confirmed by X-ray diffraction (CCDC number = 1984925) as shown below.



**Figure 31.** Crystal structure of compound **67d**.

**3-Fluoro-5,6,14-tris(4-fluorophenyl)benzo[5,6]indolo[2,1-*a*]isoquinoline-8,13-dione (67e)**



The general procedure A was followed by using **59a** (43 mg, 0.20 mmol) and **56e** (171 mg, 0.80 mmol) as starting material. Purification by column chromatography on silica gel (Hexane/EtOAc 4:1) yielded **67e** (procedure A: 32 mg, 27%; procedure B: 73 mg, 62%) as an orange solid.

**Melting point:** 283-285 °C.

**<sup>1</sup>H NMR (400 MHz, CDCl<sub>3</sub>) δ:** 8.02-7.99 (m, 1H), 7.67-7.62 (m, 2H), 7.58-7.51 (m, 4H), 7.32 (t, *J* = 8.0 Hz, 2H), 7.22-7.18 (m, 2H), 7.08-6.99 (m, 5H), 6.92-6.86 (m, 3H).

**<sup>13</sup>C NMR (100 MHz, CDCl<sub>3</sub>) δ:** 182.2 (C<sub>q</sub>), 172.9 (C<sub>q</sub>), 163.0 (d, <sup>1</sup>*J*<sub>C-F</sub> = 247.8 Hz, C<sub>q</sub>), 162.4 (d, <sup>1</sup>*J*<sub>C-F</sub> = 248.3 Hz, C<sub>q</sub>), 162.1 (d, <sup>1</sup>*J*<sub>C-F</sub> = 249.2 Hz, 2 × C<sub>q</sub>), 136.2 (C<sub>q</sub>), 135.5 (C<sub>q</sub>), 135.4 (C<sub>q</sub>), 133.8 (CH), 133.6 (C<sub>q</sub>), 133.5 (C<sub>q</sub>), 132.8 (d, <sup>3</sup>*J*<sub>C-F</sub> = 8.1 Hz, CH), 132.7 (CH), 132.5 (d, <sup>4</sup>*J*<sub>C-F</sub> = 3.7 Hz, C<sub>q</sub>), 132.0 (d, <sup>3</sup>*J*<sub>C-F</sub> = 8.0 Hz, CH), 131.6 (d, <sup>4</sup>*J*<sub>C-F</sub> = 3.6 Hz, C<sub>q</sub>), 130.8 (d, <sup>3</sup>*J*<sub>C-F</sub> = 8.3 Hz, CH), 130.5 (d, <sup>4</sup>*J*<sub>C-F</sub> = 3.5 Hz, C<sub>q</sub>), 129.0 (C<sub>q</sub>), 128.0 (d, <sup>4</sup>*J*<sub>C-F</sub> = 3.5 Hz, C<sub>q</sub>), 127.5 (C<sub>q</sub>), 126.8 (d, <sup>3</sup>*J*<sub>C-F</sub> = 8.7 Hz, CH), 126.6 (CH), 126.4 (CH), 122.1 (d, <sup>4</sup>*J*<sub>C-F</sub> = 2.2 Hz, C<sub>q</sub>), 119.0 (C<sub>q</sub>), 116.9 (d, <sup>2</sup>*J*<sub>C-F</sub> = 23.3 Hz, CH), 116.7 (d, <sup>2</sup>*J*<sub>C-F</sub> = 21.5 Hz, CH), 115.9 (d, <sup>2</sup>*J*<sub>C-F</sub> = 21.6 Hz, CH), 115.1 (d, <sup>2</sup>*J*<sub>C-F</sub> = 21.9 Hz, CH), 112.4 (d, <sup>2</sup>*J*<sub>C-F</sub> = 23.4 Hz, CH).

**IR (ATR):** 1660 (*s*, C=O), 1270 (*s*, C–N), 1221 (*s*, C–F), 735 (*m*, C–H<sub>Ar</sub>) cm<sup>-1</sup>.

**HRMS-ESI (+):** 595.1423 [M+H]<sup>+</sup>. **Calc. for (C<sub>38</sub>H<sub>20</sub>F<sub>4</sub>NO<sub>2</sub>)<sup>+</sup>:** 595.1425.

The structure of the product was also confirmed by X-ray diffraction (CCDC number = 1984926) as shown below.

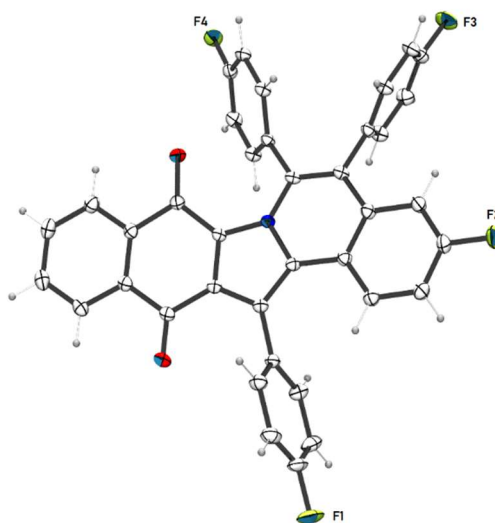
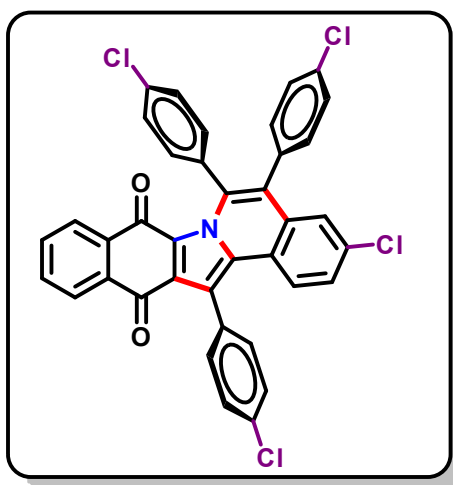


Figure 32. Crystal structure of compound 67e.

**3-Chloro-5,6,14-tris(4-chlorophenyl)benzo[5,6]indolo[2,1-*a*]isoquinoline-8,13-dione (67f)**



The general procedure A was followed by using **59a** (43 mg, 0.20 mmol) and **56f** (198 mg, 0.80 mmol) as starting material. Purification by column chromatography on silica gel (Hexane/EtOAc 4:1) yielded **67f** (procedure A: 34 mg, 26%; procedure B: 42 mg, 32%) as an orange solid.

**Melting point:** 347-350 °C.

**<sup>1</sup>H NMR (400 MHz, CDCl<sub>3</sub>) δ:** 8.02-7.99 (m, 1H), 7.69-7.66 (m, 1H), 7.61-7.57 (m, 5H), 7.48 (d, *J* = 8.2 Hz, 2H), 7.36 (d, *J* = 8.2 Hz, 2H), 7.24 (br s, 1H), 7.18-7.13 (m, 5H), 7.05 (d, *J* = 8.2 Hz, 2H).

$^{13}\text{C}$  NMR (100 MHz,  $\text{CDCl}_3$ )  $\delta$ : 182.0 ( $\text{C}_q$ ), 173.0 ( $\text{C}_q$ ), 135.8 ( $\text{C}_q$ ), 135.4 ( $\text{C}_q$ ), 135.0 ( $\text{C}_q$ ), 134.9 ( $\text{C}_q$ ), 134.8 ( $\text{C}_q$ ), 134.8 ( $\text{C}_q$ ), 134.4 ( $\text{C}_q$ ), 134.2 ( $\text{C}_q$ ), 133.9 ( $\text{C}_q$ ), 133.9 (CH), 133.5 ( $\text{C}_q$ ), 133.1 ( $\text{C}_q$ ), 132.9 (CH), 132.5 (CH), 132.4 ( $\text{C}_q$ ), 131.7 (CH), 130.2 (CH), 129.9 (CH), 129.2 (CH), 129.0 (CH), 128.9 ( $\text{C}_q$ ), 128.4 (CH), 127.8 ( $\text{C}_q$ ), 127.6 ( $\text{C}_q$ ), 126.7 (CH), 126.4 (CH), 126.4 (CH), 125.8 (CH), 123.9 ( $\text{C}_q$ ), 119.4 ( $\text{C}_q$ ).

IR (ATR): 1655 (*s*, C=O), 1272 (*m*, C–N), 821 (*s*, C–Cl), 754 (*m*, C–H<sub>Ar</sub>)  $\text{cm}^{-1}$ .

HRMS-ESI (+): 662.0217 [ $^{35}\text{Cl}$ , M+H] $^+$ . Calc. for  $(\text{C}_{38}\text{H}_{20}\text{Cl}_4\text{NO}_2)^+$ : 662.0243.

The structure of the product was also confirmed by X-ray diffraction (CCDC number = 1984927) as shown below.

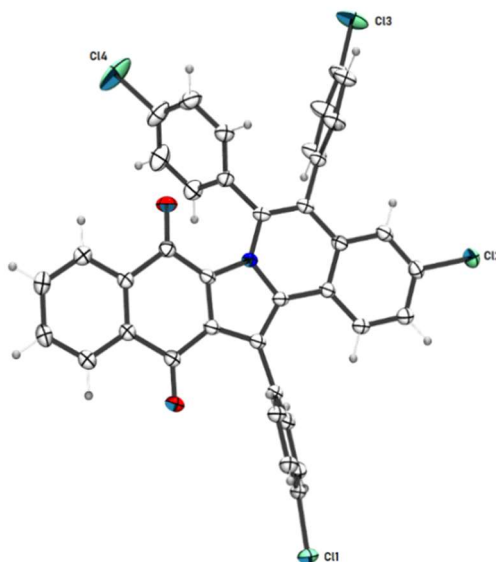
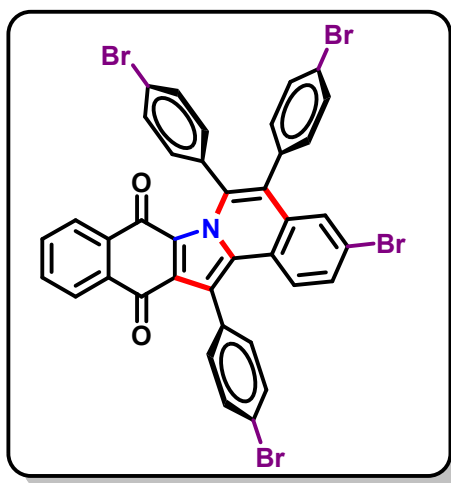


Figure 33. Crystal structure of compound 67f.

**3-Bromo-5,6,14-tris(4-bromophenyl)benzo[5,6]indolo[2,1-a]isoquinoline-8,13-dione (67g)**



The general procedure A was followed by using **59a** (43 mg, 0.20 mmol) and **56g** (269 mg, 0.80 mmol) as starting material. Purification by column chromatography on silica gel (*n*-Hexane/EtOAc 4:1) yielded **67g** (procedure A: 35 mg, 21%; procedure B: 65 mg, 39%) as an orange solid.

**Melting point:** > 370 °C.

**<sup>1</sup>H NMR (400 MHz, CDCl<sub>3</sub>) δ:** 8.02-7.99 (m, 1H), 7.76-7.73 (m, 2H), 7.69-7.66 (m, 1H), 7.61-7.56 (m, 2H), 7.54-7.50 (m, 3H), 7.43-7.39 (m, 3H), 7.34-7.31 (m, 3H), 7.09-7.06 (m, 2H), 7.00-6.97 (m, 2H).

**<sup>13</sup>C NMR (100 MHz, CDCl<sub>3</sub>) δ:** 181.9 (C<sub>q</sub>), 173.0 (C<sub>q</sub>), 135.7 (C<sub>q</sub>), 135.4 (C<sub>q</sub>), 135.2 (C<sub>q</sub>), 134.9 (C<sub>q</sub>), 134.3 (C<sub>q</sub>), 133.9 (CH), 133.5 (C<sub>q</sub>), 133.4 (C<sub>q</sub>), 132.9 (CH), 132.8 (CH), 132.8 (CH), 132.5 (C<sub>q</sub>), 132.2 (CH), 131.9 (CH), 131.8 (CH), 131.4 (CH), 130.4 (CH), 129.4 (CH), 128.9 (C<sub>q</sub>), 127.8 (C<sub>q</sub>), 127.5 (C<sub>q</sub>), 126.7 (CH), 126.4 (CH), 125.9 (CH), 124.2 (C<sub>q</sub>), 123.2 (C<sub>q</sub>), 123.0 (C<sub>q</sub>), 122.6 (C<sub>q</sub>), 122.5 (C<sub>q</sub>), 119.5 (C<sub>q</sub>).

**IR (ATR):** 1713 (s, C=O), 1702 (s, C=O), 1222 (s, C–N) cm<sup>-1</sup>.

**HRMS-ESI (+):** 837.8182 [<sup>79</sup>Br, M+H]<sup>+</sup>. **Calc. for (C<sub>38</sub>H<sub>20</sub>Br<sub>4</sub>NO<sub>2</sub>)<sup>+</sup>:** 837.8222.

*The structure of the product was also confirmed by X-ray diffraction (CCDC number = 1984928) as shown below.*

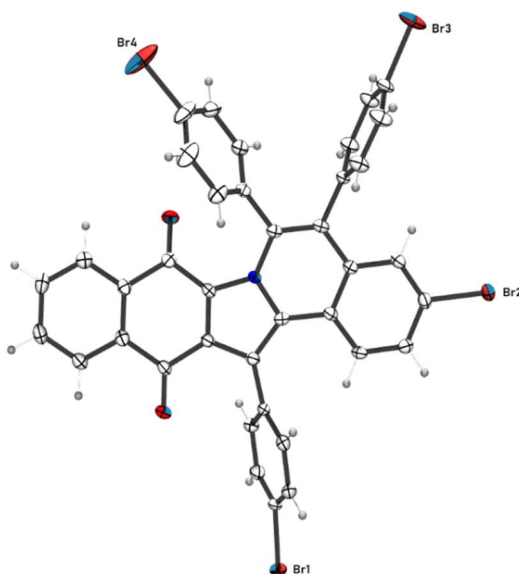
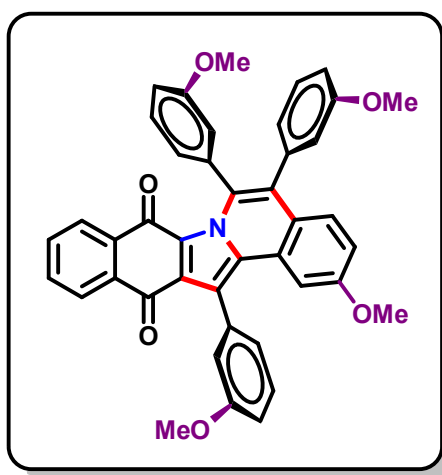


Figure 34. Crystal structure of compound **67g**.

**2-Methoxy-5,6,14-tris(3-methoxyphenyl)benzo[5,6]indolo[2,1-*a*]isoquinoline-8,13-dione  
(67h)**



The general procedure A was followed by using **59a** (43 mg, 0.20 mmol) and **56h** (191 mg, 0.80 mmol) as starting material. Purification by column chromatography on silica gel (Hexane/EtOAc 4:1) yielded **67h** (procedure A: 66 mg, 51%; procedure B: 102 mg, 79%) as a red solid.

**Melting point:** 183-185 °C.

**<sup>1</sup>H NMR (400 MHz, CDCl<sub>3</sub>)**  $\delta$ : 8.03-8.01 (m, 1H), 7.70-7.68 (m, 1H), 7.57-7.53 (m, 3H), 7.29-7.20 (m, 3H), 7.17-7.14 (m, 2H), 7.09-7.03 (m, 2H), 6.93-6.75 (m, 5H), 6.70-6.54 (m, 2H), 3.87 (s, 3H), 3.72-3.64 (m, 3H), 3.57 (s, 3H), 3.40 (s, 3H).

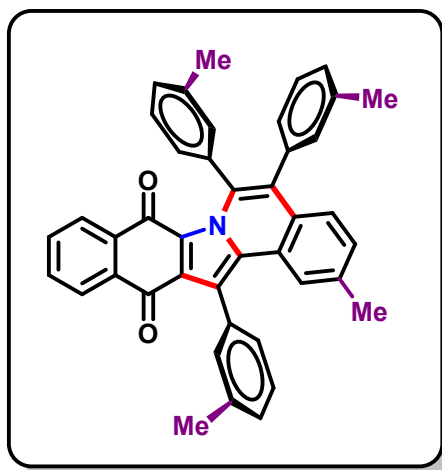


**<sup>13</sup>C NMR (100 MHz, CDCl<sub>3</sub>) δ:** 182.2 (C<sub>q</sub>), 172.9 (C<sub>q</sub>), 160.5 (C<sub>q</sub>), 159.3 (C<sub>q</sub>), 159.1 (C<sub>q</sub>), 138.2 (C<sub>q</sub>), 137.0 (C<sub>q</sub>), 135.9 (C<sub>q</sub>), 135.2 (C<sub>q</sub>), 133.7 (C<sub>q</sub>), 133.5 (CH), 133.2 (C<sub>q</sub>), 132.3 (CH), 130.4 (CH), 129.5 (CH), 129.2 (CH), 128.8 (CH), 128.7 (CH), 128.2 (C<sub>q</sub>), 127.4 (C<sub>q</sub>), 126.9 (C<sub>q</sub>), 126.6 (CH), 126.3 (CH), 125.2 (C<sub>q</sub>), 123.9 (CH), 122.8 (CH), 121.2 (C<sub>q</sub>), 120.6 (C<sub>q</sub>), 120.3 (C<sub>q</sub>), 118.8 (CH), 116.9 (C<sub>q</sub>), 116.4 (CH), 115.7 (CH), 114.7 (CH), 114.2 (CH), 113.7 (CH), 113.3 (CH), 105.3 (CH), 55.6 (CH<sub>3</sub>), 55.5 (2 × CH<sub>3</sub>), 55.0 (CH<sub>3</sub>).

**IR (ATR):** 1665 (*m*, C=O), 1593 (*s*, C=O), 1465 (*s*, CH<sub>3</sub>), 1217 (*s*, C–N), 1038 (*s*, C–O), 693 (*s*, C–H<sub>Ar</sub>) cm<sup>-1</sup>.

**HRMS-ESI (+):** 646.2211 [M+H]<sup>+</sup>. **Calc. for (C<sub>42</sub>H<sub>32</sub>NO<sub>6</sub>)<sup>+</sup>:** 646.2224.

### 2-Methyl-5,6,14-tri-*m*-tolylbenzo[5,6]indolo[2,1-*a*]isoquinoline-8,13-dione (67i)



The general procedure A was followed by using **59a** (43 mg, 0.20 mmol) and **56i** (165 mg, 0.80 mmol) as starting material. Purification by column chromatography on silica gel (*n*-Hexane/EtOAc 4:1) yielded **67i** (procedure A: 70 mg, 60%; procedure B: 73 mg, 63%) as an orange solid.

**Melting point:** 148-151 °C.

**<sup>1</sup>H NMR (400 MHz, CDCl<sub>3</sub>) δ:** 8.03-8.01 (*m*, 1H), 7.66-7.64 (*m*, 1H), 7.55-7.49 (*m*, 3H), 7.38 (*d*, *J* = 8.0 Hz, 4H), 7.20-7.17 (*m*, 2H), 7.13-7.09 (*m*, 2H), 7.03-7.02 (*m*, 3H), 6.96-6.88 (*m*, 3H), 2.49 (*s*, 3H), 2.30 (*s*, 3H), 2.16 (*s*, 3H), 2.14 (*s*, 3H).

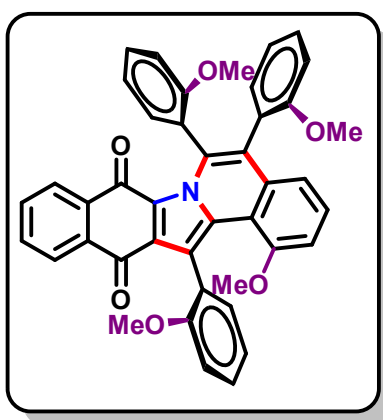
**<sup>13</sup>C NMR (100 MHz, CDCl<sub>3</sub>) δ:** 182.3 (C<sub>q</sub>), 172.8 (C<sub>q</sub>), 138.8 (C<sub>q</sub>), 137.7 (C<sub>q</sub>), 137.7 (C<sub>q</sub>), 137.1 (C<sub>q</sub>), 136.9 (C<sub>q</sub>), 136.7 (C<sub>q</sub>), 136.0 (C<sub>q</sub>), 135.7 (C<sub>q</sub>), 135.3 (C<sub>q</sub>), 134.9 (C<sub>q</sub>), 133.8 (C<sub>q</sub>), 133.3 (CH), 132.2 (CH), 132.1 (CH), 132.1 (CH), 132.0 (CH), 130.8 (CH), 129.6 (CH), 129.5 (C<sub>q</sub>), 129.3 (C<sub>q</sub>), 129.2 (CH), 129.0 (CH), 128.4 (CH), 128.4 (CH), 128.3 (C<sub>q</sub>), 128.1 (CH),

128.0 (CH), 127.5 (C<sub>q</sub>), 127.5 (CH), 127.3 (CH), 127.1 (CH), 126.4 (CH), 126.2 (CH), 125.6 (C<sub>q</sub>), 124.5 (CH), 120.8 (C<sub>q</sub>), 21.9 (CH<sub>3</sub>), 21.8 (CH<sub>3</sub>), 21.6 (CH<sub>3</sub>), 21.5 (CH<sub>3</sub>).

**IR (ATR):** 1713 (s, C=O), 1664 (s, C=O), 1467 (s, CH<sub>3</sub>), 1283 (s, C–N), 1219 (s, C–N), 766 (m, C–H<sub>Ar</sub>) cm<sup>-1</sup>.

**HRMS-ESI (+):** 582.2424 [M+H]<sup>+</sup>. **Calc. for (C<sub>42</sub>H<sub>32</sub>NO<sub>2</sub>)<sup>+</sup>:** 582.2428.

**1-Methoxy-5,6,14-tris(2-methoxyphenyl)benzo[5,6]indolo[2,1-a]isoquinoline-8,13-dione**  
(67j)



The general procedure A was followed by using **59a** (43 mg, 0.20 mmol) and **56j** (191 mg, 0.80 mmol) as starting material. Purification by column chromatography on silica gel (*n*-Hexane/EtOAc 4:1) yielded **67j** (procedure A: 71 mg, 55%; procedure B: 112 mg, 87%) as a red solid and as a mixture of atropoisomers.

**Melting point:** 194-196 °C.

**<sup>1</sup>H NMR (400 MHz, CDCl<sub>3</sub>) isomer A (38%), isomer B (33%), isomer C (17%), isomer D (12%) [ratio determined by comparative integration of the <sup>1</sup>H NMR resonances at δ = 3.84-3.74] δ:** 8.00–7.98 (m, 1H), 7.60–7.58 (m, 1H), 7.51-7.46 (m, 2H), 7.40-7.36 (m, 1H), 7.33-7.20 (m, 3H), 7.17-7.07 (m, 3H), 7.06-6.94 (m, 2H), 6.93-6.75 (m, 4H), 6.73-6.62 (m, 2H), 3.84-3.74 (m, 3H), 3.68-3.53 (m, 3H), 3.52-3.41 (m, 3H), 3.10-3.08 (m, 3H).

**<sup>13</sup>C NMR (100 MHz, CDCl<sub>3</sub>) δ:** 181.9 (C<sub>q</sub>), 181.9 (C<sub>q</sub>), 181.8 (C<sub>q</sub>), 181.8 (C<sub>q</sub>), 173.0 (C<sub>q</sub>), 172.9 (C<sub>q</sub>), 172.8 (C<sub>q</sub>), 172.7 (C<sub>q</sub>), 158.2 (C<sub>q</sub>), 157.8 (C<sub>q</sub>), 157.8 (C<sub>q</sub>), 157.7 (C<sub>q</sub>), 157.7 (C<sub>q</sub>), 157.7 (C<sub>q</sub>), 157.5 (C<sub>q</sub>), 157.3 (C<sub>q</sub>), 157.2 (C<sub>q</sub>), 157.1 (C<sub>q</sub>), 156.7 (C<sub>q</sub>), 155.9 (C<sub>q</sub>), 155.8 (C<sub>q</sub>), 155.7 (C<sub>q</sub>), 135.9 (C<sub>q</sub>), 135.9 (C<sub>q</sub>), 135.7 (C<sub>q</sub>), 135.2 (C<sub>q</sub>), 135.0 (C<sub>q</sub>), 134.8 (C<sub>q</sub>), 134.4 (C<sub>q</sub>), 134.4 (C<sub>q</sub>), 134.1 (C<sub>q</sub>), 134.0 (C<sub>q</sub>), 133.9 (C<sub>q</sub>), 133.9 (C<sub>q</sub>), 133.9 (C<sub>q</sub>), 133.6 (C<sub>q</sub>), 133.5 (C<sub>q</sub>), 133.4 (C<sub>q</sub>), 133.2 (C<sub>q</sub>), 133.0 (CH), 132.8 (CH), 132.7 (CH), 132.6 (CH), 132.0 (CH), 131.9

(CH), 131.9 (CH), 130.8 (CH), 130.5 (CH), 129.9 (CH), 129.9 (CH), 129.9 (CH), 129.7 (CH), 129.7 (CH), 129.5 (CH), 129.4 (CH), 129.3 (CH), 129.3 (CH), 129.2 (CH), 129.1 (CH), 129.0 (CH), 128.9 (CH), 128.8 (CH), 128.7 (CH), 128.7 (CH), 128.7 (CH), 128.7 (CH), 128.6 (CH), 128.6 (CH), 128.5 (CH), 128.0 (CH), 127.9 (CH), 127.9 (CH), 127.8 (CH), 127.7 (CH), 126.9 (C<sub>q</sub>), 126.7 (C<sub>q</sub>), 126.6 (C<sub>q</sub>), 126.6 (C<sub>q</sub>), 126.5 (C<sub>q</sub>), 126.5 (C<sub>q</sub>), 126.4 (C<sub>q</sub>), 126.2 (CH), 126.2 (CH), 126.2 (CH), 126.1 (CH), 126.1 (CH), 125.9 (C<sub>q</sub>), 125.7 (C<sub>q</sub>), 125.7 (C<sub>q</sub>), 120.3 (CH), 120.2 (CH), 120.2 (CH), 120.1 (CH), 119.9 (CH), 119.7 (CH), 119.6 (CH), 119.5 (CH), 119.5 (CH), 119.0 (C<sub>q</sub>), 119.0 (C<sub>q</sub>), 118.9 (C<sub>q</sub>), 118.6 (CH), 118.5 (CH), 118.3 (CH), 118.3 (CH), 117.9 (CH), 117.4 (C<sub>q</sub>), 116.1 (C<sub>q</sub>), 116.1 (C<sub>q</sub>), 116.0 (C<sub>q</sub>), 116.0 (C<sub>q</sub>), 110.8 (CH), 110.7 (CH), 110.5 (CH), 110.4 (CH), 110.4 (CH), 110.4 (CH), 110.3 (CH), 110.1 (CH), 110.0 (CH), 108.6 (CH), 108.5 (CH), 108.5 (CH), 108.4 (CH), 56.1 (CH<sub>3</sub>), 56.1 (CH<sub>3</sub>), 56.1 (CH<sub>3</sub>), 56.0 (CH<sub>3</sub>), 55.4 (CH<sub>3</sub>), 55.4 (CH<sub>3</sub>), 55.3 (CH<sub>3</sub>), 55.3 (CH<sub>3</sub>), 55.3 (CH<sub>3</sub>), 55.2 (CH<sub>3</sub>), 54.1 (CH<sub>3</sub>), 54.0 (CH<sub>3</sub>), 54.0 (CH<sub>3</sub>), 54.0 (CH<sub>3</sub>).

**IR (ATR):** 1663 (*m*, C=O), 1464 (*s*, CH<sub>3</sub>), 1238 (*s*, C–N), 1026 (*s*, C–O), 748 (*s*, C–H<sub>Ar</sub>) cm<sup>-1</sup>.

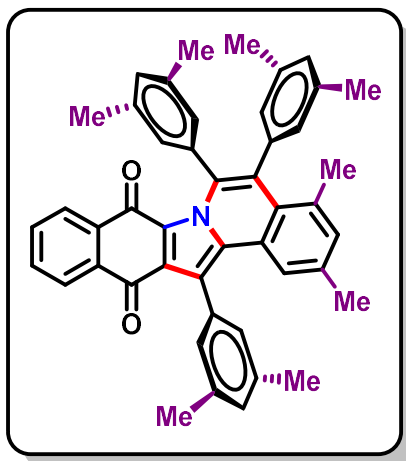
**HRMS-ESI (+):** 646.2220 [M+H]<sup>+</sup>. **Calc. for (C<sub>42</sub>H<sub>32</sub>NO<sub>6</sub>)<sup>+</sup>:** 646.2224.

*Due to the position of the methoxy group, the final material obtained from this reaction presents a mixture of four atropoisomers, which, in natural conditions, convert easily into each other. As expected, the <sup>1</sup>H and <sup>13</sup>C-NMR contain all the resonances from all the four isomers.<sup>133</sup>*

---

<sup>133</sup> Ciogli, A.; Kumar, S. V.; Mancinelli, M.; Mazzanti, A.; Perumal, S.; Severi, C.; Villani, C. *Org. Biomol. Chem.*, **2016**, *14*, 11137-11147.

**5,6,14-Tris(3,5-dimethylphenyl)-2,4-dimethylbenzo[5,6]indolo[2,1-*a*]isoquinoline-8,13-dione (67k)**



The general procedure A was followed by using **59a** (43 mg, 0.20 mmol) and **56k** (187 mg, 0.80 mmol) as starting material. Purification by column chromatography on silica gel (n-Hexane/EtOAc 4:1) yielded **67k** (procedure A: 32 mg, 25%; procedure B: 82 mg, 64%) as an orange solid.

**Melting point:** 228-232 °C.

**<sup>1</sup>H NMR (400 MHz, CDCl<sub>3</sub>) δ:** 8.01-7.99 (m, 1H), 7.67-7.65 (m, 1H), 7.52-7.49 (m, 2H), 7.35 (s, 1H), 7.18 (s, 3H), 6.96 (s, 1H), 6.85-6.80 (m, 5H), 6.63 (s, 1H), 2.44 (s, 6H), 2.22 (s, 6H), 2.11 (s, 9H), 1.78 (s, 3H).

**<sup>13</sup>C NMR (100 MHz, CDCl<sub>3</sub>) δ:** 182.1 (C<sub>q</sub>), 171.9 (C<sub>q</sub>), 138.9 (C<sub>q</sub>), 138.4 (C<sub>q</sub>), 137.0 (C<sub>q</sub>), 136.7 (C<sub>q</sub>), 136.7 (C<sub>q</sub>), 136.2 (C<sub>q</sub>), 136.0 (C<sub>q</sub>), 135.9 (C<sub>q</sub>), 135.8 (C<sub>q</sub>), 135.6 (C<sub>q</sub>), 135.2 (C<sub>q</sub>), 133.8 (CH), 133.8 (C<sub>q</sub>), 133.0 (CH), 131.9 (CH), 130.1 (CH), 129.6 (CH), 129.6 (C<sub>q</sub>), 128.7 (CH), 128.5 (CH), 128.1 (C<sub>q</sub>), 127.9 (C<sub>q</sub>), 127.7 (CH), 127.7 (CH), 127.5 (C<sub>q</sub>), 127.0 (C<sub>q</sub>), 126.1 (CH), 126.0 (CH), 122.8 (CH), 120.4 (C<sub>q</sub>), 24.2 (CH<sub>3</sub>), 21.5 (CH<sub>3</sub>), 21.4 (CH<sub>3</sub>), 21.2 (CH<sub>3</sub>), 21.2 (CH<sub>3</sub>).

**IR (ATR):** 1665 (s, C=O), 1653 (s, C=O), 1447 (m, CH<sub>3</sub>), 1246 (m, C–N), 698 (s, C–H<sub>Ar</sub>) cm<sup>-1</sup>.

**HRMS-ESI (+):** 638.3042 [M+H]<sup>+</sup>. **Calc. for (C<sub>46</sub>H<sub>40</sub>NO<sub>2</sub>)<sup>+</sup>:** 638.3054.

The structure of the product was also confirmed by X-ray diffraction (CCDC number = 1984929) as shown below.

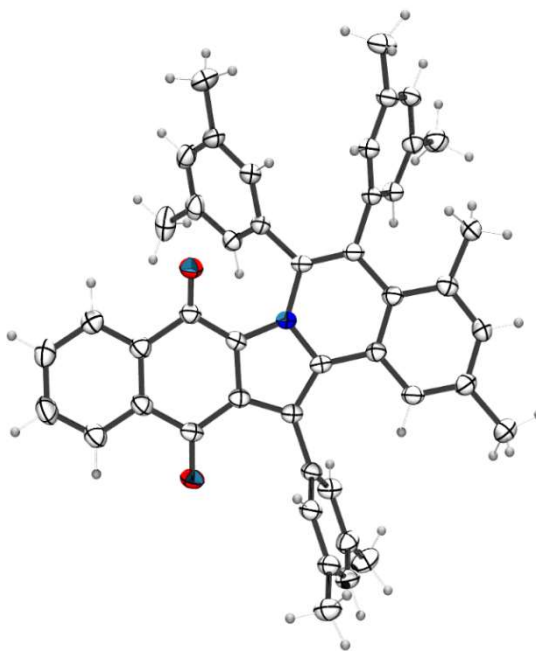
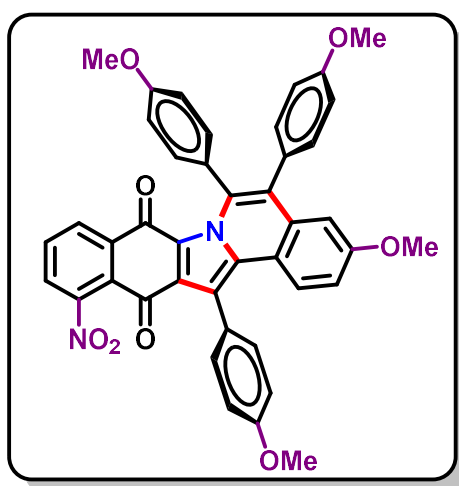


Figure 35. Crystal structure of compound 67k.

**3-Methoxy-5,6,14-tris(4-methoxyphenyl)-12-nitrobenzo[5,6]indolo[2,1-*a*]iso-quinoline-8,13-dione (68a)**



The general procedure A was followed by using **59b** (52 mg, 0.20 mmol) and **56b** (191 mg, 0.80 mmol) as starting material. Purification by column chromatography on silica gel (Hexane/EtOAc 4:1) yielded **68a** (procedure A: 16 mg, 12%; procedure B: 35 mg, 26%) as a dark brown solid.

**Melting point:** 281-284 °C.

**<sup>1</sup>H NMR (400 MHz, CDCl<sub>3</sub>) δ:** 7.84 (dd, *J* = 7.7, 0.8 Hz, 1H), 7.62-7.57 (m, 2H), 7.46 (d, *J* = 7.7 Hz, 1H), 7.41 (d, *J* = 8.7 Hz, 2H), 7.15 (d, *J* = 8.7 Hz, 2H), 7.09 (d, *J* = 8.7 Hz, 2H), 7.03

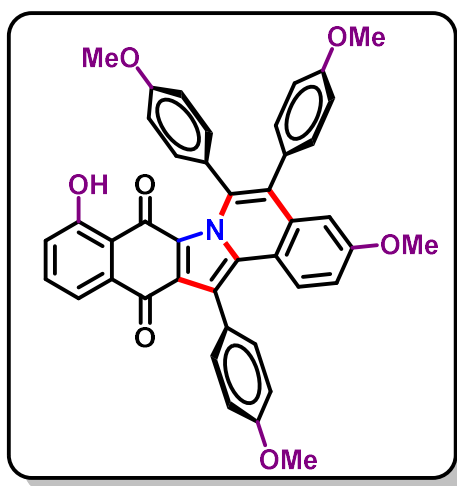
(d,  $J = 8.7$  Hz, 2H), 6.88-6.84 (m, 3H), 6.72-6.68 (m, 3H), 3.95 (s, 3H), 3.84 (s, 3H), 3.77 (s, 3H), 3.66 (s, 3H).

$^{13}\text{C}$  NMR (100 MHz,  $\text{CDCl}_3$ )  $\delta$ : 159.7 ( $\text{C}_q$ ), 158.9 ( $\text{C}_q$ ), 148.8 ( $\text{C}_q$ ), 143.5 ( $\text{C}_q$ ), 137.3 ( $\text{C}_q$ ), 136.2 ( $\text{C}_q$ ), 134.3 ( $\text{C}_q$ ), 133.7 (CH), 132.3 (CH), 131.5 (CH), 131.5 ( $\text{C}_q$ ), 130.4 ( $\text{C}_q$ ), 130.2 (CH), 129.4 ( $\text{C}_q$ ), 129.4 ( $\text{C}_q$ ), 128.8 (CH), 128.5 ( $\text{C}_q$ ), 128.5 ( $\text{C}_q$ ), 128.4 ( $\text{C}_q$ ), 126.4 (CH), 126.2 ( $\text{C}_q$ ), 125.9 (CH), 119.9 ( $\text{C}_q$ ), 119.5 ( $\text{C}_q$ ), 116.7 (CH), 115.0 (CH), 115.0 ( $\text{C}_q$ ), 114.4 ( $\text{C}_q$ ), 114.0 (CH), 113.7 ( $\text{C}_q$ ), 113.3 (CH), 109.6 (CH), 55.5 ( $\text{CH}_3$ ), 55.4 ( $2 \times \text{CH}_3$ ), 55.3 ( $\text{CH}_3$ ).

IR (ATR): 1607 (*m*, C=O), 1538 (*m*,  $\text{NO}_2$ ), 1457 (*m*,  $\text{CH}_3$ ), 1367 (*m*,  $\text{NO}_2$ ), 1244 (*s*, C–N), 1026 (*s*, C–O), 726 (*s*, C–H<sub>Ar</sub>)  $\text{cm}^{-1}$ .

HRMS-ESI (+): 691.2081  $[\text{M}+\text{H}]^+$ . Calc. for  $(\text{C}_{42}\text{H}_{31}\text{NO}_6)^+$ : 691.2075.

**9-Hydroxy-3-methoxy-5,6,14-tris(4-methoxyphenyl)benzo[5,6]indolo[2,1-*a*]iso-quinoline-8,13-dione (68b)**



The general procedure A was followed by using **59c** (46 mg, 0.20 mmol) and **56b** (191 mg, 0.80 mmol) as starting material. Purification by column chromatography on silica gel (*n*-Hexane/EtOAc 4:1) yielded **68b** (with NaOPiv as additive: 24 mg, 18%; without NaOPiv as additive: 48 mg, 36%) as a dark red solid and **68c** (with NaOPiv as additive: 28 mg, 19%; without NaOPiv as additive: not observed) as a dark red solid.

**Melting point:** 280-285 °C.

$^1\text{H}$  NMR (400 MHz,  $\text{CDCl}_3$ )  $\delta$ : 11.75 (s, 1H), 7.65 (d,  $J = 9.0$  Hz, 1H), 7.53 (dd,  $J = 8.0, 0.7$  Hz, 1H), 7.46 (d,  $J = 8.0$  Hz, 2H), 7.38 (t,  $J = 8.0$  Hz, 1H), 7.14 (d,  $J = 2.8$  Hz, 2H), 7.12 (d,  $J$

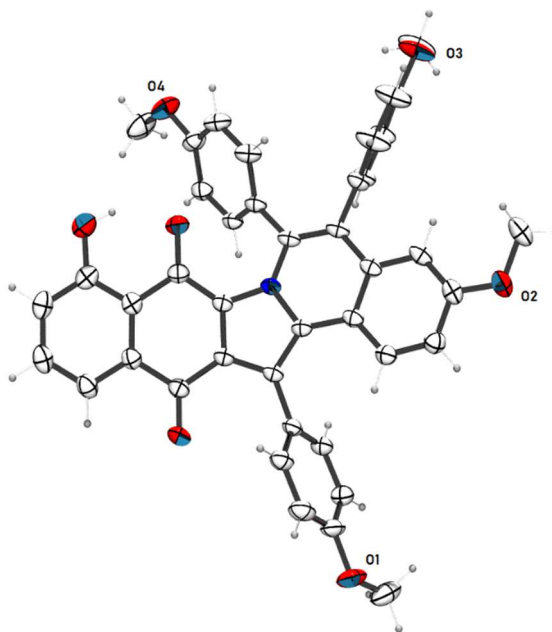
= 2.8 Hz, 2H), 7.03 (d,  $J$  = 8.0 Hz, 3H), 6.88-6.85 (m, 3H), 6.71 (d,  $J$  = 2.8 Hz, 1H), 6.67 (d,  $J$  = 9.0 Hz, 2H), 3.96 (s, 3H), 3.84 (s, 3H), 3.75 (s, 3H), 3.66 (s, 3H).

**$^{13}\text{C}$  NMR (100 MHz,  $\text{CDCl}_3$ )  $\delta$ :** 182.0 ( $\text{C}_q$ ), 176.4 ( $\text{C}_q$ ), 161.2 ( $\text{C}_q$ ), 159.7 ( $\text{C}_q$ ), 159.6 ( $\text{C}_q$ ), 159.0 ( $\text{C}_q$ ), 158.9 ( $\text{C}_q$ ), 137.5 ( $\text{C}_q$ ), 136.6 ( $\text{C}_q$ ), 134.2 ( $\text{C}_q$ ), 134.2 ( $\text{C}_q$ ), 134.1 (CH), 132.3 (CH), 131.5 (CH), 130.1 (CH), 129.7 ( $\text{C}_q$ ), 129.4 ( $\text{C}_q$ ), 129.2 ( $\text{C}_q$ ), 128.7 ( $\text{C}_q$ ), 126.9 ( $\text{C}_q$ ), 126.3 (CH), 125.7 ( $\text{C}_q$ ), 124.0 (CH), 119.9 ( $\text{C}_q$ ), 119.6 ( $\text{C}_q$ ), 118.5 (CH), 117.4 ( $\text{C}_q$ ), 116.7 (CH), 114.9 (CH), 114.0 (CH), 113.3 (CH), 109.4 (CH), 55.5 ( $\text{CH}_3$ ), 55.4 ( $3 \times \text{CH}_3$ ).

**IR (ATR):** 2953 (*w*, O-H), 1664 (*m*, C=O), 1606 (*s*, C=O), 1512 (*s*,  $\text{CH}_3$ ), 1462 (*s*,  $\text{CH}_3$ ), 1389 (*m*, O- $\text{H}_{\text{Ar}}$ ), 1244 (*s*, C-N), 1023 (*s*, C-O), 773 (*s*, C- $\text{H}_{\text{Ar}}$ )  $\text{cm}^{-1}$ .

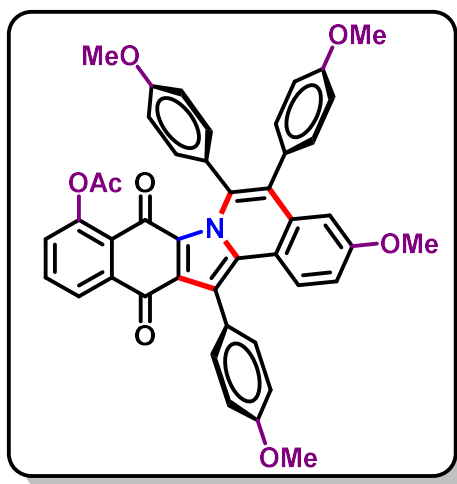
**HRMS-ESI (+):** 662.2188  $[\text{M}+\text{H}]^+$ . **Calc. for  $(\text{C}_{42}\text{H}_{32}\text{NO}_7)^+$ :** 662.2173.

The structure of the product was also confirmed by X-ray diffraction (CCDC number = 1984930) as shown below.



**Figure 36.** Crystal structure of compound **68b**.

**3-Methoxy-5,6,14-tris(4-methoxyphenyl)-8,13-dioxo-8,13-dihydrobenzo[5,6]indolo-[2,1-*a*]isoquinolin-9-yl acetate (68c)**



The general procedure A was followed by using **59c** (46 mg, 0.20 mmol) and **56b** (191 mg, 0.80 mmol) as starting material. Purification by column chromatography on silica gel (*n*-Hexane/EtOAc 4:1) yielded **68c** (with NaOPiv as additive: 28 mg, 19%; without NaOPiv as additive: not observed) as a dark red solid and **68b** (with NaOPiv as additive: 24 mg, 18%; without NaOPiv as additive: 48 mg, 36%) as a dark red solid.

**Melting point:** 280-285 °C.

**<sup>1</sup>H NMR (400 MHz, CDCl<sub>3</sub>) δ:** 8.07 (dd, *J* = 8.0, 1.2 Hz, 1H), 7.95 (dd, *J* = 8.0, 1.2 Hz, 1H), 7.84 (s, 1H), 7.79 (t, *J* = 7.7 Hz, 1H), 7.64 (d, *J* = 9.2 Hz, 1H), 7.52-7.47 (m, 1H), 7.46 (dd, *J* = 6.6, 2.2 Hz, 1H), 7.35 (dd, *J* = 8.0, 1.2 Hz, 1H), 7.16-7.15 (m, 2H), 7.13-7.12 (m, 2H), 7.04-7.02 (m, 1H), 7.01-7.00 (m, 1H), 6.87-6.83 (m, 2H), 6.70-6.67 (m, 2H), 3.95 (s, 3H), 3.83 (s, 3H), 3.79 (s, 3H), 3.65 (s, 3H), 2.06 (s, 3H).

**<sup>13</sup>C NMR (100 MHz, CDCl<sub>3</sub>) δ:** 180.9 (C<sub>q</sub>), 171.2 (C<sub>q</sub>), 170.2 (C<sub>q</sub>), 159.4 (C<sub>q</sub>), 159.3 (C<sub>q</sub>), 158.8 (C<sub>q</sub>), 158.8 (C<sub>q</sub>), 149.6 (C<sub>q</sub>), 138.2 (C<sub>q</sub>), 136.9 (C<sub>q</sub>), 136.3 (CH), 134.1 (C<sub>q</sub>), 133.9 (C<sub>q</sub>), 132.4 (CH), 131.7 (CH), 130.3 (CH), 129.6 (CH), 129.4 (C<sub>q</sub>), 128.9 (C<sub>q</sub>), 128.5 (C<sub>q</sub>), 127.9 (C<sub>q</sub>), 127.3 (C<sub>q</sub>), 126.2 (CH), 125.0 (CH), 124.9 (CH), 119.6 (C<sub>q</sub>), 119.1 (C<sub>q</sub>), 116.3 (C<sub>q</sub>), 114.7 (CH), 113.9 (CH), 113.2 (CH), 109.5 (CH), 55.5 (CH<sub>3</sub>), 55.4 (CH<sub>3</sub>), 55.4 (CH<sub>3</sub>), 55.3 (CH<sub>3</sub>), 21.5 (CH<sub>3</sub>).

**IR (ATR):** 1767 (*s*, C=O), 1659 (*s*, C=O), 1512 (*m*, CH<sub>3</sub>), 1460 (*m*, CH<sub>3</sub>), 1244 (*s*, C–N), 1181 (*s*, C–O<sub>Ac</sub>), 1027 (*s*, C–O), 773 (*m*, C–H<sub>Ar</sub>) cm<sup>-1</sup>.

**HRMS-ESI (+):** 704.2294 [M+H]<sup>+</sup>. **Calc. for (C<sub>44</sub>H<sub>34</sub>NO<sub>8</sub>)<sup>+</sup>:** 704.2279.



The structure of the product was also confirmed by X-ray diffraction (CCDC number = 1984931) as shown below.

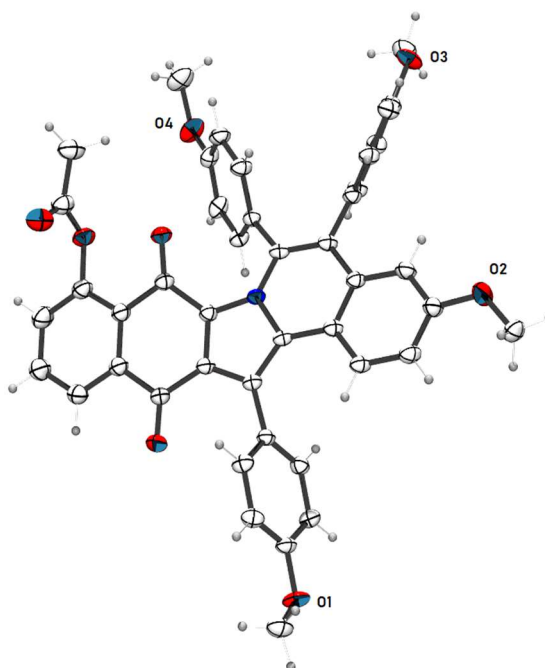
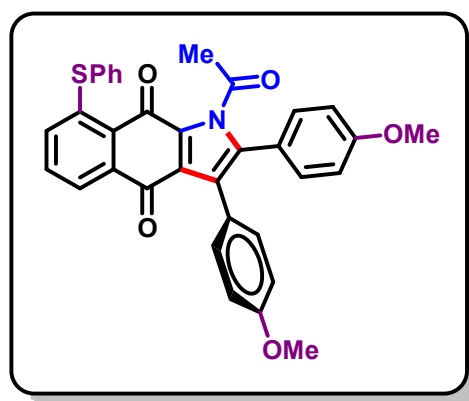


Figure 37. Crystal structure of compound **68c**.

### 1-Acetyl-2,3-bis(4-methoxyphenyl)-8-(phenylthio)-1H-benzo[f]indole-4,9-dione (**68d**)



The general procedure A was followed by using **59d** (65 mg, 0.20 mmol) and **56b** (191 mg, 0.80 mmol) as starting material. Purification by column chromatography on silica gel (*n*-Hexane/EtOAc 4:1) yielded **68d** (procedure A: 27 mg, 24%; procedure B: 46 mg, 41%) as a red solid.

**Melting point:** 205-207 °C.

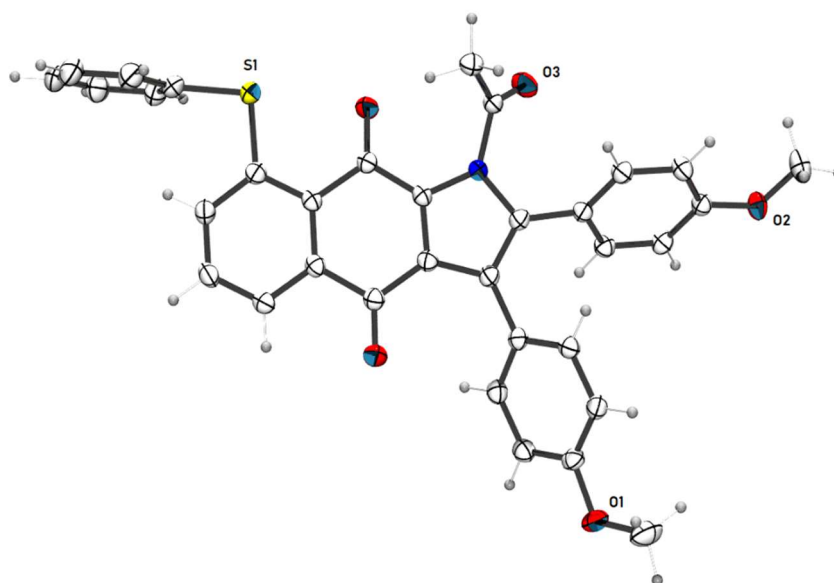
**<sup>1</sup>H NMR (400 MHz, CDCl<sub>3</sub>) δ:** 7.96-7.93 (m, 1H), 7.63-7.61 (m, 2H), 7.50-7.49 (m, 3H), 7.38-7.32 (m, 1H), 7.25-7.17 (m, 4H), 7.01-6.98 (m, 1H), 6.87-6.82 (m, 4H), 3.81 (s, 3H), 3.80 (s, 3H), 2.55 (s, 3H).

**<sup>13</sup>C NMR (100 MHz, CDCl<sub>3</sub>) δ:** 180.2 (C<sub>q</sub>), 176.0 (C<sub>q</sub>), 173.7 (C<sub>q</sub>), 160.2 (C<sub>q</sub>), 158.9 (C<sub>q</sub>), 145.4 (C<sub>q</sub>), 137.8 (C<sub>q</sub>), 136.2 (C<sub>q</sub>), 136.1 (CH), 132.4 (CH), 132.0 (CH), 131.8 (CH), 131.8 (CH), 131.7 (C<sub>q</sub>), 131.1 (CH), 130.0 (CH), 129.7 (C<sub>q</sub>), 127.1 (C<sub>q</sub>), 124.4 (CH), 124.2 (C<sub>q</sub>), 123.7 (C<sub>q</sub>), 123.2 (C<sub>q</sub>), 120.9 (C<sub>q</sub>), 114.1 (CH), 113.3 (CH), 55.3 (CH<sub>3</sub>), 55.2 (CH<sub>3</sub>), 29.0 (CH<sub>3</sub>).

**IR (ATR):** 1759 (*s*, C=O), 1632 (*s*, C=O), 1609 (*s*, C=O), 1471 (*m*, CH<sub>3</sub>), 1419 (*s*, CH<sub>3</sub>), 1213 (*s*, C–N), 1023 (*s*, C–O), 753 (*s*, C–H<sub>Ar</sub>), 692 (*m*, S–Ph) cm<sup>-1</sup>.

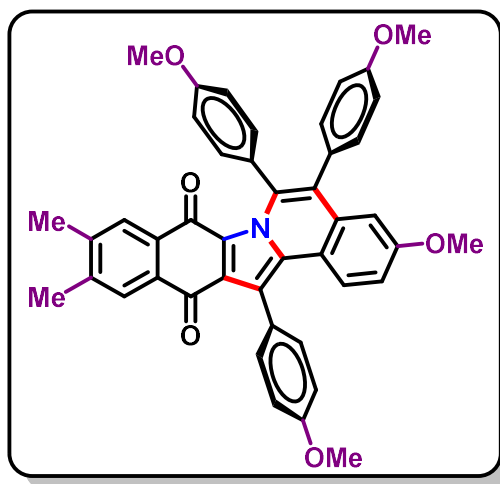
**HRMS-ESI (+):** 560.1528 [M+H]<sup>+</sup>. **Calc. for (C<sub>34</sub>H<sub>26</sub>SNO<sub>5</sub>)<sup>+</sup>:** 560.1526.

The structure of the product was also confirmed by X-ray diffraction (CCDC number = 1984932) as shown below.



**Figure 38.** Crystal structure of compound **68d**.

**3-Methoxy-5,6,14-tris(4-methoxyphenyl)-10,11-dimethylbenzo[5,6]indolo[2,1-*a*]isoquinoline-8,13-dione (68e)**



The general procedure A was followed by using **59e** (49 mg, 0.20 mmol) and **56b** (191 mg, 0.80 mmol) as starting material. Purification by column chromatography on silica gel (<sup>n</sup>Hexane/EtOAc 4:1) yielded **68e** (procedure A: 96 mg, 71%; procedure B: 101 mg, 75%) as a dark orange solid.

**Melting point:** 330-334 °C.

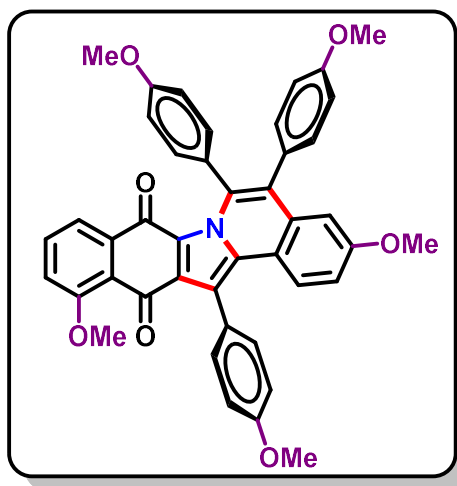
**<sup>1</sup>H NMR (400 MHz, CDCl<sub>3</sub>) δ:** 7.74 (br s, 1H), 7.67-7.63 (m, 1H), 7.47-7.42 (m, 3H), 7.17-7.12 (m, 4H), 7.03-7.01 (m, 2H), 6.87-6.82 (m, 3H), 6.70-6.67 (m, 3H), 3.96 (s, 3H), 3.84 (s, 3H), 3.77 (s, 3H), 3.65 (s, 3H), 2.28 (s, 3H), 2.27 (s, 3H).

**<sup>13</sup>C NMR (100 MHz, CDCl<sub>3</sub>) δ:** 182.8 (C<sub>q</sub>), 172.6 (C<sub>q</sub>), 159.5 (C<sub>q</sub>), 159.2 (C<sub>q</sub>), 158.8 (C<sub>q</sub>), 158.7 (C<sub>q</sub>), 143.0 (C<sub>q</sub>), 141.4 (C<sub>q</sub>), 136.4 (C<sub>q</sub>), 136.2 (C<sub>q</sub>), 133.9 (C<sub>q</sub>), 133.9 (C<sub>q</sub>), 132.4 (CH), 131.7 (C<sub>q</sub>), 131.6 (CH), 130.2 (CH), 129.9 (C<sub>q</sub>), 129.1 (C<sub>q</sub>), 129.0 (C<sub>q</sub>), 128.5 (C<sub>q</sub>), 127.6 (CH), 127.4 (C<sub>q</sub>), 127.4 (CH), 127.2 (C<sub>q</sub>), 126.1 (CH), 119.8 (C<sub>q</sub>), 118.8 (C<sub>q</sub>), 116.2 (CH), 114.8 (CH), 113.9 (CH), 113.1 (CH), 109.5 (CH), 55.5 (CH<sub>3</sub>), 55.4 (CH<sub>3</sub>), 55.4 (CH<sub>3</sub>), 55.3 (CH<sub>3</sub>), 20.2 (CH<sub>3</sub>), 20.1 (CH<sub>3</sub>).

**IR (ATR):** 1713 (*m*, C=O), 1655 (*m*, C=O), 1597 (*s*, CH<sub>3</sub>), 1456 (*s*, CH<sub>3</sub>), 1244 (*s*, C–N), 1028 (*s*, C–O), 829 (*m*, C–H<sub>Ar</sub>) cm<sup>-1</sup>.

**HRMS-ESI (+):** 674.2539 [M+H]<sup>+</sup>. **Calc. for (C<sub>44</sub>H<sub>36</sub>NO<sub>6</sub>)<sup>+</sup>:** 674.2537.

**3,12-Dimethoxy-5,6,14-tris(4-methoxyphenyl)benzo[5,6]indolo[2,1-*a*]isoquinoline-8,13-dione (68f)**



The general procedure A was followed by using **59f** (49 mg, 0.20 mmol) and **56b** (191 mg, 0.80 mmol) as starting material. Purification by column chromatography on silica gel (<sup>n</sup>Hexane/EtOAc 4:1) yielded **68f** (procedure A: 53 mg, 39%; procedure B: 91 mg, 67%) as a dark red solid.

**Melting point:** 260-263 °C.

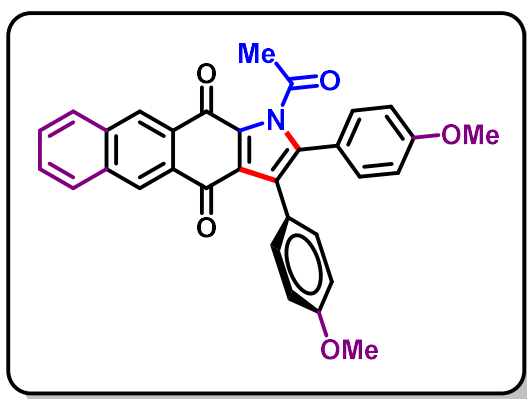
**<sup>1</sup>H NMR (300 MHz, CDCl<sub>3</sub>) δ:** 7.77-7.73 (m, 1H), 7.54 (d, *J* = 9.1 Hz, 1H), 7.43 (d, *J* = 8.4 Hz, 3H), 7.28 (br s, 1H), 7.16 (d, *J* = 8.6 Hz, 2H), 7.10 (d, *J* = 8.6 Hz, 3H), 7.02 (d, *J* = 8.6 Hz, 2H), 6.89-6.80 (m, 3H), 6.70-6.67 (m, 2H), 3.94 (s, 3H), 3.90 (s, 3H), 3.83 (s, 3H), 3.76 (s, 3H), 3.65 (s, 3H).

**<sup>13</sup>C NMR (75 MHz, CDCl<sub>3</sub>) δ:** 182.0 (C<sub>q</sub>), 172.0 (C<sub>q</sub>), 160.1 (C<sub>q</sub>), 159.4 (C<sub>q</sub>), 159.2 (C<sub>q</sub>), 158.8 (C<sub>q</sub>), 158.7 (C<sub>q</sub>), 138.9 (C<sub>q</sub>), 136.9 (C<sub>q</sub>), 136.3 (C<sub>q</sub>), 134.3 (C<sub>q</sub>), 134.0 (C<sub>q</sub>), 133.0 (C<sub>q</sub>), 132.4 (CH), 131.6 (CH), 130.3 (CH), 129.7 (C<sub>q</sub>), 129.0 (C<sub>q</sub>), 128.1 (C<sub>q</sub>), 127.7 (C<sub>q</sub>), 126.3 (C<sub>q</sub>), 126.0 (C<sub>q</sub>), 121.3 (C<sub>q</sub>), 119.8 (CH), 119.2 (CH), 119.1 (CH), 116.3 (CH), 114.9 (CH), 114.3 (CH), 113.9 (CH), 113.2 (CH), 109.5 (CH), 56.4 (CH<sub>3</sub>), 55.5 (CH<sub>3</sub>), 55.4 (CH<sub>3</sub>), 55.4 (CH<sub>3</sub>), 55.3 (CH<sub>3</sub>).

**IR (ATR):** 1660 (*m*, C=O), 1607 (*m*, C=O), 1511 (*s*, CH<sub>3</sub>), 1461 (*s*, CH<sub>3</sub>), 1243 (*s*, C–N), 1027 (*s*, C–O), 735 (*m*, C–H<sub>Ar</sub>) cm<sup>-1</sup>.

**HRMS-ESI (+):** 676.2315 [M+H]<sup>+</sup>. **Calc. for (C<sub>43</sub>H<sub>34</sub>NO<sub>7</sub>)<sup>+</sup>:** 676.2330.

**1-Acetyl-2,3-bis(4-methoxyphenyl)-1*H*-naphtho[2,3-*f*]indole-4,11-dione (68g)**



The general procedure A was followed by using **59g** (53 mg, 0.20 mmol) and **56b** (191 mg, 0.80 mmol) as starting material. Purification by column chromatography on silica gel (*n*-Hexane/EtOAc 4:1) yielded **68g** (procedure A: 13 mg, 13%; procedure B: 44 mg, 44%) as an orange solid.

**Melting point:** 205-207 °C.

**<sup>1</sup>H NMR (400 MHz, CDCl<sub>3</sub>) δ:** 8.66 (d, *J* = 2.4 Hz, 2H), 8.06-8.01 (m, 2H), 7.65 (dd, *J* = 6.2, 3.2 Hz, 2H), 7.24 (d, *J* = 8.8 Hz, 2H), 7.18 (d, *J* = 8.8 Hz, 2H), 6.86 (d, *J* = 2.4 Hz, 2H), 6.84 (d, *J* = 2.4 Hz, 2H), 3.82 (s, 3H), 3.81 (s, 3H), 2.55 (s, 3H).

**<sup>13</sup>C NMR (100 MHz, CDCl<sub>3</sub>) δ:** 180.5 (C<sub>q</sub>), 174.9 (C<sub>q</sub>), 173.8 (C<sub>q</sub>), 160.2 (C<sub>q</sub>), 158.9 (C<sub>q</sub>), 138.4 (C<sub>q</sub>), 134.9 (C<sub>q</sub>), 134.6 (C<sub>q</sub>), 132.2 (CH), 132.0 (CH), 131.8 (C<sub>q</sub>), 131.0 (C<sub>q</sub>), 130.2 (CH), 130.0 (CH), 129.8 (C<sub>q</sub>), 129.3 (CH), 129.2 (CH), 129.1 (CH), 128.5 (CH), 125.7 (C<sub>q</sub>), 125.1 (C<sub>q</sub>), 123.8 (C<sub>q</sub>), 120.9 (C<sub>q</sub>), 114.1 (CH), 113.3 (CH), 55.3 (CH<sub>3</sub>), 55.2 (CH<sub>3</sub>), 28.9 (CH<sub>3</sub>).

**IR (ATR):** 1767 (*m*, C=O), 1670 (*m*, C=N), 1643 (*m*, C=O), 1613 (*s*, C=O), 1407 (*s*, CH<sub>3</sub>), 1241 (*s*, C–N), 1182 (*s*, C–O<sub>im</sub>), 1024 (*s*, C–O), 768 (*s*, C–H<sub>Ar</sub>) cm<sup>-1</sup>.

**HRMS-ESI (+):** 502.1649 [M+H]<sup>+</sup>. **Calc. for (C<sub>32</sub>H<sub>24</sub>NO<sub>5</sub>)<sup>+</sup>:** 502.1649.

*The structure of the product was also confirmed by X-ray diffraction (CCDC number = 1984933) as shown below.*

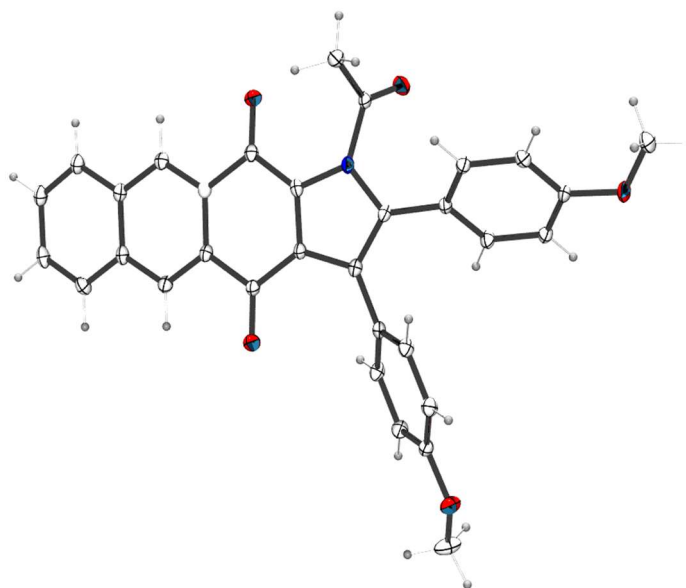
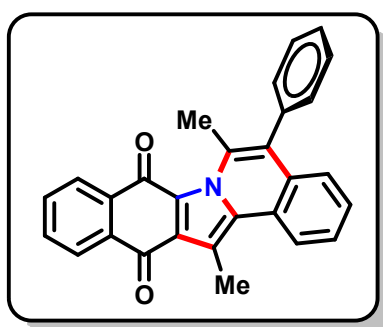


Figure 39. Crystal structure of compound **68g**.

#### 6,14-Dimethyl-5-phenylbenzo[5,6]indolo[2,1-*a*]isoquinoline-8,13-dione (**69a**)



The general procedure A was followed by using **59a** (43 mg, 0.20 mmol) and prop-1-yn-1-ylbenzene (**71**) (100 $\mu$ L, 93 mg, 0.80 mmol) as starting material. Purification by column chromatography on silica gel (Hexane/EtOAc 4:1) yielded **69a** (procedure A: 24 mg, 30%; procedure B: 30 mg, 38%) as an orange solid and **69b** (procedure A: 27 mg, 34%; procedure B: 32 mg, 41%) as an orange solid.

**Melting point:** 300-302 °C.

**<sup>1</sup>H NMR (400 MHz, CDCl<sub>3</sub>)  $\delta$ :** 8.60 (d,  $J$  = 8.0 Hz, 1H), 8.20 (d,  $J$  = 7.0 Hz, 1H), 8.15 (d,  $J$  = 7.0 Hz, 1H), 7.72-7.64 (m, 2H), 7.63-7.59 (m, 1H), 7.57-7.50 (m, 3H), 7.47-7.43 (m, 1H), 7.38 (d,  $J$  = 8.0 Hz, 2H), 7.30 (d,  $J$  = 8.1 Hz, 1H), 3.22 (s, 3H), 2.52 (s, 3H).

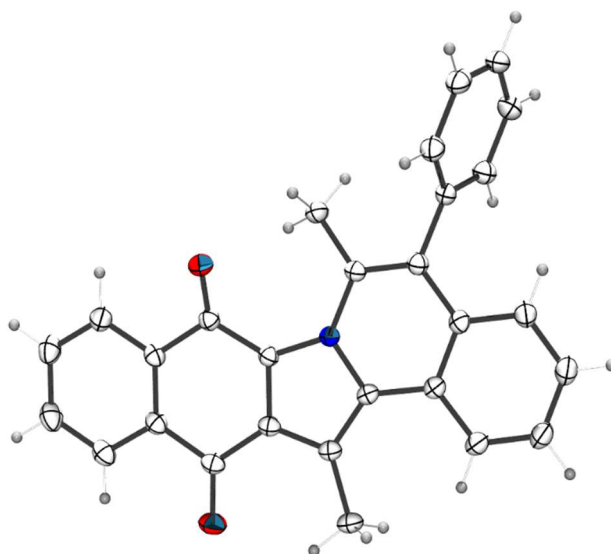
**<sup>13</sup>C NMR (100 MHz, CDCl<sub>3</sub>)  $\delta$ :** 184.4 (C<sub>q</sub>), 173.4 (C<sub>q</sub>), 137.8 (C<sub>q</sub>), 136.5 (C<sub>q</sub>), 136.2 (C<sub>q</sub>), 134.2 (C<sub>q</sub>), 134.0 (C<sub>q</sub>), 133.6 (CH), 132.4 (CH), 131.3 (C<sub>q</sub>), 131.1 (CH), 129.5 (C<sub>q</sub>), 129.1 (C<sub>q</sub>),

129.0 (CH), 128.3 (CH), 127.9 (CH), 127.6 (CH), 126.9 (C<sub>q</sub>), 126.8 (CH), 126.8 (CH), 126.4 (CH), 126.0 (C<sub>q</sub>), 124.2 (CH), 118.3 (C<sub>q</sub>), 22.3 (CH<sub>3</sub>), 13.3 (CH<sub>3</sub>).

**IR (ATR):** 1655 (*s*, C=O), 1633 (*s*, C=O), 1437 (*s*, CH<sub>3</sub>), 1365 (*s*, CH<sub>3</sub>), 1267 (*s*, C–N), 1022 (*m*, C–O), 754 (*s*, C–H<sub>Ar</sub>) cm<sup>-1</sup>.

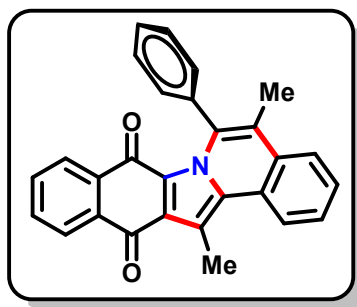
**HRMS-ESI (+):** 402.1477 [M+H]<sup>+</sup>. **Calc. for (C<sub>28</sub>H<sub>20</sub>NO<sub>2</sub>)<sup>+</sup>:** 402.1489.

The structure of the product was also confirmed by X-ray diffraction (CCDC number = 1984934) as shown below.



**Figure 40.** Crystal structure of compound **69a**.

#### 5,14-Dimethyl-6-phenylbenzo[5,6]indolo[2,1-*a*]isoquinoline-8,13-dione (**69b**)



The general procedure A was followed by using **59a** (43 mg, 0.20 mmol) and prop-1-yn-1-ylbenzene (**71**) (100 μL, 93 mg, 0.80 mmol) as starting material. Purification by column chromatography on silica gel (Hexane/EtOAc 4:1) yielded **69b** (procedure A: 27 mg, 34%; procedure B: 32 mg, 41%) as an orange solid and **69a** (procedure A: 24 mg, 30%; procedure B: 30 mg, 38%) as an orange solid.

**Melting point:** 240-242 °C.

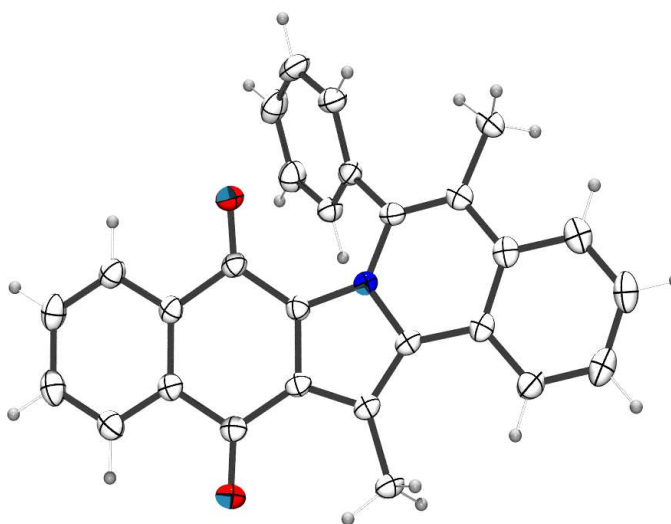
**<sup>1</sup>H NMR (400 MHz, CDCl<sub>3</sub>) δ:** 8.53 (d, *J* = 8.0 Hz, 1H), 8.13-8.11 (m, 1H), 7.94-7.92 (m, 1H), 7.67-7.50 (m, 5H), 7.47-7.41 (m, 4H), 7.38-7.33 (m, 1H), 3.16 (s, 3H), 2.42 (s, 3H).

**<sup>13</sup>C NMR (100 MHz, CDCl<sub>3</sub>) δ:** 184.1 (C<sub>q</sub>), 172.2 (C<sub>q</sub>), 137.4 (C<sub>q</sub>), 135.9 (C<sub>q</sub>), 135.9 (C<sub>q</sub>), 135.3 (C<sub>q</sub>), 134.0 (C<sub>q</sub>), 133.3 (CH), 132.1 (CH), 131.3 (C<sub>q</sub>), 129.4 (CH), 128.3 (CH), 128.1 (CH), 128.0 (CH), 128.0 (CH), 127.0 (C<sub>q</sub>), 126.9 (C<sub>q</sub>), 126.3 (CH), 126.2 (CH), 125.1 (CH), 124.4 (CH), 121.7 (C<sub>q</sub>), 117.2 (C<sub>q</sub>), 16.5 (CH<sub>3</sub>), 13.2 (CH<sub>3</sub>).

**IR (ATR):** 1651 (*s*, C=O), 1591 (*m*, C=O), 1443 (*m*, CH<sub>3</sub>), 1390 (*m*, CH<sub>3</sub>), 1228 (*s*, C–N), 753 (*s*, C–H<sub>Ar</sub>) cm<sup>-1</sup>.

**HRMS-ESI (+):** 402.1484 [M+H]<sup>+</sup>. **Calc. for (C<sub>28</sub>H<sub>20</sub>NO<sub>2</sub>)<sup>+</sup>:** 402.1489.

*The structure of the product was also confirmed by X-ray diffraction (CCDC number = 1984935) as shown below.*



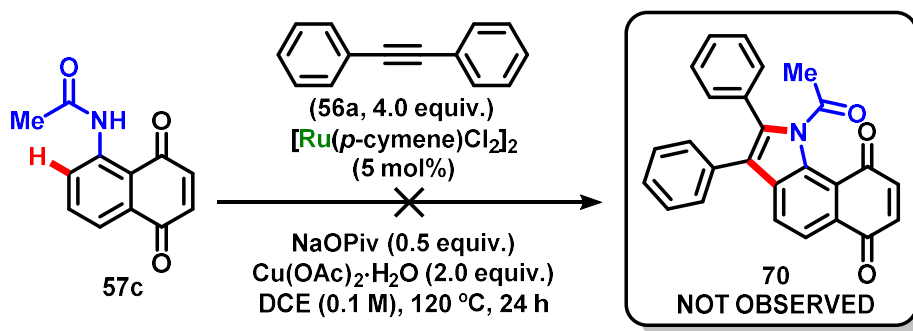
**Figure 41.** Crystal structure of compound **69b**.

Compound **64** was submitted to a procedure similar to Procedure A described above for the ruthenium-catalyzed double annulation of quinones, priorly to the optimization of the method, from which the product **67a** (36mg, 34%) was successfully achieved.

Compounds 6, 58a, 60, 61 and 62 (as substrates, 0.2 mmol) and compounds 5, 34, 44-48, 56l-s (as annulating agents, 0.8 mmol) were submitted to the general procedures A and B described above, however, in all cases, only the respective starting materials were observed. Therefore, no reaction was achieved in these cases.



### 1-acetyl-2,3-diphenyl-1H-benzo[g]indole-6,9-dione (70)



Under an atmosphere of N<sub>2</sub>, a 10 mL Schlenk tube was charged with the corresponding naphthoquinone **57c** (43 mg, 0.20 mmol), Cu(OAc)<sub>2</sub>·H<sub>2</sub>O (80 mg, 0.40 mmol), diphenylacetylene (**56a**, 142 mg, 0.80 mmol) and [RuCl<sub>2</sub>(p-cymene)]<sub>2</sub> (6 mg, 5 mol %). Then, DCE (2 mL, 0.1 M) was added *via* a syringe. The reaction mixture was heated to 120 °C for 24 h. The mixture was then cooled to room temperature, filtered through a pad of celite and the solvent was removed under reduced pressure. No product was observed in this reaction, only compound **57c** was obtained back. The reaction was repeated for a higher temperature (140 °C), but still no product was obtained.

#### 5.4. Computational data

All calculations were performed using Gaussian 16, Revision B.01 package.<sup>134</sup> Geometry optimizations were performed at the ωB97XD<sup>135</sup> level of theory. Ruthenium was described with def2-SVPP<sup>136</sup> basis set together with the def2-ECP<sup>137</sup> effective core potential,

<sup>134</sup> Frisch, M. J.; Trucks, G. W.; Schlegel, H. B.; Scuseria, G. E.; Robb, M. A.; Cheeseman, J. R.; Scalmani, G.; Barone, V.; Petersson, G. A.; Nakatsuji, H.; Li, X.; Caricato, M.; Marenich, A. V.; Bloino, J.; Janesko, B. G.; Gomperts, R.; Mennucci, B.; Hratchian, H. P.; Ortiz, J. V.; Izmaylov, A. F.; Sonnenberg, J. L.; Williams-Young, D.; Ding, F.; Lipparini, F.; Egidi, F.; Goings, J.; Peng, B.; Petrone, A.; Henderson, T.; Ranasinghe, D.; Zakrzewski, V. G.; Gao, J.; Rega, N.; Zheng, G.; Liang, W.; Hada, M.; Ehara, M.; Toyota, K.; Fukuda, R.; Hasegawa, J.; Ishida, M.; Nakajima, T.; Honda, Y.; Kitao, O.; Nakai, H.; Vreven, T.; Throssell, K.; Montgomery, J. A., Jr.; Peralta, J. E.; Ogliaro, F.; Bearpark, M. J.; Heyd, J. J.; Brothers, E. N.; Kudin, K. N.; Staroverov, V. N.; Keith, T. A.; Kobayashi, R.; Normand, J.; Raghavachari, K.; Rendell, A. P.; Burant, J. C.; Iyengar, S. S.; Tomasi, J.; Cossi, M.; Millam, J. M.; Klene, M.; Adamo, C.; Cammi, R.; Ochterski, J. W.; Martin, R. L.; Morokuma, K.; Farkas, O.; Foresman, J. B.; Fox, D. J. Gaussian, *Gaussian 16*, 2016, Revision C.01, Inc., Wallingford CT.

<sup>135</sup> Chai, J.-D.; Head-Gordon, M. *Phys. Chem. Chem. Phys.*, **2008**, *10*, 6615-6620.

<sup>136</sup> Weigend, F.; Ahlrichs, R. *Phys. Chem. Chem. Phys.*, **2005**, *7*, 3297-3305.

<sup>137</sup> Andrae, D.; Häußermann, U.; Dolg, M.; Stoll, H.; Preuß, H. *Theor. Chim. Acta*, **1990**, *77*, 123-141.

while on all other atoms def2-SVPP basis set was used. All stationary points were fully characterized by analytical frequency calculations as either a minimum or a transition state (only one imaginary frequency). Intrinsic Reaction Coordinate (IRC) calculations<sup>138,139,140</sup> were used to confirm the intermediates linked by each transition state. Single point calculations were performed at the  $\omega$ B97XD and M06<sup>141</sup> (including D3<sup>142</sup> dispersion corrections) levels of theory with def2-TZVPP basis set and def2-ECP on ruthenium, and def2-TZVPP basis set on all other atoms. Solvent effects were taken into consideration in the single point calculations through the use of the SMD<sup>143</sup> continuum solvation model with 1,2-dichloroethane ( $\epsilon = 10.125$ ) as implemented in Gaussian. Unless otherwise stated all reported energies are Gibbs free energies in kcal mol<sup>-1</sup>, which were calculated by adding the gas-phase Gibbs free energy correction ( $\Delta\Delta G$ ) at 393 K and 1 atm to the single point energies. Images of 3D structure were created using CYLView.<sup>144</sup> Plots of frontier orbitals of **59a**, **67a'** and **67a** were constructed by using Chemissian software,<sup>145</sup> and were obtained for the optimized structures at the B3LYP<sup>146</sup> (including D3 dispersion corrections with Becke-Johnson<sup>147</sup> damping scheme) level of theory with def2-TZVPP basis set and SMD (solvent = 1,2-dichloroethane).

---

<sup>138</sup> Fukui, K. *Acc. Chem. Res.*, **1981**, *14*, 363-368.

<sup>139</sup> Hratchian, H. P.; Schlegel, H. B. *J. Chem. Phys.*, **2004**, *120*, 9918-9924.

<sup>140</sup> Hratchian, H. P.; Schlegel, H. B. *J. Chem. Theory Comput.*, **2005**, *1*, 61-69.

<sup>141</sup> Zhao, Y.; Truhlar, D. G. *Theor. Chem. Acc.*, **2008**, *120*, 215-241.

<sup>142</sup> Grimme, S.; Antony, J.; Ehrlich, S.; Krieg, H. *J. Chem. Phys.*, **2010**, *132*, 154104.

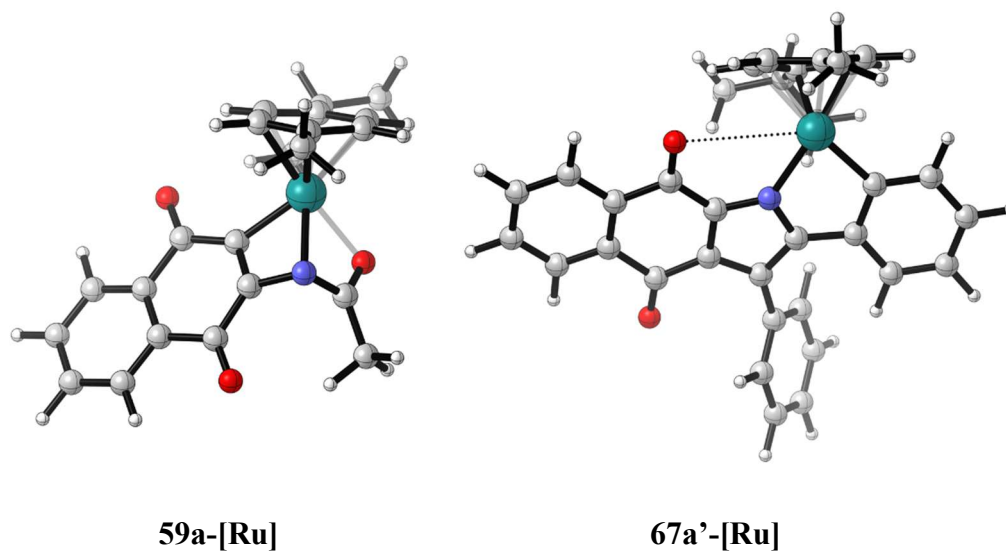
<sup>143</sup> Marenich, A. V.; Cramer, C. J.; Truhlar, D. G. *J. Phys. Chem. B*, **2009**, *113*, 6378-6396.

<sup>144</sup> Legault, C.Y. *CYLview 1.0b*, Université de Sherbrooke, **2009** (<http://www.cylview.org>).

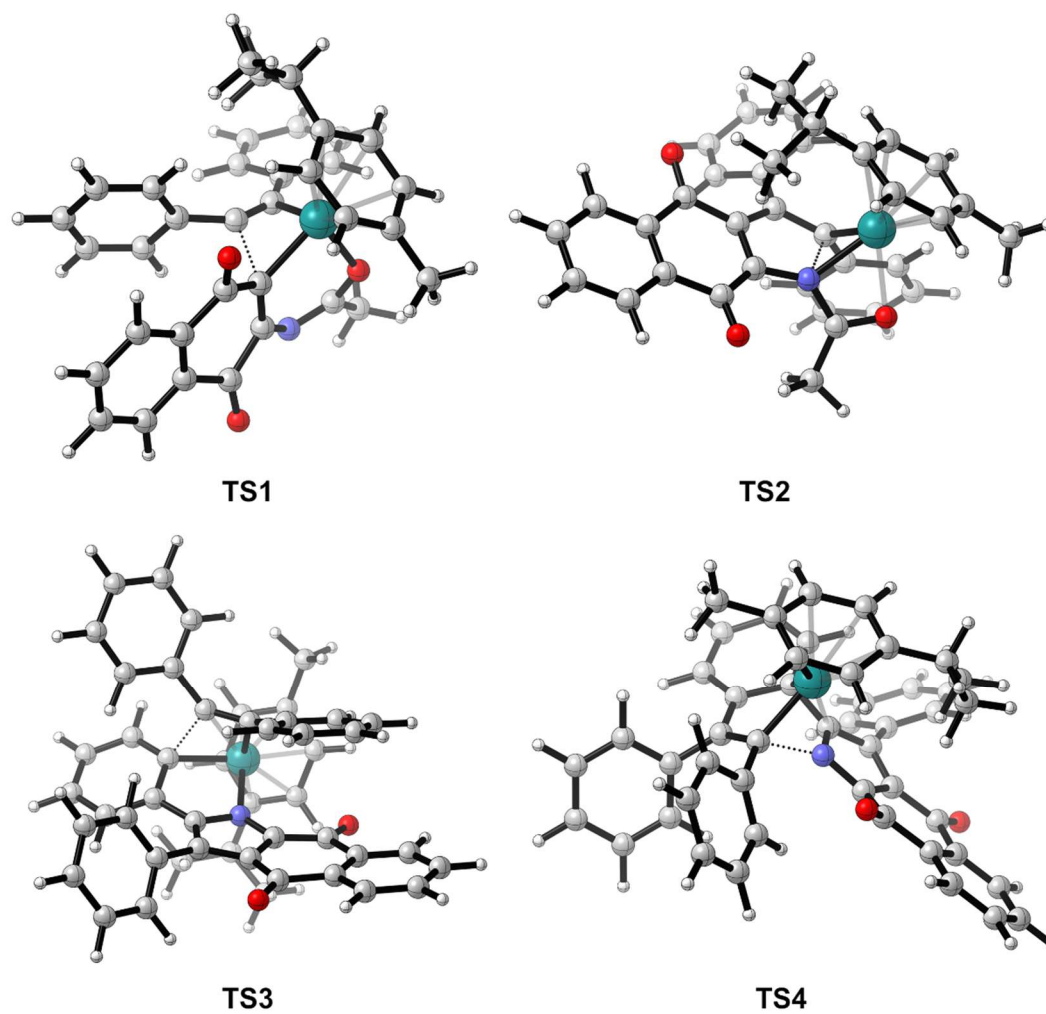
<sup>145</sup> Skripnikov, L. *Chemissian 4.60*, **2018** (<http://www.chemissian.com>).

<sup>146</sup> (a) Vosko, S. H.; Wilk, L.; Nusair, M. *Can. J. Phys.*, **1980**, *58*, 1200-1211; (b) Lee, C.; Yang, W.; Parr, R. G. *Phys. Rev. B*, **1988**, *37*, 785-789; (c) Becke, A. D. *J. Chem. Phys.*, **1993**, *98*, 5648-5652; (d) Stephens, P. J.; Devlin, F. J.; Chabalowski, C. F.; Frisch, M. J. *J. Phys. Chem.*, **1994**, *98*, 11623-11627.

<sup>147</sup> Grimme, S.; Ehrlich, S.; Goerigk, L. *J. Comput. Chem.*, **2011**, *32*, 1456-1465.



**Figure 42.** 3D images of the key intermediates **59a-[Ru]** and **67a'-[Ru]**.



**Figure 43.** 3D images of the transition states **TS1-4** associated with the C–C and C–N coupling steps.

## 5.5. Antitumor assays

Compounds were tested for cytotoxic activity in cell culture *in vitro* using seven cancer cell lines (**HCT-116**: human colon cancer cell line, **L929**: mouse fibroblast cell line, **MCF-7**: human breast cancer cell line, **HL-60**: human leukemia cell line, **SNB-19**: human glioblastoma cell line, **NCI-H460**: human lung cancer cell line, **PC3**: human prostatic cell line). The human cancer cell lines used in this work were obtained from the National Cancer Institute (Bethesda, MD, USA). The mouse fibroblast cell line (L929) was purchased from Rio de Janeiro Cell Bank (Rio de Janeiro, Brazil). The cells were maintained in RPMI 1640 medium supplemented with 10% fetal bovine serum, 2 mM glutamine, 100 U mL<sup>-1</sup> penicillin, 100 µg mL<sup>-1</sup> streptomycin at 37 °C with 5% CO<sub>2</sub>. The cytotoxicity of the samples was evaluated using the MTT method (1). The cells were plated in 96-well test plates in the following densities: 0.3 x 10<sup>6</sup> (HL-60), 0.5 x 10<sup>5</sup> (NCI-H460), 0.7 x 10<sup>5</sup> (HCT-116), 0.1 x 10<sup>6</sup> (SNB-19), 0.1x10<sup>6</sup> (MCF-7), 0.1 x 10<sup>6</sup> (PC3) and 0.7 x 10<sup>5</sup> (L929). The samples were incubated for 72 h in a concentration range of 0.04-5 µg/mL. Doxorubicin (0.001-1.10 µM) was used as the positive control, and negative control groups received the same amount of vehicle (DMSO). The cell viability was determined by reduction of the yellow dye 3-(4,5-dimethyl-2-thiazol)-2,5-diphenyl-2*H*-tetrazolium bromide (MTT) to a purple formazan product as described by Mosmann.<sup>148</sup> At the end of the incubation time (72 h), the plates were centrifuged and the medium was replaced by fresh medium (200 µL) containing 0.5 mg/mL MTT. Three hours later, the MTT formazan product was dissolved in DMSO (150 µL) and the absorbance was measured using a multiplate reader (Spectra Count, Packard, Ontario, Canada). The influence of the compound on cell proliferation and survival was quantified as the percentage of control absorbance of the reduced dye at 550 nm. The experiments were analyzed using averages and the corresponding confidence intervals based on the non-linear regression generated using GraphPad Prism. Each sample was tested in triplicate in at least three independent experiments. An intensity scale was used to evaluate the cytotoxic potential of the tested samples. All cells were mycoplasma-free. All observed results are presented in **Table 15**.

---

<sup>148</sup> Mosmann, T. *J. Immunol. Methods*, **1983**, 65, 55-63.

**Table 15.** Activity of products **67a-k**, **68a-b**, **69a** and **69b** against seven cancer cell lines.

Compound	IC <sub>50</sub> (μM)						
	HCT-116	L929	MCF-7	HL-60	SNB-19	NCI-H460	PC3
<b>67a</b>	>15	>15	>15	>15	>15	>15	>15
<b>67b</b>	>15	>15	>15	>15	>15	>15	>15
<b>67c</b>	>15	>15	>15	>15	>15	>15	>15
<b>67d</b>	>15	>15	>15	2.92	>15	>15	>15
<b>67e</b>	>15	>15	>15	>15	>15	>15	>15
<b>67f</b>	>15	>15	>15	>15	>15	>15	>15
<b>67g</b>	>15	>15	>15	>15	>15	>15	>15
<b>67h</b>	>15	>15	>15	>15	>15	>15	>15
<b>67i</b>	>15	>15	>15	>15	>15	>15	>15
<b>67j</b>	>15	>15	>15	13.19	>15	>15	>15
<b>67k</b>	>15	>15	>15	>15	>15	>15	>15
<b>68a</b>	>15	>15	>15	8.45	>15	>15	>15
<b>68b</b>	>15	>15	>15	>15	>15	>15	>15
<b>68c</b>	>15	>15	>15	>15	>15	>15	>15
<b>68d</b>	>15	>15	>15	>15	>15	>15	>15
<b>68e</b>	>15	>15	>15	>15	>15	>15	>15
<b>68f</b>	>15	>15	>15	>15	>15	>15	>15
<b>68g</b>	>15	>15	>15	3.17	>15	>15	>15
<b>69a</b>	>15	>15	>15	>15	>15	>15	>15
<b>69b</b>	>15	>15	>15	>15	>15	>15	>15
<b>Doxorubicin</b>	0.21	1.72	0.15	0.02	2.05	0.15	0.76

## REFERENCES

- 1 Weaver, M. G.; Pettus, T. R. R. Synthesis of *para*- and *ortho*-Quinones. *Comprehensive Organic Synthesis*, **2014**, 2<sup>nd</sup> ed., 7, 373-410.
- 2 (a) Ke, F.; Yu, J.; Chen, W.; Si, X.; Li, X.; Yang, F.; Liao, Y.; Zuo, Z. The anti-malarial atovaquone selectively increases chemosensitivity in retinoblastoma via mitochondrial dysfunction-dependent oxidative damage and Akt/AMPK/mTOR inhibition. *Biochem. Biophys. Res. Commun.*, **2018**, 504, 374-379; (b) Devadevi, N.; Rajkumar, K.; Vijaylakshmi, P. Efficacy of buparvaquone in the treatment of bovine benign theileriosis. *Int. J. Chem. Stud.*, **2018**, 6, 1-3.
- 3 Jardim, G. A. M.; Bozzi, I. A. O.; Oliveira, W. X. C.; Mesquita-Rodrigues, C.; Menna-Barreto, R. F. S.; Kumar, R. A.; Gravel, E.; Doris, E.; Braga, A. L.; Silva Júnior, E. N. Copper complexes and carbon nano tube-copper ferrite-catalyzed benzenoid A-ring selenation of quinones: an efficient method for the synthesis of trypanocidal agents. *New J. Chem.*, **2019**, 43, 13751-13763.
- 4 Kharma, A.; Jacob, C.; Bozzi, I. A. O.; Jardim, G. A. M.; Braga, A. L.; Salomão, K.; Gatto, C. C.; Silva, M. F. S.; Pessoa, C.; Stangier, M.; Ackermann, L.; Silva Júnior, E. N. Electrochemical selenation/cyclization of quinones: a rapid, green and efficient access to functionalized trypanocidal and antitumor compounds. *Eur. J. Org. Chem.*, **2020**, 2020, 4474-4486.
- 5 Gaultier, J.; Hauw, C. Structure of 1' $\alpha$ -Naphthoquinone. *Acta Cryst.*, **1965**, 18, 179-183.
- 6 Tikkanen, L.; Matsushima, T.; Natori, S.; Yoshihira, K. Mutagenicity of natural naphthoquinones and benzoquinones in the *Salmonella*/microsome test. *Mut. Res.*, **1983**, 124, 25-34.
- 7 Hussain, H.; Krohn, K.; Ahmad, V. U.; Miana, G. A.; Green, I. R. Lapachol: an overview. *Arkivoc*, **2007**, 2, 145-171.

- 8 Arnaudon, M. Reserches sur un novel acide extrait du bois du Paraguay. *C. R. Acad. Sci. (Paris)*, **1858**, *46*, 1152-1156.
- 9 Fieser, L. F. The alkylation of hydroxynaphthoquinone III. A synthesis of lapachol. *J. Am. Chem. Soc.*, **1927**, *49*, 857-864
- 10 Oliveira, L. G.; Silva, M. M.; Paula, F. C. S.; Pereira-Maia, E. C.; Donnici, C. L.; Simone, C. A.; Frézard, F.; da Silva Júnior, E. N.; Demicheli, C. Antimony(IV) and bismuth(V) complexes of lapachol: synthesis, Crystal structure and cytotoxic activity. *Molecules*, **2011**, *16*, 10314-10323.
- 11 Moura, K. G. C.; Emery, F. S.; Pinto, C. N.; Pinto, M. C. F. R.; Dantas, A. P.; Salomão, K.; Castro, S. L.; Pinto, A. V. Trypanocidal activity of isolated naphthoquinones from *Tabebuia* and some heterocyclic derivatives: a review from an interdisciplinary situdy. *J. Braz. Chem. Soc.*, **2001**, *12*, 325-338.
- 12 Andrade-Neto, V. F.; Goulart, M. O. F.; Filho, J. F. S.; Silva, M. J.; Pinto, M. C. F. R.; Pinto, A. V.; Zalis, M. G.; Carvalho, L. H.; Krettli, A. U. Antimalarial acitivity of phenazines from lapachol,  $\beta$ -lapachone, and its derivatives against *Plasmodium falciparum* *in vitro* and *Plasmodium berghei* *in vivo*. *Bioorg. Med. Chem. Lett.*, **2004**, *14*, 1145-1149.
- 13 Hirota, Y. Study on Mechanism Underlying Metabolic Biotransformation of Vitamin K. *Vitamins (Japan)*, **2017**, *92*, 63-72.
- 14 Garber, A. K.; Binkley, N. C.; Krueger, D. C.; Suttie, J. W. Comparison of phylloquinone bioavailability from food sources or a supplement in human subjects. *J. Nutr.*, **1999**, *129*, 1201-1203.
- 15 Schurgers, L. J.; Vermeer, C. Determination of phylloquinone and menaquinones in food: effect of food matrix on circulating vitamin K concentrations. *Haemostasis*, **2000**, *30*, 298-307.
- 16 (a) Jardim, G. A. M.; Silva, T. L.; Goulart, M. O. F.; Carlos A. de Simone, C. A.; Barbosa, J. M. C.; Salomão, K.; Solange L. de Castro, S. L.; Bower, J. F.; da Silva Júnior, E. N. Rhodium-catalyzed C–H bond activation for the synthesis of quinonoid compounds: significant anti-*Trypanosoma cruzi* activities and electrochemical studies

- of functionalized quinones. *Eur. J. Med. Chem.*, **2017**, *136*, 406-419; (b) Dumanska, Y.; Shakh, Y.; Kudrinetska, A.; Bolibrukh, K.; Karkhut, A.; Lytvyn, B.; Kovalchuk, O.; Marshalok, O.; Platonov, M.; Polovkovych, S.; Novikov, V. Synthesis of new fused tricyclic quinoid systems and studying of their biological activity *in-silico*. *Res. J. Pharm. Biol. Chem. Sci.*, **2013**, *4*, 1471-1479; (c) Nasiri, H. R.; Madej, G.; Panish, R.; Lafontaine, M.; Bats, J. W.; Lancaster, C. R. D.; Schwalbe, H. Design, synthesis, and biological testing of novel naphthoquinones as substrate-based inhibitors of the quinol/fumarate reductase from *Wolinella succinogenes*. *J. Med. Chem.*, **2013**, *56*, 9530-9541; (d) Dias, G. G.; Rogge, T.; Kuniyil, R.; Jacob, C.; Menna-Barreto, R. F. S.; da Silva Junior, E. N.; Ackermann, L. Ruthenium-catalyzed C–H oxygenation of quinones by weak O-coordination for potent trypanocidal agents. *Chem. Commun.*, **2018**, *54*, 12840-12843; (e) Su, J.; Zhang, Y.; Chen, M.; Li, W.; Qin, X.; Xie, Y.; Qin, L.; Huang, S.; Zhang, M. A copper halide promoted regioselective halogenation of coumarins using *N*-halosuccinimide as halide source. *Synlett*, **2019**, *30*, 630-634.
- 17 (a) Perchellet, E. M.; Sperfslage, B. J.; Wang, Y.; Huang, X.; Tamura, M.; Hua, D. H.; Perchellet, J.-P. Among substituted 9,10-dihydro-9,10-[1,2]benzenoanthracene-1,4,5,8-tetraones, the lead antitumor triptycene bisquinone TT24 blocks nucleoside transport, induces apoptotic DNA fragmentation and decreases the viability of L1210 leukemic cells in the nanomolar range of daunorubicin *in vitro*. *Anti-Cancer Drugs*, **2002**, *13*, 567-581; (b) Perchellet, E. M.; Wang, Y.; Weber, R. L.; Lou, K.; Hua, D. H.; Perchellet, J.-P. H. Antitumor triptycene bisquinones induce a caspase-independent release of mitochondrial cytochrome c and a caspase-2-mediated activation of initiator caspase-8 and -9 in HL-60 cells by a mechanism which does not involve Fas signaling. *Anti-Cancer Drugs*, **2004**, *15*, 929-946; (c) Dolfi, S. C.; Yang, Z.; Lee, M.-J.; Guan, F.; Hong, J.; Yang, C. S. Inhibitory effects of different forms of tocopherols, tocopherol phosphates, and tocopherol quinones on growth of colon cancer cell. *J. Agric. Food Chem.*, **2013**, *61*, 8533-8540.
- 18 (a) Ramírez-Macías, I.; Marín, C.; Es-Samti, H.; Fernández, A.; Guardia, J. J.; Zentar, H.; Agil, A.; Chahboun, R.; Alvarez-Manzaneda, E.; Sánchez-Moreno, M. Taiwaniaquinoid and abietane quinone derivatives with trypanocidal activity against *T. cruzi* and *Leishmania* spp. *Parasitol. Intern.*, **2012**, *61*, 405-413; (b) Sarkhosh, M.; Khorshidi, N.; Niazi, A.; Leardi, R. Application of genetic algorithms for pixel selection in multivariate image analysis for a QSAR study of trypanocidal activity for quinone



- compounds and design new quinone compounds. *Chemomet. Intell. Lab. Sys.*, **2014**, *139*, 168-174.
- 19 (a) Caro, D.; Florez, M.; Gaitan, R.; Martinez, E.; Baldiris, R.; Vivas-Reyes, R. Study of relationship chemical structure antimalaria activity of quinoidal compounds obtained by synthesis. *Afinidad*, **2017**, *74*, 185-193; (b) Ahenkorah, S.; Coertzen, D.; Tong, J. X.; Fridianto, K.; Wittlin, S.; Birkholtz, L.-M.; Tan, K. S. W.; Lam, Y.; Go, M.-L.; Haynes, R. K. Antimalarial  $N^1, N^3$ -dialkyldioxonaphthoimidazoliums: synthesis, biological activity, and structure–activity relationships. *ACS Med. Chem. Lett.*, **2020**, *11*, 49-55.
- 20 (a) Wolfbeis, O. S.; Furlinger, E. Absorption, fluorescence and fluorimetric detection limits of naturally occurring quinoid antibiotics and dyes. *Microchim. Acta*, **1983**, *81*, 385-398; (b) Krohn, K. Biomimetic synthesis of deca- and dodecaketide-derived quinone antibiotics. *Eur. J. Org. Chem.*, **2002**, *2002*, 1351-1362.
- 21 (a) Muronetz, V. I.; Asryants, R. A.; Semenyuk, P. I.; Mishchenko, N. P.; Vasilieva, E. A.; Fedoreyev, S. A.; Schmalhausen, E. V. Natural quinones: antioxidant and antiaggregant action towards glyceraldehyde-3-phosphate dehydrogenase. *Curr. Org. Chem.*, **2017**, *21*, 2125-2133; (b) Maringer, L.; Roiser, L.; Wallner, G.; Nitsche, D.; Buchberger, W. The role of quinoid derivatives in the UV-initiated synergistic interaction mechanism of HALS and phenolic antioxidants. *Polym. Degrad. Stab.*, **2016**, *131*, 91-97.
- 22 Stagliano, K. W.; Emadi, A.; Lu, Z.; Malinakova, H. C.; Twenter, B.; Yu, M.; Holland, L. E.; Rom, A. M.; Harwood, J. S.; Amin, R.; Johnson, A. A.; Pommier, Y. Regiocontrolled synthesis and HIV inhibitory activity of unsymmetrical binaphthoquinone and trimeric naphthoquinone derivatives of conocurvone. *Bioorg. Med. Chem.*, **2006**, *14*, 5651-5665.
- 23 Shukla, H.; Chitrakar, R.; Bibi, H. A.; Gaje, G.; Koucheki, A.; Trush, M. A.; Zhu, H.; Li, R.; Jia, Z. Reactive oxygen species production by BP-1,6-quinone and its effects on the endothelial dysfunction: Involvement of the mitochondria. *Toxicol. Lett.*, **2020**, *322*, 120-130.
- 24 (a) Waugh, T. M.; Masters, J.; Aliev, A. E.; Marson, C. M. Monocyclic Quinone Structure-Activity Patterns: Synthesis of Catalytic Inhibitors of Topoisomerase II with

- Potent Antiproliferative Activity. *ChemMedChem*, **2002**, *15*, 114-124; (b) Zhou, D.-C.; Lu, Y.-T.; Mai, Y.-W.; Zhang, C.; Xia, J.; Yao, P.-F.; Wang, H.-G.; Huang, S.-L.; Huang, Z.-S. Design, synthesis and biological evaluation of novel perimidine *o*-quinone derivatives as non-intercalative topoisomerase II catalytic inhibitors. *Bioorg. Chem.*, **2019**, *91*, 103131.
- 25 (a) Hanchate, V.; Devarajappa, R.; Prabhu, K. R. Sulfoxonium-ylide-directed C–H activation and tandem (4 + 1) annulation. *Org. Lett.*, **2020**, *8*, 2878-2882; (b) Ma, X.; Zhao, X.; Zhu, R.; Zhang, D. Computational study on why and how of nonconventional *meta*-C–H arylation of electron-rich arenes *via* Pd/quinoxaline-based ligand/norbornene cooperative catalysis. *J. Org. Chem.*, **2020**, *85*, 5995-6007; (c) Sagadevan, A.; Charitou, A.; Wang, F.; Ivanona, M.; Vuagnat, M.; Greaney, M. F. *Ortho* C–H arylation of arenes at room temperature using visible light ruthenium C–H activation. *Chem. Sci.*, **2020**, *11*, 4439-4443; (d) Thombal, R. S.; Lee, Y. R. Palladium-catalyzed direct oxidative C–H activation/annulation for regioselective construction of *N*-acylindoles. *Org. Lett.*, **2020**, *22*, 3397-3401.
- 26 (a) Yuan, S.; Chang, J.; Yu, B. Construction of biologically important biaryl scaffolds through direct C–H bond activation: advances and prospects. *Top. Curr. Chem.*, **2020**, *378*, 23; (b) Zhang, X.; Bai, R.; Xiong, H.; Xu, H.; Hou, W. Meeting organometallic chemistry with drug discovery: C–H activation enabled discovery of a new ring system of 12*H*-indazolo[2,1-*a*]cinnolin-12-ones with anti-proliferation activity. *Bioorg. Med. Chem. Lett.*, **2020**, *30*, 126916.
- 27 Dimroth, O. Ueber die Mercurirung aromatischer Verbindungen. *Berichte Deut. Chem. Gesell.*, **1902**, *35*, 2032-2045.
- 28 (a) Murahashi, S. Synthesis of phthalimidines from Schiff bases and carbon monoxide. *J. Am. Chem. Soc.*, **1955**, *77*, 6403-6404; (b) Bianchini, C.; Mealli, C.; Peruzzini, M.; Vizza, F.; Zanobini, F. Activation of C–H bonds in acetylene and terminal alkynes by rhodium(I) species. Crystal structure of *cis*-(ethynyl) hydride [(NP<sub>3</sub>)Rh(H)(≡CH)]BPh<sub>4</sub>·1.5C<sub>4</sub>H<sub>8</sub>O (NP<sub>3</sub> = N(CH<sub>2</sub>CH<sub>2</sub>PPh<sub>2</sub>)<sub>3</sub>). *J. Organometal. Chem.*, **1988**, *346*, C53-C57.

- 29 Janowicz, A. H.; Bergman, R. G. Carbon-hydrogen activation in completely saturated hydrocarbons: direct observation of  $M + R-H \rightarrow M(R)(H)$ . *J. Am. Chem. Soc.*, **1982**, *104*, 352-354.
- 30 Agasti, S.; Pal, T.; Achar, T. K.; Maiti, S.; Pal, D.; Mandal, S.; Daud, K.; Lahiri, G. K.; Maiti, D. Regioselective synthesis of fused furans by decarboxylative annulation of  $\alpha,\beta$ -alkenyl carboxylic acid with cyclic ketone: synthesis of di-heteroaryl derivatives. *Angew. Chem. Int. Ed.*, **2019**, *58*, 11039-11043.
- 31 Zhu, C.; Kuniyil, R.; Jei, B. B.; Ackermann, L. Domino C–H activation/directing group migration/alkyne annulation: unique selectivity by  $d^6$ -cobalt(III) catalysts. *ACS Catal.*, **2020**, *10*, 4444-4450.
- 32 Lu, Q.; Mondal, S.; Cembellín, S.; Greßies, S.; Glorius, F. Site-selective C–H activation and regiospecific annulation using propargylic carbonates. *Chem. Sci.*, **2019**, *10*, 6560-6564.
- 33 Wang, S.-G.; Liu, Y.; Cramer, N. Asymmetric alkenyl C–H functionalization by  $Cp^*Rh^{III}$  forms 2*H*-pyrrol-2-ones through [4+1]-annulation of acryl amides and allenes. *Angew. Chem. Int. Ed.*, **2019**, *58*, 18136-18140.
- 34 Carvalho, R. L.; Dias, G. G.; Pereira, C. L. M.; Ghosh, P.; Maiti, D.; da Silva Júnior, E. N. A catalysis guide focusing on C–H activation processes. *J. Braz. Chem. Soc.*, **2021**, *32*, 917-952.
- 35 Ess, D. H.; Goddard III, W. A.; Periana, R. A. Electrophilic, ambiphilic, and nucleophilic C–H bond activation: understanding the electronic continuum of C–H bond activation through transition-state and reaction pathway interaction energy decompositions. *Organometallics*, **2010**, *29*, 6459-6472.
- 36 (a) Arockiam, P. B.; Bruneau, C.; Dixneuf, P. H. Ruthenium(II)-catalyzed C–H bond activation and functionalization. *Chem. Rev.*, **2012**, *112*, 5879-5918; (b) Duarah, G.; Kaishap, P. P.; Begum, T.; Gogoi, S. Recent advances in ruthenium(II)-catalyzed C–H bond activation and alkyne annulation reactions. *Adv. Synth. Catal.*, **2019**, *361*, 654-672.

- 37 (a) Colby, D. A.; Bergman, R. G.; Ellman, J. A. Rhodium-catalyzed C–C bond formation *via* heteroatom-directed C–H bond activation. *Chem. Rev.*, **2010**, *110*, 624-655; (b) Song, L.; Tian, G.; Van der Eycken, E. V. Rhodium(III)-catalyzed intermolecular cascade annulation through C–H activation: concise synthesis of rosettacin. *Mol. Catal.*, **2018**, *459*, 129-134; (c) Wang, Z.; Xu, H. Rhodium-catalyzed C–H activation/cyclization of enamines with sulfoxonium ylides toward polysubstituted naphthalenes. *Tetrahedron Lett.*, **2019**, *60*, 664-667.
- 38 (a) Li, B.-J.; Yang, S.-D.; Shi, Z.-J. Recent advances in direct arylation *via* palladium-catalyzed aromatic C–H activation. *Synlett*, **2008**, *7*, 949-957; (b) Chen, X.; Engle, K. M.; Wang, D.-H.; Yu, J.-Q. Palladium(II)-catalyzed C–H activation/C–C cross-coupling reaction: versatility and practicality. *Angew. Chem. Int. Ed.*, **2009**, *48*, 5094-5115; (c) Engelin, C. J.; Fristrup, P. Palladium catalyzed allylic C–H alkylation: a mechanistic perspective. *Molecules*, **2011**, *16*, 951-969.
- 39 (a) Slugovc, C.; Padilla-Martínez, I.; Sirol, S.; Carmona, E. Rhodium- and Iridium-trispyrazolylborate complexes: C–H activation and coordination chemistry. *Coord. Chem. Rev.*, **2001**, *213*, 129-157; (b) Tenn, W. J.; Young, K. J. H.; Bhalla, G.; Oxgaard, J.; Goddard, W. A.; Periana, R. A. C–H Activation with an O-donor Iridium-methoxo complex. *J. Am. Chem. Soc.*, **2005**, *127*, 14172-14173; (c) Wu, X.; Sun, S.; Yu, J.-T.; Cheng, J. Recent applications of  $\alpha$ -carbonyl sulfoxonium ylides in rhodium- and iridium-catalyzed C–H functionalizations. *Synlett*, **2019**, *30*, 21-29.
- 40 (a) Zhang, J. J.; Zhang, M.; Lu, M.; He, Y.; Li, S.; Fan, L.; Zhang, X.; Wu, J.-K.; Yang, X. Synthesis of spiropyrans *via* the Rh(III)-catalyzed annulation of 3-aryl-2*H*-benzo[*b*][1,4]oxazines with diazo ketoesters. *Chem. Commun.*, **2022**, *58*, 5144-5147; (b) Li, X.; Li, D.; Zhang, X. Ru(II)-Catalyzed C–H bond activation/annulation of *N*-iminopyridinium ylides with sulfoxonium ylides. *Org. Biomol. Chem.*, **2022**, *20*, 1475-1479; (c) Singh, A.; Shukla, R. K.; Volla, C. M. R. Rh(III)-catalyzed [5+1] annulation of 2-alkenylanilides and 2-alkenylphenols with allenyl acetates. *Chem. Sci.*, **2022**, *13*, 2043-2049; (d) Li, J.; Xu, X.; Luo, Z.; Yao, Z.; Yang, J.; Zhang, X.; Xu, L.; Wang, P.; Shi, Q. Rhodium(III)-catalyzed regioselective C–H annulation and alkenylation of 2-pyridones with terminal alkynes. *Adv. Synth. Catal.*, **2022**, *364*, 1264-1270.

- 41 (a) Zhang, S.-S.; Liu, Y.-Z.; Zheng, Y.-C.; Xie, H.; Chen, S.-Y.; Song, J.-L.; Shu, B. Rhodium(III)-catalyzed regioselective C–H allylation and phenylation of indoles at C4-position. *Adv. Synth. Catal.*, **2022**, *364*, 64-70; (b) Wu, M.-S.; Ruan, X.-Y.; Han, Z.-Y.; Gong, L.-Z. Palladium-catalyzed cascade C–H functionalization/asymmetric allylation reaction of aryl  $\alpha$ -diazoamides and allenes: Lewis acid makes a difference. *Chem. Eur. J.*, **2022**, *28*, e202104218; (c) Xiong, Q.; Xiao, L.; Dong, X.-Q.; Wang, C.-J. Asymmetric synthesis of chiral aza-macrolactones *via* iridium-catalyzed cascade allylation/macrolactonization. *Org. Lett.*, **2022**, *24*, 2579-2584.
- 42 (a) Bakthadoss, M.; Reddy, T. T.; Agarwal, V.; Sharada, D. S. Ester-directed orthogonal dual C–H activation and ortho aryl C–H alkenylation *via* distal weak coordination. *Chem. Commun.*, **2022**, *58*, 1406-1409; (b) Zhao, H.; Luo, Z.; Yang, J.; Li, B.; Han, J.; Xu, L.; Lai, W.; Walsh, P. J. Ligand-promoted Rh(I)-catalyzed C2-selective C–H alkenylation and polyenylation of imidazoles with alkenyl carboxylic acids. *Chem. Eur. J.*, **2022**, *in press*, DOI: 10.1002/chem.202200441; (c) Xiong, P.; Hemming, M.; Ivlev, S. I.; Meggers, E. Electrochemical enantioselective nucleophilic  $\alpha$ -C(sp<sup>3</sup>)–H alkenylation of 2-acyl imidazoles. *J. Am. Chem. Soc.*, **2022**, *144*, 6964-6971.
- 43 (a) Deng, K.-Z. Jia, W.-L.; Fernández-Ibáñez, M. A. Selective *para*-C–H alkynylation of aniline derivatives by Pd/S,O-ligand catalysis. *Chem. Eur. J.*, **2022**, *28*, e202104107; (b) Ma, L.; Zhang, X.; Tuo, Y.; Zheng, Q.-Z. Cp\*Rh(III)-Catalyzed regioselective C(sp<sup>2</sup>)–H mono- and dialkynylation of thioamides by sulfur coordination. *J. Org. Chem.*, **2022**, *87*, 3691-3700; (c) Tan, E.; Nannini, J.; Stoica, O.; Echavarren, A. M. Rh-Catalyzed *ortho* C–H alkynylation of aromatic aldehydes. *Org. Lett.*, **2021**, *23*, 1263-1268.
- 44 (a) Gao, T.-H.; Xiong, Y.; Guo, P.; Liu, F.-S.; Zhao, L. Rigid  $\alpha$ -diimine palladium complexes as direct C–H arylation precatalysts for thiophenes and heteroaryl bromides. *Inorg. Chem. Commun.*, **2022**, *140*, 109403; (b) Xu, Y.-X.; Liang, Y.-Q.; Cai, Z.-J.; Ji, S.-J. Ruthenium(II)-catalyzed chelation-assisted desulfurative arylation of benzo[h]quinolines with arylsulfonyl chlorides. *Org. Lett.*, **2022**, *24*, 2601-2606; (c) Li, H.-L.; Yang, D.-F.; Jing, H.-Q.; Antilla, J. C.; Kuninobu, Y. Palladium-catalyzed enantioselective C(sp<sup>3</sup>)–H arylation of 2-propyl azaaryls enabled by an amino acid ligand. *Org. Lett.*, **2022**, *24*, 1286-1291.

- 45 (a) Shi, Y.; Yang, Y.; Xu, S. Iridium-catalyzed enantioselective C(sp<sup>3</sup>)–H borylation of aminocyclopropanes. *Angew. Chem. Int. Ed.*, **2022**, *61*, e202201463; (b) Wang, T.-C.; Wang, P.-S.; Chen, D.-F.; Gong, L.-Z. Access to chiral homoallylic vicinal diols from carbonyl allylation of aldehydes with allyl ethers *via* palladium-catalyzed allylic C–H borylation. *Sci. China Chem.*, **2022**, *65*, 298-303; (c) Lu, S.; Zheng, T.; Ma, J.; Deng, Z.; Qin, S.; Chen, Y.; Liang, Y. *para*-Selective C–H Borylation of Aromatic Quaternary Ammonium and Phosphonium Salts. *Angew. Chem. Int. Ed.*, **2022**, *61*, e202201285.
- 46 (a) Li, D.-K.; Zhang, B.; Ye, Q.; Deng, W.; Xu, Z.-Y. Synthesis of indenones *via* palladium-catalyzed carbonylation with Mo(CO)<sub>6</sub> as a CO surrogate. *Organometallics*, **2022**, *41*, 441-449; (b) Cheng, M.; Huang, X.-Y.; Yang, F.; Zhao, D.-M.; Ji, K.; Chen, Z.-S. Palladium-catalyzed carbene migratory insertion/carbonylation cascade reaction: synthesis of 2-indolones with a C3 all-carbon quaternary center. *Org. Lett.*, **2022**, *24*, 1237-1242; (c) Yang, Y.-Z.; He, D.-L.; Li, J.-H. Rhodium-catalyzed reductive *trans*-alkylacylation of internal alkynes *via* a formal carborhodation/C–H carbonylation cascade. *Org. Lett.*, **2022**, *23*, 5039-5043.
- 47 Jardim, G. A. M.; de Carvalho, R. L.; Nunes, M. P.; Machado, L. A.; Almeida, L. D.; Bahou, K. A.; Bower, J. B.; da Silva Júnior, E. N. Looking deep into C–H functionalization: the synthesis and application of cyclopentadienyl and related metal catalysts. *Chem. Commun.*, **2022**, *58*, 3101-3121.
- 48 de Carvalho, R. L.; de Miranda, A. S.; Nunes, M. P.; Gomes, R. S.; Jardim, G. A. M.; da Silva Júnior, E. N. On the application of 3d metals for C–H activation toward bioactive compounds: The key step for the synthesis of silver bullets. *Beilstein J. Org. Chem.*, **2021**, *17*, 1849-1938.
- 49 (a) Zhang, H.; Sun, M.-C.; Yang, D.; Li, T.; Song, M.-P.; Niu, J.-L. Cobalt(II)-catalyzed activation of C(sp<sup>3</sup>)–H bonds: organic oxidant enabled selective functionalization. *ACS Catal.*, **2022**, *12*, 1650-1656; (b) Ghosh, P.; Schoch, R.; Bauer, M. Selective benzylic CH-borylations by tandem cobalt catalysis. *Angew. Chem. Int. Ed.*, **2022**, *134*, e202110821; (c) Yao, Q.-J.; Chen, J.-H.; Song, H.; Huang, F.-R.; Shi, B.-F. Cobalt/Salox-catalyzed enantioselective C–H functionalization of arylphosphinamides. *Angew. Chem. Int. Ed.*, **2022**, *61*, e202202892.

- 50 (a) Yao, C.; Zhang, T.; Gonçalves, T. P.; Huang, K.-W. Selective benzylic C<sub>sp3</sub>-H bond activations mediated by a phosphorus-nitrogen PN<sup>3</sup>P-nickel complex. *Chem. Commun.*, **2022**, 58, 1593-1596; (b) Campbell, M. W.; Yuan, M.; Polites, V. C.; Gutierrez, O.; Molander, G. A. Photochemical C – H activation enables nickel-catalyzed olefin dicarbofunctionalization. *J. Am. Chem. Soc.*, **2021**, 143, 3901-3910; (c) Murugesan, V.; Ganguly, A.; Karthika, A.; Rasappan, R. C–H alkylation of aldehydes by merging TBADT hydrogen atom transfer with nickel catalysis. *Org. Lett.*, **2021**, 23, 5389-5393.
- 51 (a) Sahoo, K.; Panda, N. Iron(III) chloride mediated *para*-selective C–H functionalization: access to C5-chloro and C5,C7-dichloro/dianisyl substituted 2-arylbenzoxazoles. *Adv. Synth. Catal.*, **2022**, 364, 1023-1030; (b) Yu, Z.; Li, G.; Zhang, J.; Liu, L. Iron-catalysed chemo- and *ortho*-selective C–H bond functionalization of phenols with  $\alpha$ -aryl- $\alpha$ -diazoacetates. *Org. Chem. Front.*, **2021**, 8, 3770-3775; (c) Dey, D.; Patra, M.; Al-Hunaiti, A.; Yadav, H. R.; Al-mherat, A.; Arar, S.; Maji, M.; Choudhury, A. R.; Biswas, B. Synthesis, structural characterization and C–H activation property of a tetra-iron(III) cluster. *J. Mol. Struct.*, **2019**, 1180, 220-226.
- 52 Murali, K.; Machado, L. A.; de Carvalho, R. L.; Pedrosa, L. F.; Mukherjee, R.; da Silva Júnior, E. N.; Maiti, D. Decoding directing groups and their pivotal role in C–H activation. *Chem. Eur. J.*, **2021**, 27, 12453-12508.
- 53 Kumar, S.; Kumar, A.; Sharma, D.; Das, P. Free Amine, hydroxyl and sulfhydryl directed C–H functionalization and annulation: application to heterocycle synthesis. *Chem. Rec.*, **2022**, 22, e202100171.
- 54 Achar, T. K.; Zhang, X.; Mondal, R.; Shanavas, M. S.; Maiti, S.; Maity, S.; Pal, N.; Paton, R. S.; Maiti, D. Palladium-catalyzed directed meta-selective C – H allylation of arenes: unactivated internal olefins as allyl surrogates. *Angew. Chem. Int. Ed.*, **2019**, 58, 10353-10360.
- 55 Ahmad, M. S.; Meguellati, K. Recent advances in metal catalyzed C–H functionalization with a wide range of directing groups. *ChemistrySelect*, **2022**, 7, e202103716.
- 56 (a) Ramadoss, B.; Jin, Y.; Asako, S.; Ilies, L. Remote steric control for undirected meta-selective C–H activation of arenes. *Science*, **2022**, 375, 658-663; (b) Bellina, F.; La

- Manna, M.; Rosadoni, E. Undirected, selective C<sub>sp2</sub>-H alkynylation of five-membered heteroarenes. *Curr. Org. Chem.*, **2021**, *25*, 2116-2141.
- 57 (a) Hammarback, A.; Bishop, A. L.; Jordan, C.; Athavan, G.; Eastwood, J. B.; Burden, T. J.; Bray, J. T. W.; Clarke, F.; Robinson, A.; Krieger, J.-P.; Whitwood, A.; Clark, I. P.; Towrie, M.; Lynam, J. M.; Fairlamb, I. J. S. Manganese-mediated C-H bond activation of fluorinated aromatics and the *ortho*-fluorine effect: kinetic analysis by *in situ* infrared spectroscopic analysis and time-resolved methods. *ACS Catal.*, **2022**, *12*, 1532-1544; (b) Wang, Y.; Wang, H.; Yang, Q.; Xie, S.; Zhu, H. Quinazoline-assisted *ortho*-halogenation with *N*-halosuccinimides through Pd(II)-catalyzed C(sp<sup>2</sup>)-H activation. *Eur. J. Org. Chem.*, **2022**, DOI: 10.1002/ejoc.202200316.
- 58 (a) Dutta, U.; Maiti, D. Emergence of pyrimidine-based *meta*-directing group: journey from weak to strong coordination in diversifying *meta*-C-H functionalization. *Acc. Chem. Res.*, **2022**, *55*, 354-372; (b) Luan, Y.-Y.; Gou, X.-Y.; Shi, W.-Y.; Liu, H.-C.; Chen, X.; Liang, Y.-M. Three-component ruthenium-catalyzed *meta*-C-H alkylation of phenol derivatives. *Org. Lett.*, **2022**, *24*, 1136-1140.
- 59 Dutta, U.; Maiti, S.; Pimparkar, S.; Maiti, S.; Gahan, L. R.; Krenske, E. H.; Lupton, D. W.; Maiti, D. Rhodium catalyzed template-assisted distal *para*-C-H olefination. *Chem. Sci.*, **2019**, *10*, 7426-7432.
- 60 de Carvalho, R. L.; Almeida, R. G.; Murali, K.; Machado, L. A.; Pedrosa, L. F.; Dolui, P.; Maiti, D.; da Silva Júnior, E. N. Removal and modification of directing groups used in metal-catalyzed C-H functionalization: the magical step of conversion into 'conventional' functional groups. *Org. Biomol. Chem.*, **2021**, *19*, 525-547.
- 61 (a) Chen, Y.; Lyu, H.; Quan, Y.; Xie, Z. Fe-catalyzed intramolecular B-H/C-H dehydrogenative coupling: synthesis of carborane-fused nitrogen heterocycles. *Org. Lett.*, **2021**, *23*, 4163-4167; (b) Liao, Y.; Zhou, Y.; Zhang, Z.; Fan, J.; Liu, F.; Shi, Z. Intramolecular oxidative coupling between unactivated aliphatic C-H and aryl C-H bonds. *Org. Lett.*, **2021**, *23*, 1251-1257.
- 62 Singh, A.; Dey, A.; Pal, K.; Dash, O. P.; Volla, C. M. R. Pd(II)-catalyzed transient directing group-assisted regioselective diverse C4-H functionalizations of indoles. *Org. Lett.*, **2022**, *24*, 1941-1946.



- 63 Wang, Q.; Nie, Y.-H. Liu, C.-X.; Zhang, W.-W.; Wu, Z.-J.; Gu, Q.; Zheng, C.; You, S.-L. Rhodium(III)-catalyzed enantioselective C–H activation/annulation of ferrocenecarboxamides with internal alkynes. *ACS Catal.*, **2022**, *12*, 3083-3093.
- 64 Yin, C.; Li, L.; Yu, C. Rh(III)-catalyzed C–H annulation of sulfoxonium ylides with iodonium ylides towards isocoumarins. *Org. Biomol. Chem.*, **2022**, *20*, 1112-1116.
- 65 Zeng, Z.; Yan, F.; Dai, M.; Yu, Z.; Liu, F.; Zhao, Z.; Bai, R.; Lan, Y. Mechanistic investigation of Cu-catalyzed asymmetric alkynylation of cyclic *N*-sulfonyl ketimines with terminal alkynes. *Organometallics*, **2022**, *41*, 270-277.
- 66 Guo, L.-Y.; Li, Q.; Liu, Y.-T.; Li, L.; Ni, Y.-Q.; Li, Y.; Pan, F. Palladium-catalyzed alkynylation of alkenes *via* C–H activation for the preparation of conjugated 1,3-enynes. *Adv. Synth. Catal.*, **2022**, *364*, 1109-1116.
- 67 Han, C.; Tian, X.; Zhang, H.; Rominger, F.; Hashmi, S. K. Tetrasubstituted 1,3-enynes by gold-catalyzed direct C(sp<sup>2</sup>)–H alkynylation of acceptor-substituted enamines. *Org. Lett.*, **2021**, *23*, 4764-4768.
- 68 (a) Rodrigues, T.; Werner, M.; Roth, J.; da Cruz, E. H. G.; Marques, M. C.; Akkapeddi, P.; Lobo, S. A.; Koeberle, A.; Corzana, F.; da Silva Júnior, E. N.; Werz, O.; Bernardes, G. J. L. Machine intelligence decrypts  $\beta$ -lapachone as an allosteric 5-lipoxygenase inhibitor. *Chem. Sci.*, **2018**, *9*, 6899-6903; (b) de Castro, S. L.; Emery, F. S.; da Silva Júnior, E. N. Synthesis of quinoidal molecules: strategies towards bioactive compounds with an emphasis on lapachones. *Eur. J. Med. Chem.*, **2013**, *69*, 678-700; (c) Kallifidas, D.; Kang, H.-S.; Brady, S. F. Tetarimycin A, an MRSA-active antibiotic identified through induced expression of environmental DNA gene clusters. *J. Am. Chem. Soc.*, **2012**, *134*, 19552-19555; (d) Powis, G. Metabolism and reactions of quinoid anticancer agents. *Pharmacol. Ther.*, **1987**, *35*, 57; (e) O'Brien, P. J. Molecular mechanisms of quinone cytotoxicity. *Chem. Biol. Interact.*, **1991**, *80*, 1; (f) Hillard, E. A.; Abreu, F. C.; Ferreira, D. C.; Jaouen, G.; Goulart, M. O. F.; Amatore, C. Electrochemical parameters and techniques in drug development, with an emphasis on quinones and related compounds. *Chem. Commun.*, **2008**, *23*, 2612.

- 69 Wood, J. M.; da Silva Júnior, E. N.; Bower, J. F. Rh-Catalyzed [2+2+2] cycloadditions with benzoquinones: de novo access to naphthoquinones for lignan and type II polyketide synthesis. *Org. Lett.*, **2020**, *22*, 265-269.
- 70 (a) Ambler, B. R.; Turnbull, B. W. H.; Suravarapu, S. R.; Uteuliyev, M. M.; Huynh, N. O.; Krische, M. J. Enantioselective ruthenium-catalyzed benzocyclobutenone–ketol cycloaddition: merging C–C bond activation and transfer hydrogenative coupling for type II polyketide construction. *J. Am. Chem. Soc.*, **2018**, *140*, 9091-9094; (b) Bender, M.; Turnbull, B. W. H.; Ambler, B. R.; Krische, M. J. Ruthenium-catalyzed insertion of adjacent diol carbon atoms into C–C bonds: Entry to type II polyketides. *Science*, **2017**, *357*, 779-781.
- 71 (a) Arisawa, M.; Fujii, Y.; Kato, H.; Fukuda, H.; Matsumoto, T.; Ito, M.; Abe, H.; Ito, Y.; Shuto, S. One-pot ring-closing metathesis/1,3-dipolar cycloaddition through assisted tandem ruthenium catalysis: synthesis of a dye with isoindolo[2,1-*a*]quinoline structure. *Angew. Chem. Int. Ed.*, **2013**, *52*, 1003-1007; (b) Fujii, Y.; Takehara, T.; Suzuki, T.; Fujioka, H.; Shuto, S.; Arisawa, M. One-Pot olefin isomerization/aliphatic enamine ring-closing metathesis/oxidation/1,3-dipolar cycloaddition for the synthesis of isoindolo[1,2-*a*]isoquinolines. *Adv. Synth. Catal.*, **2015**, *357*, 4055-4062.
- 72 Liu, Y.; Sun, J.-W. Copper(II)-catalyzed synthesis of benzo[*f*]pyrido[1,2-*a*]indole-6,11-dione derivatives via naphthoquinone difunctionalization reaction. *J. Org. Chem.*, **2012**, *77*, 1191-1197.
- 73 Suematsu, N.; Ninomiya, M.; Sugiyama, H.; Udagawa, T.; Tanaka, K.; Koketsu, M. Synthesis of carbazoloquinone derivatives and their antileukemic activity via modulating cellular reactive oxygen species. *Bioorg. Med. Chem. Lett.*, **2019**, *29*, 2243-2247.
- 74 Jardim, G. A. M.; da Silva Júnior, E. N.; Bower, J. F. Overcoming naphthoquinone deactivation: rhodium-catalyzed C-5 selective C–H iodination as a gateway to functionalized derivatives. *Chem. Sci.*, **2016**, *7*, 3780-3784.
- 75 Dias, G. G.; do Nascimento, T. A.; de Almeida, A. K. A.; Bombaça, A. C. S.; Menna-Barreto, R. F. S.; Jacob, C.; Warratz, S.; da Silva Júnior, E. N.; Ackermann, L.

- Ruthenium(II)-catalyzed C–H alkenylation of quinones: diversity-oriented strategy for trypanocidal compounds. *Eur. J. Org. Chem.*, **2019**, 2019, 2344-2353.
- 76 Jardim, G. A. M.; Oliveira, W. X. C.; de Freitas, R. P.; Menna-Barreto, R. F. S.; Silva, T. L.; Goulart, M. O. F.; da Silva Júnior, E. N. Direct sequential C–H iodination/organoyl-thiolation for the benzenoid A-ring modification of quinonoid deactivated systems: a new protocol for potent trypanocidal quinones. *Org. Biomol. Chem.*, **2018**, *16*, 1686-1691.
- 77 (a) Ackermann, L. Carboxylate-assisted ruthenium-catalyzed alkyne annulations by C–H/Het–H bond functionalizations. *Acc. Chem. Res.*, **2014**, *47*, 281-295; (b) Rouquet, G.; Chatani, N. Catalytic functionalization of C(sp<sup>2</sup>)–H and C(sp<sup>3</sup>)–H bonds by using bidentate directing groups. *Angew. Chem. Int. Ed.*, **2013**, *52*, 11726-11743; (c) Peng, S.; Liu, S.; Zhang, S.; Cao, S.; Sun, J. Synthesis of polyheteroaromatic compounds via rhodium-catalyzed multiple C–H bond activation and oxidative annulation. *Org. Lett.*, **2015**, *17*, 5032-5035; (d) Jayakumar, J.; Parthasarathy, K.; Chen, Y.-H.; Lee, T.-H.; Chuang, S.-C.; Cheng, C.-H. One-pot synthesis of highly substituted polyheteroaromatic compounds by rhodium(III)-catalyzed multiple C-H activation and annulation. *Angew. Chem. Int. Ed.*, **2014**, *53*, 9889-9892; (e) Rakshit, S.; Patureau, F. W.; Glorius, F. Pyrrole synthesis via allylic sp<sup>3</sup> C–H activation of enamines followed by intermolecular coupling with unactivated alkynes. *J. Am. Chem. Soc.*, **2010**, *132*, 9585-9587; (f) Song, G.; Chen, D.; Pan, C.-L.; Crabtree, R. H.; Li, X. Rh-Catalyzed oxidative coupling between primary and secondary benzamides and alkynes: synthesis of polycyclic amides. *J. Org. Chem.*, **2010**, *75*, 7487-7490; (g) Satoshi, M.; Nobuyoshi, U.; Koji, H.; Tetsuya, S.; Masahiro, M. Rhodium-catalyzed oxidative coupling/cyclization of benzamides with alkynes via C–H bond cleavage. *Chem. Lett.*, **2010**, *39*, 744-746; (h) Kong, W.-J.; Finger, L. H.; Messinis, A. M.; Kuniyil, R.; Oliveira, J. C. A.; Ackermann, L. Flow rhodaelectro-catalyzed alkyne annulations by versatile C–H activation: mechanistic support for rhodium(III/IV). *J. Am. Chem. Soc.*, **2019**, *141*, 17198-17206; (i) Zhu, C.; Kuniyil, R.; Ackermann, L. Manganese(I)-catalyzed C-H activation/Diels-Alder/retro-Diels-Alder domino alkyne annulation featuring transformable pyridines. *Angew. Chem. Int. Ed.*, **2019**, *58*, 5338-5342; (j) Tian, C.; Dhawa, U.; Scheremetjew, A.; Ackermann, L. Cupraelectro-catalyzed alkyne annulation: evidence for distinct C–H alkynylation and decarboxylative C–H/C–C manifolds. *ACS Catal.*, **2019**, *9*, 7690-7696; (k) Mei, R.; Koeller, J.; Ackermann, L.

- Electrochemical ruthenium-catalyzed alkyne annulations by C–H/Het–H activation of aryl carbamates or phenols in protic media. *Chem. Commun.*, **2018**, *54*, 12879-12882;
- (l) Mei, R.; Wang, H.; Warratz, S.; Macgregor, S. A.; Ackermann, L. Cobalt-catalyzed oxidase C–H/N–H alkyne annulation: mechanistic insights and access to anticancer agents. *Chem. Eur. J.*, **2016**, *22*, 6759-6763; (m) Ma, W.; Ackermann, L. Silver-mediated alkyne annulations by C–H/P–H functionalizations: step-economical access to benzophospholes. *Synthesis*, **2014**, *46*, 2297-2304; (n) Li, J.; Ackermann, L. Ruthenium-catalyzed oxidative alkyne annulation by C–H activation on ketimines. *Tetrahedron*, **2014**, *70*, 3342-3348; (o) Song, W.; Ackermann, L. Nickel-catalyzed alkyne annulation by anilines: versatile indole synthesis by C–H/N–H functionalization. *Chem. Commun.*, **2013**, *49*, 6638-6640; (p) Kornhaaß, C.; Li, J.; Ackermann, L. Cationic ruthenium catalysts for alkyne annulations with oximes by C–H/N–O functionalizations. *J. Org. Chem.*, **2012**, *77*, 9190-9198.
- 78 (a) Wang, L.; Ackermann, L. Versatile pyrrole synthesis through ruthenium(II)-catalyzed alkene C–H bond functionalization on enamines. *Org. Lett.*, **2013**, *15*, 176-179; (b) Gońka, E.; Yang, L.; Steinbock, R.; Pescioioli, F.; Kuniyil, R.; Ackermann, L.  $\pi$ -Extended polyaromatic hydrocarbons by sustainable alkyne annulations through double C–H/N–H activation. *Chem. Eur. J.*, **2019**, *25*, 16246-16250.
- 79 Wang, D.; Ge, B.; Li, L.; Shan, J.; Ding, Y. Transition metal-free Direct C–H functionalization of quinones and naphthoquinones with diaryliodonium salts: synthesis of aryl naphthoquinones as  $\beta$ -secretase inhibitors. *J. Org. Chem.*, **2014**, *79*, 8607-8613.
- 80 Ma, W.; Tan, Y.; Wang, Y.; Li, Z.; Li, Z.; Gu, L.; Mei, R.; Cheng, A. Hydroxyl-directed ruthenium-catalyzed *peri*-selective C–H acylmethylation and annulation of naphthols with sulfoxonium ylides. *Org. Lett.*, **2021**, *23*, 6200-6205.
- 81 Han, B. H.; Boudjouk, P. Organic sonochemistry. Ultrasound-promoted coupling of organic halides in the presence of lithium wire. *Tetrahedron Lett.*, **1981**, *22*, 2757-2758.
- 82 Chioma, F.; Ekennia, A. C.; Ibeji, C. U.; Okafor, S. N.; Onwudiwe, D. C.; Osowole, A. A.; Ujam, O. T. Synthesis, characterization, antimicrobial activity and DFT studies of 2-(pyrimidin-2-ylamino)naphthalene-1,4-dione and its Mn(II), Co(II), Ni(II) and Zn(II) complexes. *J. Mol. Struct.*, **2018**, *1163*, 455-464.

- 83 Josey, B. J.; Inks, E. S.; Wen, X.; Chou, C. J. Structure–Activity Relationship Study of Vitamin K Derivatives Yields Highly Potent Neuroprotective Agents. *J. Med. Chem.*, **2013**, *56*, 1007-1022.
- 84 Fieser, L. F.; Hartwell, J. L. The reaction of hydrazoic acid with the naphthoquinones. *J. Am. Chem. Soc.*, **1935**, *57*, 1482-1484.
- 85 Yin, J.; Rainier, J. D. The one-pot synthesis of amidonaphthoquinones from aminonaphthoquinones. *Tetrahedron Lett.*, **2020**, *61*, 151800.
- 86 Duarah, G.; Kaishap, P. P.; Begum, T.; Gogoi, S. Recent advances in ruthenium(II)-catalyzed C–H bond activation and alkyne annulation reactions. *Adv. Synth. Catal.*, **2019**, *361*, 645-672.
- 87 Wang, Y.; Zhu, S.; Zou, L.-H. Recent advances in direct functionalization of quinones. *Eur. J. Org. Chem.*, **2019**, *2019*, 2179–2201.
- 88 (a) Bennet, M. A.; Huang, T.-N.; Matheson, T. W.; Smith, A. K. ( $\eta^6$ -Hexamethylbenzene)ruthenium complexes. *Inorg. Synth.*, **2007**, *16*, 74-78; (b) Lorion, M. M.; Ackermann, L. [Ru(O<sub>2</sub>CR)<sub>2</sub>(*p*-cymene)]. *Encycl. Reag. Org. Synth.*, **2017**, 1-3. DOI: 10.1002/047084289x.rn02097; (c) Hey, D. A.; Fischer, P. J.; Baratta, W.; Kühn, F. E. Ru(O<sub>2</sub>CCF<sub>3</sub>)<sub>2</sub> and ruthenium phosphine complexes bearing fluoroacetate ligands: synthesis, characterization and catalytic activity. *Dalton Trans.*, **2019**, *48*, 4625-4635.
- 89 (a) Chen, R.; Cui, S. Rh(III)-catalyzed C–H activation/cyclization of benzamides and diazonaphthalen-2(1*H*)-ones for synthesis of lactones. *Org. Lett.*, **2017**, *19*, 4002-4005; (b) Zheng, L.; Hua, R. Modular assembly of ring-fused and  $\pi$ -extended phenanthroimidazoles via C–H activation and alkyne annulation. *J. Org. Chem.*, **2014**, *79*, 3930-3936.
- 90 (a) Wu, B.; Gao, X.; Yan, Z.; Chen, M.-W.; Zhou, Y.-G. C–H oxidation/Michael addition/cyclization cascade for enantioselective synthesis of functionalized 2-amino-4*H*-chromenes. *Org. Lett.*, **2015**, *17*, 6134-6137; (b) Ma, W.; Weng, Z.; Fang, X.; Gu, L.; Song, Y.; Ackermann, L. Ruthenium-catalyzed C–H selenylations of benzamides. *Eur. J. Org. Chem.*, **2019**, *2019*, 41-45.

- 91 Mukherjee, K.; Shankar, M.; Ghosh, K.; Sahoo, A. K. An orchestrated unsymmetrical annulation episode of C(sp<sup>2</sup>)-H bonds with alkynes and quinones: access to spiro-isoquinolones. *Org. Lett.*, **2018**, *20*, 1914-1918.
- 92 (a) Gandeepan, P.; Koeller, J.; Korvorapun, K.; Mohr, J.; Ackermann, L. Visible-light-enabled ruthenium-catalyzed *meta*-C-H alkylation at room temperature. *Angew. Chem. Int. Ed.*, **2019**, *58*, 9820-9825; (b) Yetra, S. R.; Rogge, T.; Warratz, S.; Struwe, J.; Peng, W.; Vana, P.; Ackermann, L. Micellar catalysis for ruthenium(II)-catalyzed C-H arylation: weak-coordination-enabled C-H activation in H<sub>2</sub>O. *Angew. Chem. Int. Ed.*, **2019**, *58*, 7490-7494; (c) Qiu Y.; Tian, C.; Massignan, L.; Rogge, T.; Ackermann, L. Electrooxidative ruthenium-catalyzed C-H/O-H annulation by weak *O*-coordination. *Angew. Chem. Int. Ed.*, **2018**, *57*, 5818-5822; (d) Ma, W. Weng, Z.; Rogge, T.; Gu, L.; Lin, J.; Peng, A.; Luo, X.; Gou, X.; Ackermann, L. Ruthenium(II)-catalyzed C-H chalcogenation of anilides. *Adv. Synth. Catal.*, **2018**, *360*, 704-710.
- 93 (a) Rota, P.; Allevi, P.; Colombo, R.; Costa, M. L.; Anastasia, M. General and chemoselective *N*-transacylation of secondary amides by means of perfluorinated anhydrides. *Angew. Chem. Int. Ed.*, **2010**, *49*, 1850-1853; (b) Zhang, G.; Liu, C.; Yi, H.; Meng, Q.; Bian, C.; Chen, H.; Jian, J.-X.; Wu, L.-Z.; Lei, A. External oxidant-free oxidative cross-coupling: a photoredox cobalt-catalyzed aromatic C-H thiolation for constructing C-S bonds. *J. Am. Chem. Soc.*, **2015**, *137*, 9273-9280; (c) Guilarte, V.; Castroviejo, M. P.; García-García, P.; Fernández-Rodríguez, M. A.; Sanz, R. Approaches to the synthesis of 2,3-dihaloanilines. useful precursors of 4-functionalized-1*H*-indoles. *J. Org. Chem.*, **2011**, *76*, 3416-3437.
- 94 Mio, M. J.; Kopel, L.C.; Braun, J. B.; Gadzikwa, T. L.; Hull, K. L.; Brisbois, R. G.; Markworth, C. J.; Grieco, P. A. One-pot synthesis of symmetrical and unsymmetrical bisarylethynes by a modification of the Sonogashira coupling reaction. *Org. Lett.* **2002**, *4*, 3199-3202.
- 95 Zhou, Q.; Peng, C.; Du, F.; Zhou, L.; Shi, Y.; Du, Y.; Liu, D.; Sun, W.; Zhang, M.; Chen, G. Design, synthesis and activity of BB1608 derivatives targeting on stem cells. *Eur. J. Med. Chem.*, **2018**, *151*, 39-50.
- 96 (a) Calvo, R.; Zhang, K.; Passera, A.; Katayev, D. Facile access to nitroarenes and nitroheteroarenes using *N*-nitrosaccharin. *Nature Commun.*, **2019**, *10*, 3410; (b) Huang,

- B.; Fan, C.; Yu, H.; Ma, J.; Pan, C.; Zhang, D.; Zheng, A.; Li, Y.; Sun, Y. Sol-gel preparation of helical silicate containing palladium oxide nanoparticles and the application for nitration of aromatic compound. *Mol. Catal.*, **2018**, *446*, 140-151; (c) Hiller, M.; Sittel, T.; Wadepohl, H.; Enders, M. A new class of lanthanide complexes with three ligand centered radicals: NMR evaluation of ligand field energy splitting and magnetic coupling. *Chem. Eur. J.*, **2019**, *25*, 10668-10677; (d) Meng, G.; Zheng, M.-L.; Zheng, A.-Q.; Wang, M.; Shi, J. The novel usage of thiourea nitrate in aryl nitration. *Chin. Chem. Lett.*, **2014**, *25*, 87-89; (e) Ma, X. M.; Li, B. D.; Chen, L.; Lu, M.; Lv, C. X. Selective nitration of aromatic compounds catalyzed by H $\beta$  zeolite using N<sub>2</sub>O<sub>5</sub>. *Chin. Chem. Lett.*, **2012**, *23*, 809-812.
- 97 Brocklehurst, C. E.; Lehmann, H.; La Vecchia, L. Nitration chemistry in continuous flow using fuming nitric acid in a commercially available flow reactor. *Org. Process Res. Dev.*, **2011**, *15*, 1447-1453.
- 98 Prokopcová, H.; Kappe, C. O. The Liebeskind-Srogl C–C cross-coupling reaction. *Angew. Chem. Int. Ed.*, **2009**, *48*, 2276-2286.
- 99 Torssell, K. Diels-Alder reactions of thiophene oxides generates in situ. *Acta Chem. Scand. B*, **1976**, *30*, 353-357.
- 100 Contant, P.; Haess, M.; Riegl, J.; Scalone, M.; Visnick, M. Synthesis of racemic Frenolicin B and 5-*epi*-Frenolicin B via intramolecular palladium-catalyzed arylcarbonylation. *Synthesis*, **1999**, *5*, 821-828.
- 101 Fieser, L. F.; Dunn, J. T. The addition of dienes to halogenated and hydroxylated naphthoquinones. *J. Am. Chem. Soc.*, **1937**, *59*, 1016-1021.
- 102 Yamakado, T.; Takahashi, S.; Watanabe, K.; Matsumoto, Y.; Osuka, A.; Saito, S. Conformational planarization versus singlet fission: distinct excited-state dynamics of cyclooctatetraene-fused acene dimers. *Angew. Chem. Int. Ed.*, **2018**, *130*, 5536-5541.
- 103 Haloulos, I.; Theodorou, D.; Zannikou, Y.; Zannikos, F. Monitoring fuel quality: a case study for quinizarin marker content of unleaded petrol marketed in Greece. *Accred. Qual. Assur.*, **2016**, *21*, 203-210.

- 104 Tucker, K. B. E.; Sawyer, R.; Stockwell, P. B. The automatic extraction, identification and determination of quinizarin in hydrocarbon oils. *Analyst*, **1970**, *95*, 730-737.
- 105 Barret, R.; Daudon, M. Oxidation of phenols to quinones by bis(trifluoroacetoxy)iodobenzene. *Tetrahedron Lett.*, **1990**, *31*, 4871-4872.
- 106 Dolomanov, O. V.; Bourhis, L. J.; Gildea, R. J.; Howard, J. A. K.; Puschmann, H. OLEX2: a complete structure solution, refinement and analysis program. *J. Appl. Cryst.*, **2009**, *42*, 339-341.
- 107 Sheldrick, G. M. SHELXT - Integrated space-group and crystal-structure determination. *Acta Cryst.*, **2015**, *A71*, 3-8.
- 108 Sheldrick, G. M. A short history of SHELX. *Acta Cryst.*, **2008**, *A64*, 112-122.
- 109 Osuský, P.; Nociarová, J.; Smolíček, M.; Gyepes, R.; Georgiou, D.; Polyzos, I.; Fakis, M.; Hrobárik, P. Oxidative C–H homocoupling of push–pull benzothiazoles: an atom-economical route to highly emissive quadrupolar arylamine-functionalized 2,2'-bibenzothiazoles with enhanced two-photon absorption. *Org. Lett.*, **2021**, *23*, 5512-5517.
- 110 Fischer, A.; Golding, R. M.; Tennant, W. C. Nuclear magnetic resonance studies of some aromatic nitroso-compounds. *J. Chem. Soc.*, **1965**, *1127*, 6032-6035.
- 111 Gontijo, T. B.; de Carvalho, R. L.; Dantas-Pereira, L.; Menna-Barreto, R. F. S.; Rogge, T.; Ackermann, L. da Silva Júnior, E. N. Ruthenium(II)- and palladium(II)-catalyzed position-divergent C–H oxygenations of arylated quinones: Identification of hydroxylated quinonoid compounds with potent trypanocidal activity. *Bioorg. Med. Chem.*, **2021**, *40*, 116164.
- 112 Rahman, M.; Szostak, M. Synthesis of sulfoxonium ylides from amides by selective N–C(O) activation. *Org. Lett.*, **2021**, *23*, 4818-4822.
- 113 Melzig, L.; Metzger, A.; Knochel, P. Pd- and Ni-catalyzed cross-coupling reactions of functionalized organozinc reagents with unsaturated thioethers. *Chem. Eur. J.*, **2011**, *17*, 2948-2956.



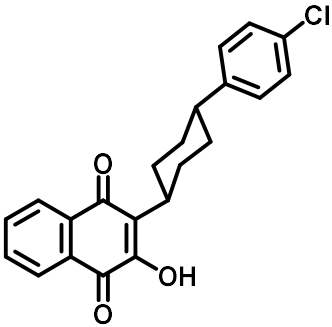
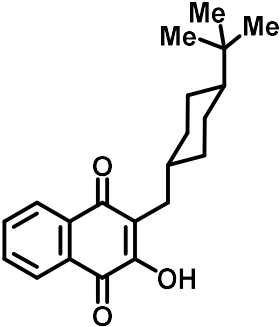
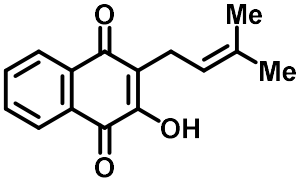
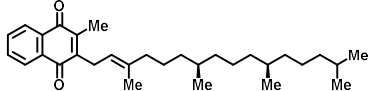
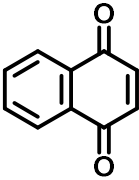
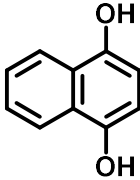
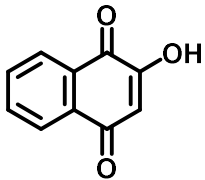
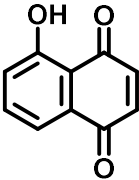
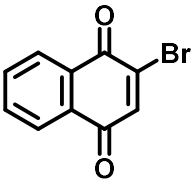
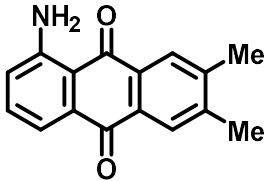

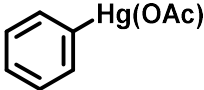
- 114 Gauthier, R.; Mamone, M.; Paquin, J.-F. Gold-catalyzed hydrofluorination of internal alkynes using aqueous HF. *Org. Lett.*, **2019**, *21*, 9024-9027.
- 115 Li, W.; Tang, J.; Li, S.; Zheng, X.; Yuan, M.; Xu, B.; Jiang, W.; Fu, H.; Li, R.; Chen, H. Stereodivergent synthesis of alkenylpyridines *via* Pd/Cu catalyzed C–H alkenylation of pyridinium salts with alkynes. *Org. Lett.*, **2020**, *22*, 7814-7819.
- 116 Mangel, N.; Snider, B. B. Efficient synthesis of the tetracyclic aminoquinone moiety of marmycin A. *Org. Lett.*, **2009**, *11*, 4926-4929.
- 117 Suchard, O.; Kane, R.; Roe, B. J.; Zimmermann, E.; Jung, C.; Waske, P. A.; Mattay, J.; Oelgemöller, M. Photooxygenations of 1-naphthols: an environmentally friendly access to 1,4-naphthoquinones. *Tetrahedron*, **2006**, *62*, 1467-1473.
- 118 Carvalho, R. L.; Jardim, G. A. M.; Santos, A. C. C.; Araujo, M. H.; Oliveira, W. X. C.; Bombaça, A. C. S.; Menna-Barreto, R. F. S.; Gopi, E.; Gravel, E.; Doris, E.; Silva Júnior, E. N. Combination of aryl diselenides/hydrogen peroxide and carbon-nanotube/rhodium nanohybrids for naphthol oxidation: an efficient route towards trypanocidal quinones. *Chem. Eur. J.*, **2018**, *57*, 15227-15235.
- 119 Zhang, L.-L.; Da, B.-C.; Xiang, S.-H.; Zhu, S.; Yuan, Z.-Y.; Guo, Z.; Tan., B. Organocatalytic double arylation of 3-isothiocyanato oxindoles: Stereocontrolled synthesis of complex spirooxindoles. *Tetrahedron*, **2019**, *75*, 1689-1696.
- 120 Bailey, D.; Williams, V. E. An efficient synthesis of substituted anthraquinones and naphthoquinones. *Tetrahedron Lett.*, **2004**, *45*, 2511-2513.
- 121 Montenegro, R. C.; Araújo, A. J.; Molina, M. T.; Filho, J. D. B. M.; Rocha, D. D.; López-Montero, E.; Goulart, M. O. F.; Bento, E. S.; Alves, A. P. N. N.; Pessoa, C.; Moraes, M. O.; Costa-Lotufo, L. V. Cytotoxic activity of naphthoquinones with special emphasis on juglone and its 5-O-methyl derivative. *Chem.-Biol. Int.*, **2010**, *184*, 439-448.
- 122 Nor, S. M. M.; Sukari, M. A. H. M.; Azziz, S. S. S. A.; Fah, W. C.; Alimon, H.; Juhan, S. F. Synthesis of New Cytotoxic Aminoanthraquinone Derivatives *via* Nucleophilic Substitution Reactions. *Molecules*, **2013**, *18*, 8046-8062.

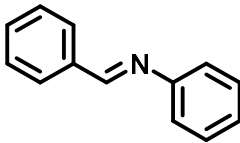
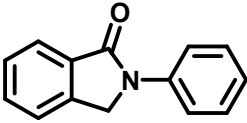
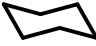
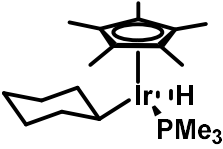
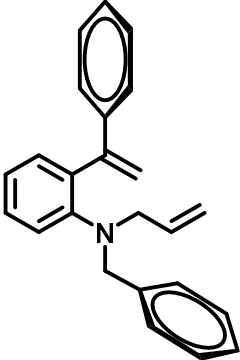
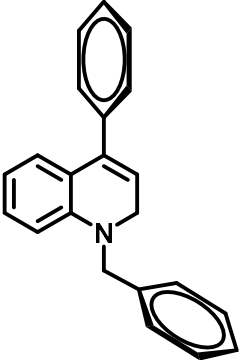
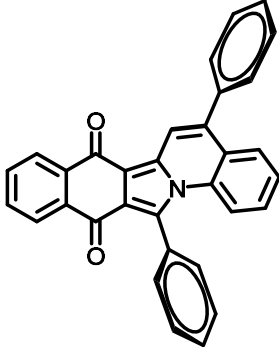
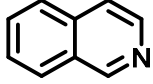
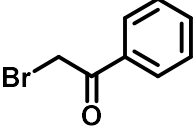
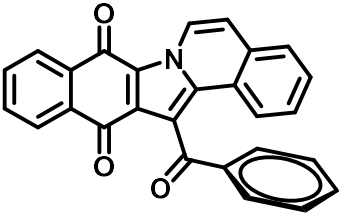
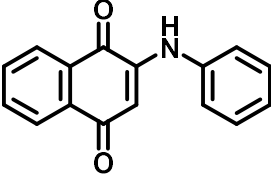
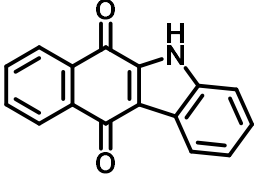
- 123 Wellauer, J.; Miladinov, D.; Buchholz, T.; Schütz, J.; Stemmler, R. T.; Medlock, J. A.; Bonrath, W.; Sparr, C. Organophotocatalytic aerobic oxygenation of phenols in a visible-light continuous-flow photoreactor. *Chem. Eur. J.*, **2021**, *27*, 9748-9752.
- 124 Zhang, J.; Chang, C.-W. T. One-pot Synthesis of 1- and 2-Substituted Naphtho[2,3-*d*][1,2,3]triazole-4,9-diones. *J. Org. Chem.*, **2009**, *74*, 4414-4417.
- 125 Bao, N.; Ou, J.; Shi, W.; Li, N.; Chen, L.; J. Sun. Highly Efficient Synthesis and Structure-Activity Relationships of a Small Library of Substituted 1,4-Naphthoquinones. *Eur. J. Org. Chem.*, **2018**, *2018*, 2254-2258.
- 126 Guo, J.; Kiran, I. N. C.; Reddy, R. S.; Gao, J.; Tang, M.; Liu, Y.; He, Y. Synthesis of Carbazolequinones by Formal [3+2] Cycloaddition of Arynes and 2-Aminoquinones. *Org. Lett.*, **2016**, *18*, 2499-2502.
- 127 Arnone, A.; Merlini, L.; Nasini, G.; Pava, O. V. Direct Amination of Naphthazarin, Juglone, and Some Derivatives. *Synth. Comm.*, **2007**, *37*, 2569-2577.
- 128 Dinda, B. K.; Basak, S.; Ghosh, B.; Mal, D. A Five-Step Cascade for the Modular and Regiodefined Synthesis of Naphth[2,1-*d*]oxazoles. *Synthesis*, **2016**, *48*, 1235-1245.
- 129 Dong, Y.; Jiang, H.; Chen, X.-L.; Ye, J.-X.; Zhou, Q.; Gao, L.-S.; Luo, Q.-Q.; Shi, Z.-C.; Li, Z.-H.; He, B. Silver-catalyzed one-pot biarylamination of quinones with arylamines: access to *N*-arylamine-functionalized *p*-iminoquinone derivatives. *Synthesis*, **2022**, *54*, 2242-2250.
- 130 Smith, R. B.; Canton, C.; Lawrence, N. S.; Livingstone, C.; Davis, J. Molecular anchors-mimicking metabolic processes in thiol analysis. *New J. Chem.*, **2006**, *30*, 1718-1724.
- 131 Zhang, C.; Chou, C. J. Metal-free direct amidation of naphthoquinones using hydroxamic acids as an amide source: application in the synthesis of an HDAC6 inhibitor. *Org. Lett.*, **2016**, *18*, 5512-5515.
- 132 Dai, W.; Wang, L.; Shang, S.; Chen, B.; Li, G.; Gao, S. Highly efficient oxidation of alcohols catalyzed by a porphyrin-inspired manganese complex. *Chem. Commun.*, **2015**, *51*, 11268-11271.

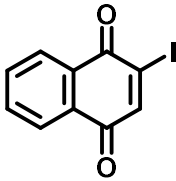
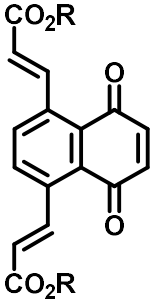
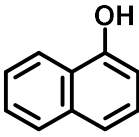
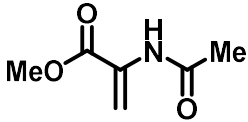
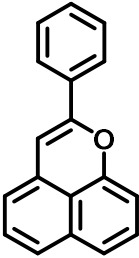
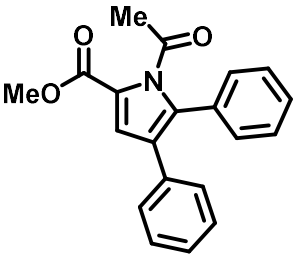
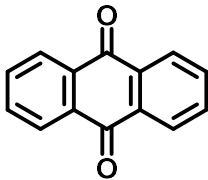
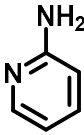
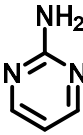
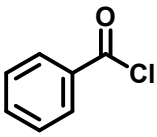
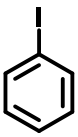
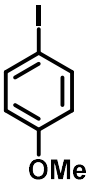
- 133 Ciogli, A.; Kumar, S. V.; Mancinelli, M.; Mazzanti, A.; Perumal, S.; Severi, C.; Villani, C. Atropisomerism in 3-arylthiazolidine-2-thiones. A combined dynamic NMR and dynamic HPLC study. *Org. Biomol. Chem.*, **2016**, *14*, 11137-11147.
- 134 Frisch, M. J.; Trucks, G. W.; Schlegel, H. B.; Scuseria, G. E.; Robb, M. A.; Cheeseman, J. R.; Scalmani, G.; Barone, V.; Petersson, G. A.; Nakatsuji, H.; Li, X.; Caricato, M.; Marenich, A. V.; Bloino, J.; Janesko, B. G.; Gomperts, R.; Mennucci, B.; Hratchian, H. P.; Ortiz, J. V.; Izmaylov, A. F.; Sonnenberg, J. L.; Williams-Young, D.; Ding, F.; Lipparini, F.; Egidi, F.; Goings, J.; Peng, B.; Petrone, A.; Henderson, T.; Ranasinghe, D.; Zakrzewski, V. G.; Gao, J.; Rega, N.; Zheng, G.; Liang, W.; Hada, M.; Ehara, M.; Toyota, K.; Fukuda, R.; Hasegawa, J.; Ishida, M.; Nakajima, T.; Honda, Y.; Kitao, O.; Nakai, H.; Vreven, T.; Throssell, K.; Montgomery, J. A., Jr.; Peralta, J. E.; Ogliaro, F.; Bearpark, M. J.; Heyd, J. J.; Brothers, E. N.; Kudin, K. N.; Staroverov, V. N.; Keith, T. A.; Kobayashi, R.; Normand, J.; Raghavachari, K.; Rendell, A. P.; Burant, J. C.; Iyengar, S. S.; Tomasi, J.; Cossi, M.; Millam, J. M.; Klene, M.; Adamo, C.; Cammi, R.; Ochterski, J. W.; Martin, R. L.; Morokuma, K.; Farkas, O.; Foresman, J. B.; Fox, D. J. Gaussian, *Gaussian 16*, **2016**, Revision C.01, Inc., Wallingford CT.
- 135 Chai, J.-D.; Head-Gordon, M. Long-range corrected hybrid density functionals with damped atom–atom dispersion corrections. *Phys. Chem. Chem. Phys.*, **2008**, *10*, 6615-6620.
- 136 Weigend, F.; Ahlrichs, R. Balanced basis sets of split valence, triple zeta valence and quadruple zeta valence quality for H to Rn: Design and assessment of accuracy. *Phys. Chem. Chem. Phys.*, **2005**, *7*, 3297-3305.
- 137 Andrae, D.; Häußermann, U.; Dolg, M.; Stoll, H.; Preuß, H. Energy-adjusted *ab initio* pseudopotentials for the second and third row transition elements. *Theor. Chim. Acta*, **1990**, *77*, 123-141.
- 138 Fukui, K. The path of chemical reactions - the IRC approach. *Acc. Chem. Res.*, **1981**, *14*, 363-368.
- 139 Hratchian, H. P.; Schlegel, H. B. Accurate reaction paths using a Hessian based predictor–corrector integrator. *J. Chem. Phys.*, **2004**, *120*, 9918-9924.

- 140 Hratchian, H. P.; Schlegel, H. B. Using Hessian updating to increase the efficiency of a Hessian based predictor-corrector reaction path following method. *J. Chem. Theory Comput.*, **2005**, *1*, 61-69.
- 141 Zhao, Y.; Truhlar, D. G. The M06 suite of density functionals for main group thermochemistry, thermochemical kinetics, noncovalent interactions, excited states, and transition elements: two new functionals and systematic testing of four M06-class functionals and 12 other functionals. *Theor. Chem. Acc.*, **2008**, *120*, 215-241.
- 142 Grimme, S.; Antony, J.; Ehrlich, S.; Krieg, H. A consistent and accurate *ab initio* parametrization of density functional dispersion correction (DFT-D) for the 94 elements H-Pu. *J. Chem. Phys.*, **2010**, *132*, 154104.
- 143 Marenich, A. V.; Cramer, C. J.; Truhlar, D. G. Universal solvation model based on solute electron density and on a continuum model of the solvent defined by the bulk dielectric constant and atomic surface tensions. *J. Phys. Chem. B*, **2009**, *113*, 6378-6396.
- 144 Legault, C.Y. *CYLview 1.0b*, Université de Sherbrooke, **2009** (<http://www.cylview.org>).
- 145 Skripnikov, L. *Chemissian 4.60*, **2018** (<http://www.chemissian.com>).
- 146 (a) Vosko, S. H.; Wilk, L.; Nusair, M. Accurate spin-dependent electron liquid correlation energies for local spin density calculations: a critical analysis. *Can. J. Phys.*, **1980**, *58*, 1200-1211; (b) Lee, C.; Yang, W.; Parr, R. G. Development of the Colle-Salvetti correlation-energy formula into a functional of the electron density. *Phys. Rev. B*, **1988**, *37*, 785-789; (c) Becke, A. D. Density-functional thermochemistry. III. The role of exact exchange. *J. Chem. Phys.*, **1993**, *98*, 5648-5652; (d) Stephens, P. J.; Devlin, F. J.; Chabalowski, C. F.; Frisch, M. J. *Ab initio* calculation of vibrational absorption and circular dichroism spectra using density functional force fields. *J. Phys. Chem.*, **1994**, *98*, 11623-11627.
- 147 Grimme, S.; Ehrlich, S.; Goerigk, L. Effect of the damping function in dispersion corrected density functional theory. *J. Comput. Chem.*, **2011**, *32*, 1456-1465.
- 148 Mosmann, T. Rapid colorimetric assay for cellular growth and survival: Application to proliferation and cytotoxicity assays. *J. Immunol. Methods*, **1983**, *65*, 55-63.






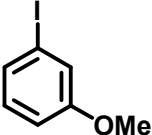
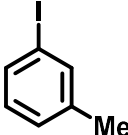
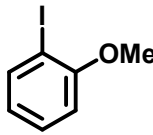
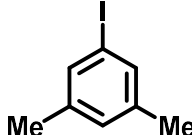

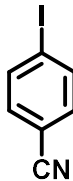
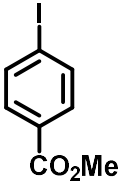
## **APPENDICES**

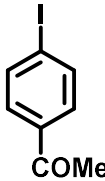
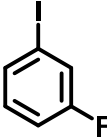
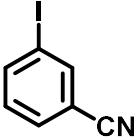
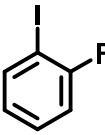
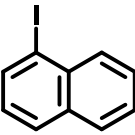

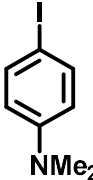
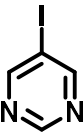


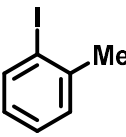
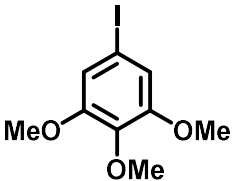
 <p>1</p>	 <p>2</p>	 <p>3</p>
 <p>4</p>	 <p>5</p>	 <p>5'</p>
 <p>6</p>	 <p>7</p>	 <p>8</p>
 <p>9</p>	 <p>10</p>	 <p>11</p>



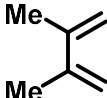
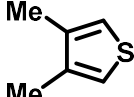
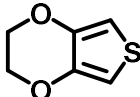
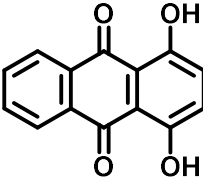
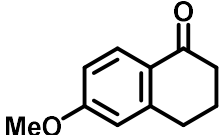
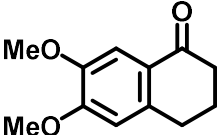
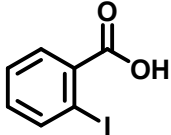
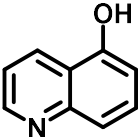
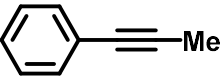
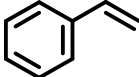
 <p>12</p>	 <p>13</p>	 <p>14</p>
 <p>15</p>	 <p>16</p>	 <p>17</p>
 <p>18</p>	 <p>19</p>	 <p>20</p>
 <p>21</p>	 <p>22</p>	 <p>23</p>

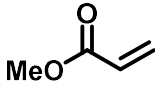
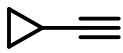
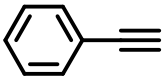
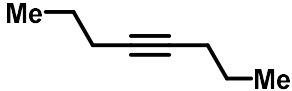
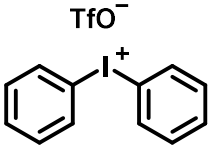
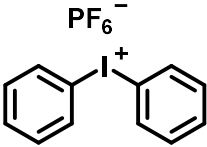
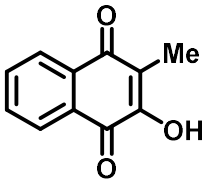
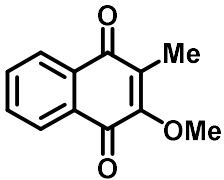
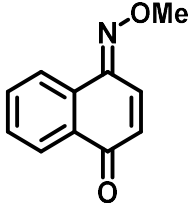
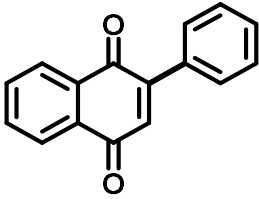
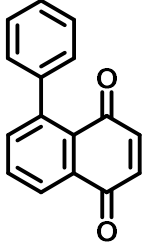
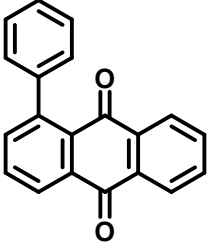
 <p>24</p>	 <p>25</p> <p>R = Me or Et</p>	 <p>26a</p>
 <p>26b</p>	 <p>27a</p>	 <p>27b</p>
 <p>28</p>	 <p>29</p>	 <p>30</p>
 <p>31</p>	 <p>32a</p>	 <p>32b</p>

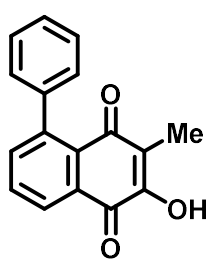
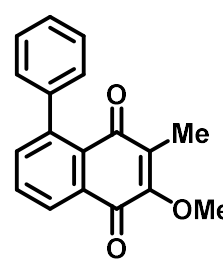
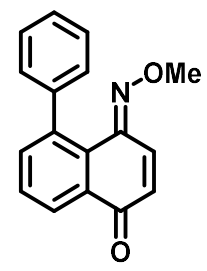
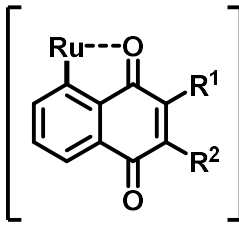
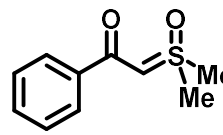
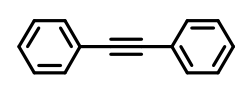
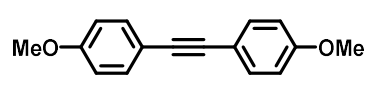
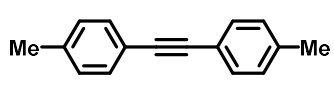
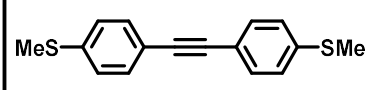
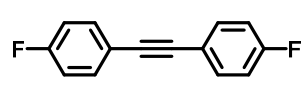
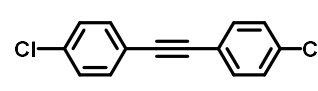
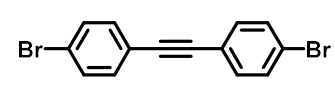


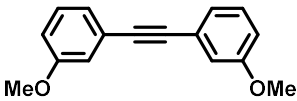
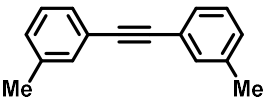
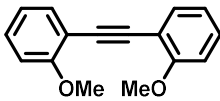
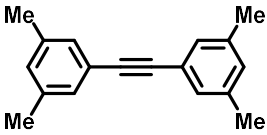
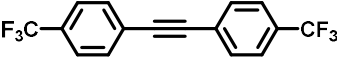
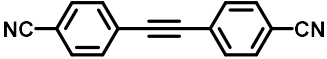
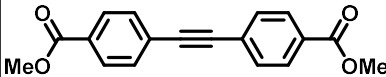
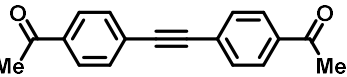
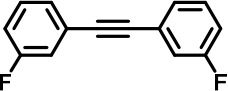
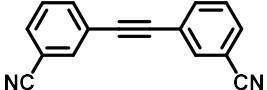
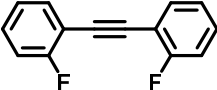
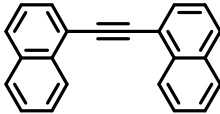
 Me	 SMe	 F
32c	32d	32e
 Cl	 Br	 OMe
32f	32g	32h
 Me	 OMe	 Me Me
32i	32j	32k
 CF <sub>3</sub>	 CN	 CO <sub>2</sub> Me
32l	32m	32n

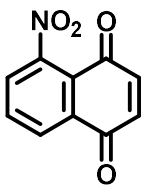
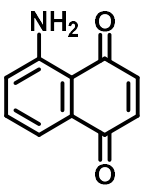
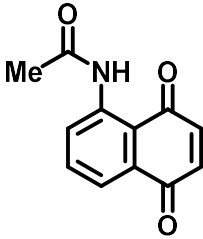
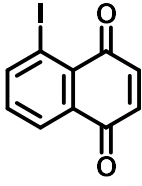
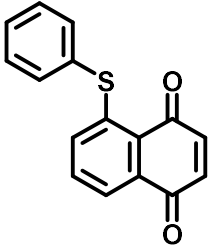
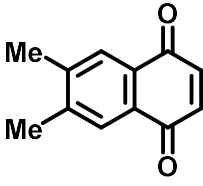
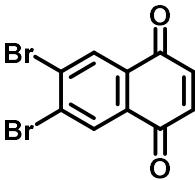
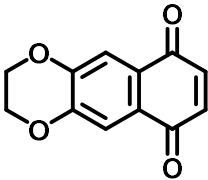
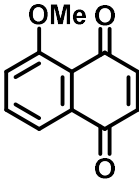
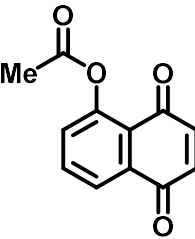
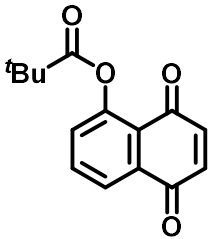
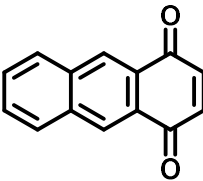
 <chem>CC(=O)c1ccc(I)cc1</chem>	 <chem>Fc1ccc(I)cc1</chem>	 <chem>N#Cc1cccc(I)c1</chem>
<b>32o</b>	<b>32p</b>	<b>32q</b>
 <chem>Fc1ccccc1I</chem>	 <chem>c1ccc2ccccc2c1I</chem>	 <chem>CCc1ccc(I)cc1</chem>
<b>32r</b>	<b>32s</b>	<b>32t</b>
 <chem>CN(C)c1ccc(I)cc1</chem>	 <chem>C1=CN=CN=C1I</chem>	 <chem>CC(C)(C)c1ccc(I)cc1</chem>
<b>32u</b>	<b>32v</b>	<b>32w</b>
 <chem>O=C(c1ccc(I)cc1)c2ccccc2</chem>	 <chem>Cc1ccccc1I</chem>	 <chem>COC1=C(OC)C(OC)C(I)=C1</chem>
<b>32x</b>	<b>32y</b>	<b>32z</b>

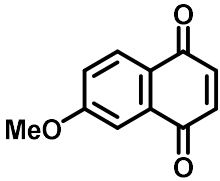
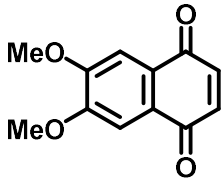
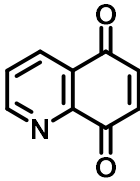
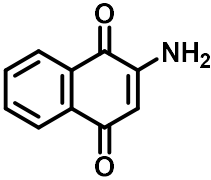
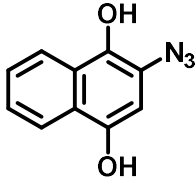
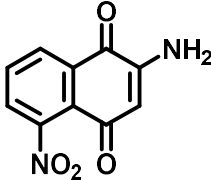
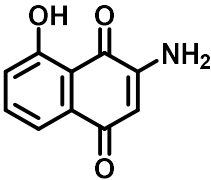
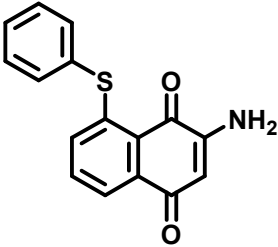
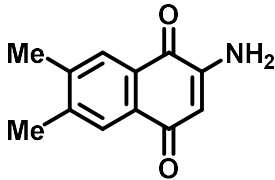
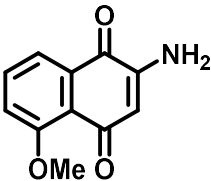
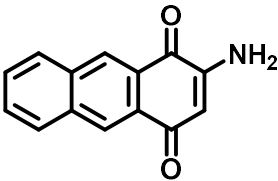
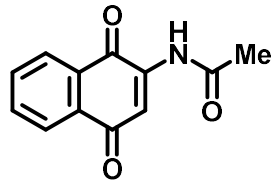
 33	 34	 35
 36	 37	 38
 39	 40	 41
 42	 43	 44

 <chem>COC(=O)C=C</chem>	 <chem>C#CCBr</chem>	 <chem>C#Cc1ccccc1</chem>
45	46	47
 <chem>CC=CC=CC</chem>	 <chem>[I+](c1ccccc1)(c2ccccc2)[O-](F)(F)F</chem>	 <chem>[I+](c1ccccc1)(c2ccccc2)[S-](F)(F)(F)(F)F</chem>
48	49	50
 <chem>CC1=C(O)C(=O)C2=CC=CC=C2C1=O</chem>	 <chem>COC1=C(C)C(=O)C2=CC=CC=C2C1=O</chem>	 <chem>CN(C)C1=CC=C2C(=O)C(=O)C=C12</chem>
51a	51b	51c
 <chem>C1=CC=C(C=C1)C2=CC=CC=C2C3=C(C)C(=O)C(=O)C=C3</chem>	 <chem>C1=CC=C(C=C1)C2=CC=CC=C2C3=C(C)C(=O)C(=O)C=C3</chem>	 <chem>C1=CC=C(C=C1)C2=CC=CC=C2C3=C(C)C(=O)C(=O)C=C3</chem>
52	53a	53b

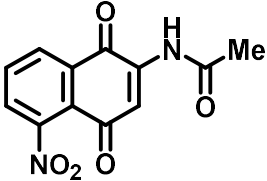
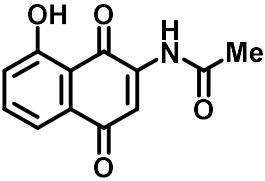
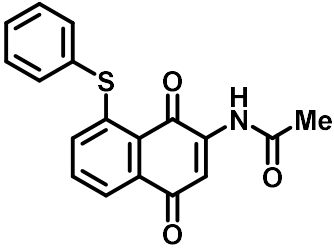
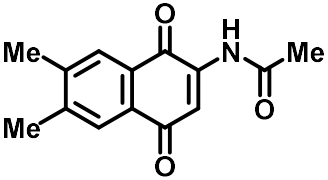
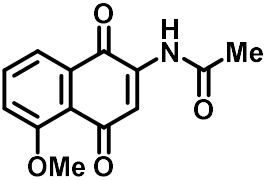
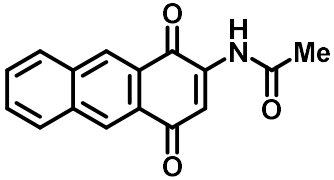
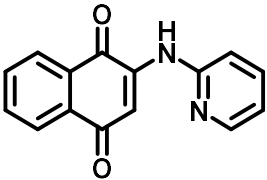
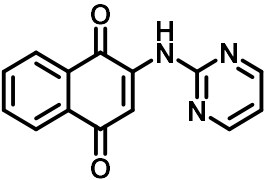
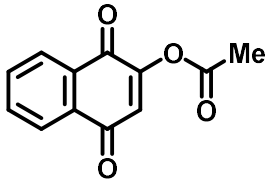
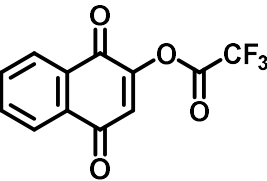
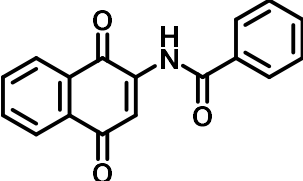
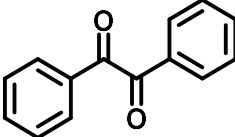
 <p>53c</p>	 <p>53d</p>	 <p>53e</p>
 <p>54</p>	 <p>55</p>	 <p>56a</p>
 <p>56b</p>	 <p>56c</p>	 <p>56d</p>
 <p>56e</p>	 <p>56f</p>	 <p>56g</p>

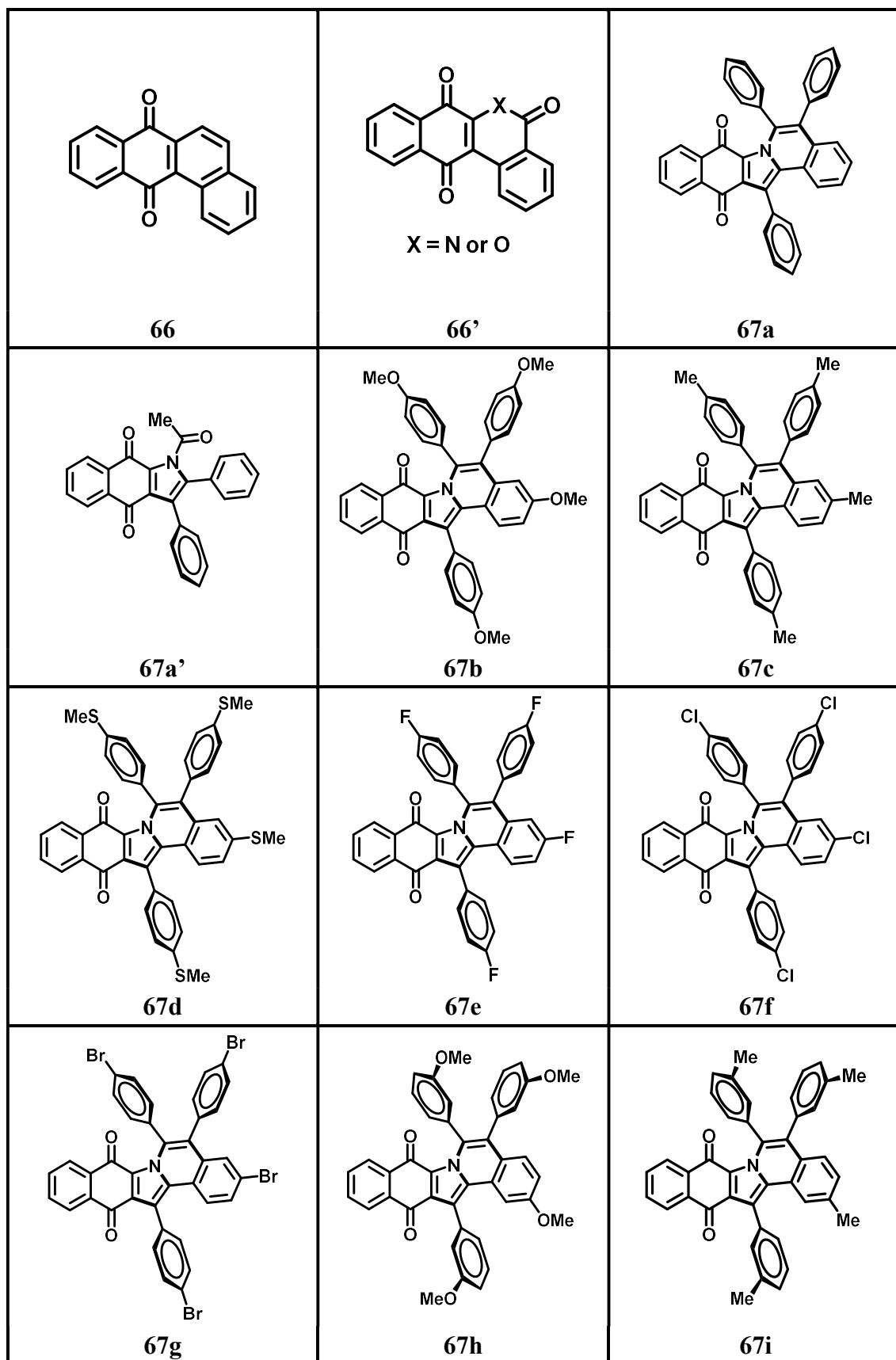
 <p>56h</p>	 <p>56i</p>	 <p>56j</p>
 <p>56k</p>	 <p>56l</p>	 <p>56m</p>
 <p>56n</p>	 <p>56o</p>	 <p>56p</p>
 <p>56q</p>	 <p>56r</p>	 <p>56s</p>

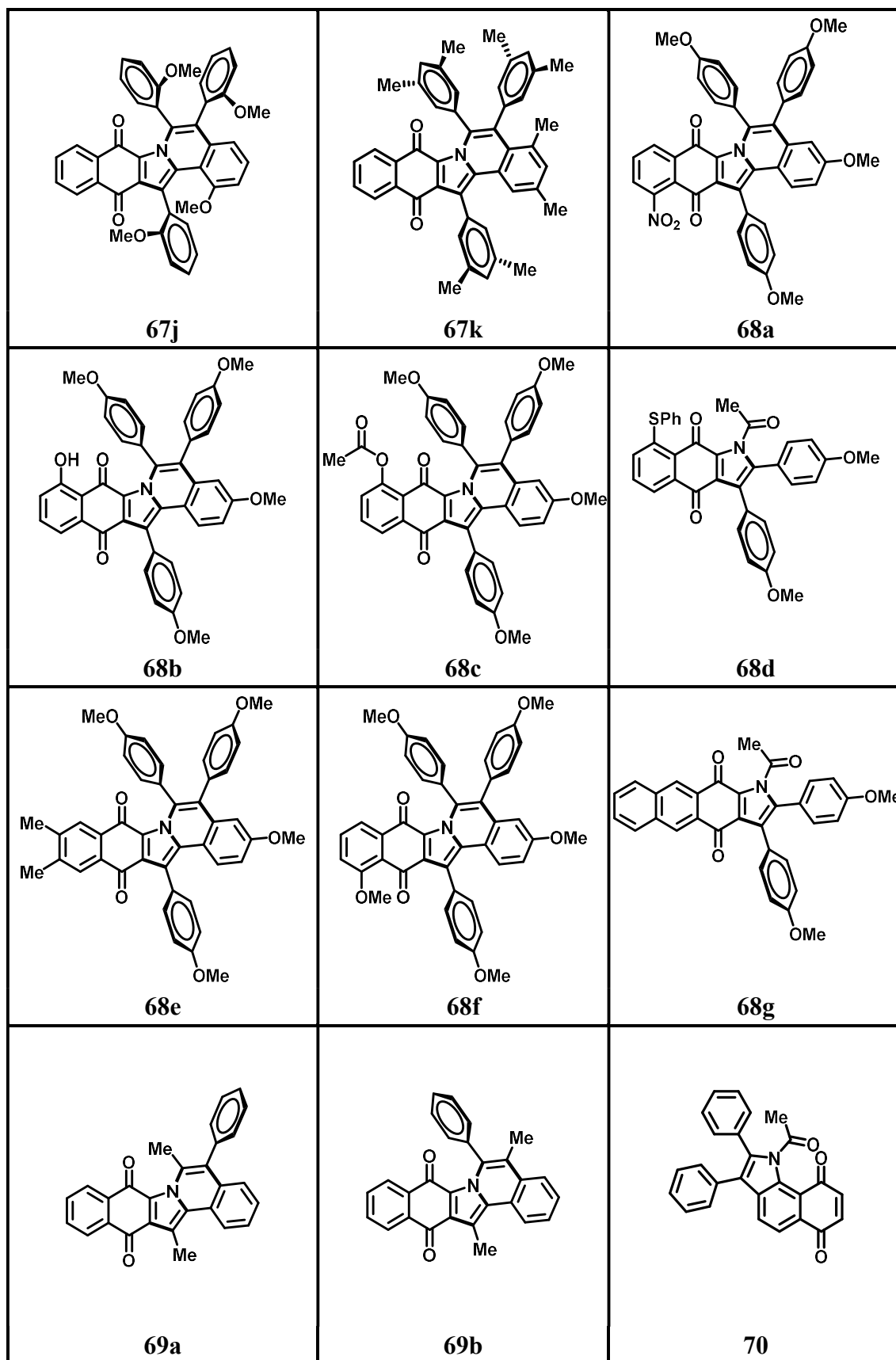
 <p>57a</p>	 <p>57b</p>	 <p>57c</p>
 <p>57d</p>	 <p>57e</p>	 <p>57f</p>
 <p>57g</p>	 <p>57h</p>	 <p>57i</p>
 <p>57j</p>	 <p>57k</p>	 <p>57l</p>

 <p>57m</p>	 <p>57n</p>	 <p>57o</p>
 <p>58a</p>	 <p>58a'</p>	 <p>58b</p>
 <p>58c</p>	 <p>58d</p>	 <p>58e</p>
 <p>58f</p>	 <p>58g</p>	 <p>59a</p>



 <p>59b</p>	 <p>59c</p>	 <p>59d</p>
 <p>59e</p>	 <p>59f</p>	 <p>59g</p>
 <p>60</p>	 <p>61</p>	 <p>62</p>
 <p>63</p>	 <p>64</p>	 <p>65</p>





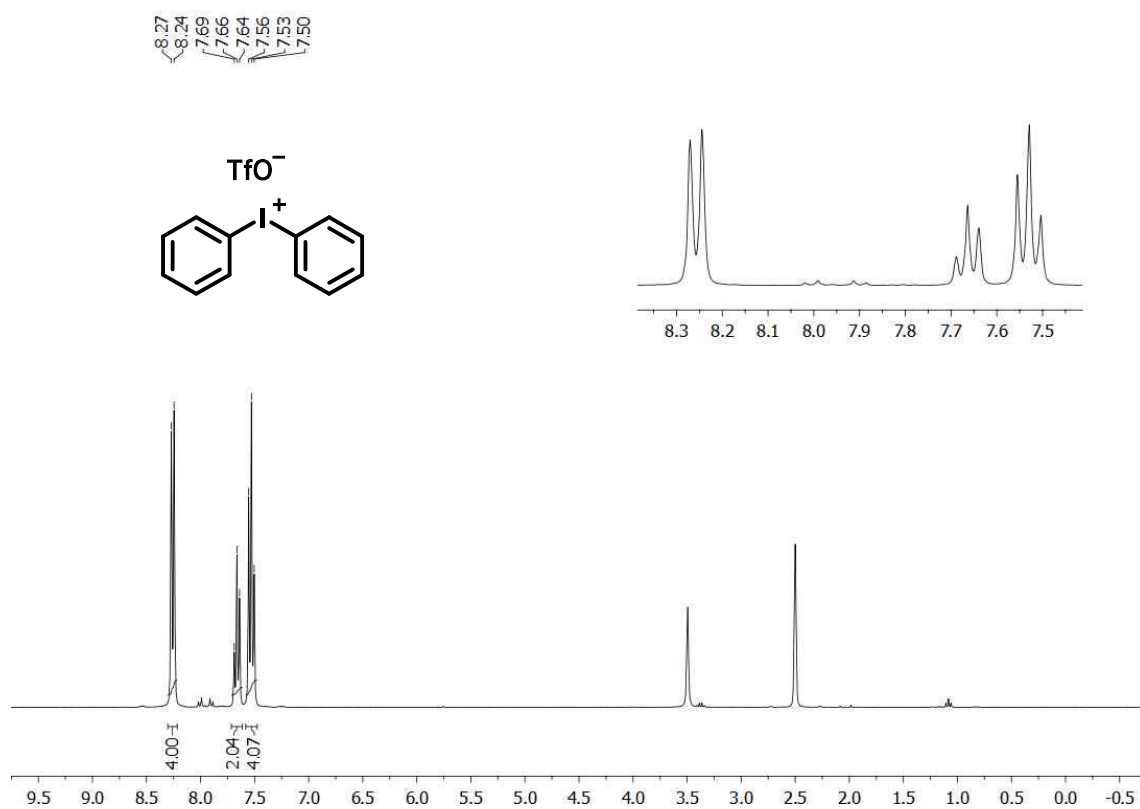


Figure A1. <sup>1</sup>H-NMR spectrum of compound 49 (DMSO-*d*<sub>6</sub>, 300 MHz).

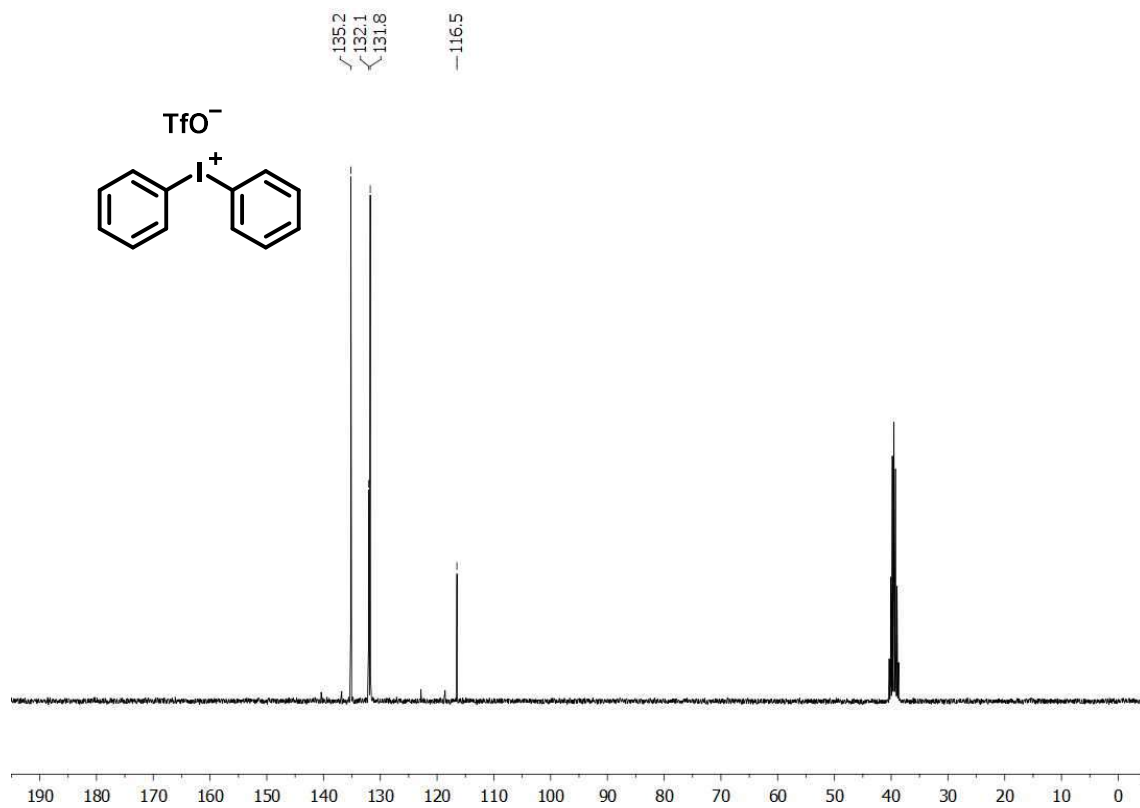
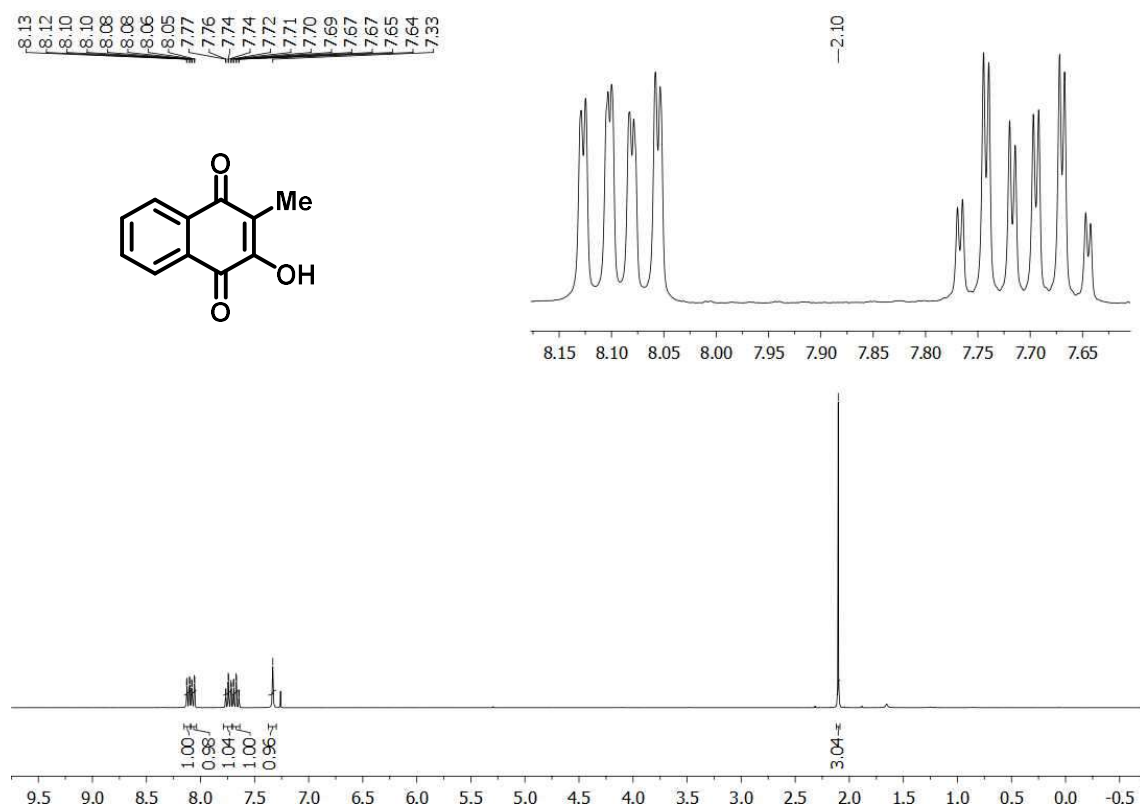
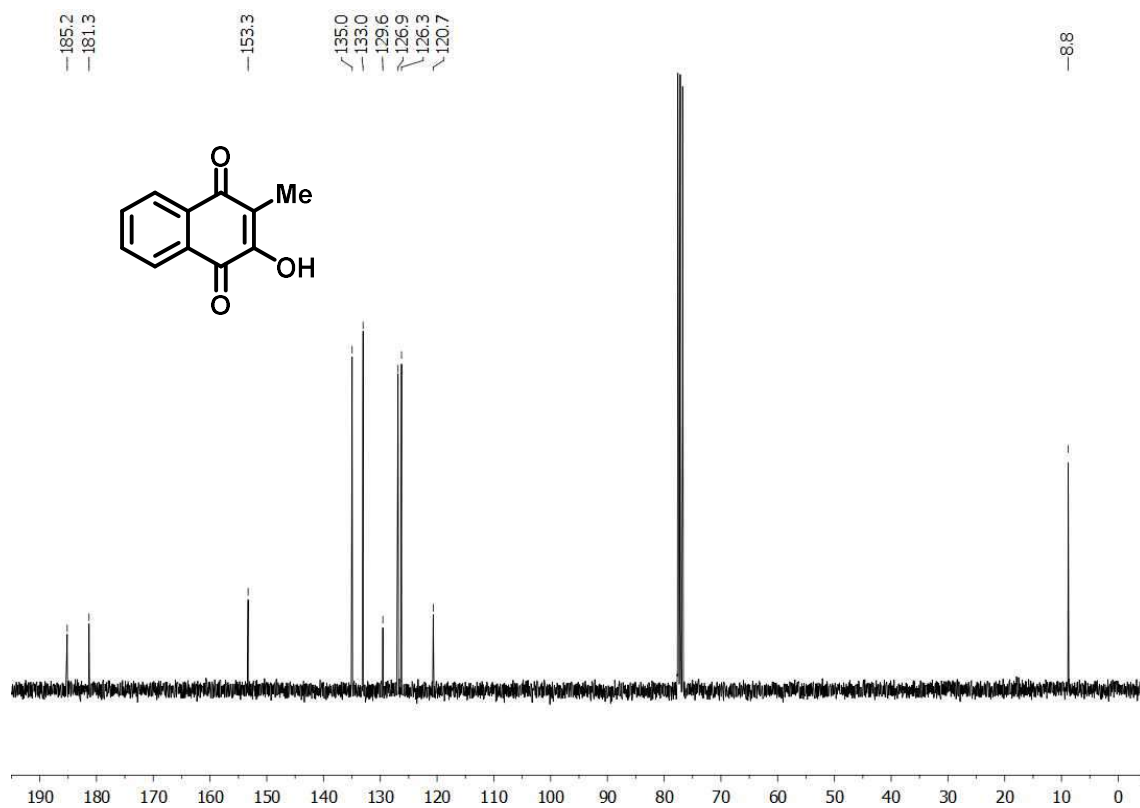


Figure A2. <sup>13</sup>C-NMR spectrum of compound 49 (DMSO-*d*<sub>6</sub>, 75 MHz).



**Figure A3.** <sup>1</sup>H-NMR spectrum of compound **51a** (CDCl<sub>3</sub>, 300 MHz).



**Figure A4.** <sup>13</sup>C-NMR spectrum of compound **51a** (CDCl<sub>3</sub>, 75 MHz).



Figure A5. <sup>1</sup>H-NMR spectrum of compound **51b** (CDCl<sub>3</sub>, 300 MHz).

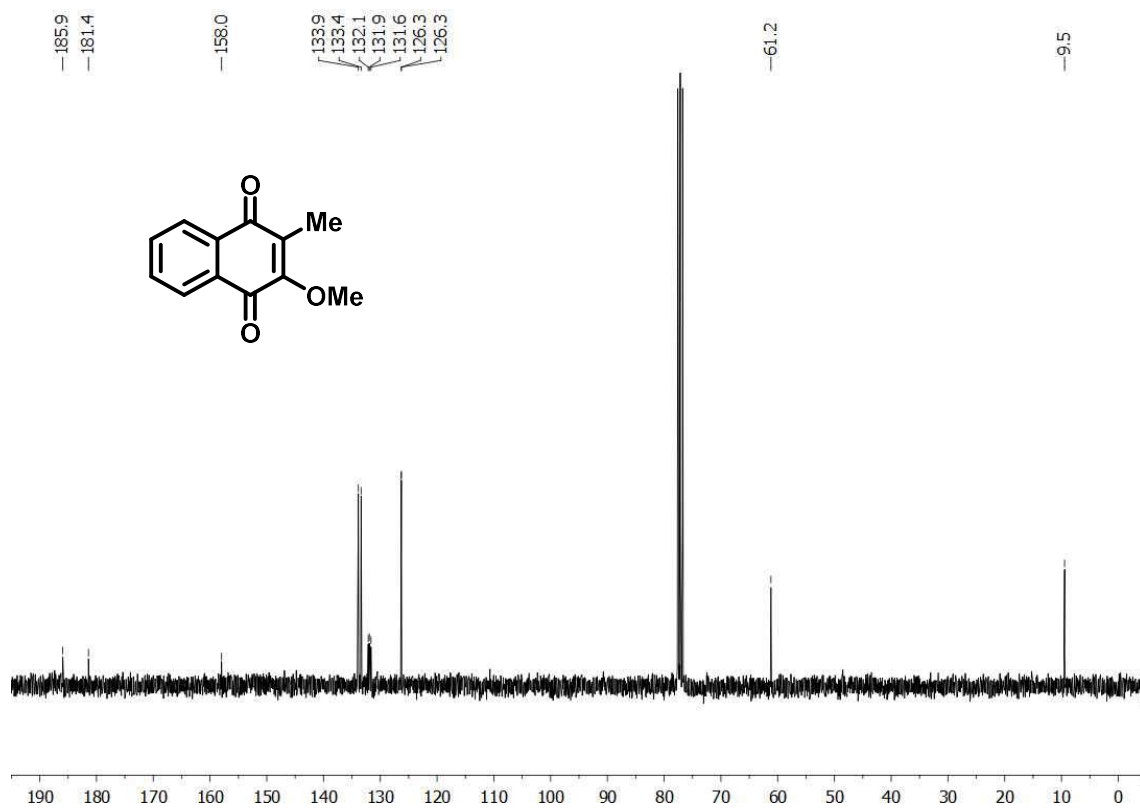


Figure A6. <sup>13</sup>C-NMR spectrum of compound **51b** (CDCl<sub>3</sub>, 75 MHz).

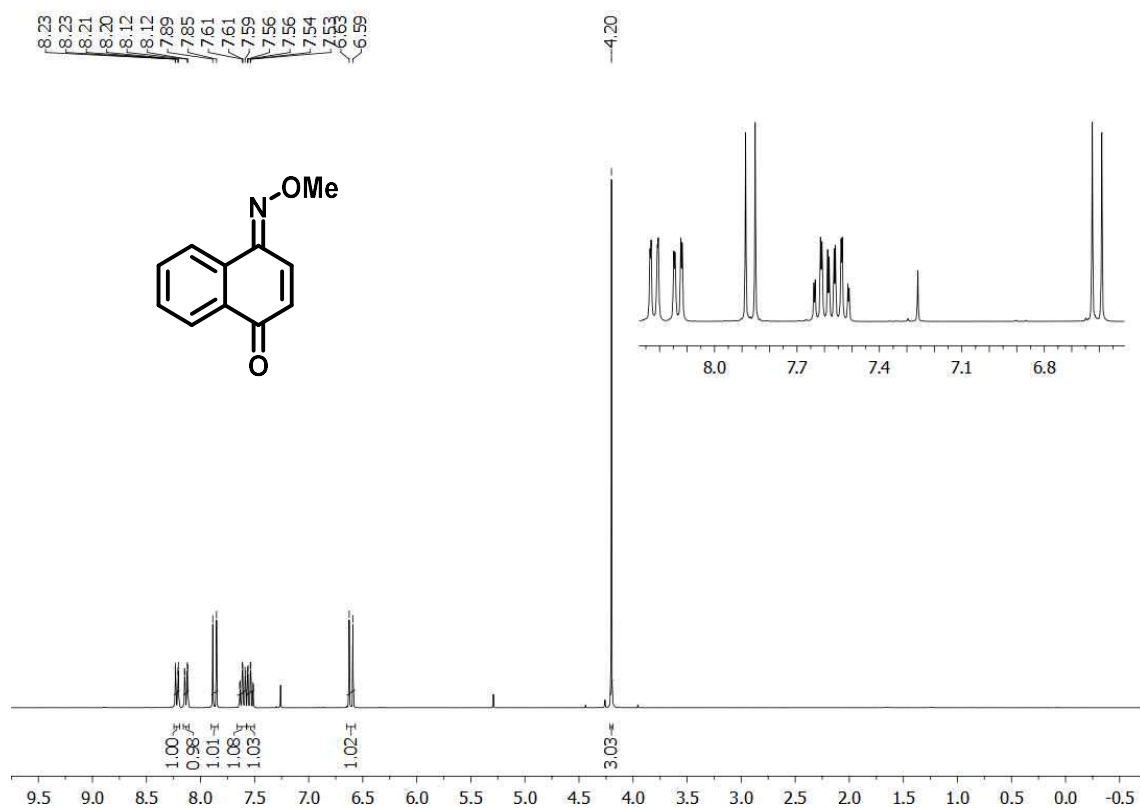


Figure A7. <sup>1</sup>H-NMR spectrum of compound 51c (CDCl<sub>3</sub>, 300 MHz).

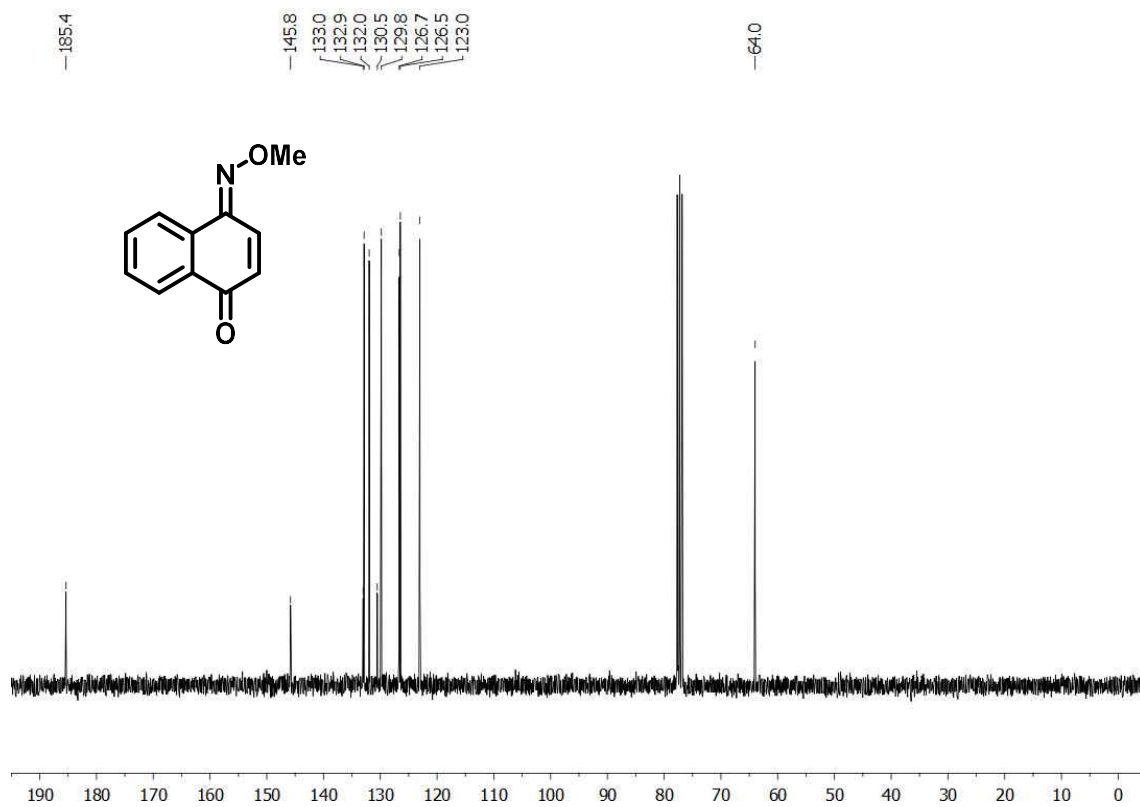


Figure A8. <sup>13</sup>C-NMR spectrum of compound 51b (CDCl<sub>3</sub>, 75 MHz).

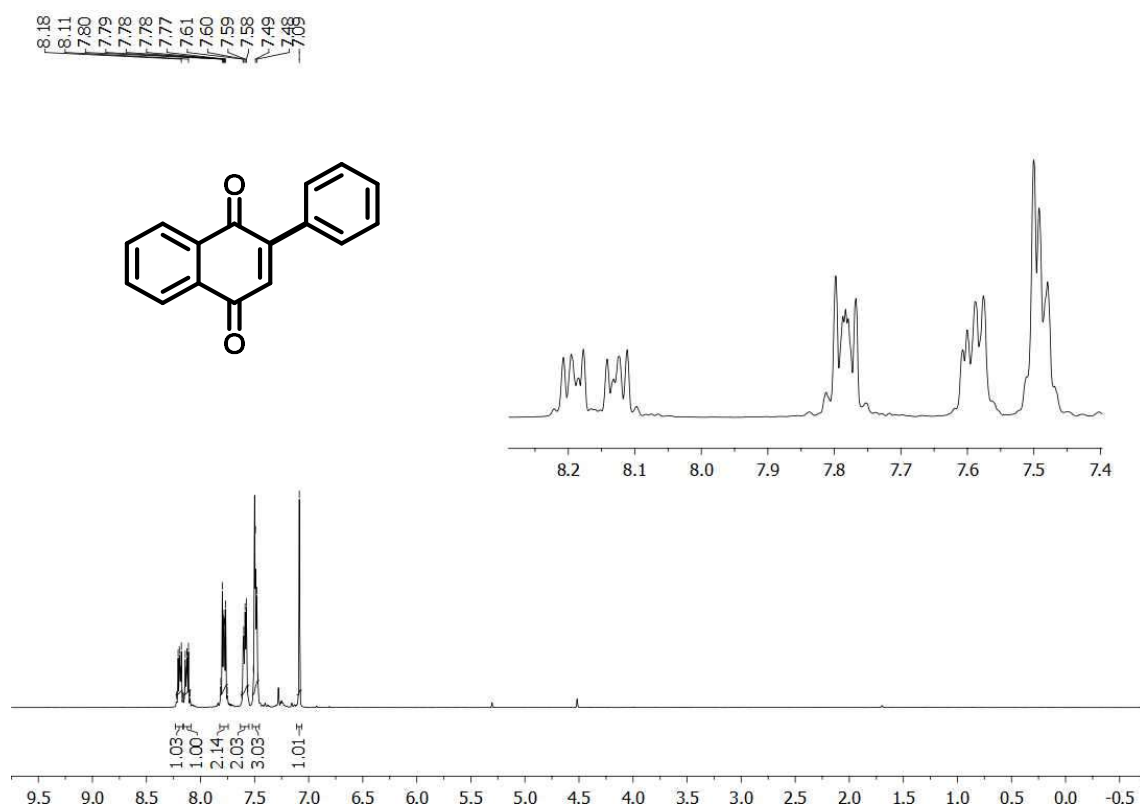


Figure A9. <sup>1</sup>H-NMR spectrum of compound 52 (CDCl<sub>3</sub>, 300 MHz).

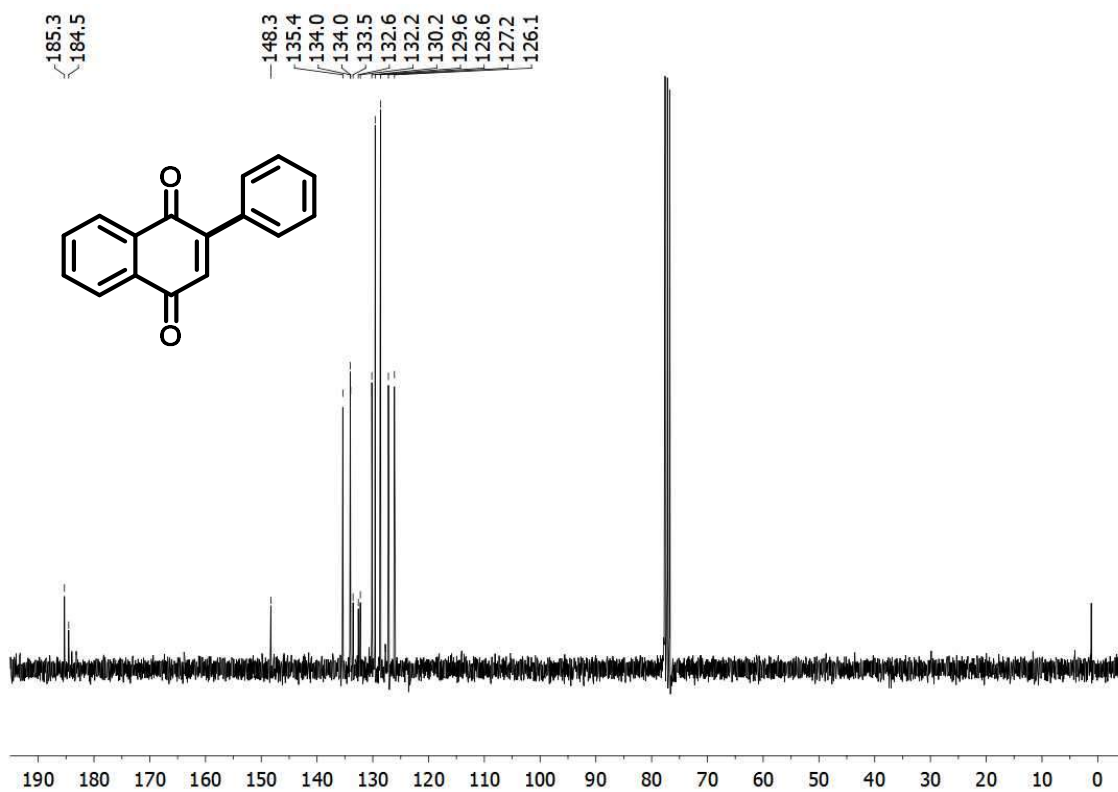


Figure A10. <sup>13</sup>C-NMR spectrum of compound 52 (CDCl<sub>3</sub>, 75 MHz).



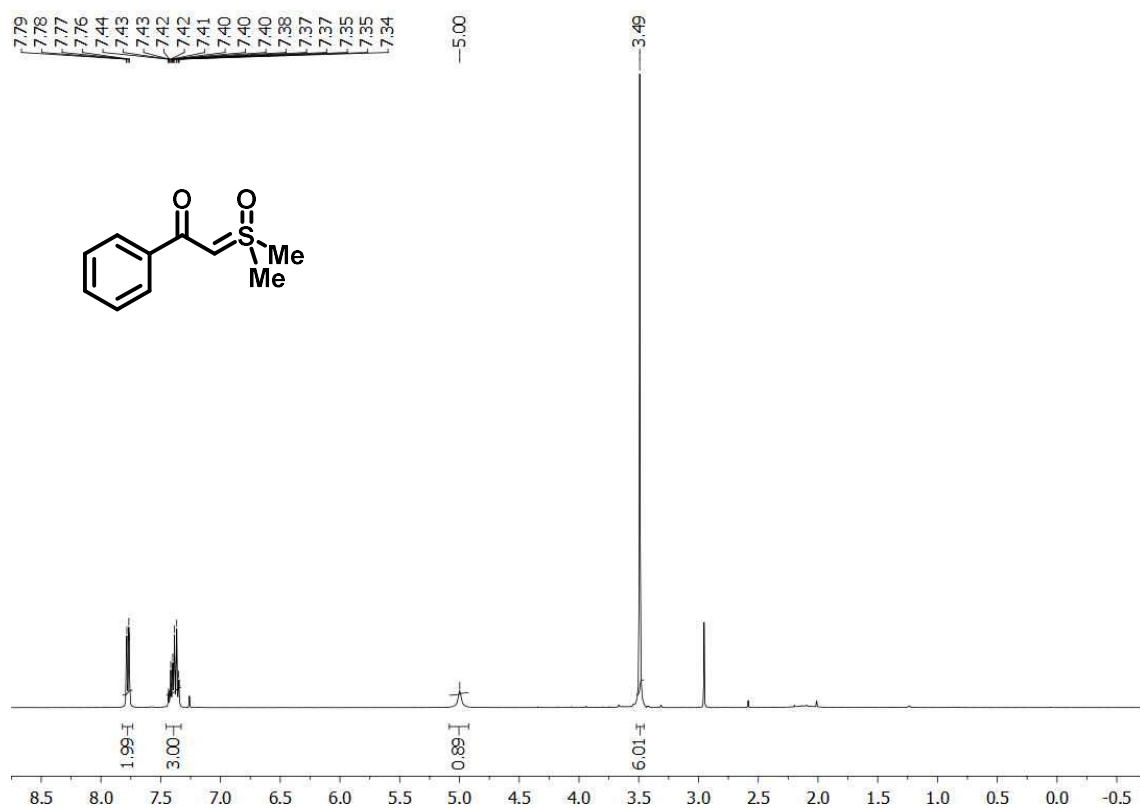


Figure A11. <sup>1</sup>H-NMR spectrum of compound **55** (CDCl<sub>3</sub>, 300 MHz).

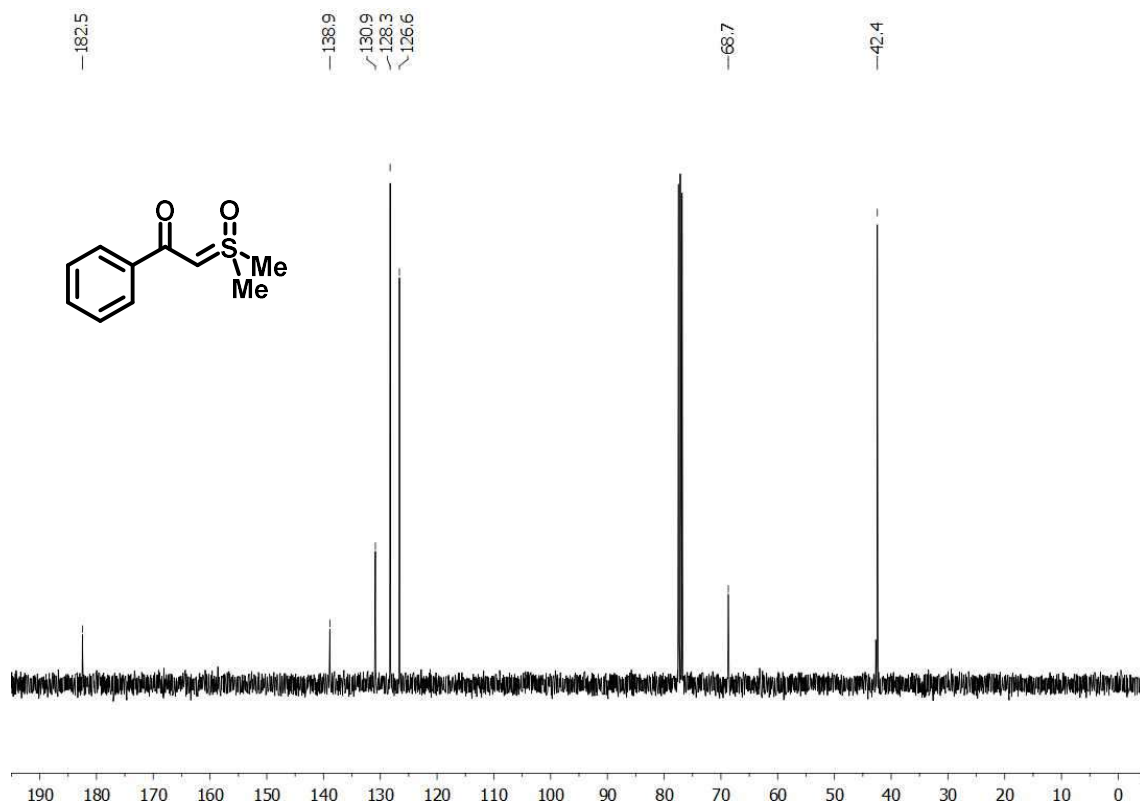
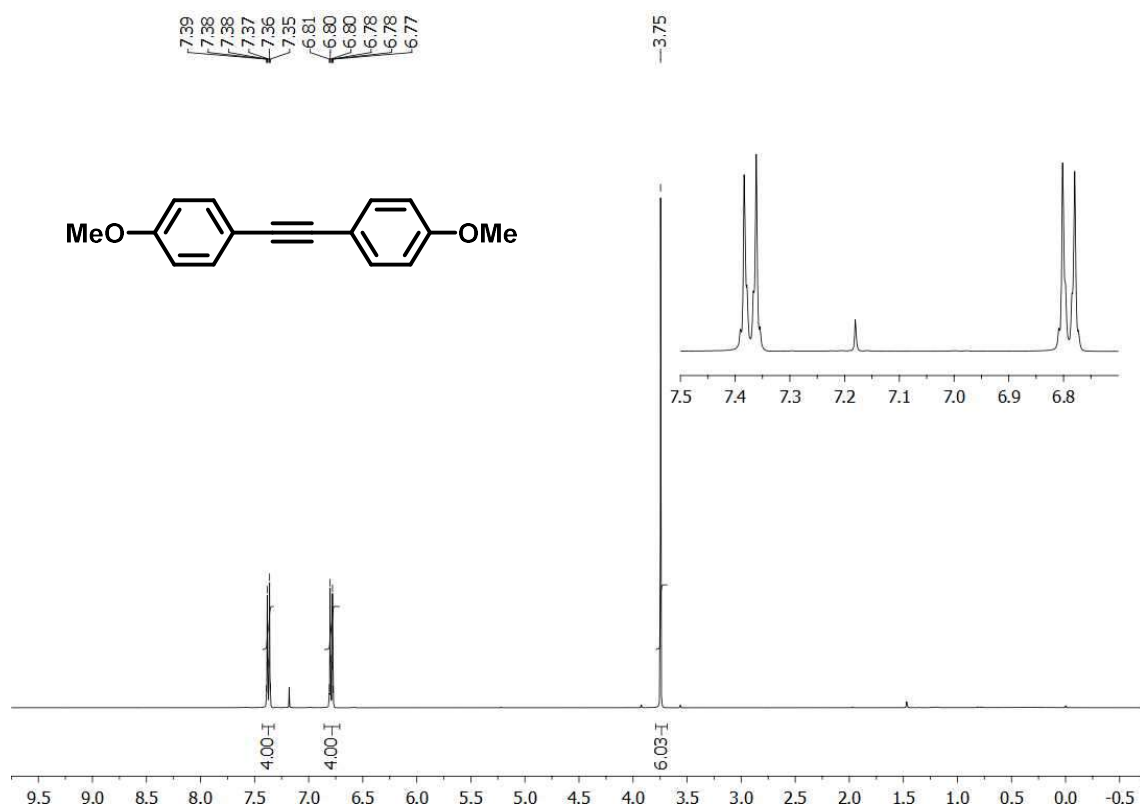
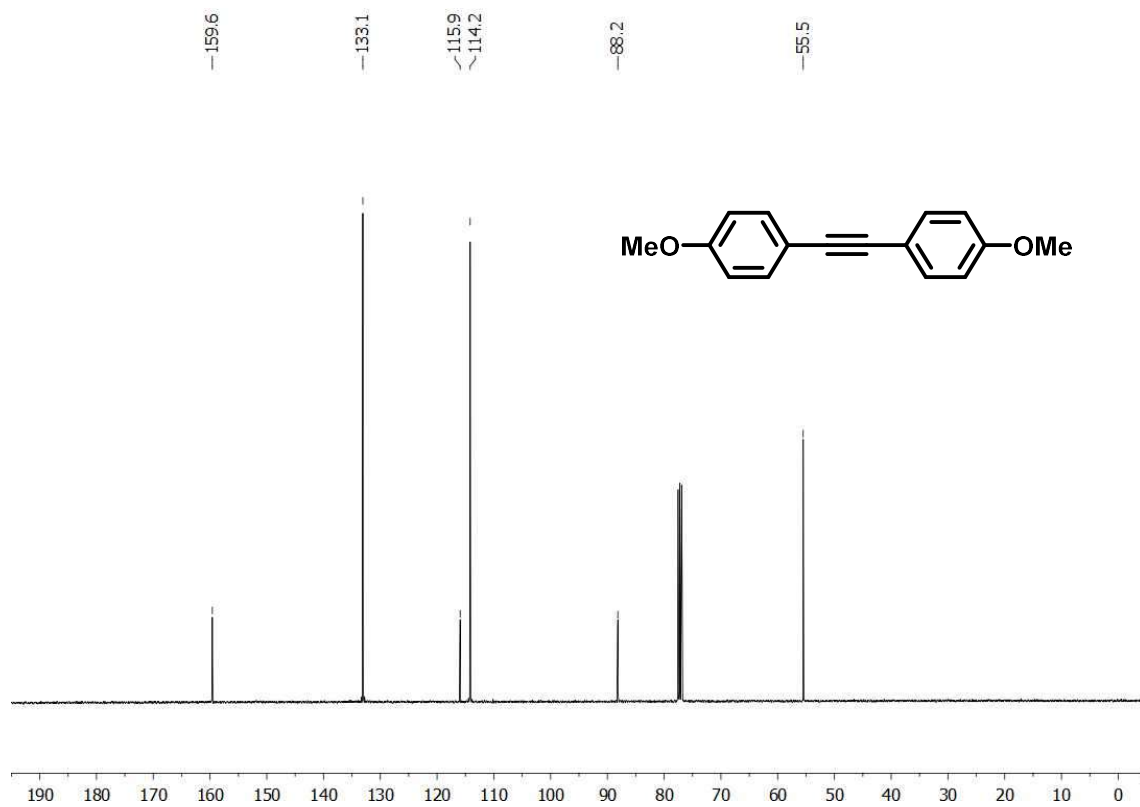


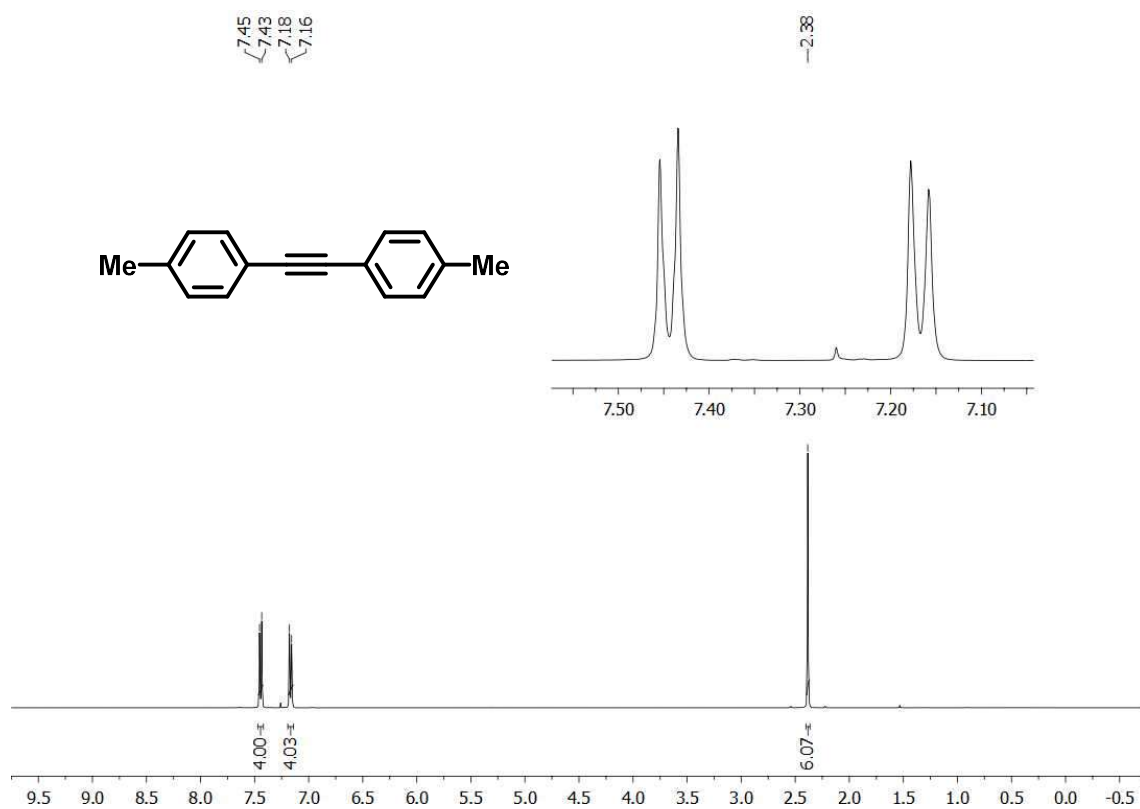
Figure A12. <sup>13</sup>C-NMR spectrum of compound **55** (CDCl<sub>3</sub>, 75 MHz).



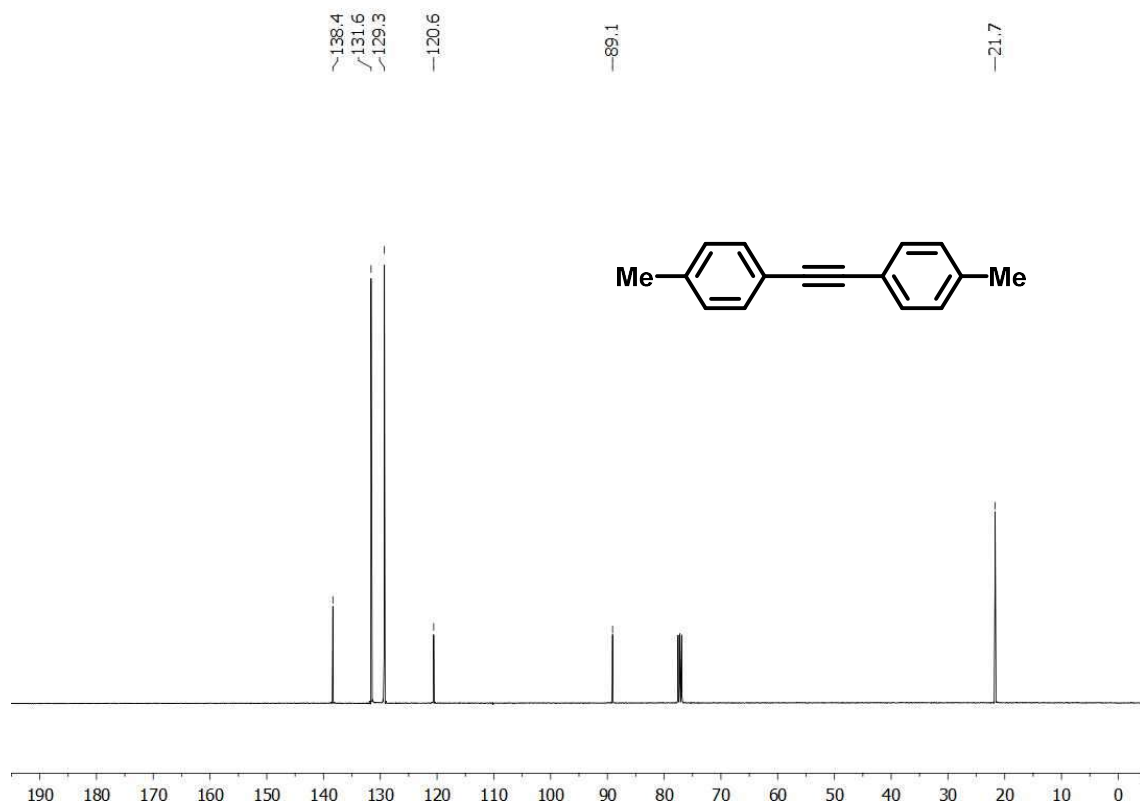
**Figure A13.** <sup>1</sup>H-NMR spectrum of compound **56b** (CDCl<sub>3</sub>, 400 MHz).



**Figure A14.** <sup>13</sup>C-NMR spectrum of compound **56b** (CDCl<sub>3</sub>, 100 MHz).



**Figure A15.** <sup>1</sup>H-NMR spectrum of compound **56c** (CDCl<sub>3</sub>, 400 MHz).



**Figure A16.** <sup>13</sup>C-NMR spectrum of compound **56c** (CDCl<sub>3</sub>, 100 MHz).

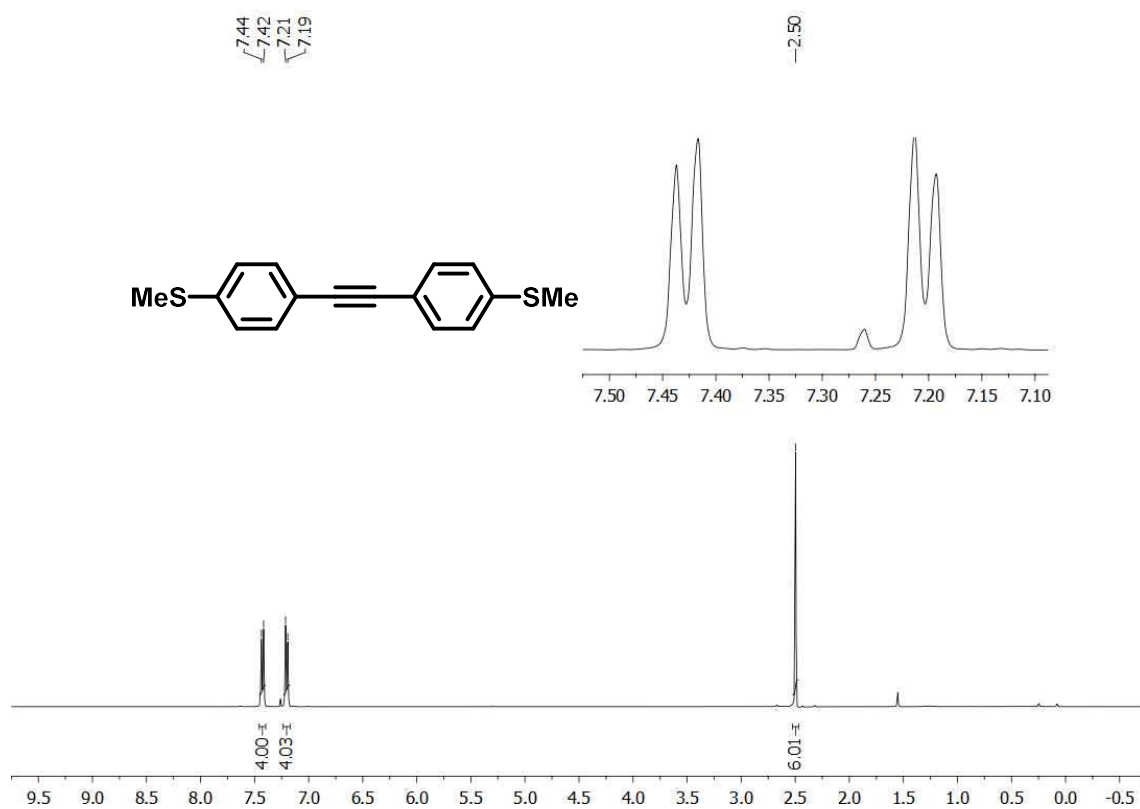


Figure A17. <sup>1</sup>H-NMR spectrum of compound **56d** (CDCl<sub>3</sub>, 400 MHz).

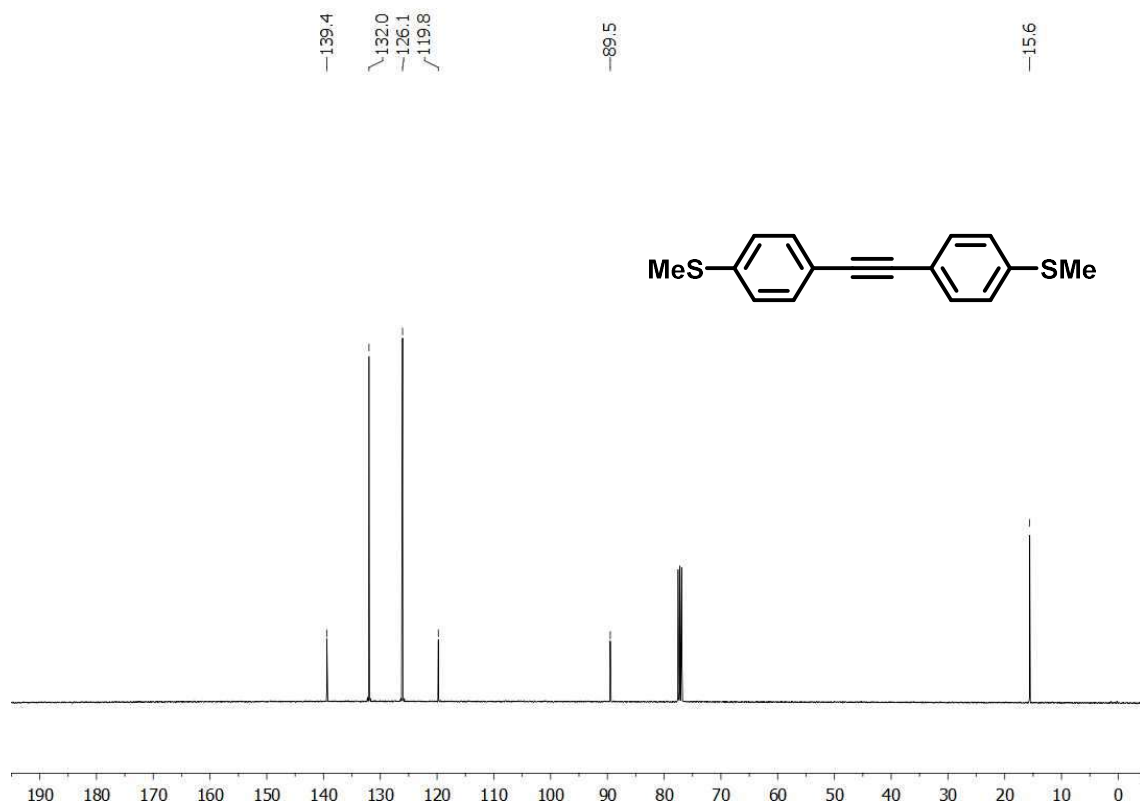


Figure A18. <sup>13</sup>C-NMR spectrum of compound **56d** (CDCl<sub>3</sub>, 100 MHz).

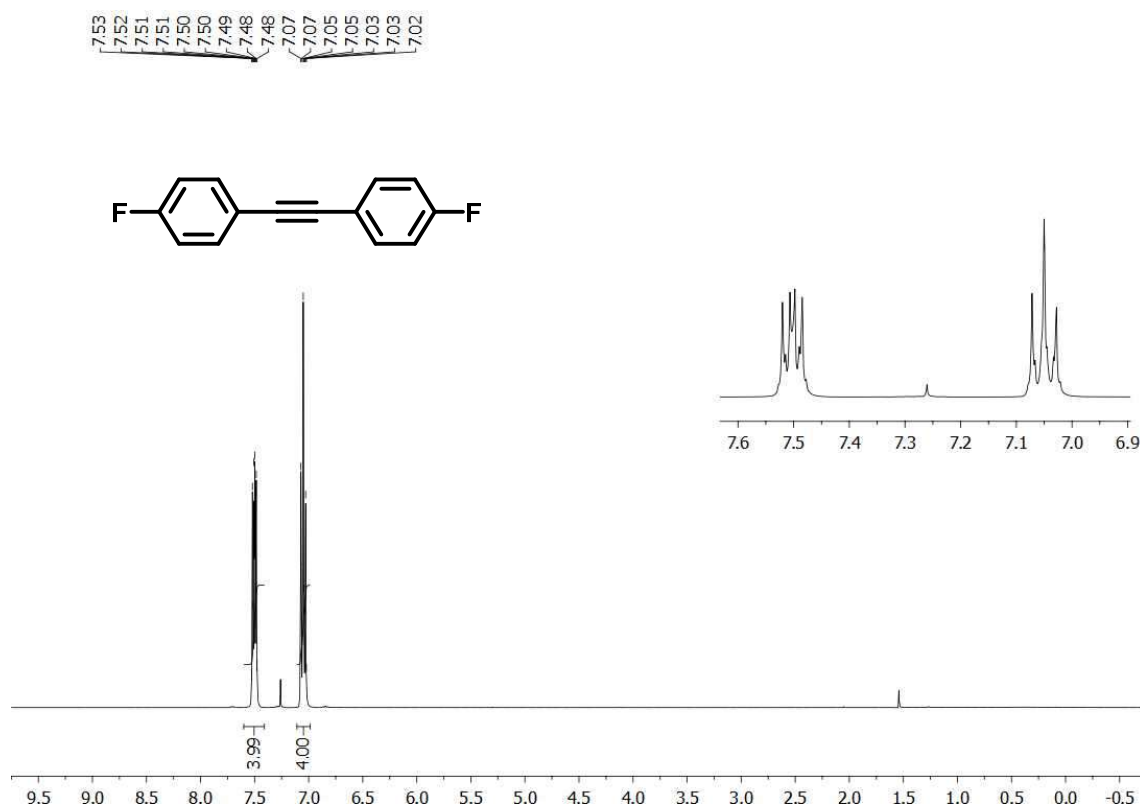


Figure A19. <sup>1</sup>H-NMR spectrum of compound 56e (CDCl<sub>3</sub>, 400 MHz).

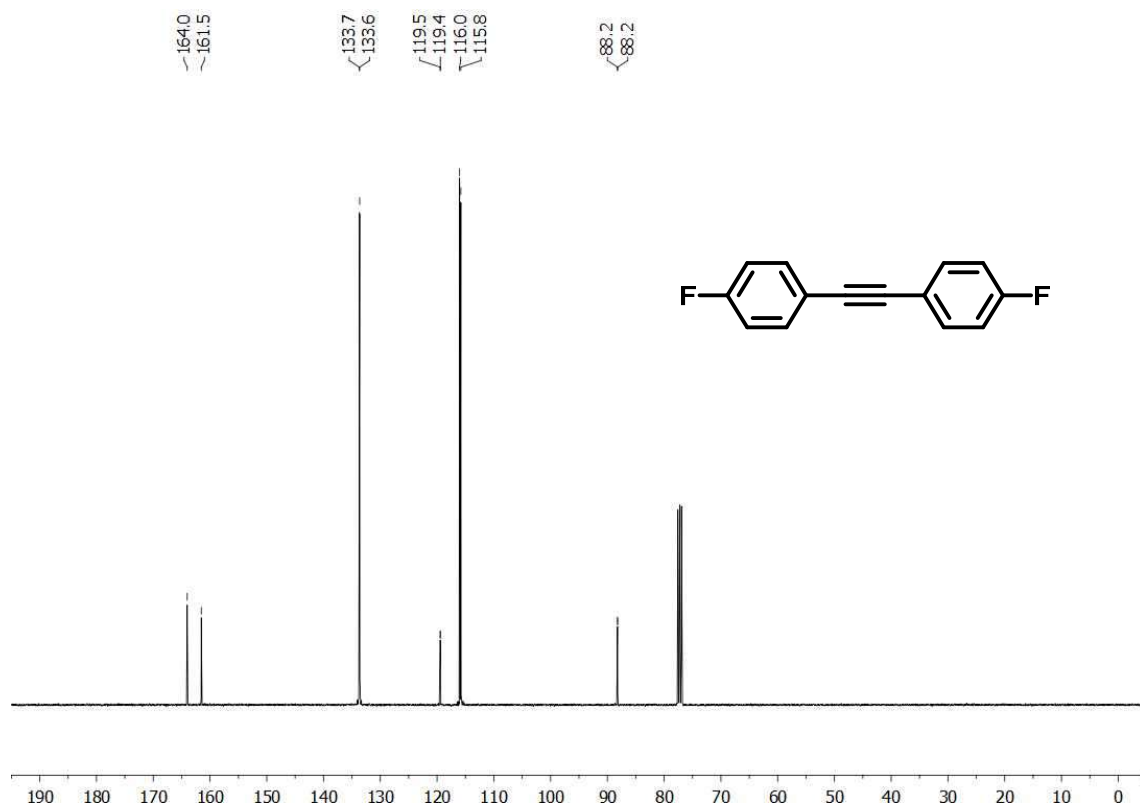
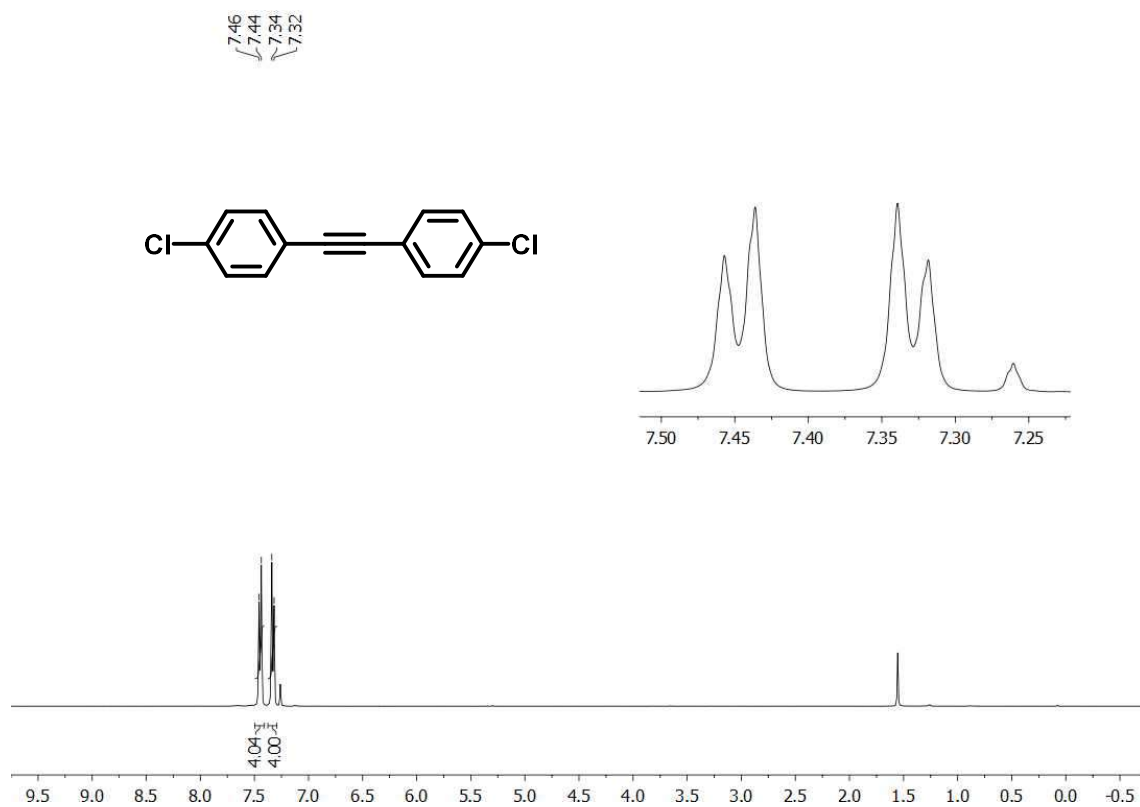
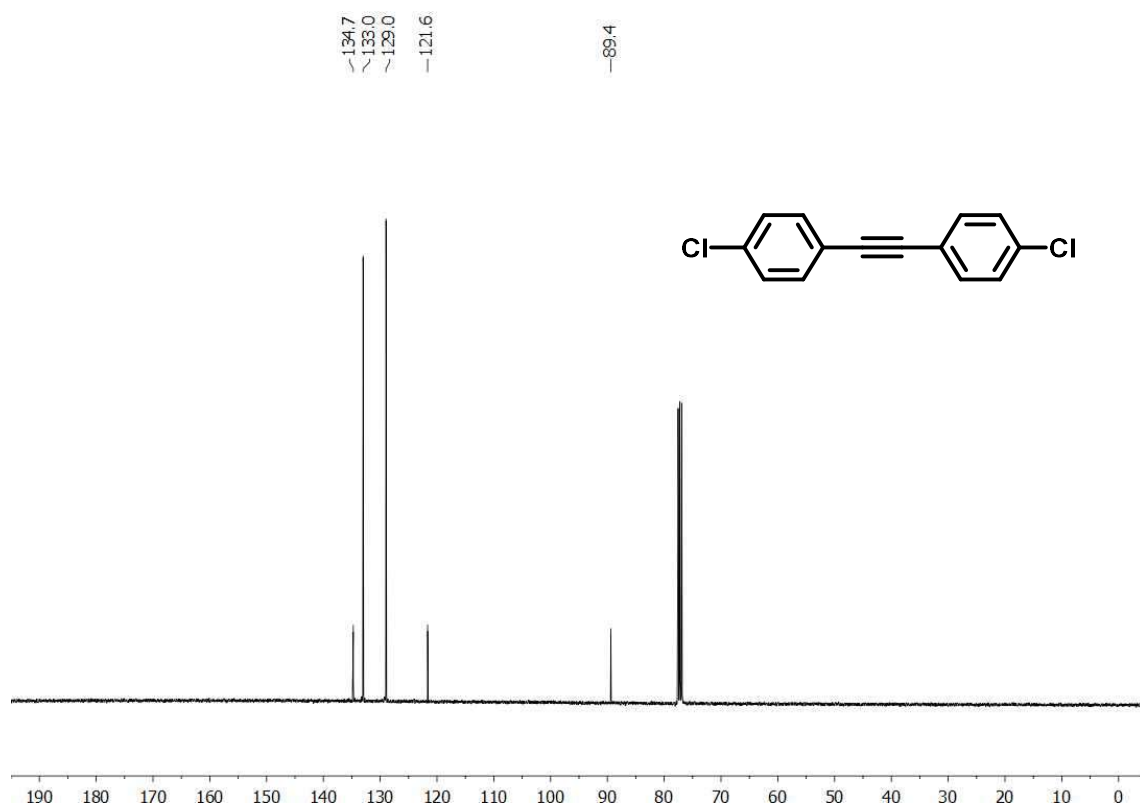


Figure A20. <sup>13</sup>C-NMR spectrum of compound 56e (CDCl<sub>3</sub>, 100 MHz).



**Figure A21.** <sup>1</sup>H-NMR spectrum of compound **56f** (CDCl<sub>3</sub>, 400 MHz).



**Figure A22.** <sup>13</sup>C-NMR spectrum of compound **56f** (CDCl<sub>3</sub>, 100 MHz).

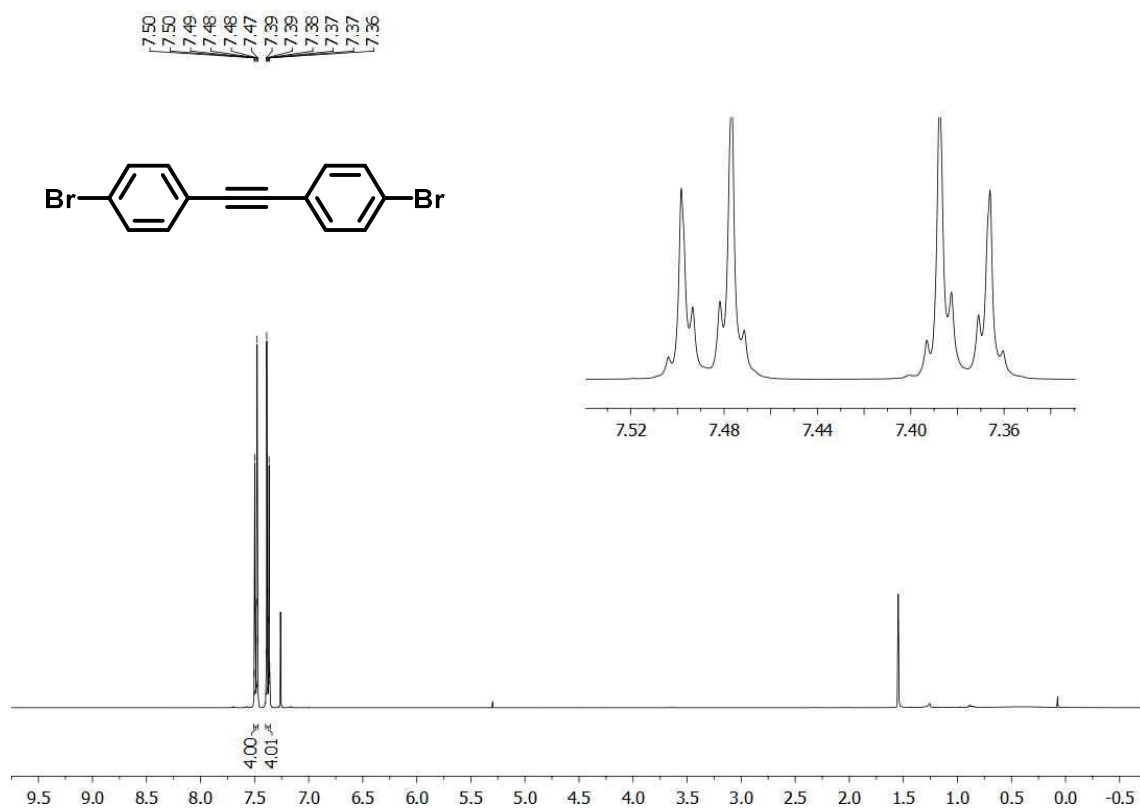


Figure A23. <sup>1</sup>H-NMR spectrum of compound **56g** (CDCl<sub>3</sub>, 400 MHz).

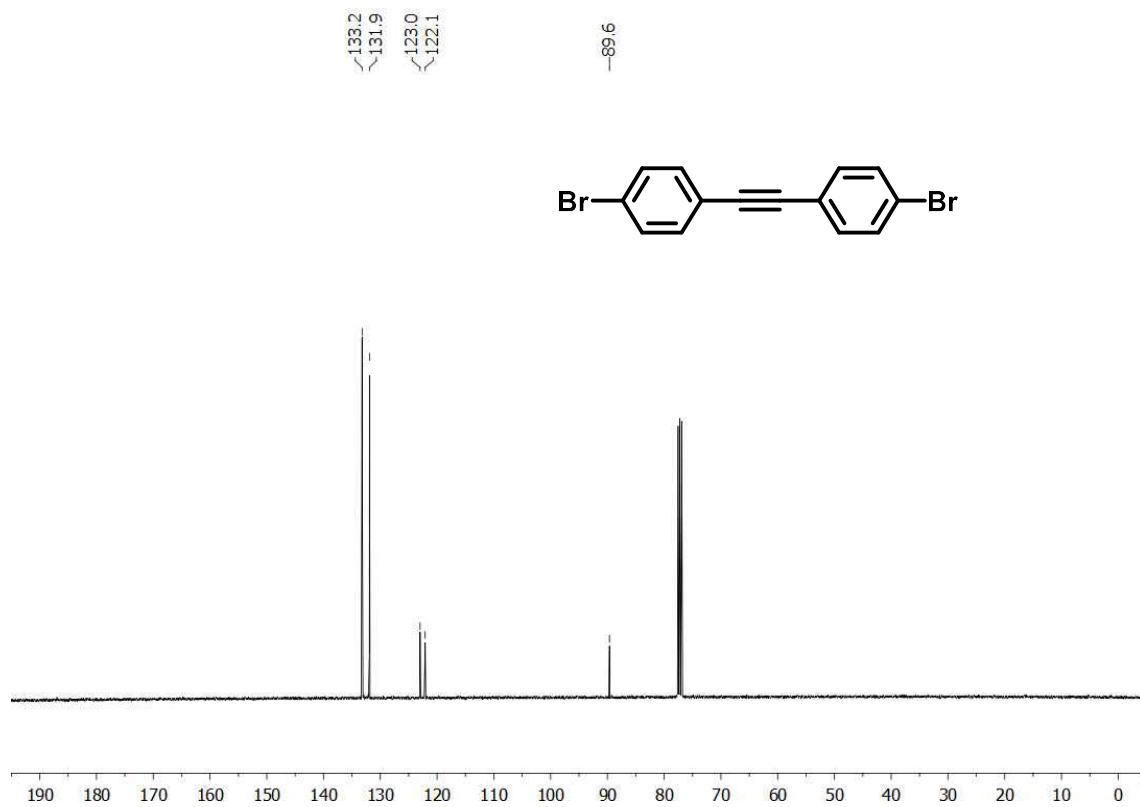


Figure A24. <sup>13</sup>C-NMR spectrum of compound **56g** (CDCl<sub>3</sub>, 100 MHz).

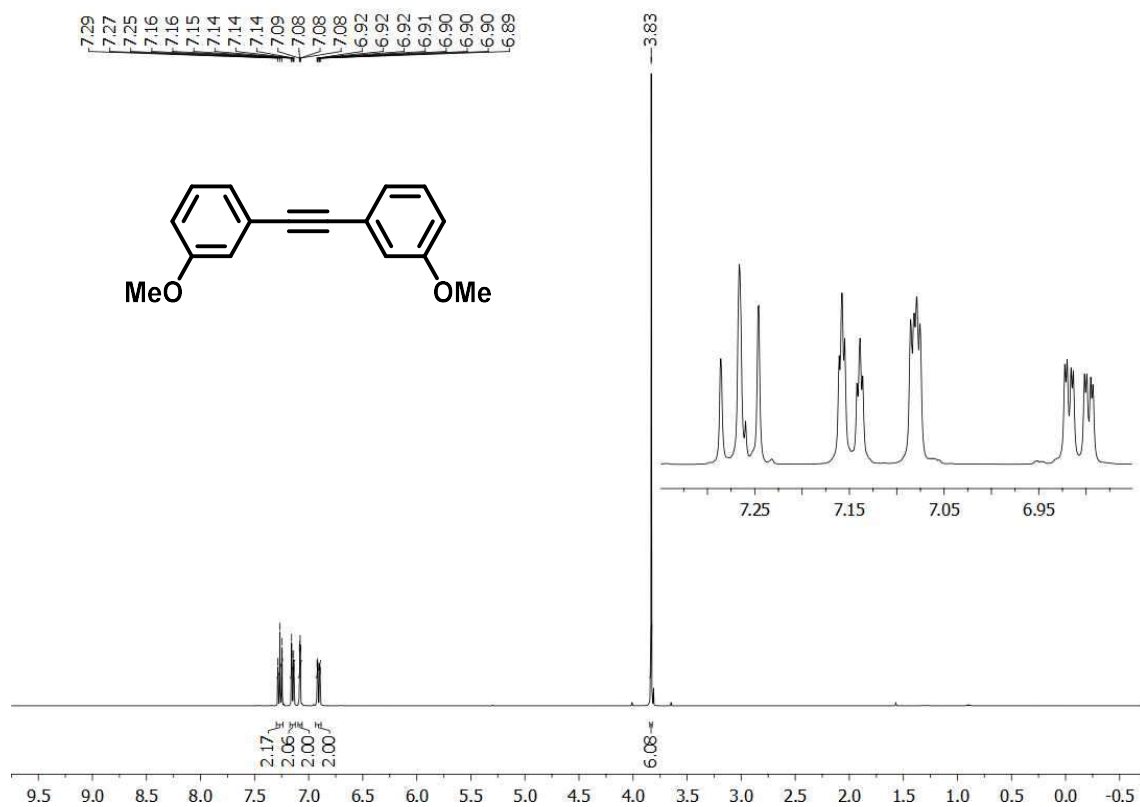


Figure A25. <sup>1</sup>H-NMR spectrum of compound **56h** (CDCl<sub>3</sub>, 400 MHz).

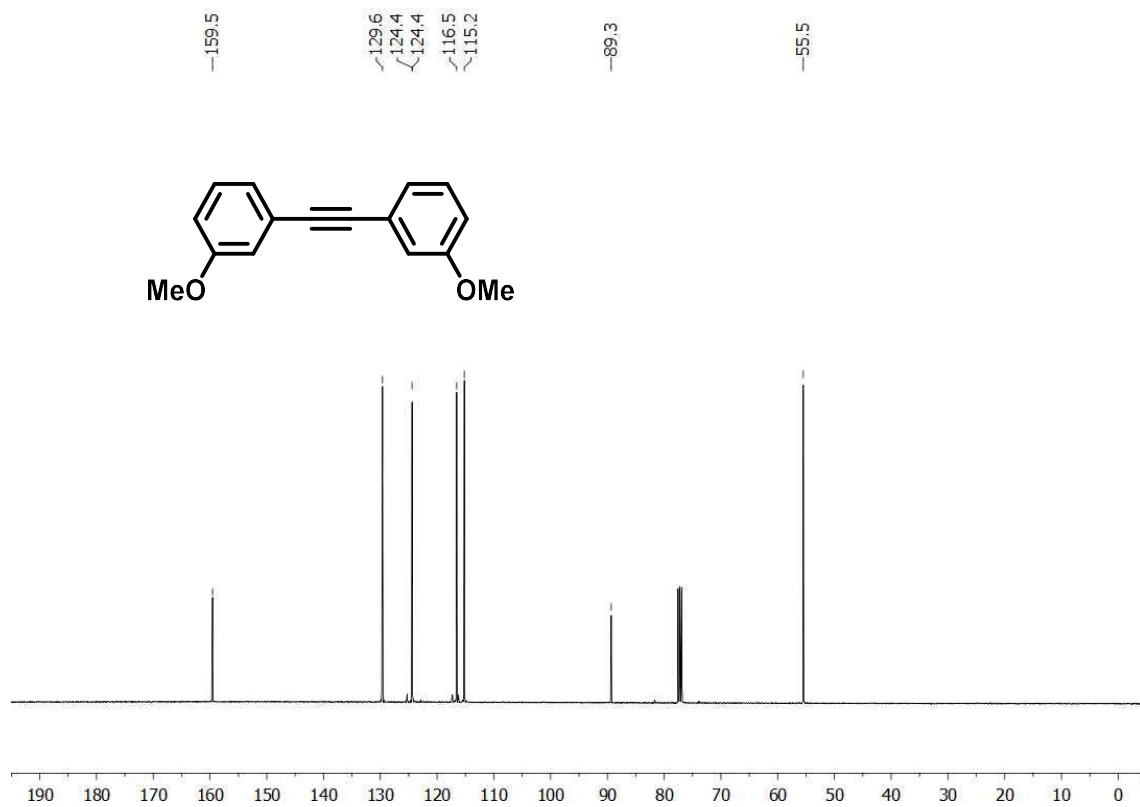
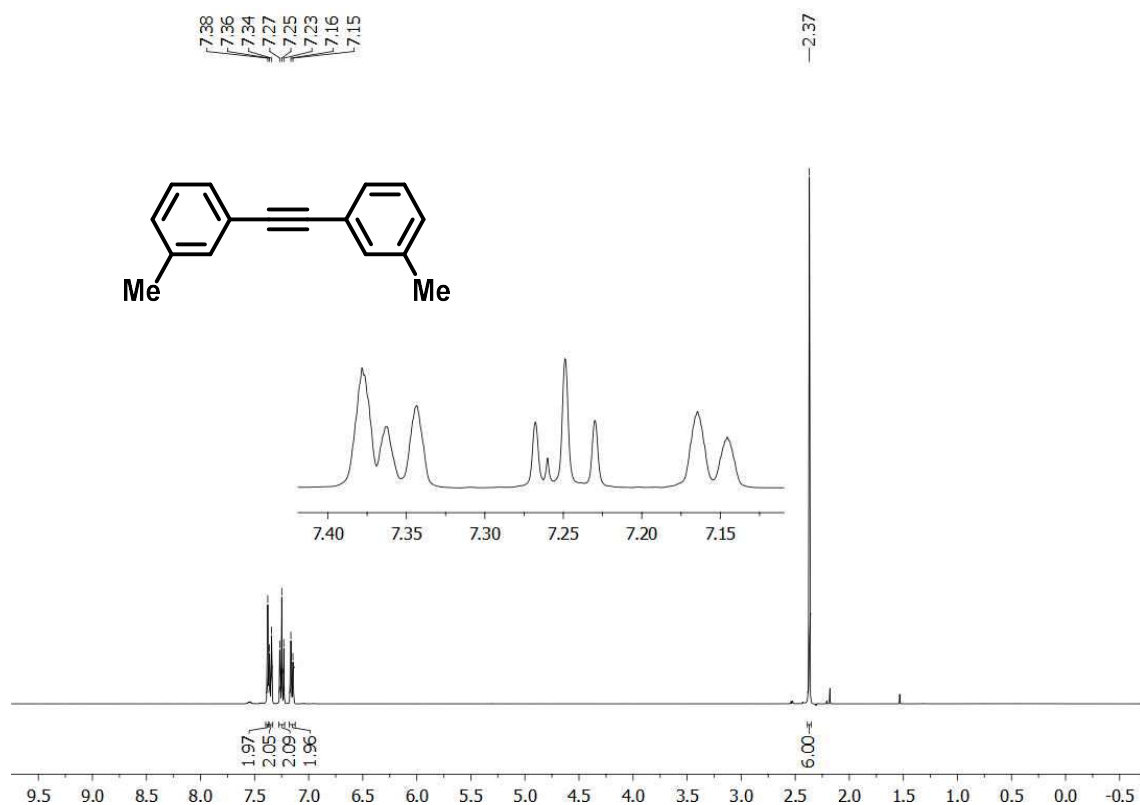
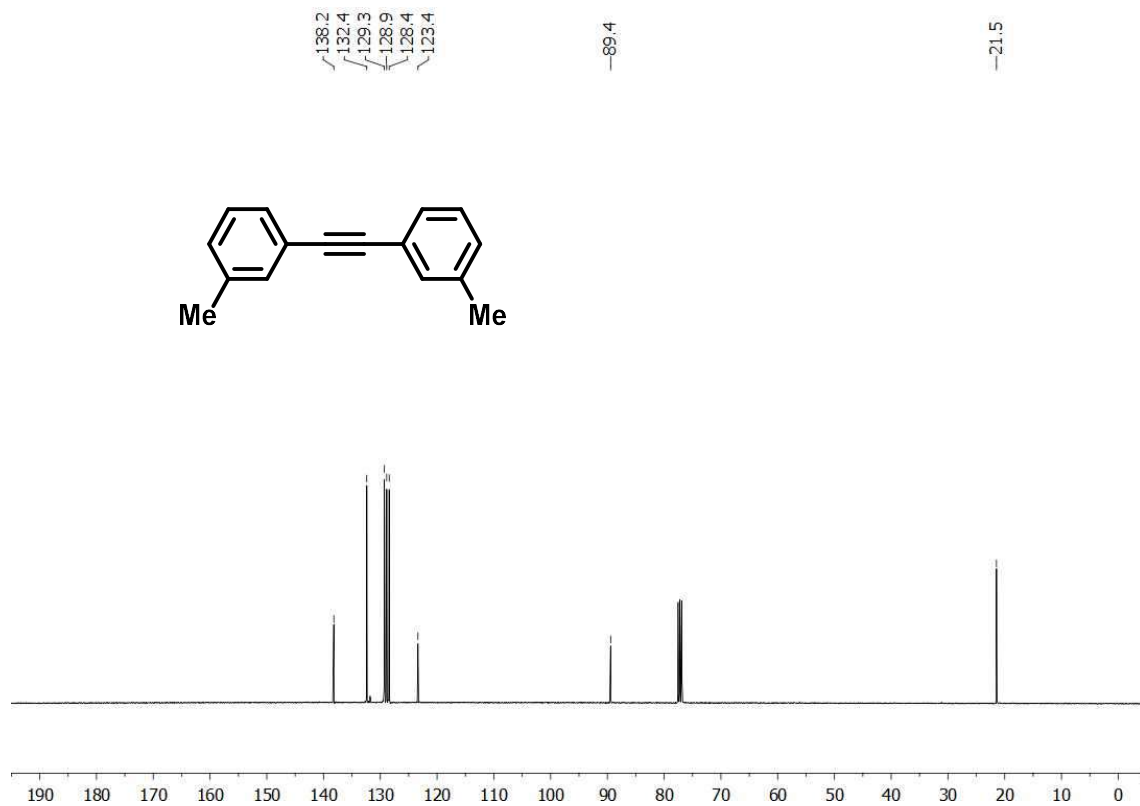


Figure A26. <sup>13</sup>C-NMR spectrum of compound **56h** (CDCl<sub>3</sub>, 100 MHz).





**Figure A27.** <sup>1</sup>H-NMR spectrum of compound **56i** (CDCl<sub>3</sub>, 400 MHz).



**Figure A28.** <sup>13</sup>C-NMR spectrum of compound **56i** (CDCl<sub>3</sub>, 100 MHz).

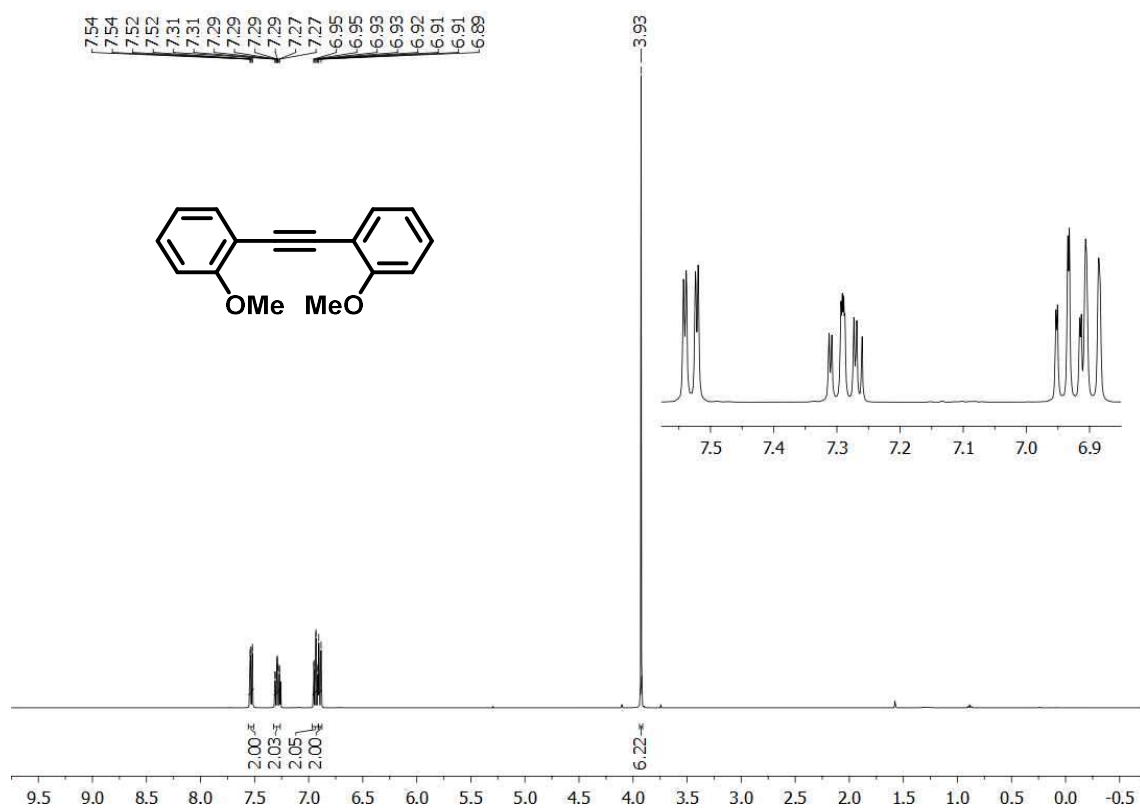


Figure A29. <sup>1</sup>H-NMR spectrum of compound **56j** (CDCl<sub>3</sub>, 400 MHz).

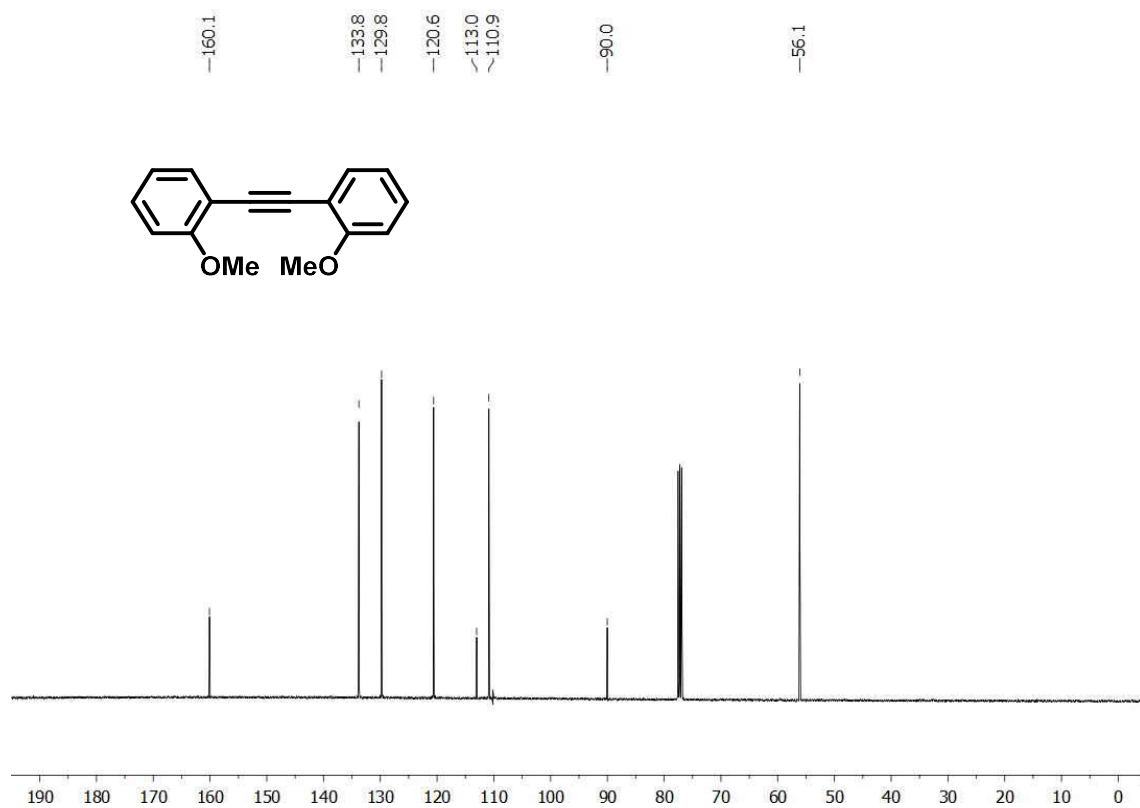


Figure A30. <sup>13</sup>C-NMR spectrum of compound **56j** (CDCl<sub>3</sub>, 100 MHz).

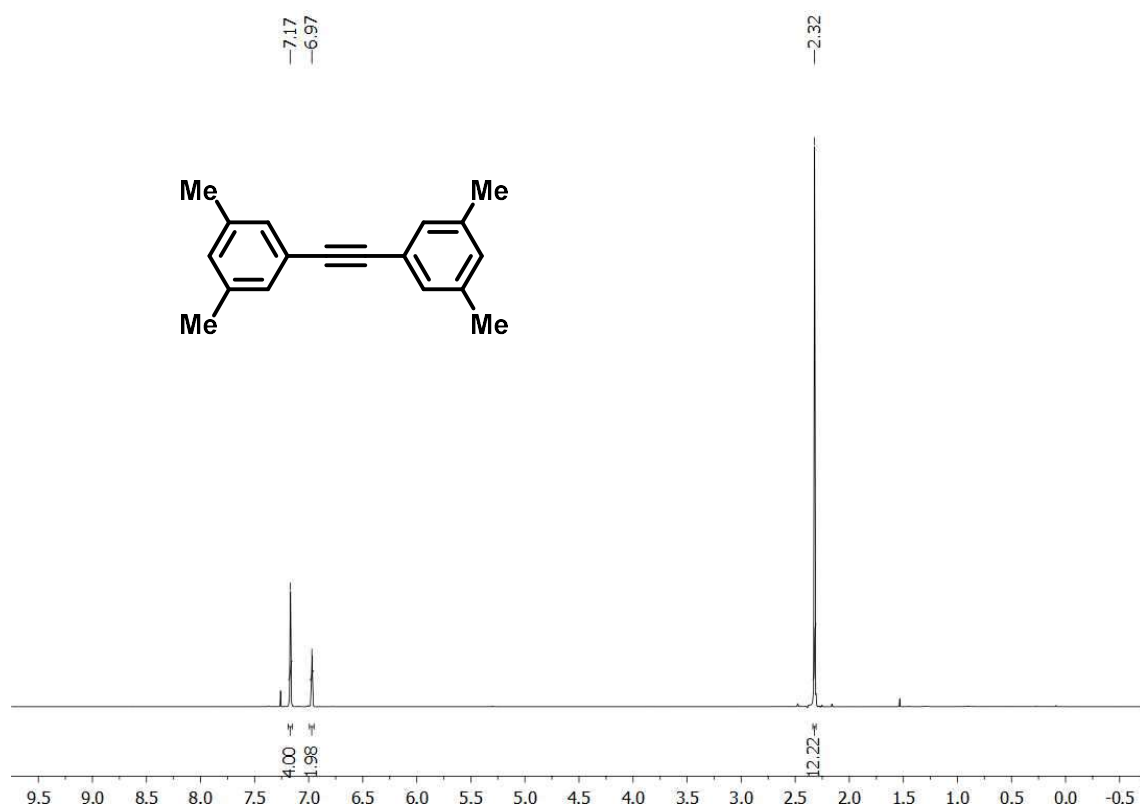


Figure A31. <sup>1</sup>H-NMR spectrum of compound 56k (CDCl<sub>3</sub>, 400 MHz).

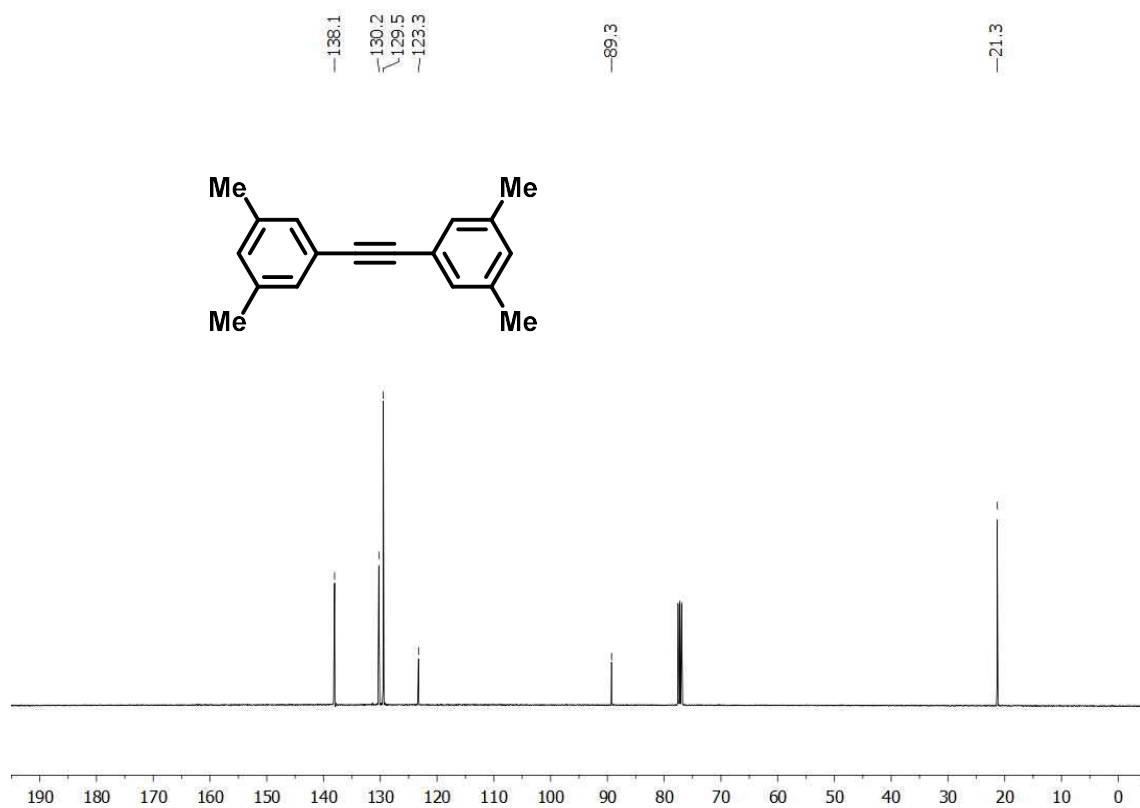
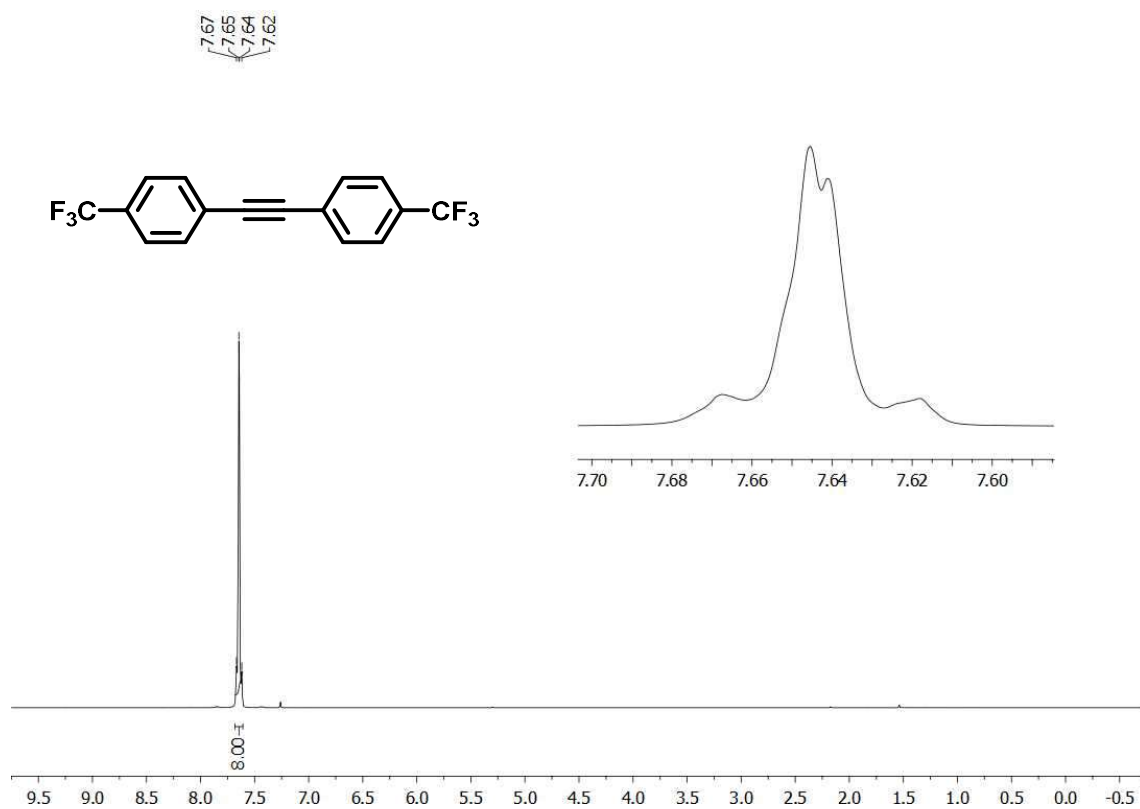
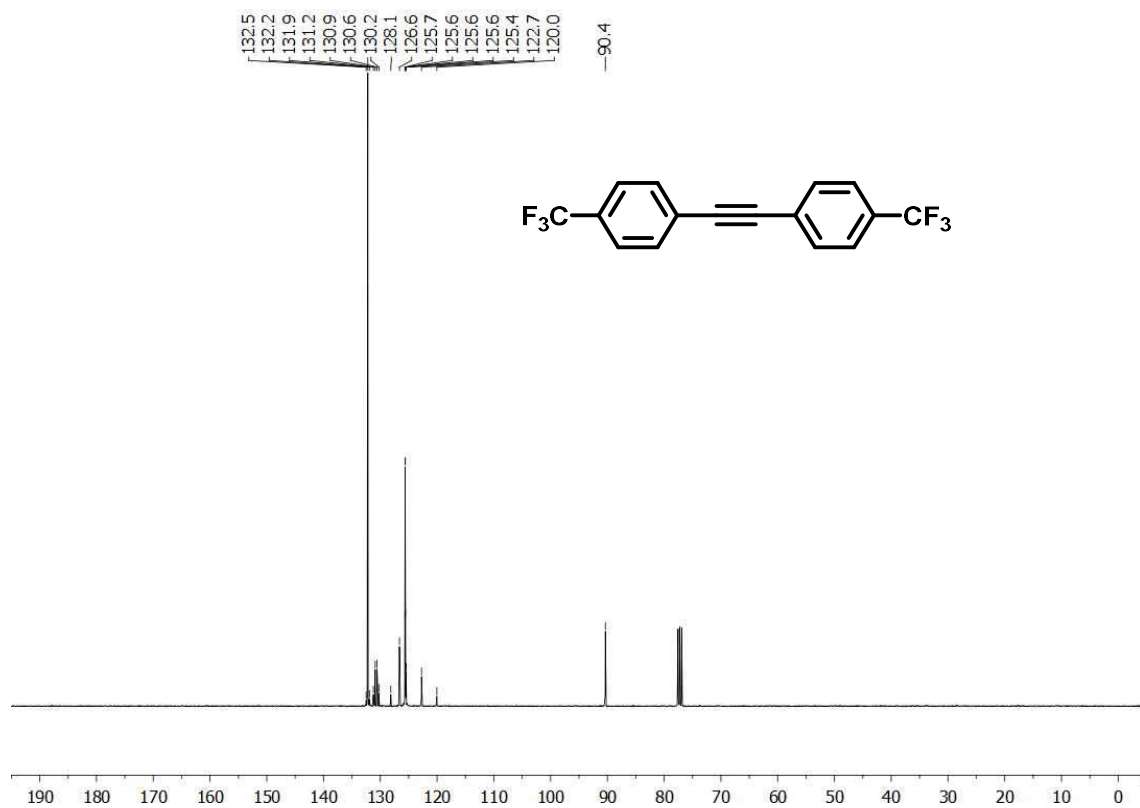


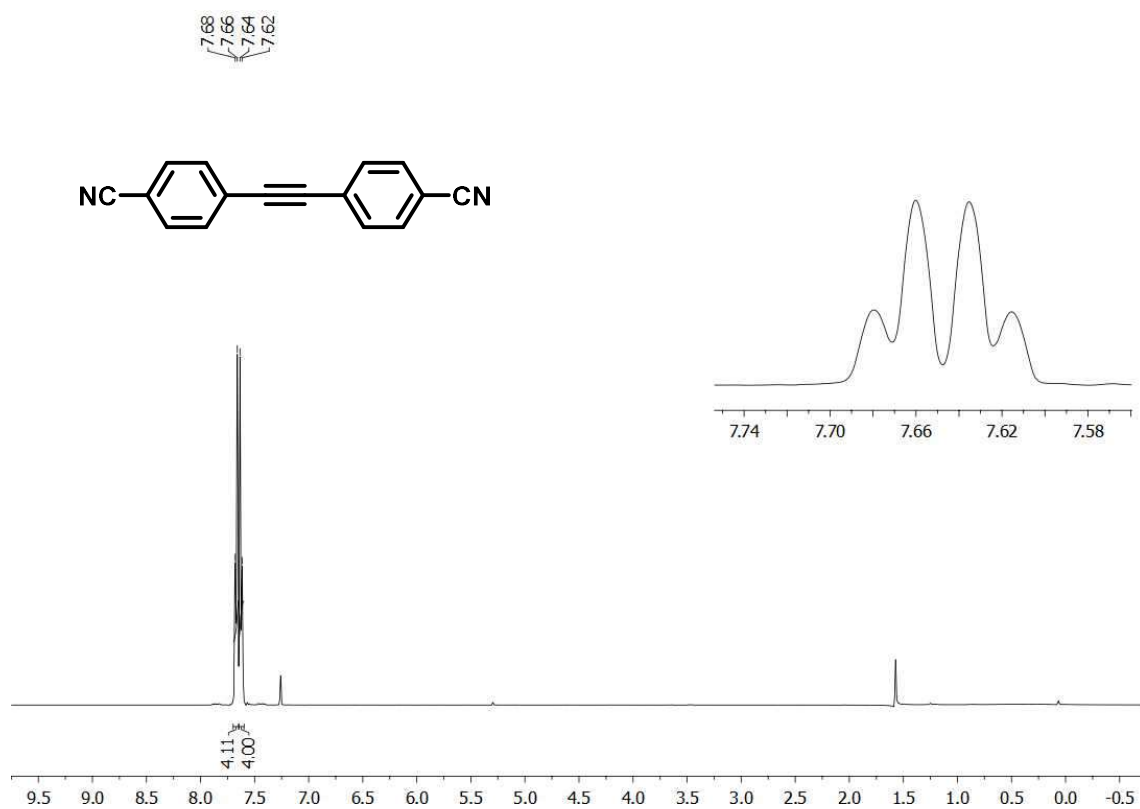
Figure A32. <sup>13</sup>C-NMR spectrum of compound 56k (CDCl<sub>3</sub>, 100 MHz).



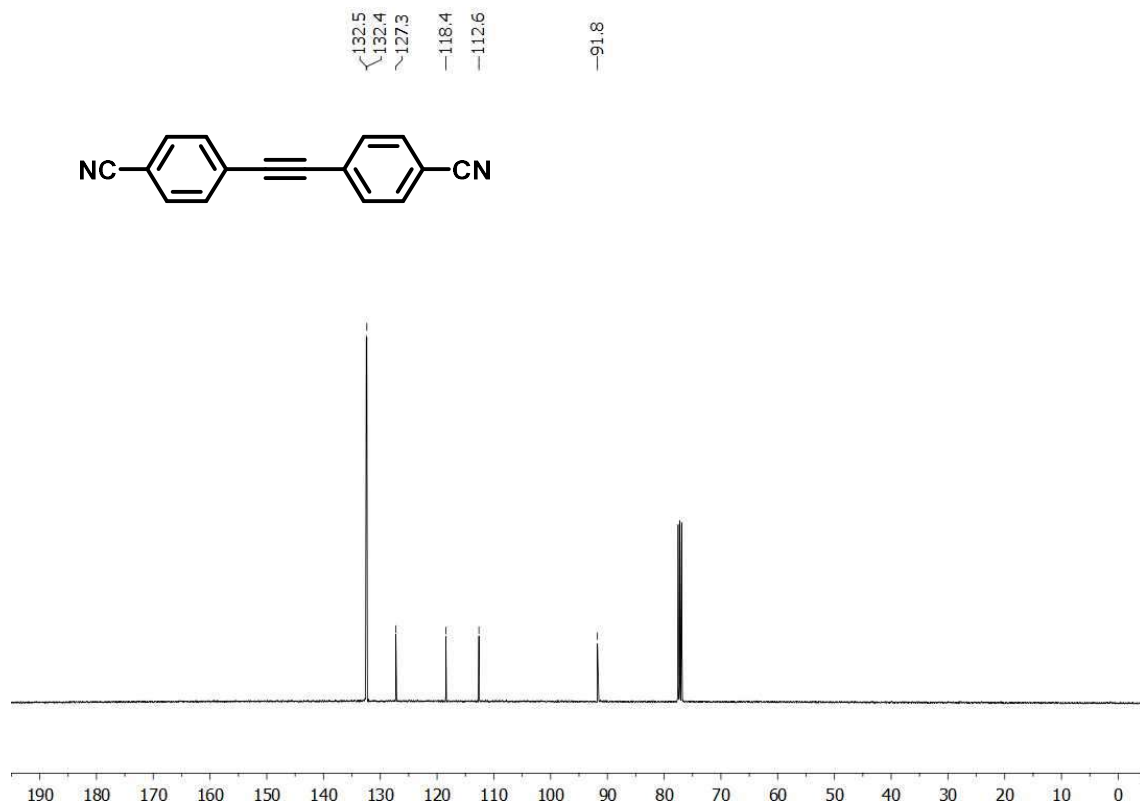
**Figure A33.** <sup>1</sup>H-NMR spectrum of compound **561** (CDCl<sub>3</sub>, 400 MHz).



**Figure A34.** <sup>13</sup>C-NMR spectrum of compound **561** (CDCl<sub>3</sub>, 100 MHz).



**Figure A35.** <sup>1</sup>H-NMR spectrum of compound **56m** (CDCl<sub>3</sub>, 400 MHz).



**Figure A36.** <sup>13</sup>C-NMR spectrum of compound **56m** (CDCl<sub>3</sub>, 100 MHz).

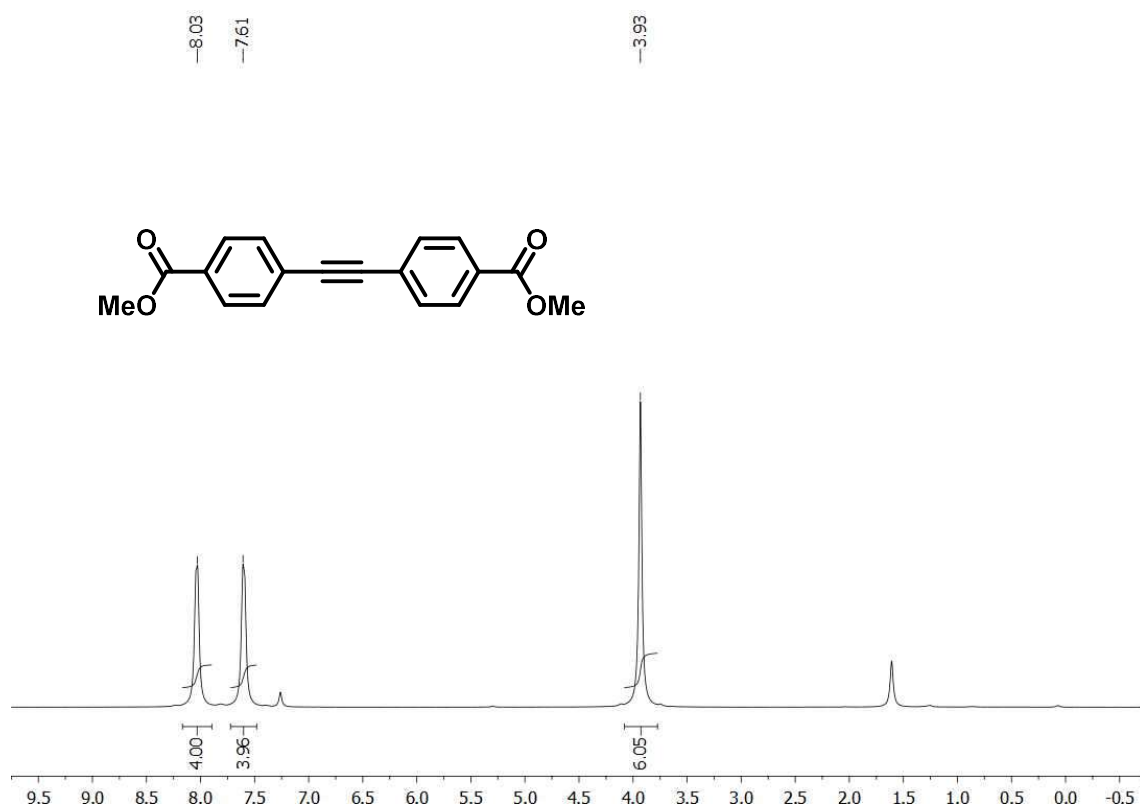


Figure A37. <sup>1</sup>H-NMR spectrum of compound 56n (CDCl<sub>3</sub>, 400 MHz).

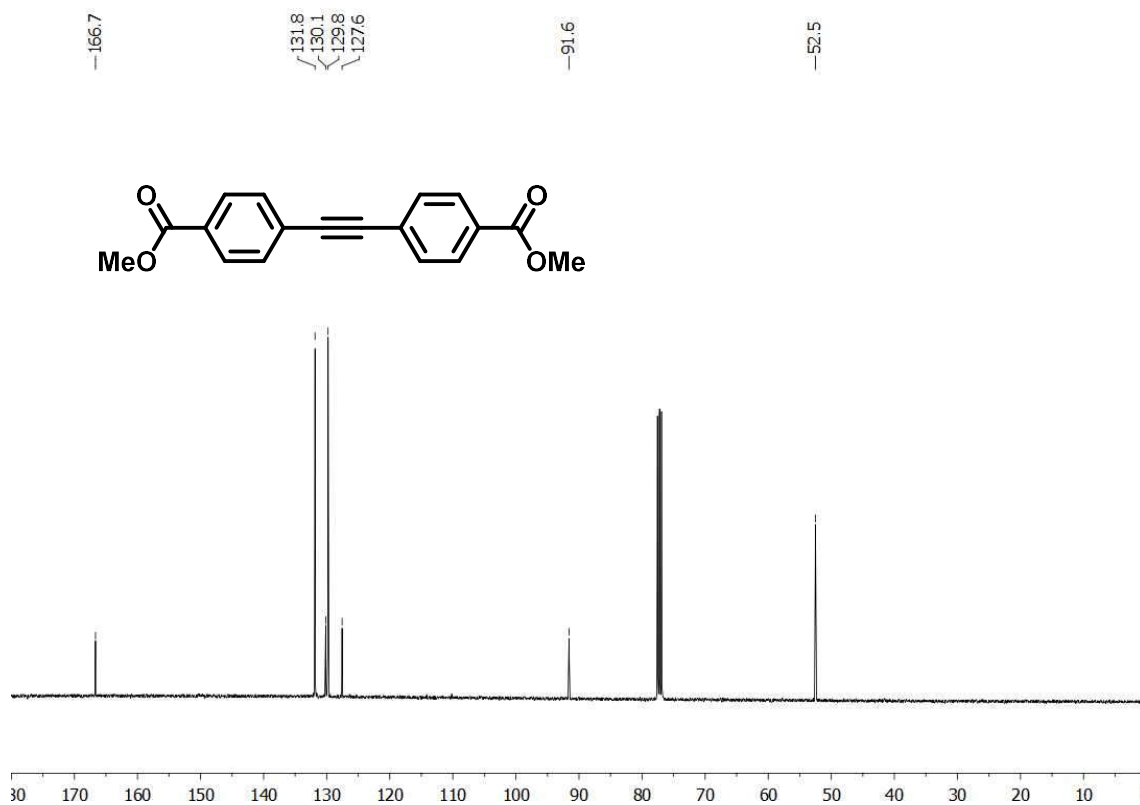
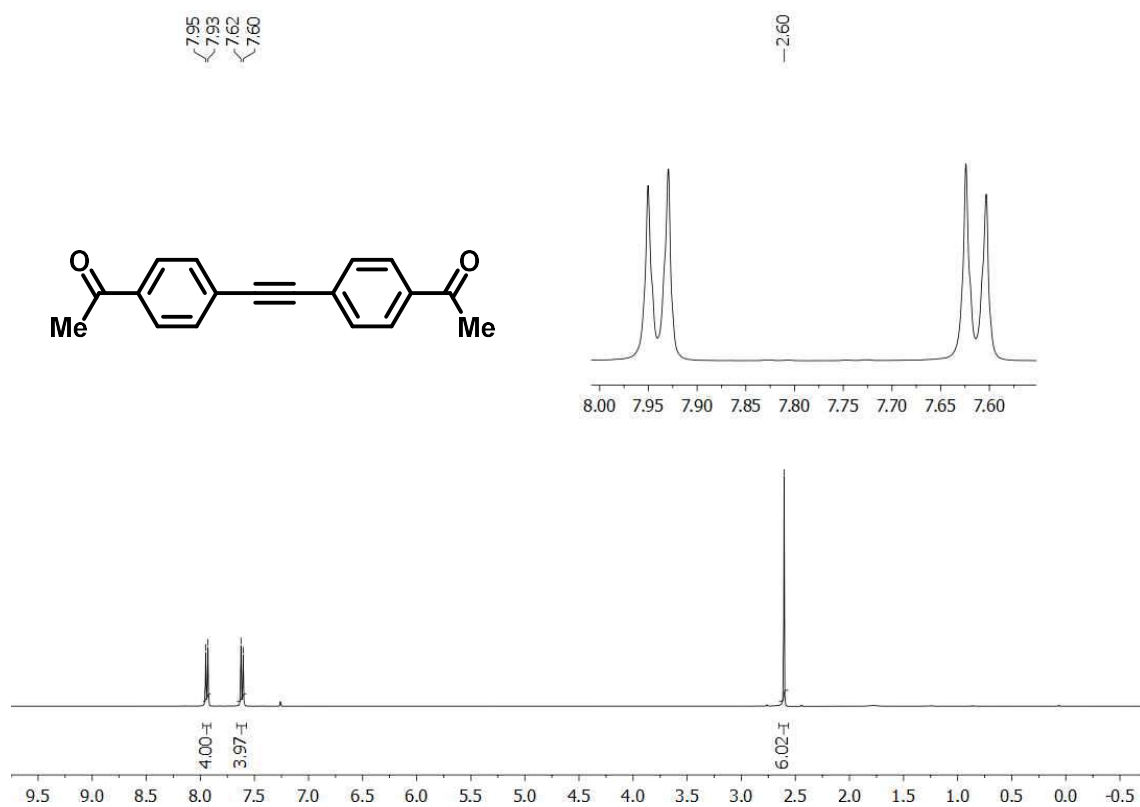
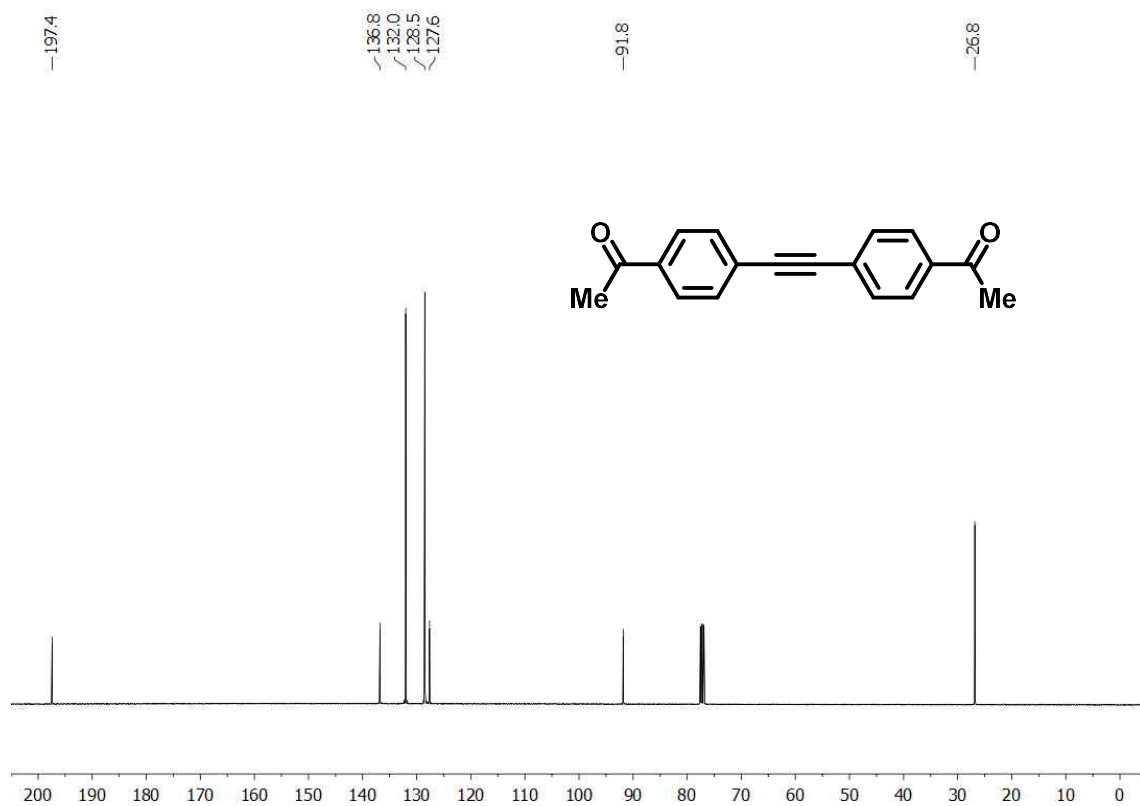


Figure A38. <sup>13</sup>C-NMR spectrum of compound 56n (CDCl<sub>3</sub>, 100 MHz).



**Figure A39.** <sup>1</sup>H-NMR spectrum of compound **56o** (CDCl<sub>3</sub>, 400 MHz).



**Figure A40.** <sup>13</sup>C-NMR spectrum of compound **56o** (CDCl<sub>3</sub>, 100 MHz).

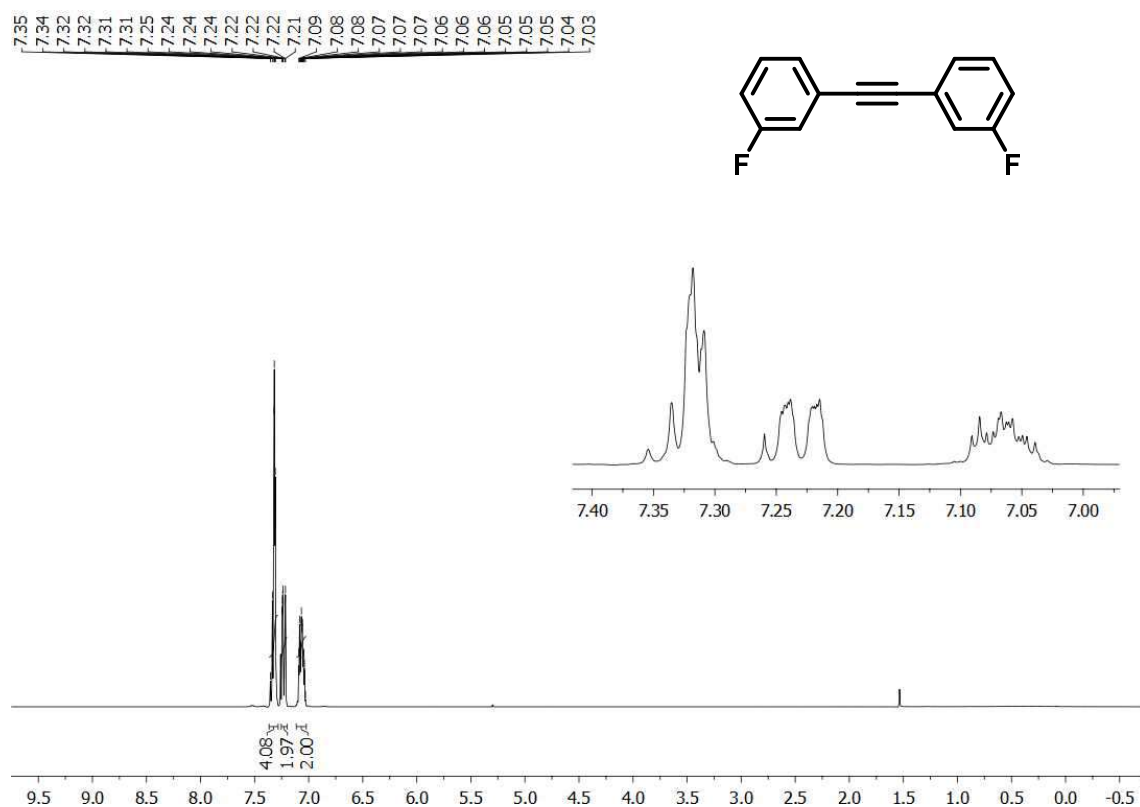
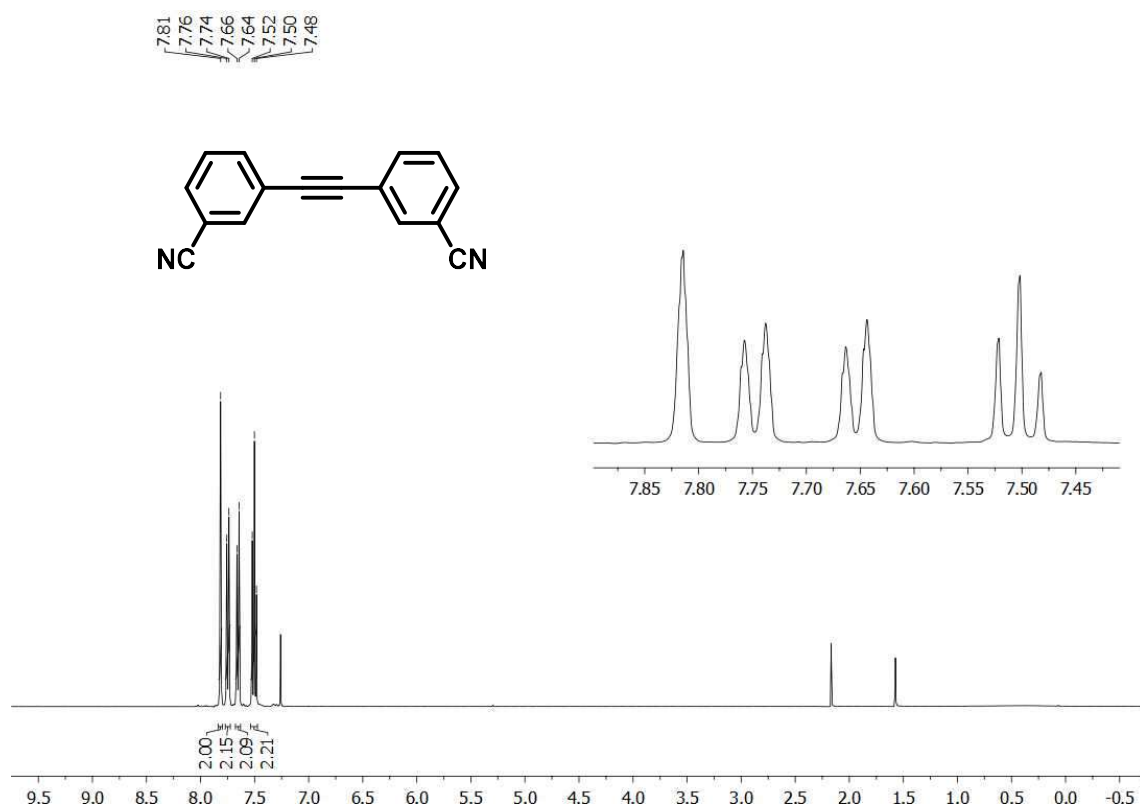


Figure A41. <sup>1</sup>H-NMR spectrum of compound 56p (CDCl<sub>3</sub>, 400 MHz).

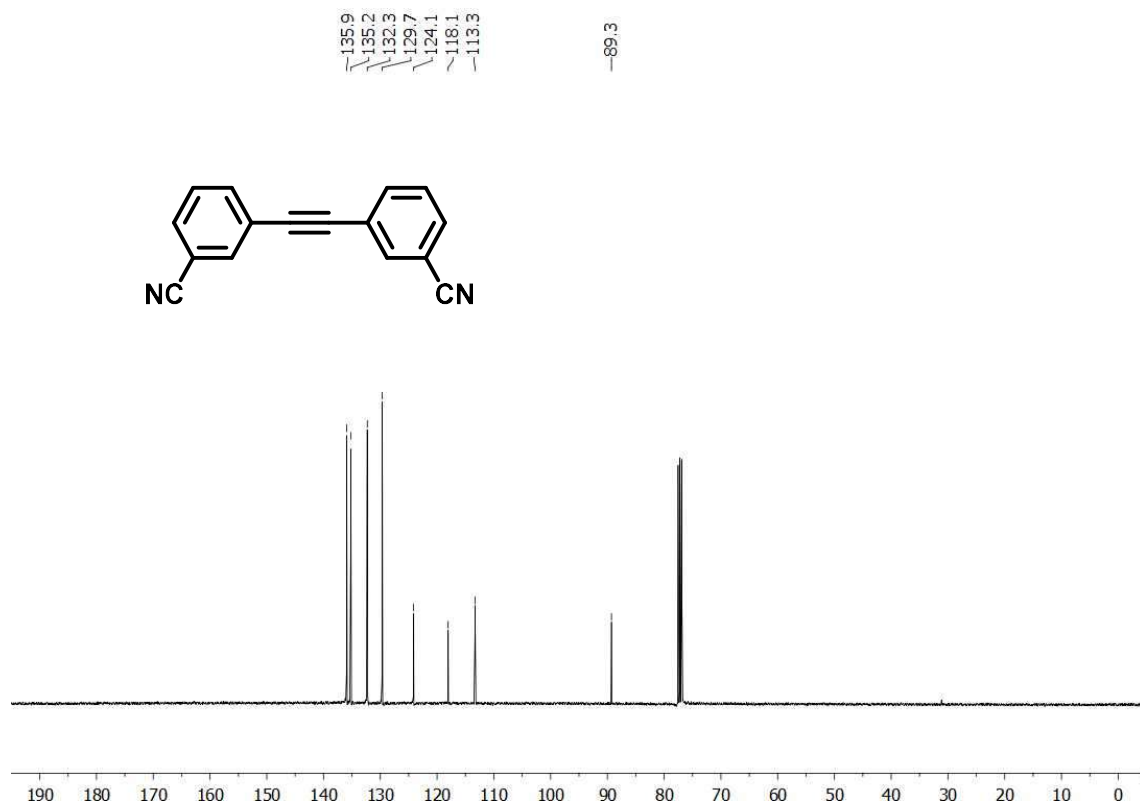


Figure A42. <sup>13</sup>C-NMR spectrum of compound 56p (CDCl<sub>3</sub>, 100 MHz).





**Figure A43.** <sup>1</sup>H-NMR spectrum of compound **56q** (CDCl<sub>3</sub>, 400 MHz).



**Figure A44.** <sup>13</sup>C-NMR spectrum of compound **56q** (CDCl<sub>3</sub>, 100 MHz).

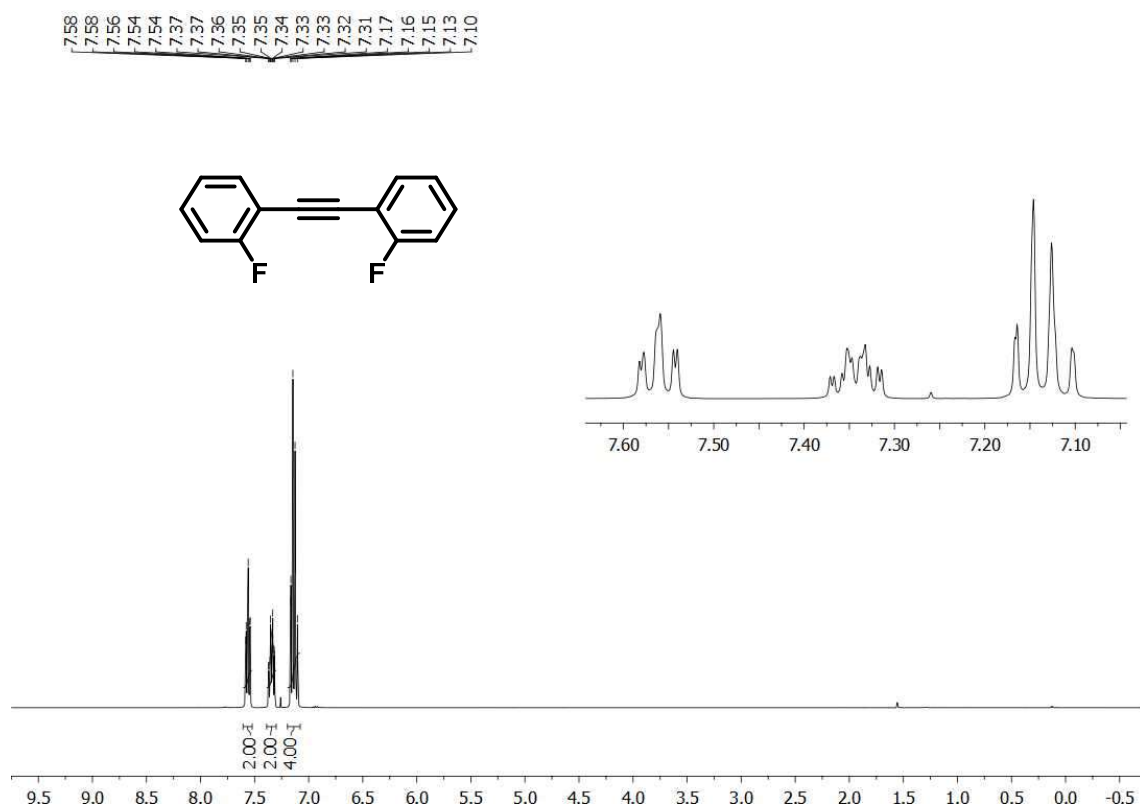


Figure A45. <sup>1</sup>H-NMR spectrum of compound **56r** (CDCl<sub>3</sub>, 400 MHz).

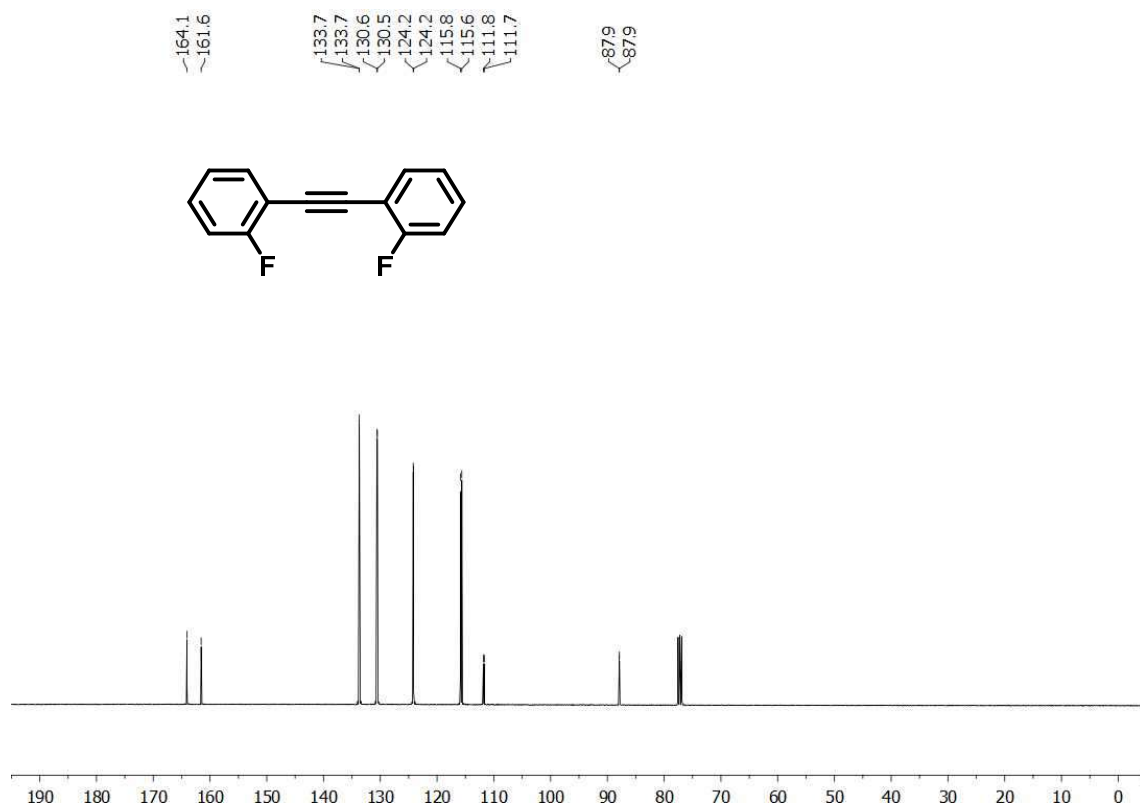
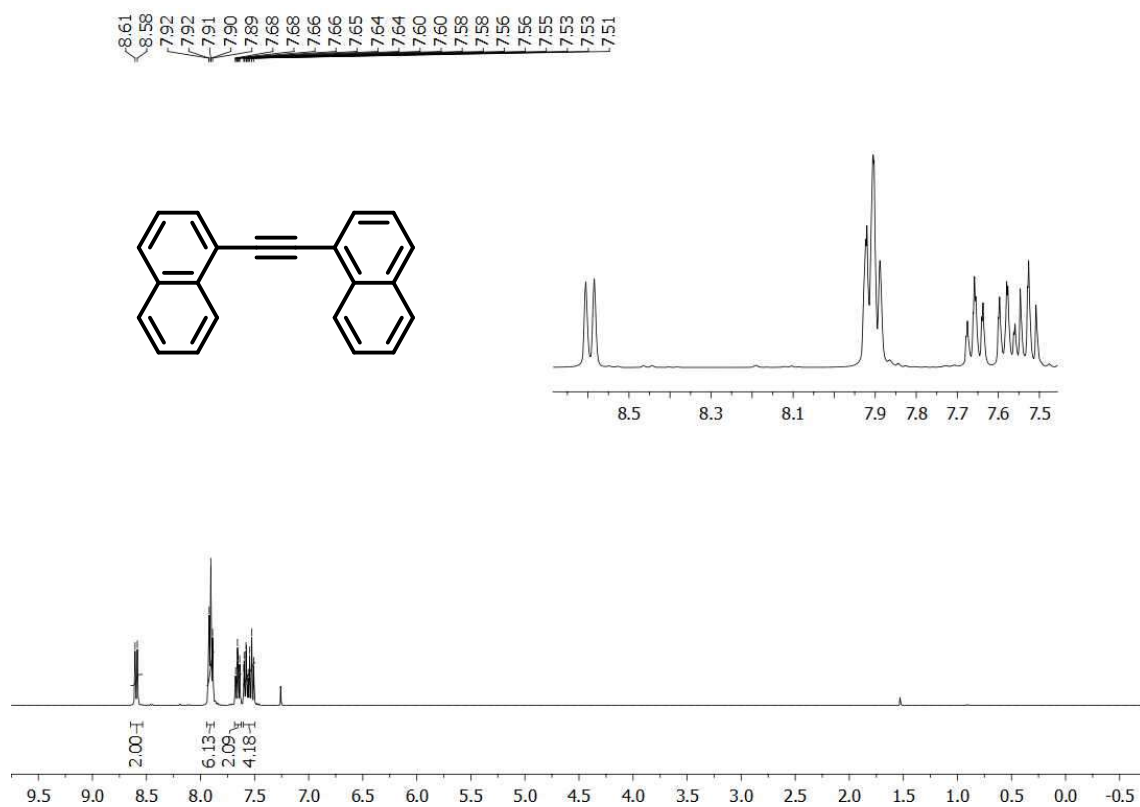
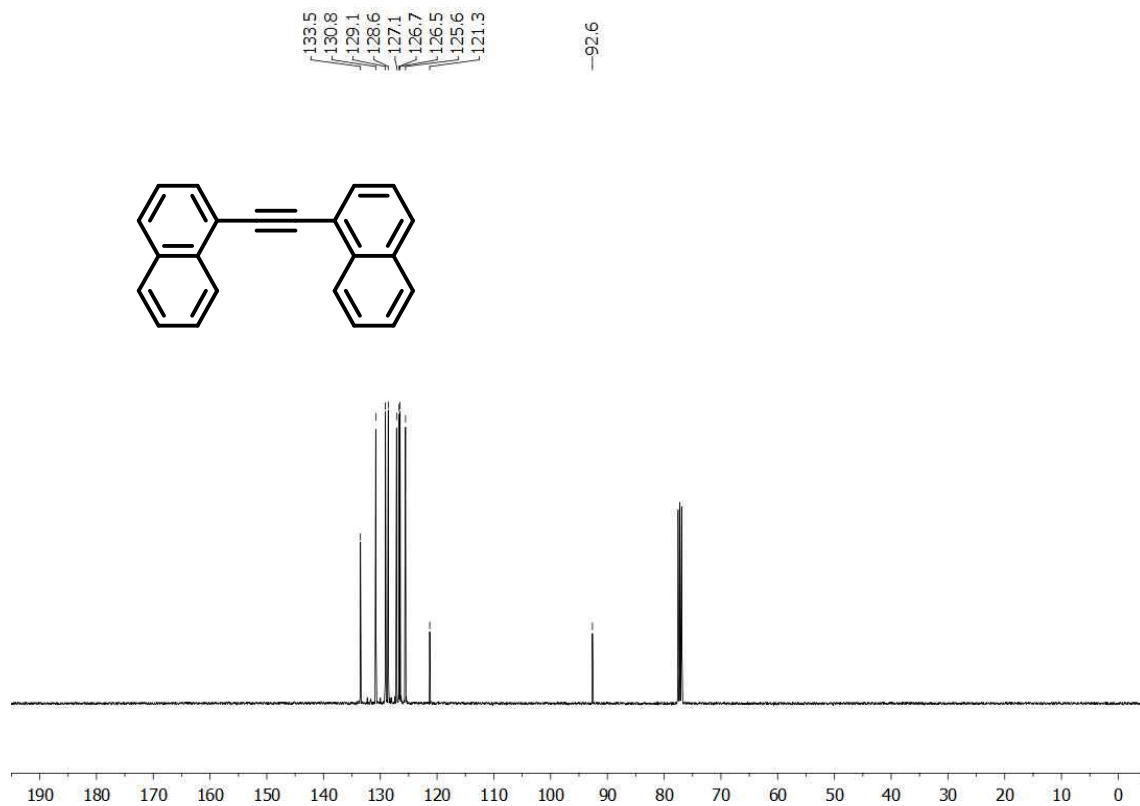


Figure A46. <sup>13</sup>C-NMR spectrum of compound **56r** (CDCl<sub>3</sub>, 100 MHz).



**Figure A47.** <sup>1</sup>H-NMR spectrum of compound **56s** (CDCl<sub>3</sub>, 400 MHz).



**Figure A48.** <sup>13</sup>C-NMR spectrum of compound **56s** (CDCl<sub>3</sub>, 100 MHz).

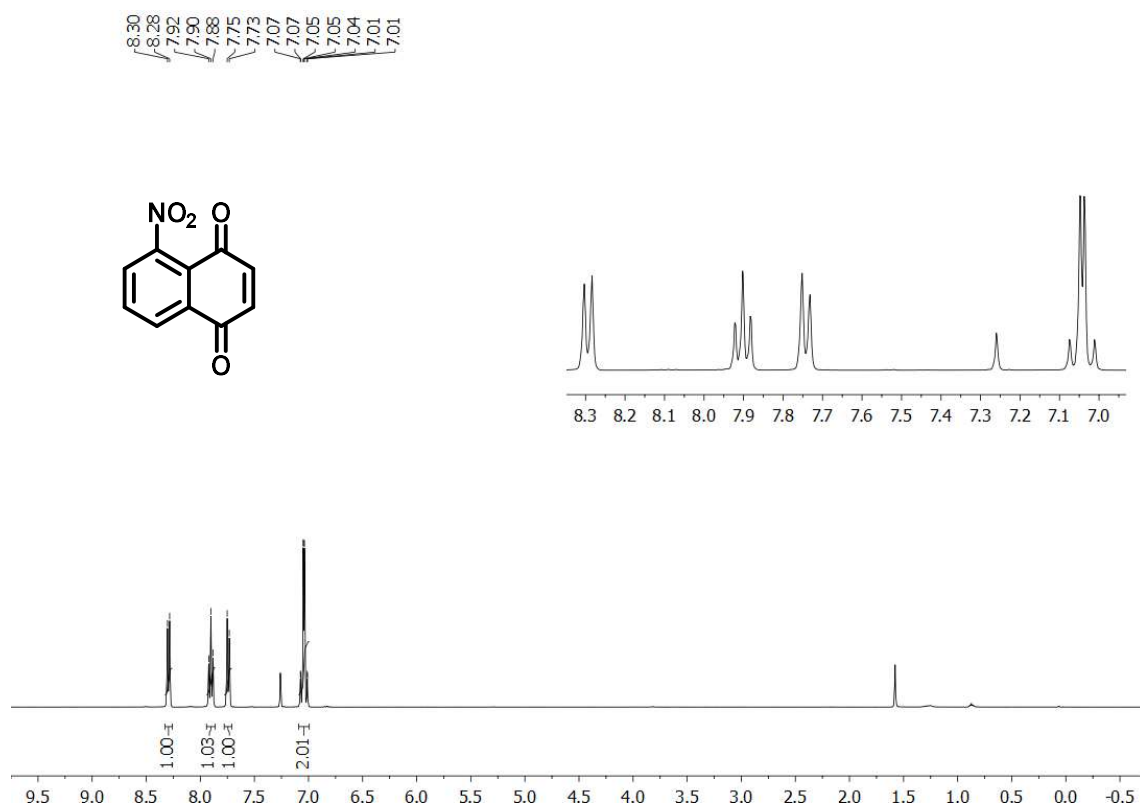


Figure A49. <sup>1</sup>H-NMR spectrum of compound 57a (CDCl<sub>3</sub>, 400 MHz).

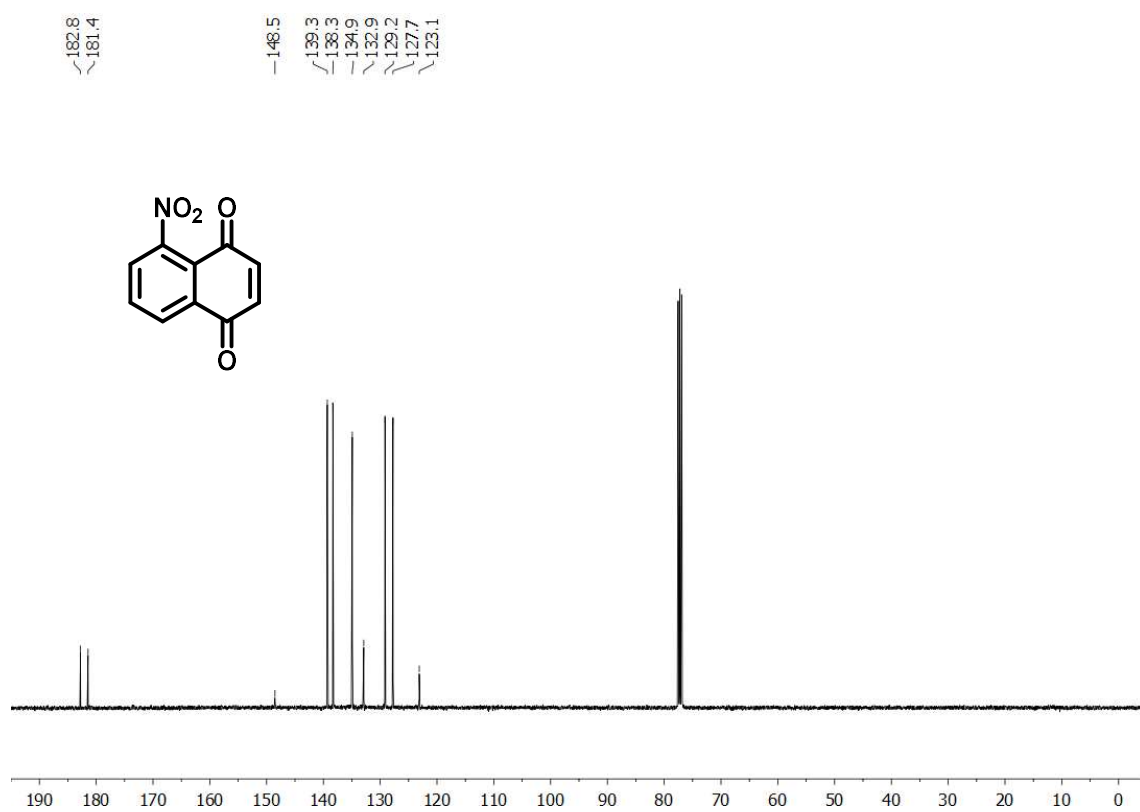


Figure A50. <sup>13</sup>C-NMR spectrum of compound 57a (CDCl<sub>3</sub>, 100 MHz).

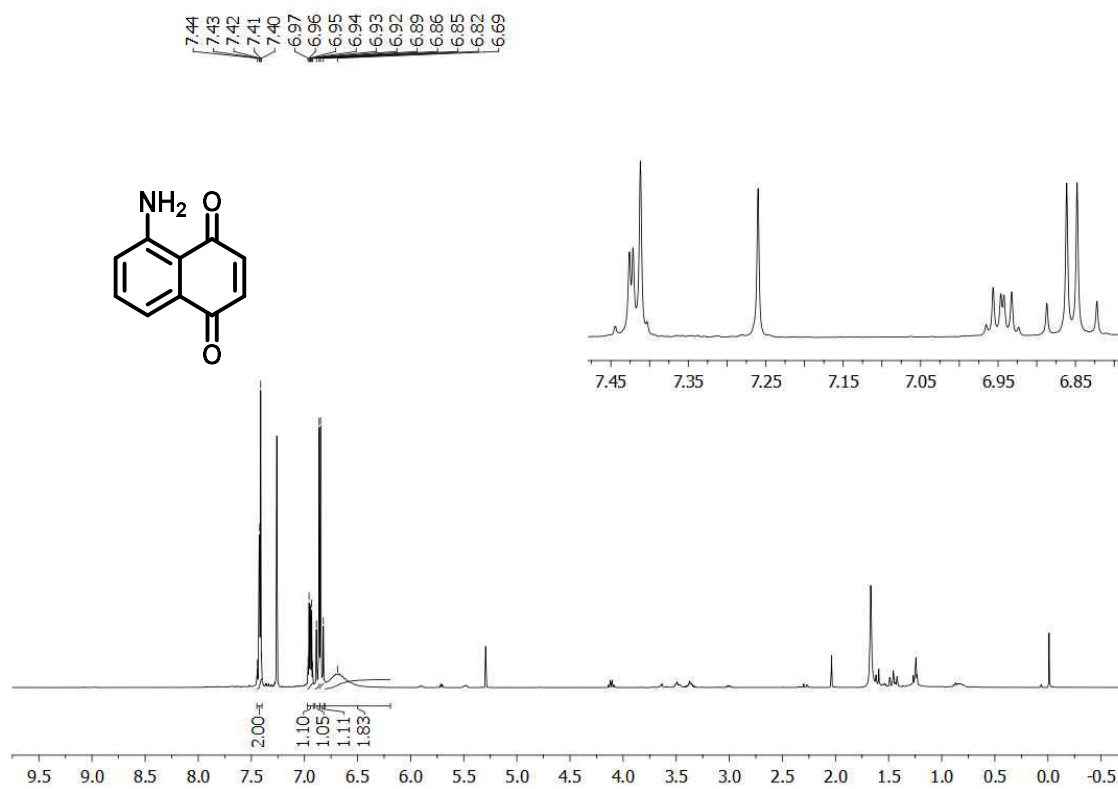


Figure A51. <sup>1</sup>H-NMR spectrum of compound **57b** (CDCl<sub>3</sub>, 400 MHz).

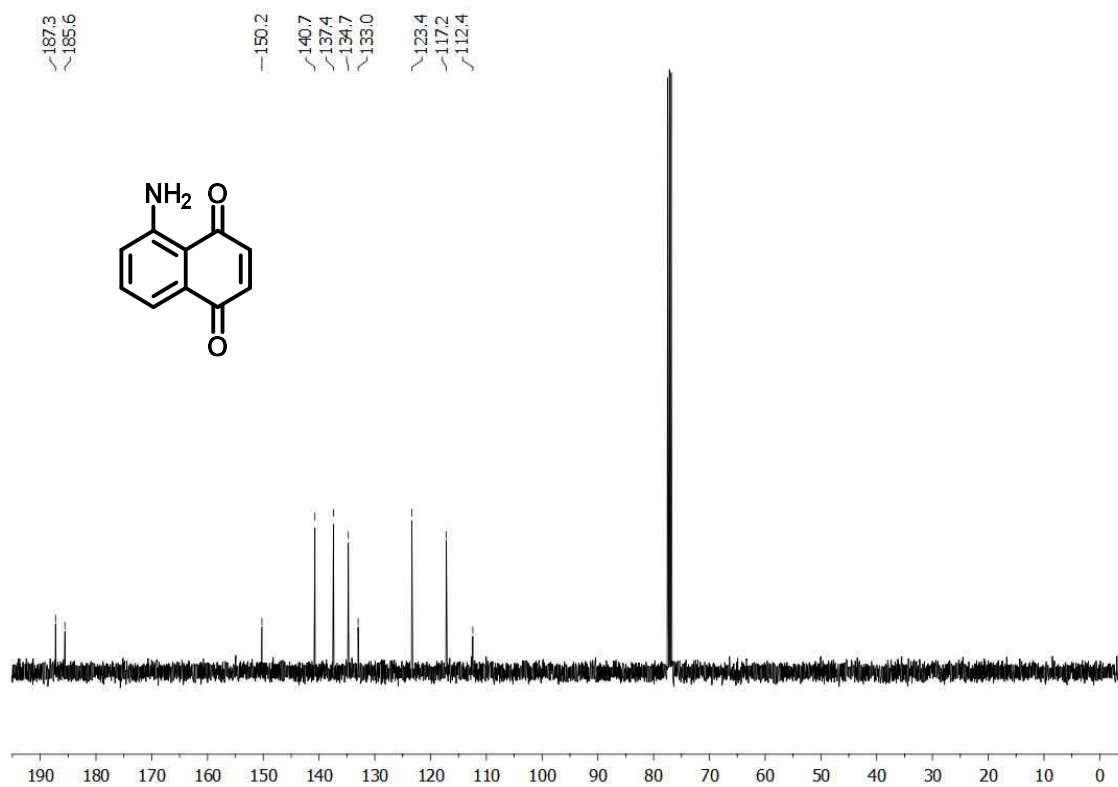


Figure A52. <sup>13</sup>C-NMR spectrum of compound **57b** (CDCl<sub>3</sub>, 100 MHz).

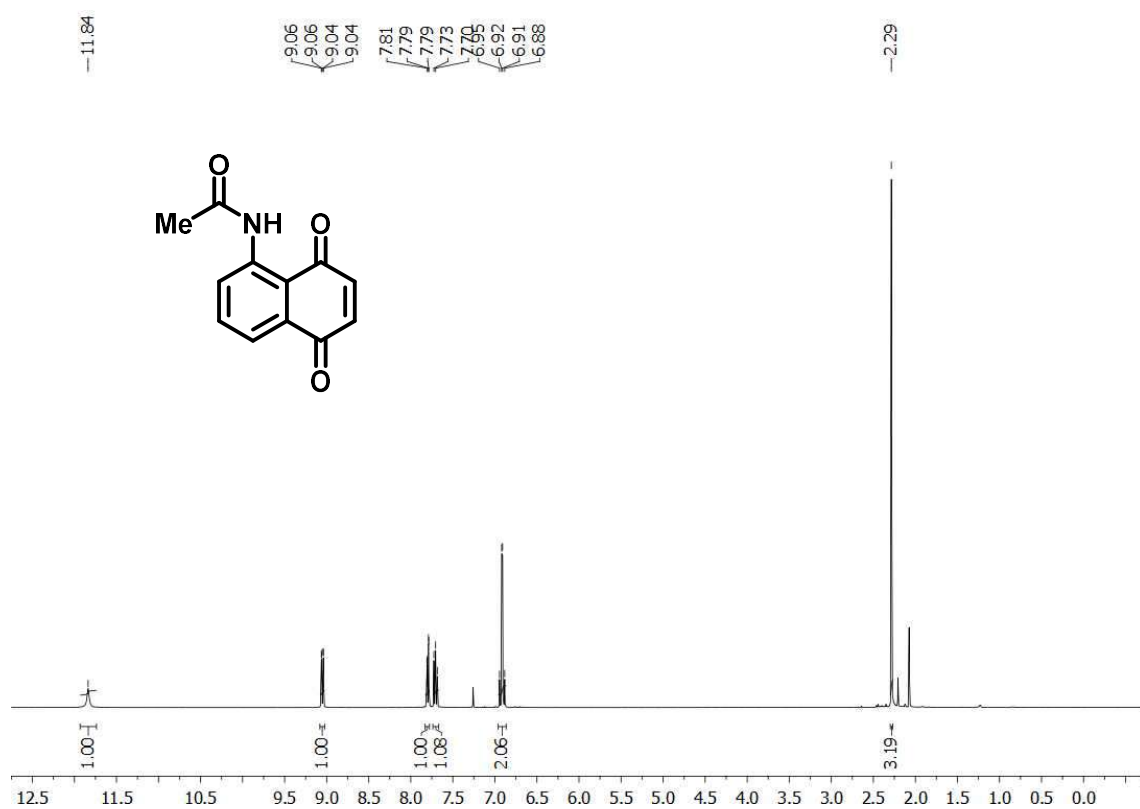


Figure A53. <sup>1</sup>H-NMR spectrum of compound 57c (CDCl<sub>3</sub>, 400 MHz).

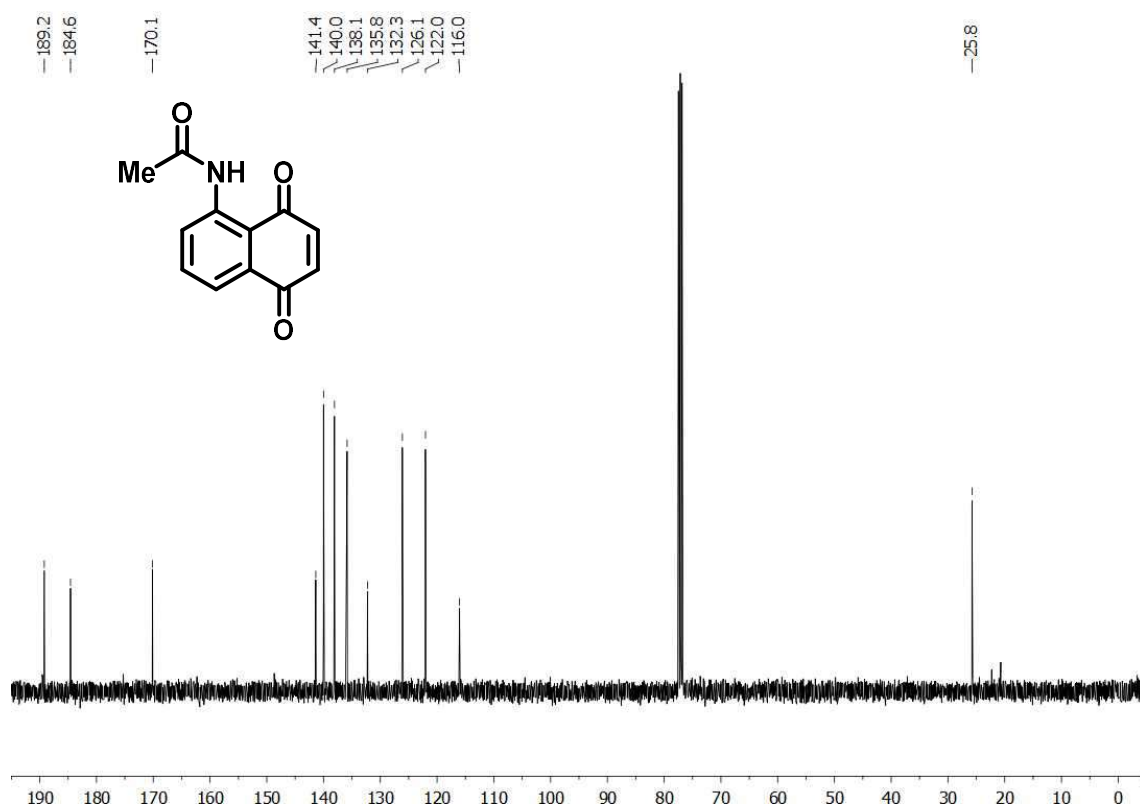


Figure A54. <sup>13</sup>C-NMR spectrum of compound 57c (CDCl<sub>3</sub>, 100 MHz).

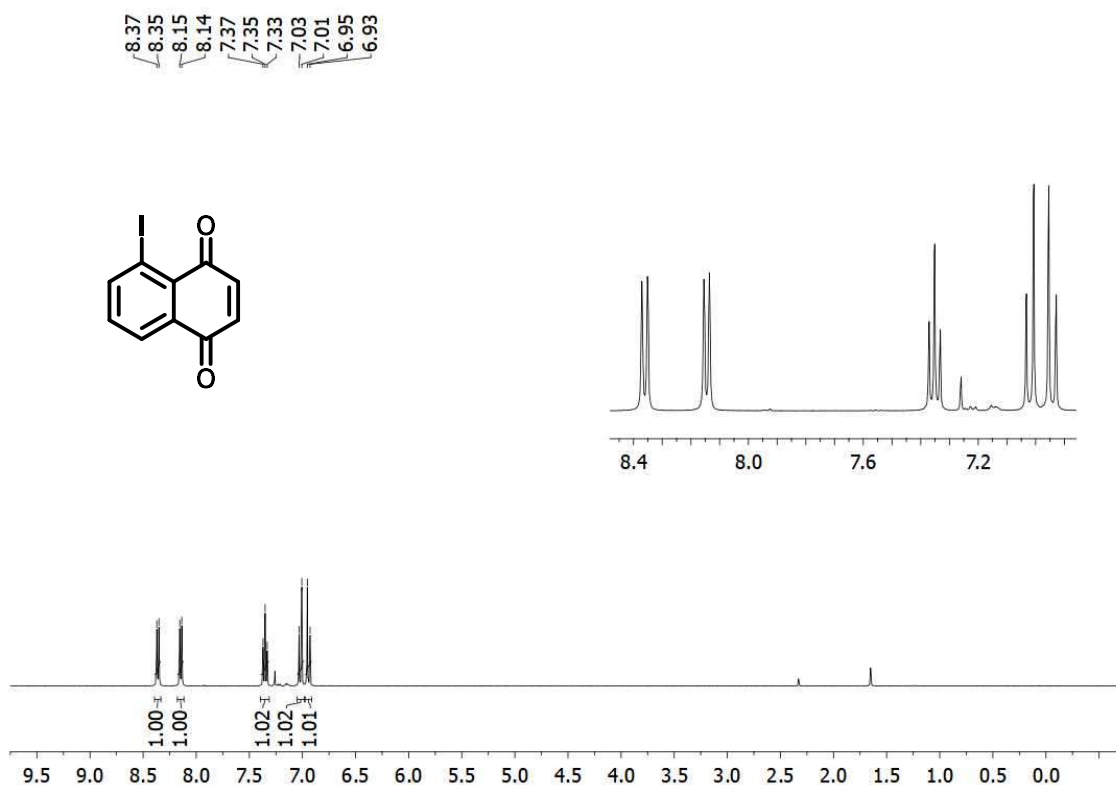


Figure A55. <sup>1</sup>H-NMR spectrum of compound **57d** (CDCl<sub>3</sub>, 400 MHz).

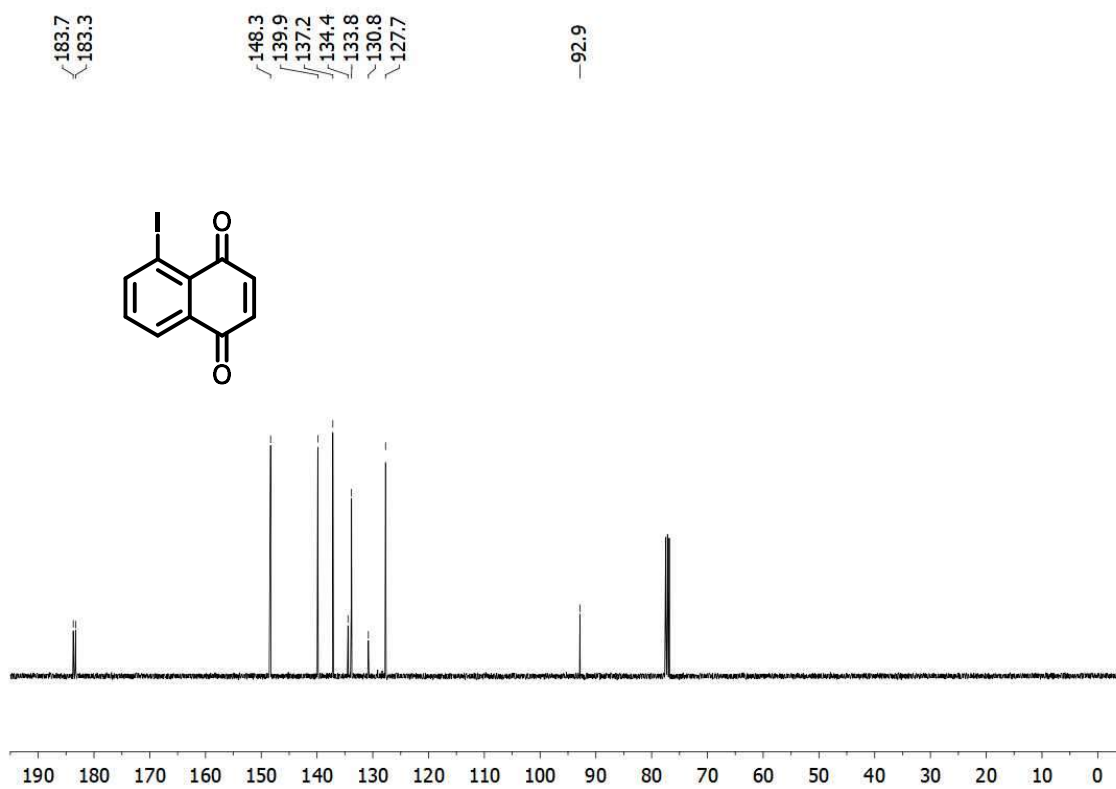


Figure A56. <sup>13</sup>C-NMR spectrum of compound **57d** (CDCl<sub>3</sub>, 100 MHz).

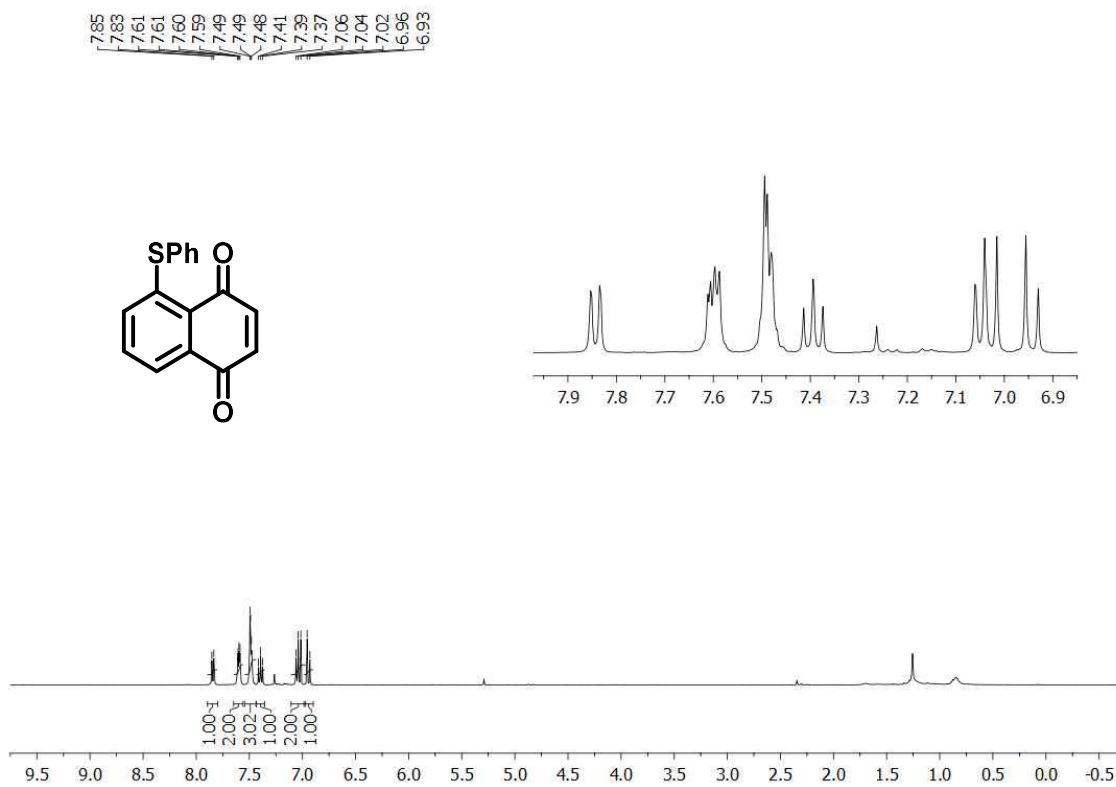


Figure A57. <sup>1</sup>H-NMR spectrum of compound 57e (CDCl<sub>3</sub>, 400 MHz).

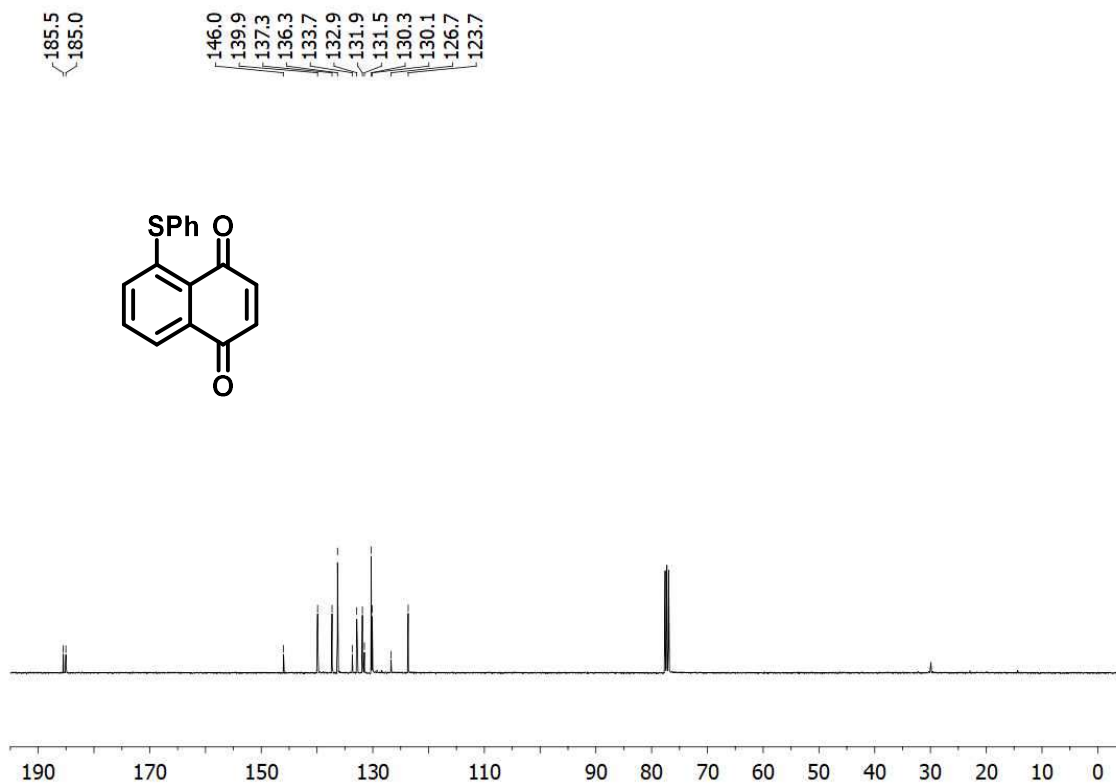
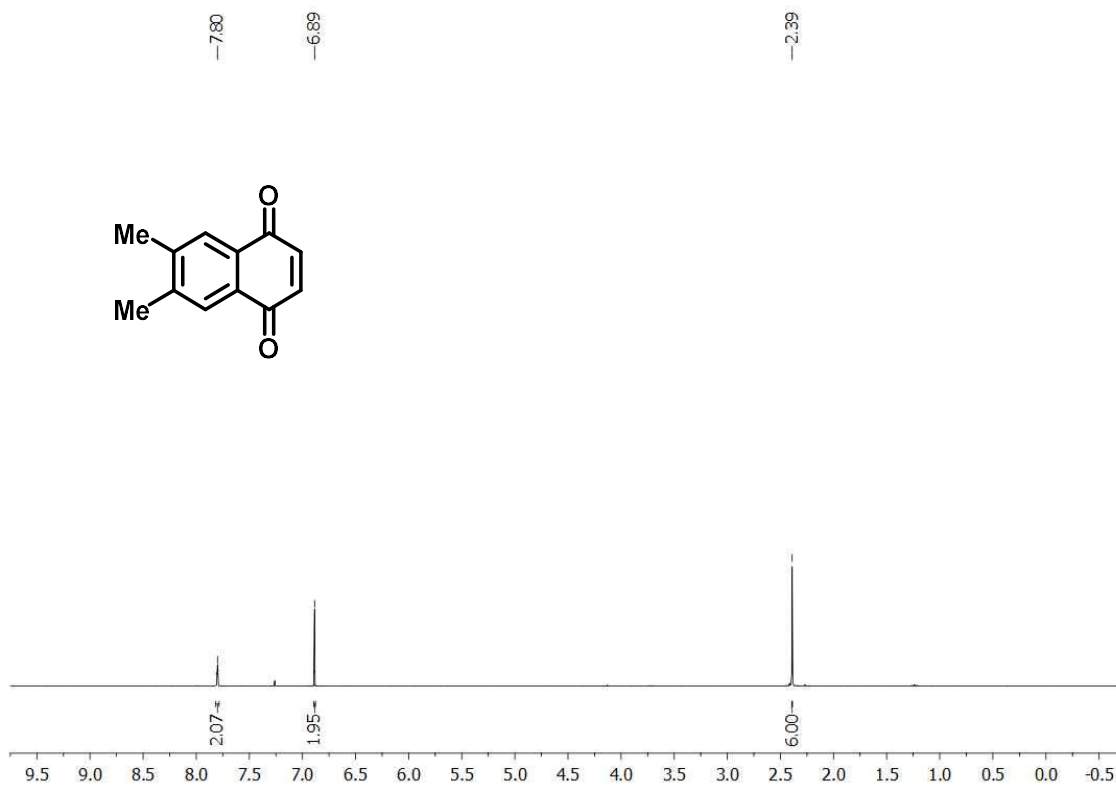
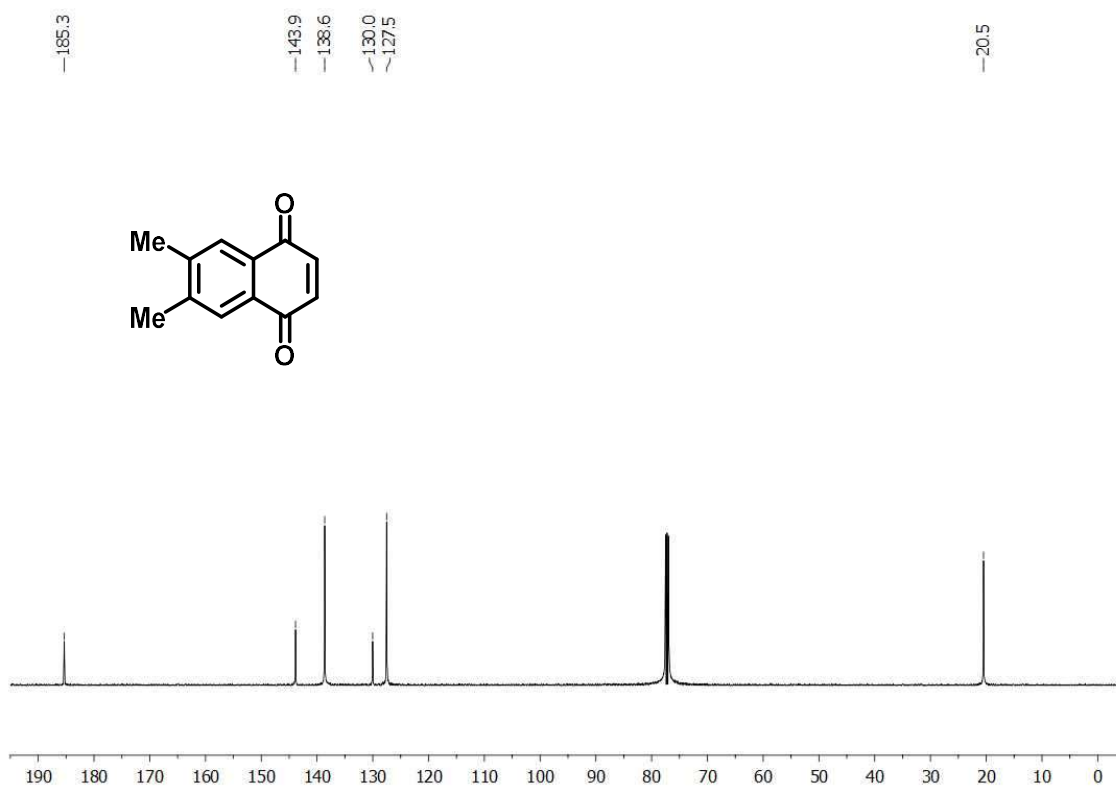


Figure A58. <sup>13</sup>C-NMR spectrum of compound 57e (CDCl<sub>3</sub>, 100 MHz).





**Figure A59.** <sup>1</sup>H-NMR spectrum of compound **57f** (CDCl<sub>3</sub>, 300 MHz).



**Figure A60.** <sup>13</sup>C-NMR spectrum of compound **57f** (CDCl<sub>3</sub>, 75 MHz).

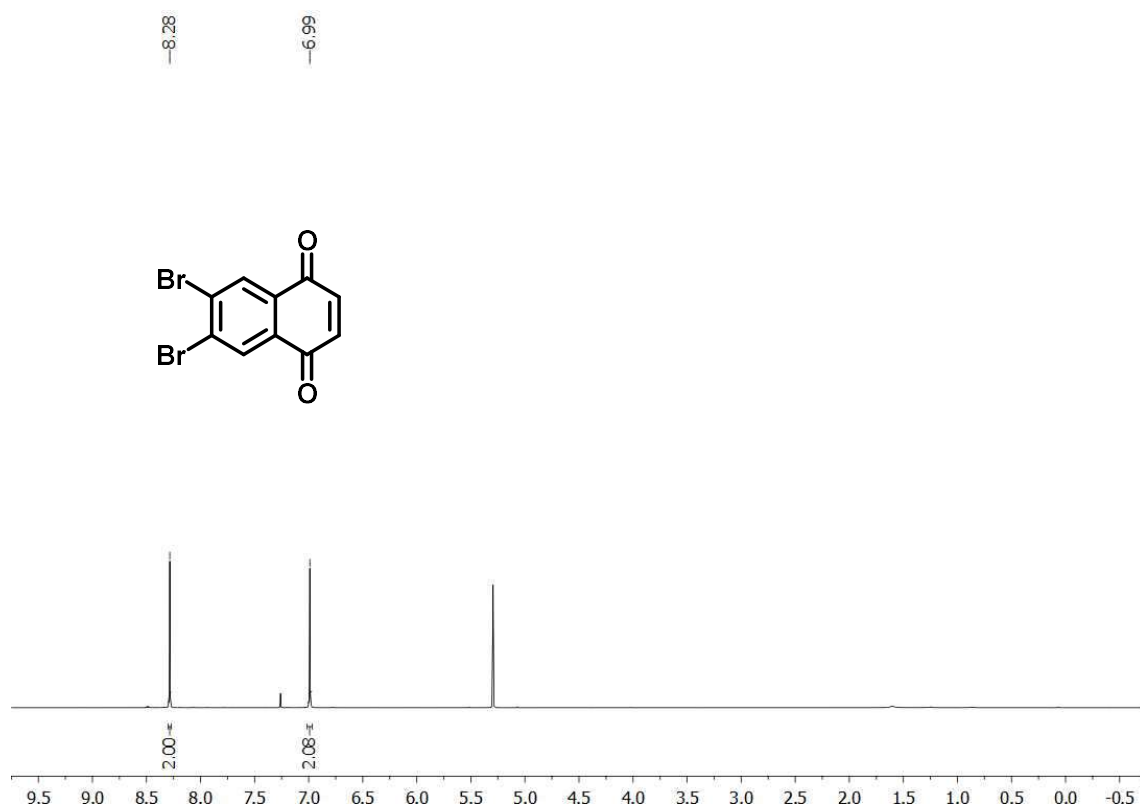


Figure A61. <sup>1</sup>H-NMR spectrum of compound 57g (CDCl<sub>3</sub>, 400 MHz).

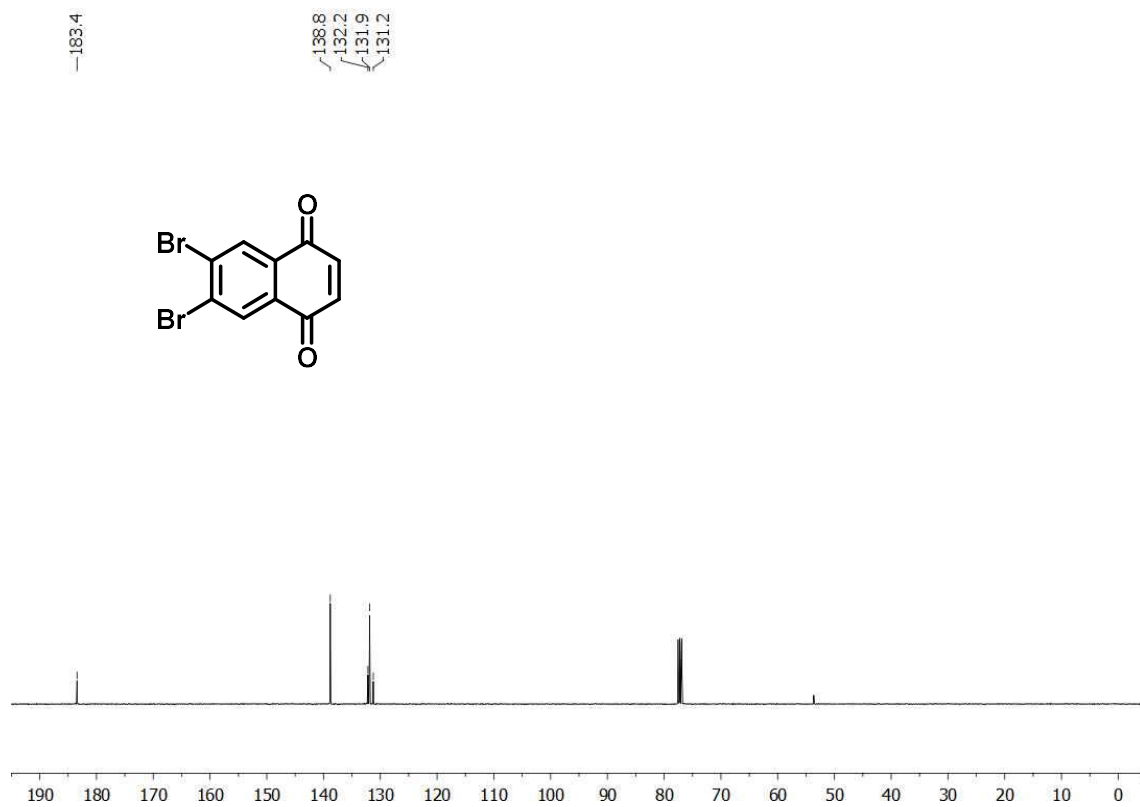
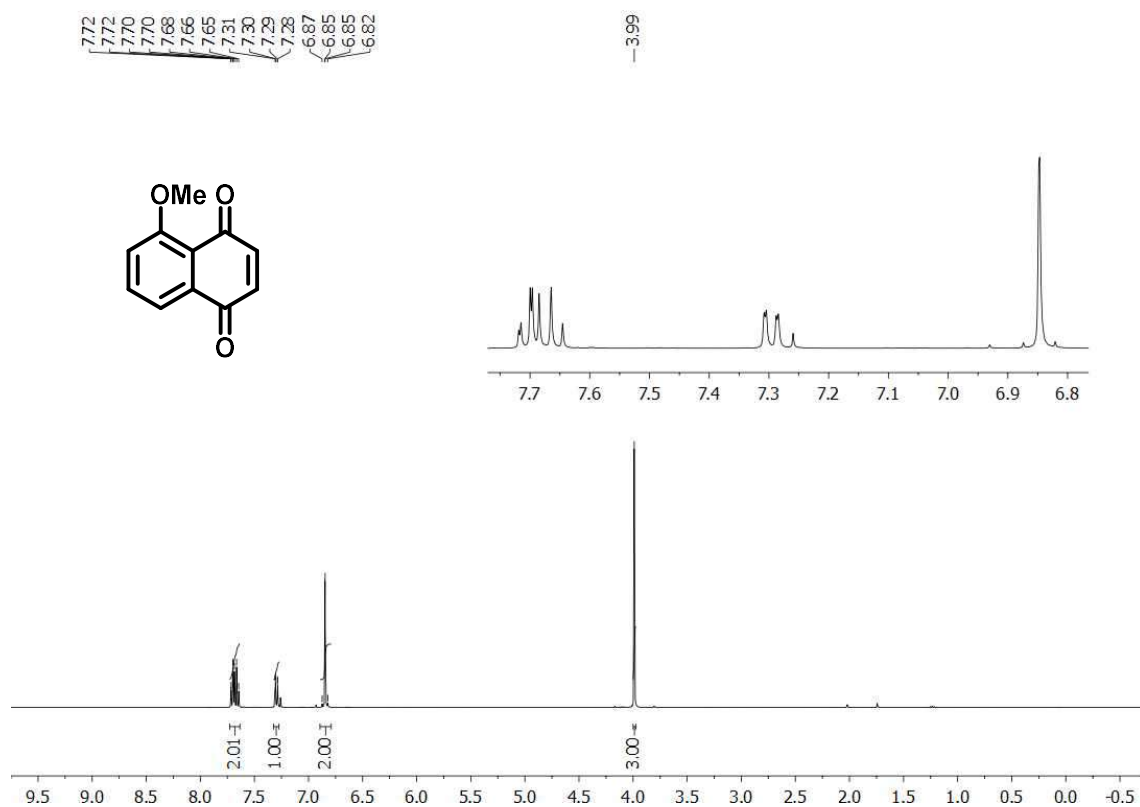
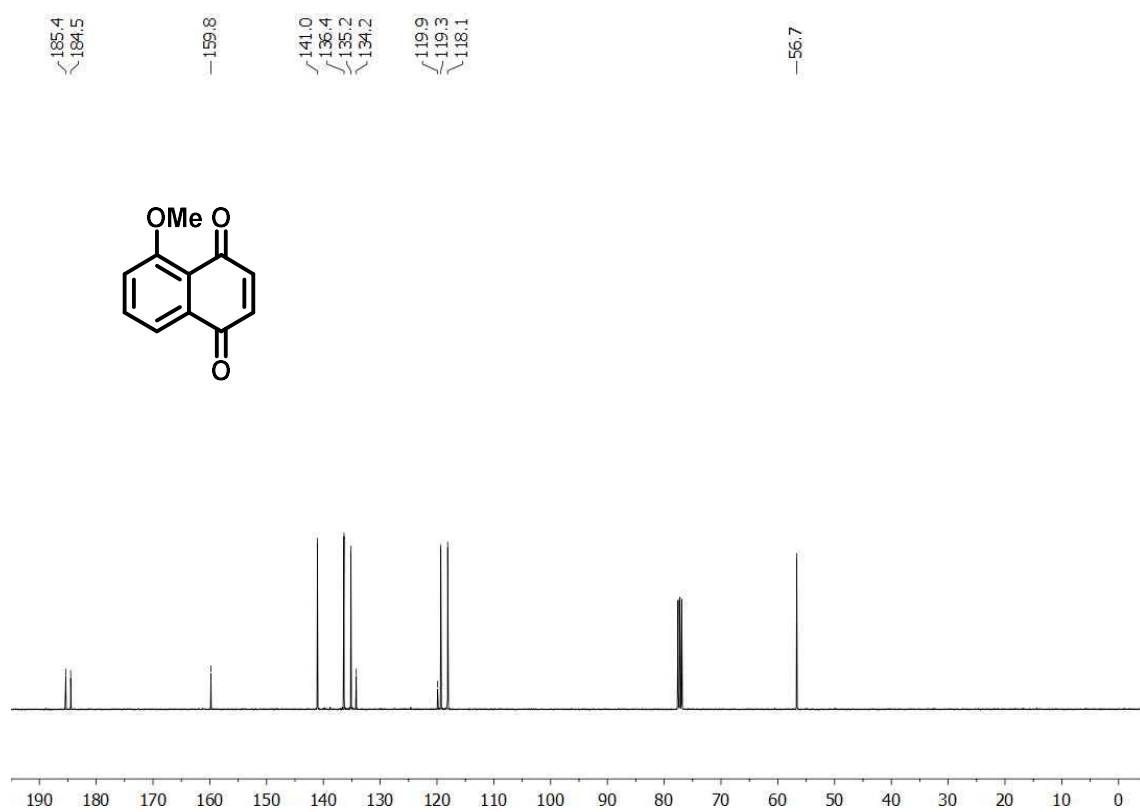


Figure A62. <sup>13</sup>C-NMR spectrum of compound 57g (CDCl<sub>3</sub>, 100 MHz).



**Figure A63.** <sup>1</sup>H-NMR spectrum of compound **57i** (CDCl<sub>3</sub>, 400 MHz).



**Figure A64.** <sup>13</sup>C-NMR spectrum of compound **57i** (CDCl<sub>3</sub>, 100 MHz).

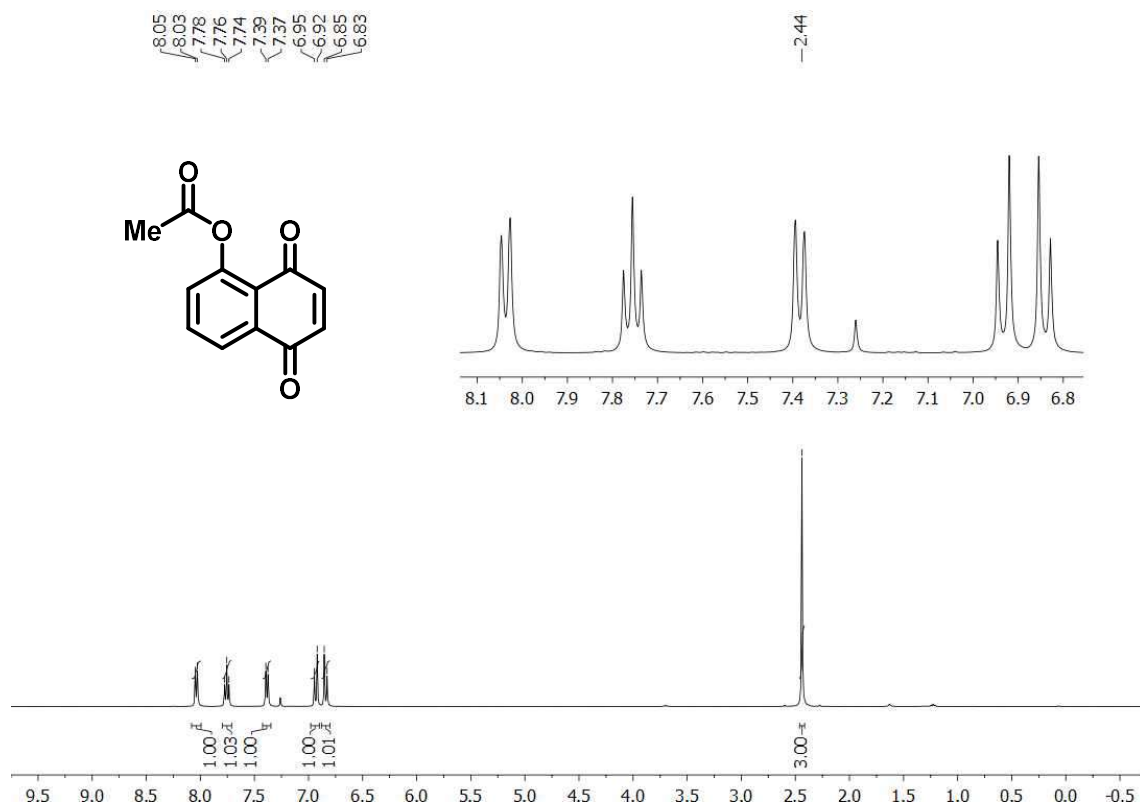


Figure A65. <sup>1</sup>H-NMR spectrum of compound **57j** (CDCl<sub>3</sub>, 400 MHz).

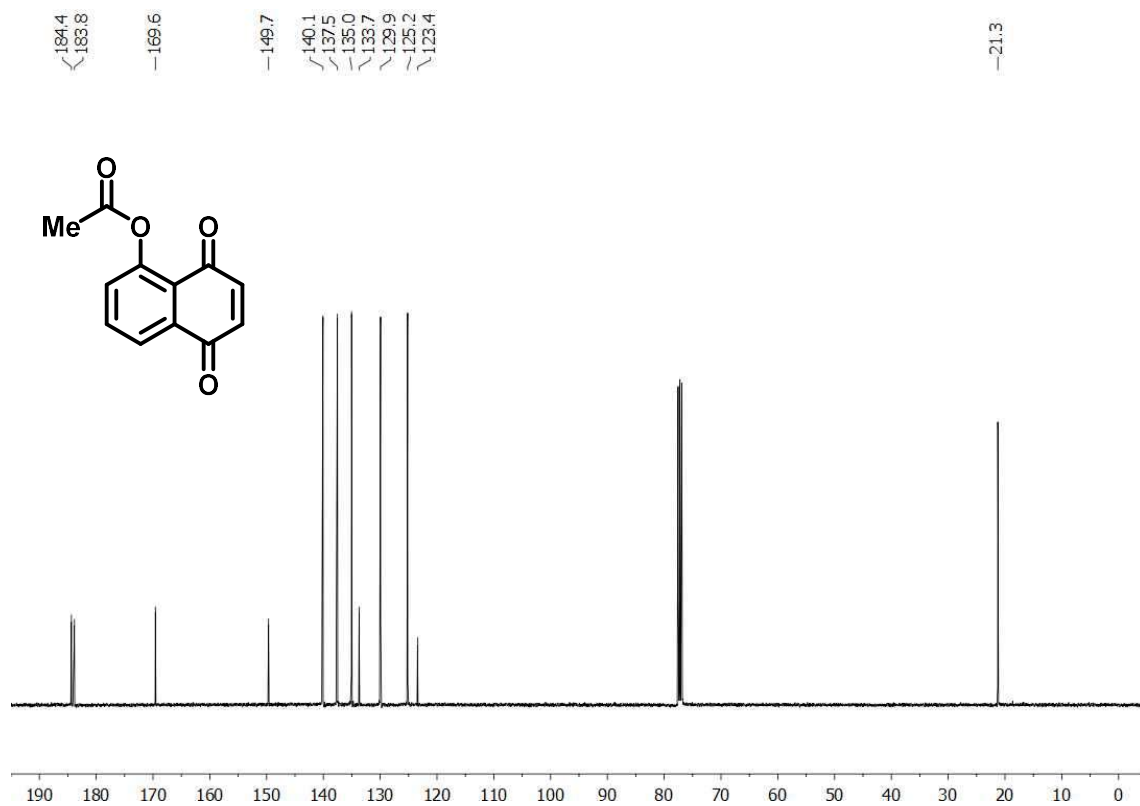
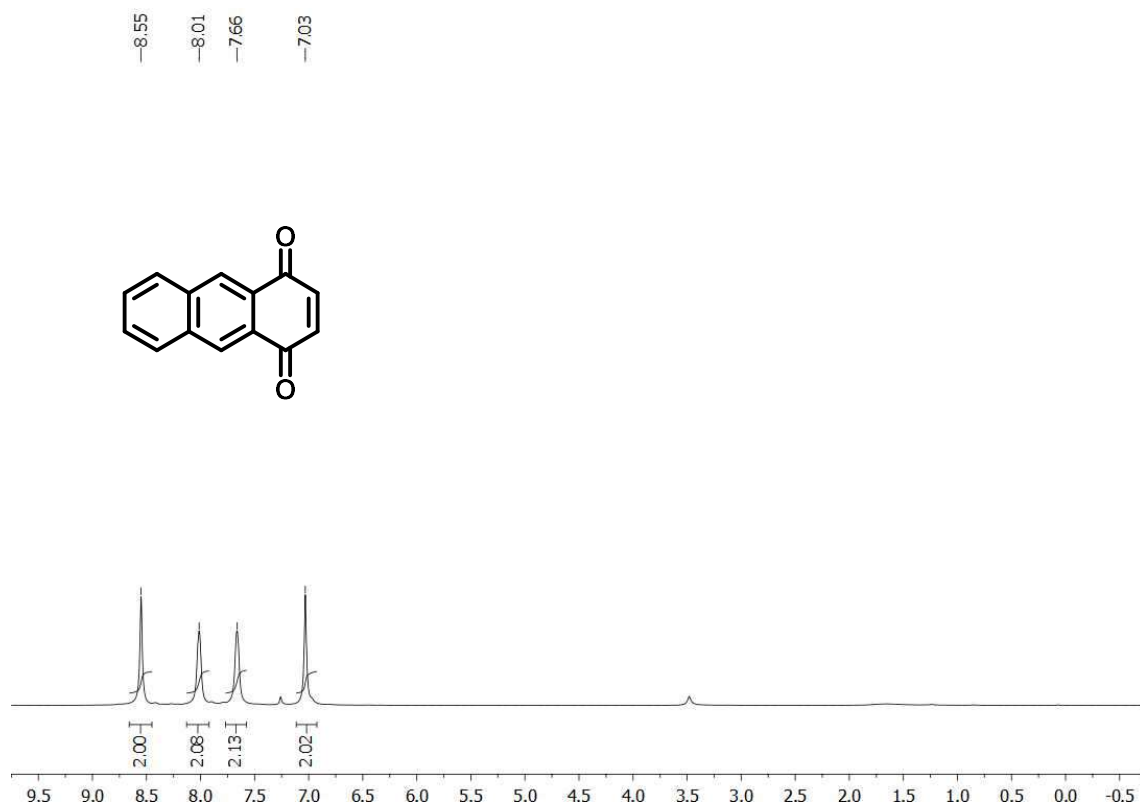
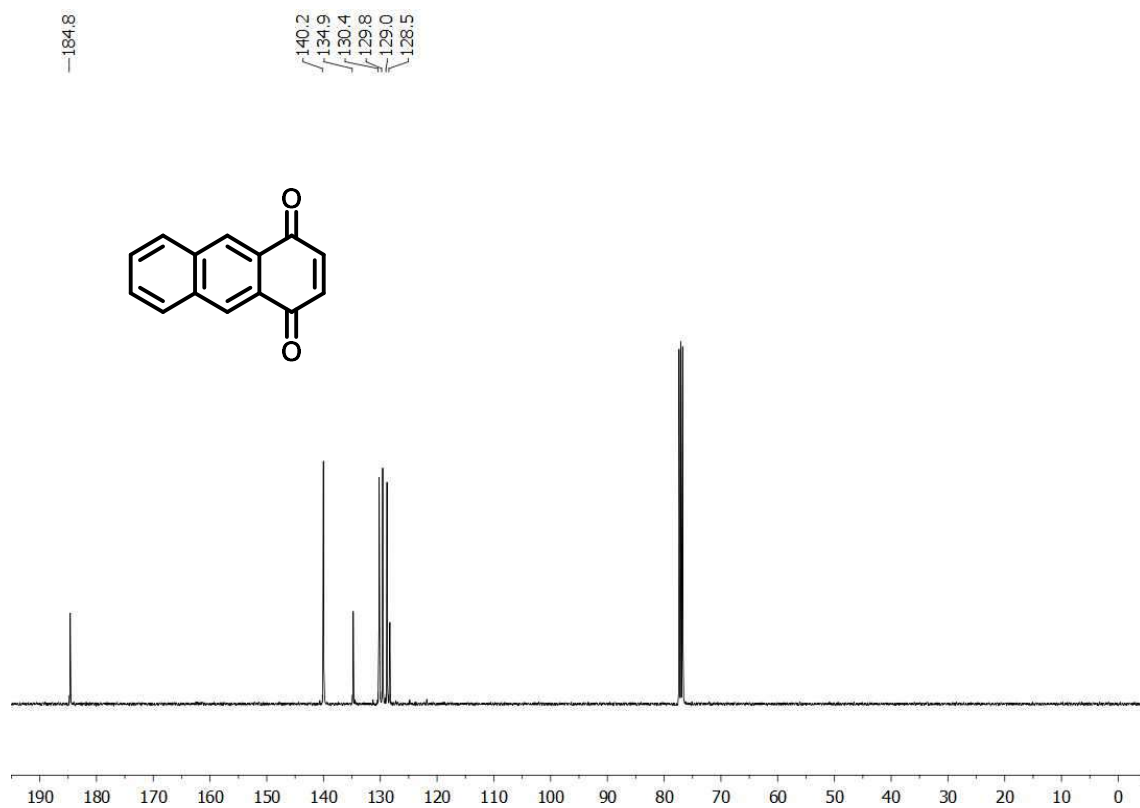


Figure A66. <sup>13</sup>C-NMR spectrum of compound **57j** (CDCl<sub>3</sub>, 100 MHz).



**Figure A67.** <sup>1</sup>H-NMR spectrum of compound **571** (CDCl<sub>3</sub>, 400 MHz).



**Figure A68.** <sup>13</sup>C-NMR spectrum of compound **571** (CDCl<sub>3</sub>, 100 MHz).

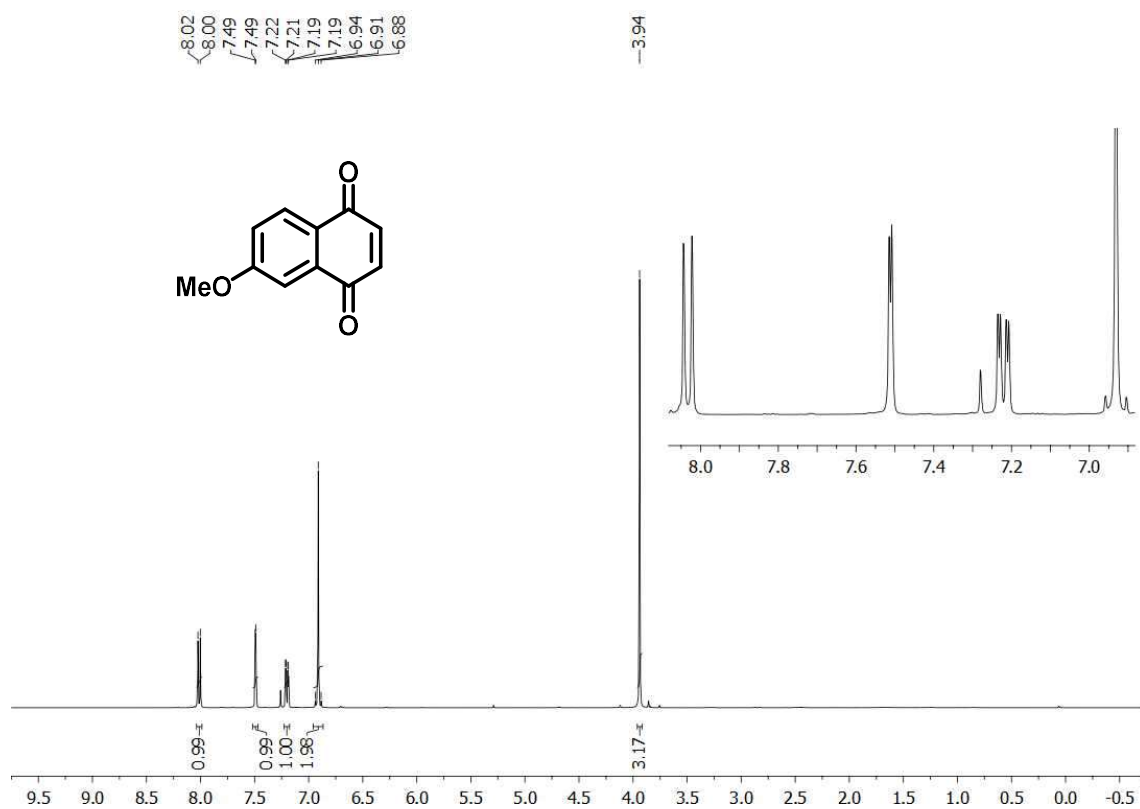


Figure A69. <sup>1</sup>H-NMR spectrum of compound **57m** (CDCl<sub>3</sub>, 400 MHz).

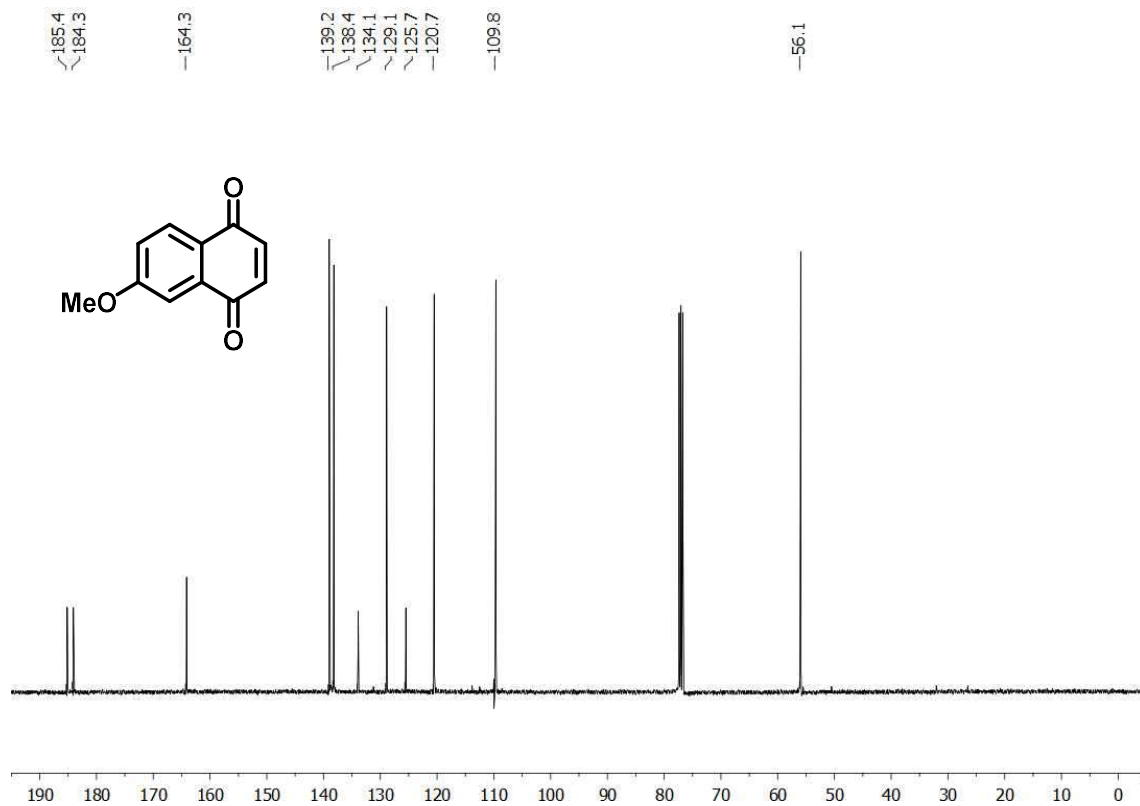
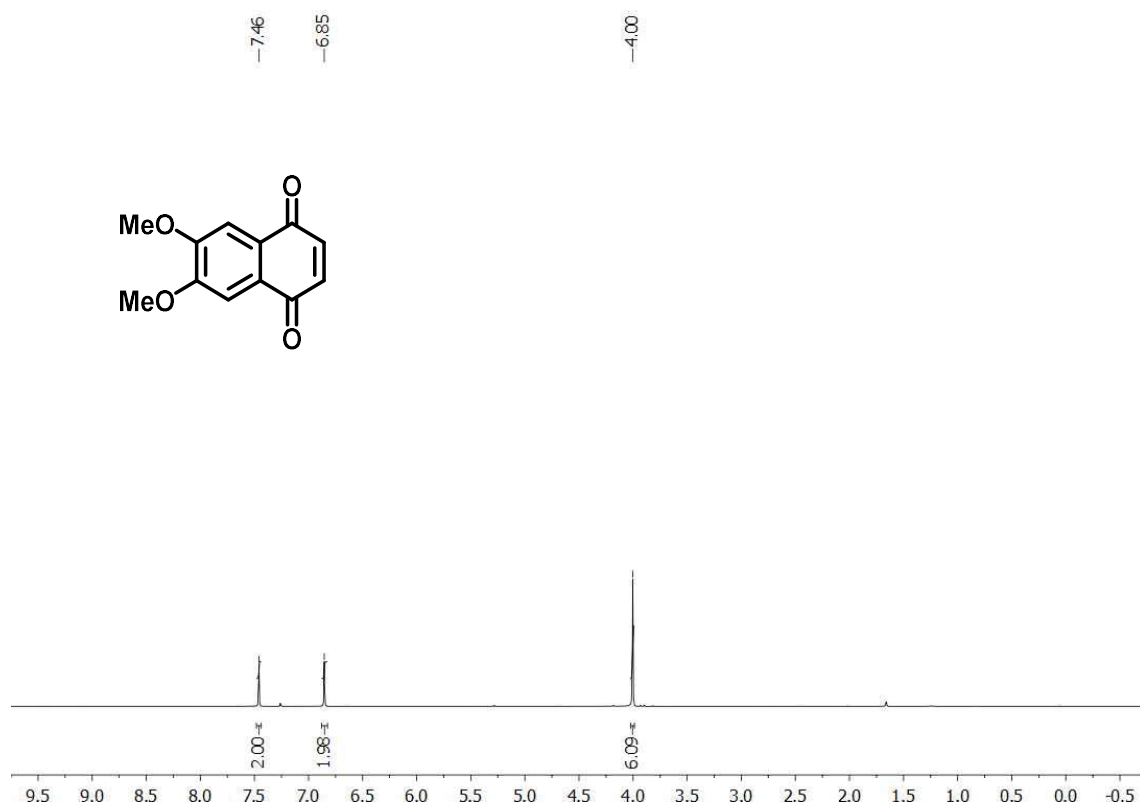
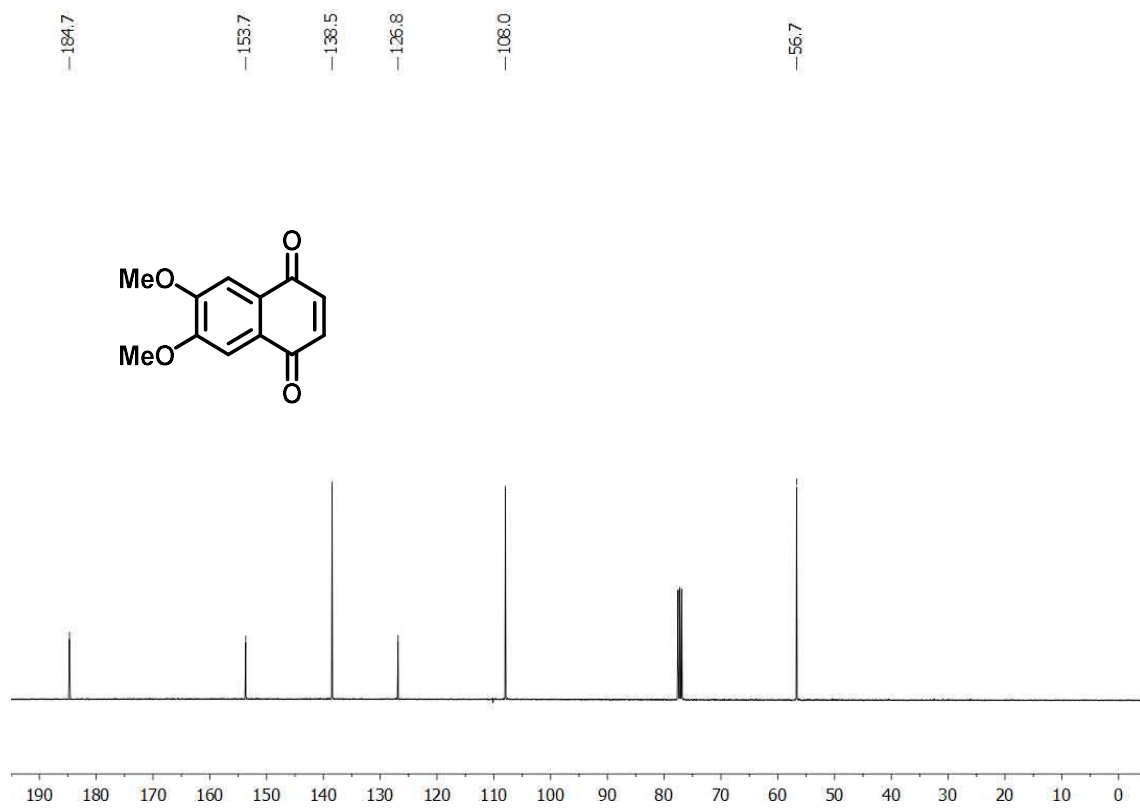


Figure A70. <sup>13</sup>C-NMR spectrum of compound **57m** (CDCl<sub>3</sub>, 100 MHz).



**Figure A71.** <sup>1</sup>H-NMR spectrum of compound **57n** (CDCl<sub>3</sub>, 400 MHz).



**Figure A72.** <sup>13</sup>C-NMR spectrum of compound **57n** (CDCl<sub>3</sub>, 100 MHz).

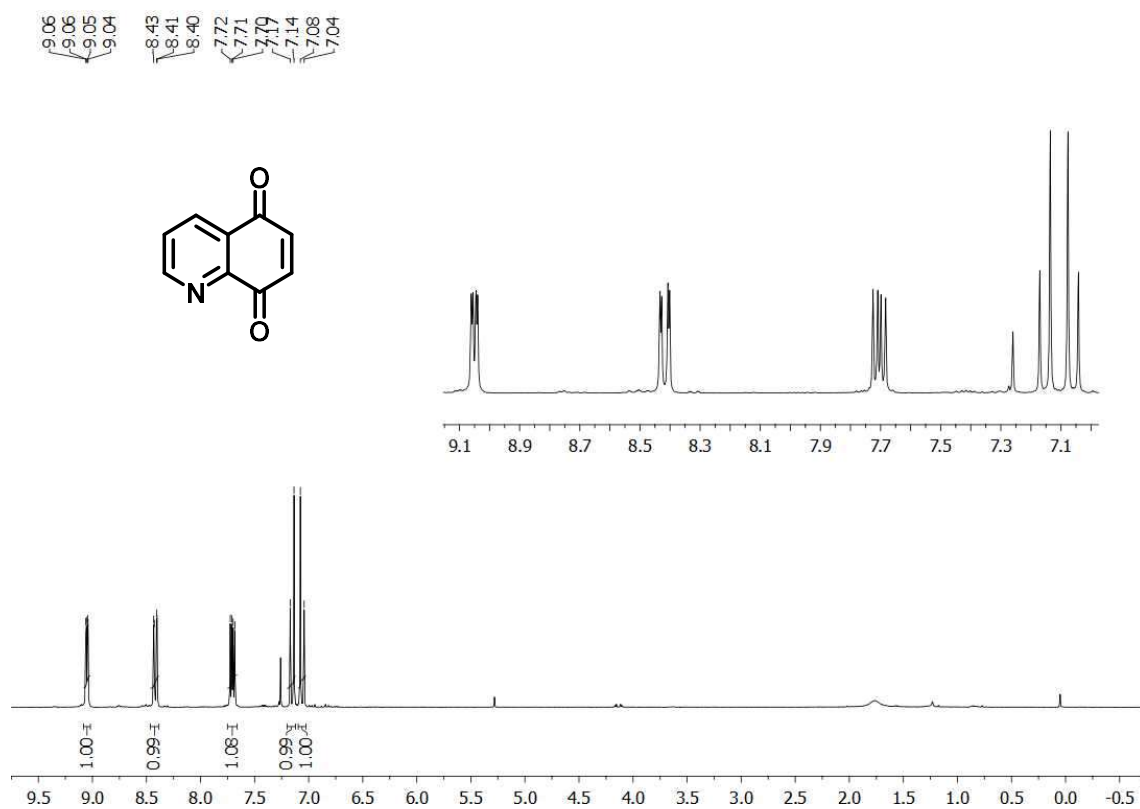


Figure A73. <sup>1</sup>H-NMR spectrum of compound **57o** (CDCl<sub>3</sub>, 400 MHz).

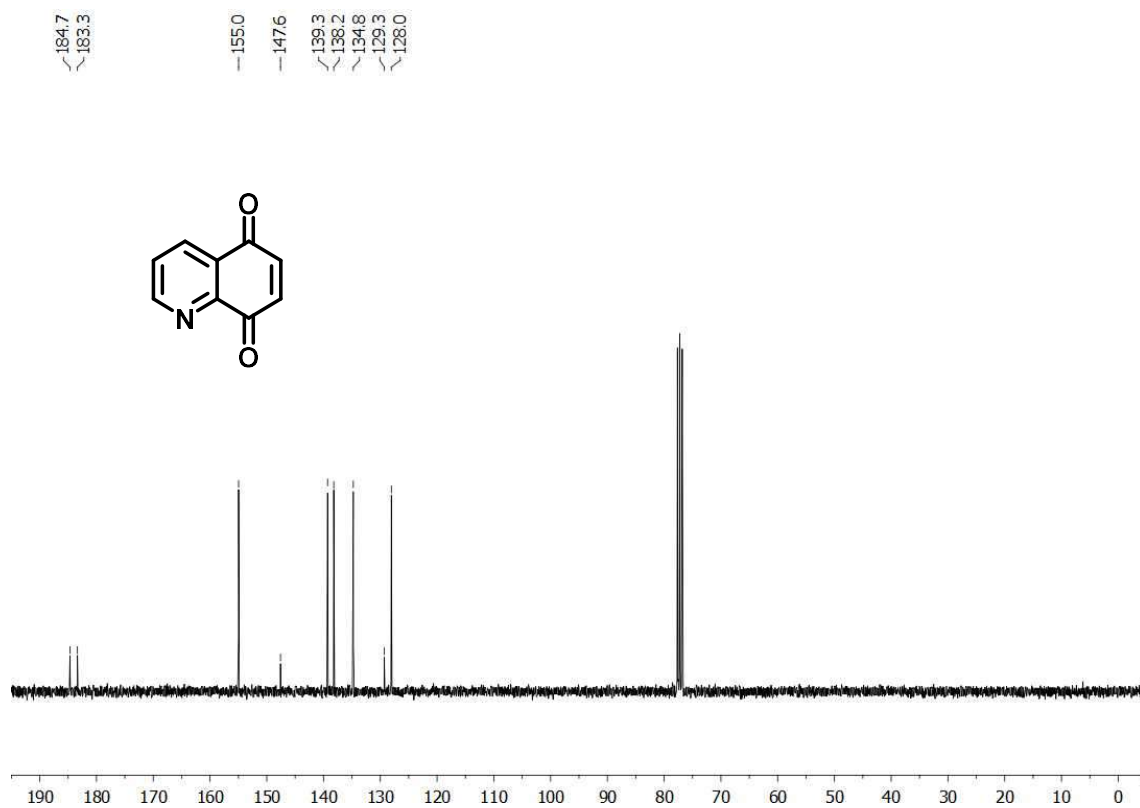


Figure A74. <sup>13</sup>C-NMR spectrum of compound **57o** (CDCl<sub>3</sub>, 100 MHz).



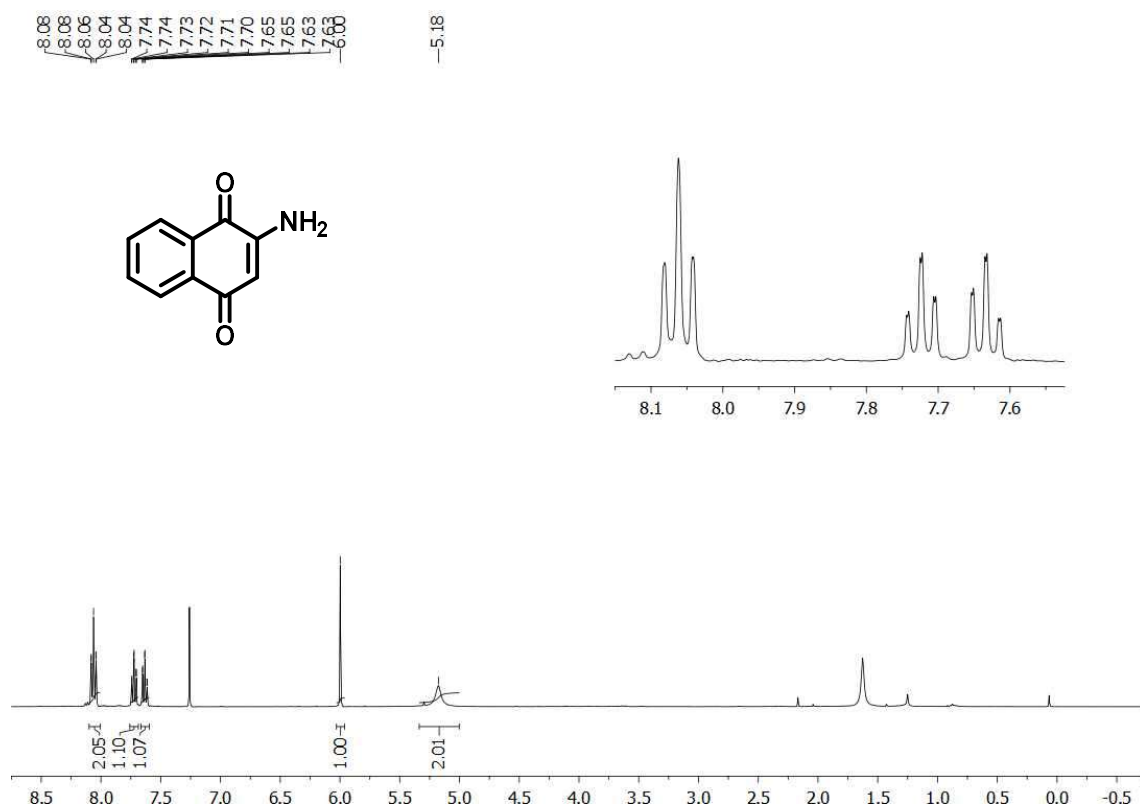


Figure A75. <sup>1</sup>H-NMR spectrum of compound 58a (CDCl<sub>3</sub>, 400 MHz).

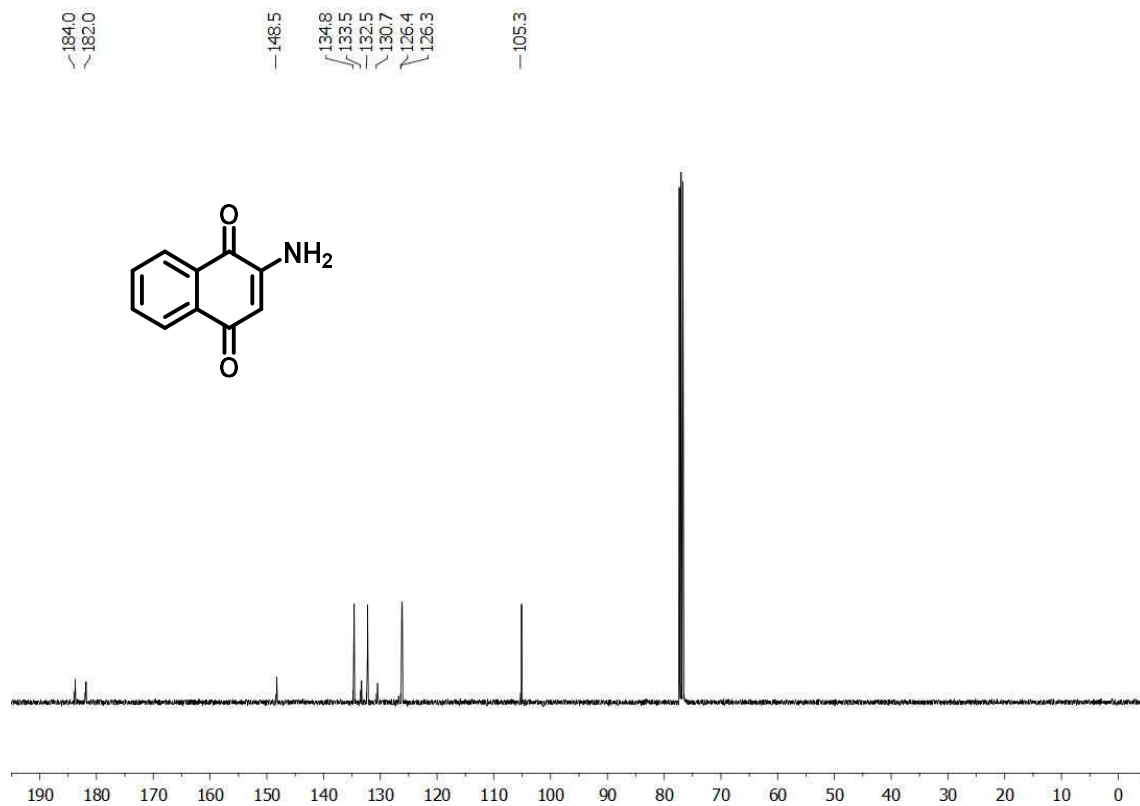


Figure A76. <sup>13</sup>C-NMR spectrum of compound 58a (CDCl<sub>3</sub>, 100 MHz).

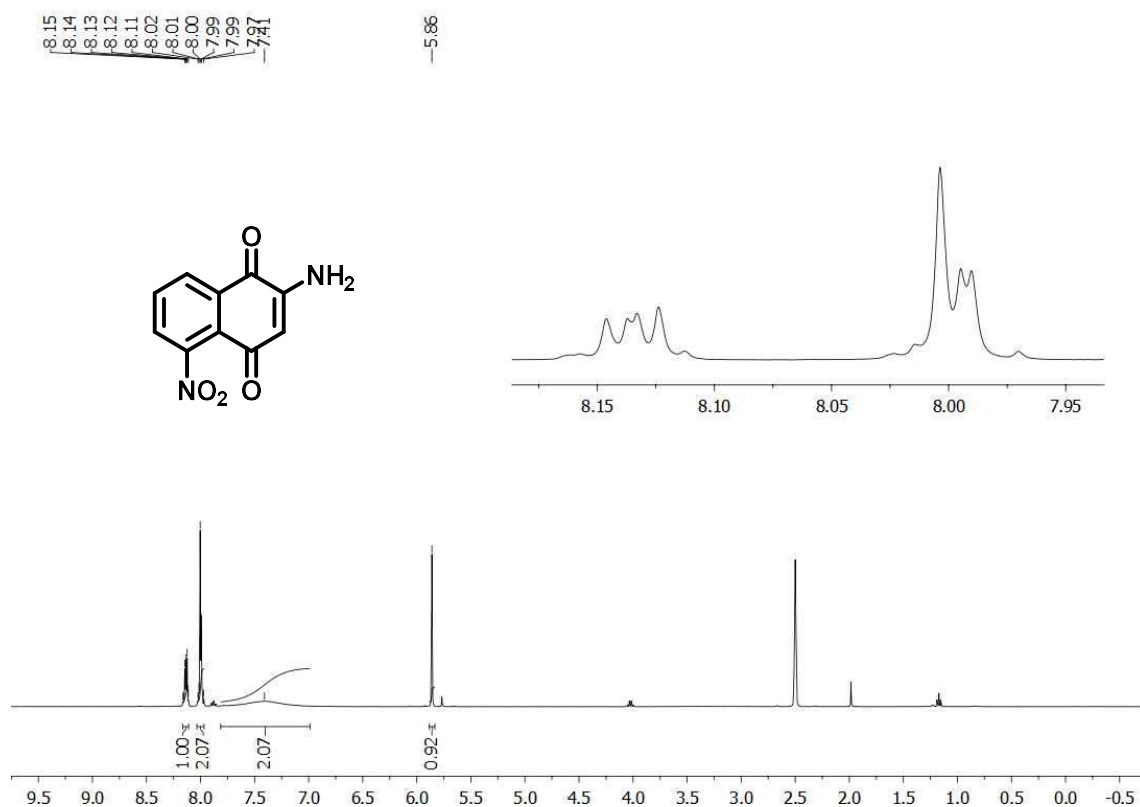


Figure A77. <sup>1</sup>H-NMR spectrum of compound **58b** (DMSO-*d*<sub>6</sub>, 300 MHz).

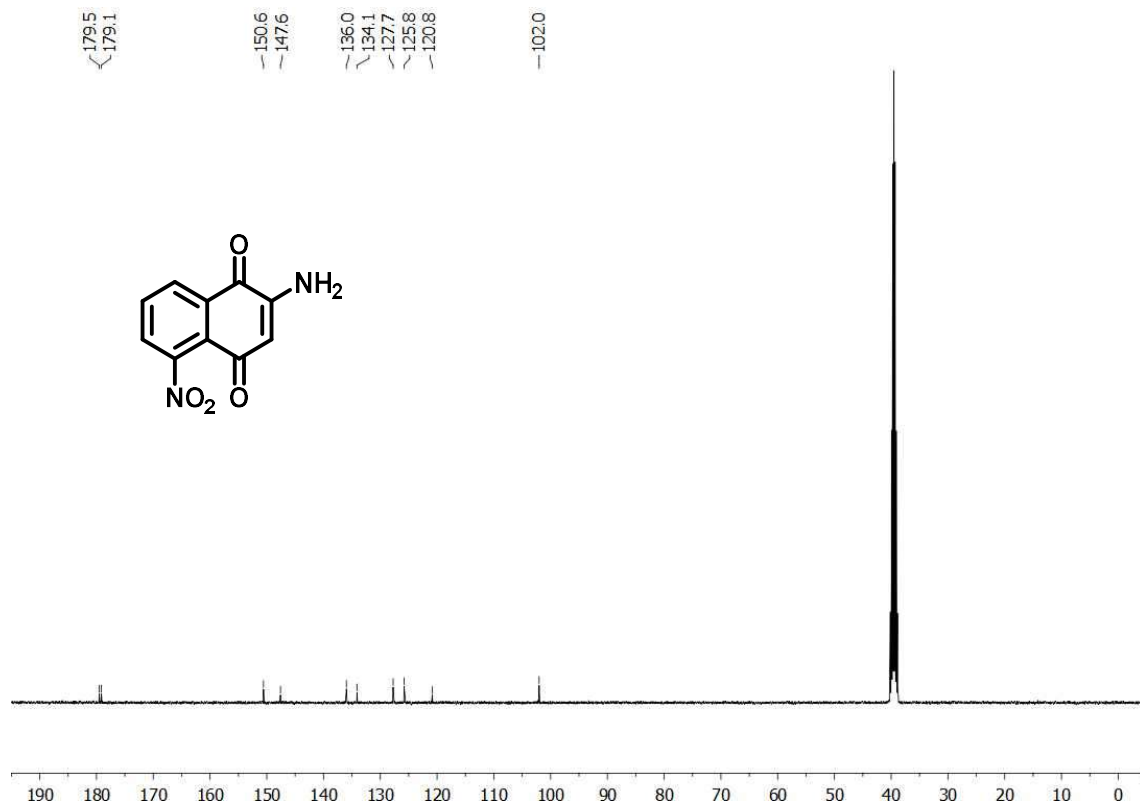
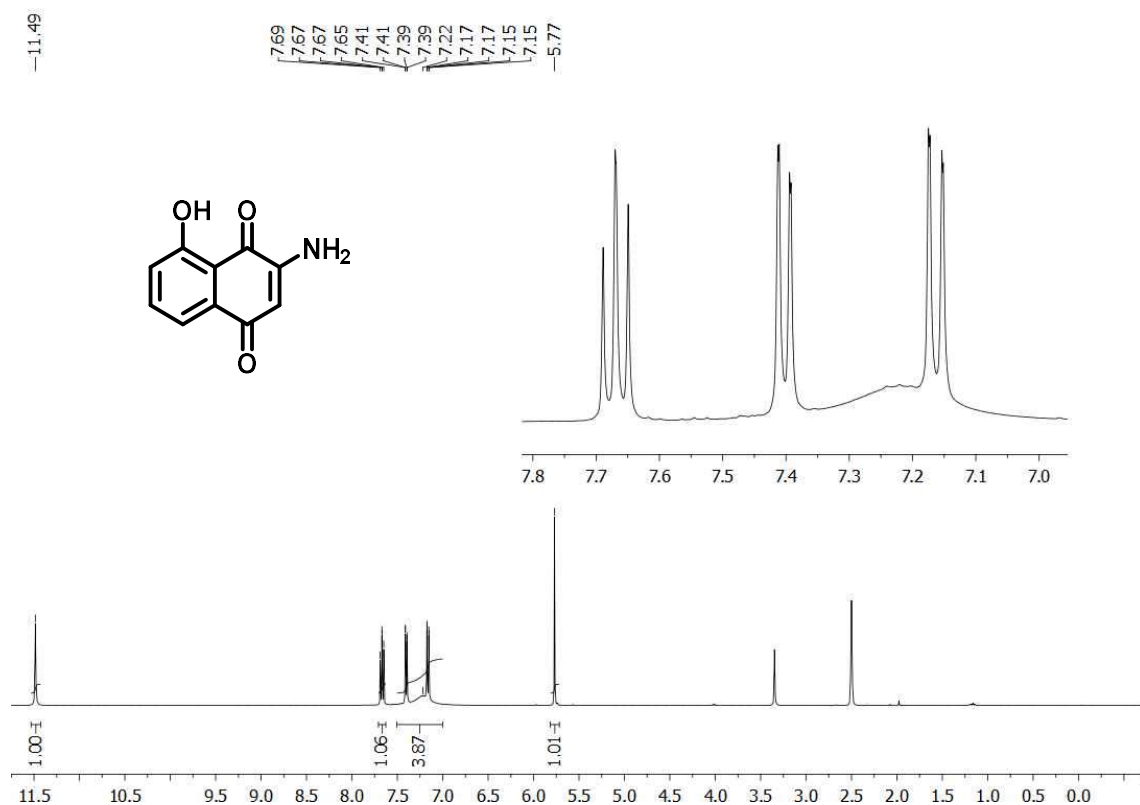
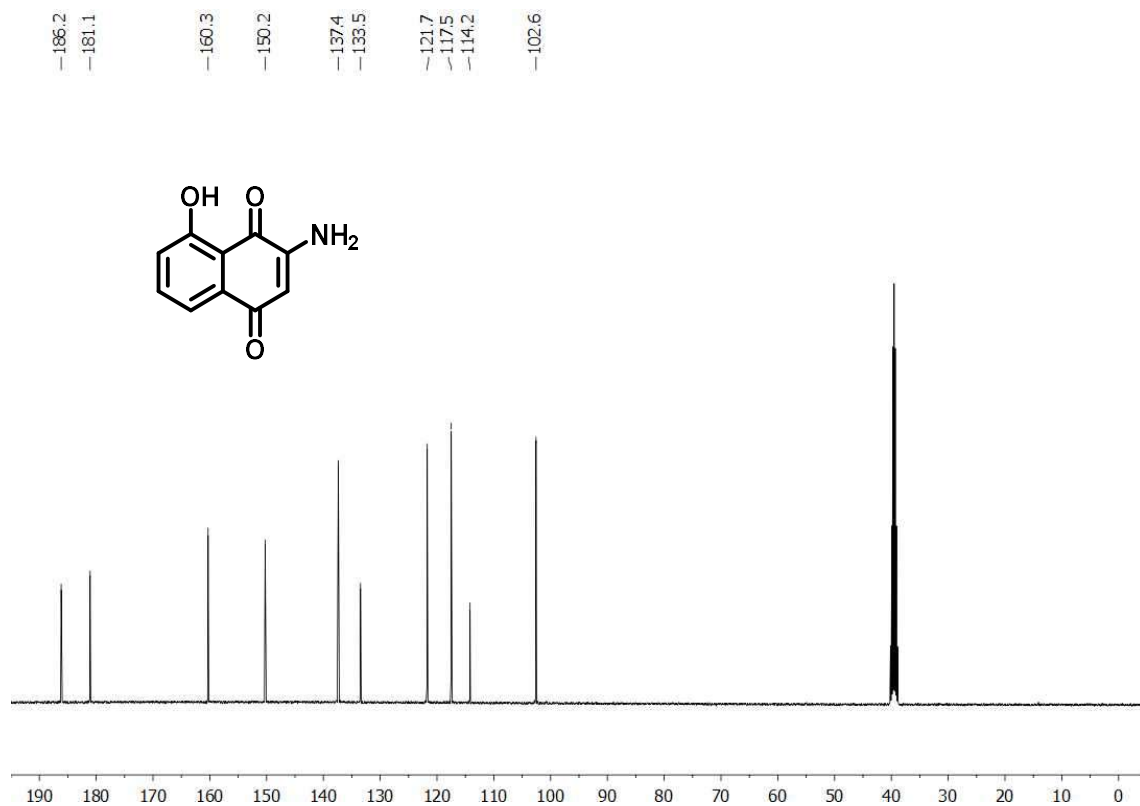


Figure A78. <sup>13</sup>C-NMR spectrum of compound **58b** (DMSO-*d*<sub>6</sub>, 75 MHz).



**Figure A79.** <sup>1</sup>H-NMR spectrum of compound **58c** (DMSO-*d*<sub>6</sub>, 400 MHz).



**Figure A80.** <sup>13</sup>C-NMR spectrum of compound **58c** (DMSO-*d*<sub>6</sub>, 100 MHz).

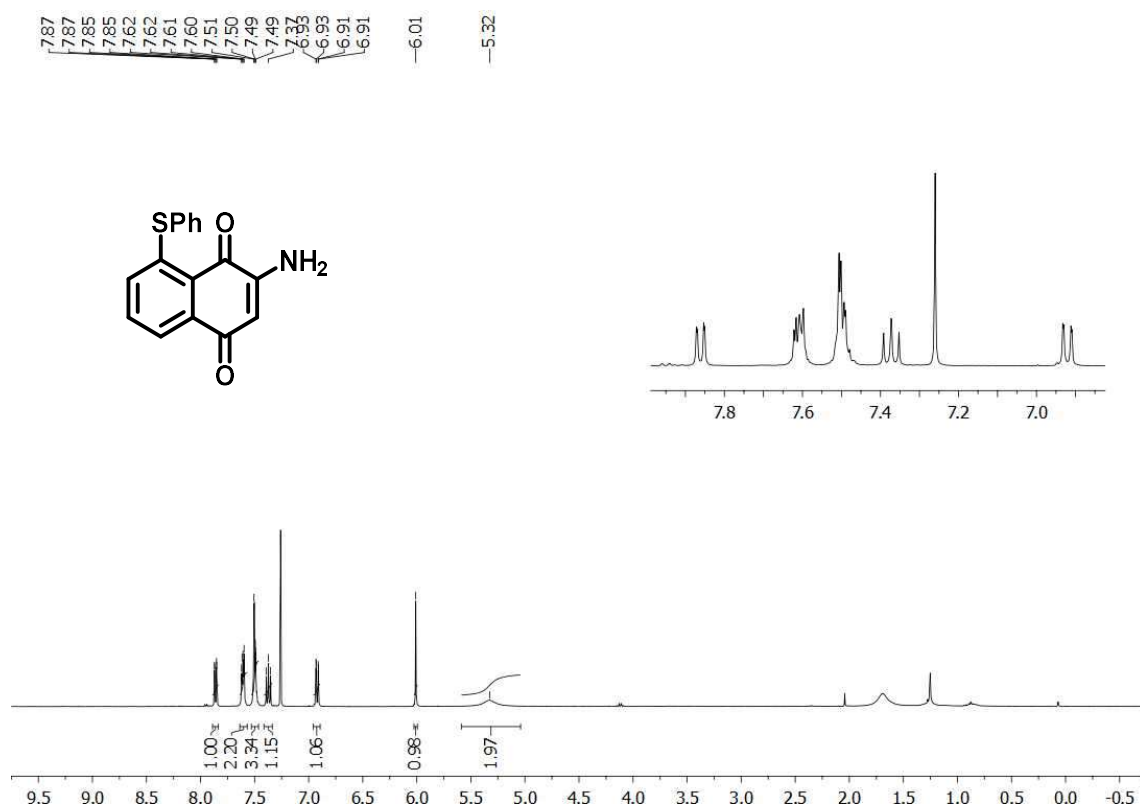


Figure A81. <sup>1</sup>H-NMR spectrum of compound **58d** (CDCl<sub>3</sub>, 400 MHz).

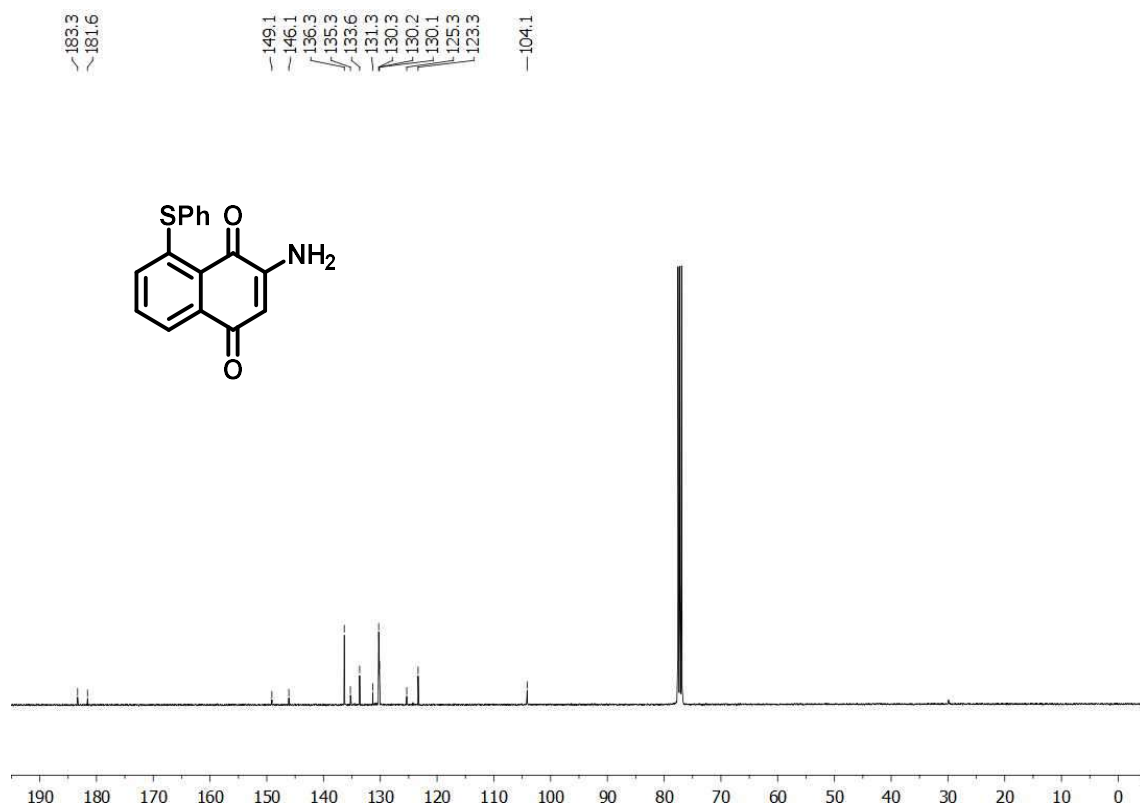


Figure A82. <sup>13</sup>C-NMR spectrum of compound **58d** (CDCl<sub>3</sub>, 100 MHz).

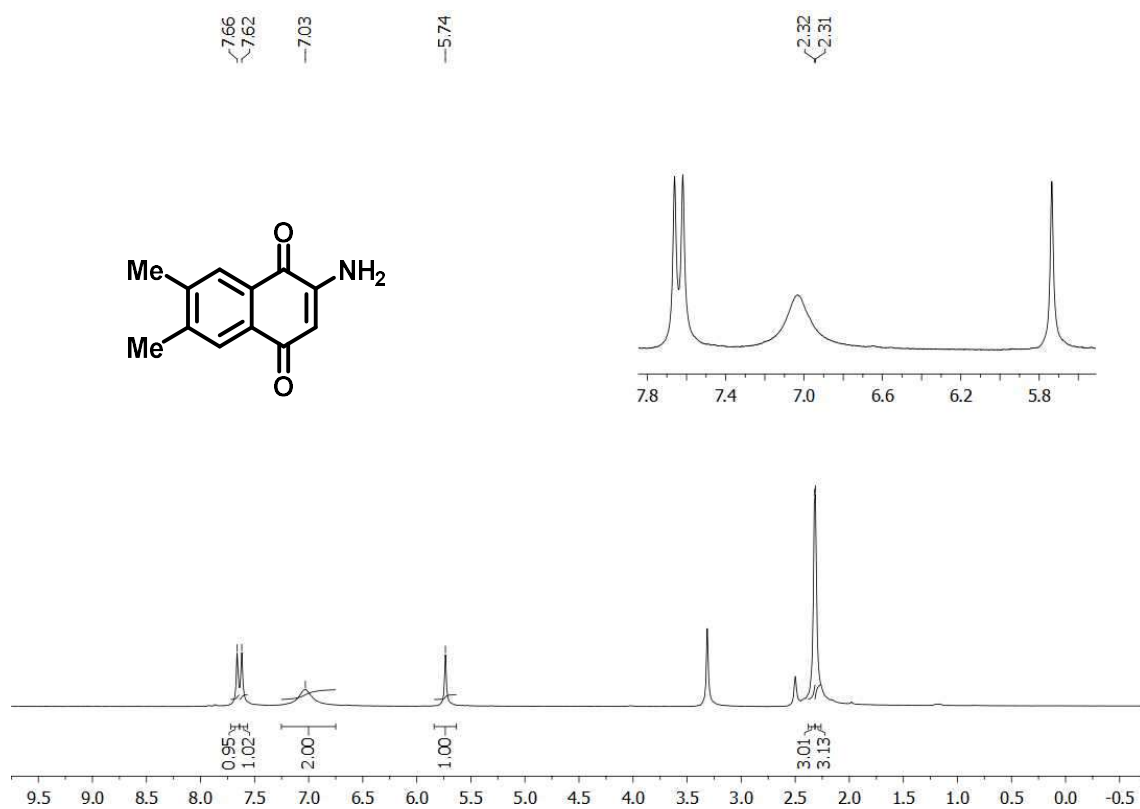


Figure A83. <sup>1</sup>H-NMR spectrum of compound 58e (DMSO-*d*<sub>6</sub>, 400 MHz).

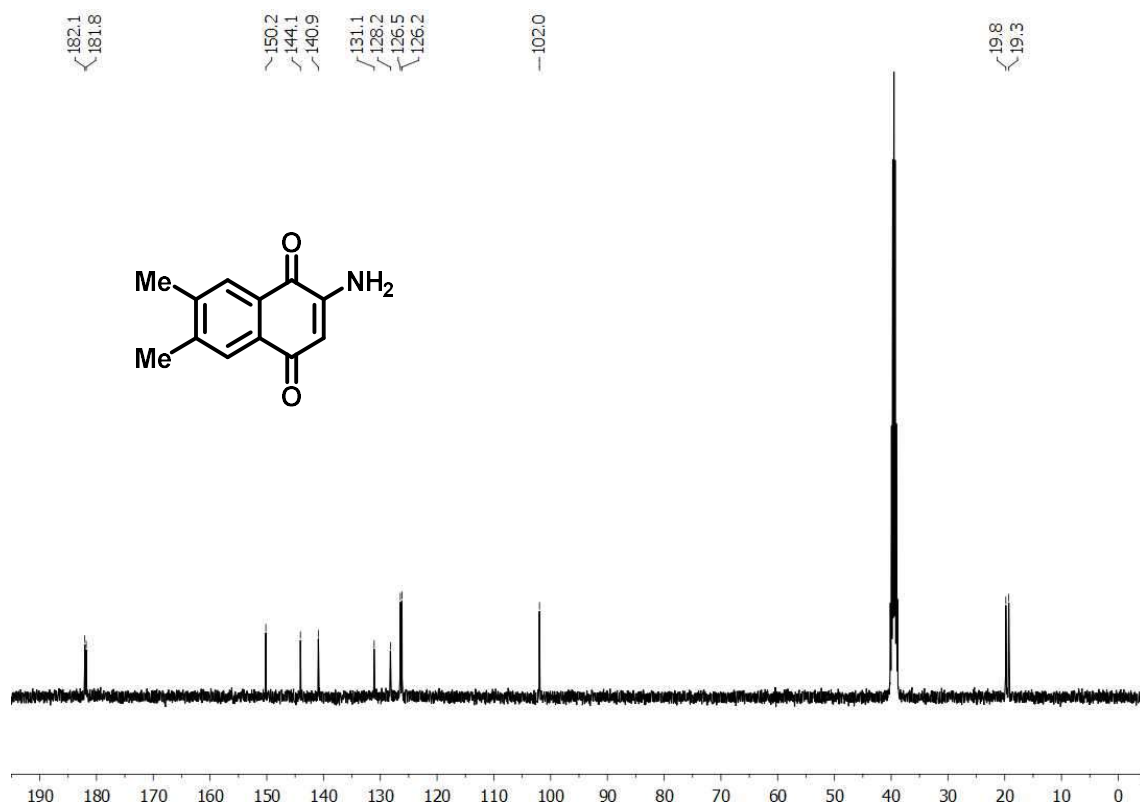


Figure A84. <sup>13</sup>C-NMR spectrum of compound 58e (DMSO-*d*<sub>6</sub>, 100 MHz).

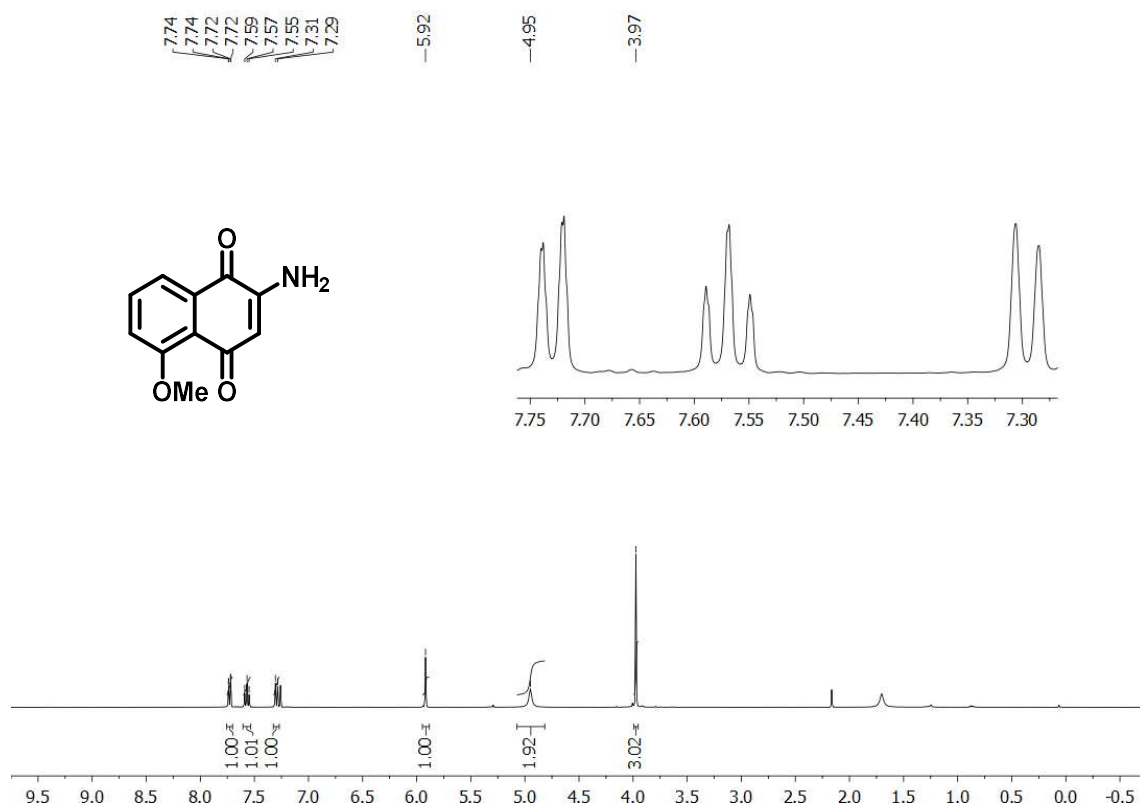


Figure A85. <sup>1</sup>H-NMR spectrum of compound **58f** (CDCl<sub>3</sub>, 400 MHz).

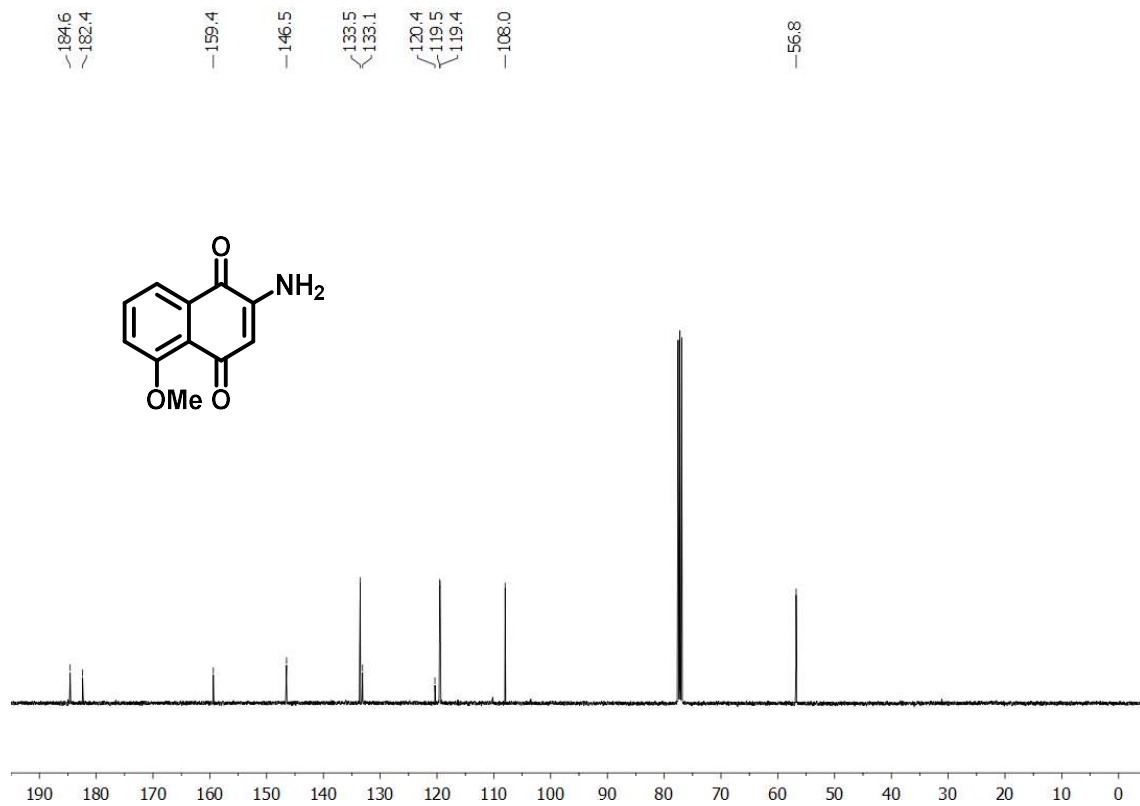


Figure A86. <sup>13</sup>C-NMR spectrum of compound **58f** (CDCl<sub>3</sub>, 100 MHz).

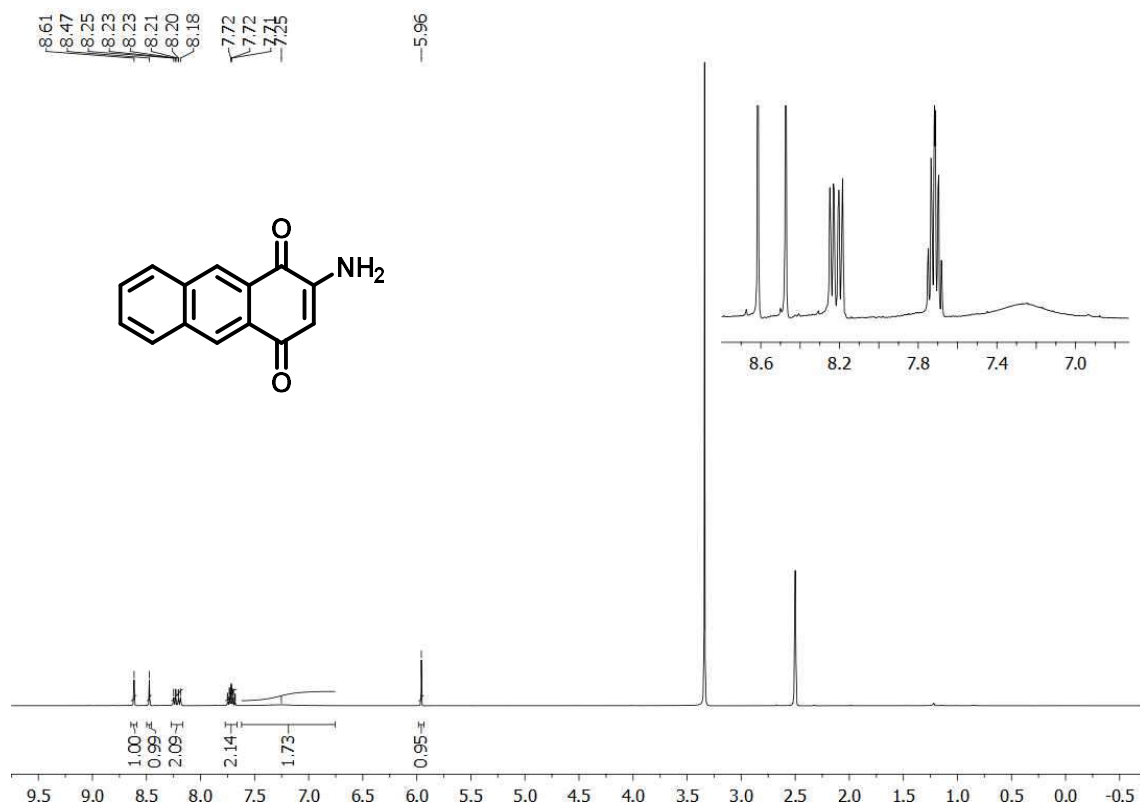


Figure A87. <sup>1</sup>H-NMR spectrum of compound 58g (DMSO-*d*<sub>6</sub>, 400 MHz).

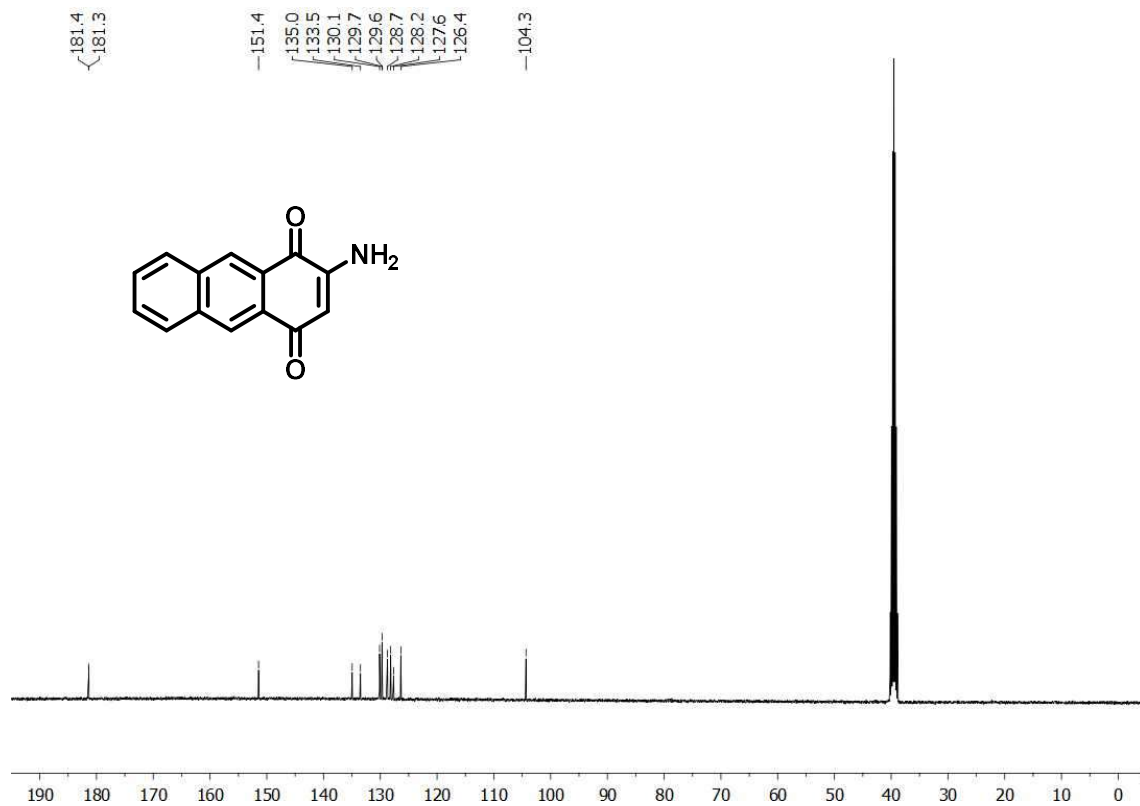


Figure A88. <sup>13</sup>C-NMR spectrum of compound 58g (DMSO-*d*<sub>6</sub>, 100 MHz).

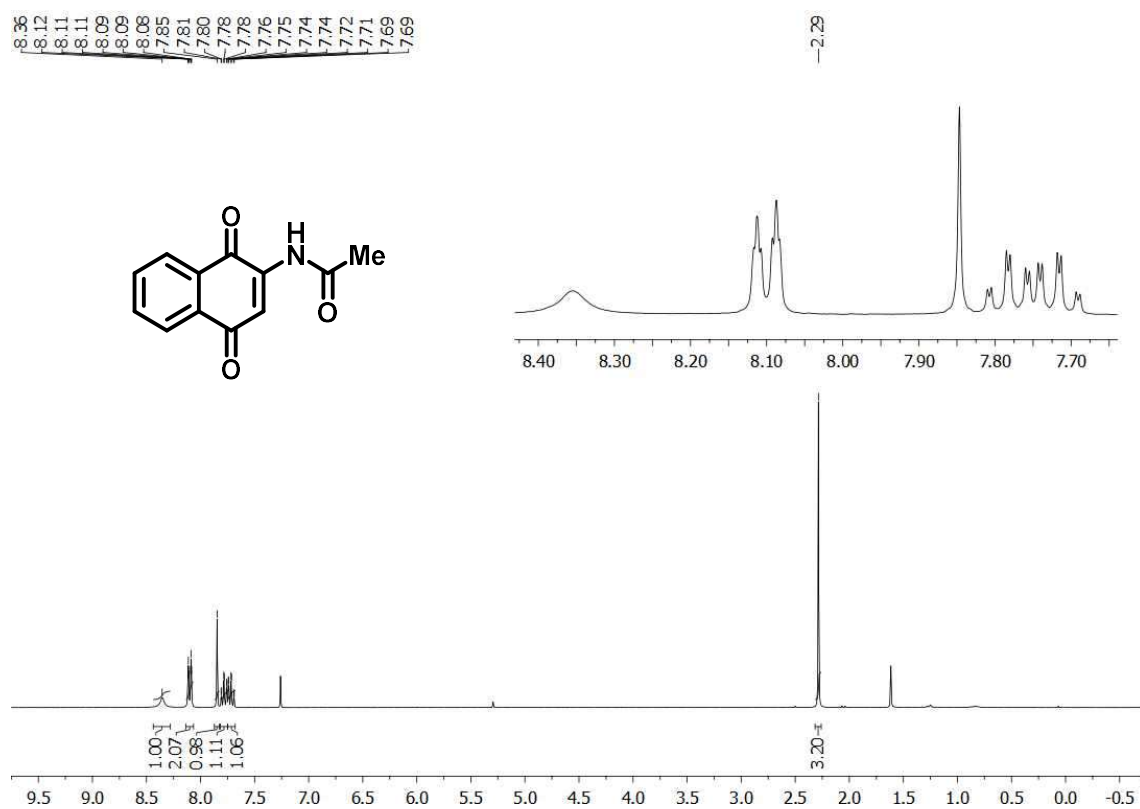


Figure A89. <sup>1</sup>H-NMR spectrum of compound 59a (CDCl<sub>3</sub>, 400 MHz).

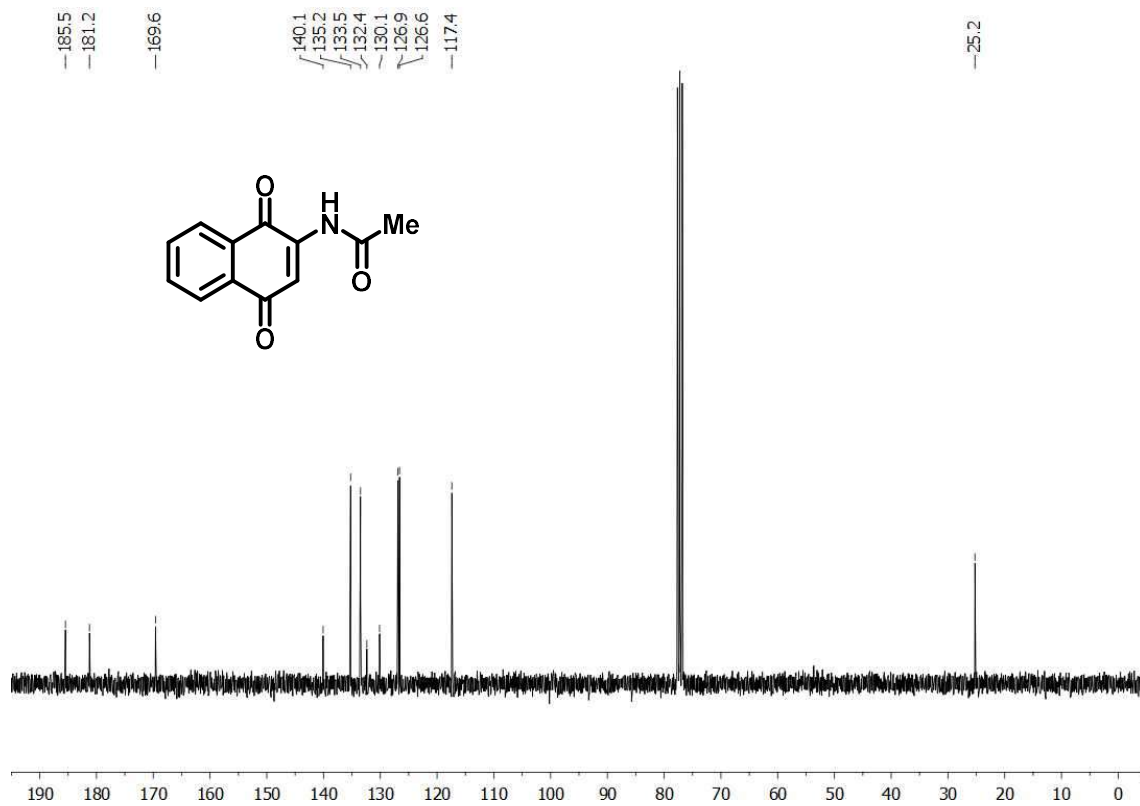


Figure A90. <sup>13</sup>C-NMR spectrum of compound 59a (CDCl<sub>3</sub>, 100 MHz).



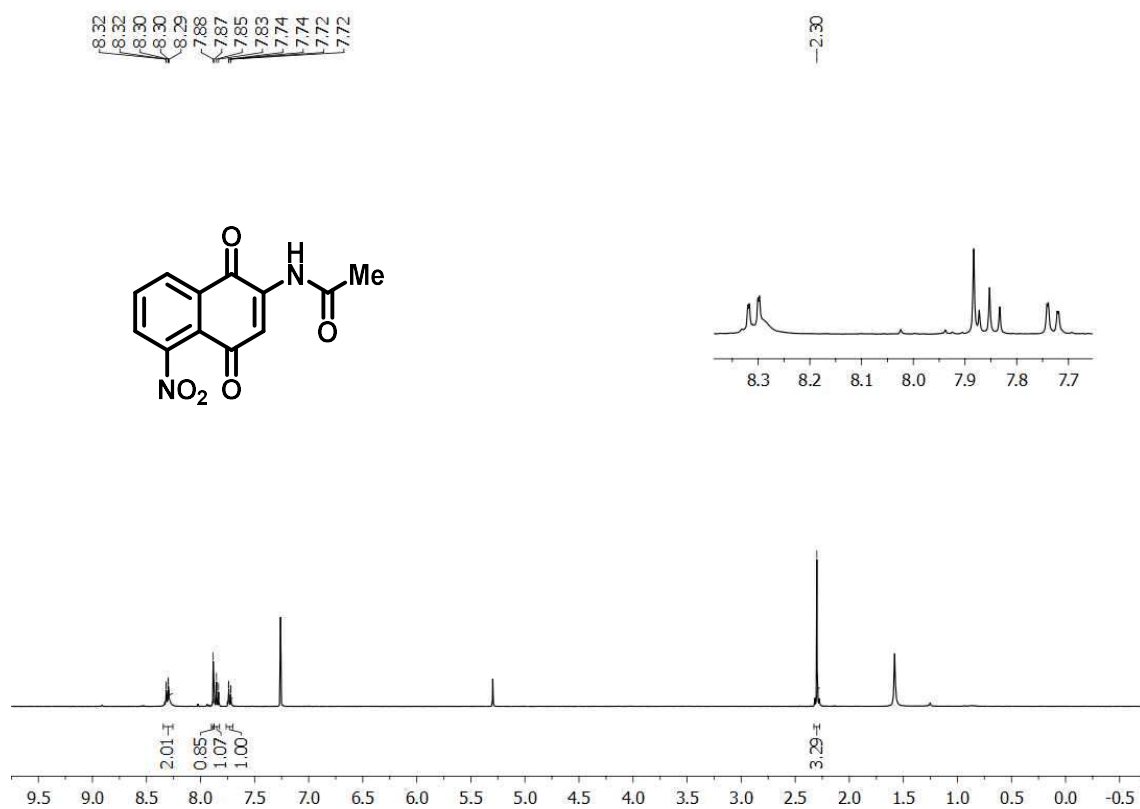


Figure A91. <sup>1</sup>H-NMR spectrum of compound **59b** (CDCl<sub>3</sub>, 400 MHz).



Figure A92. <sup>13</sup>C-NMR spectrum of compound **59b** (CDCl<sub>3</sub>, 100 MHz).

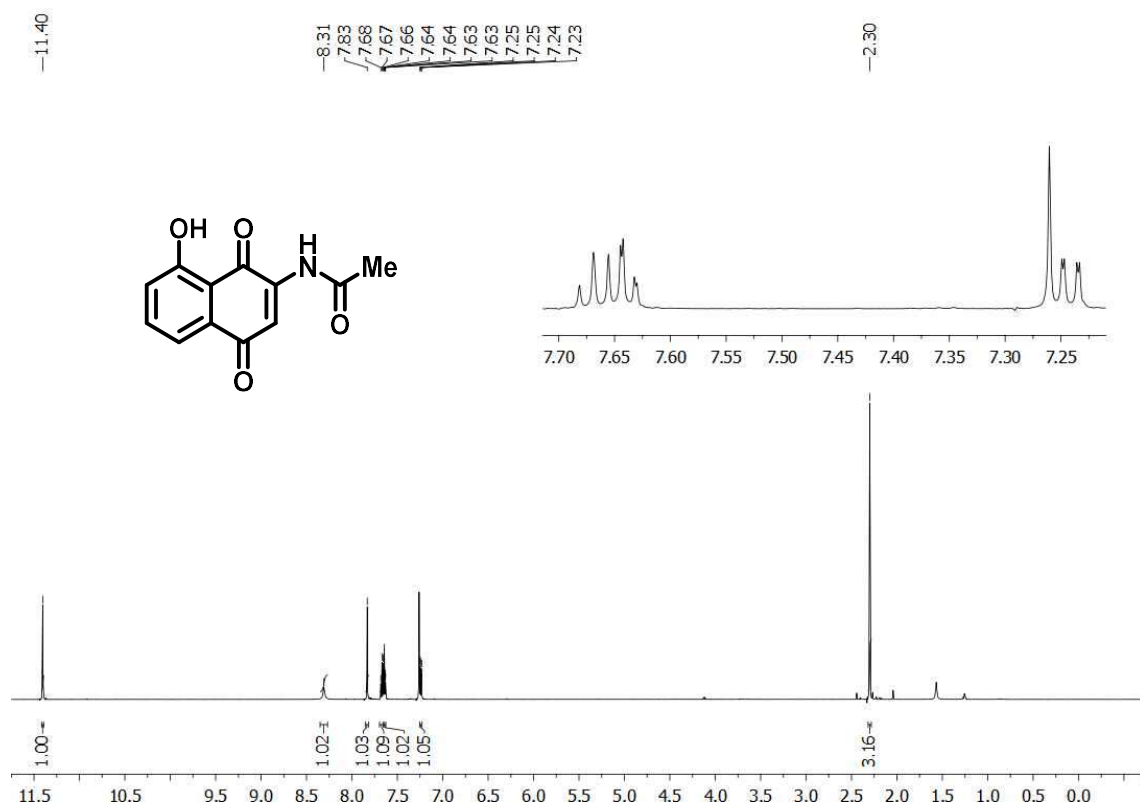


Figure A93. <sup>1</sup>H-NMR spectrum of compound 59c (CDCl<sub>3</sub>, 600 MHz).

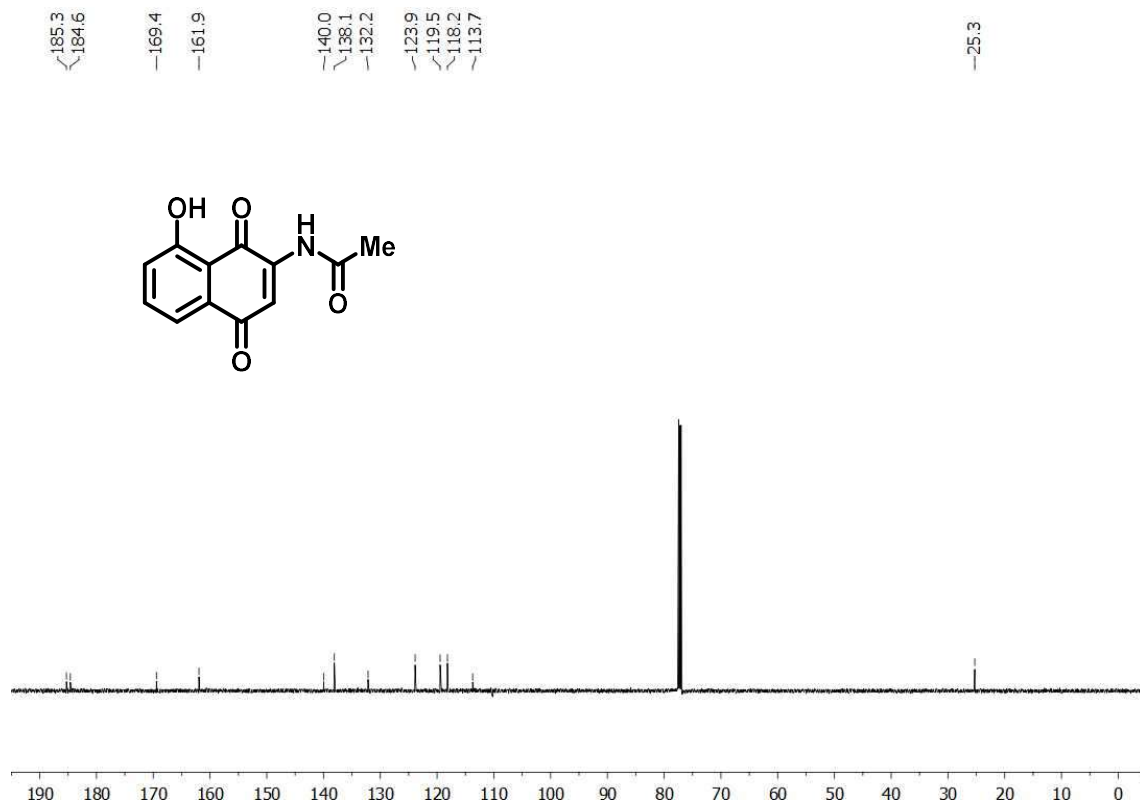


Figure A94. <sup>13</sup>C-NMR spectrum of compound 59c (CDCl<sub>3</sub>, 150 MHz).

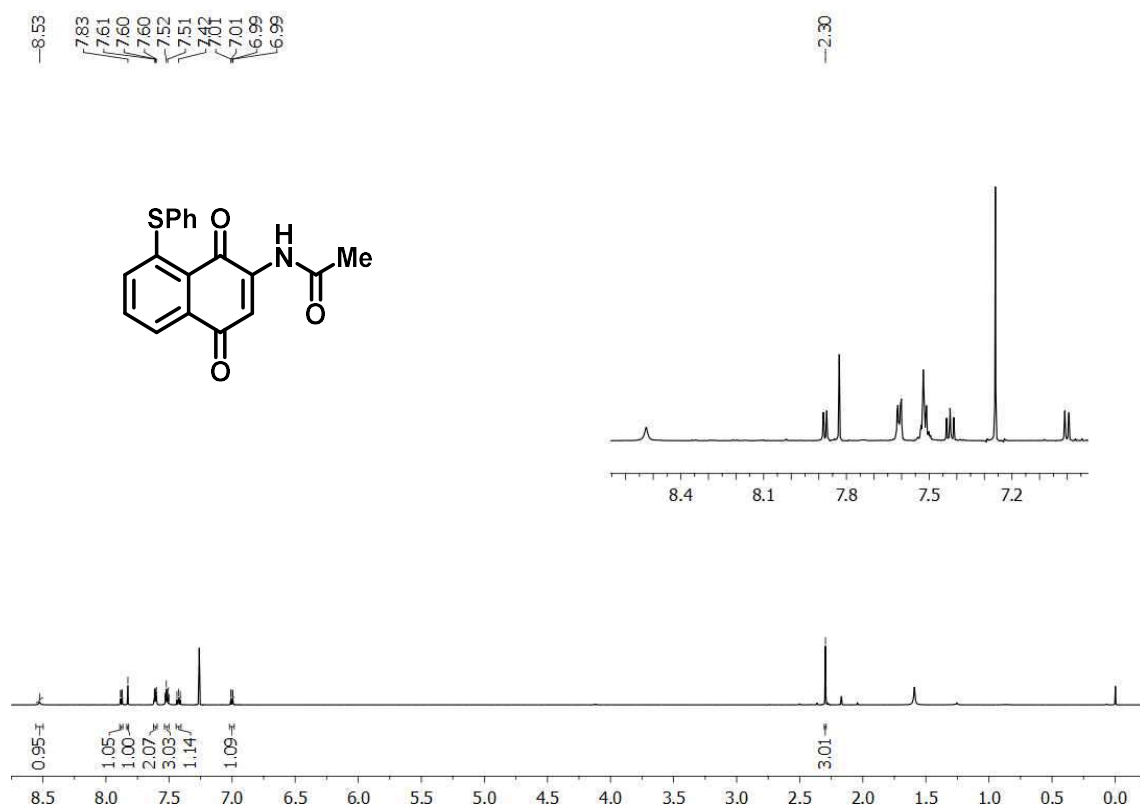


Figure A95. <sup>1</sup>H-NMR spectrum of compound **59d** (CDCl<sub>3</sub>, 600 MHz).

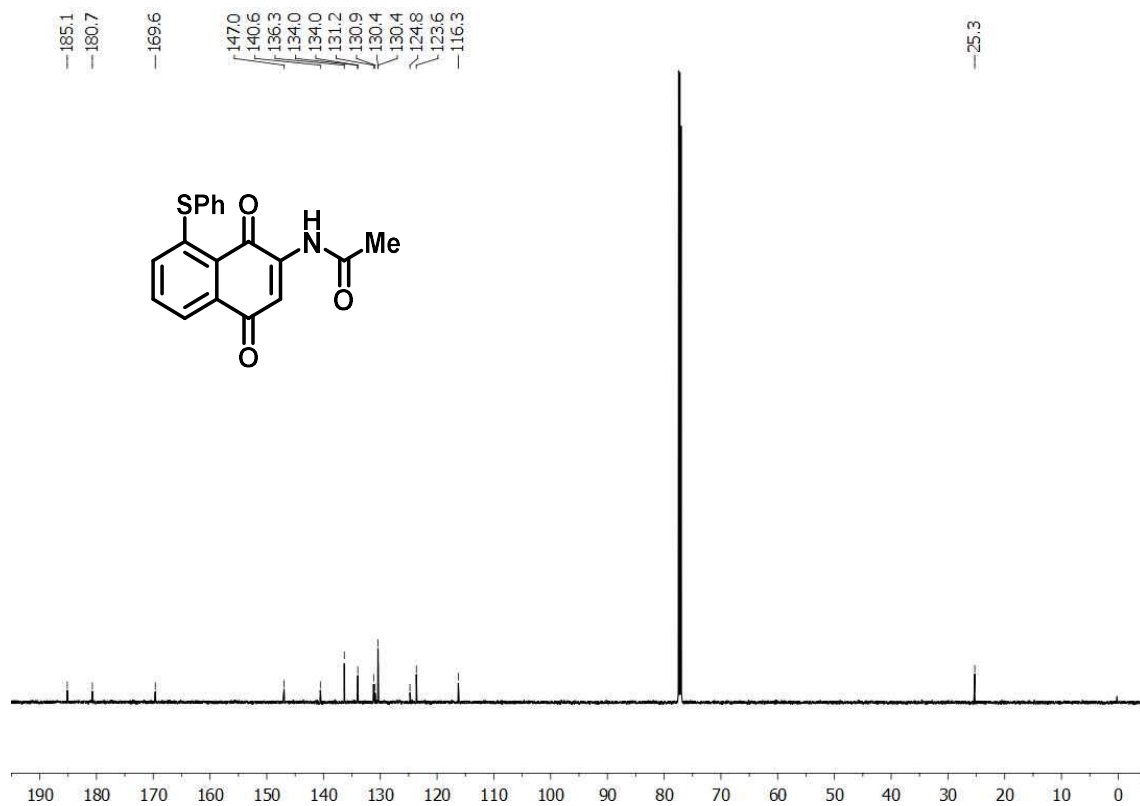


Figure A96. <sup>13</sup>C-NMR spectrum of compound **59d** (CDCl<sub>3</sub>, 150 MHz).

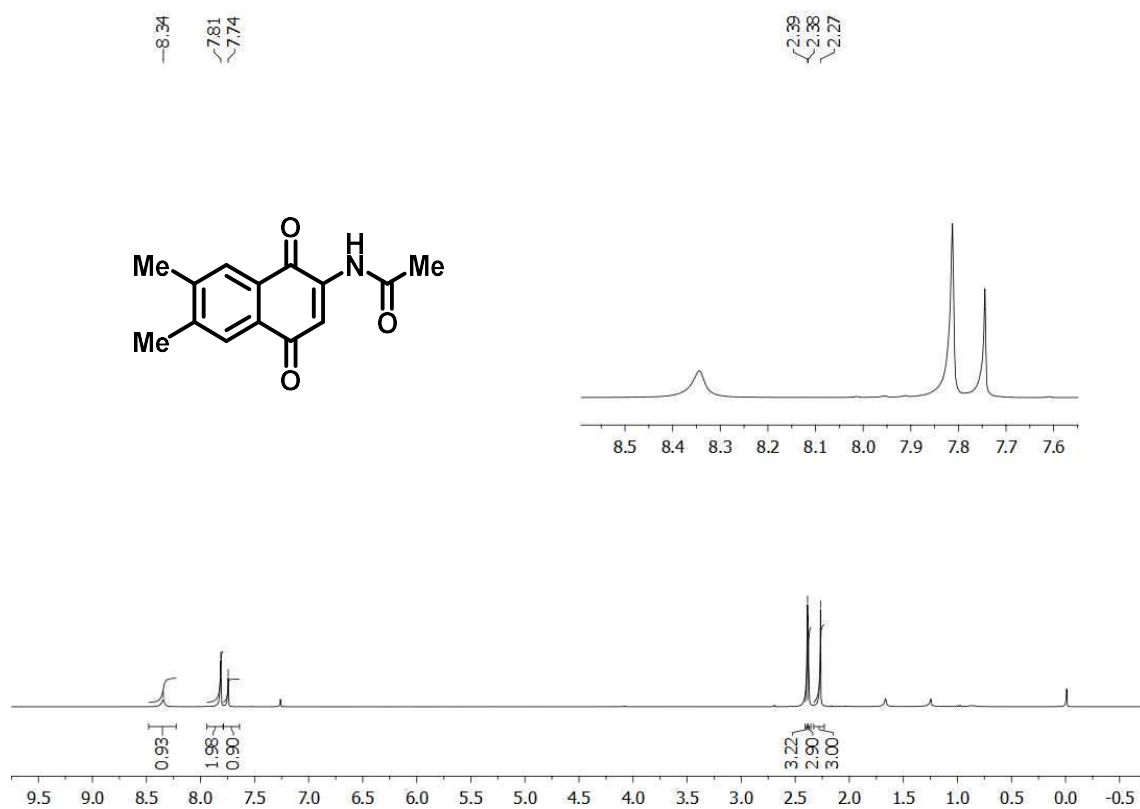


Figure A97. <sup>1</sup>H-NMR spectrum of compound **59e** (CDCl<sub>3</sub>, 400 MHz).

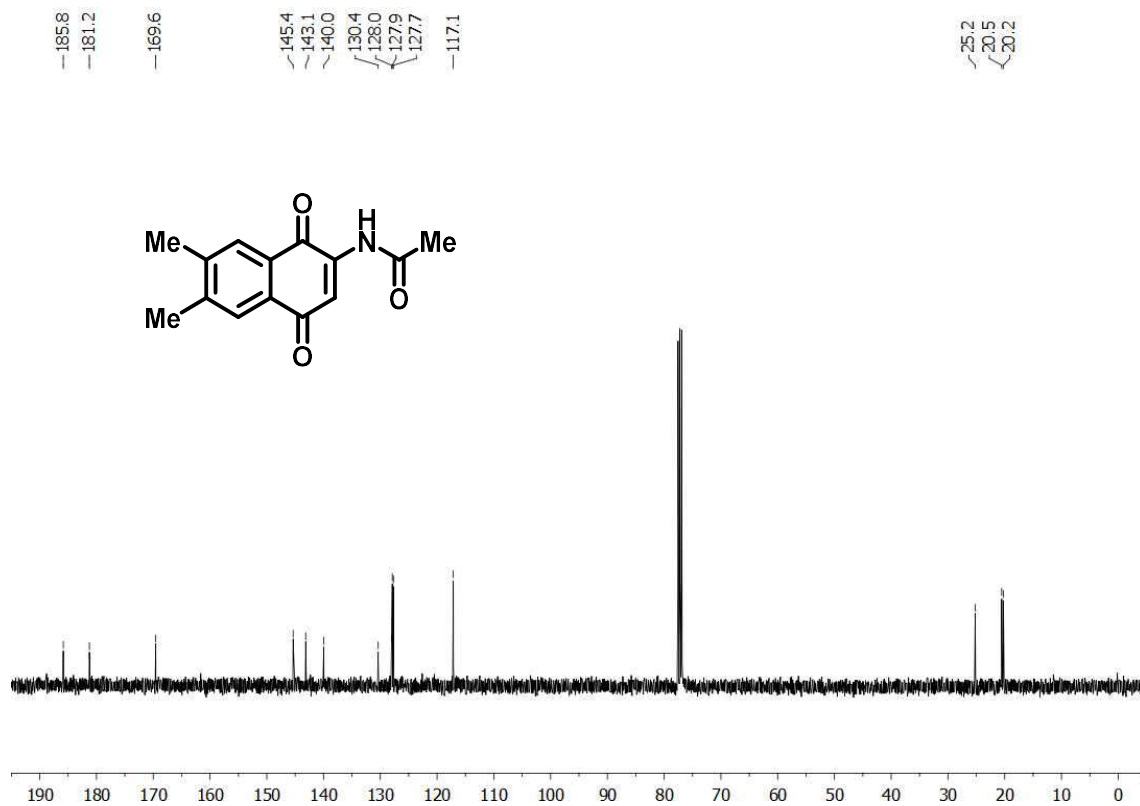


Figure A98. <sup>13</sup>C-NMR spectrum of compound **59e** (CDCl<sub>3</sub>, 100 MHz).

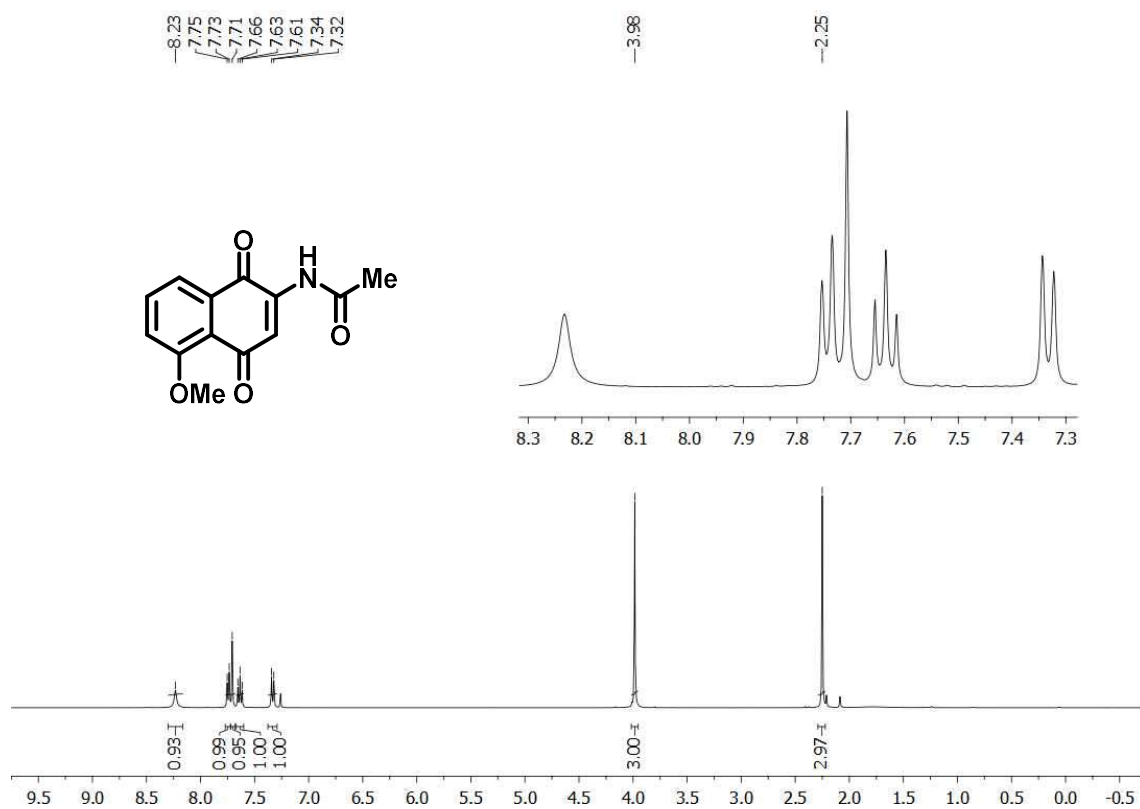


Figure A99. <sup>1</sup>H-NMR spectrum of compound 59f (CDCl<sub>3</sub>, 400 MHz).

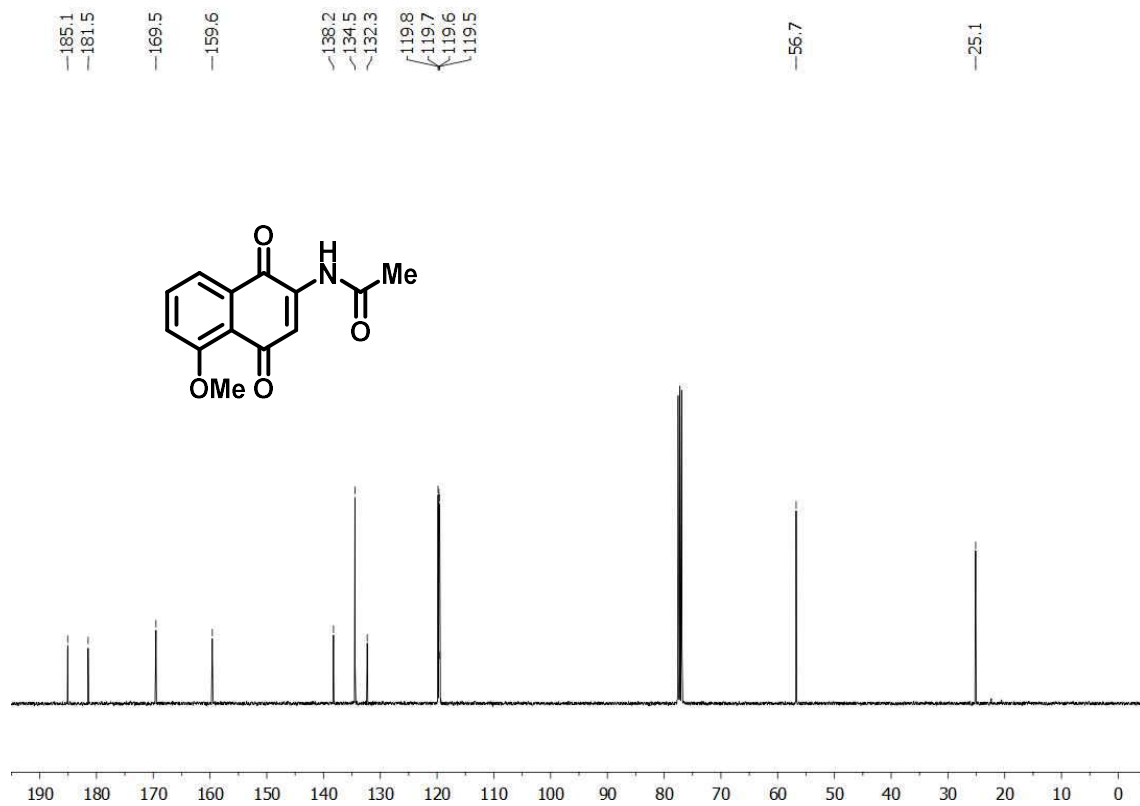


Figure A100. <sup>13</sup>C-NMR spectrum of compound 59f (CDCl<sub>3</sub>, 100 MHz).

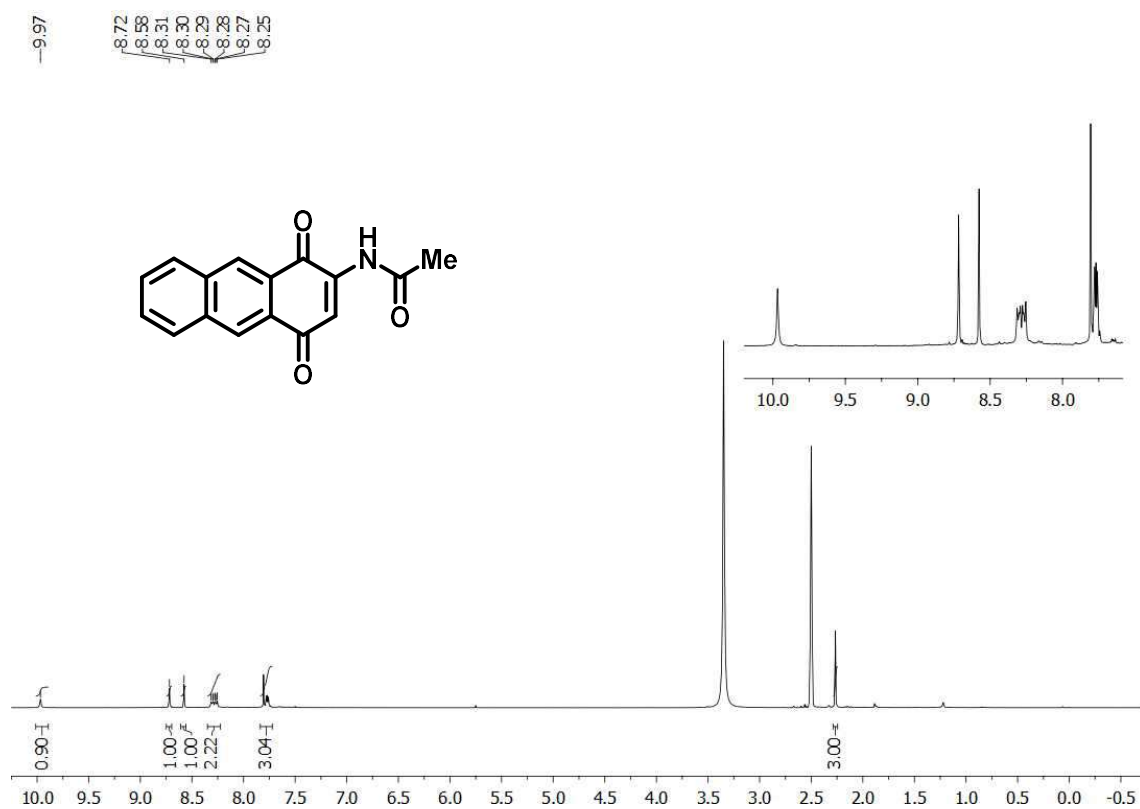


Figure A101. <sup>1</sup>H-NMR spectrum of compound 59g (DMSO-*d*<sub>6</sub>, 400 MHz).

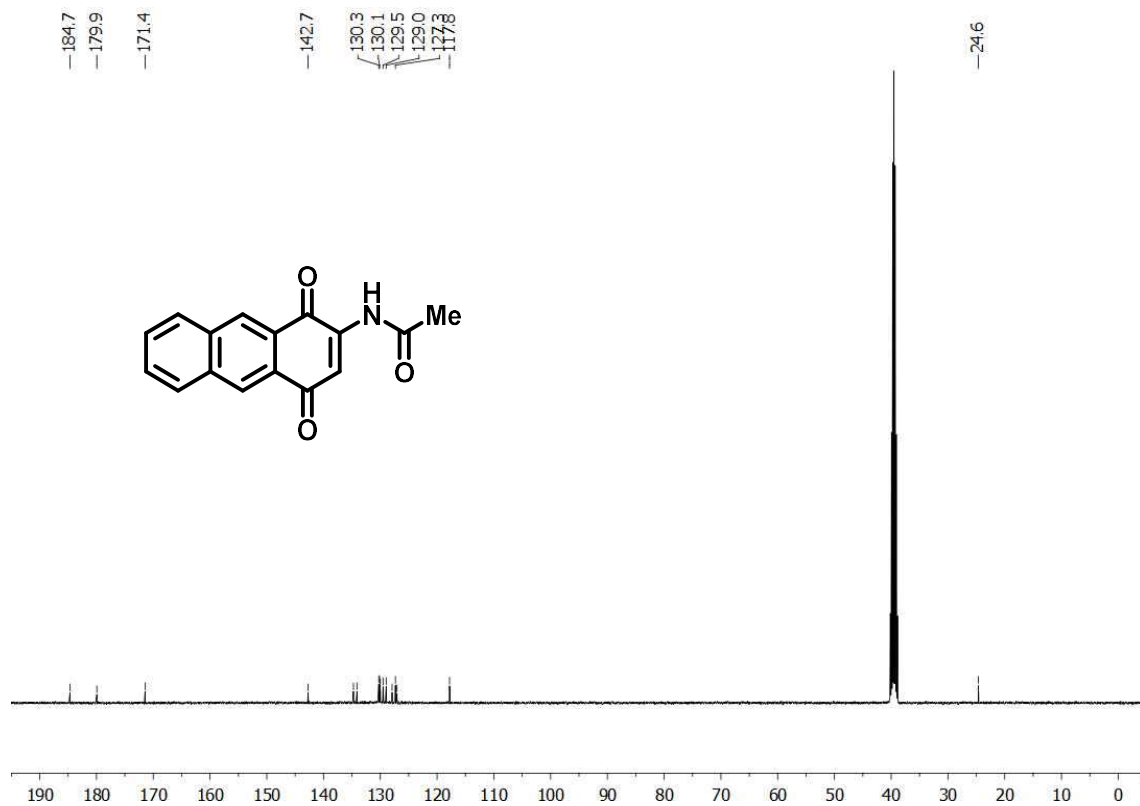
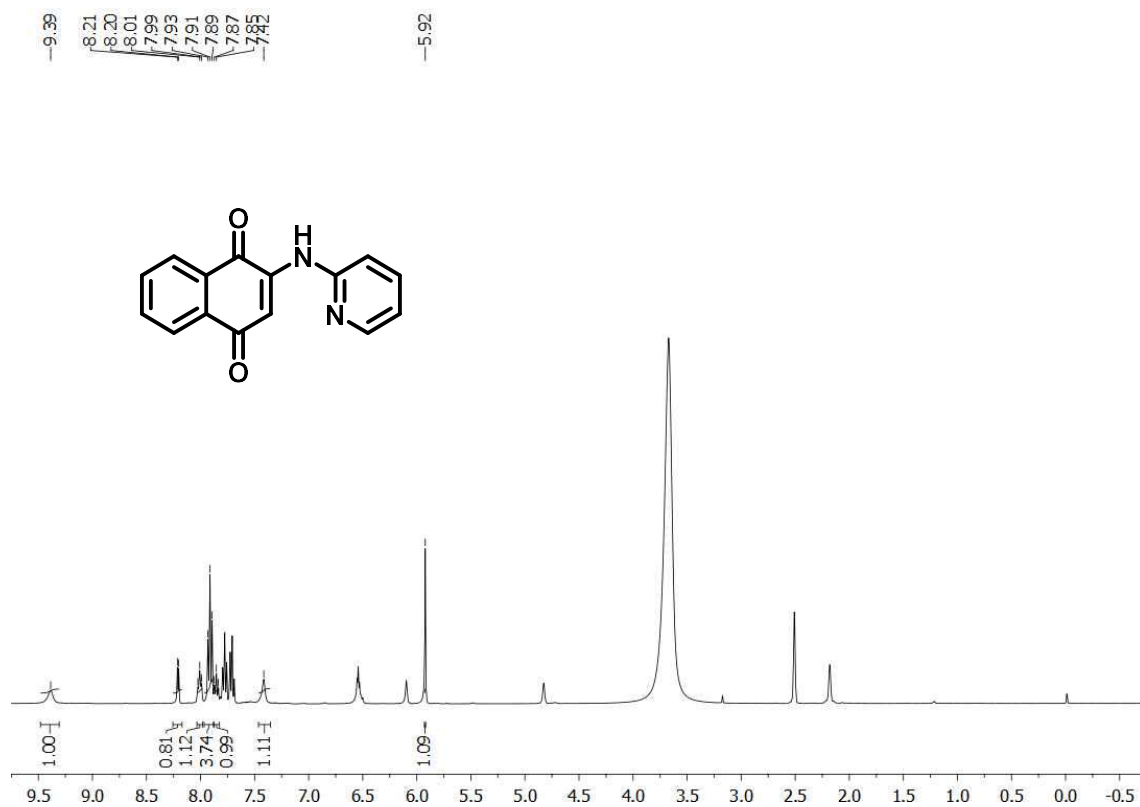
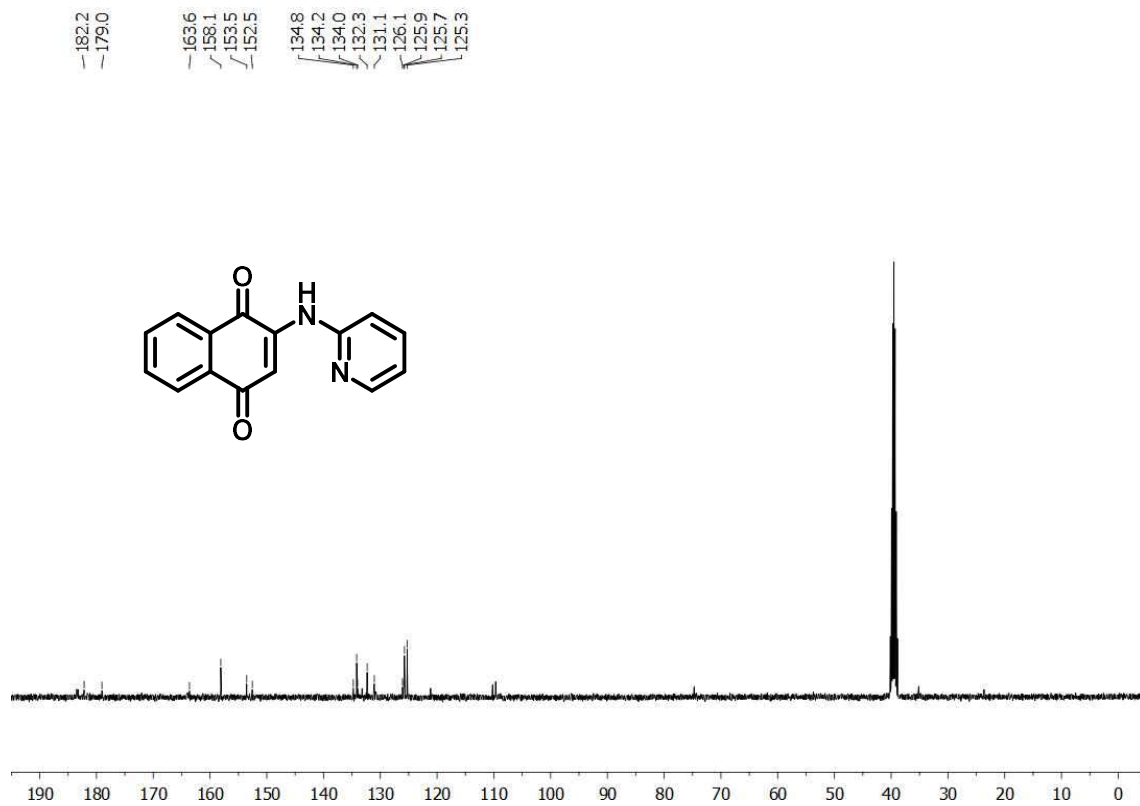


Figure A102. <sup>13</sup>C-NMR spectrum of compound 59g (DMSO-*d*<sub>6</sub>, 100 MHz).



**Figure A103.**  $^1\text{H-NMR}$  spectrum of compound **60** (DMSO- $d_6$ , 400 MHz).



**Figure A104.**  $^{13}\text{C-NMR}$  spectrum of compound **60** (DMSO- $d_6$ , 100 MHz).

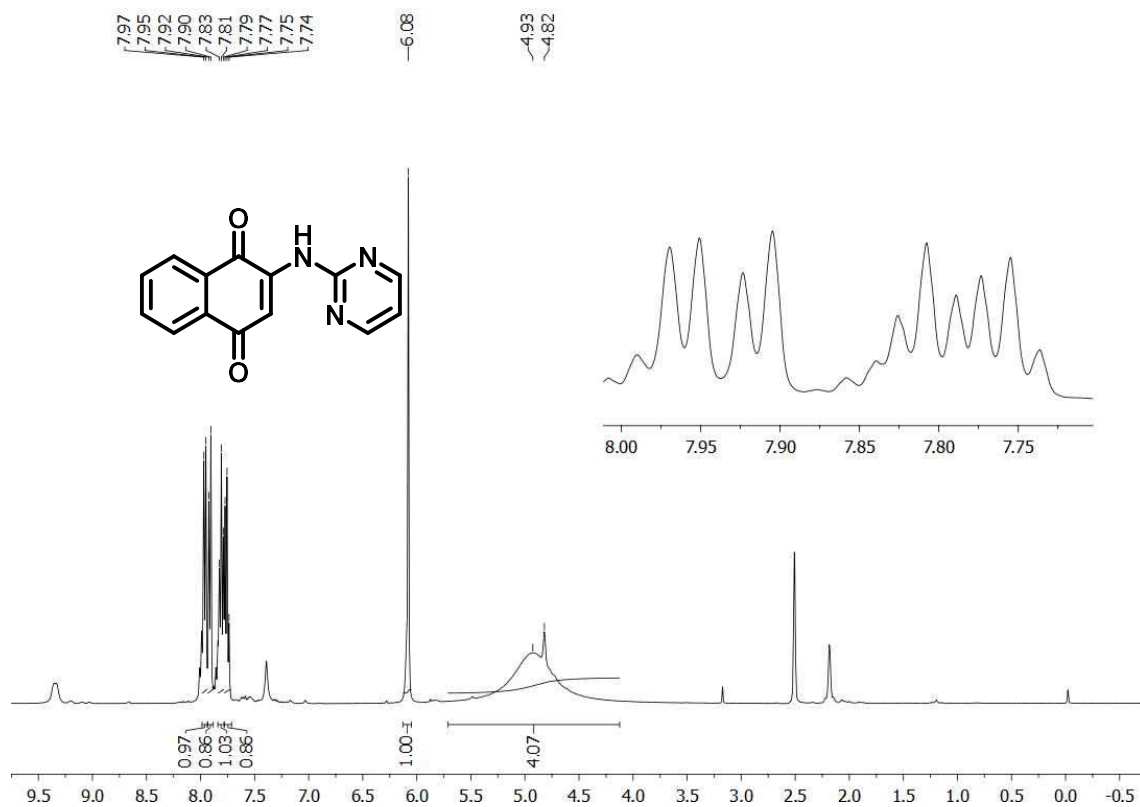


Figure A105.  $^1\text{H-NMR}$  spectrum of compound **61** (DMSO- $d_6$ , 400 MHz).

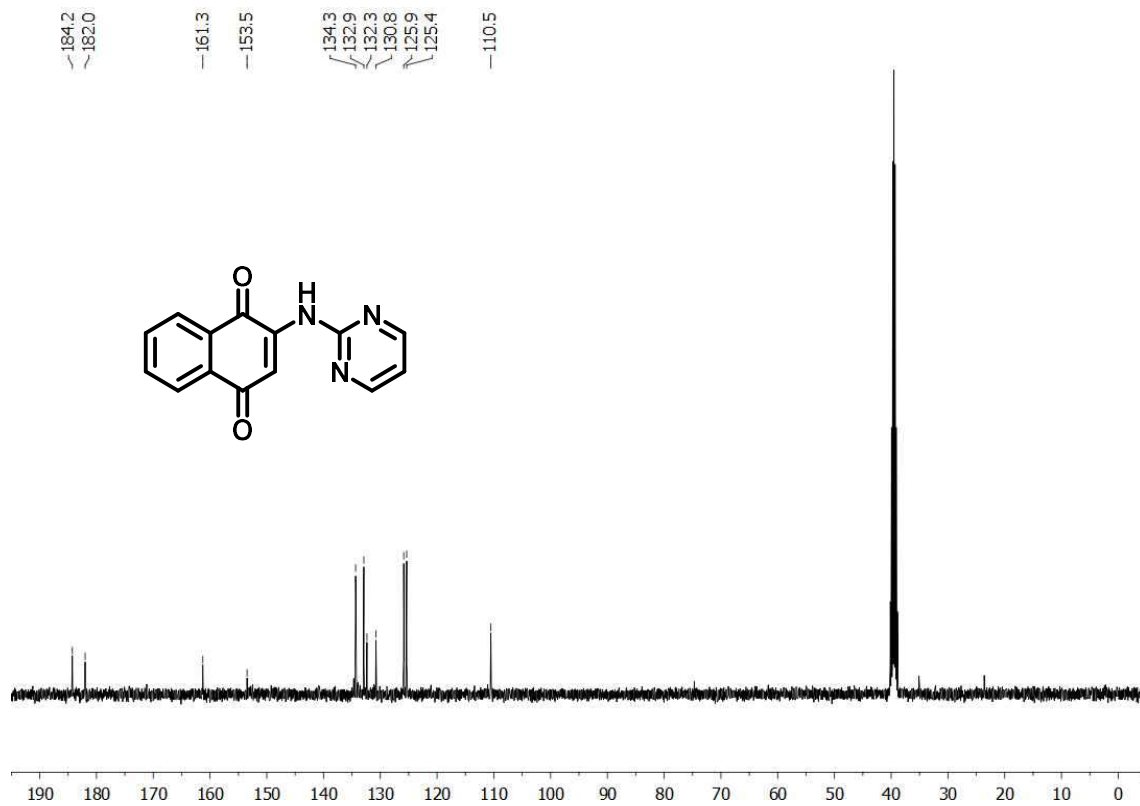


Figure A106.  $^{13}\text{C-NMR}$  spectrum of compound **61** (DMSO- $d_6$ , 100 MHz).



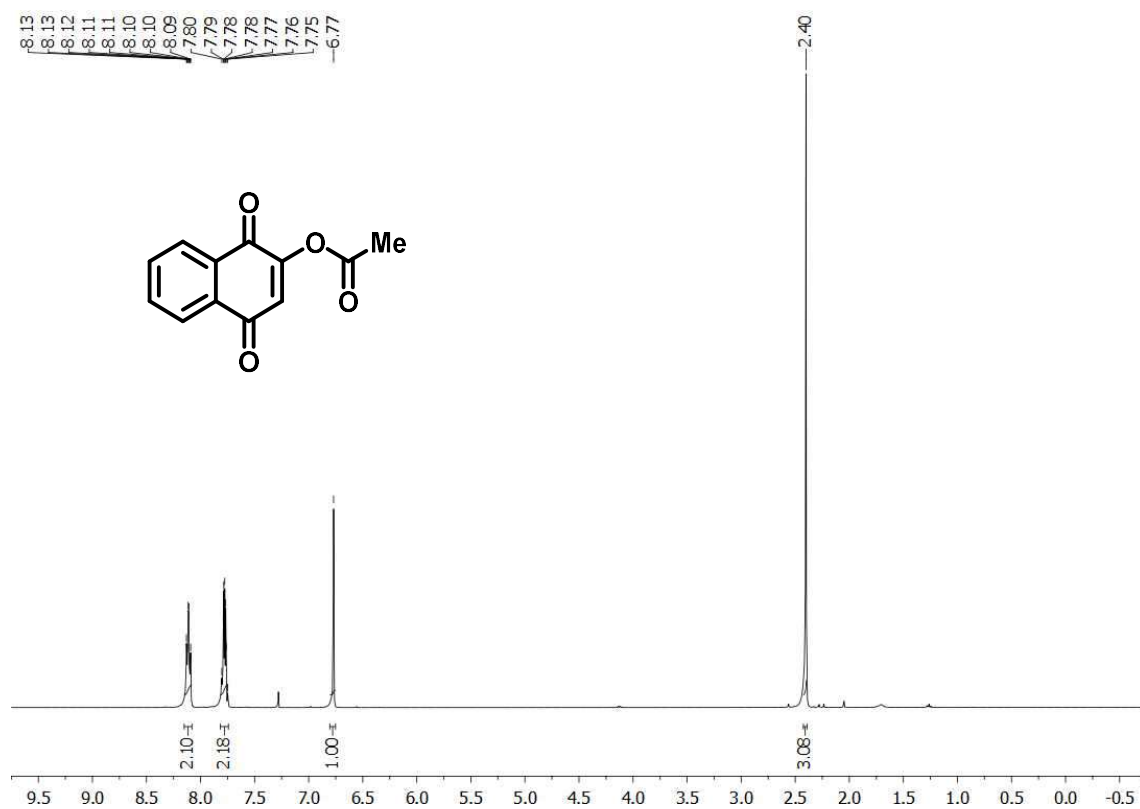


Figure A107. <sup>1</sup>H-NMR spectrum of compound **62** (CDCl<sub>3</sub>, 400 MHz).

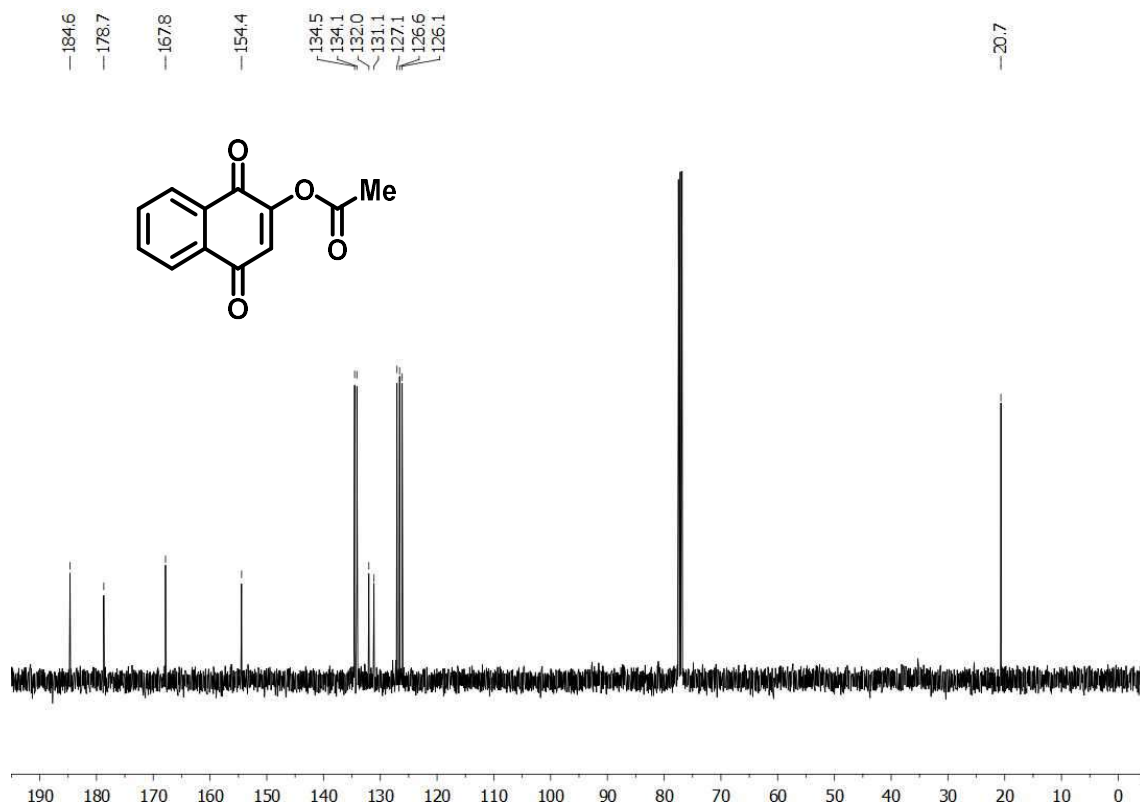


Figure A108. <sup>13</sup>C-NMR spectrum of compound **62** (CDCl<sub>3</sub>, 100 MHz).

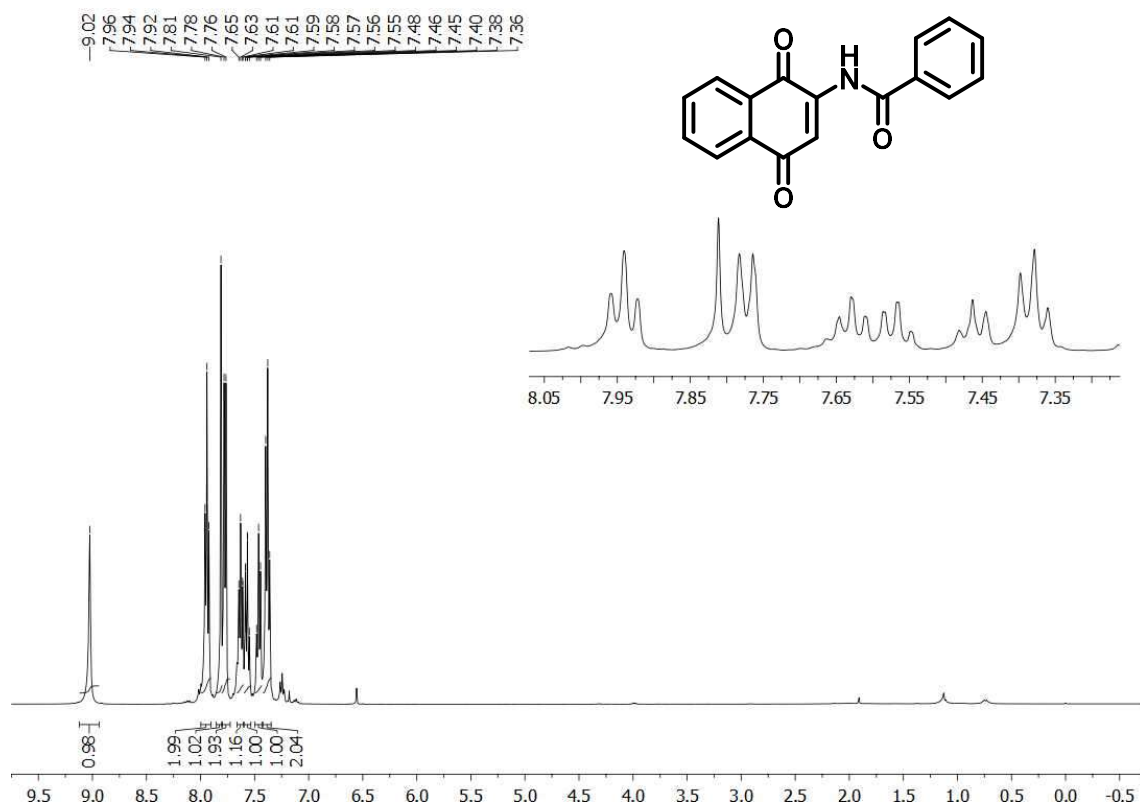


Figure A109. <sup>1</sup>H-NMR spectrum of compound 64 (CDCl<sub>3</sub>, 400 MHz).

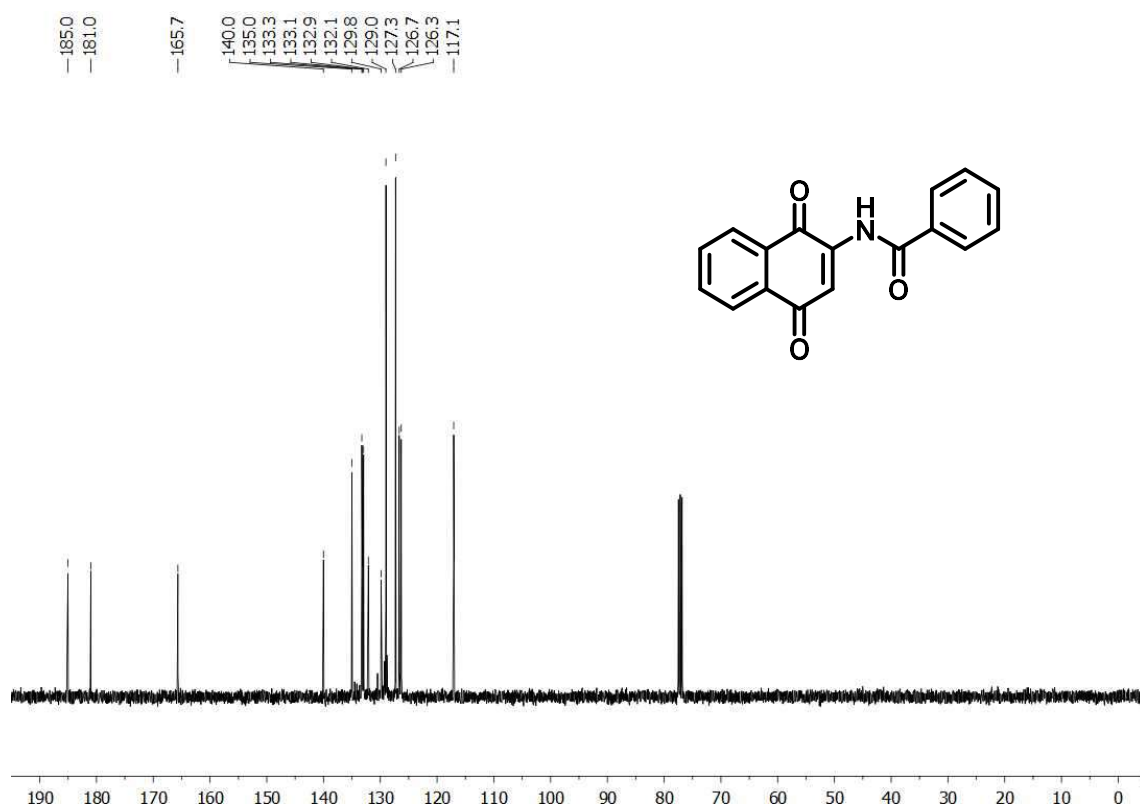


Figure A110. <sup>13</sup>C-NMR spectrum of compound 64 (CDCl<sub>3</sub>, 100 MHz).

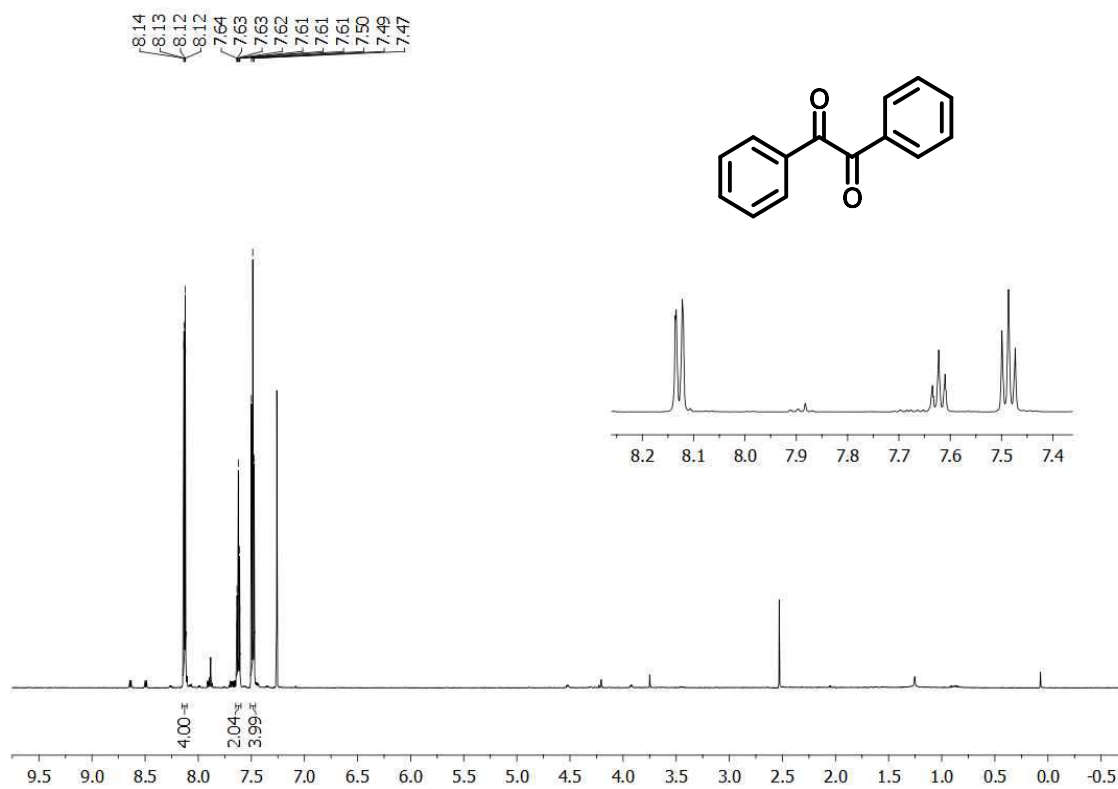


Figure A111. <sup>1</sup>H-NMR spectrum of compound **65** (CDCl<sub>3</sub>, 400 MHz).

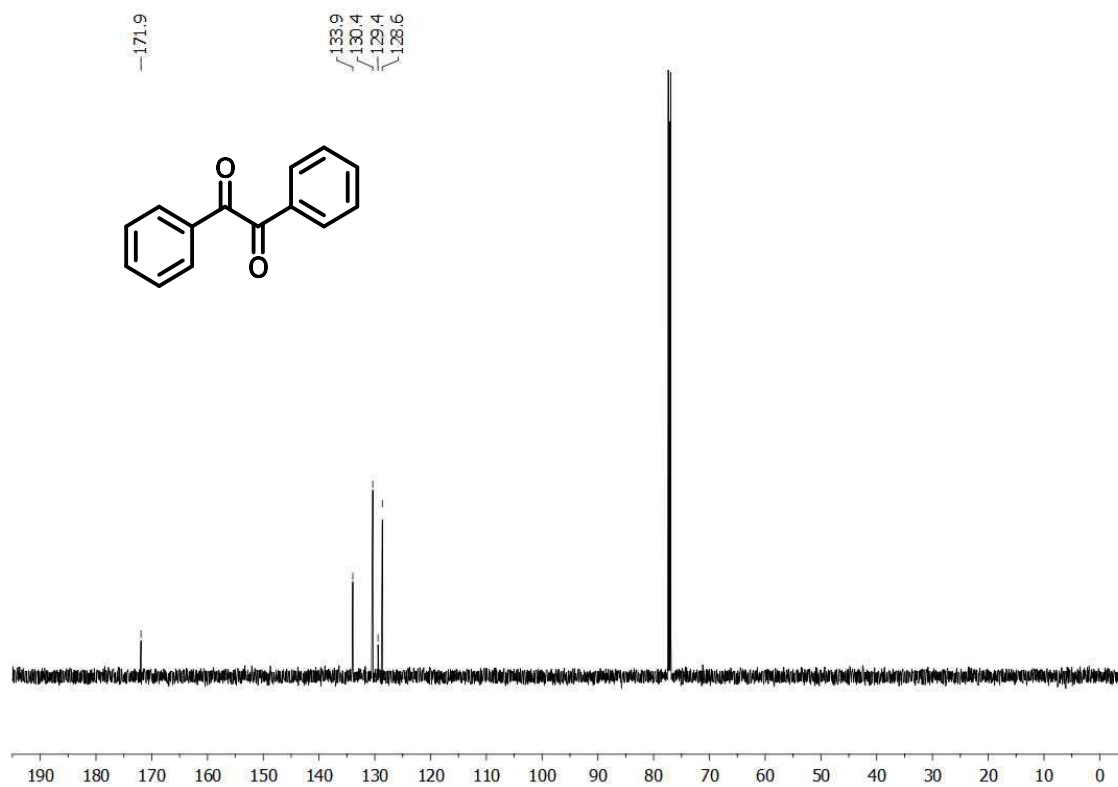


Figure A112. <sup>13</sup>C-NMR spectrum of compound **65** (CDCl<sub>3</sub>, 100 MHz).

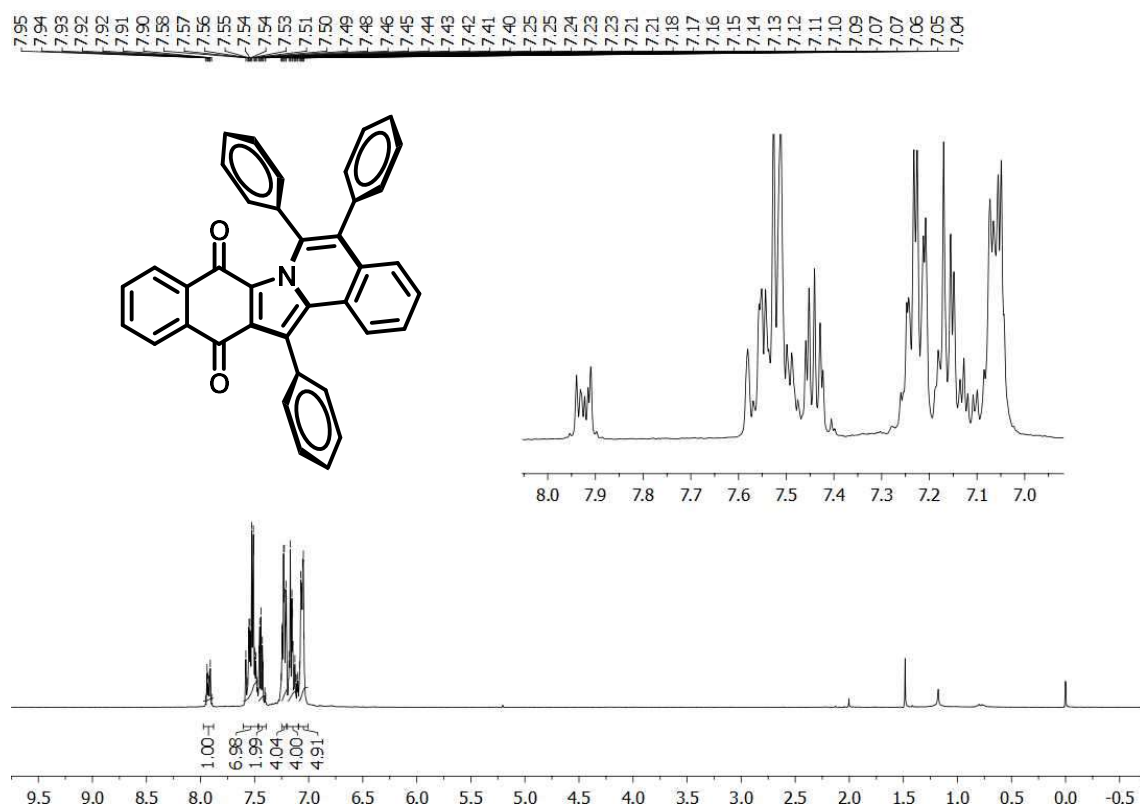


Figure A113. <sup>1</sup>H-NMR spectrum of compound 67a (CDCl<sub>3</sub>, 400 MHz).

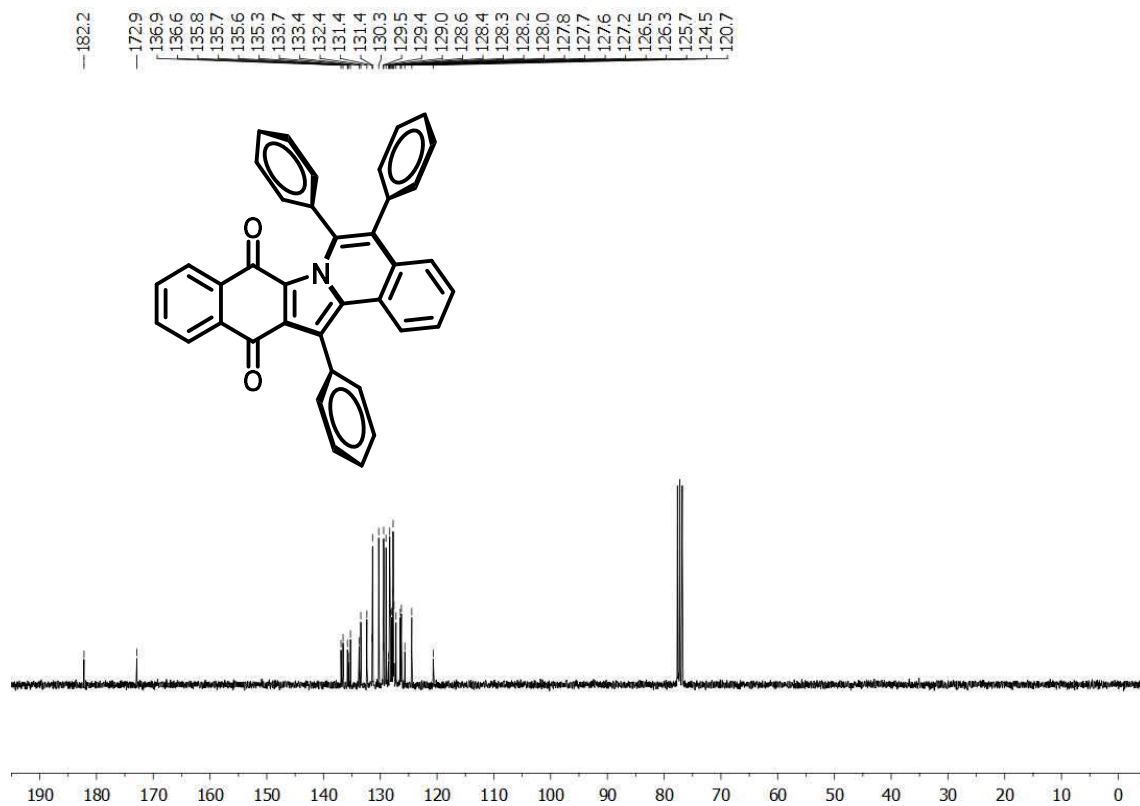


Figure A114. <sup>13</sup>C-NMR spectrum of compound 67a (CDCl<sub>3</sub>, 100 MHz).

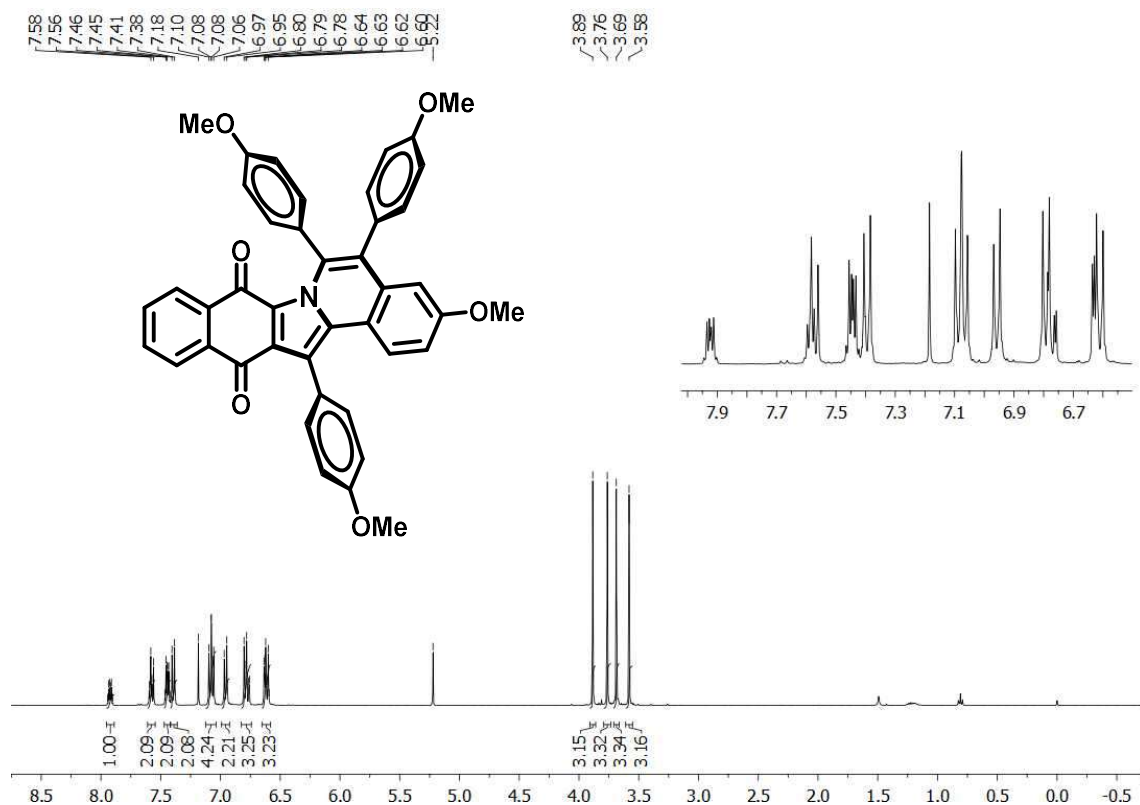


Figure A115.  $^1\text{H}$ -NMR spectrum of compound **67b** ( $\text{CDCl}_3$ , 400 MHz).

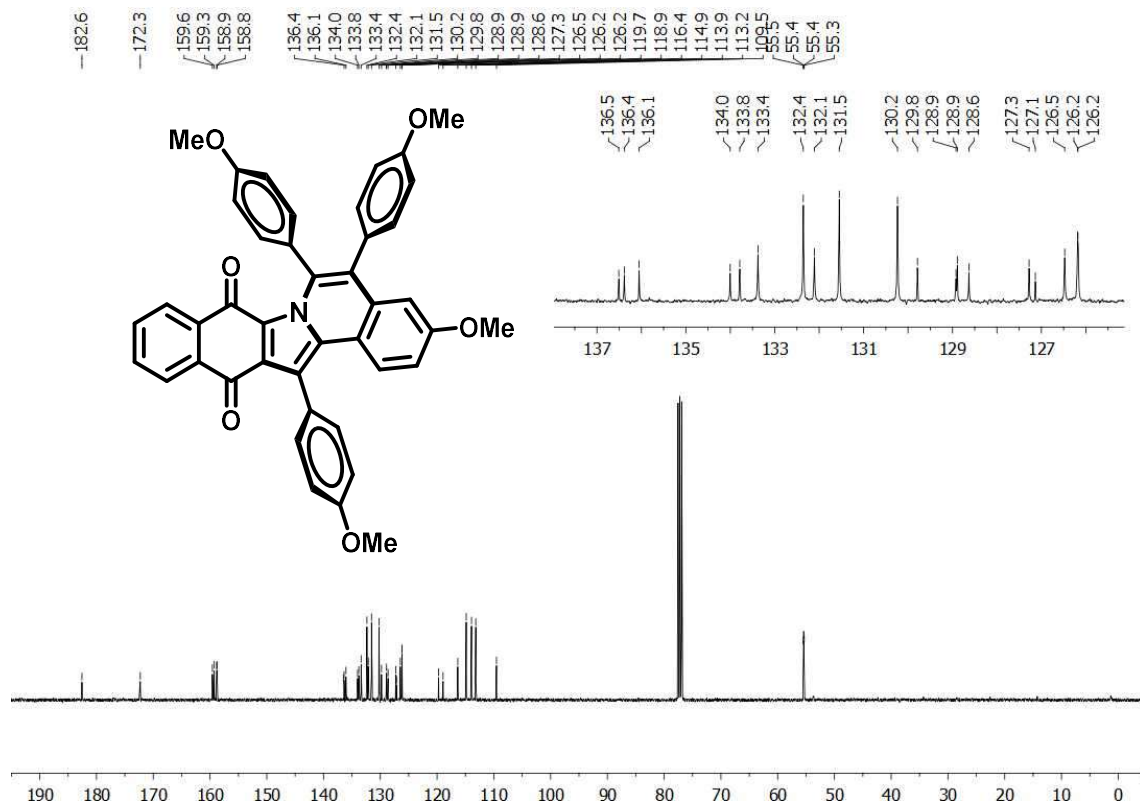


Figure A116.  $^{13}\text{C}$ -NMR spectrum of compound **67b** ( $\text{CDCl}_3$ , 100 MHz).

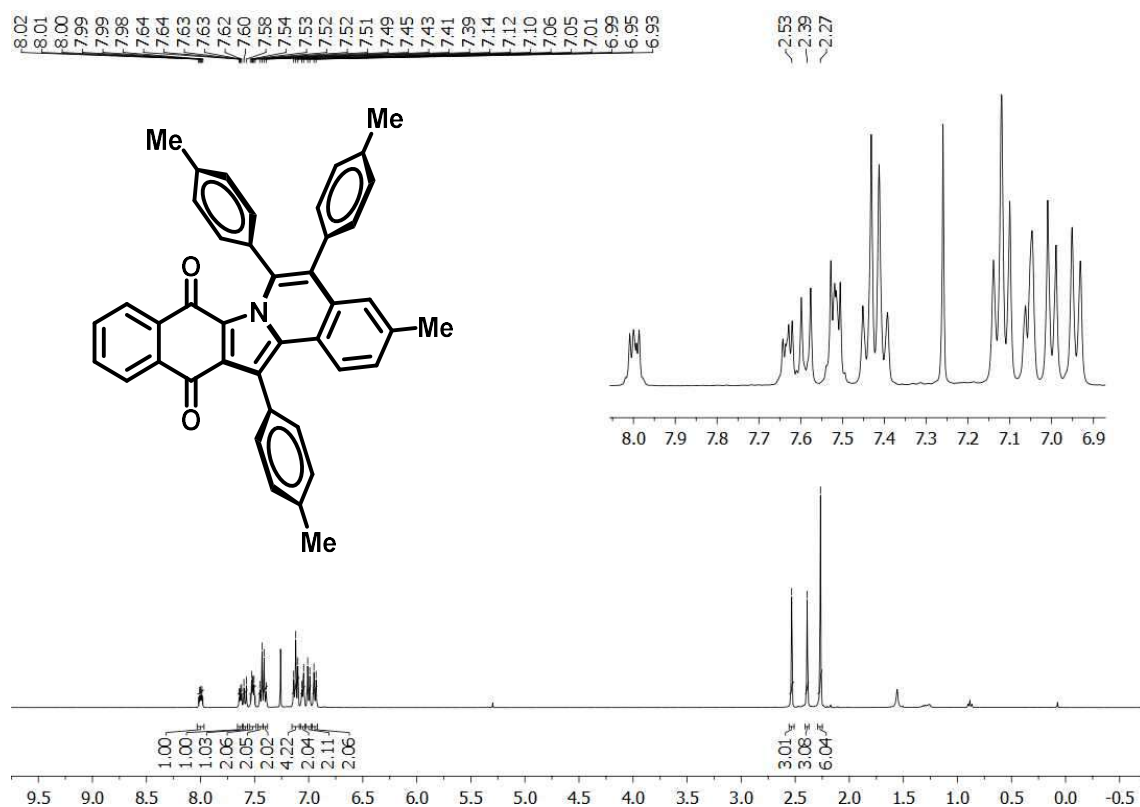


Figure A117. <sup>1</sup>H-NMR spectrum of compound 67c (CDCl<sub>3</sub>, 400 MHz).

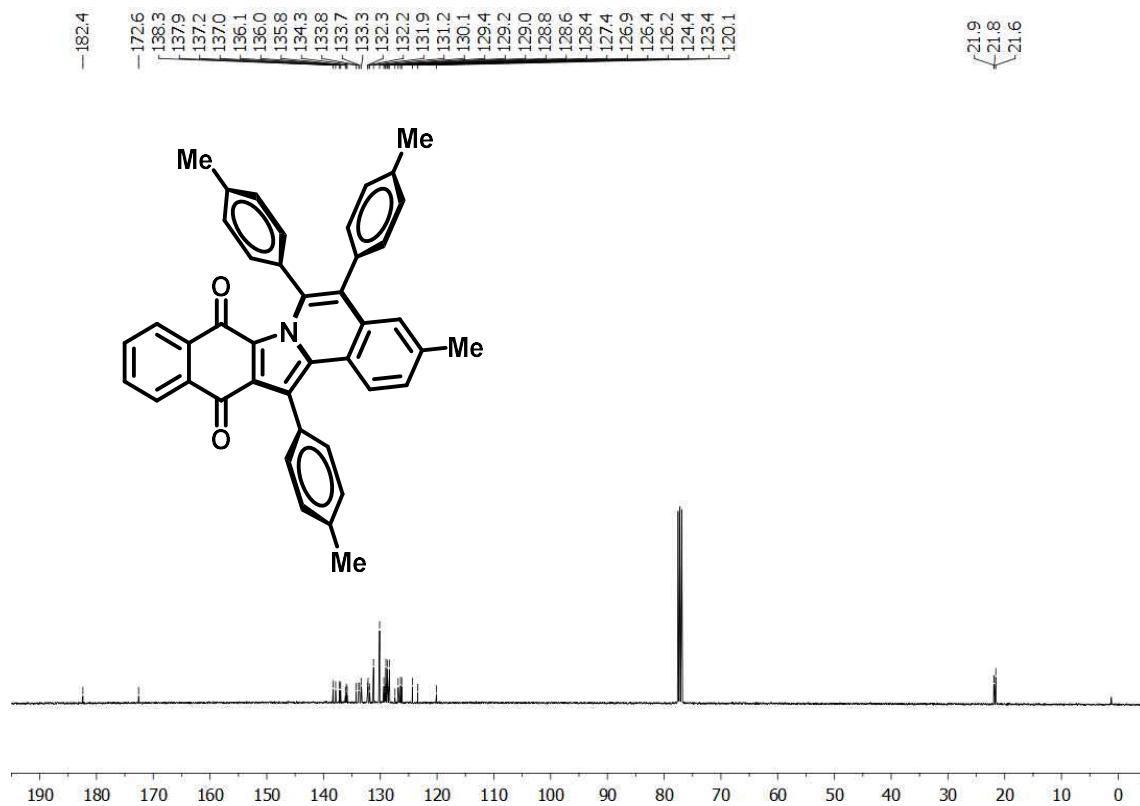


Figure A118. <sup>13</sup>C-NMR spectrum of compound 67c (CDCl<sub>3</sub>, 100 MHz)

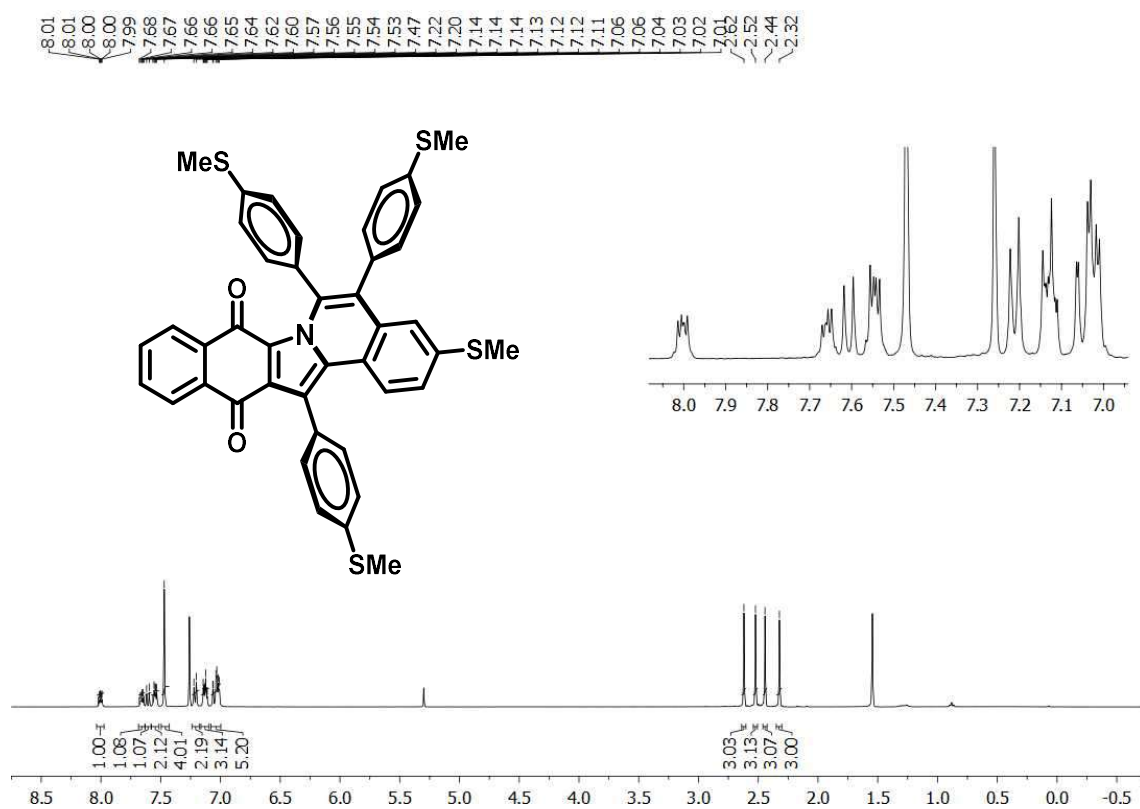


Figure A119. <sup>1</sup>H-NMR spectrum of compound 67d (CDCl<sub>3</sub>, 400 MHz).

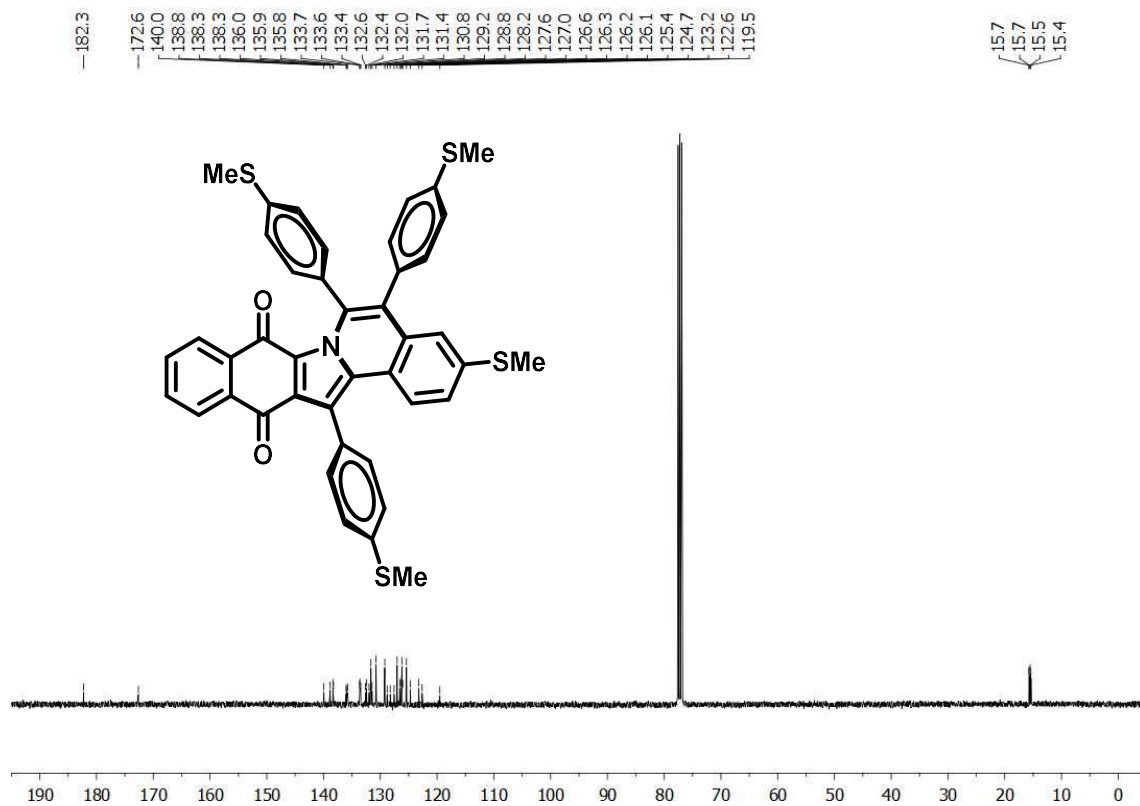


Figure A120. <sup>13</sup>C-NMR spectrum of compound 67d (CDCl<sub>3</sub>, 100 MHz).

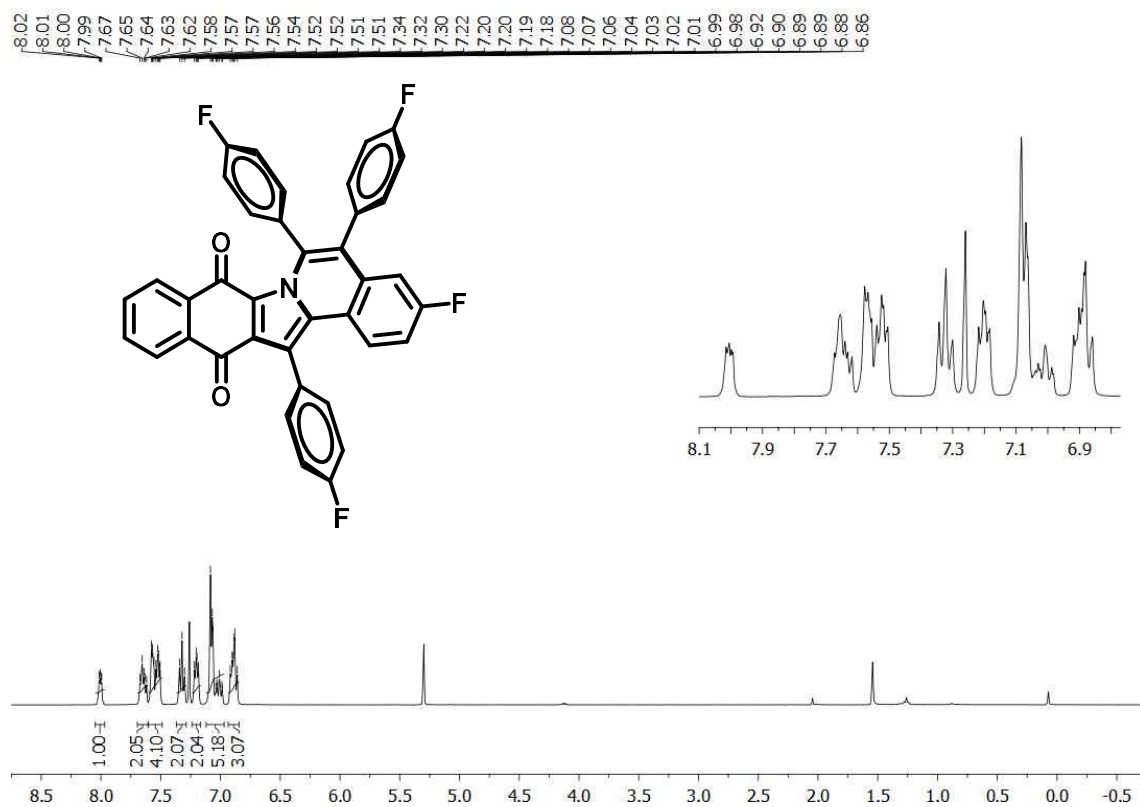


Figure A121. <sup>1</sup>H-NMR spectrum of compound 67e (CDCl<sub>3</sub>, 400 MHz).

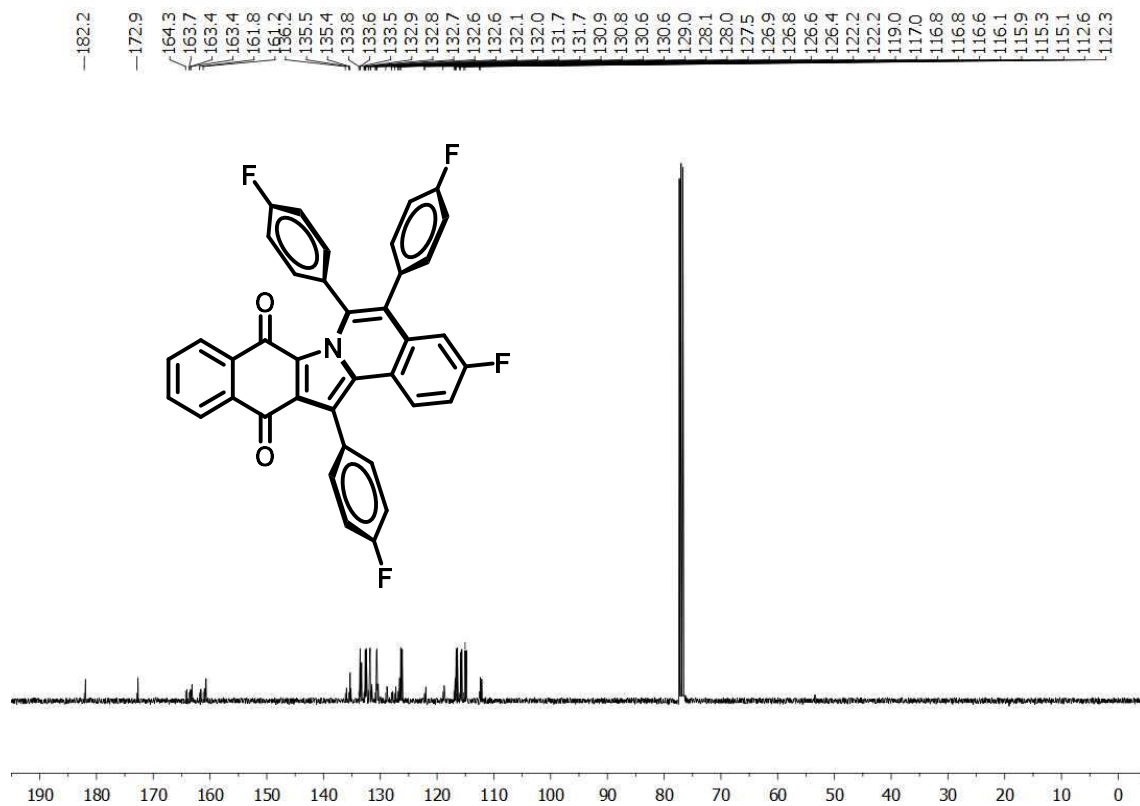


Figure A122. <sup>13</sup>C-NMR spectrum of compound 67e (CDCl<sub>3</sub>, 100 MHz).



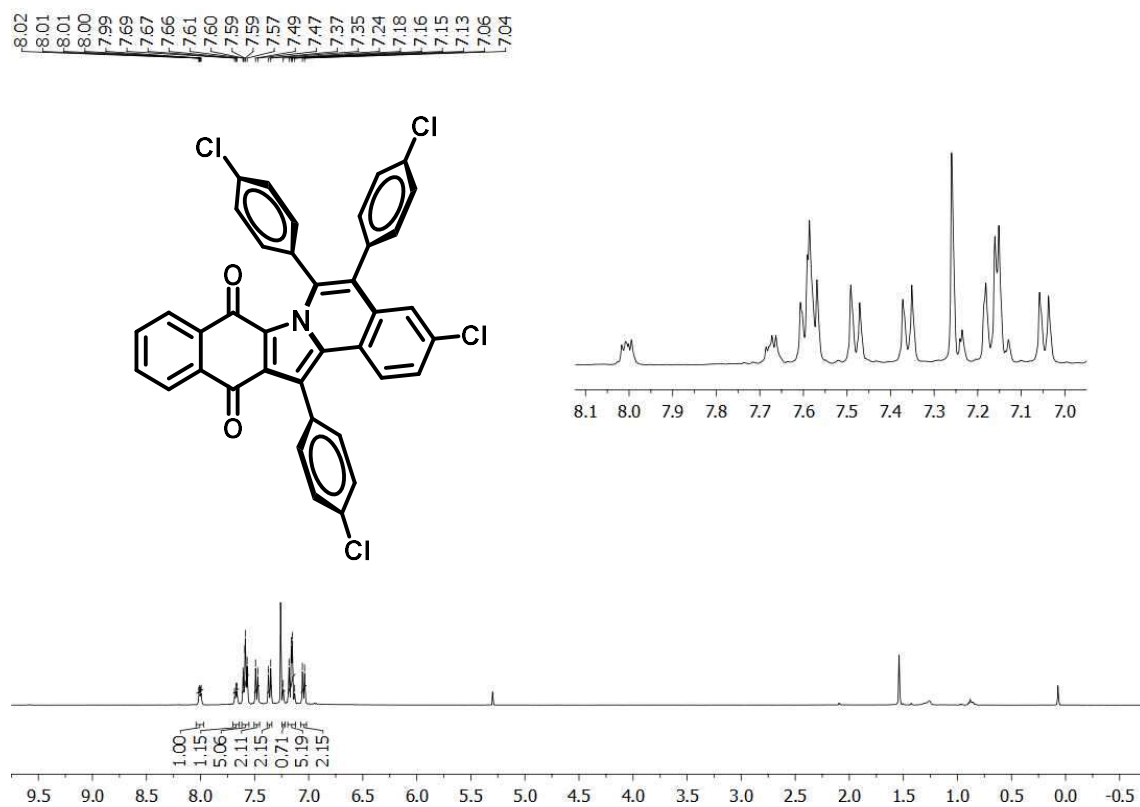


Figure A123. <sup>1</sup>H-NMR spectrum of compound 67f (CDCl<sub>3</sub>, 400 MHz).

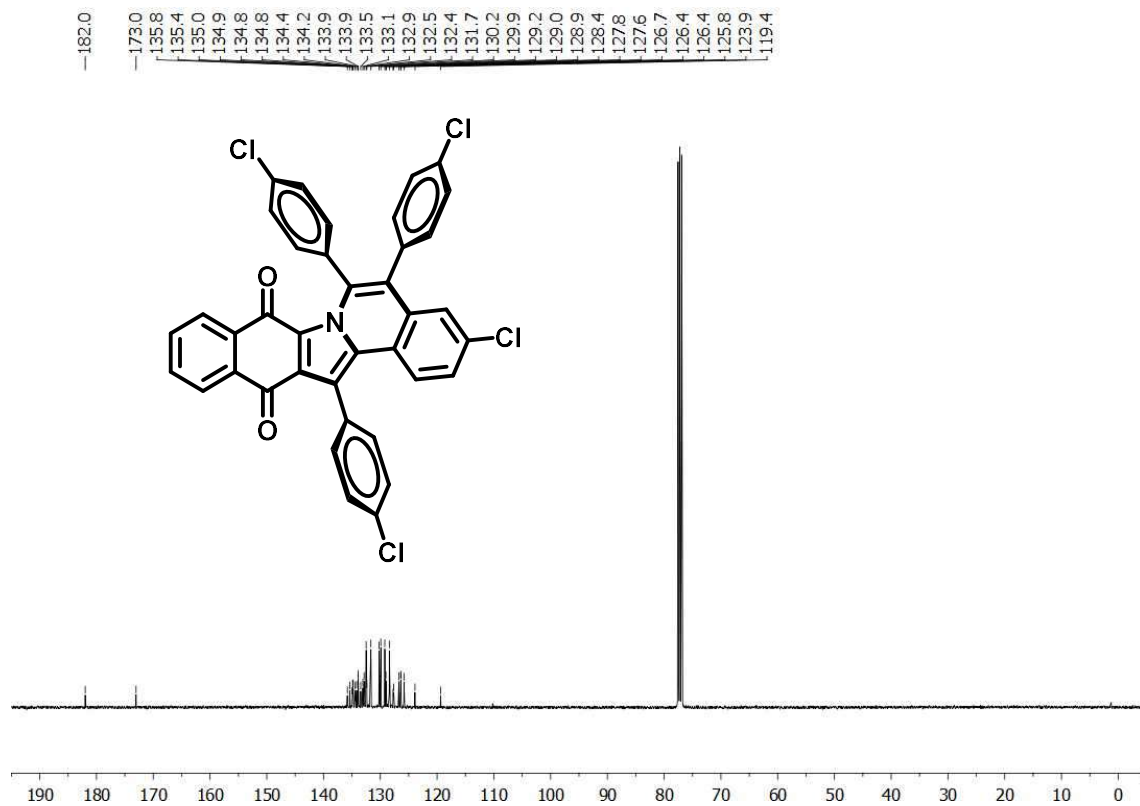


Figure A124. <sup>13</sup>C-NMR spectrum of compound 67f (CDCl<sub>3</sub>, 100 MHz)

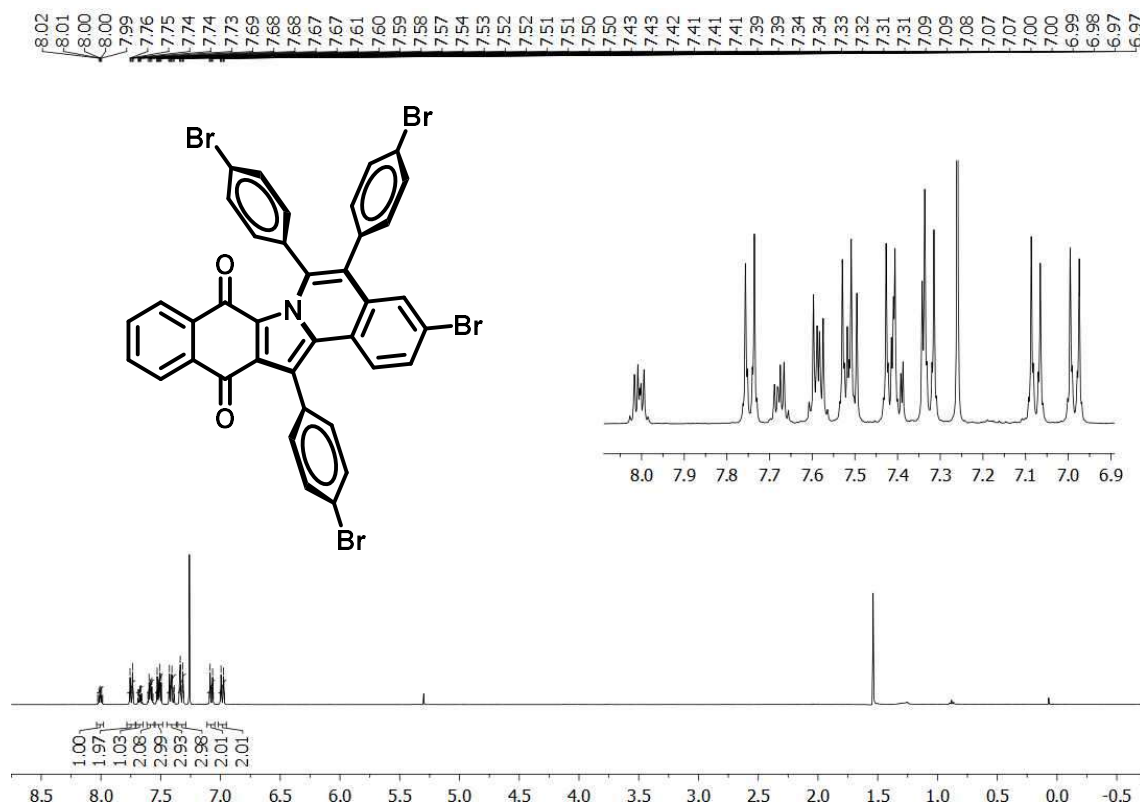


Figure A125. <sup>1</sup>H-NMR spectrum of compound 67g (CDCl<sub>3</sub>, 400 MHz).

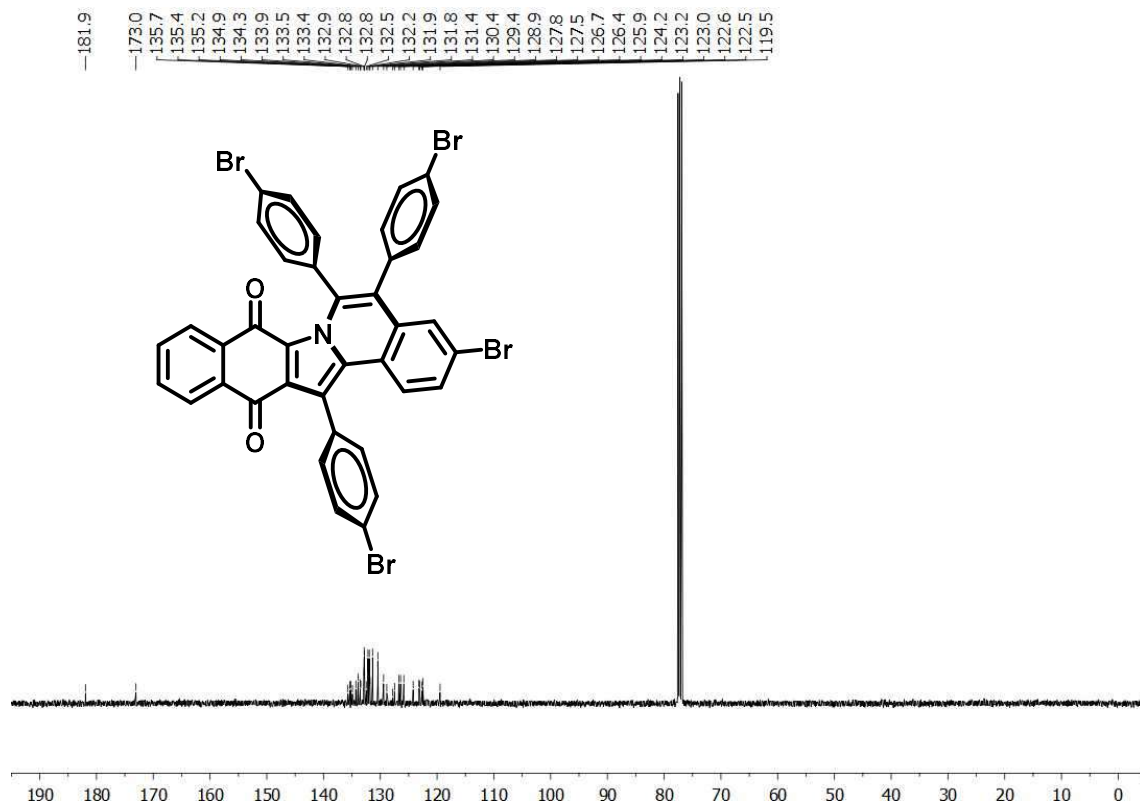


Figure A126. <sup>13</sup>C-NMR spectrum of compound 67g (CDCl<sub>3</sub>, 100 MHz).

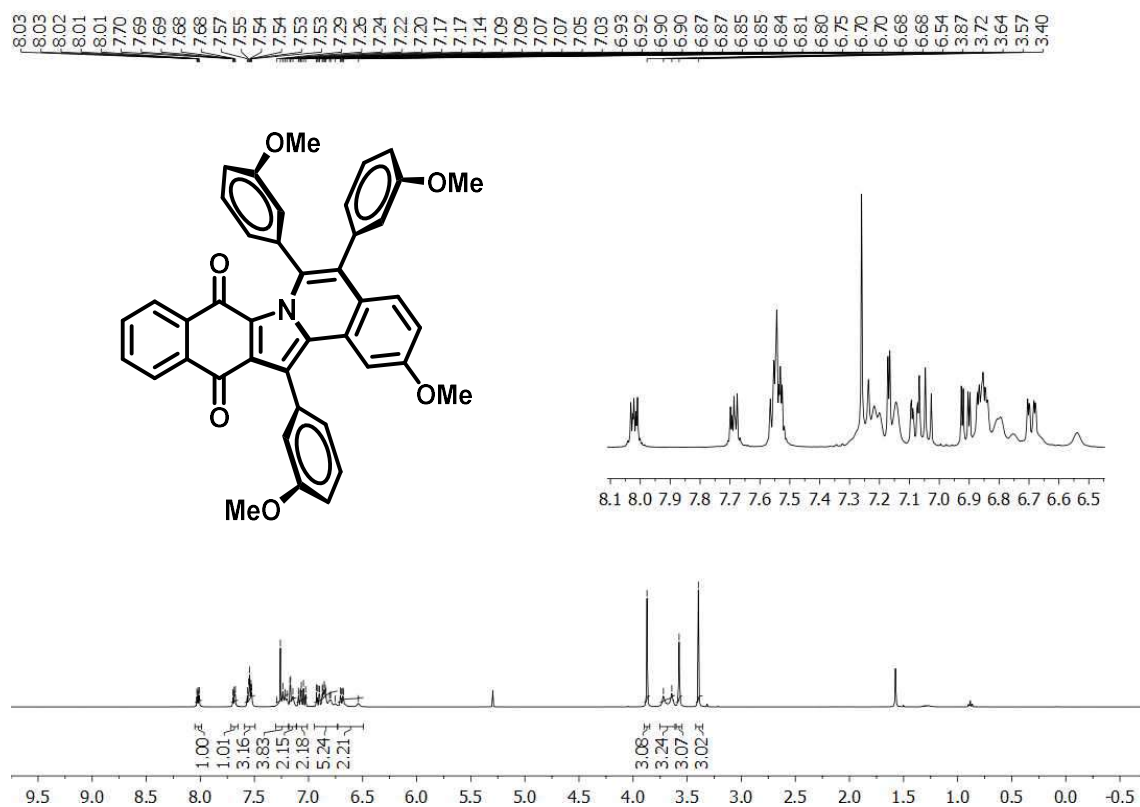


Figure A127. <sup>1</sup>H-NMR spectrum of compound 67h (CDCl<sub>3</sub>, 400 MHz).

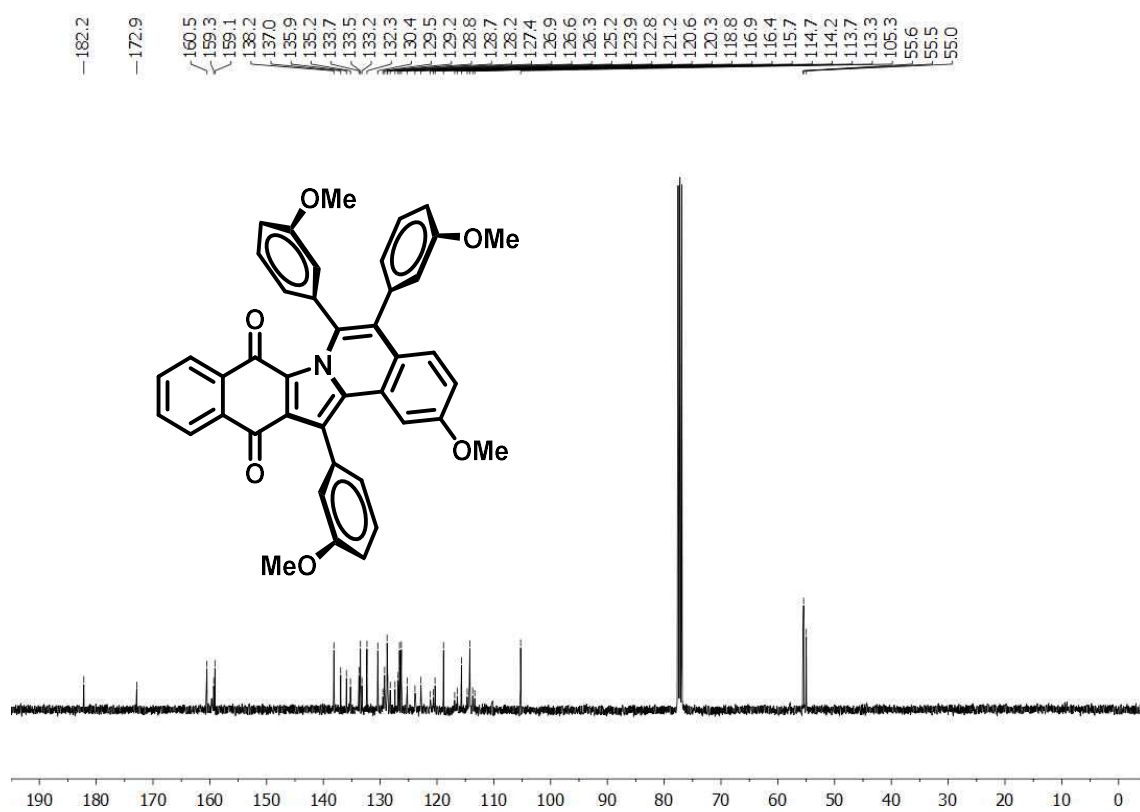


Figure A128. <sup>13</sup>C-NMR spectrum of compound 67h (CDCl<sub>3</sub>, 100 MHz).

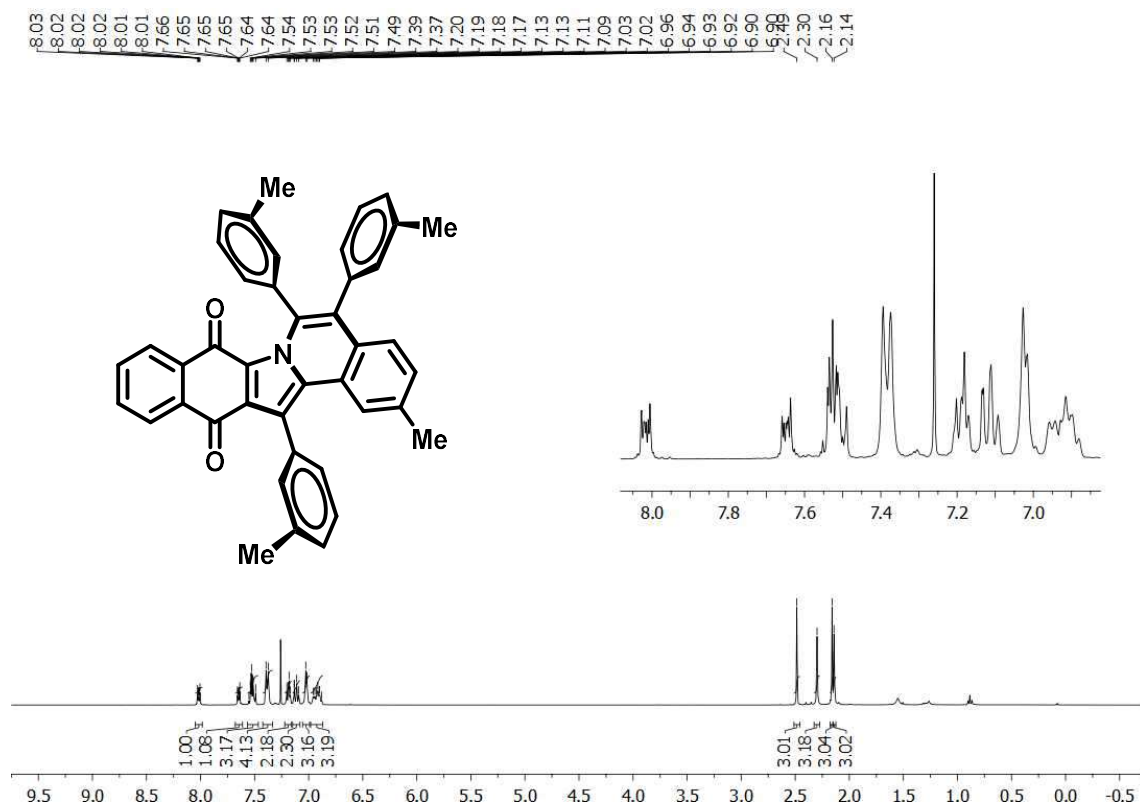


Figure A129. <sup>1</sup>H-NMR spectrum of compound 67i (CDCl<sub>3</sub>, 400 MHz).

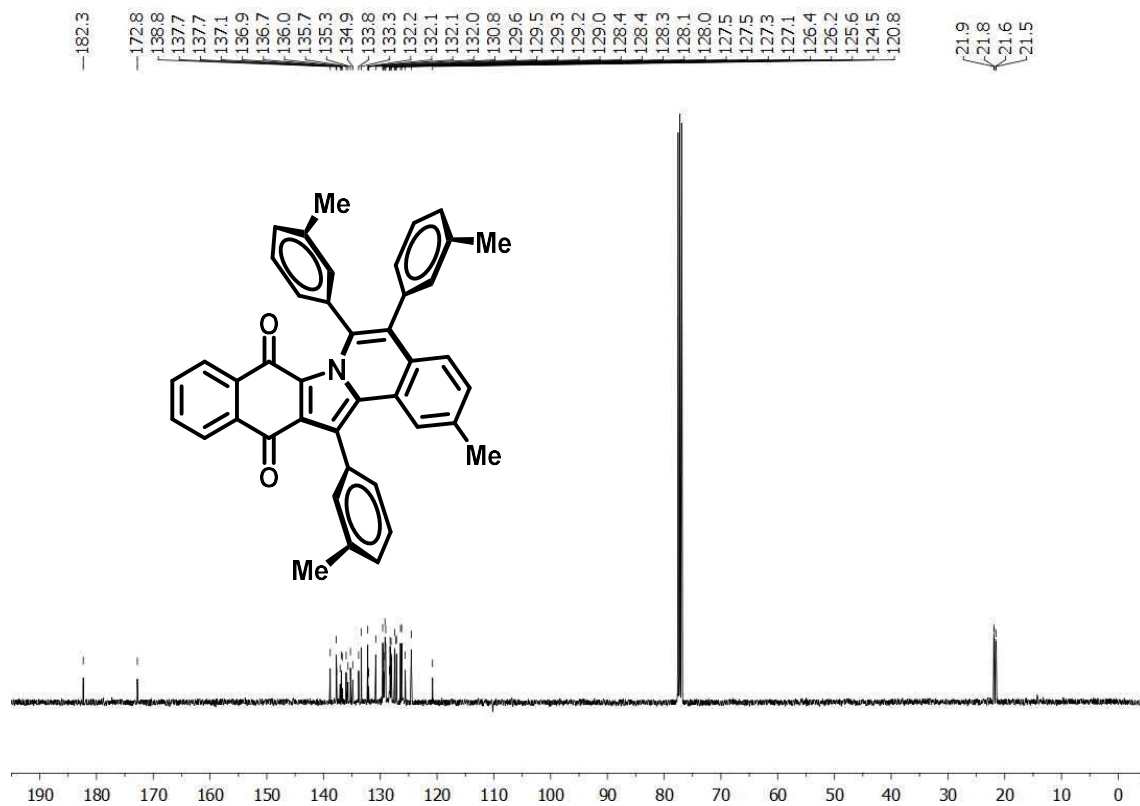


Figure A130. <sup>13</sup>C-NMR spectrum of compound 67i (CDCl<sub>3</sub>, 100 MHz).

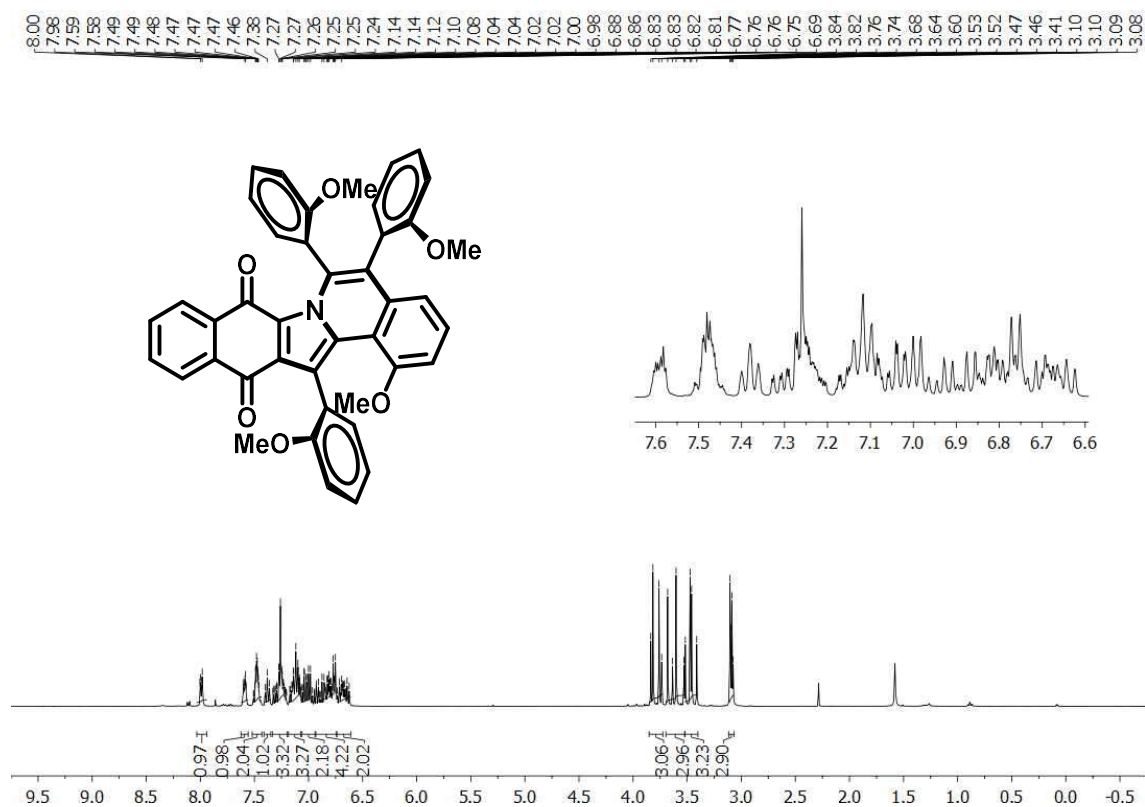


Figure A131. <sup>1</sup>H-NMR spectrum of compound 67j (CDCl<sub>3</sub>, 400 MHz).

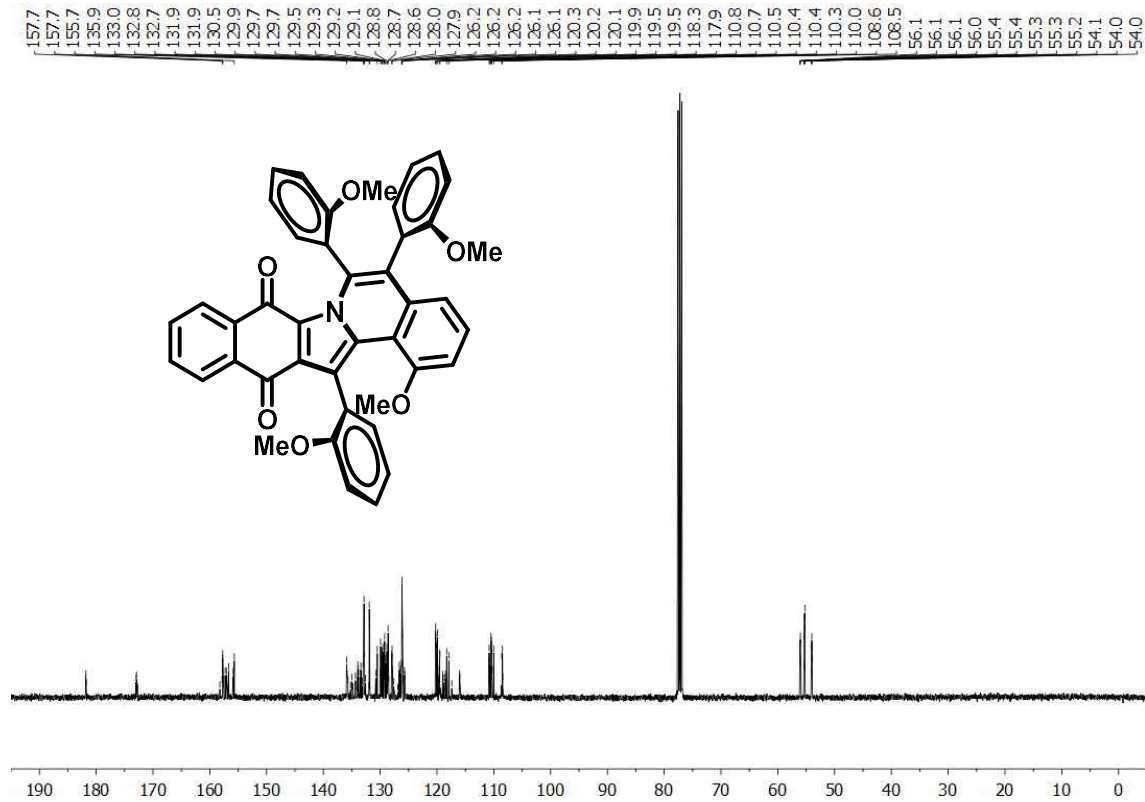


Figure A132. <sup>13</sup>C-NMR spectrum of compound 67j (CDCl<sub>3</sub>, 100 MHz).

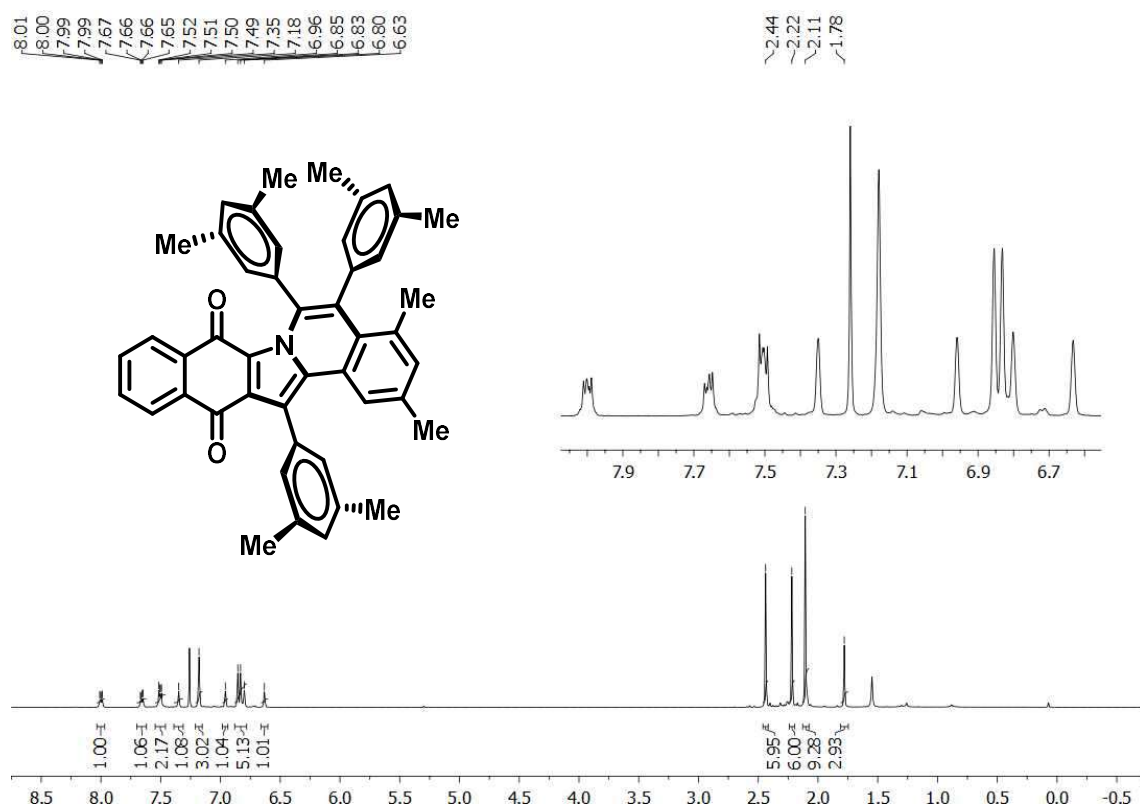


Figure A133. <sup>1</sup>H-NMR spectrum of compound 67k (CDCl<sub>3</sub>, 400 MHz).

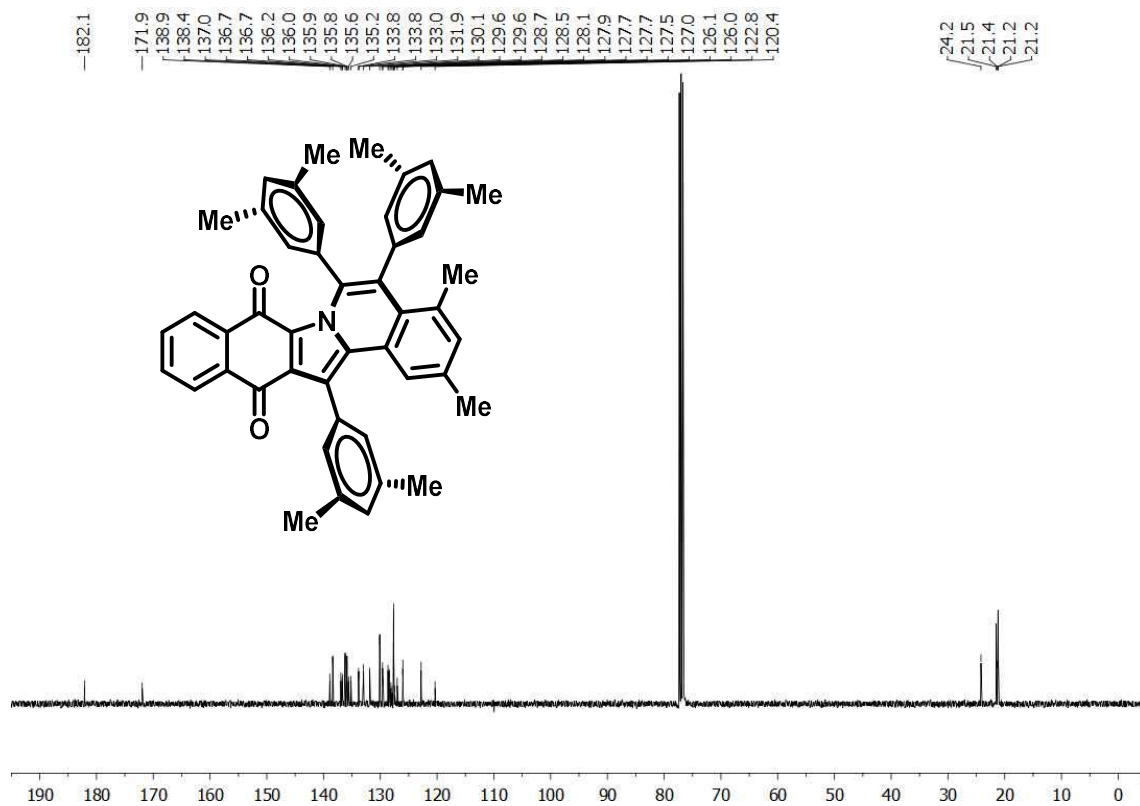


Figure A134. <sup>13</sup>C-NMR spectrum of compound 67k (CDCl<sub>3</sub>, 100 MHz).

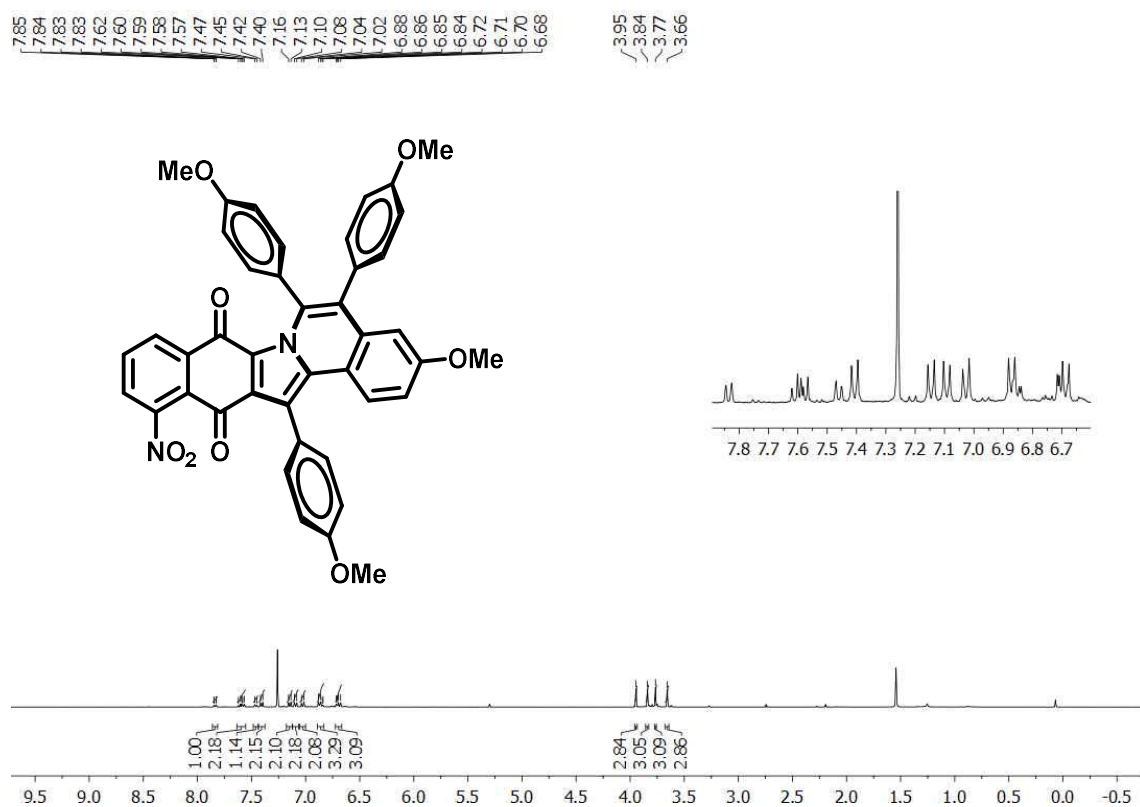


Figure A135. <sup>1</sup>H-NMR spectrum of compound 68a (CDCl<sub>3</sub>, 400 MHz).

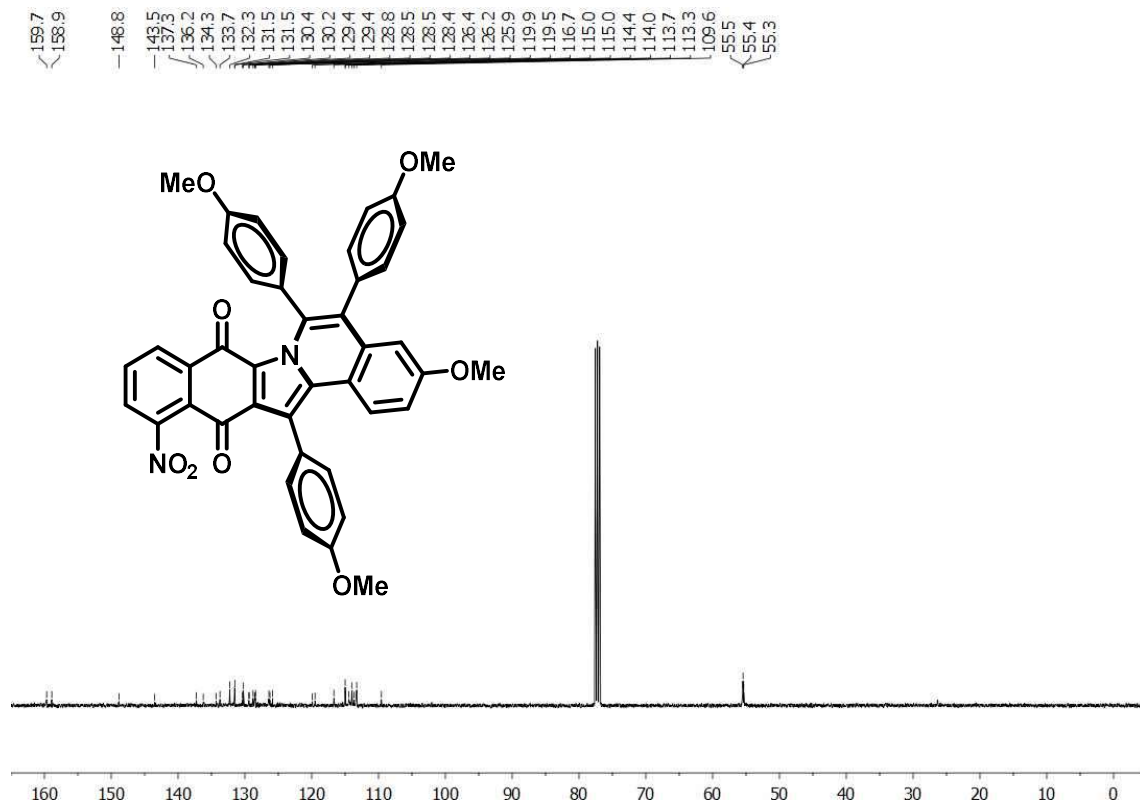


Figure A136. <sup>13</sup>C-NMR spectrum of compound 68a (CDCl<sub>3</sub>, 100 MHz).

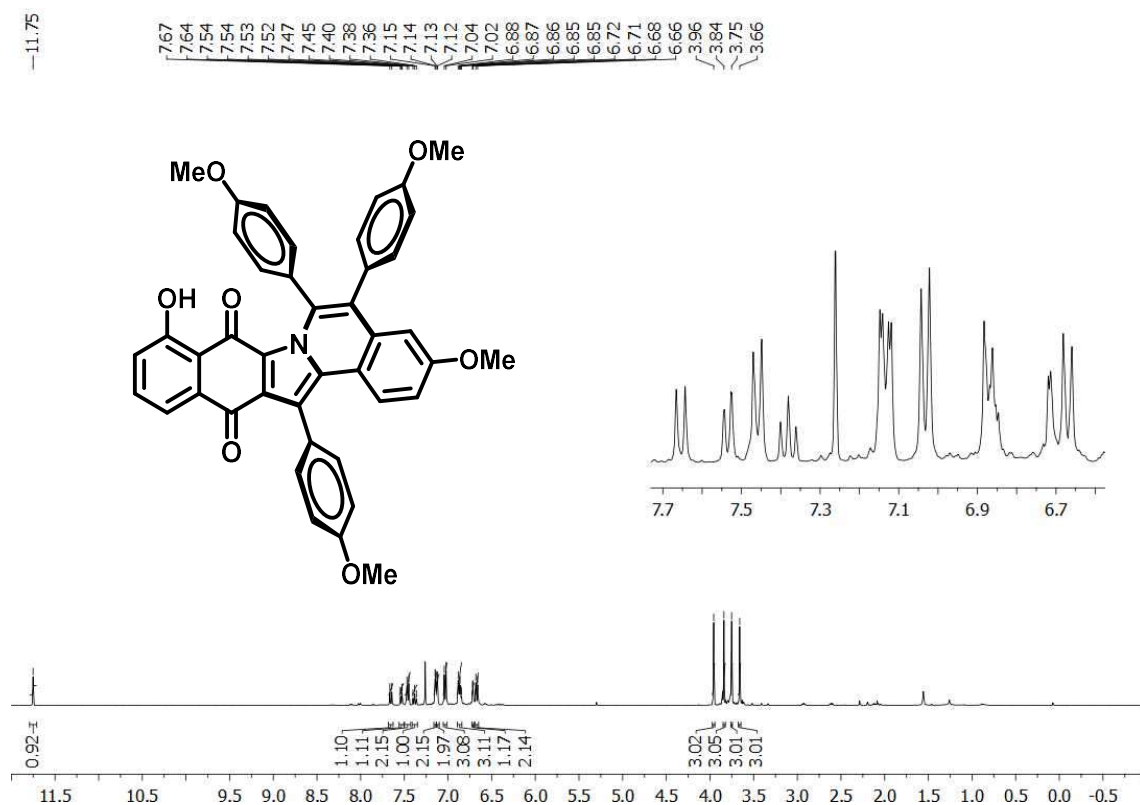


Figure A137. <sup>1</sup>H-NMR spectrum of compound **68b** (CDCl<sub>3</sub>, 400 MHz).

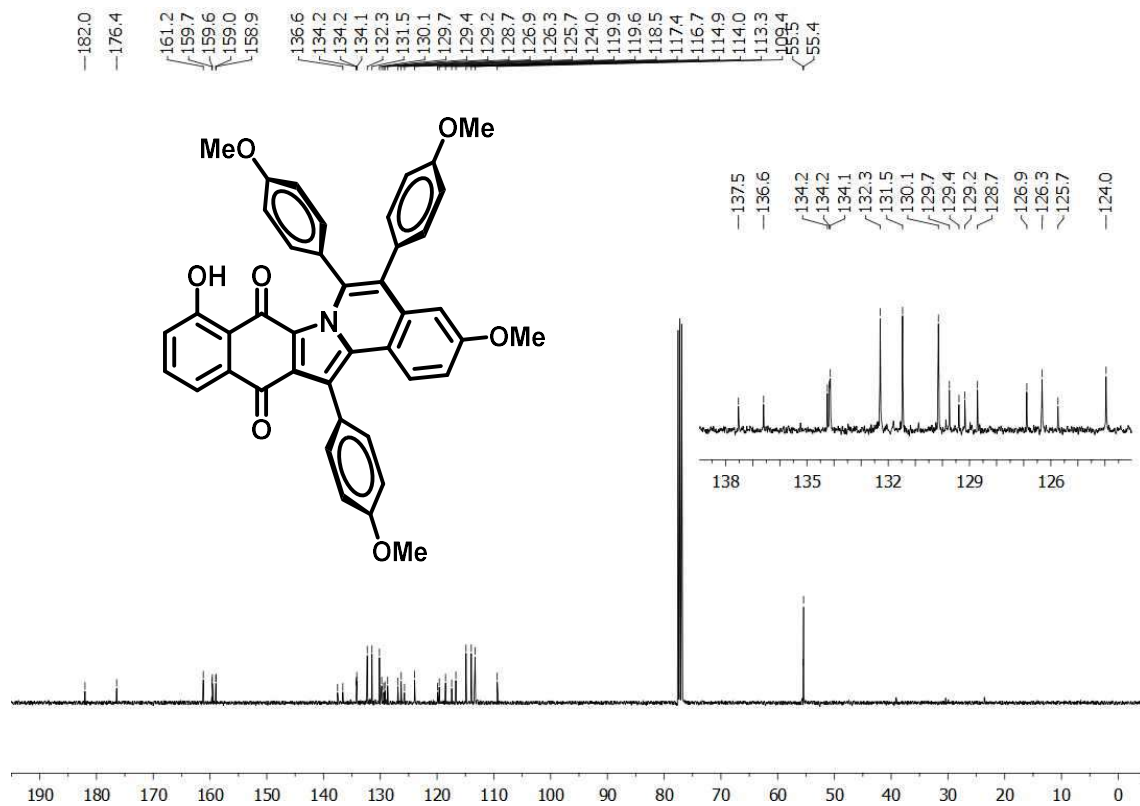


Figure A138. <sup>13</sup>C-NMR spectrum of compound **68b** (CDCl<sub>3</sub>, 100 MHz).



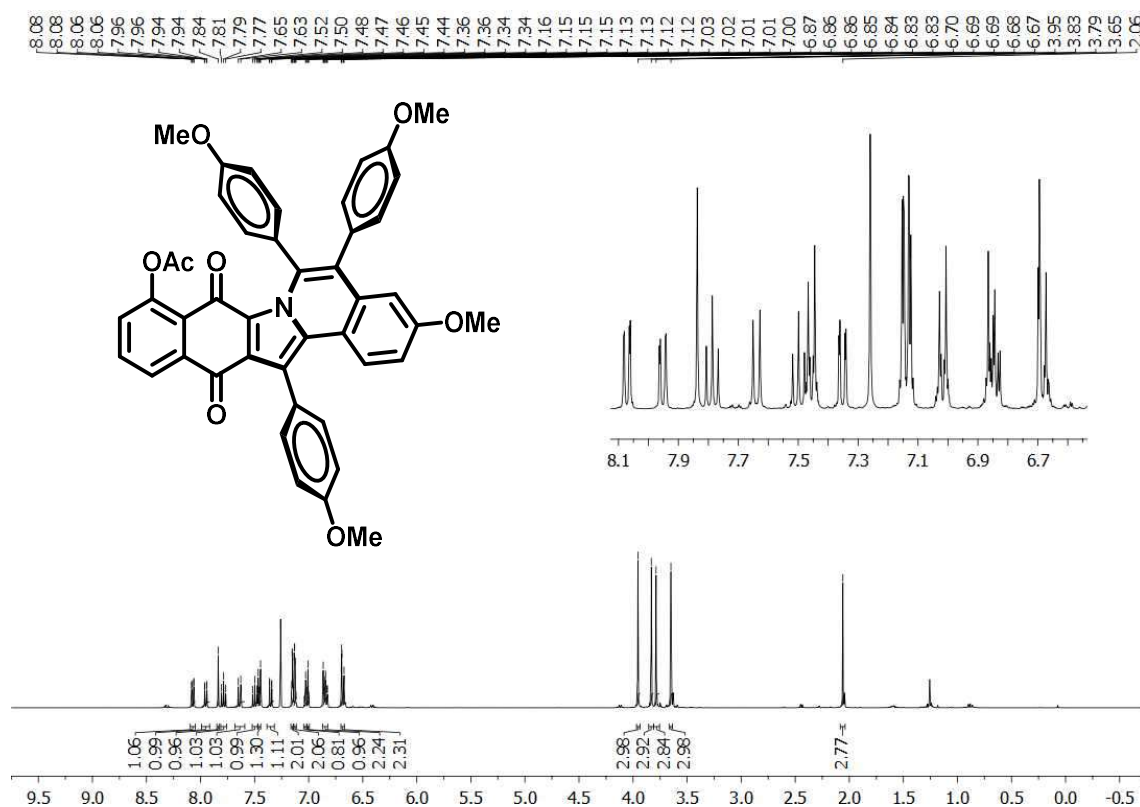


Figure A139. <sup>1</sup>H-NMR spectrum of compound **68c** (CDCl<sub>3</sub>, 400 MHz).

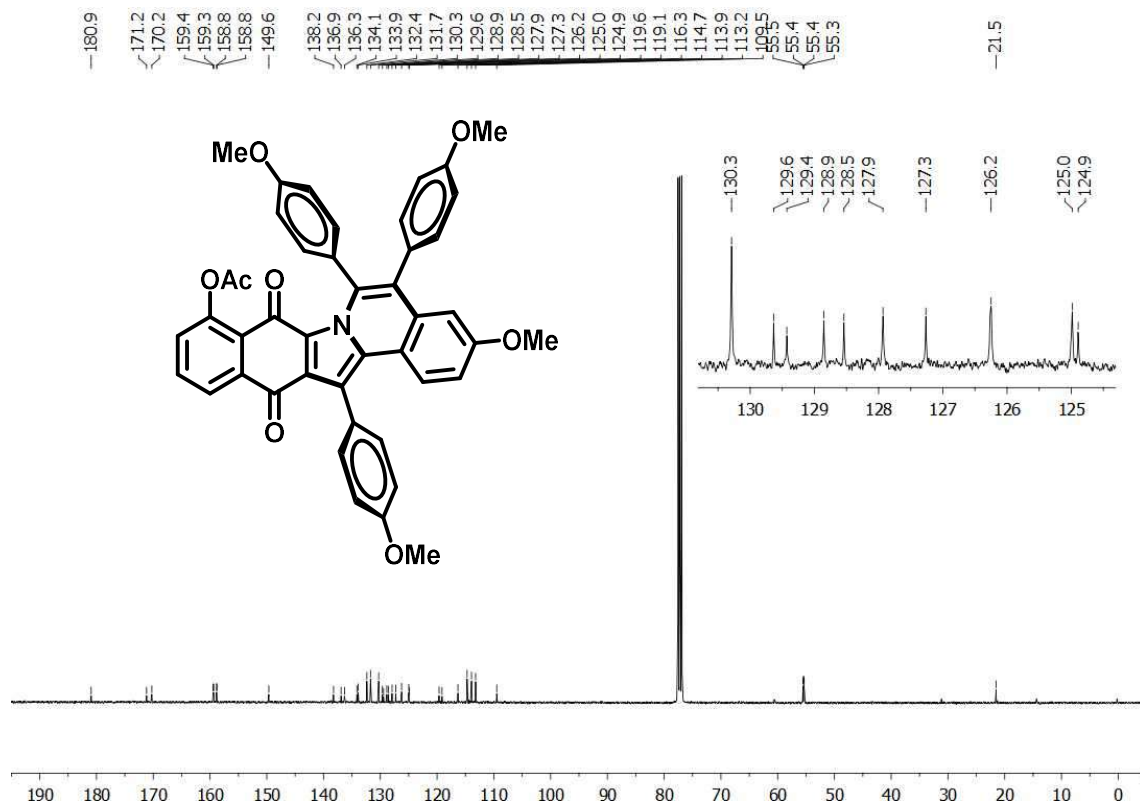


Figure A140. <sup>13</sup>C-NMR spectrum of compound **68c** (CDCl<sub>3</sub>, 100 MHz).

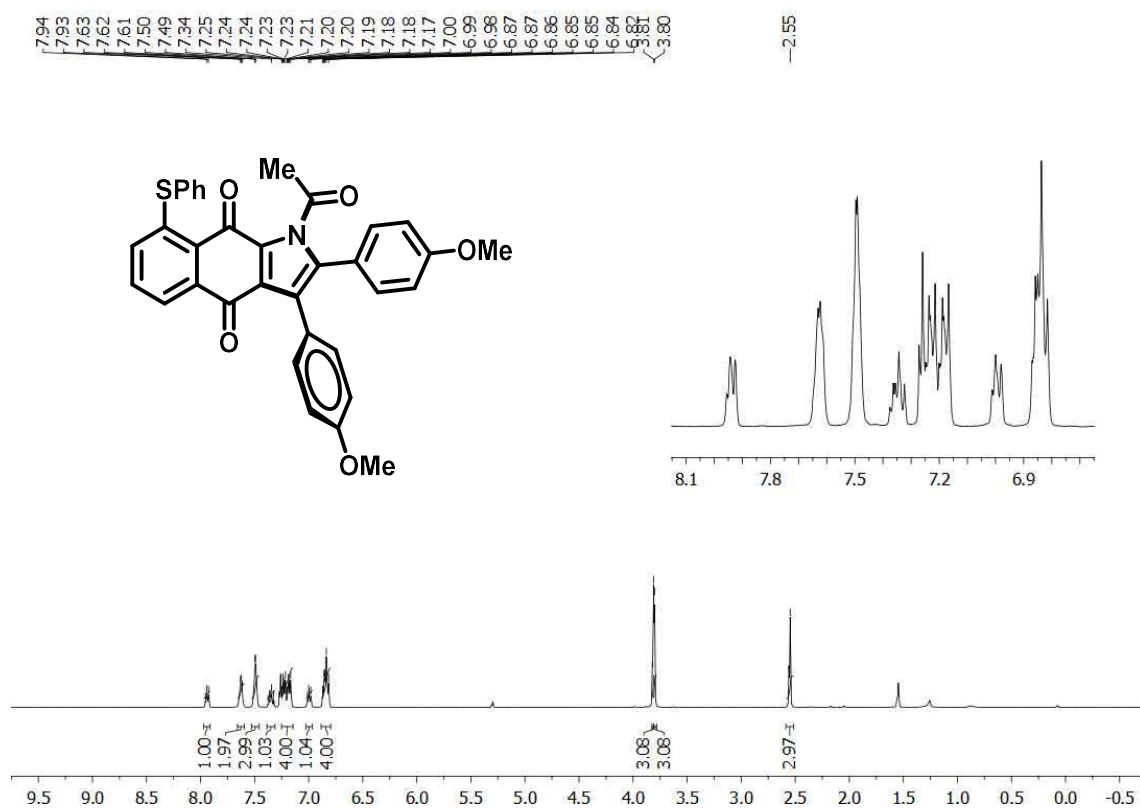


Figure A141. <sup>1</sup>H-NMR spectrum of compound **68d** (CDCl<sub>3</sub>, 400 MHz).

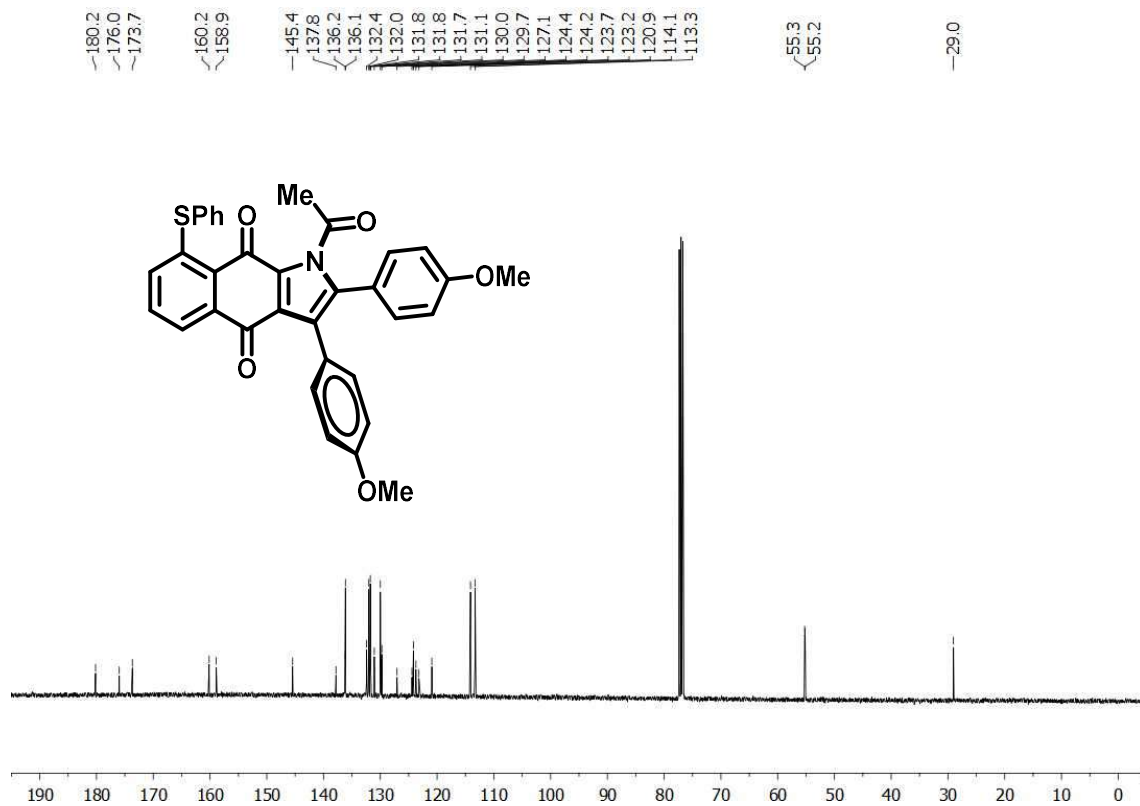


Figure A142. <sup>13</sup>C-NMR spectrum of compound **68d** (CDCl<sub>3</sub>, 100 MHz).

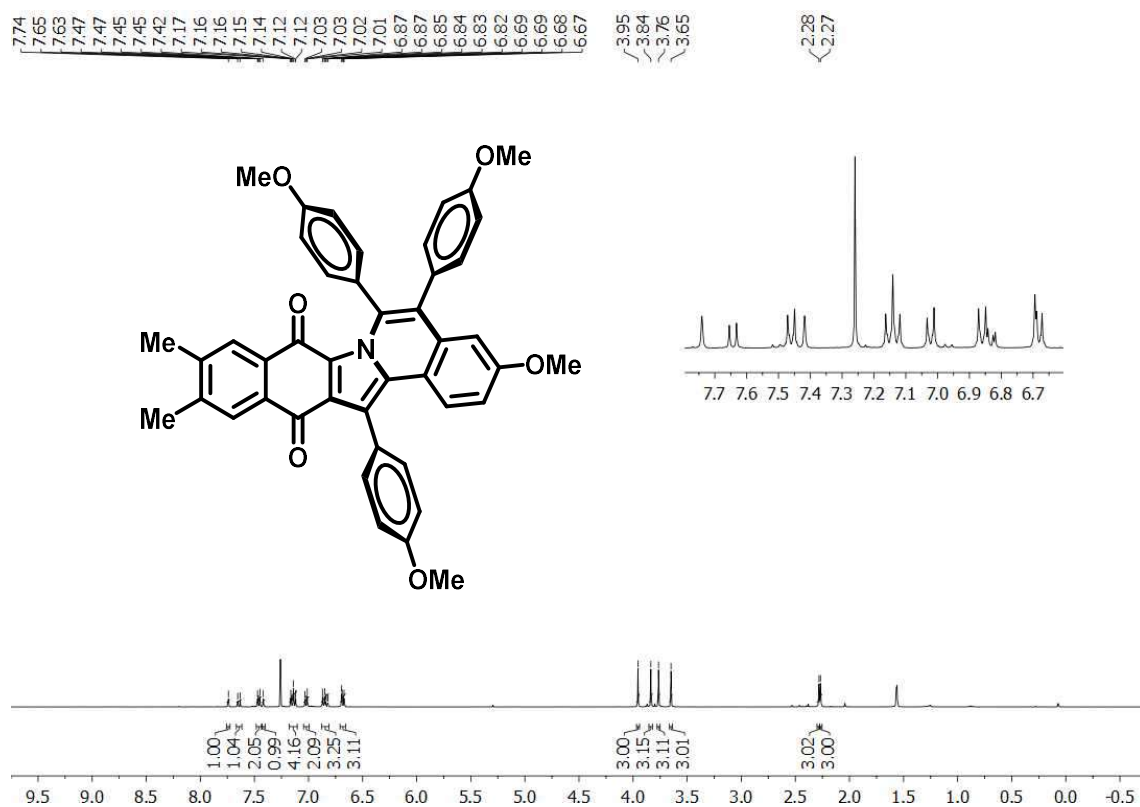


Figure A143. <sup>1</sup>H-NMR spectrum of compound **68e** (CDCl<sub>3</sub>, 400 MHz).

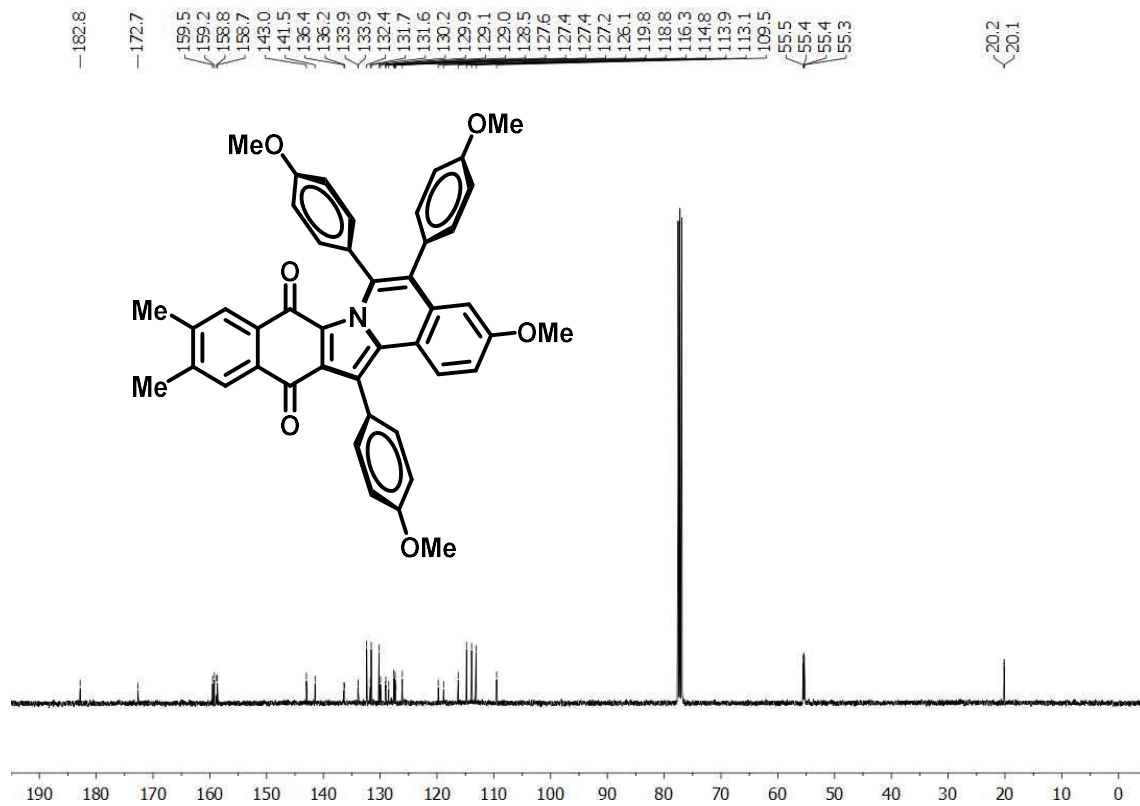


Figure A144. <sup>13</sup>C-NMR spectrum of compound **68e** (CDCl<sub>3</sub>, 100 MHz).

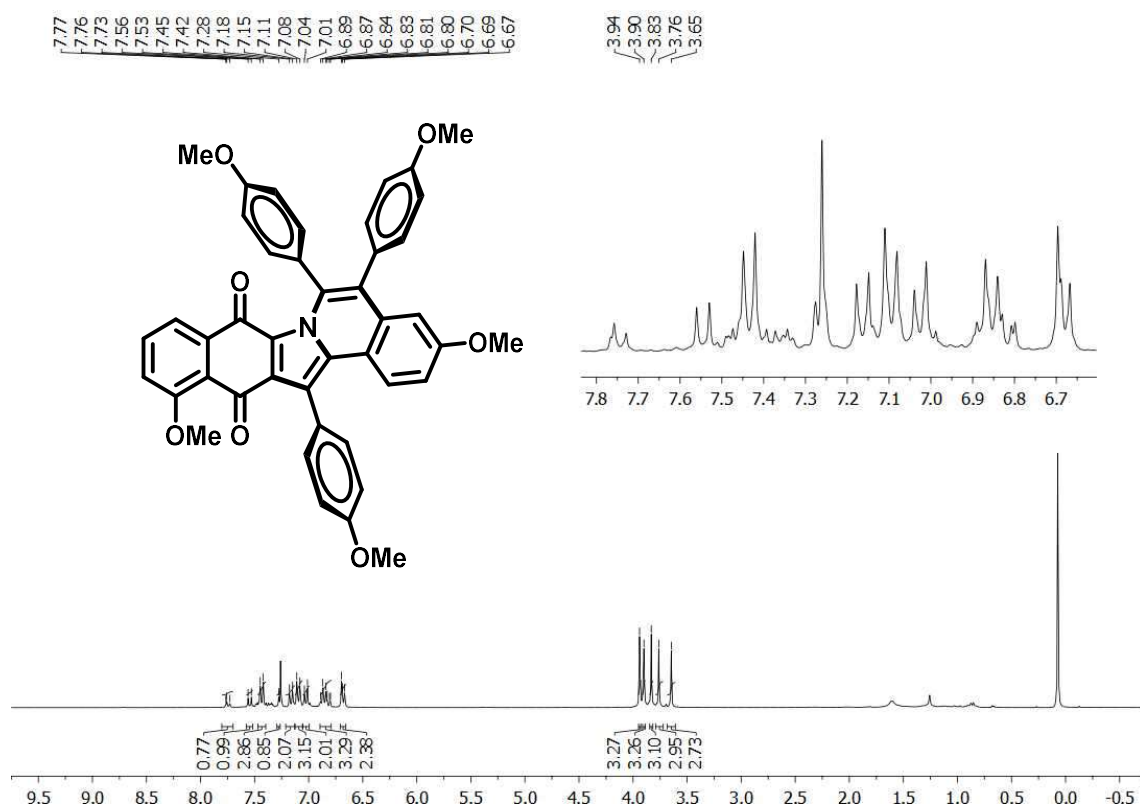


Figure A145. <sup>1</sup>H-NMR spectrum of compound 68f (CDCl<sub>3</sub>, 300 MHz).

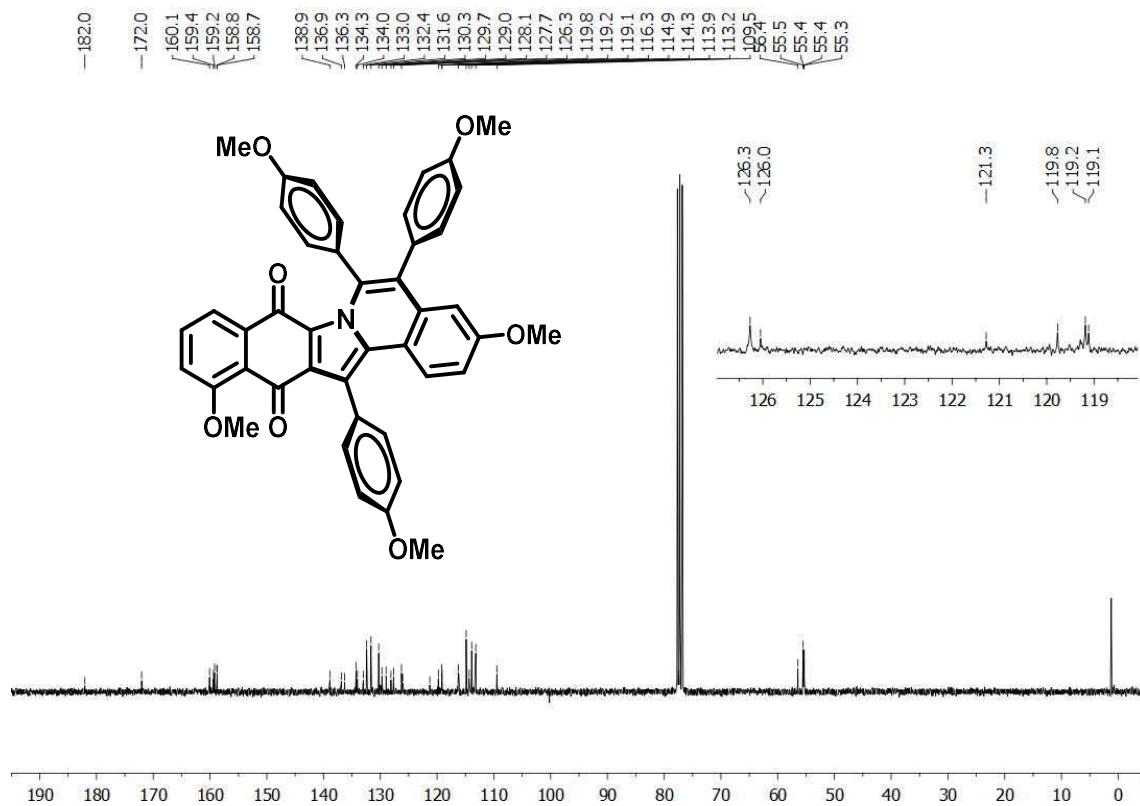


Figure A146. <sup>13</sup>C-NMR spectrum of compound 68f (CDCl<sub>3</sub>, 75 MHz)

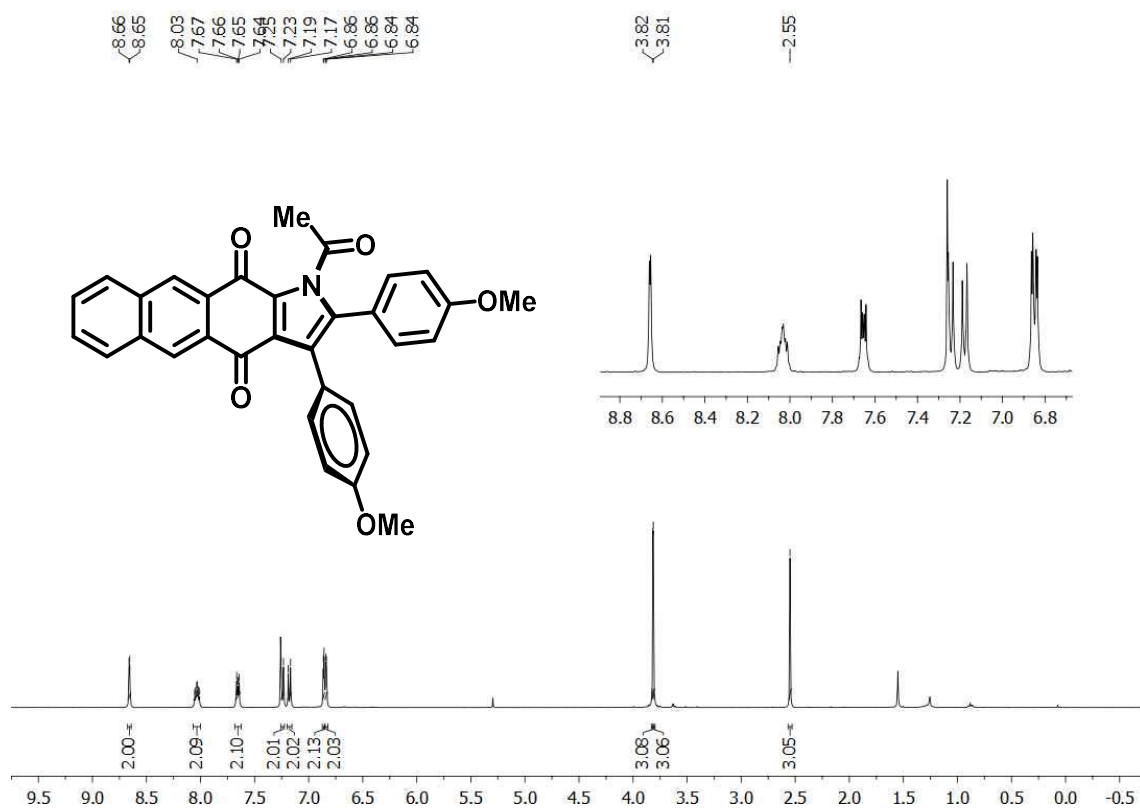


Figure A147. <sup>1</sup>H-NMR spectrum of compound **68g** (CDCl<sub>3</sub>, 400 MHz).

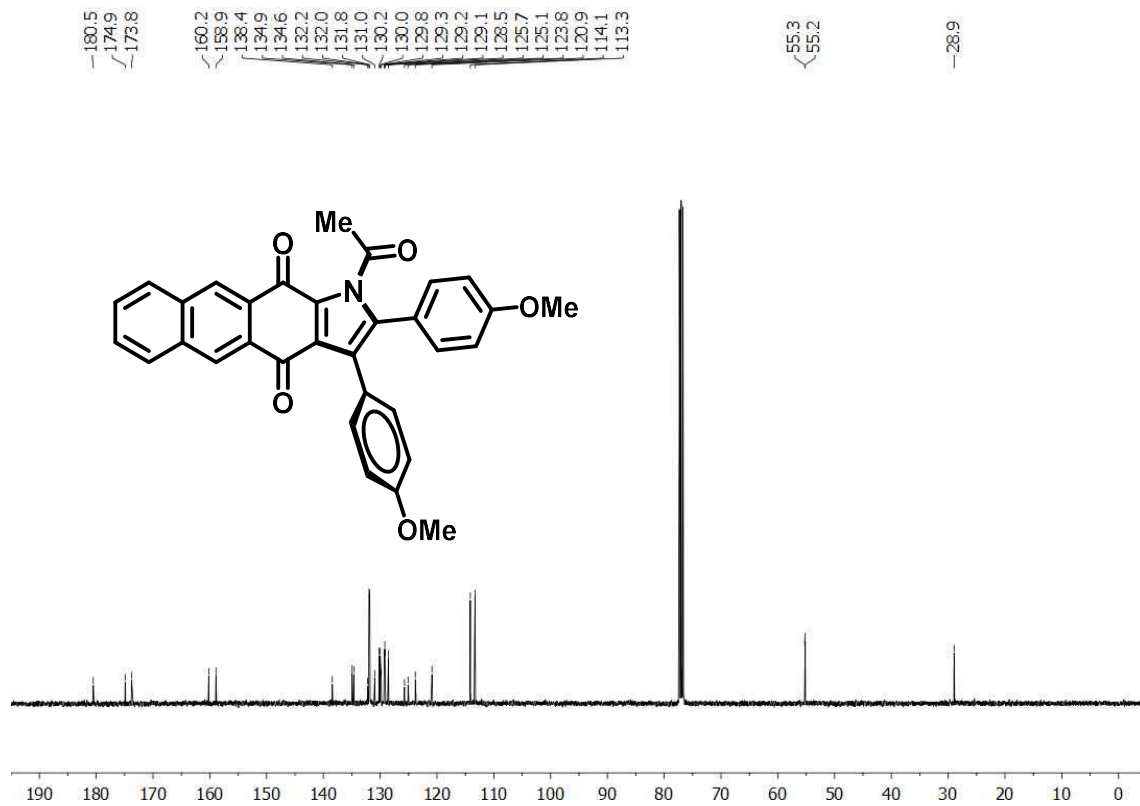


Figure A148. <sup>13</sup>C-NMR spectrum of compound **68g** (CDCl<sub>3</sub>, 100 MHz).

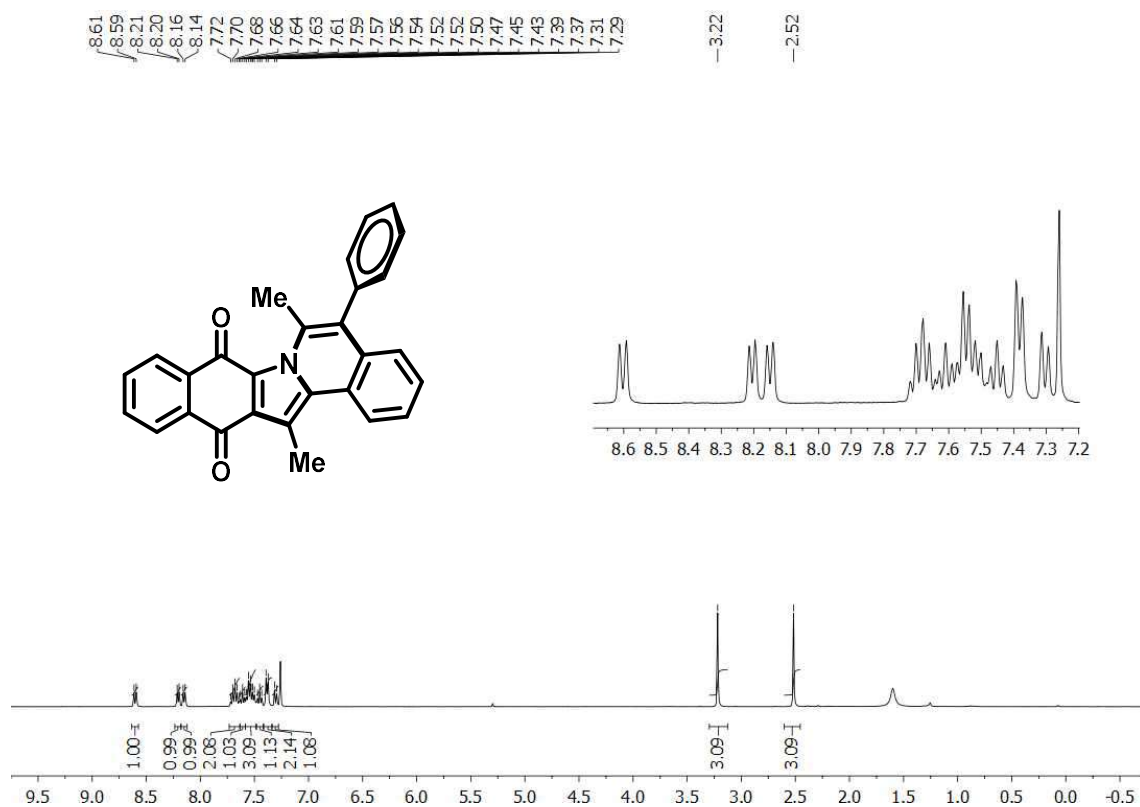


Figure A149. <sup>1</sup>H-NMR spectrum of compound **69a** (CDCl<sub>3</sub>, 400 MHz).

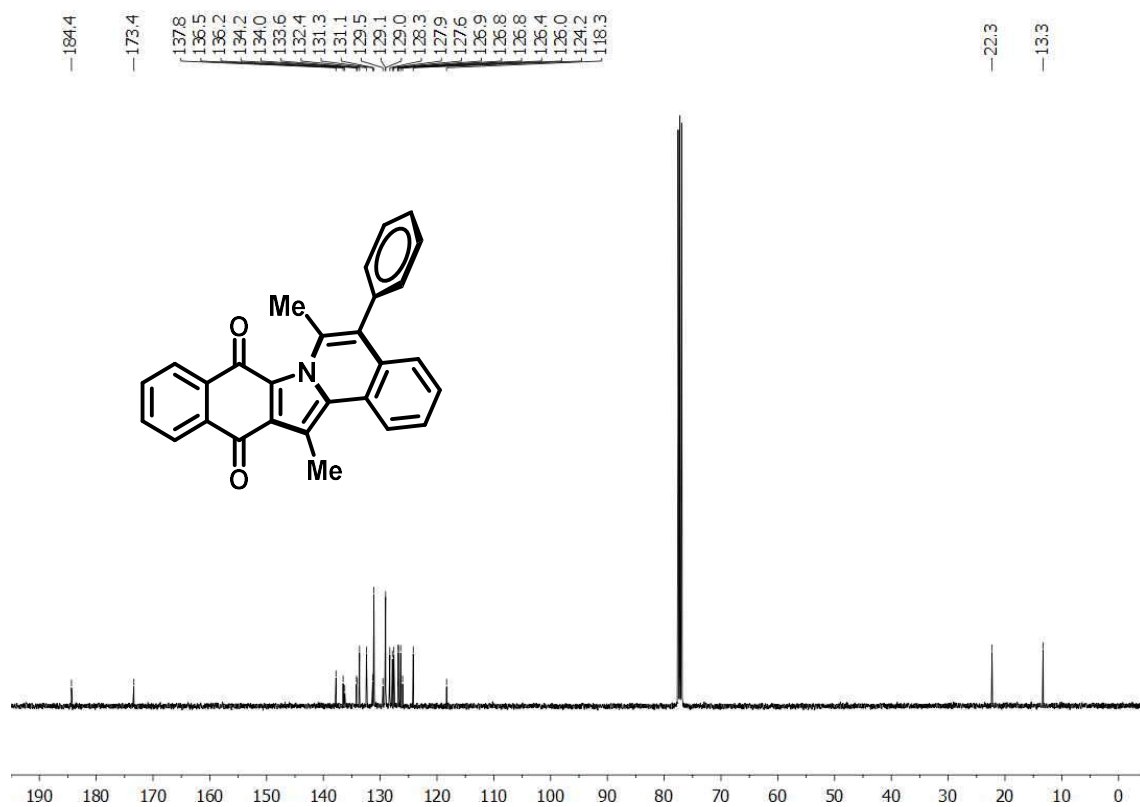


Figure A150. <sup>13</sup>C-NMR spectrum of compound **69a** (CDCl<sub>3</sub>, 100 MHz).

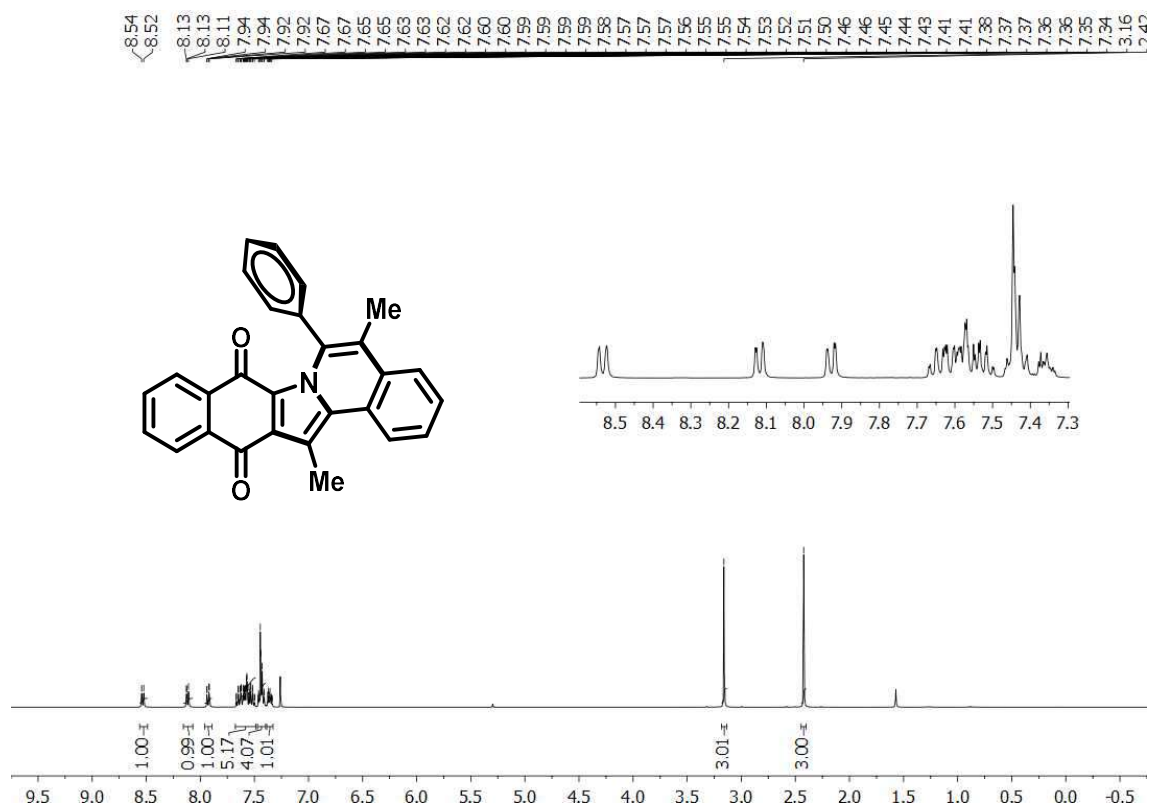


Figure A151. <sup>1</sup>H-NMR spectrum of compound **69b** (CDCl<sub>3</sub>, 400 MHz).

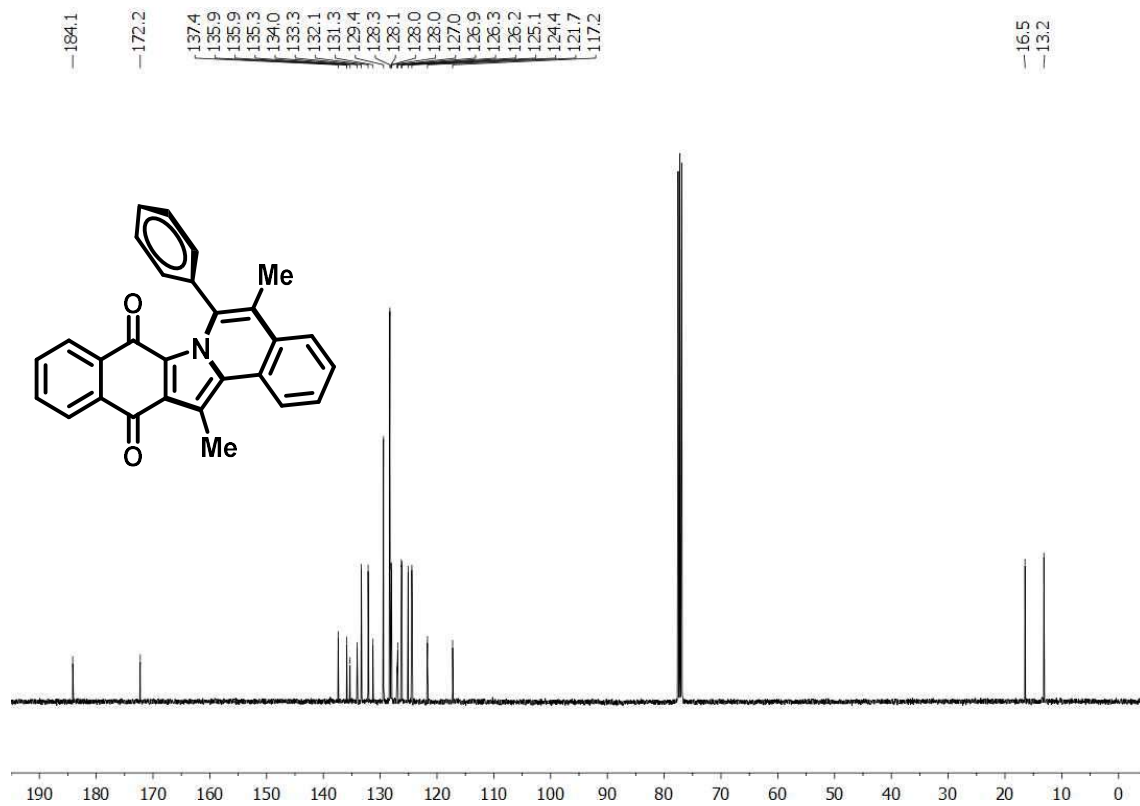
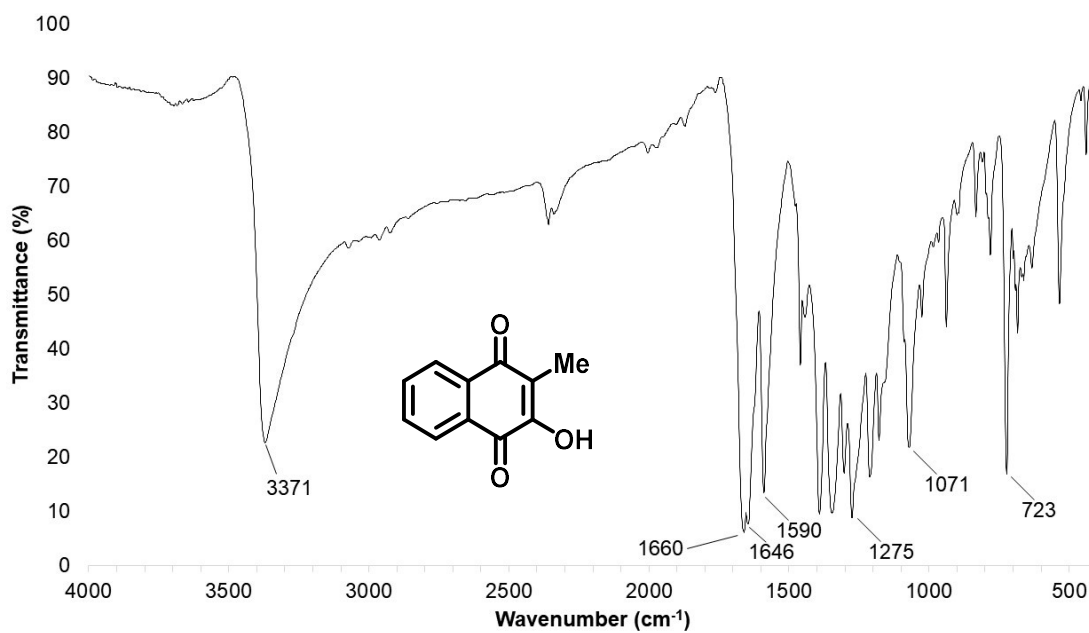
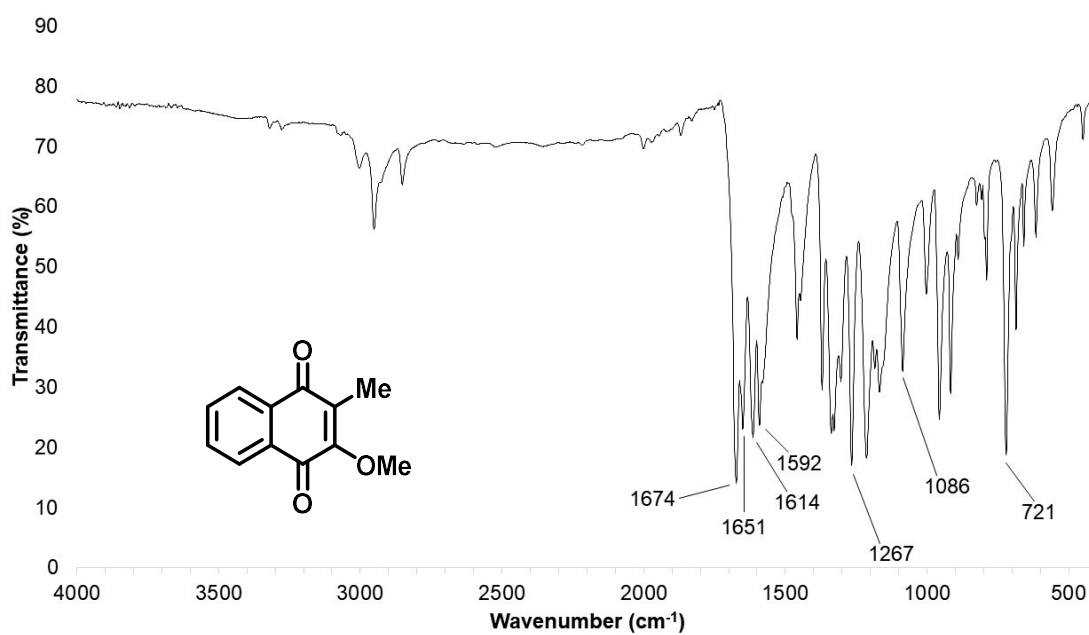


Figure A152. <sup>13</sup>C-NMR spectrum of compound **69b** (CDCl<sub>3</sub>, 100 MHz).



**Figure B1.** Infrared spectrum (IR-KBr) of the compound **51a**.



**Figure B2.** Infrared spectrum (IR-KBr) of the compound **51b**.



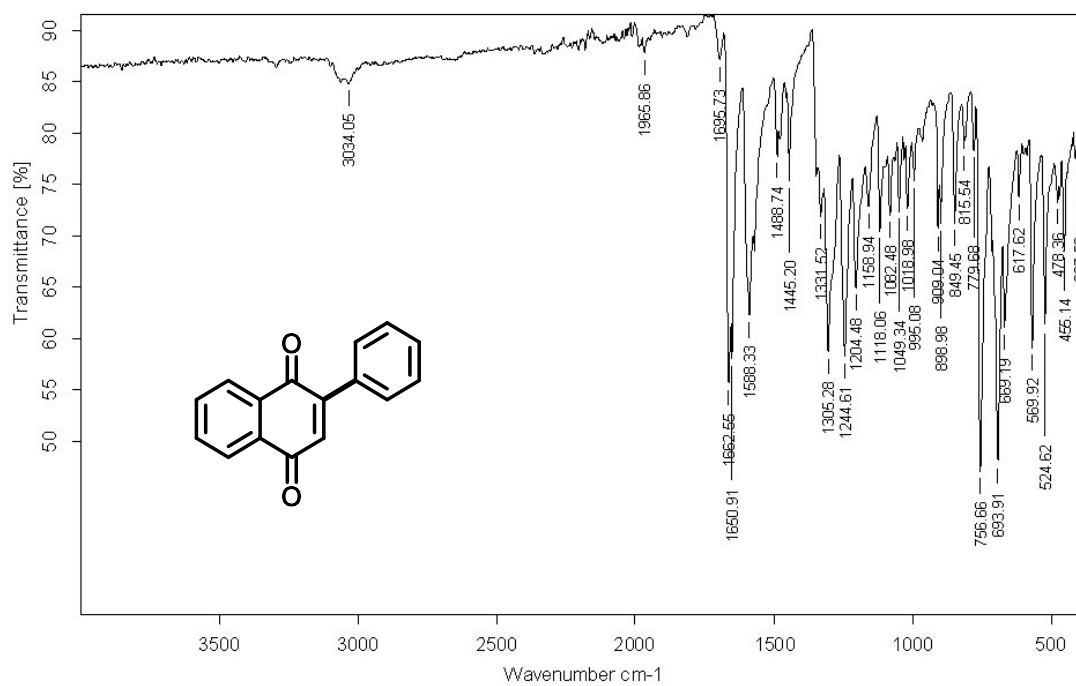


Figure B3. Infrared spectrum (ATR) of the compound 52.

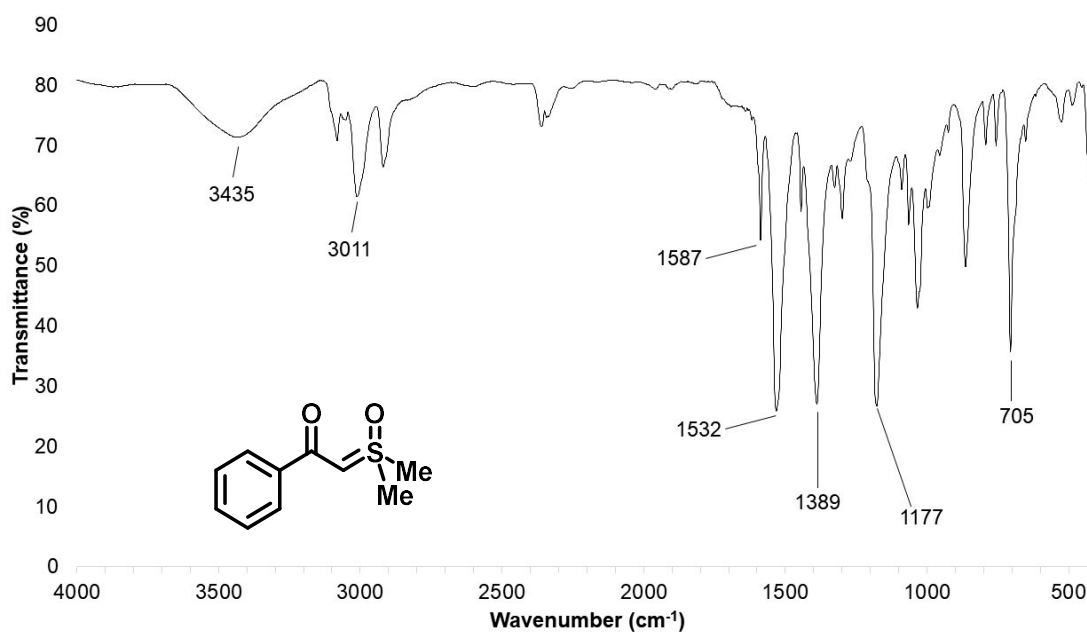
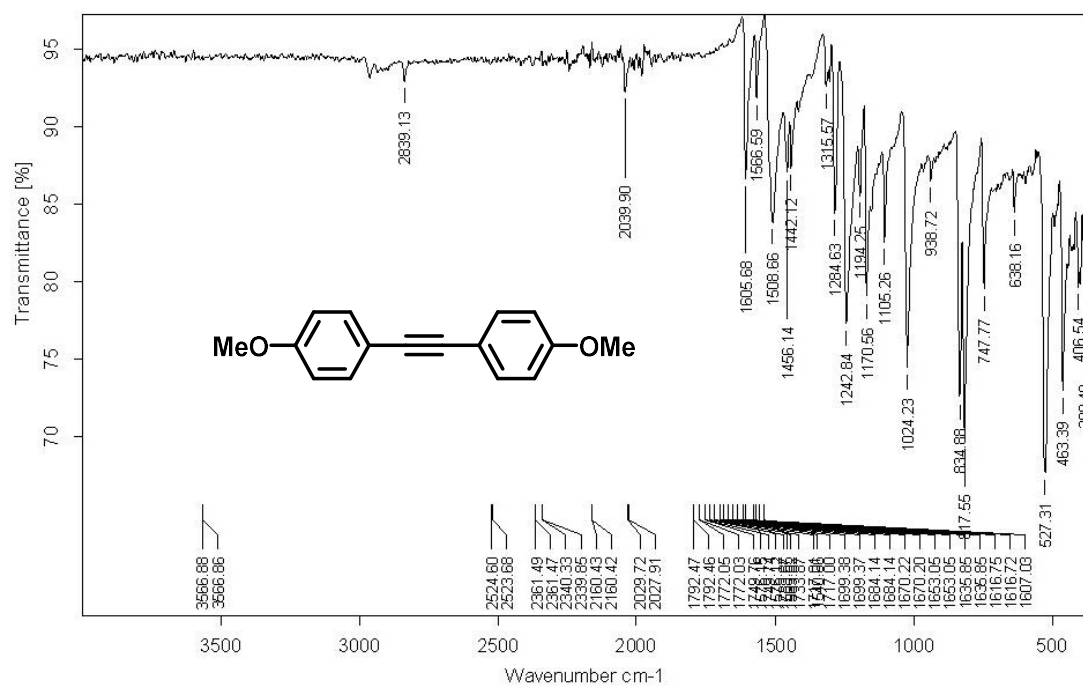
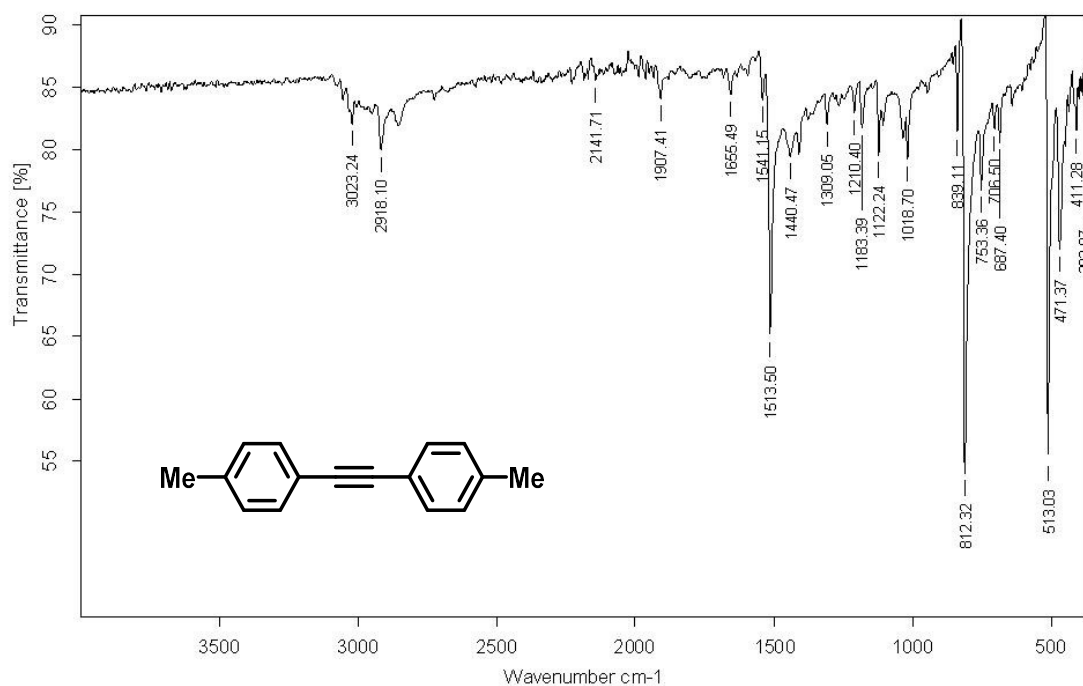


Figure B4. Infrared spectrum (IR-KBr) of the compound 55.



**Figure B5.** Infrared spectrum (IR-ATR) of the compound **56b**.



**Figure B6.** Infrared spectrum (IR-ATR) of the compound **56c**.

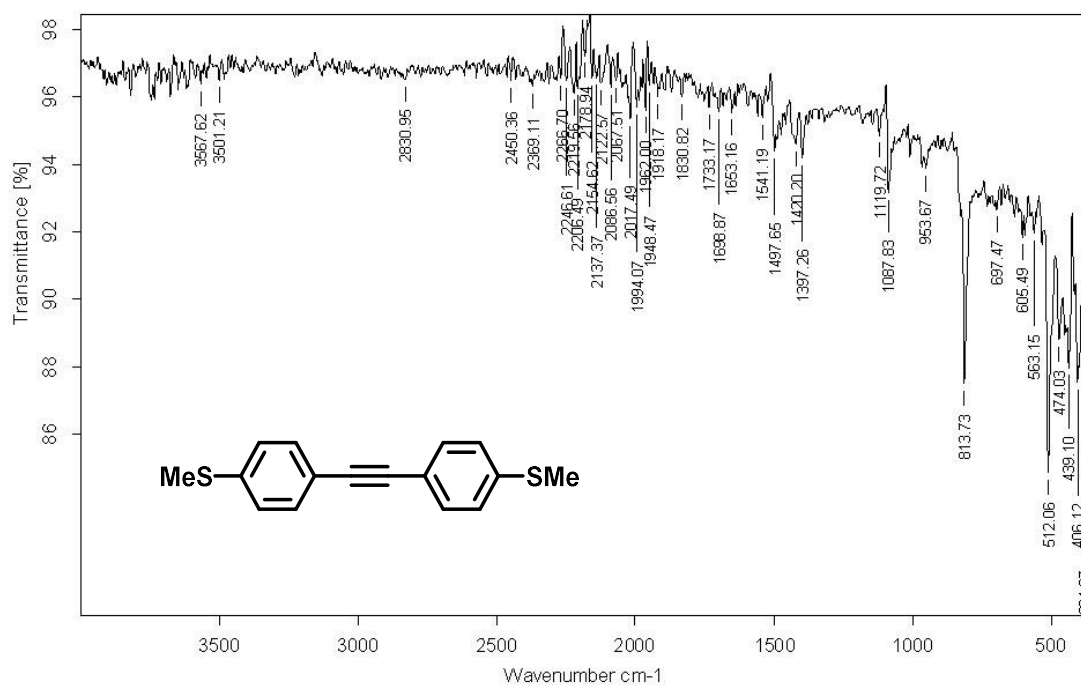


Figure B7. Infrared spectrum (IR-ATR) of the compound 56d.

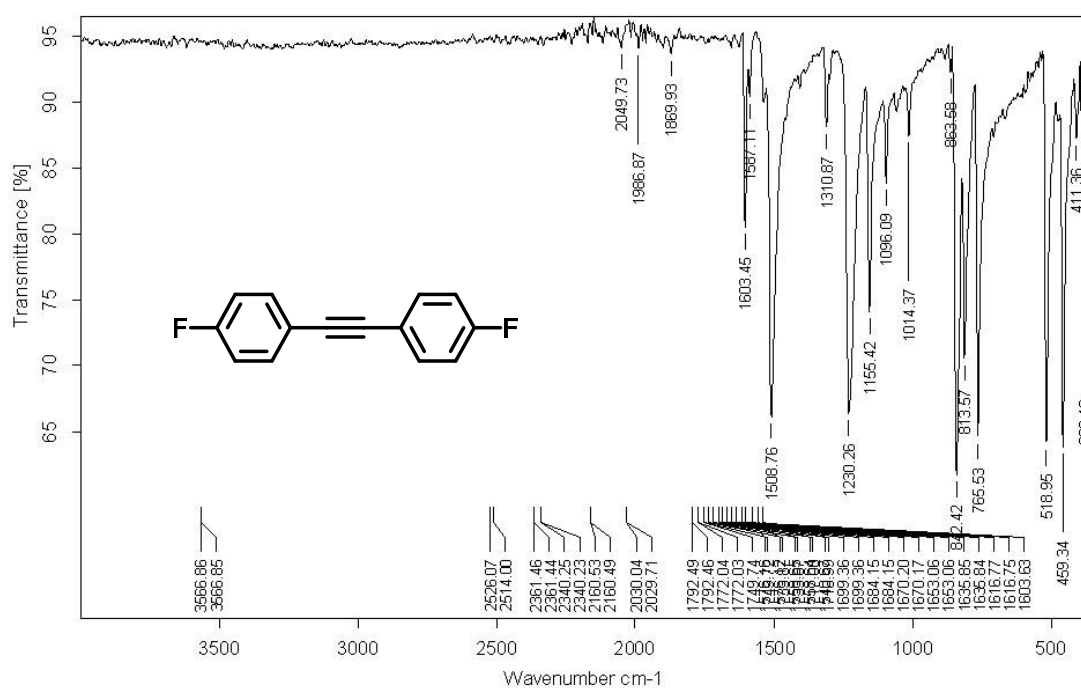
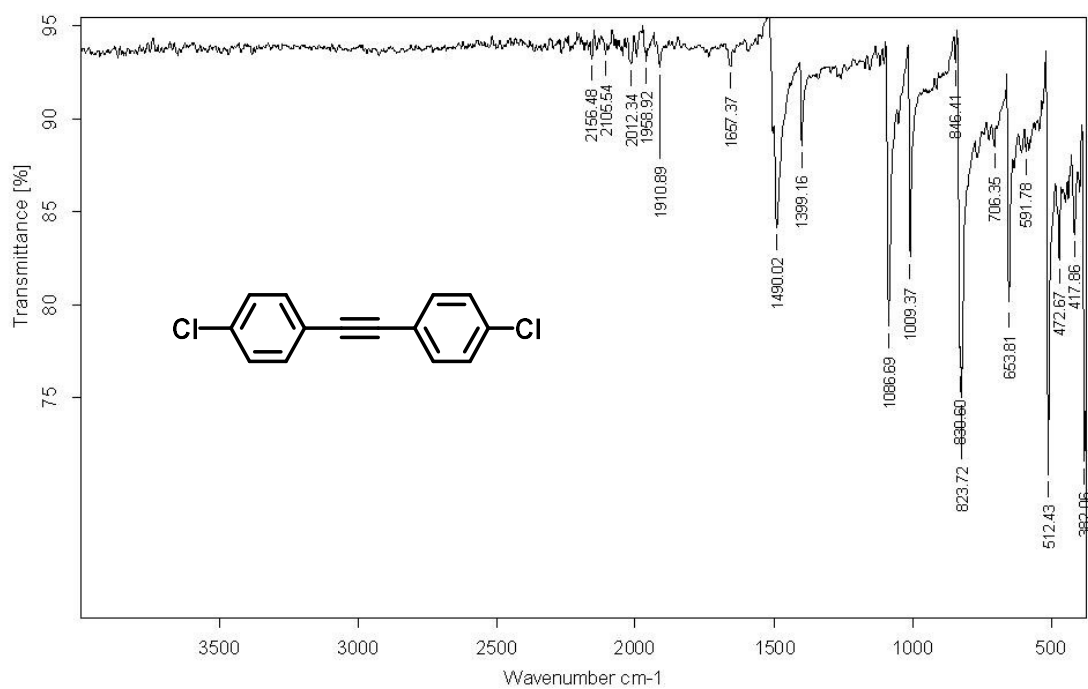
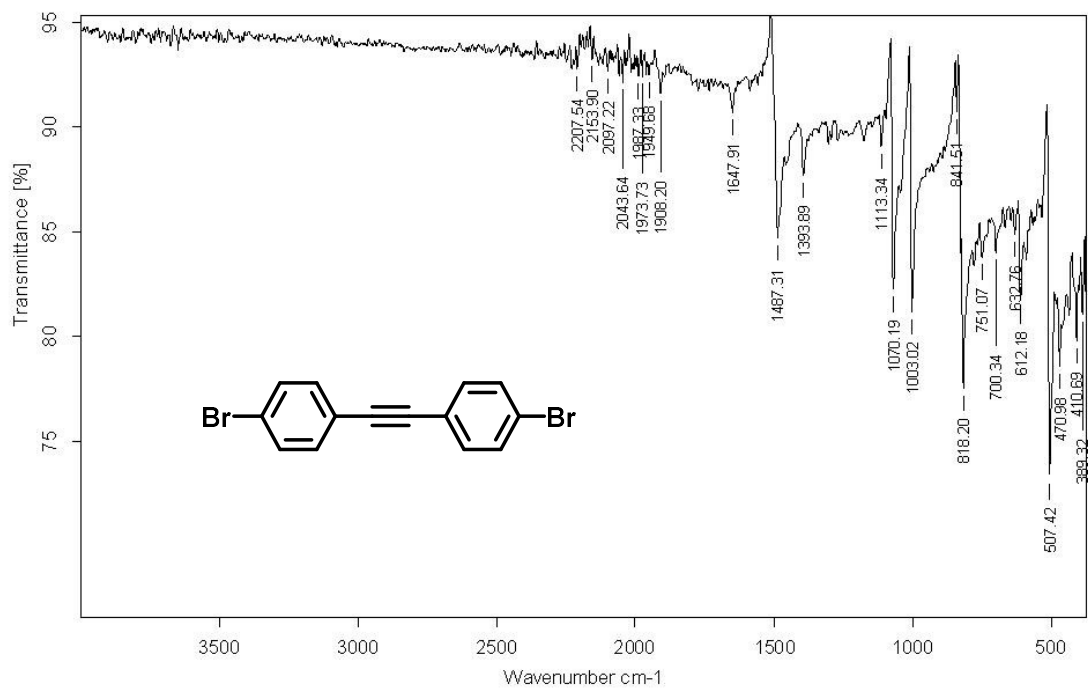


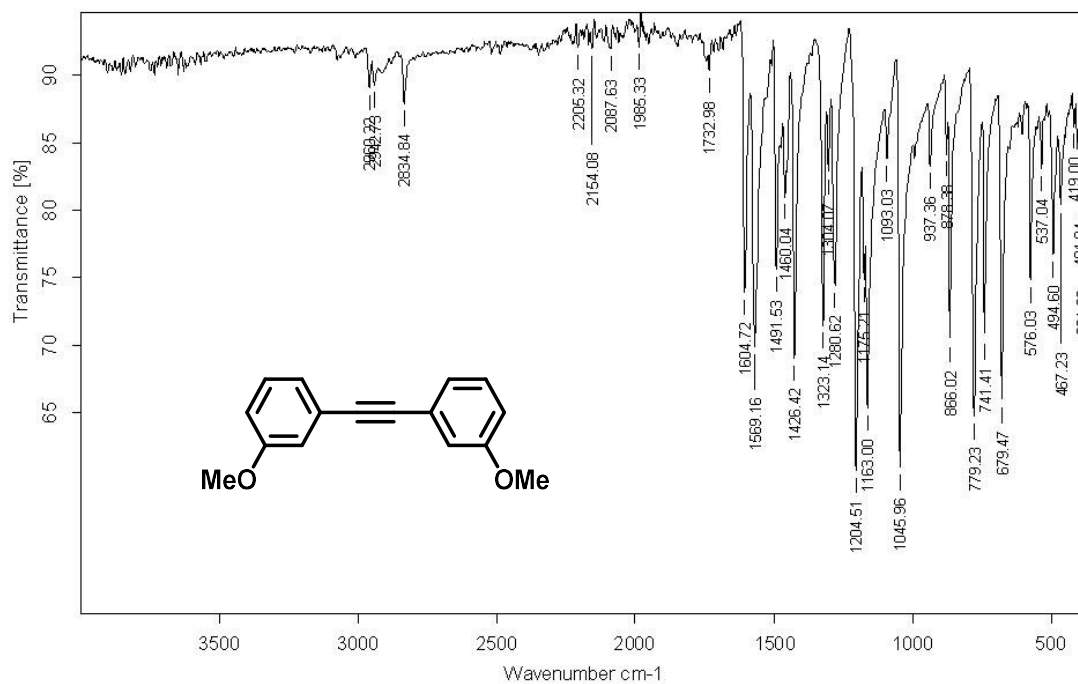
Figure B8. Infrared spectrum (IR-ATR) of the compound 56e.



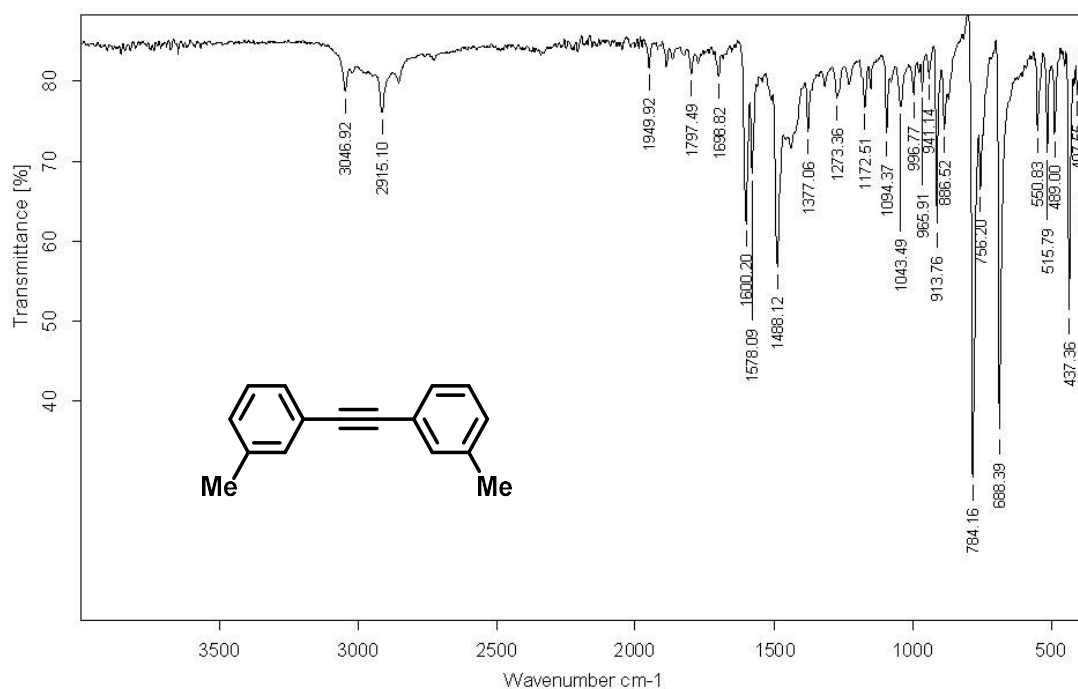
**Figure B9.** Infrared spectrum (IR-ATR) of the compound **56f**.



**Figure B10.** Infrared spectrum (IR-ATR) of the compound **56g**.



**Figure B11.** Infrared spectrum (IR-ATR) of the compound **56h**.



**Figure B12.** Infrared spectrum (IR-ATR) of the compound **56i**.

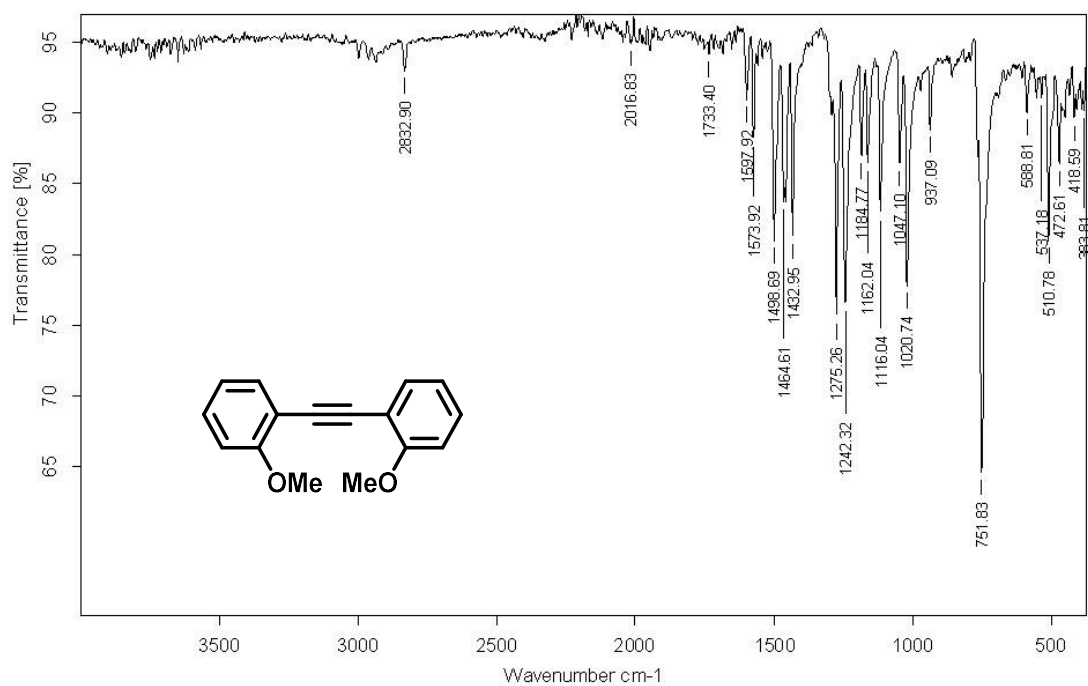


Figure B13. Infrared spectrum (IR-ATR) of the compound 56j.

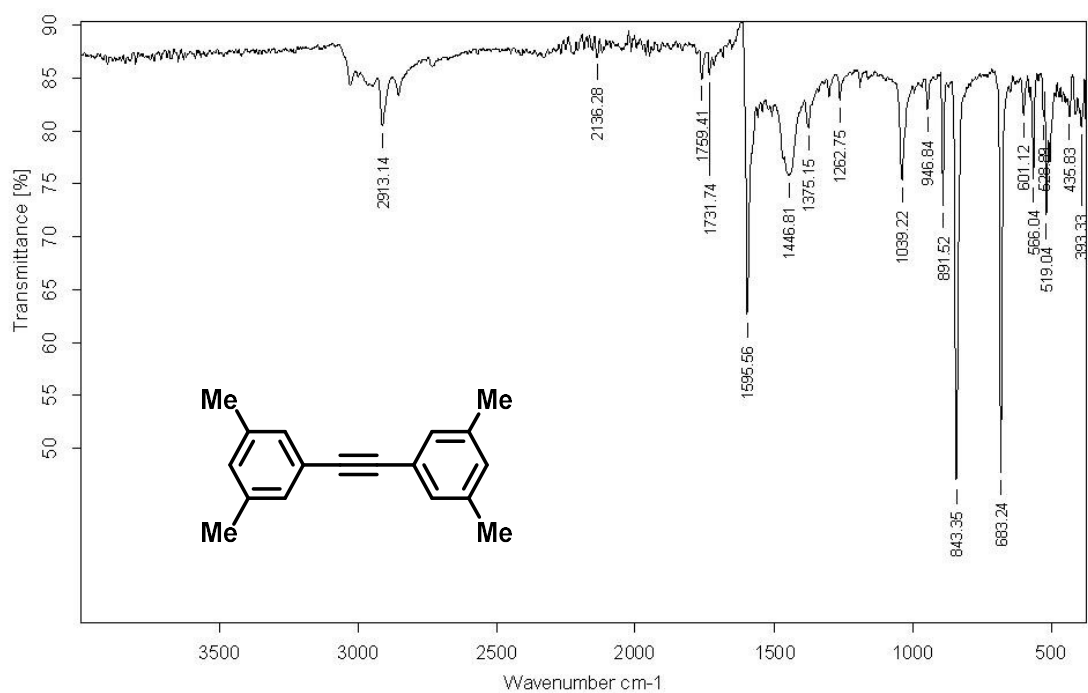
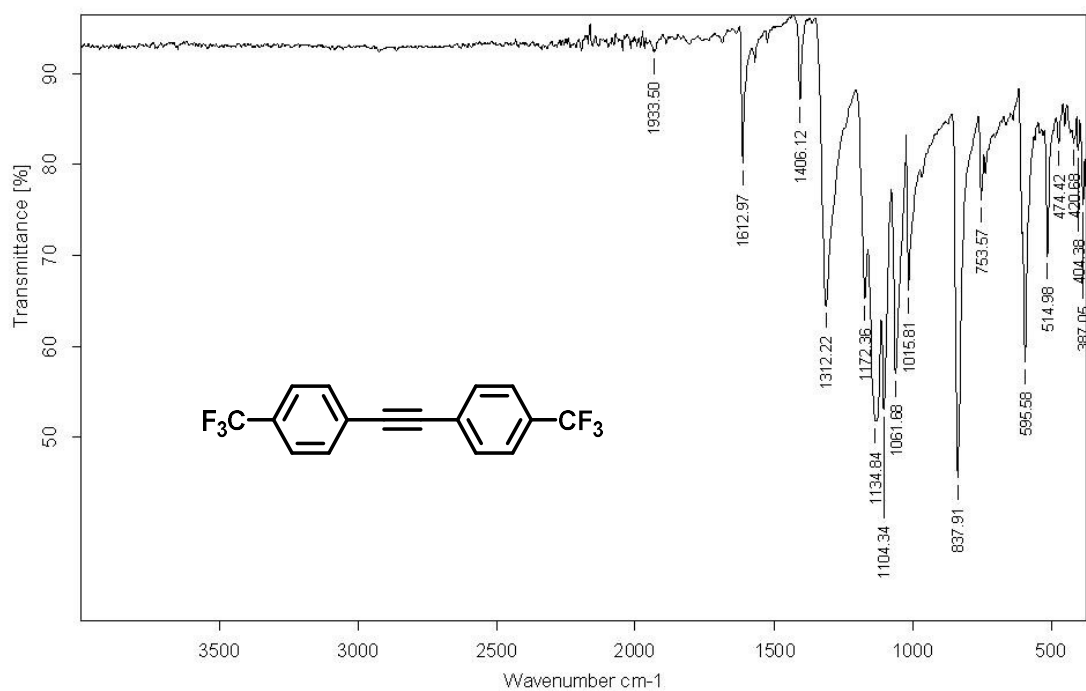
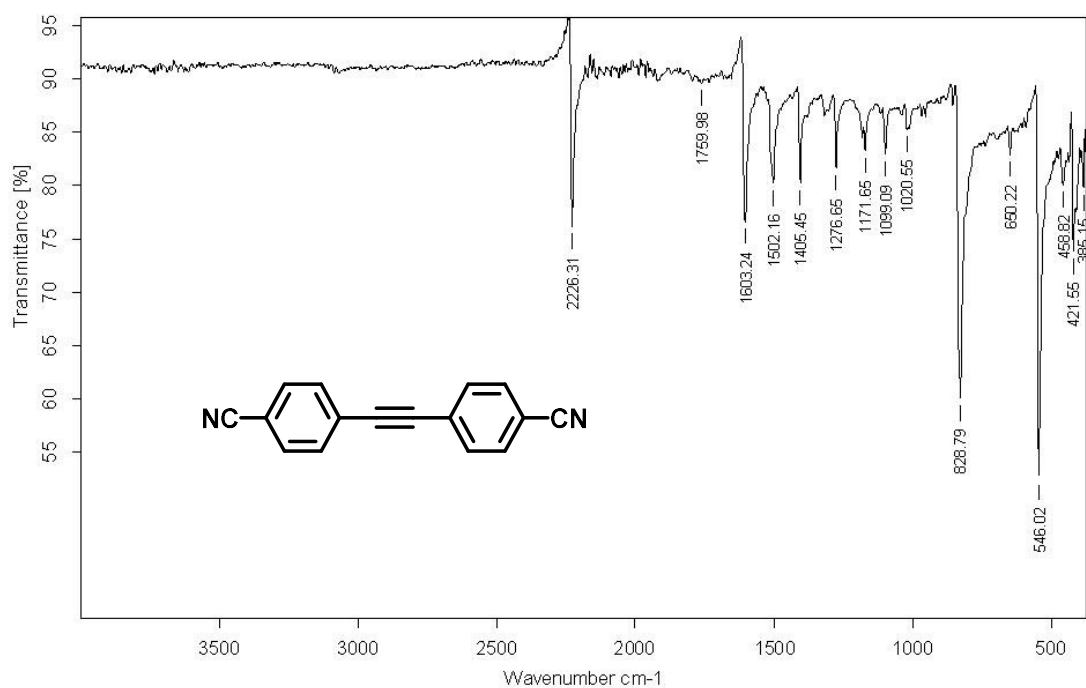


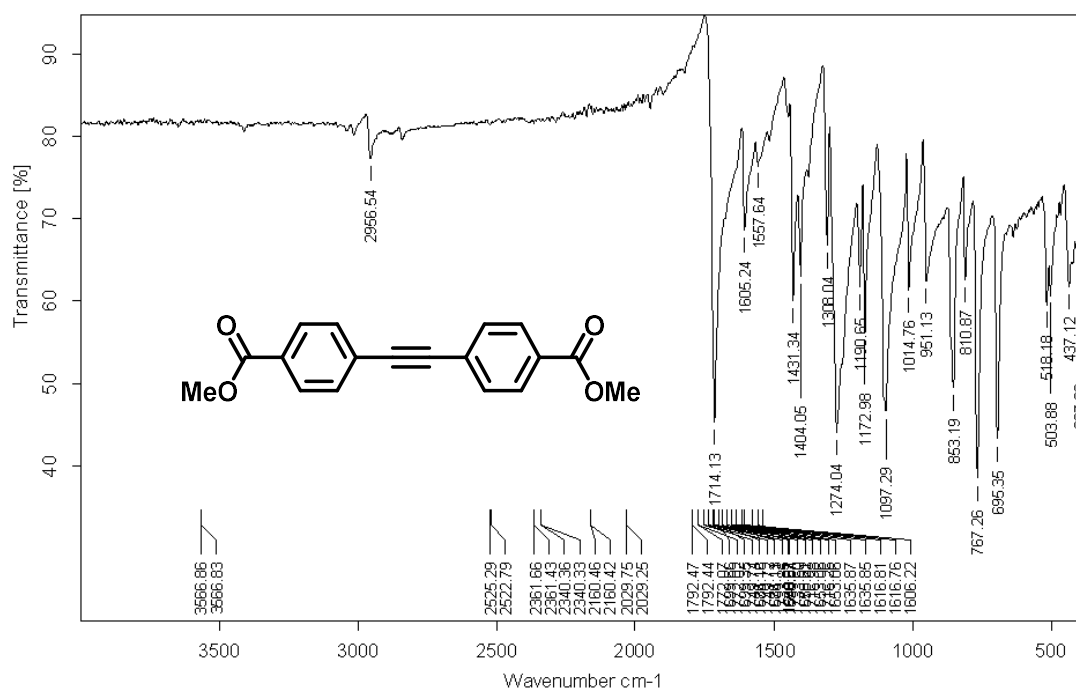
Figure B14. Infrared spectrum (IR-ATR) of the compound 56k.



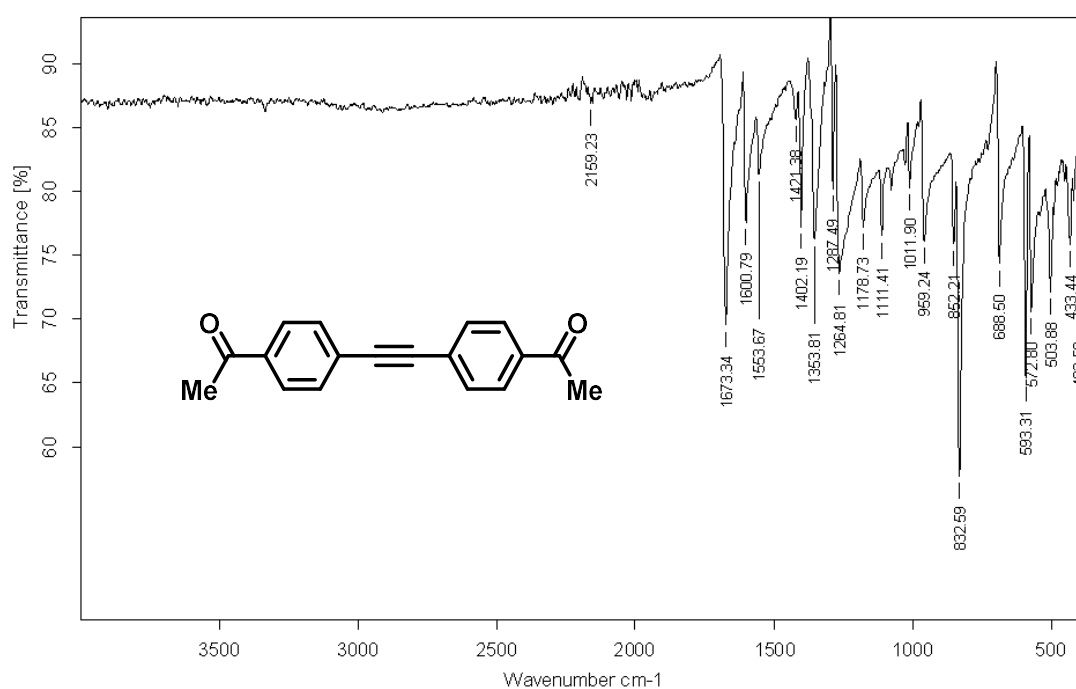
**Figure B15.** Infrared spectrum (IR-ATR) of the compound **56l**.



**Figure B16.** Infrared spectrum (IR-ATR) of the compound **56m**.



**Figure B17.** Infrared spectrum (IR-ATR) of the compound 56n.



**Figure B18.** Infrared spectrum (IR-ATR) of the compound 56o.



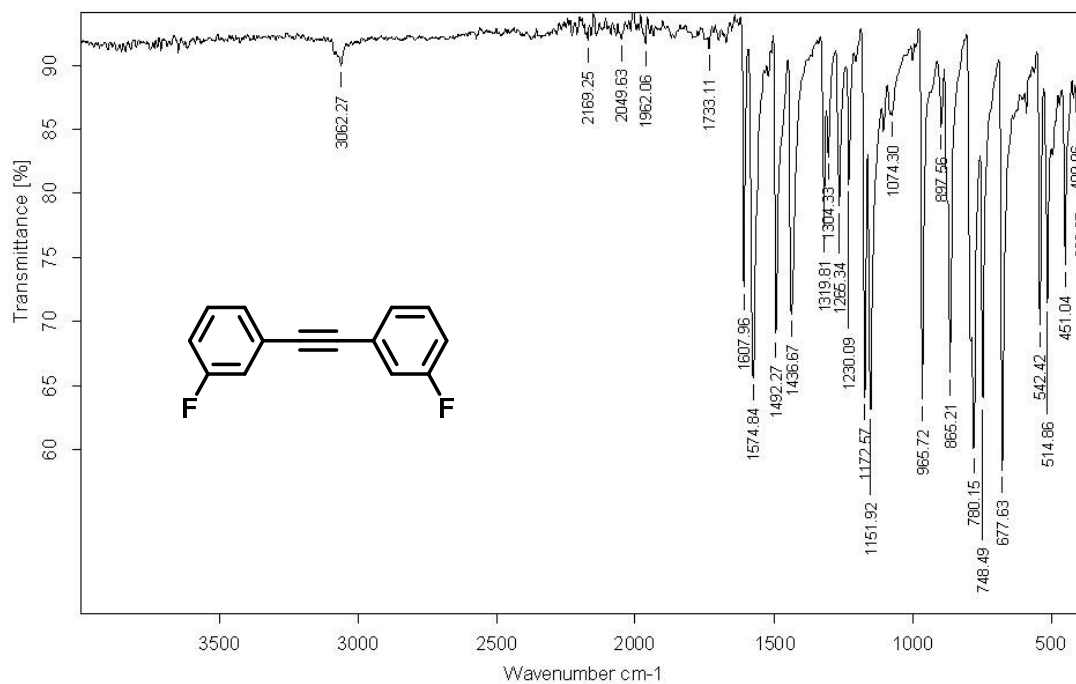


Figure B19. Infrared spectrum (IR-ATR) of the compound 56p.

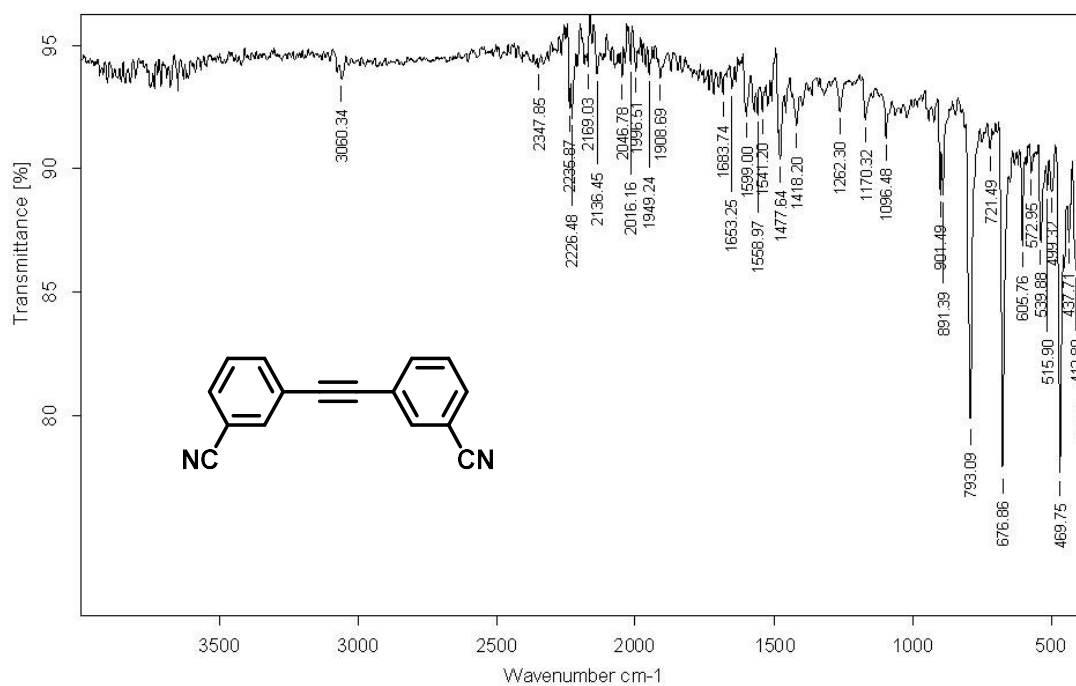


Figure B20. Infrared spectrum (IR-ATR) of the compound 56q.

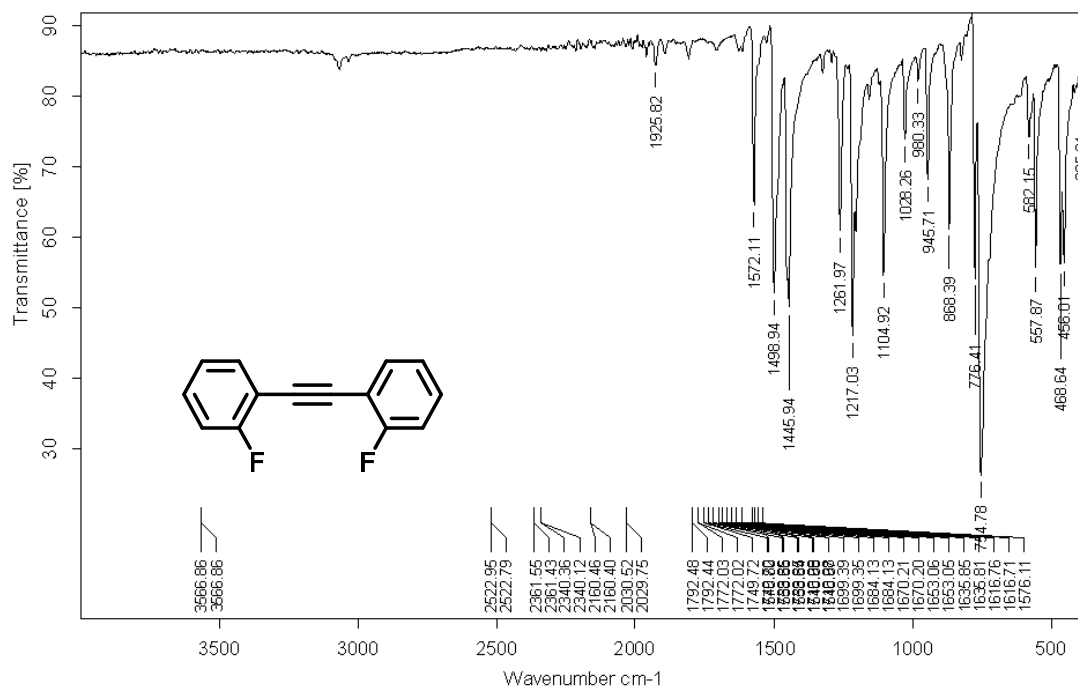


Figure B21. Infrared spectrum (IR-ATR) of the compound **56r**.

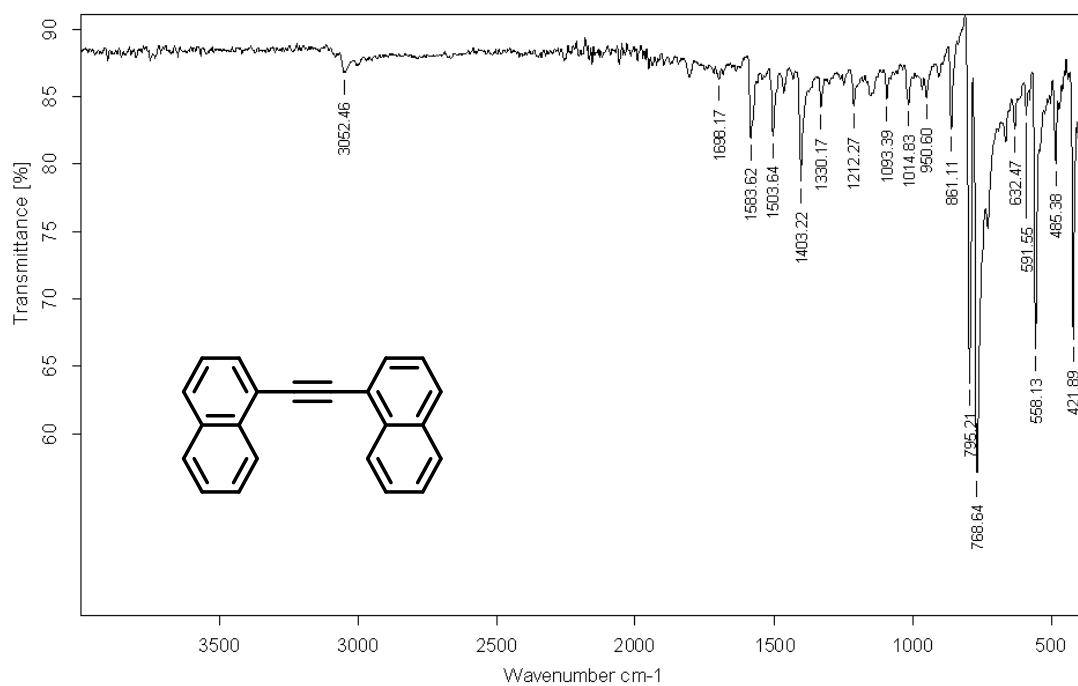


Figure B22. Infrared spectrum (IR-ATR) of the compound **56s**.

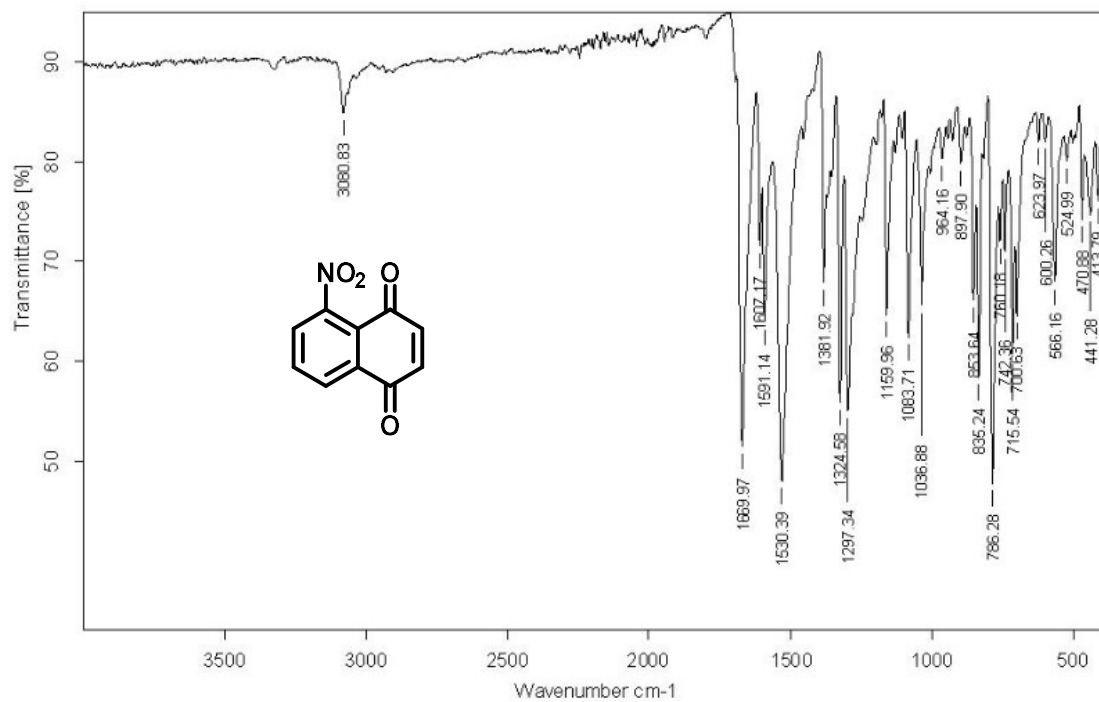


Figure B23. Infrared spectrum (IR-ATR) of the compound 57a.

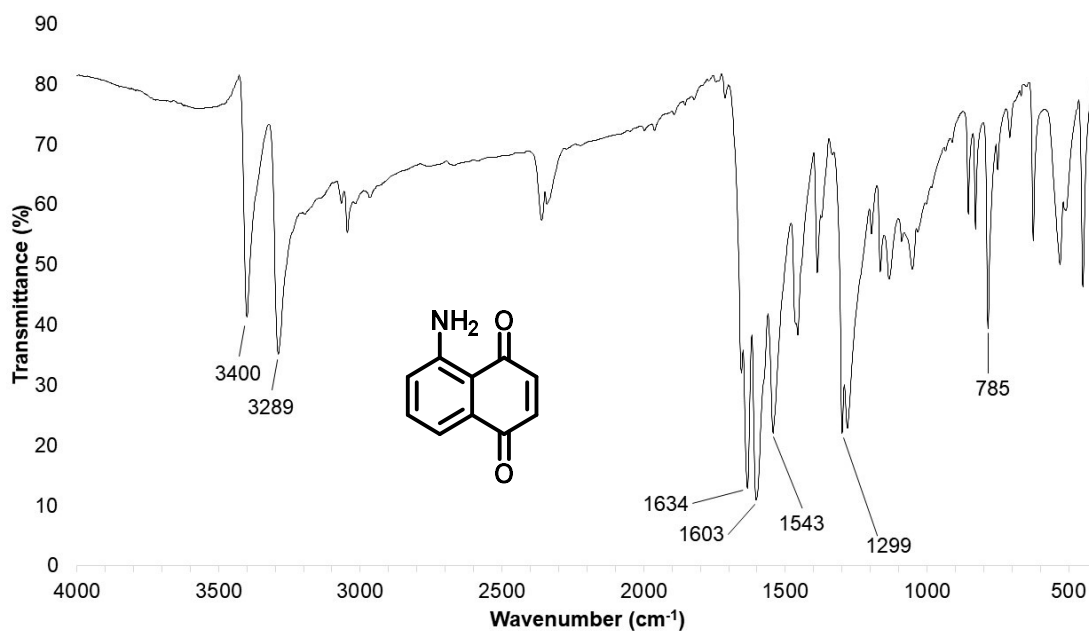
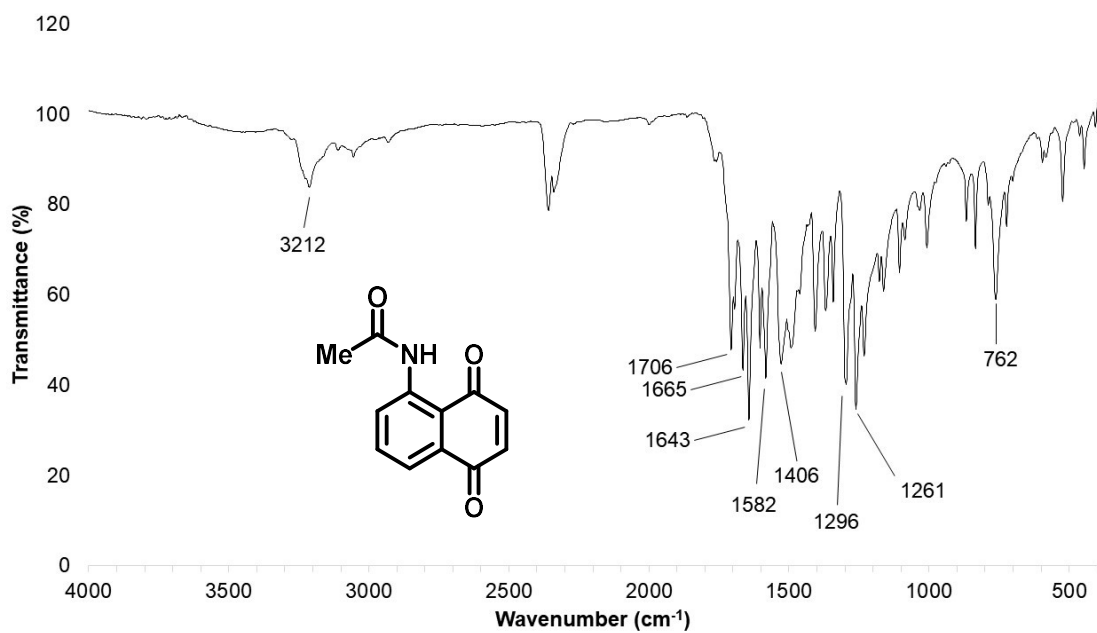
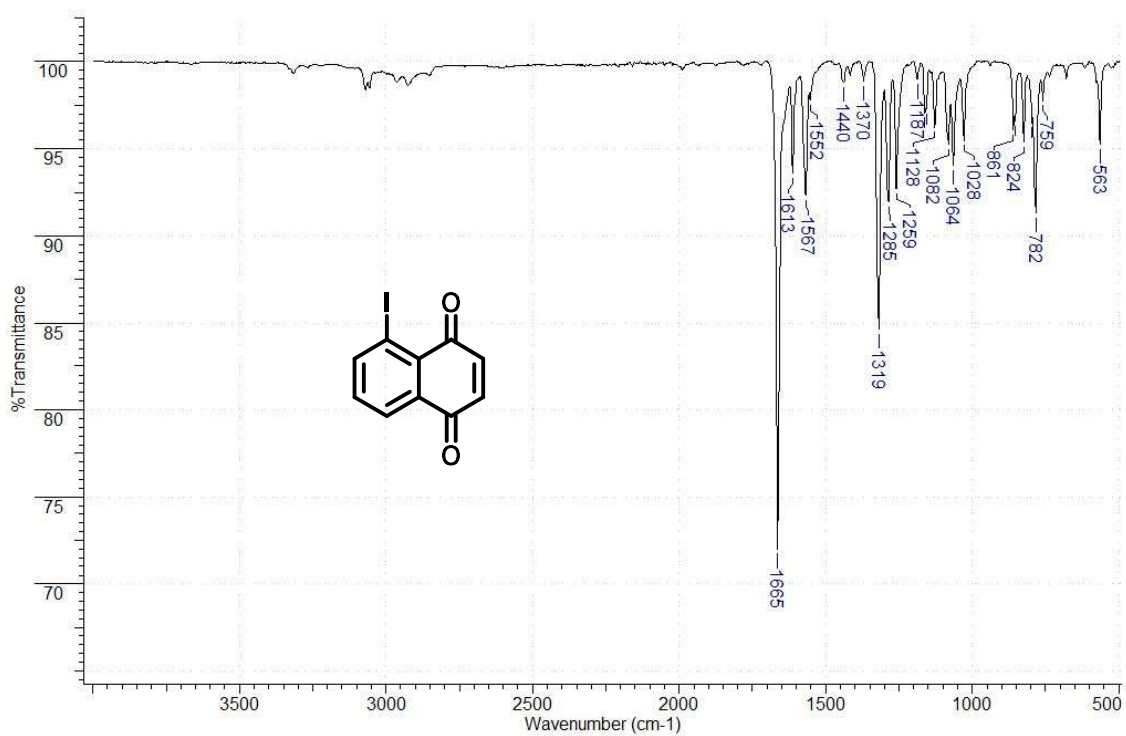


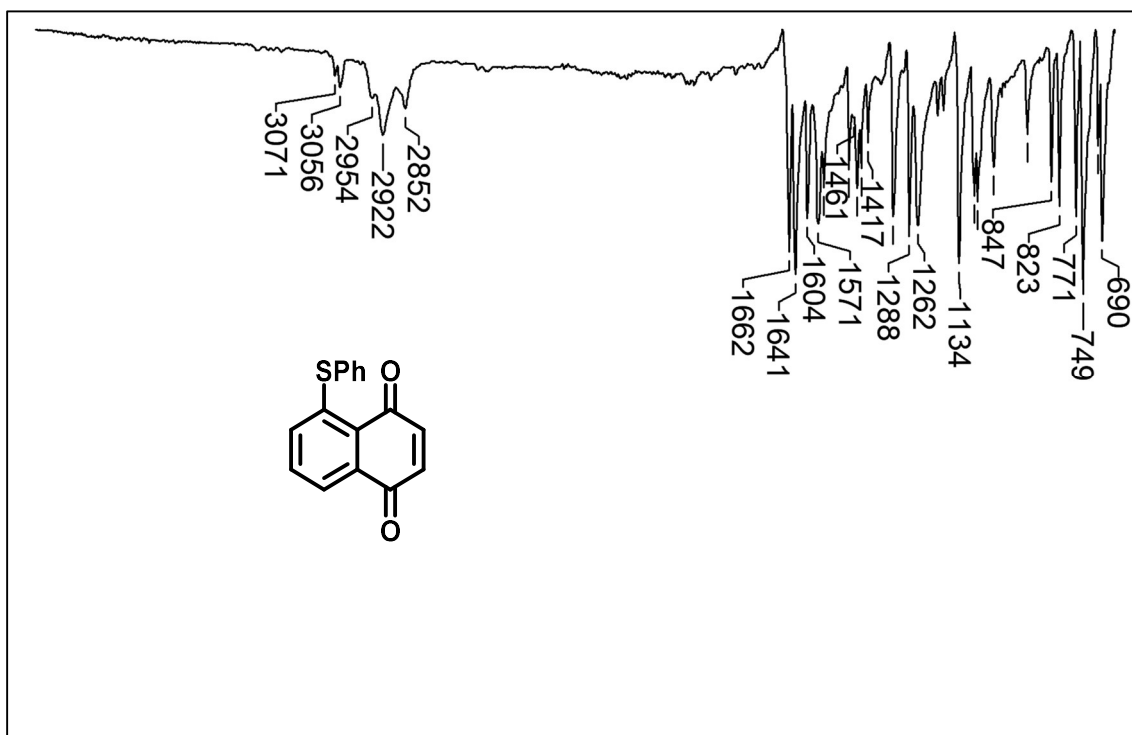
Figure B24. Infrared spectrum (IR-KBr) of the compound 57b.



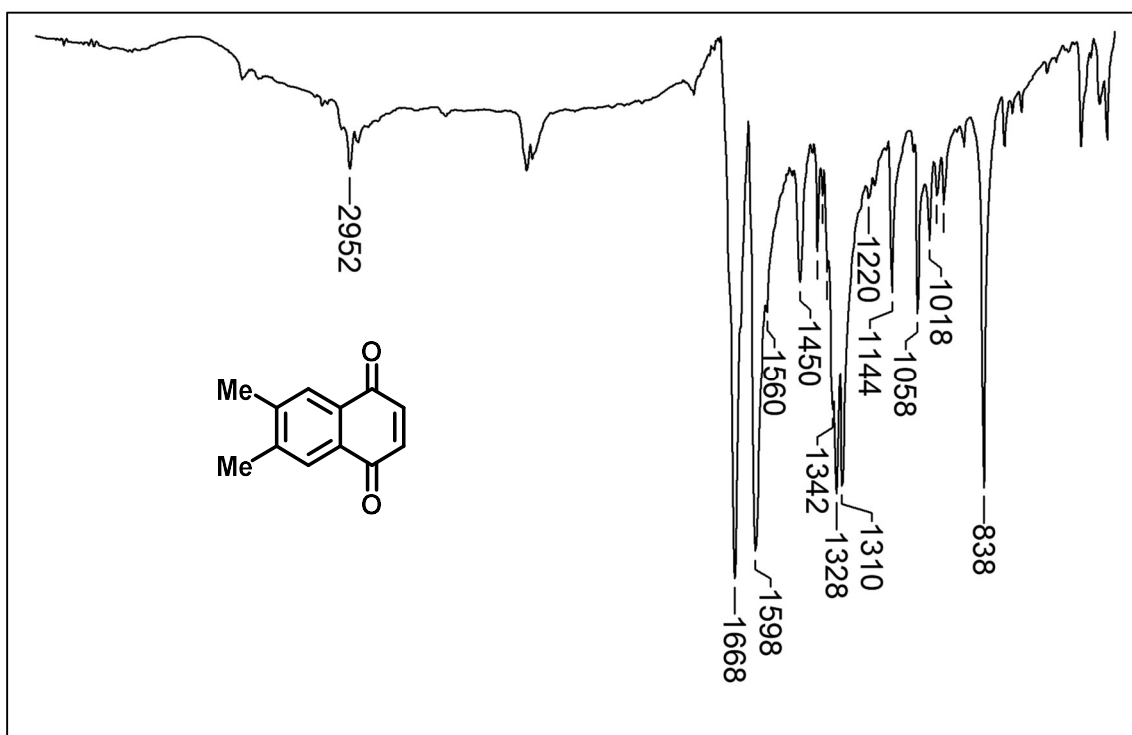
**Figure B25.** Infrared spectrum (IR-KBr) of the compound **57c**.



**Figure B26.** Infrared spectrum (IR-ATR) of the compound **57d**.



**Figure B27.** Infrared spectrum (IR-KBr) of the compound **57e**.



**Figure B28.** Infrared spectrum (IR-KBr) of the compound **57f**.

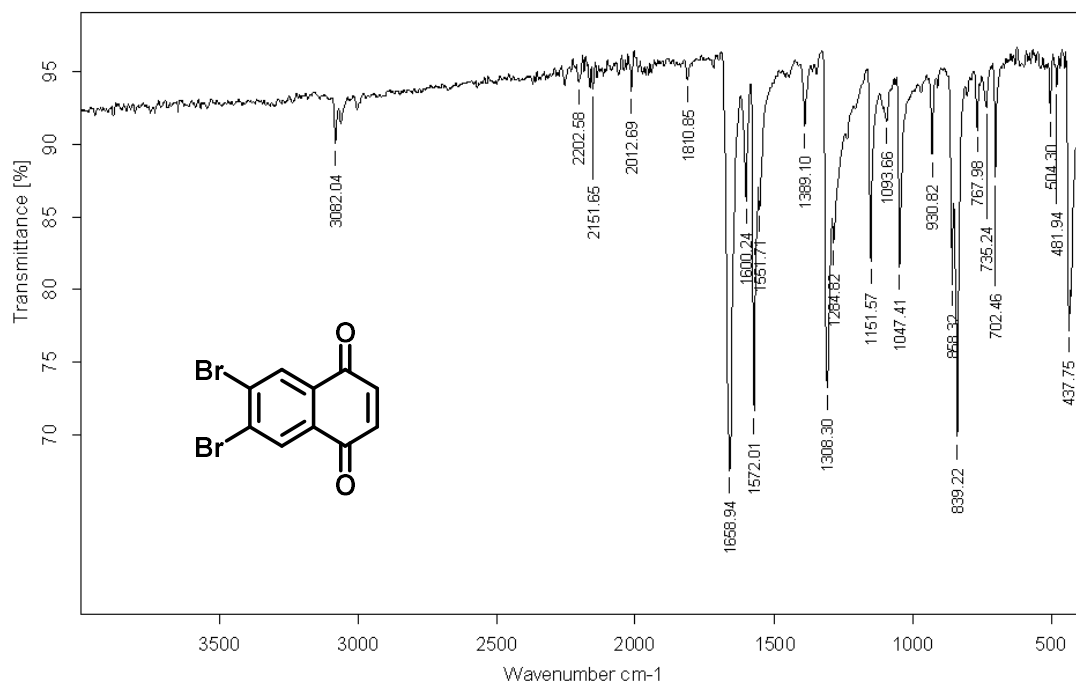


Figure B29. Infrared spectrum (IR-ATR) of the compound **57g**.

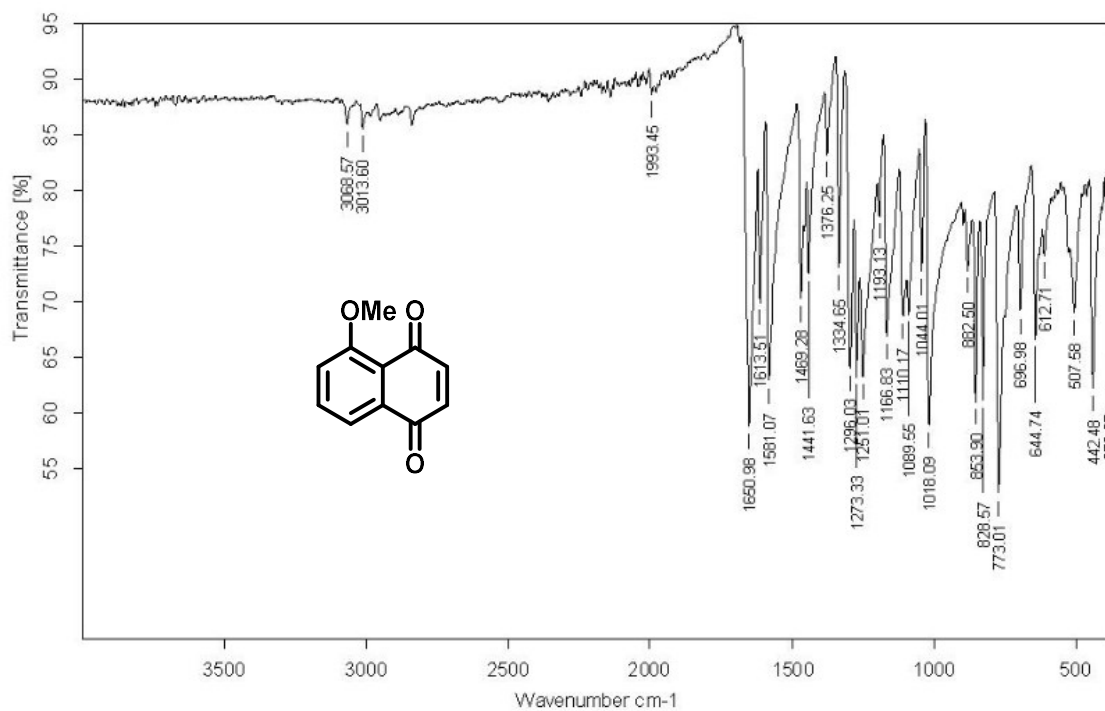
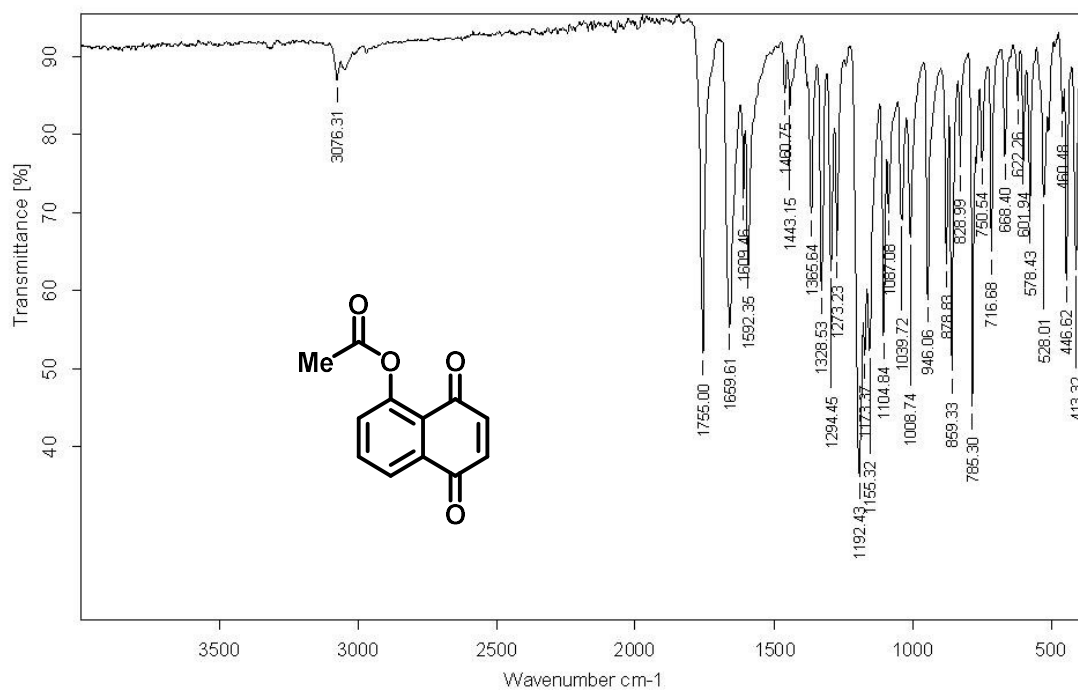
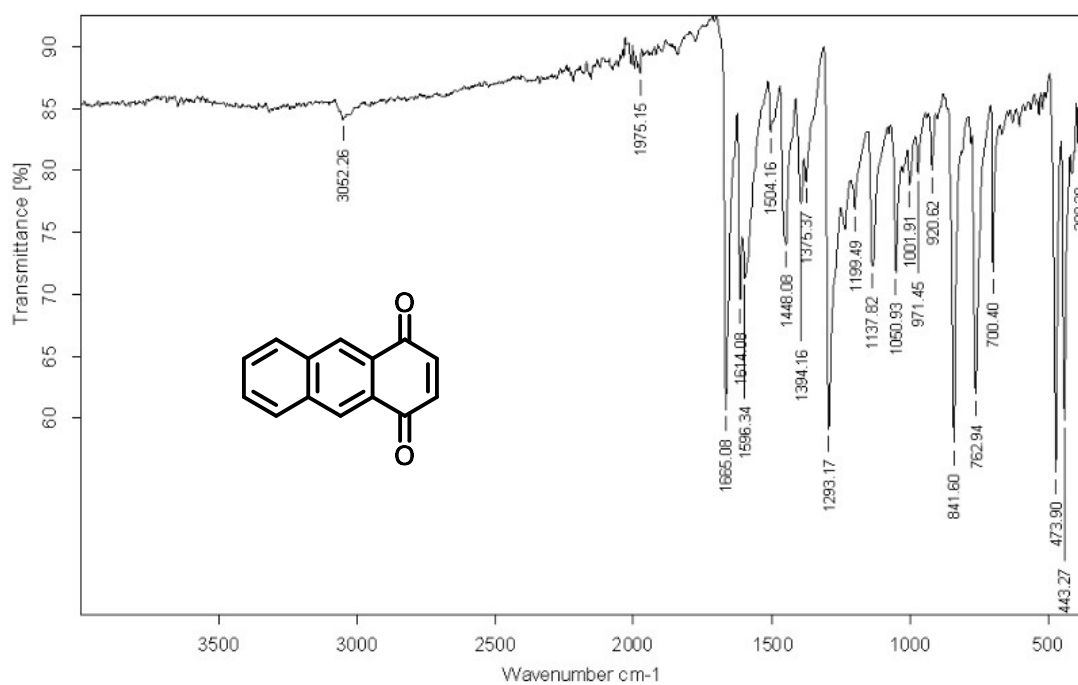


Figure B30. Infrared spectrum (IR-ATR) of the compound **57i**.



**Figure B31.** Infrared spectrum (IR-ATR) of the compound **57j**.



**Figure B32.** Infrared spectrum (IR-ATR) of the compound **57l**.

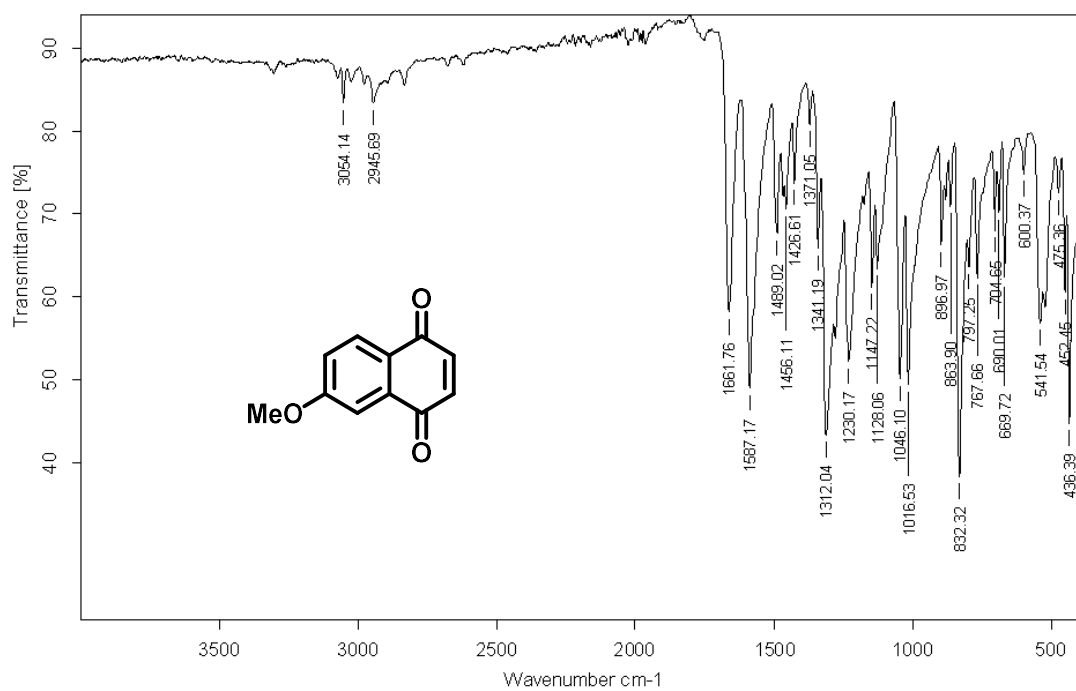


Figure B33. Infrared spectrum (IR-ATR) of the compound 57m.

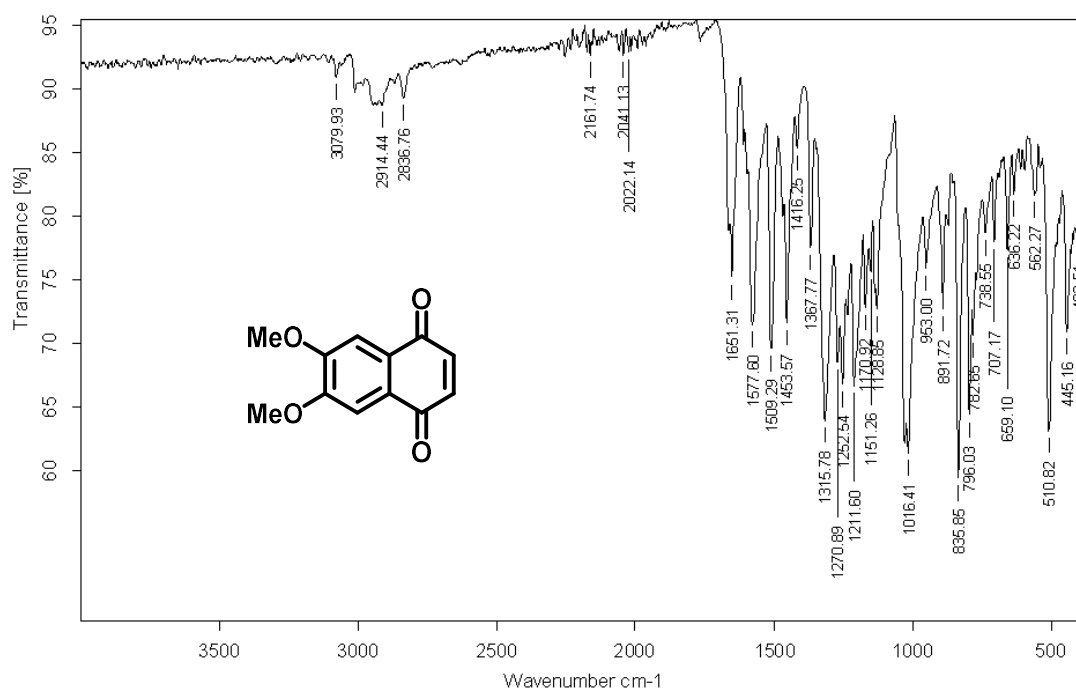


Figure B34. Infrared spectrum (IR-ATR) of the compound 57n.



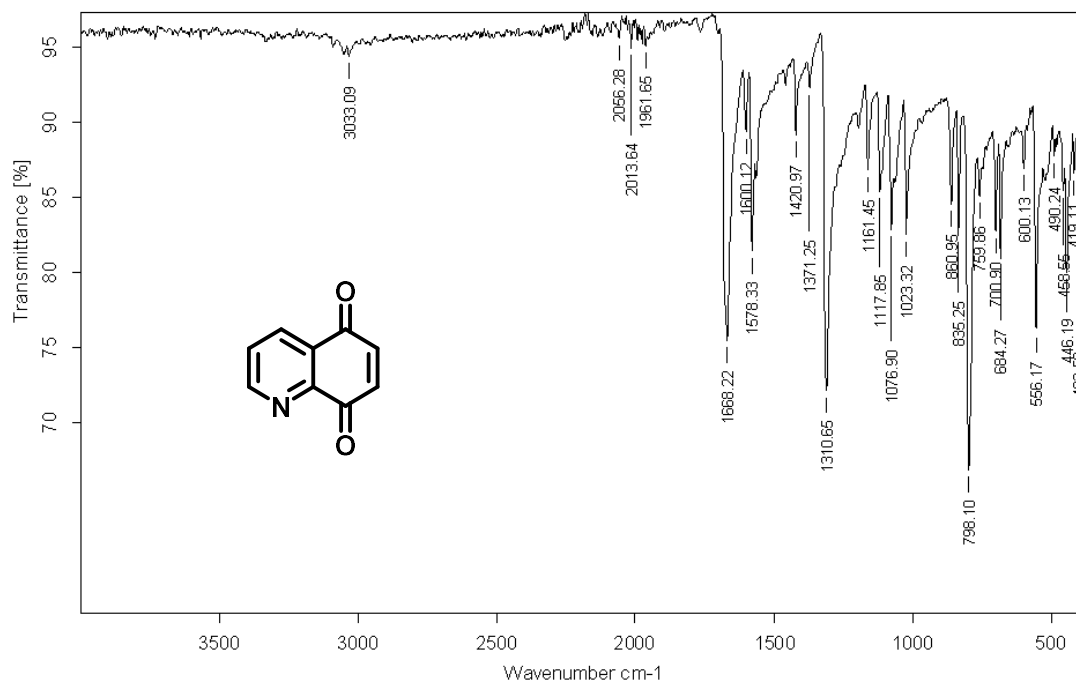


Figure B35. Infrared spectrum (IR-ATR) of the compound 57o.

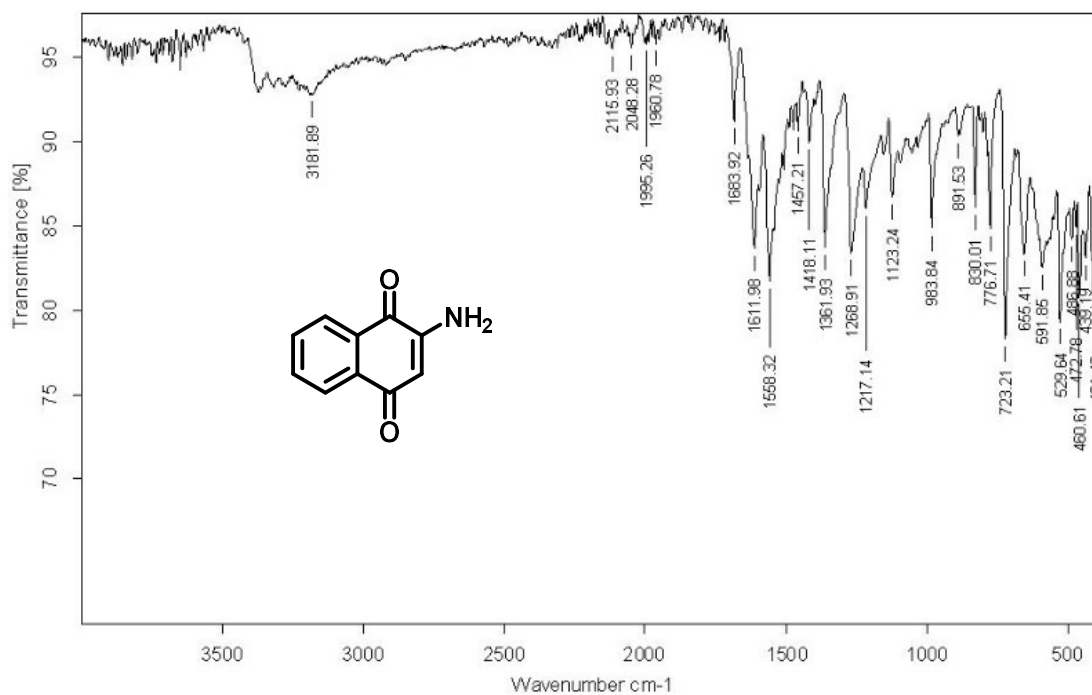
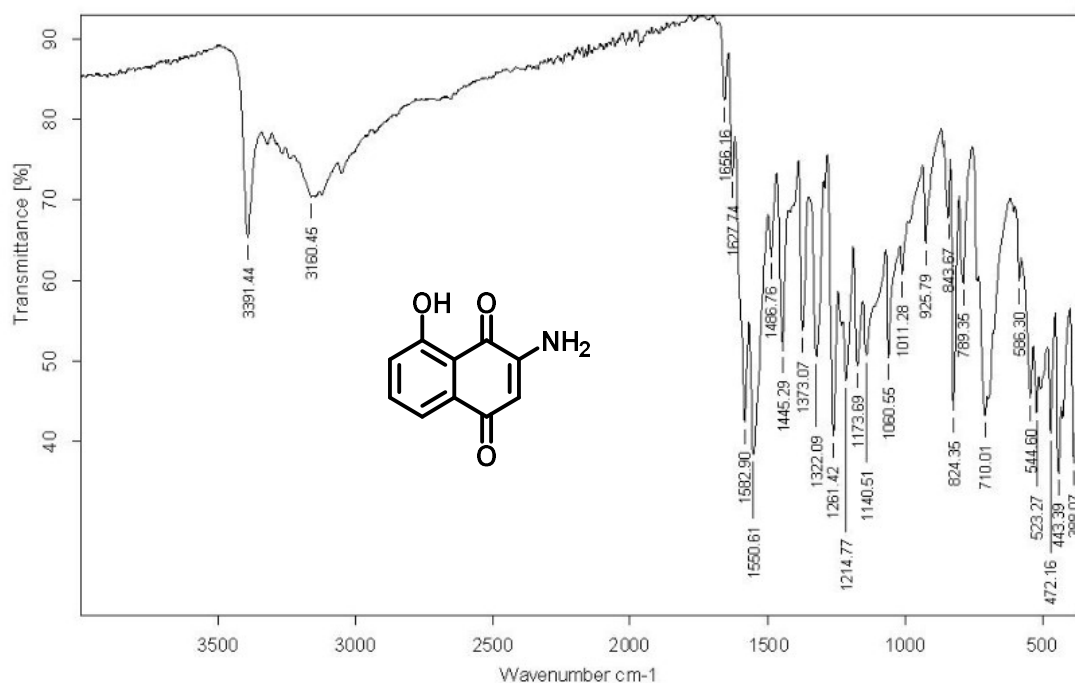
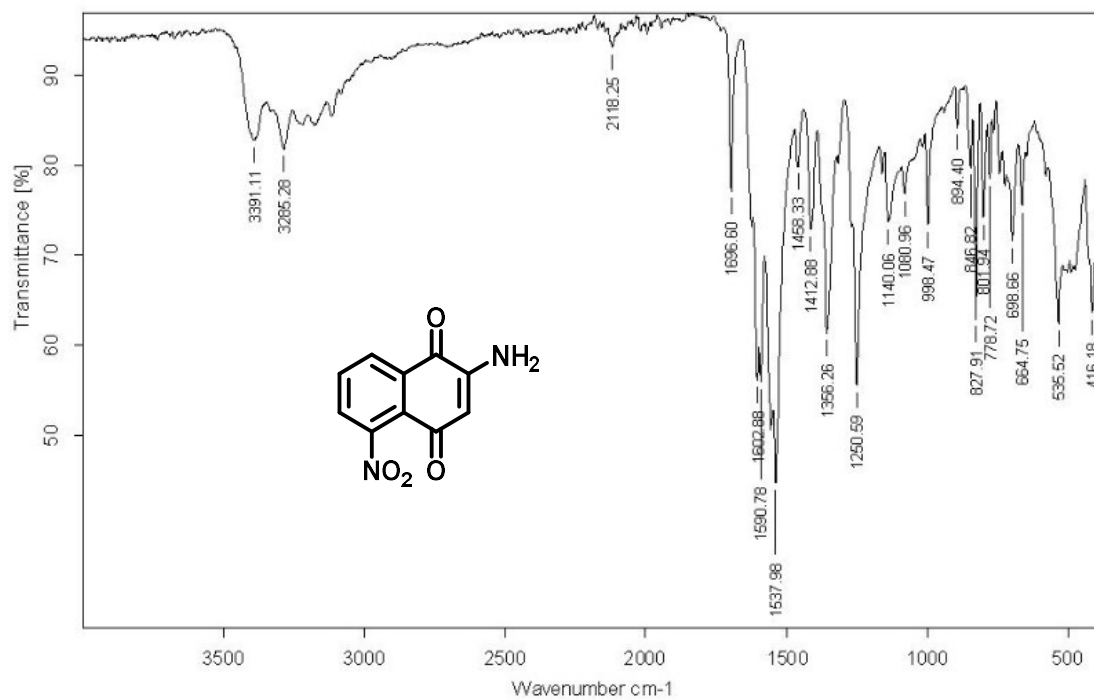
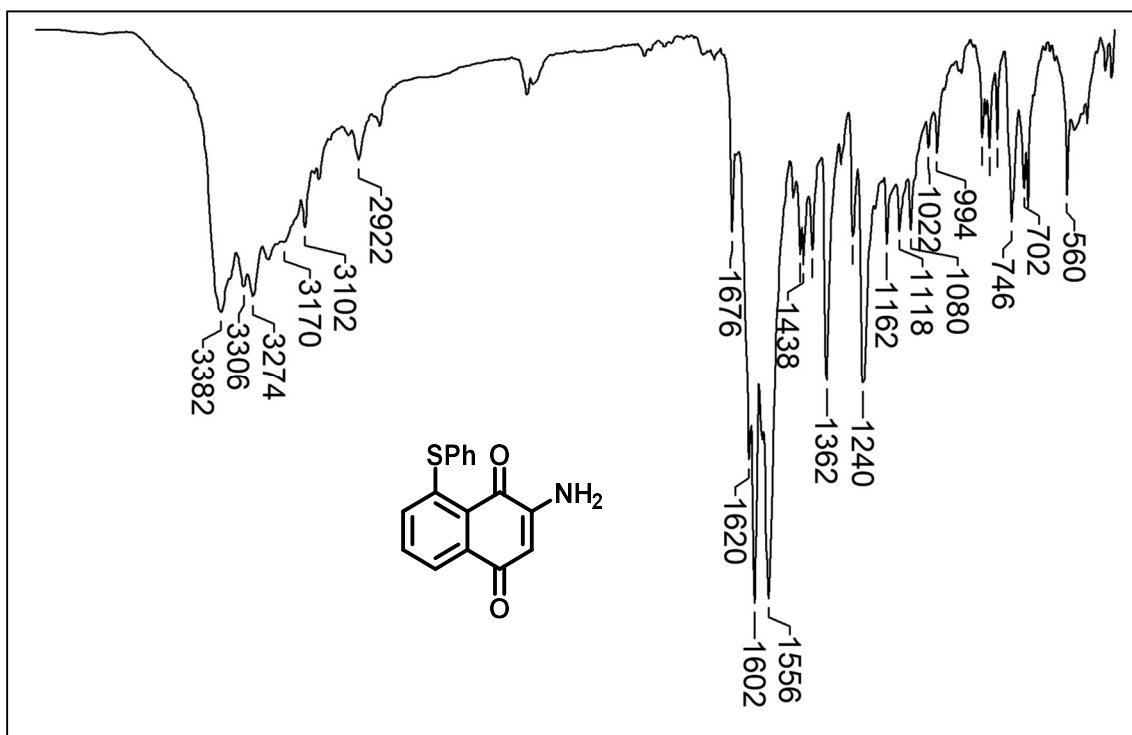
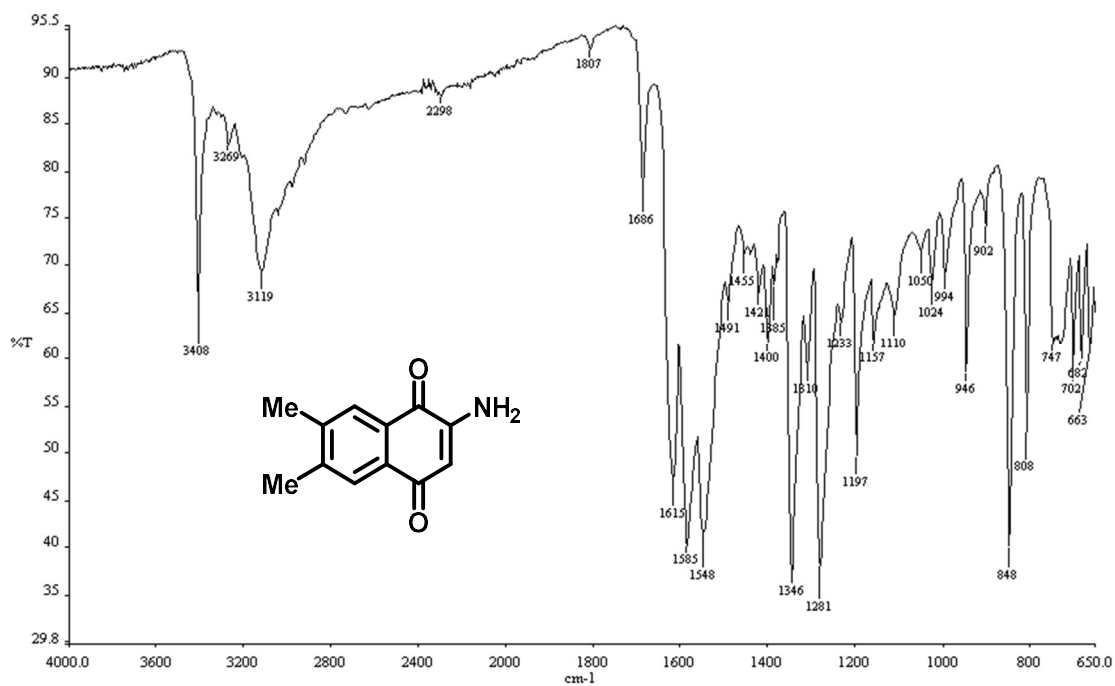


Figure B36. Infrared spectrum (IR-ATR) of the compound 58a.





**Figure B39.** Infrared spectrum (IR-KBr) of the compound **58d**.



**Figure B40.** Infrared spectrum (IR-KBr) of the compound **58e**.

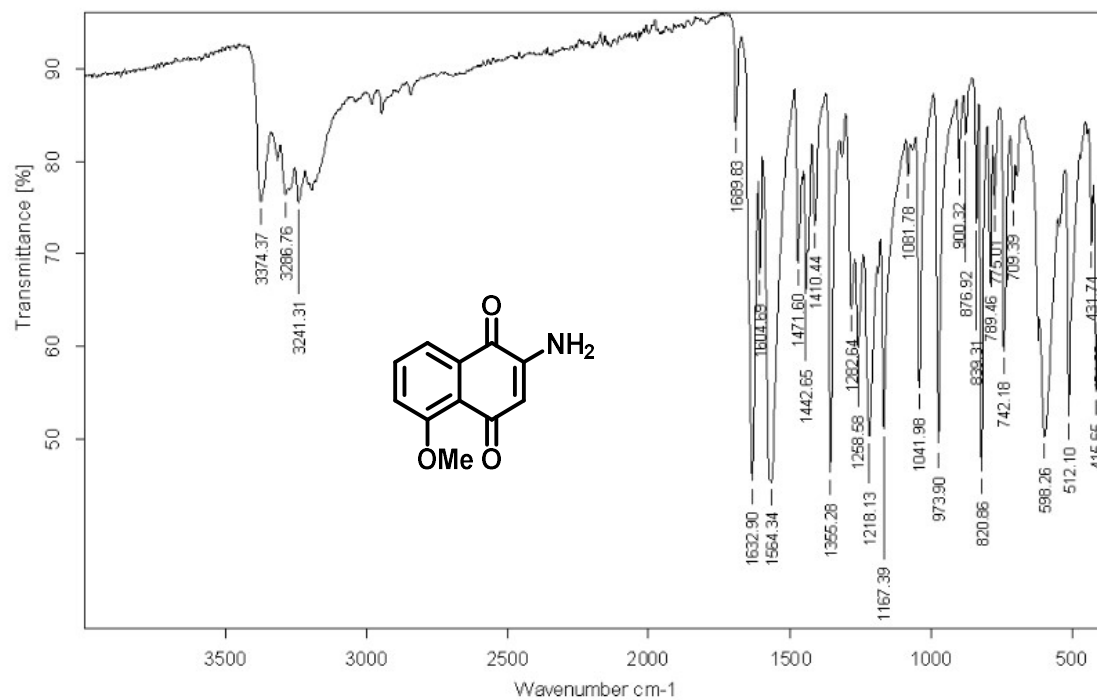


Figure B41. Infrared spectrum (IR-ATR) of the compound 58f.

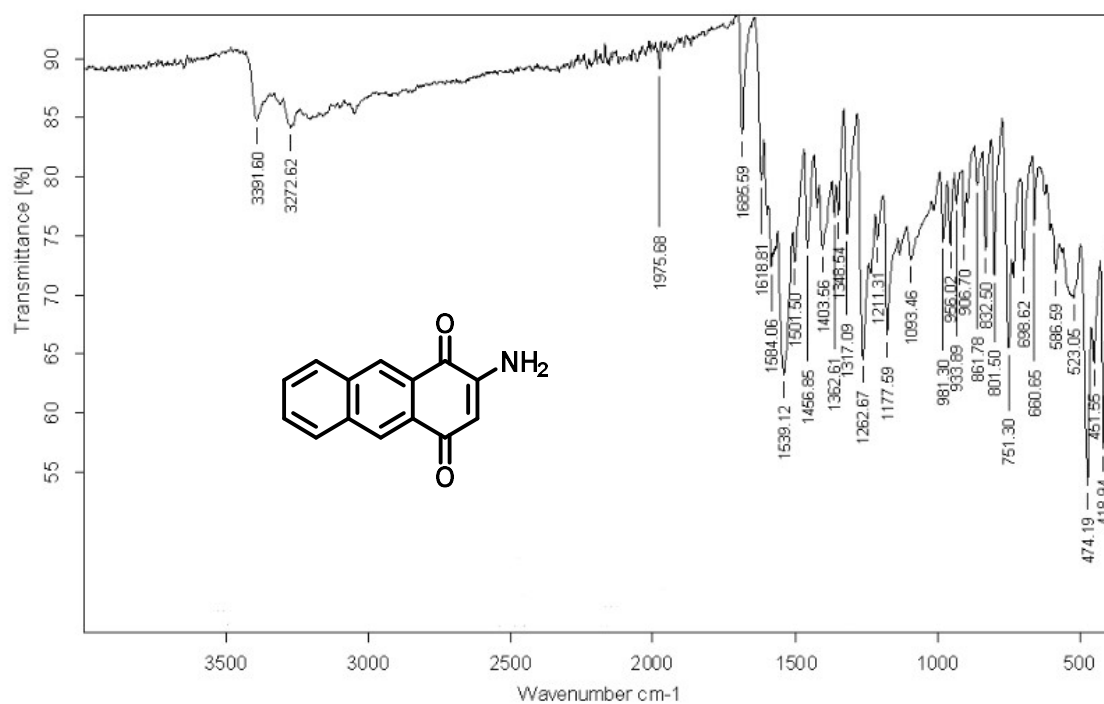


Figure B42. Infrared spectrum (IR-ATR) of the compound 58g.

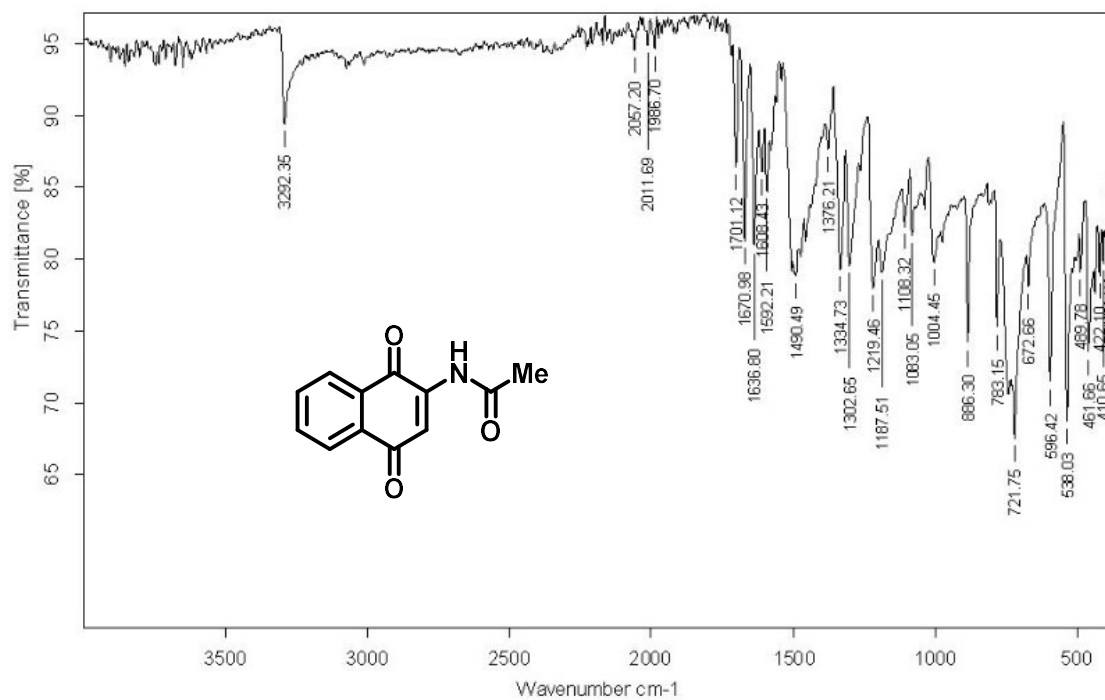


Figure B43. Infrared spectrum (IR-ATR) of the compound 59a.

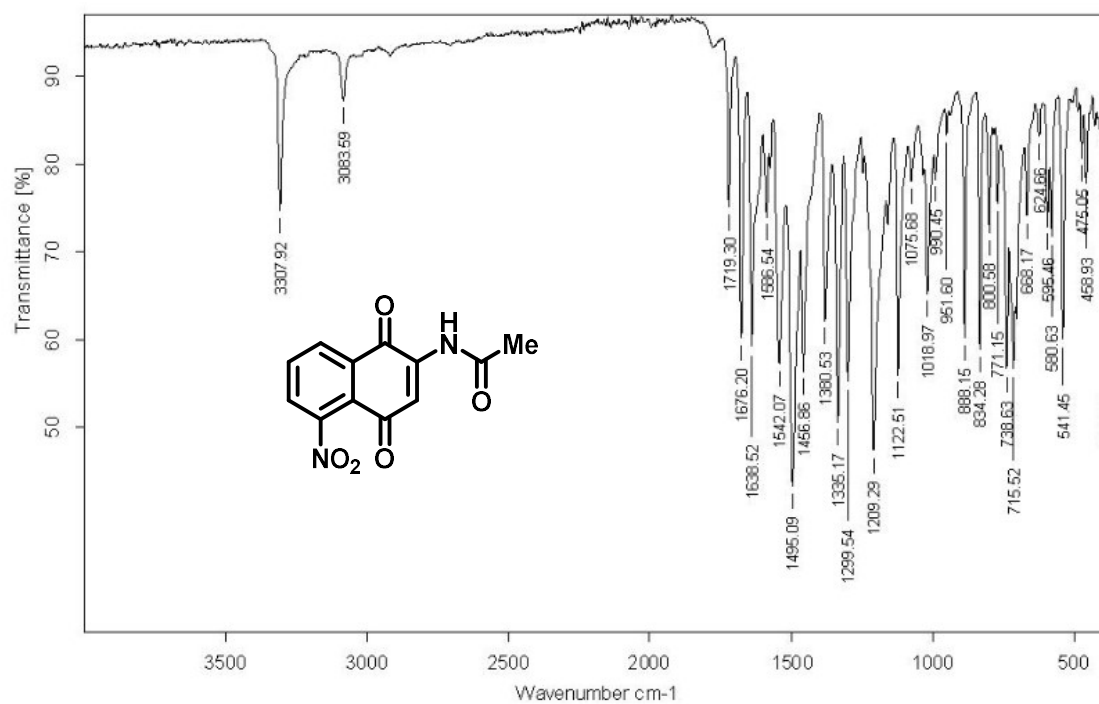


Figure B44. Infrared spectrum (IR-ATR) of the compound 59b.

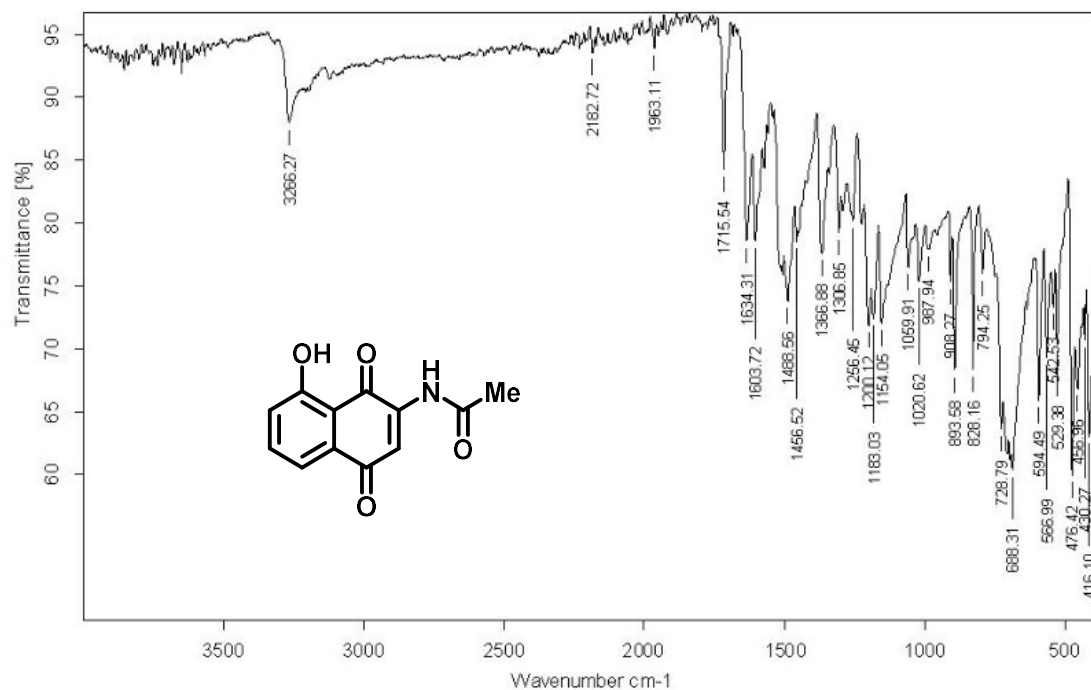


Figure B45. Infrared spectrum (IR-ATR) of the compound 59c.

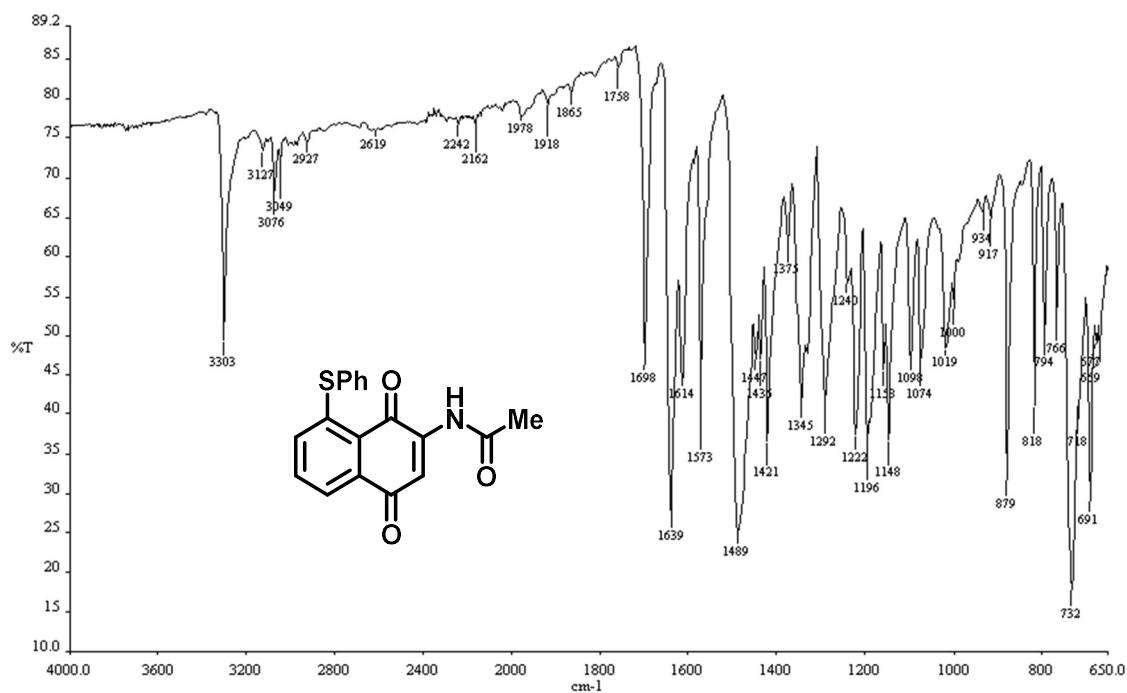


Figure B46. Infrared spectrum (IR-KBr) of the compound 59d.

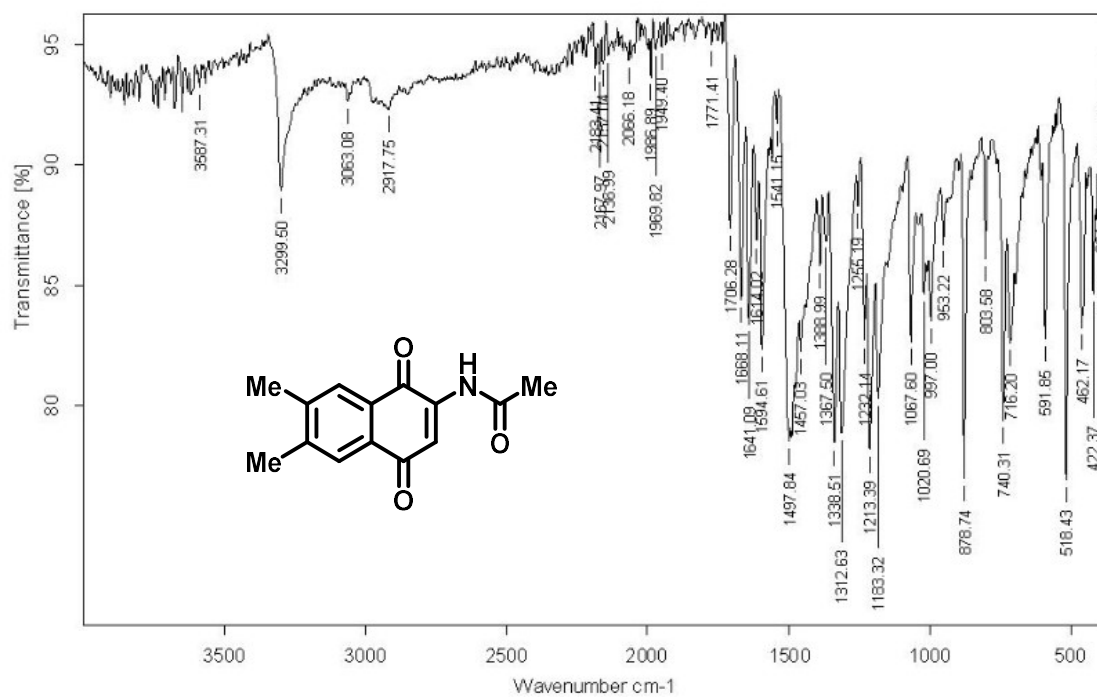


Figure B47. Infrared spectrum (IR-ATR) of the compound 59e.

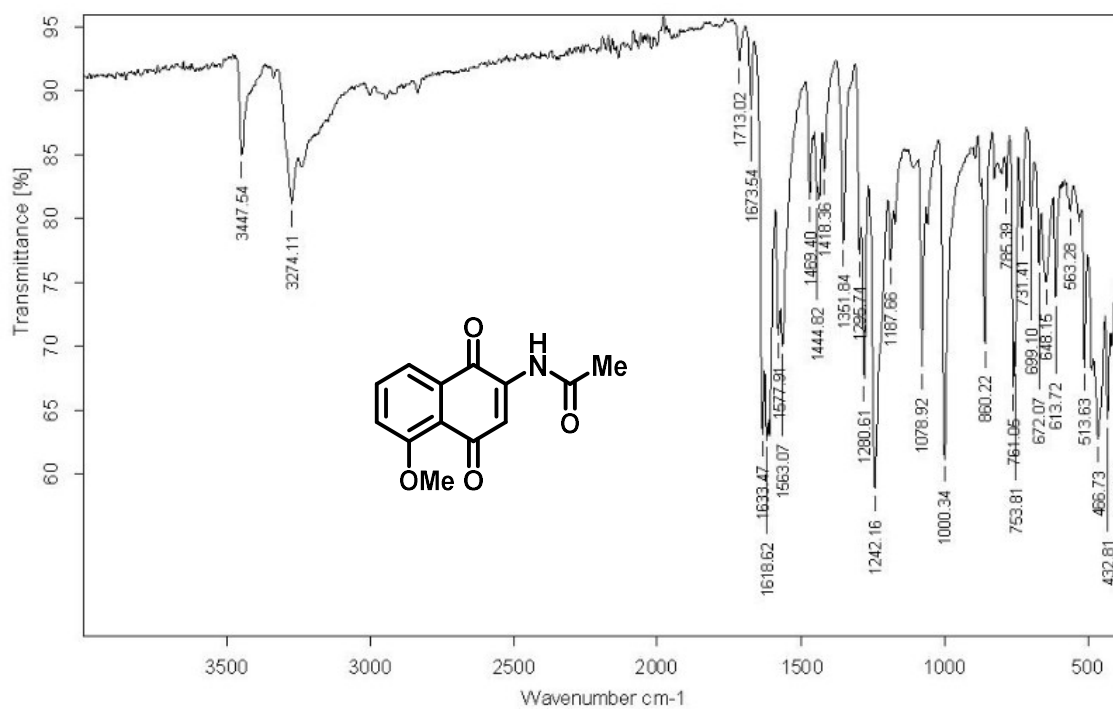
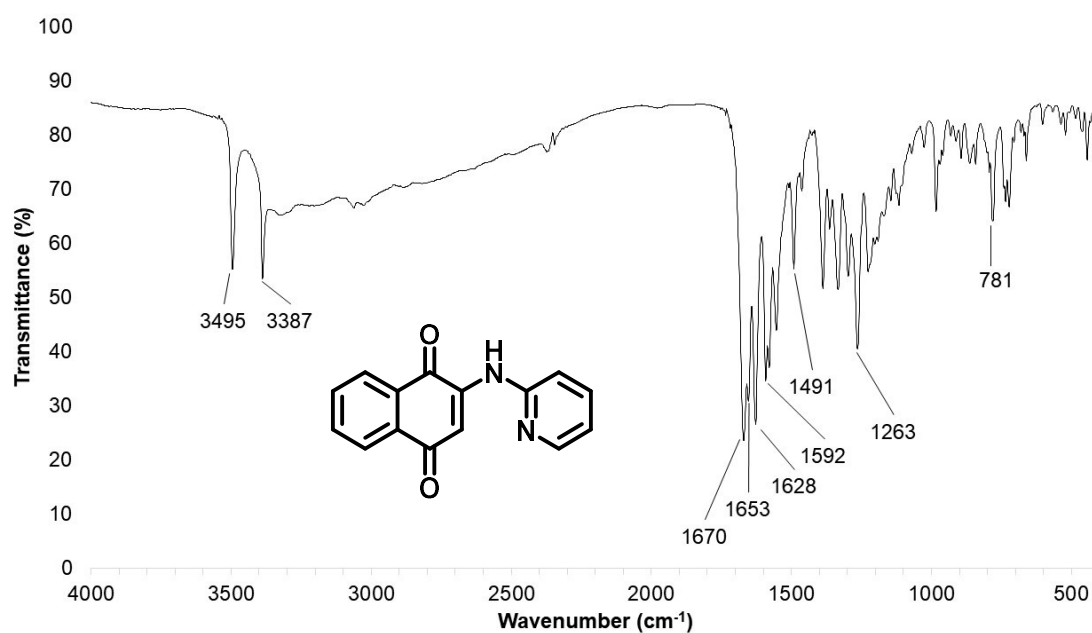
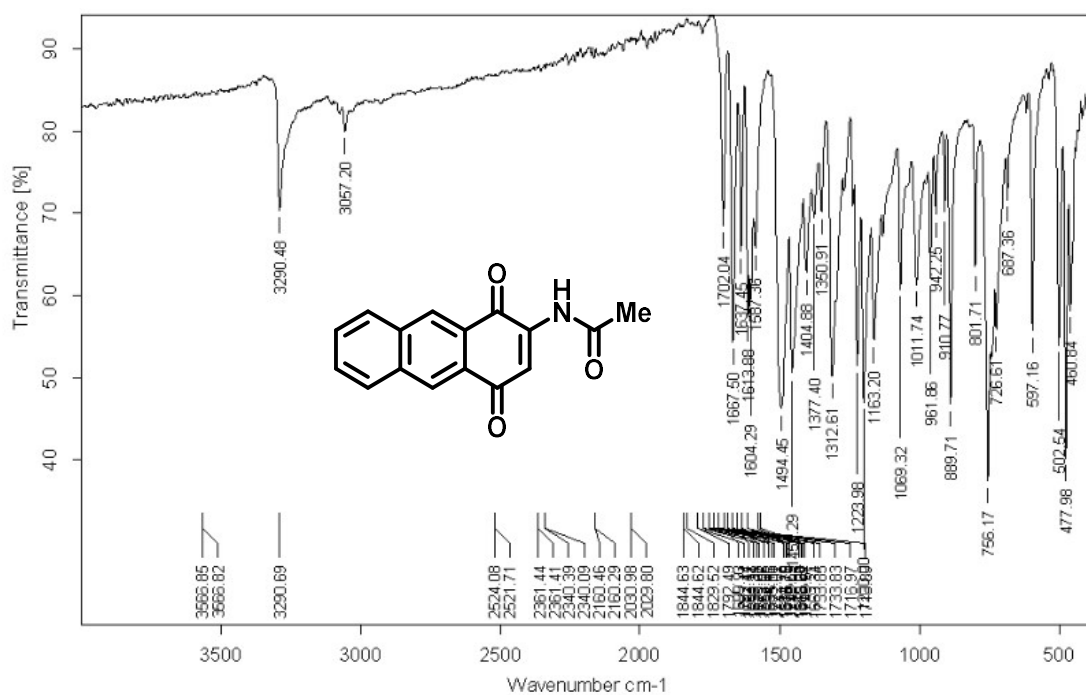
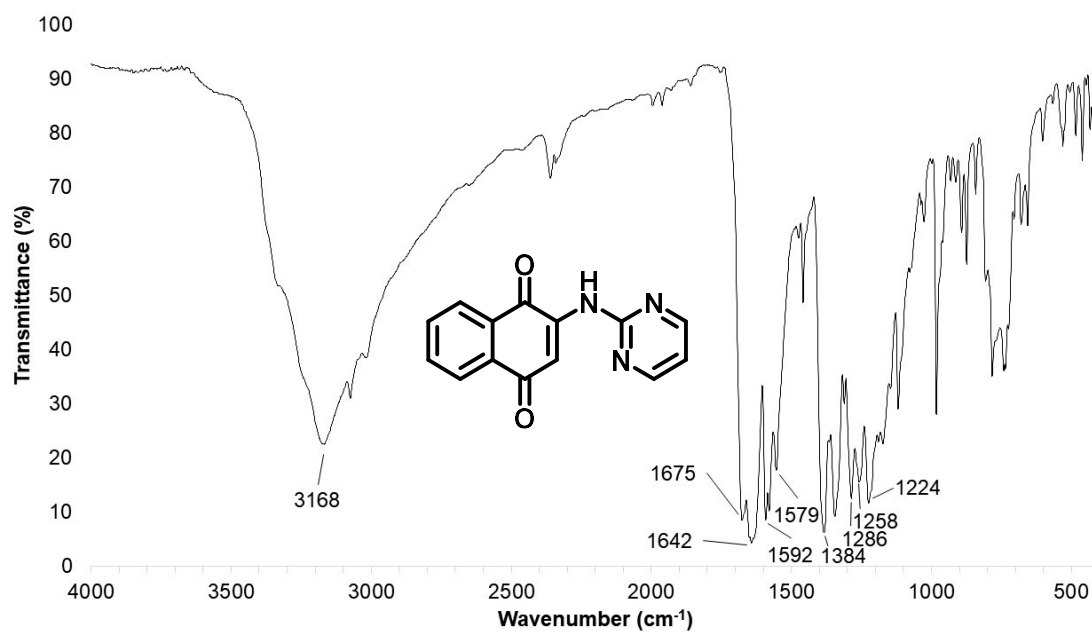


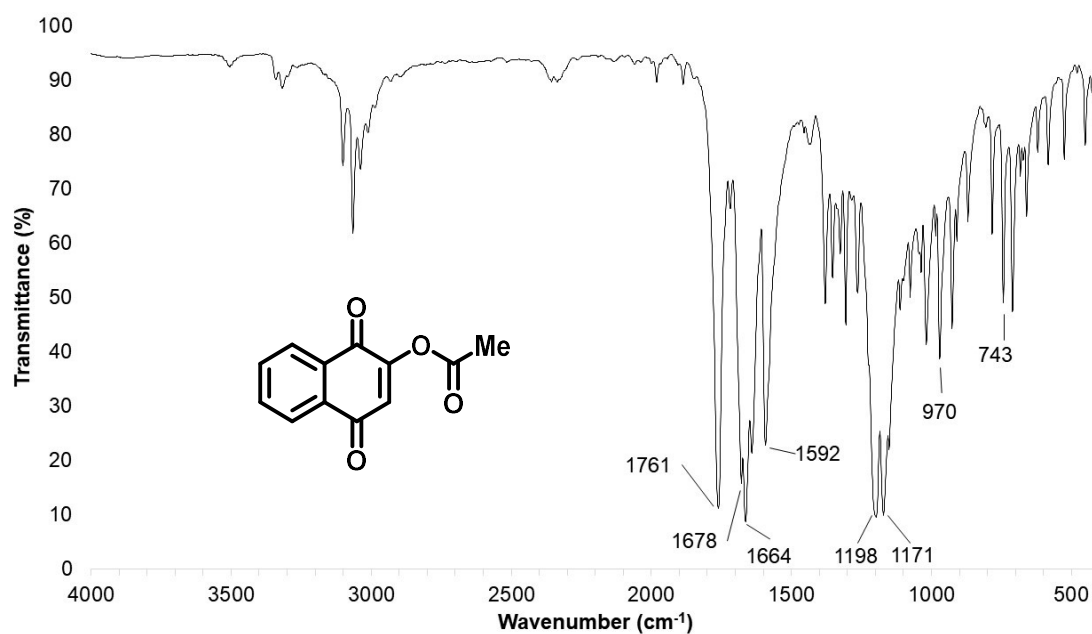
Figure B48. Infrared spectrum (IR-ATR) of the compound 59f.







**Figure B51.** Infrared spectrum (IR-KBr) of the compound **61**.



**Figure B52.** Infrared spectrum (IR-KBr) of the compound **62**.

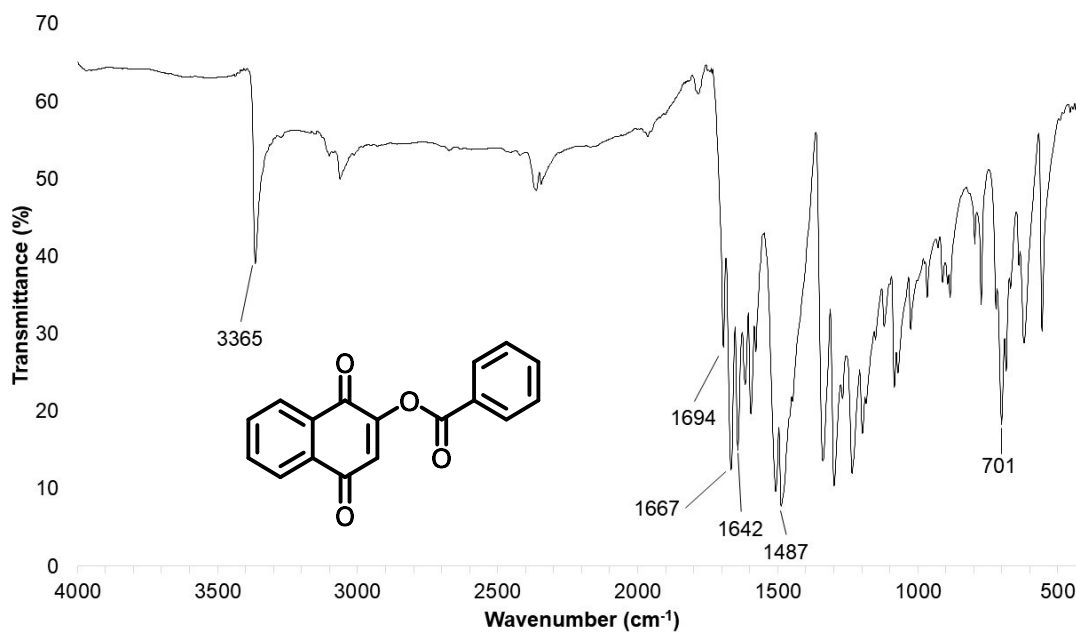


Figure B53. Infrared spectrum (IR-KBr) of the compound 64.

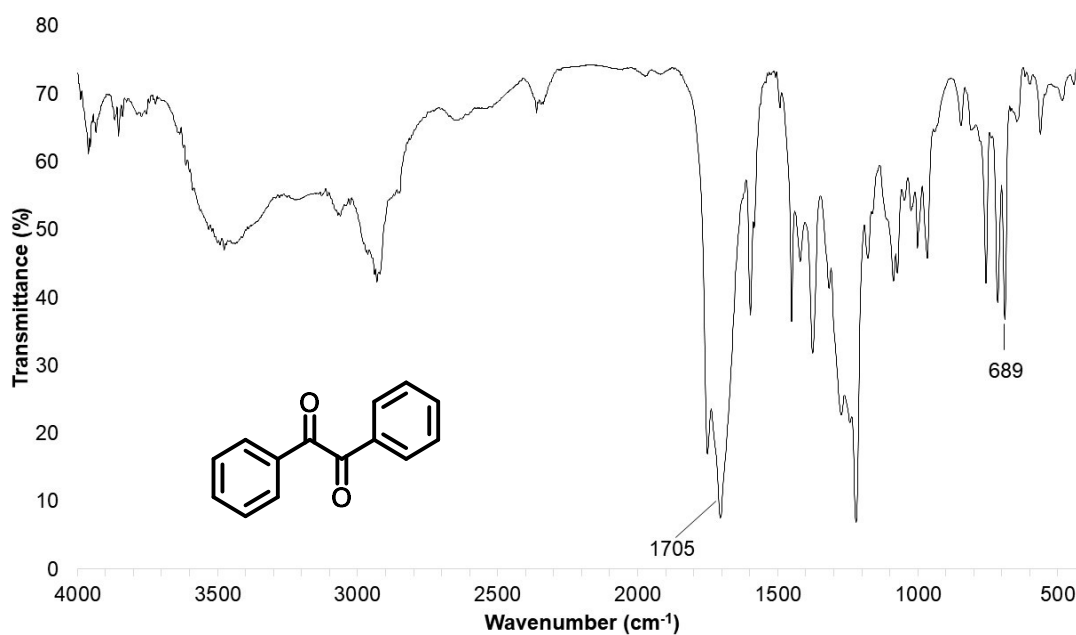


Figure B54. Infrared spectrum (IR-KBr) of the compound 65.

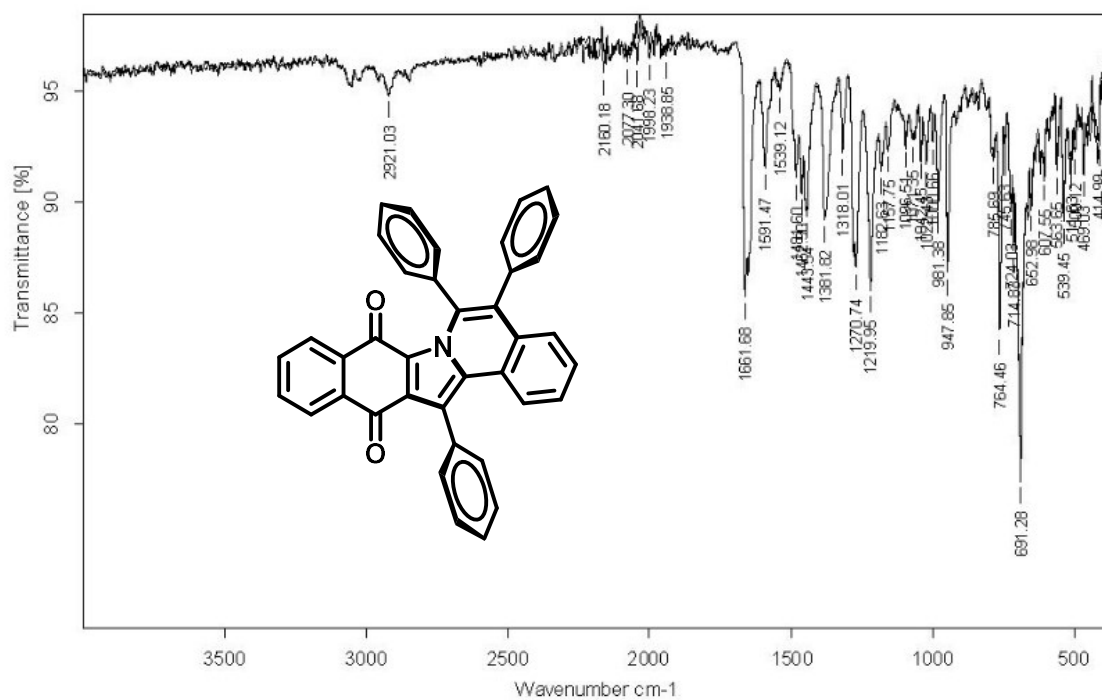


Figure B55. Infrared spectrum (IR-ATR) of the compound 67a.

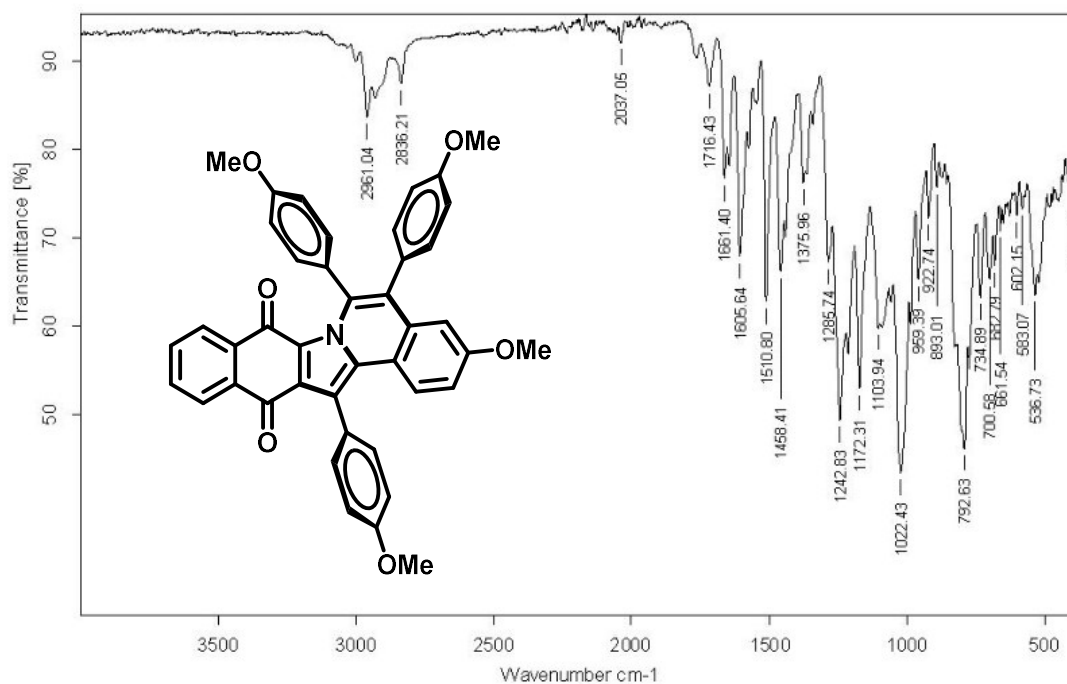


Figure B56. Infrared spectrum (IR-ATR) of the compound 67b.

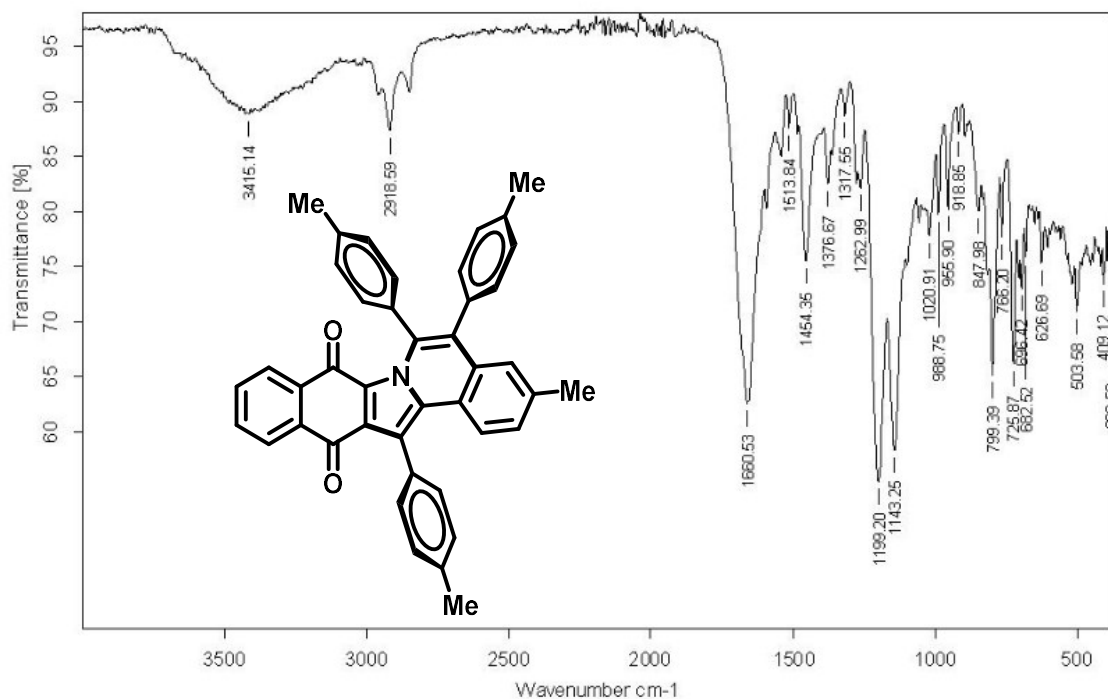


Figure B57. Infrared spectrum (IR-ATR) of the compound 67c.

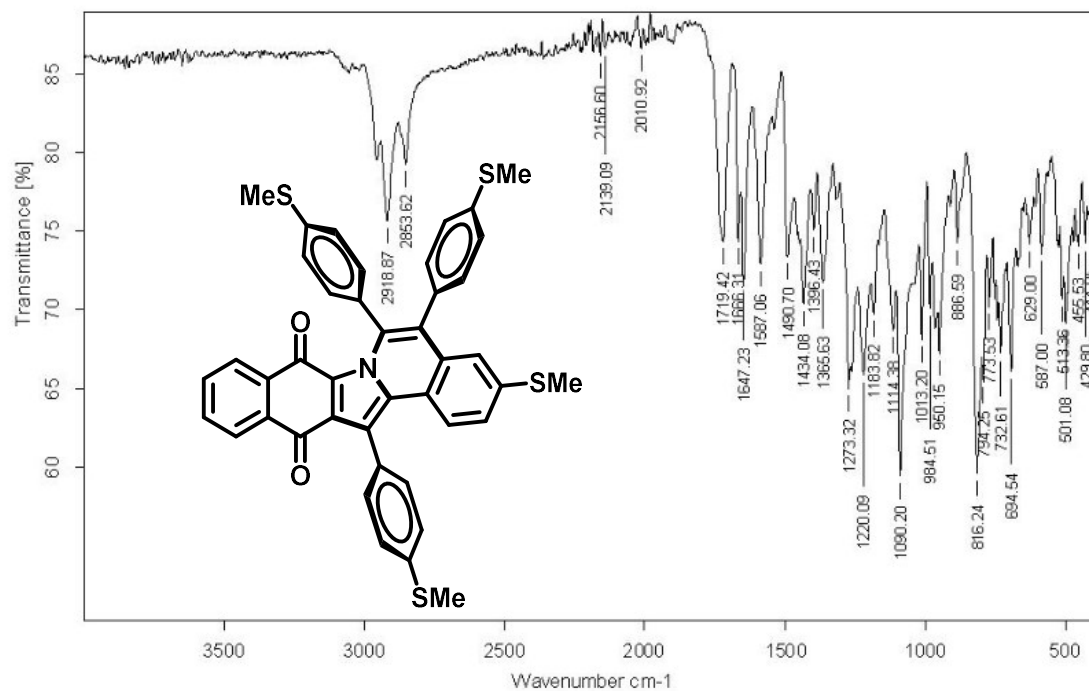


Figure B58. Infrared spectrum (IR-ATR) of the compound 67d.

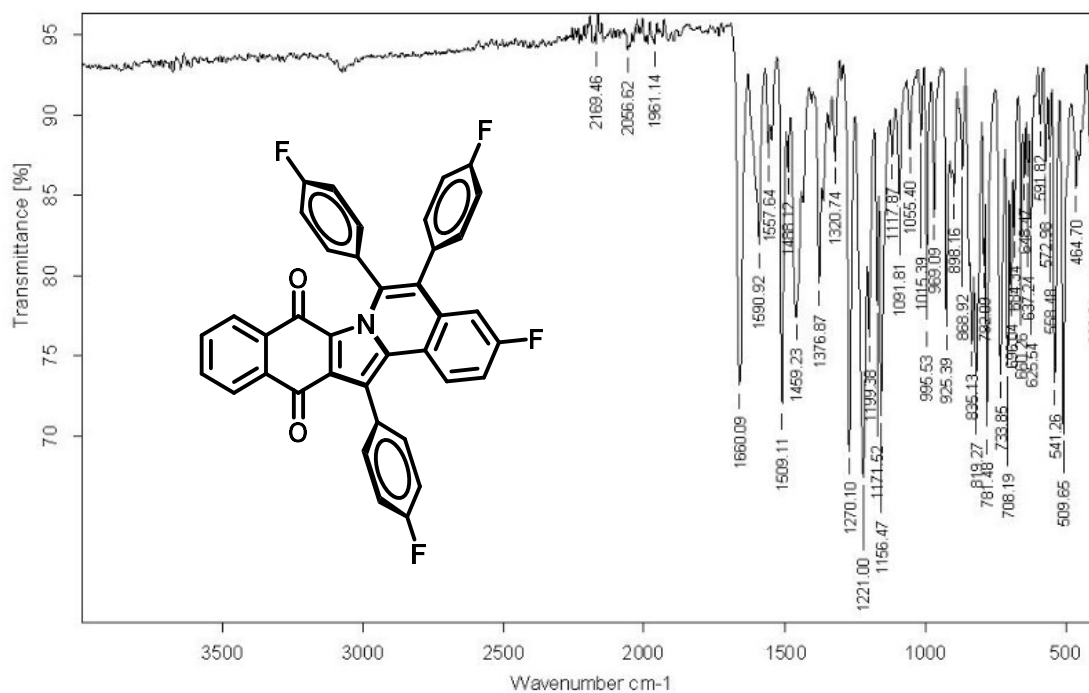


Figure B59. Infrared spectrum (IR-ATR) of the compound 67e.

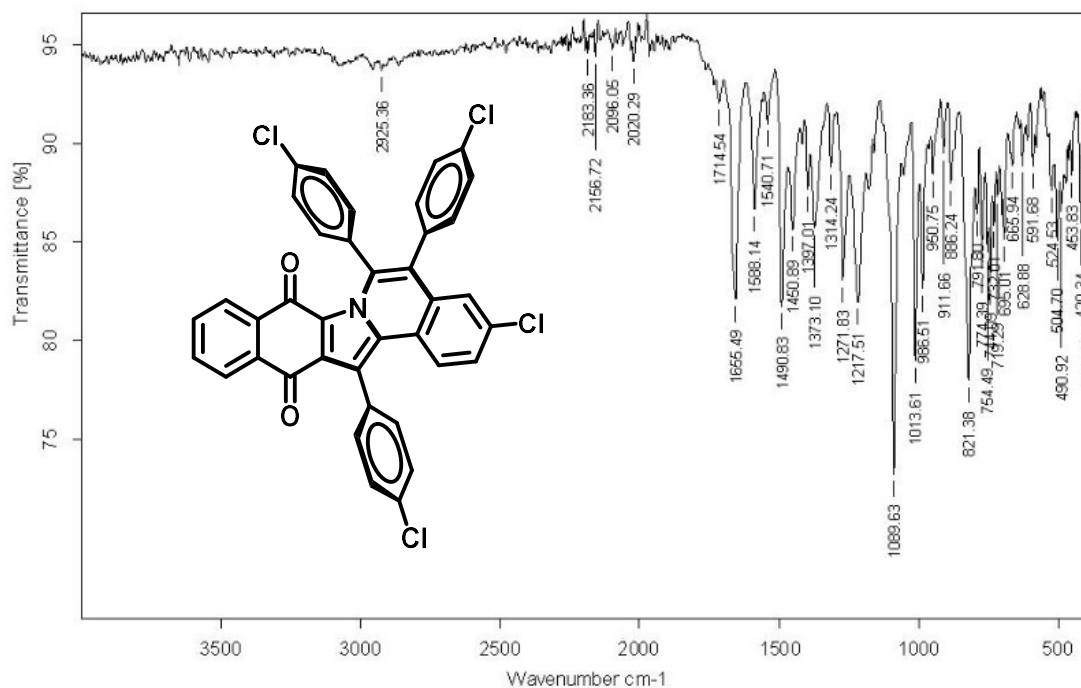


Figure B60. Infrared spectrum (IR-ATR) of the compound 67f.

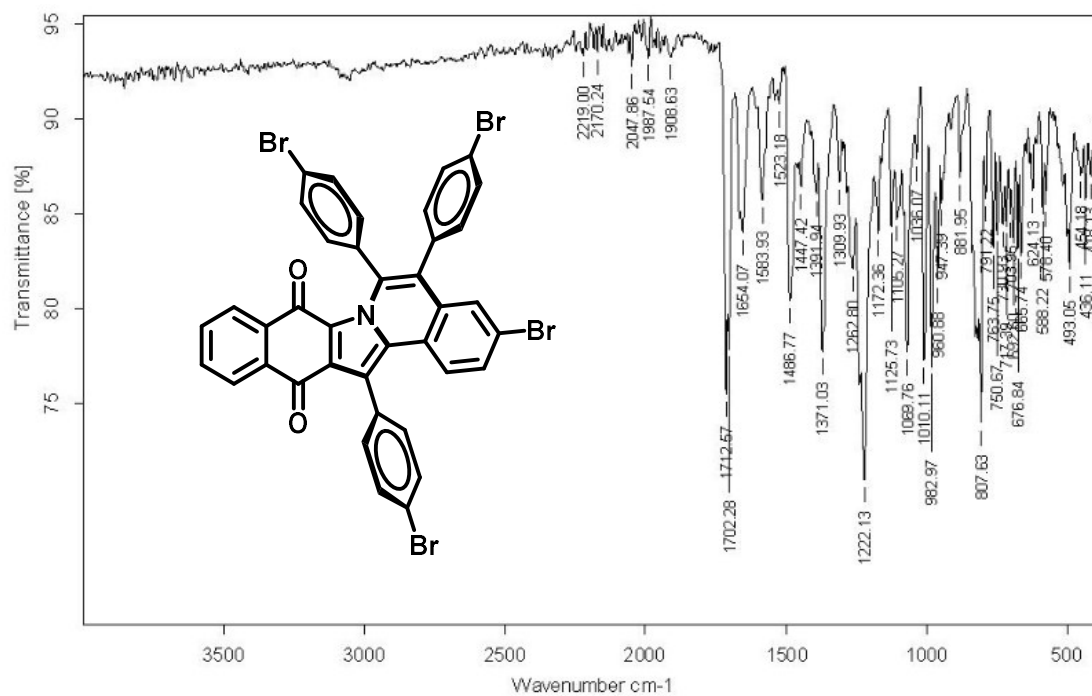


Figure B61. Infrared spectrum (IR-ATR) of the compound 67g.

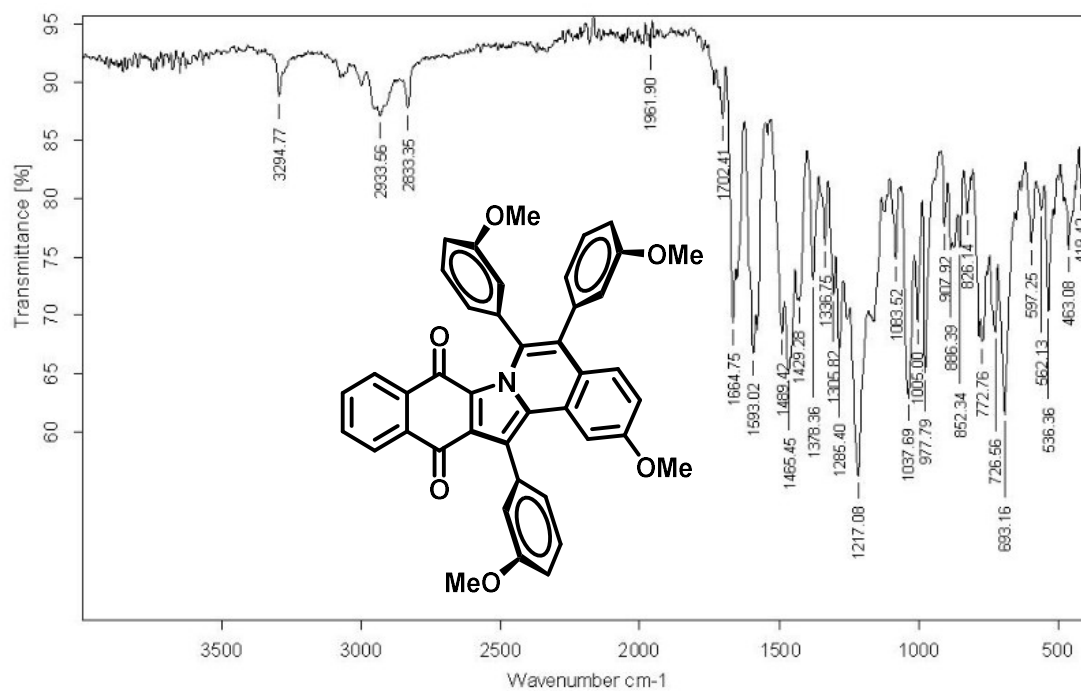
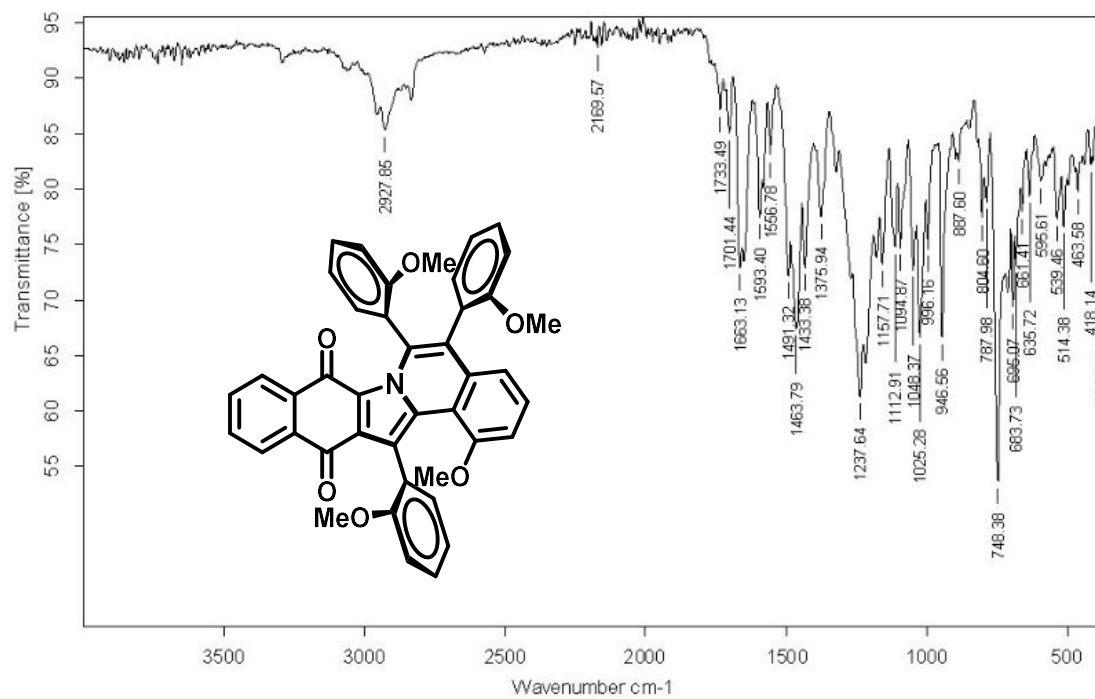
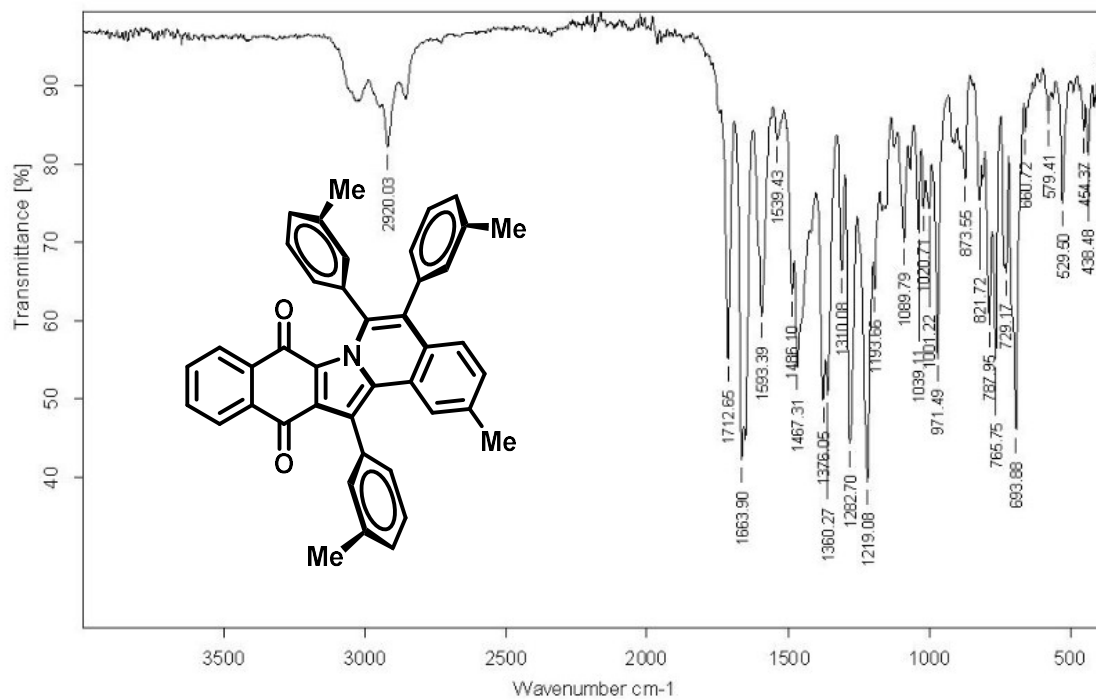


Figure B62. Infrared spectrum (IR-ATR) of the compound 67h.



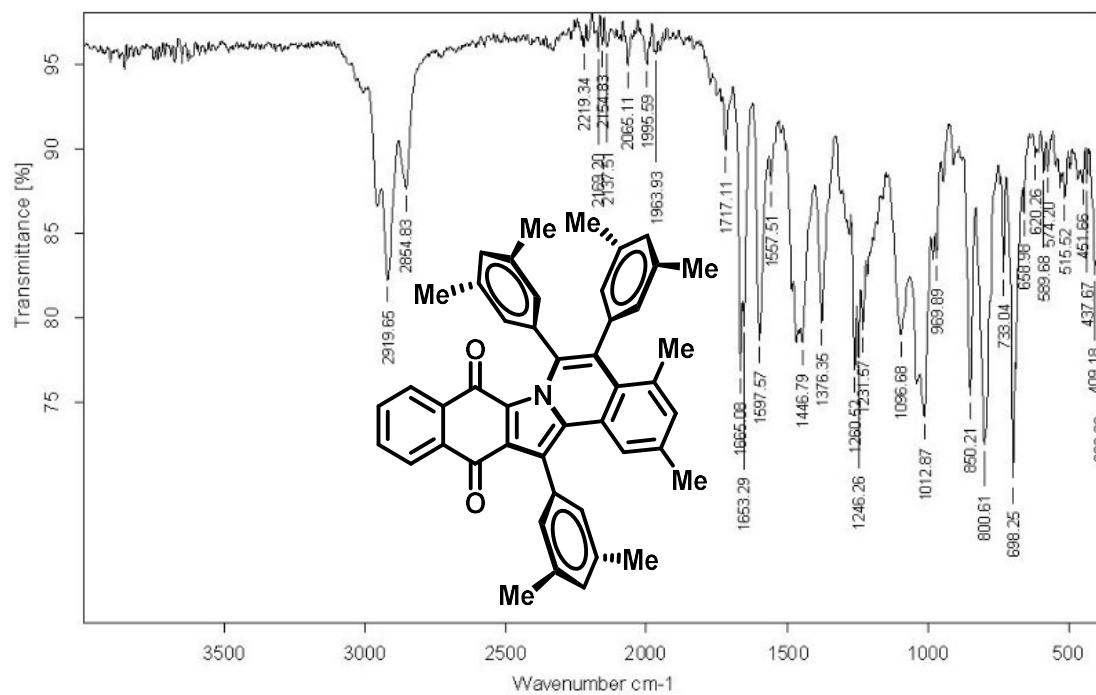


Figure B65. Infrared spectrum (IR-ATR) of the compound 67k.

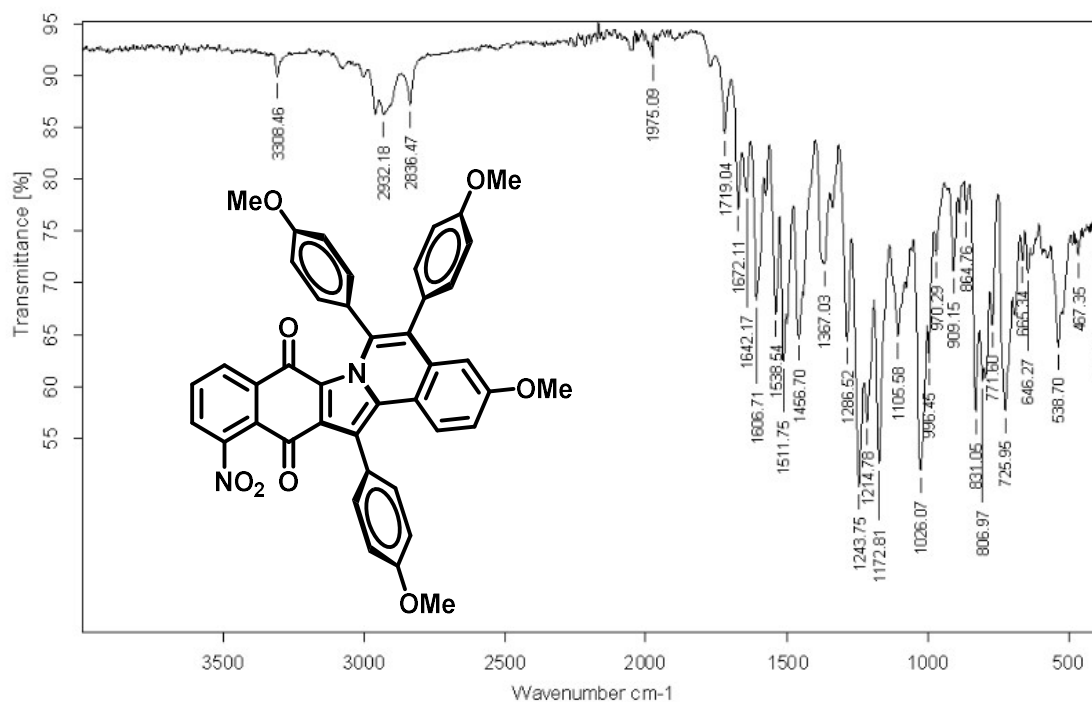


Figure B66. Infrared spectrum (IR-ATR) of the compound 68a.



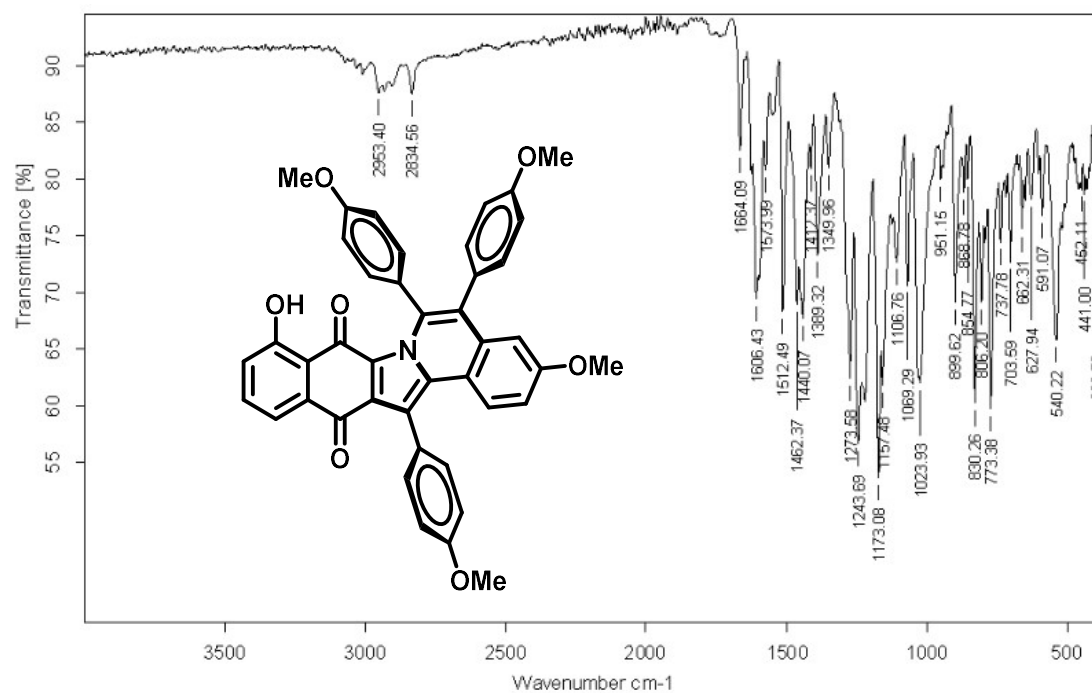


Figure B67. Infrared spectrum (IR-ATR) of the compound **68b**.

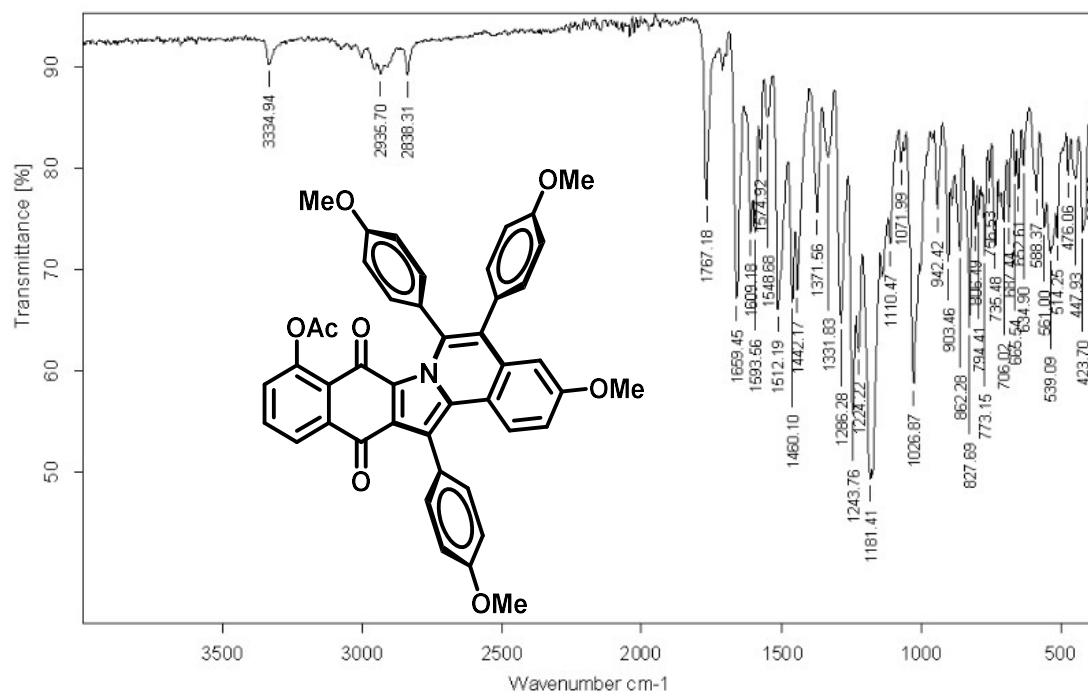


Figure B68. Infrared spectrum (IR-ATR) of the compound **68c**.

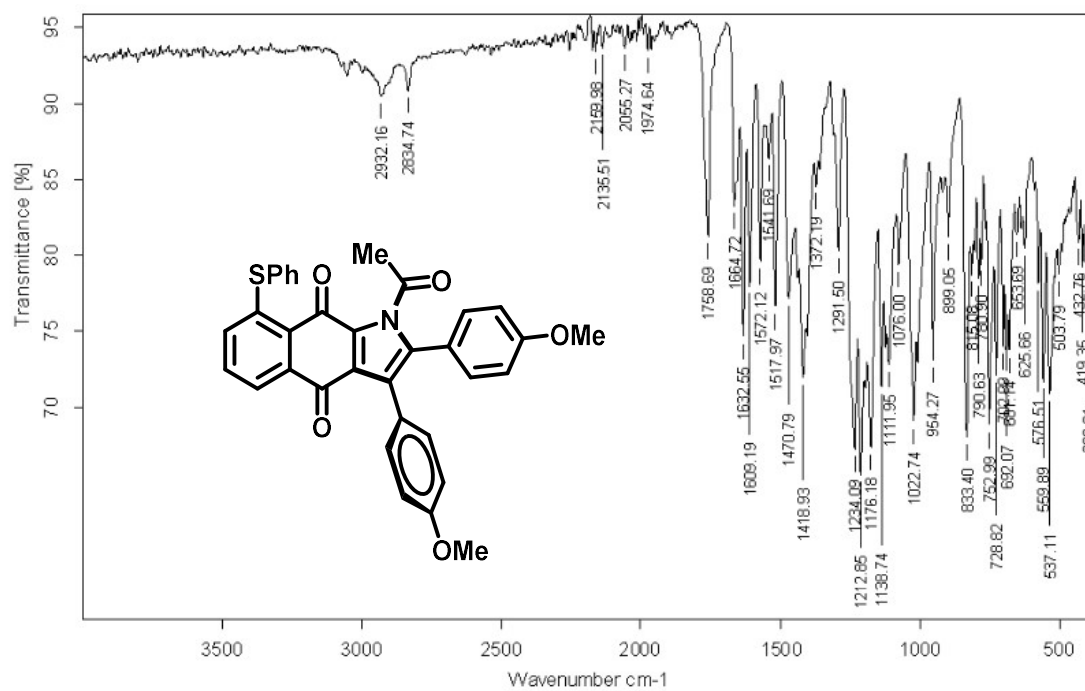


Figure B69. Infrared spectrum (IR-ATR) of the compound 68d.

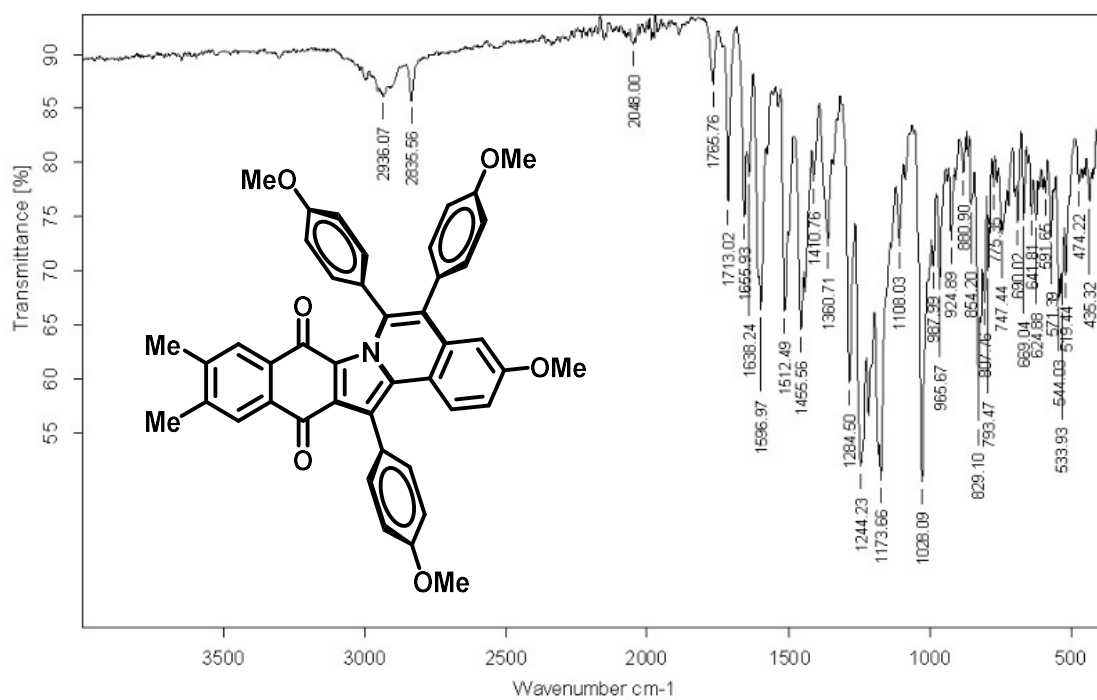


Figure B70. Infrared spectrum (IR-ATR) of the compound 68e.

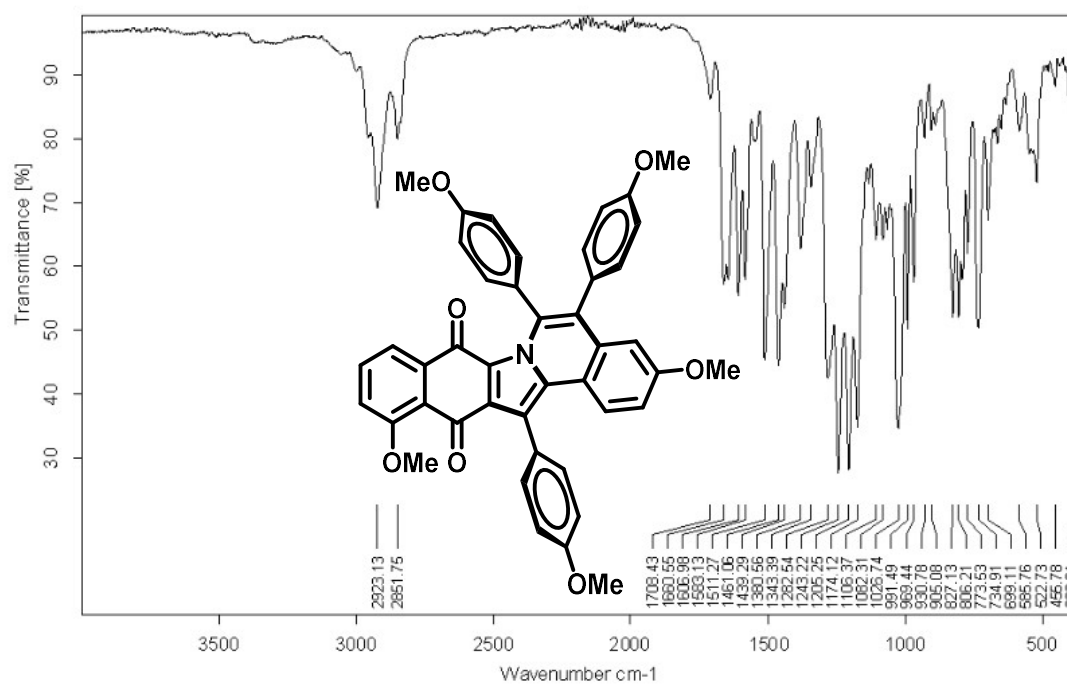


Figure B71. Infrared spectrum (IR-ATR) of the compound **68f**.

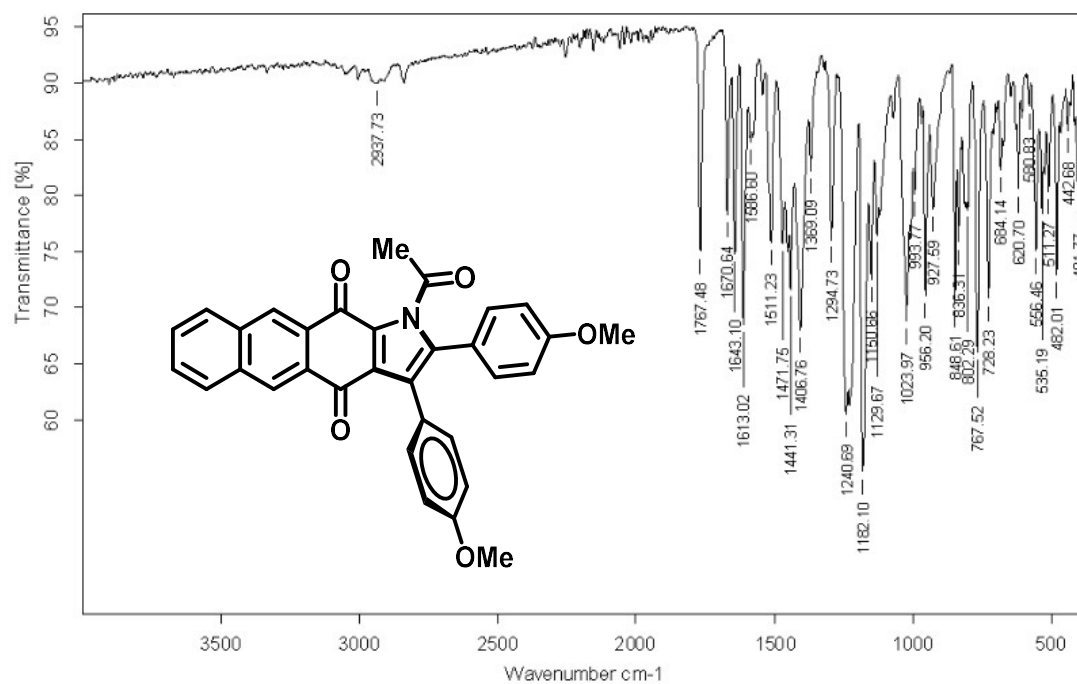


Figure B72. Infrared spectrum (IR-ATR) of the compound **68g**.

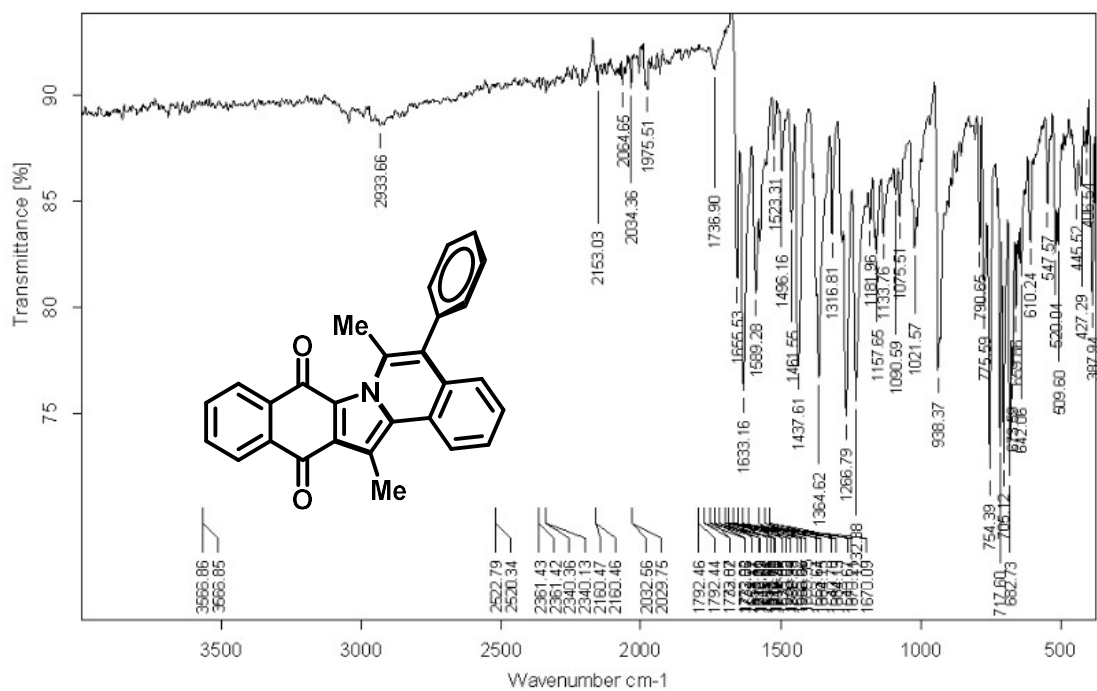


Figure B73. Infrared spectrum (IR-ATR) of the compound 69a.

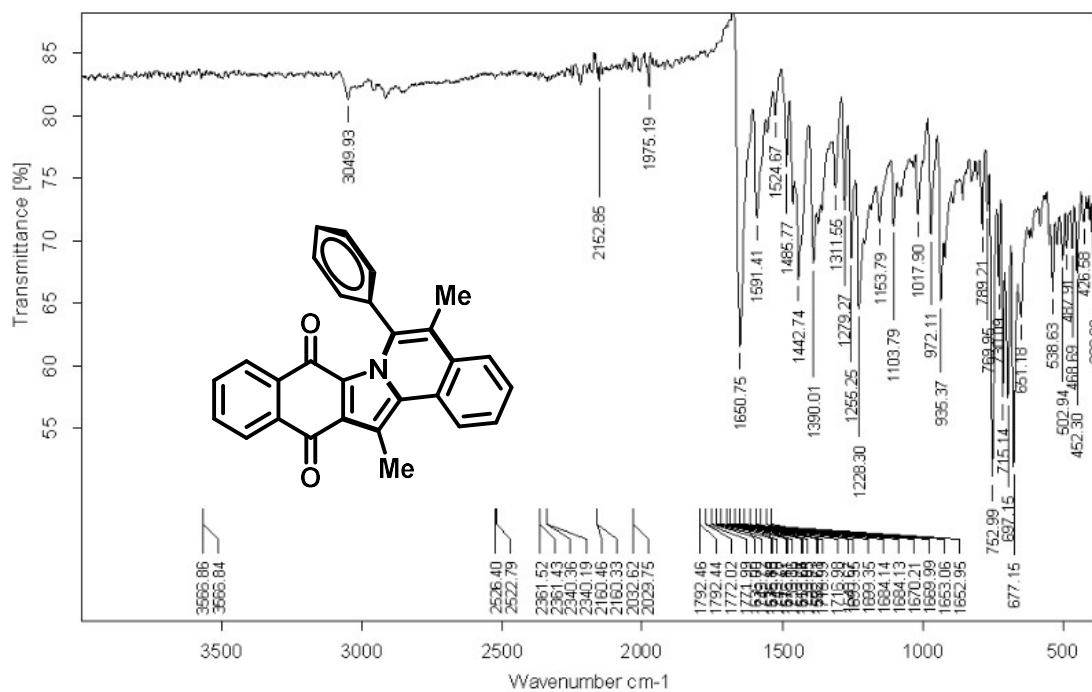


Figure B74. Infrared spectrum (IR-ATR) of the compound 69b.

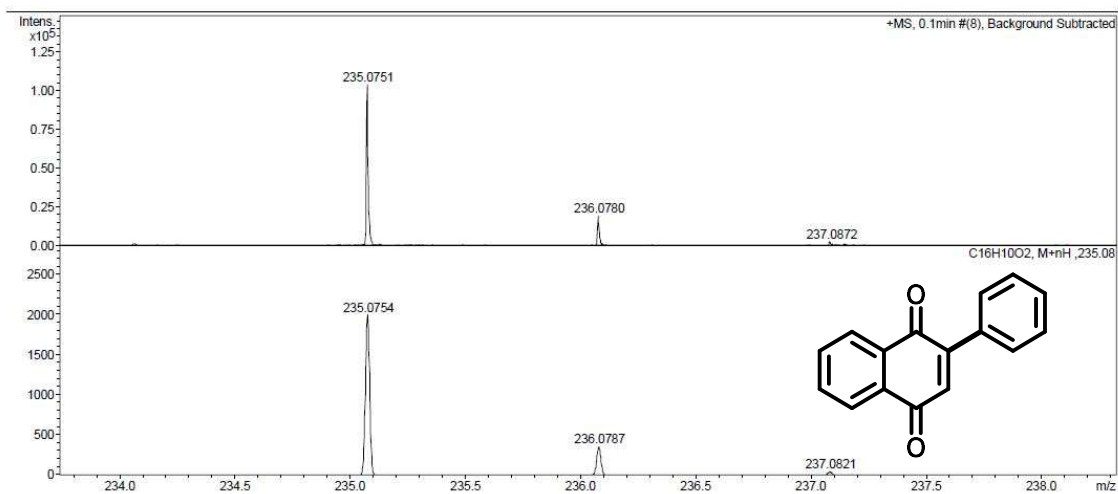


Figure C1. HRMS-ESI (+) of compound 52.

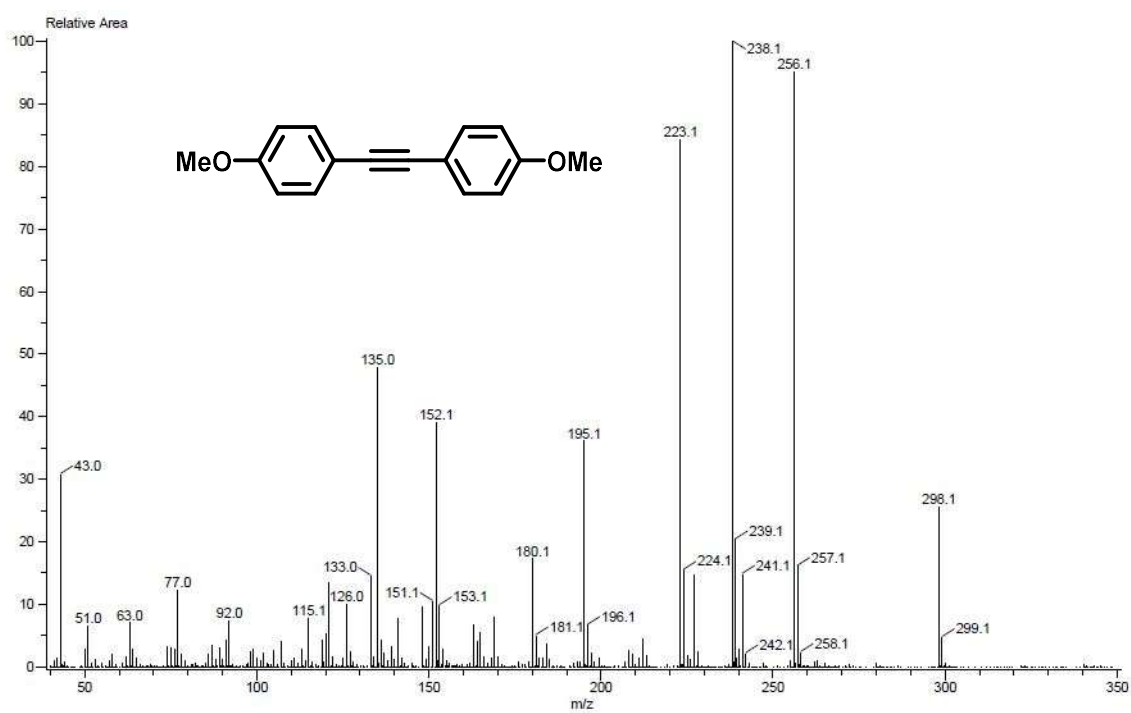
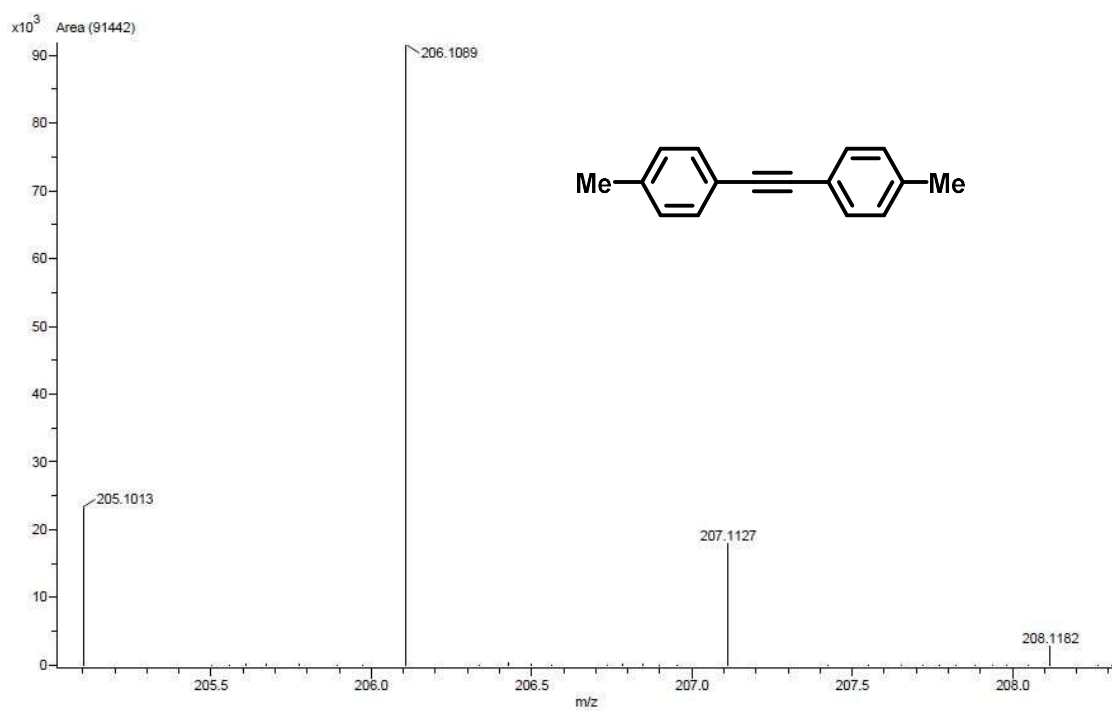
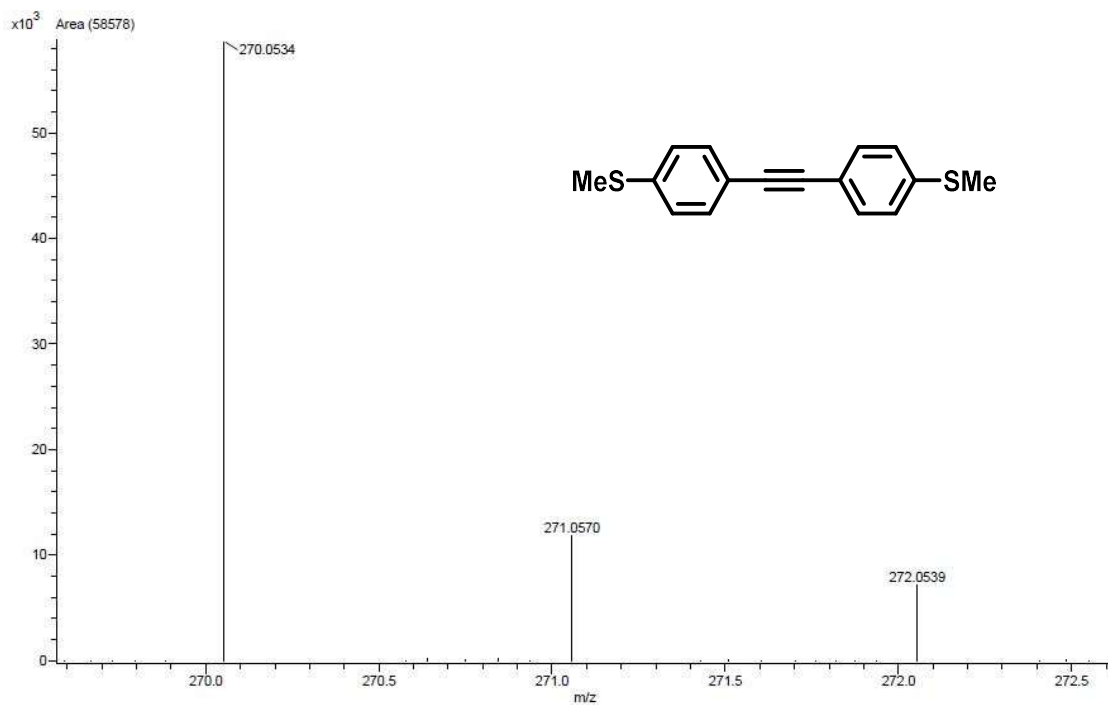


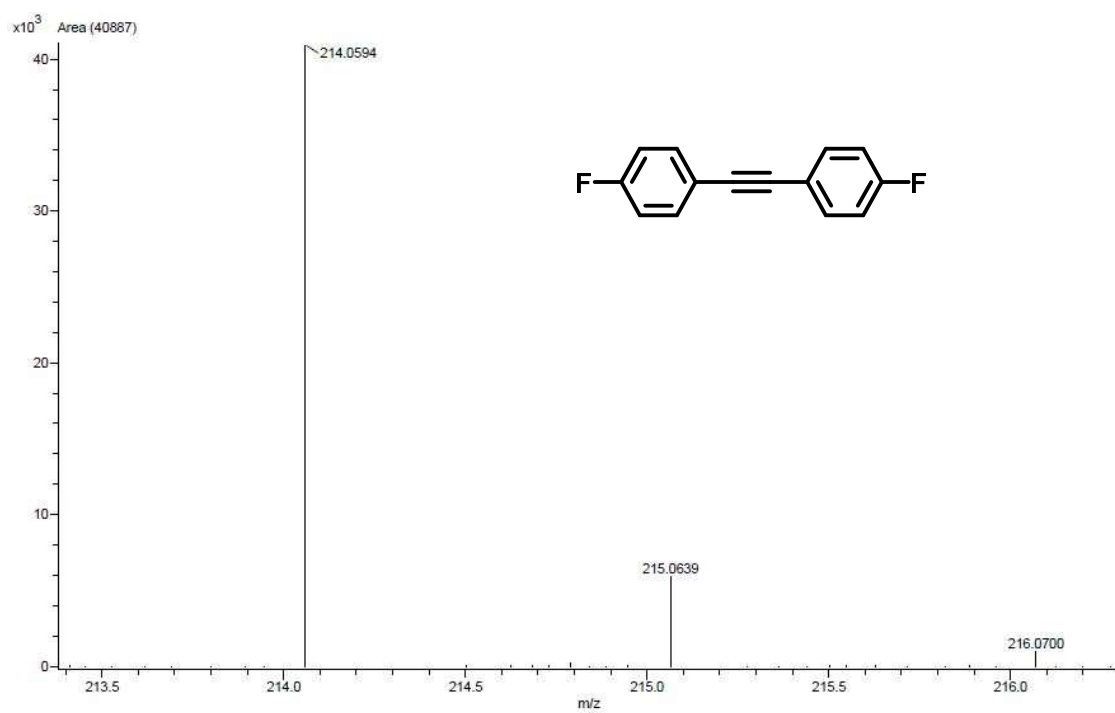
Figure C2. MS-EI (+) of compound 56b.



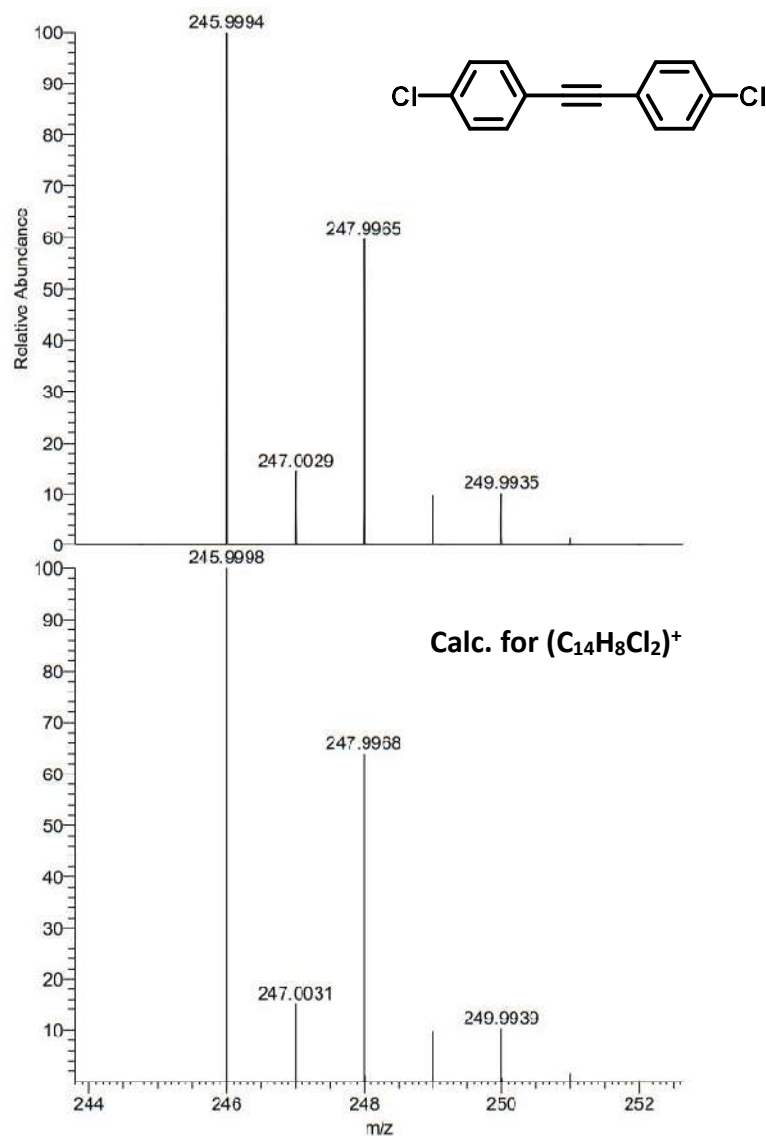
**Figure C3.** HRMS-EI (+) of compound **56c**.



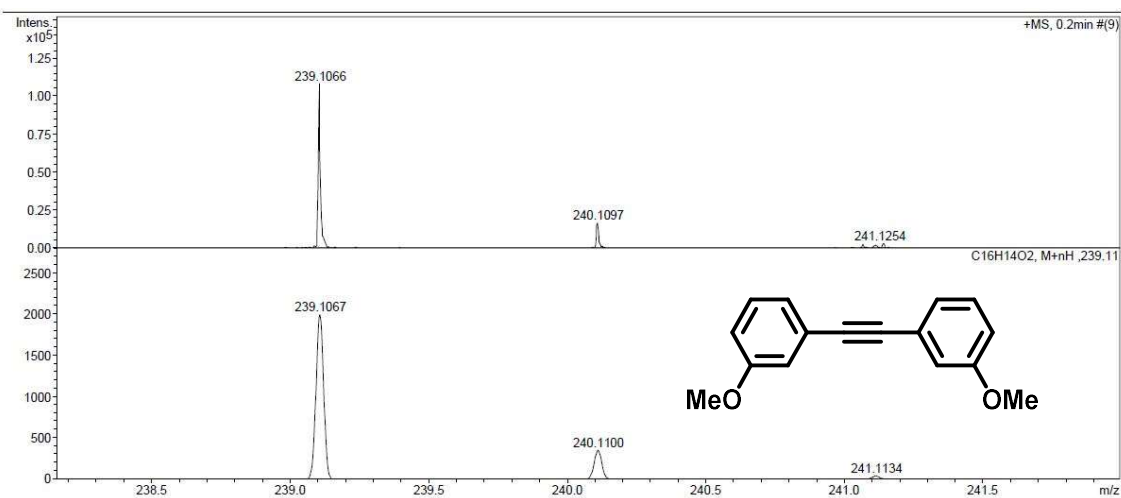
**Figure C4.** HRMS-EI (+) of compound **56d**.



**Figure C5.** HRMS-EI (+) of compound 56e.



**Figure C6.** HRMS-EI (+) of compound **56f**.



**Figure C7.** HRMS-ESI (+) of compound **56h**.



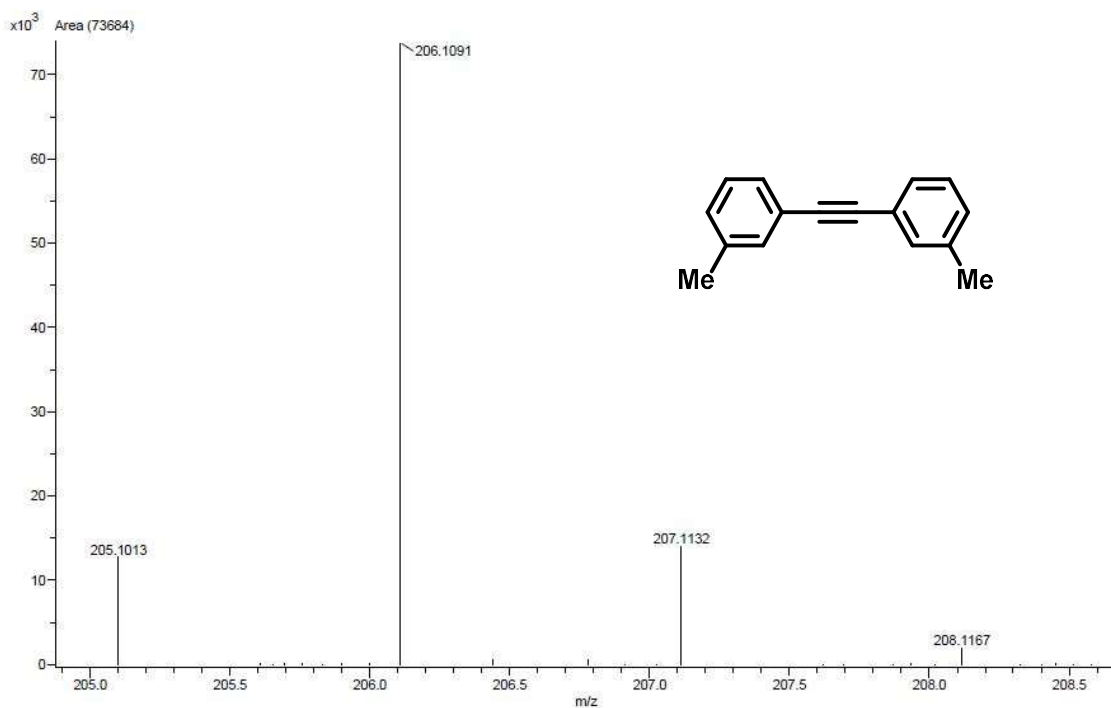


Figure C8. HRMS-EI (+) of compound 56i.

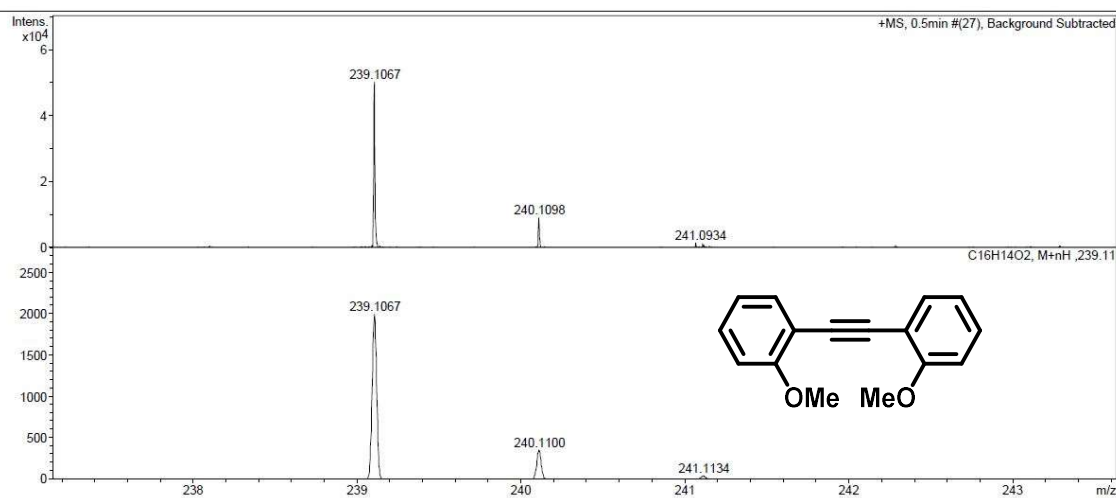


Figure C9. HRMS-ESI (+) of compound 56j.

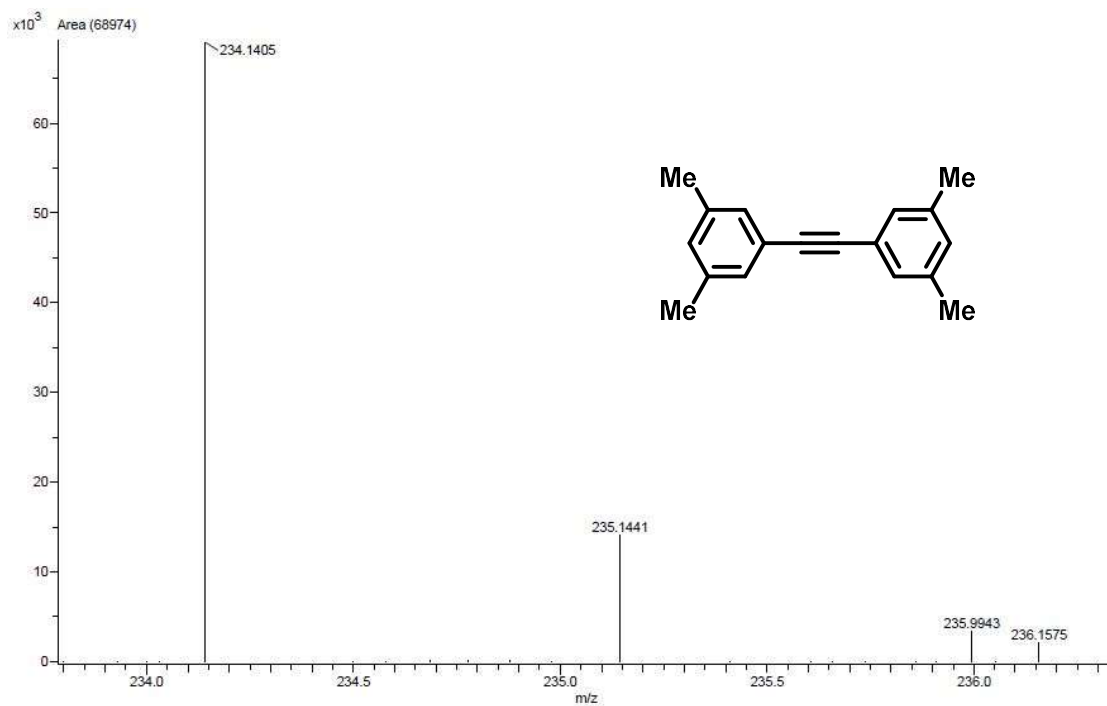


Figure C10. HRMS-EI (+) of compound 56k.

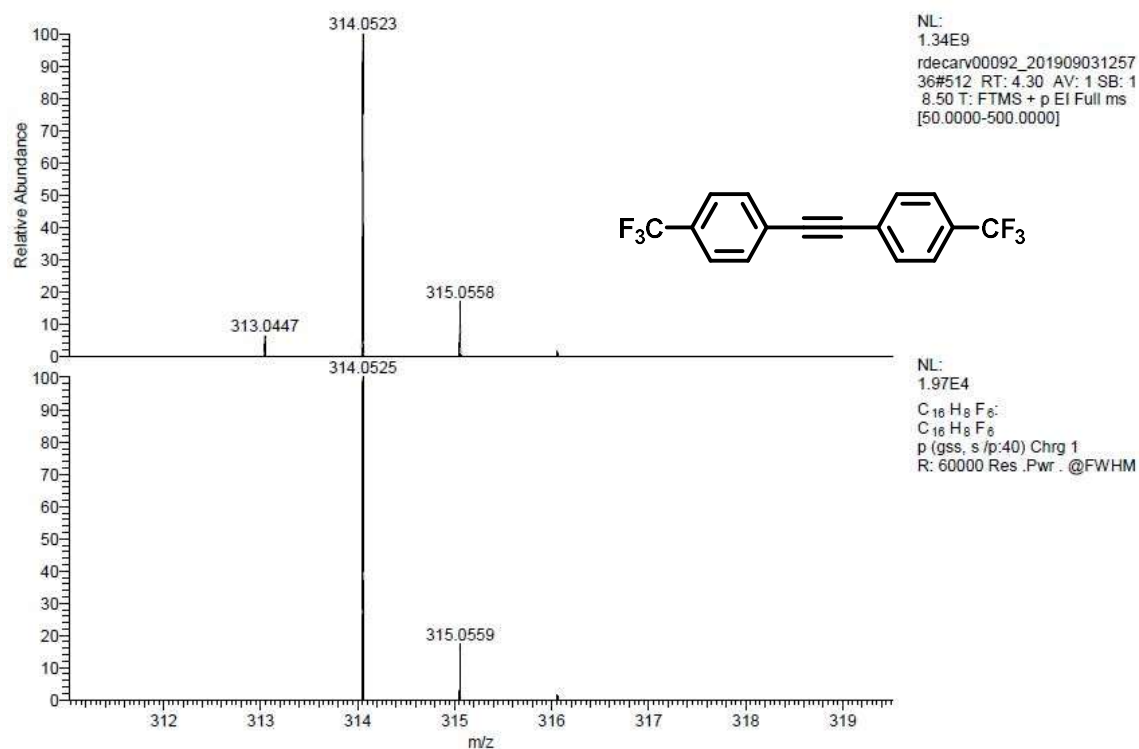


Figure C11. HRMS-EI (+) of compound 56l.

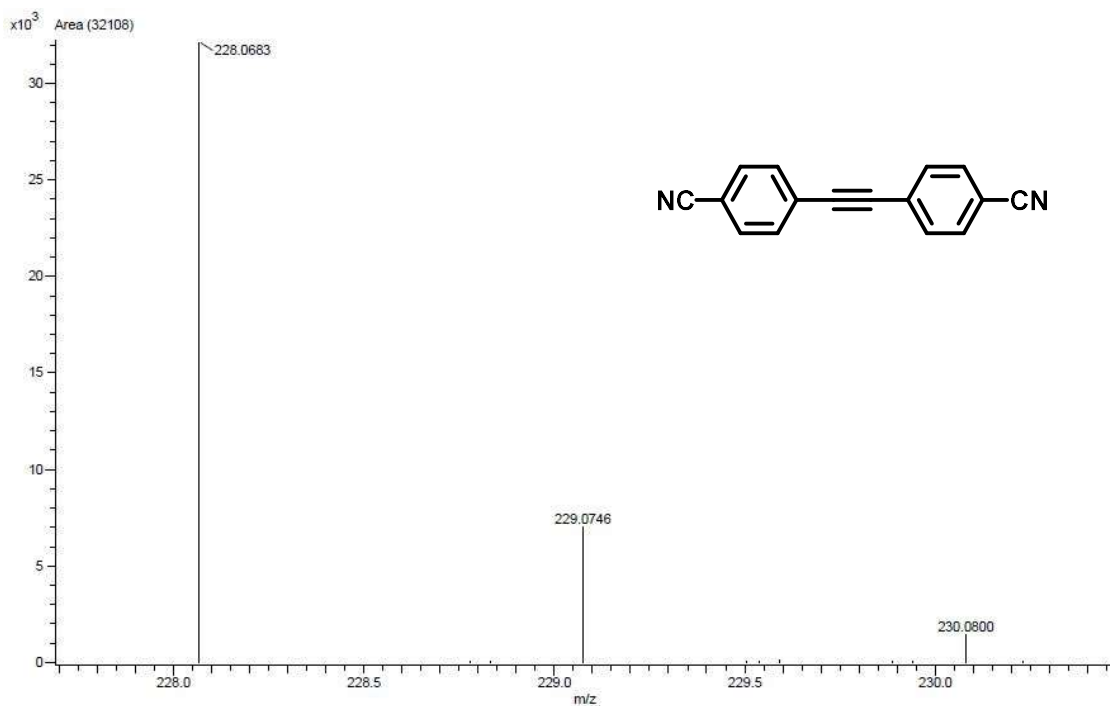


Figure C12. HRMS-EI (+) of compound 56m.

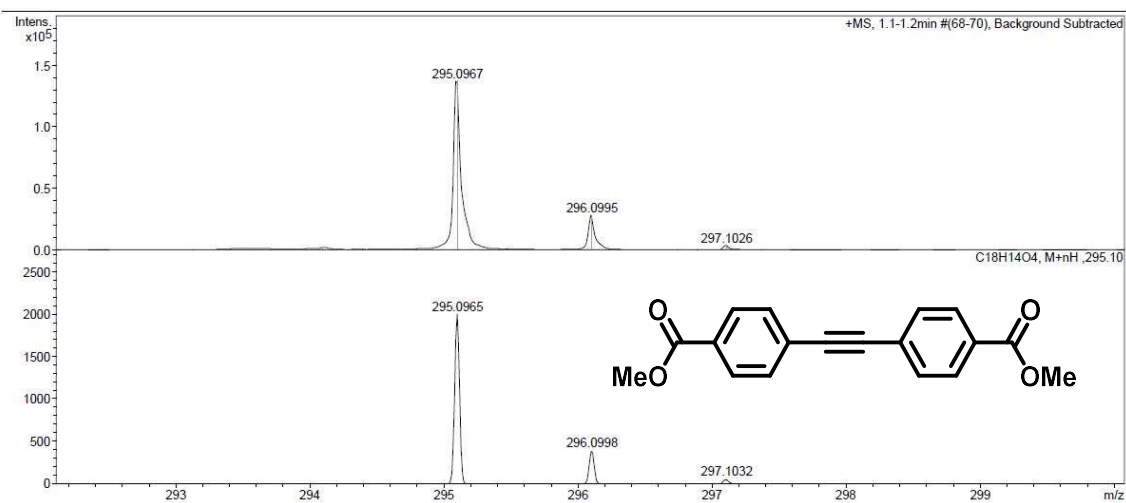


Figure C13. HRMS-ESI (+) of compound 56n.

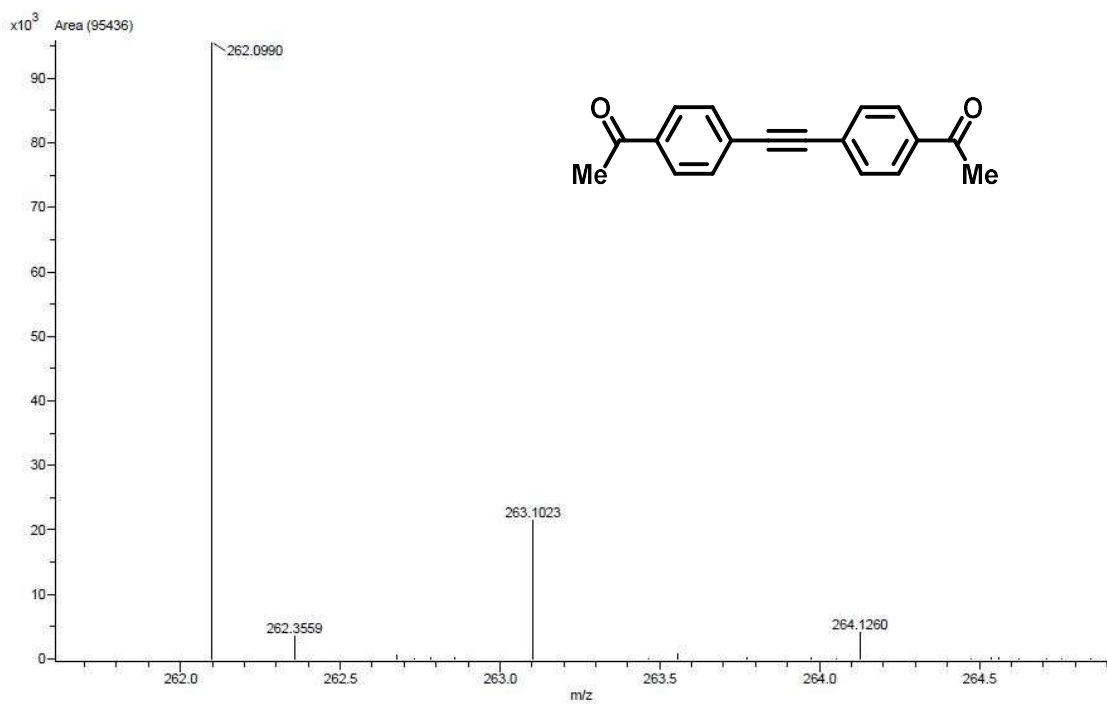


Figure C14. HRMS-EI (+) of compound 560.

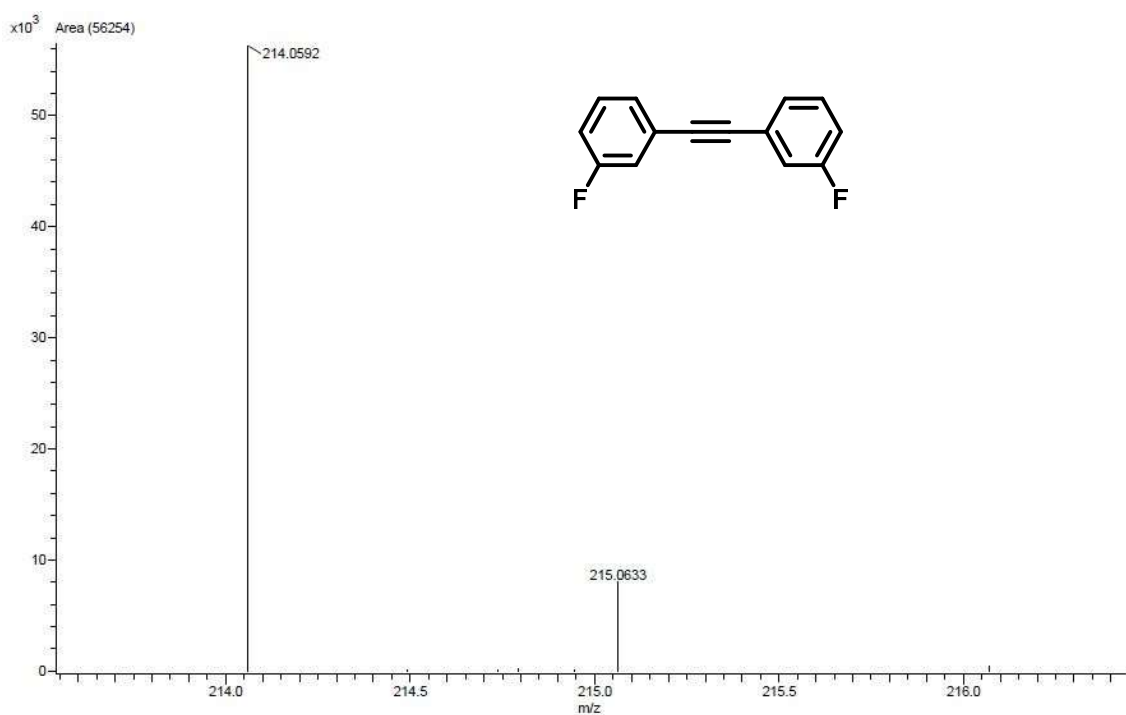
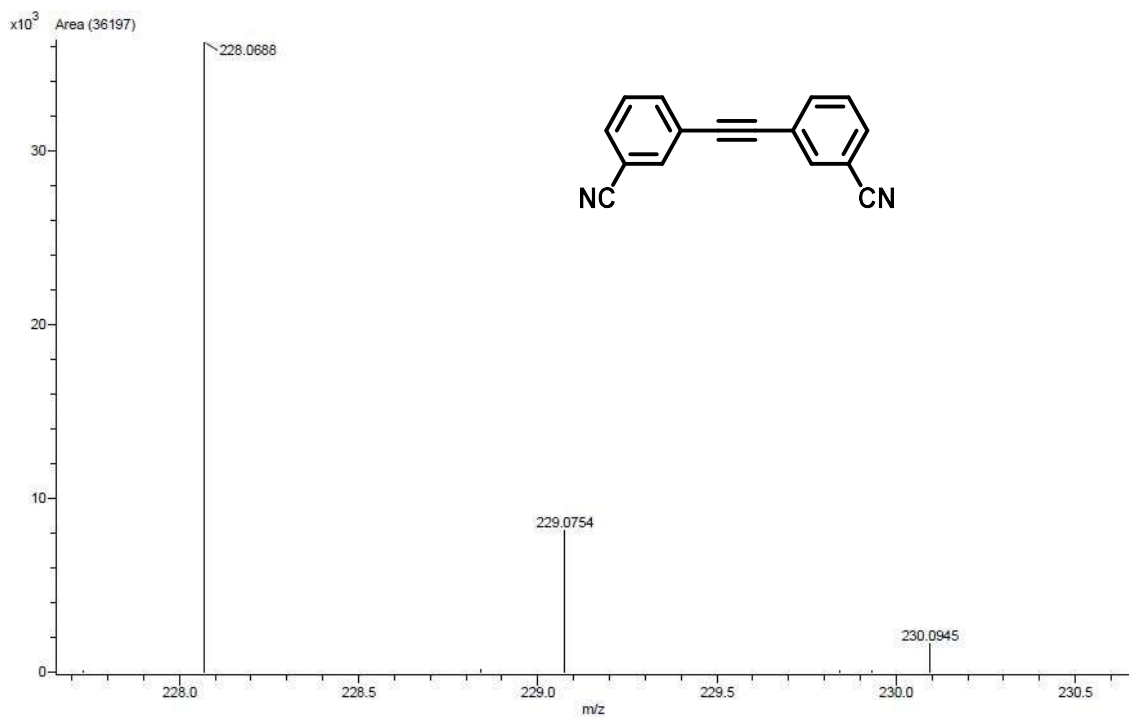
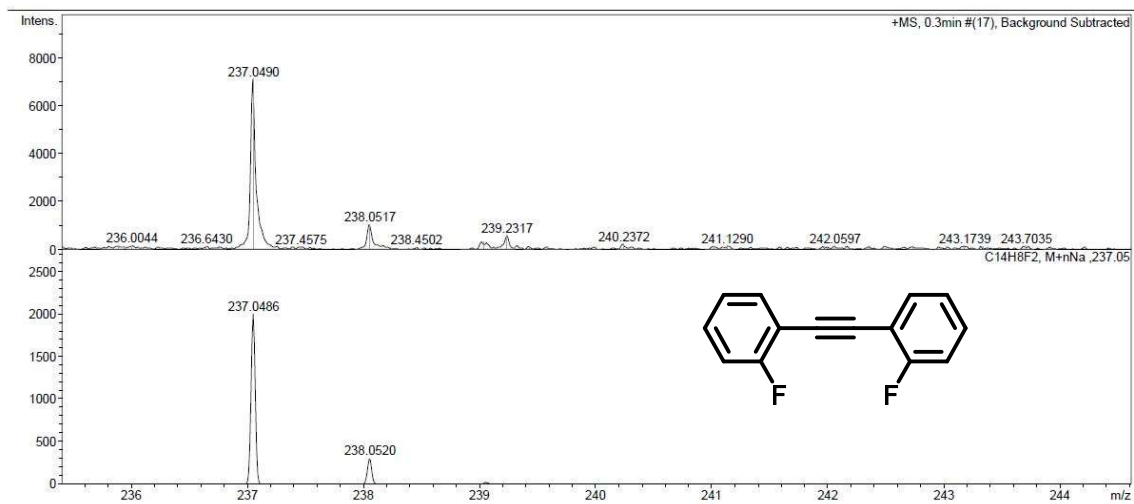


Figure C15. HRMS-EI (+) of compound 56p.



**Figure C16.** HRMS-EI (+) of compound **56q**.



**Figure C17.** HRMS-ESI (+) of compound **56r**.

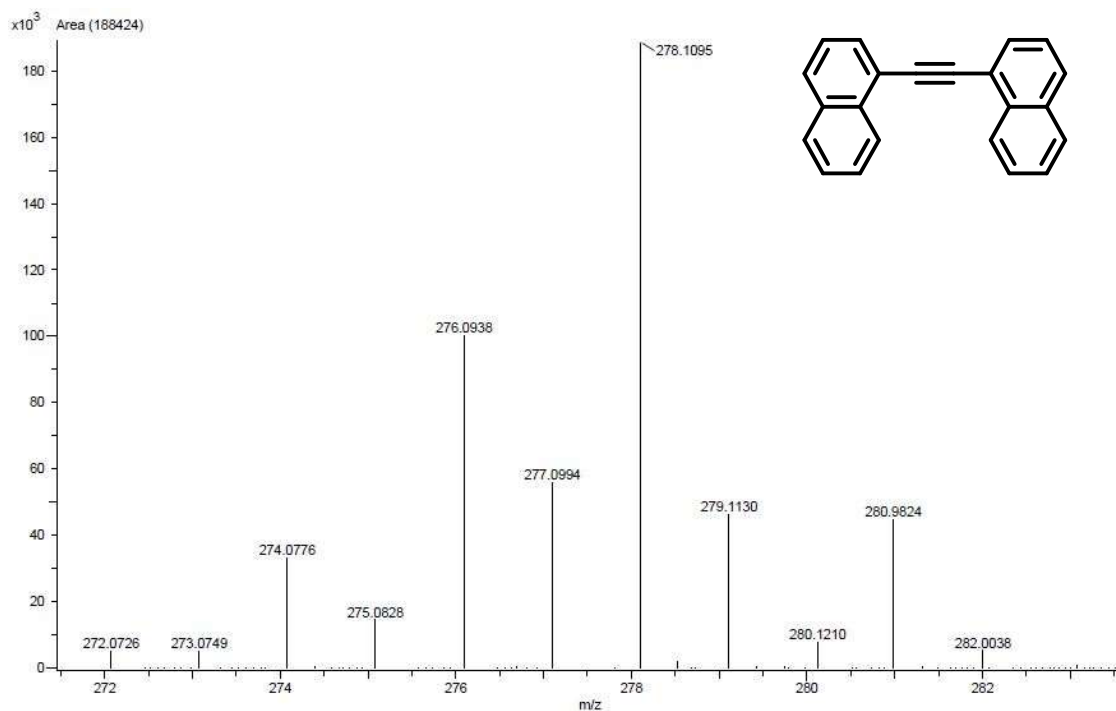


Figure C18. HRMS-EI (+) of compound 56s.

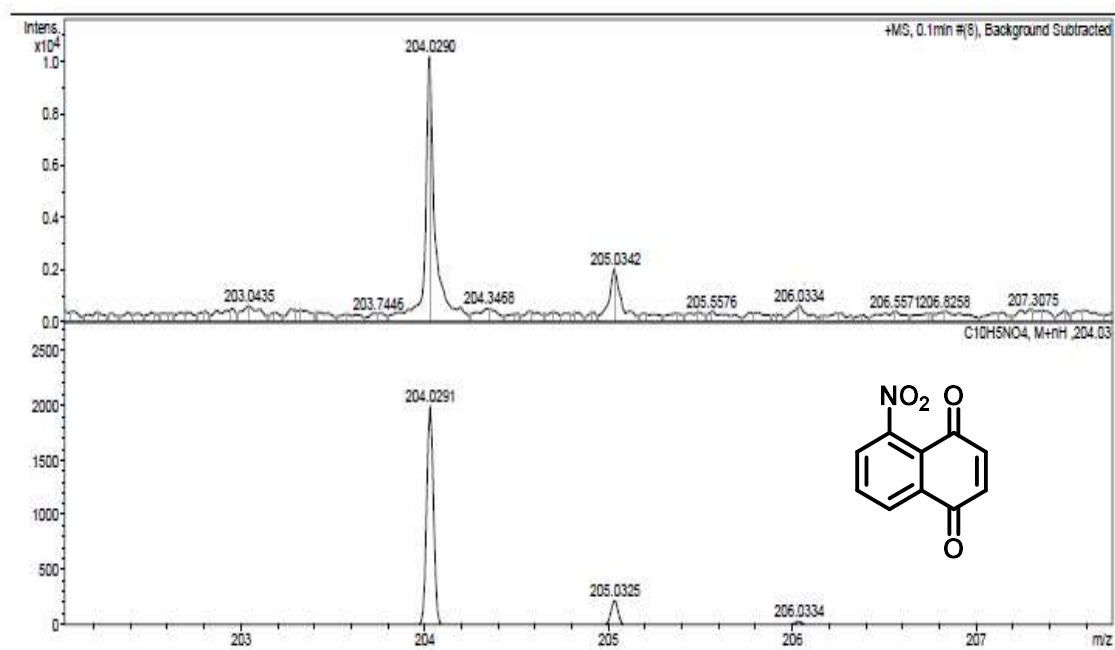


Figure C19. HRMS-ESI (+) of compound 57a.

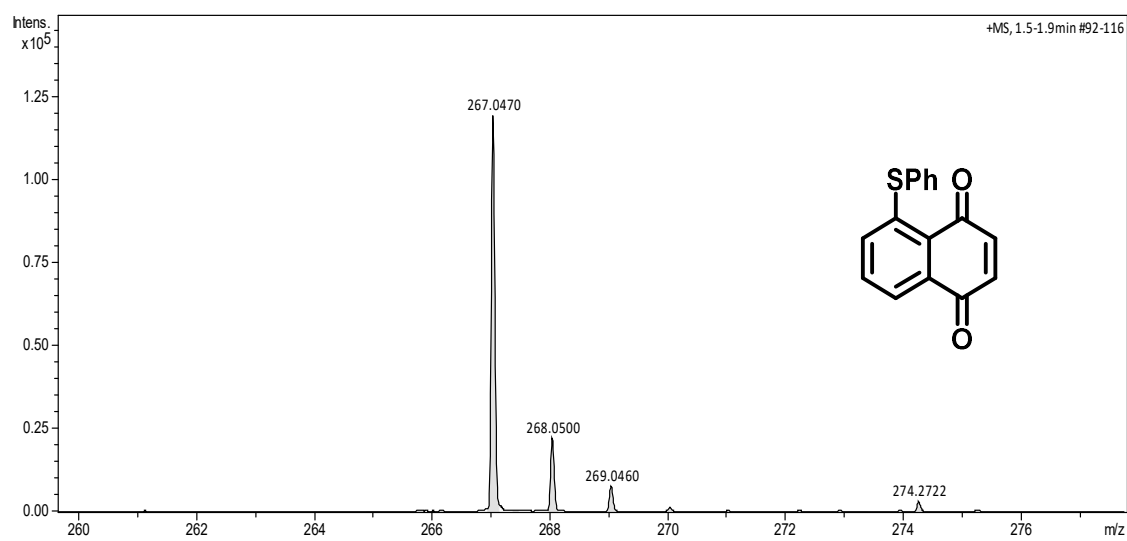


Figure C20. HRMS-ESI (+) of compound 57e.

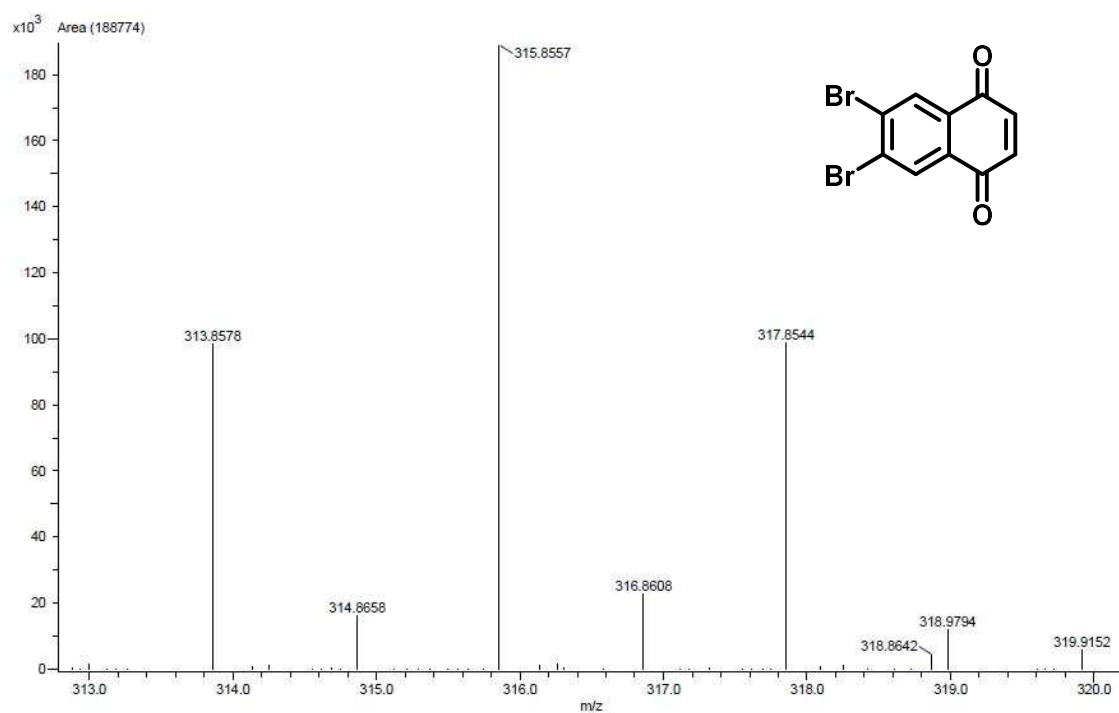


Figure C21. HRMS-EI (+) of compound 57g.

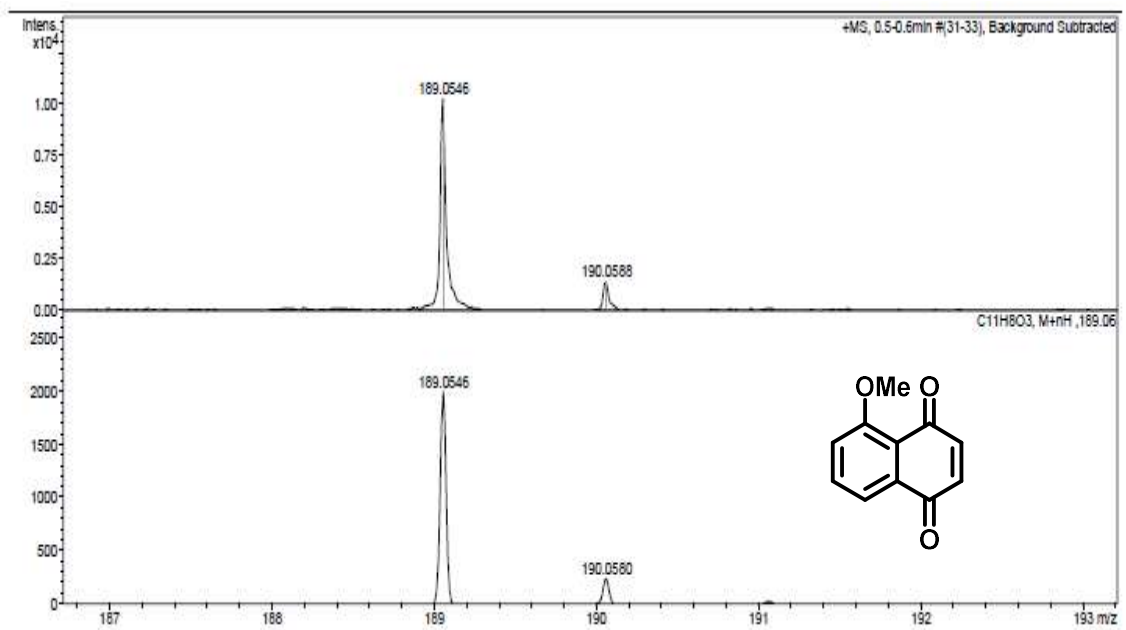


Figure C22. HRMS-ESI (+) of compound 57i.

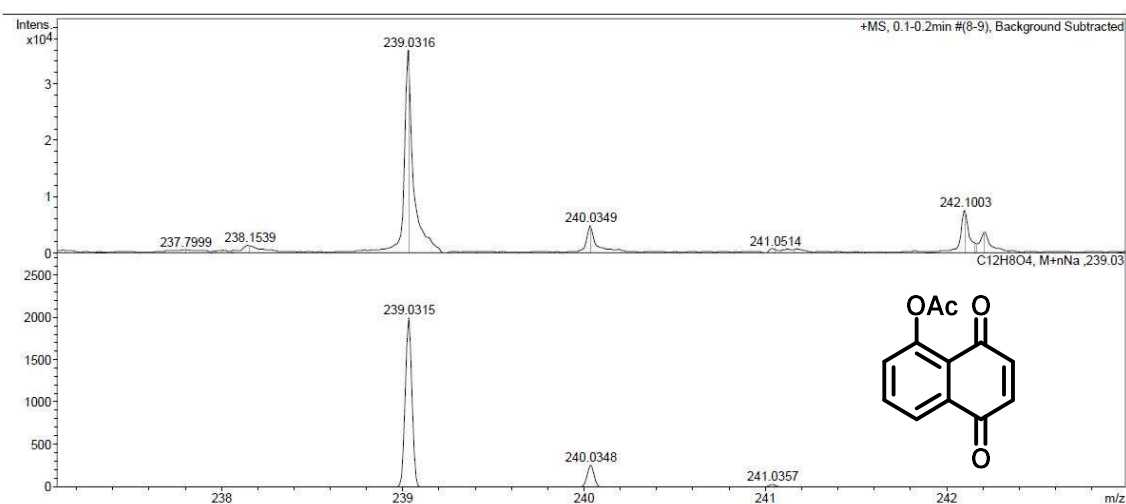


Figure C23. HRMS-ESI (+) of compound 57j.



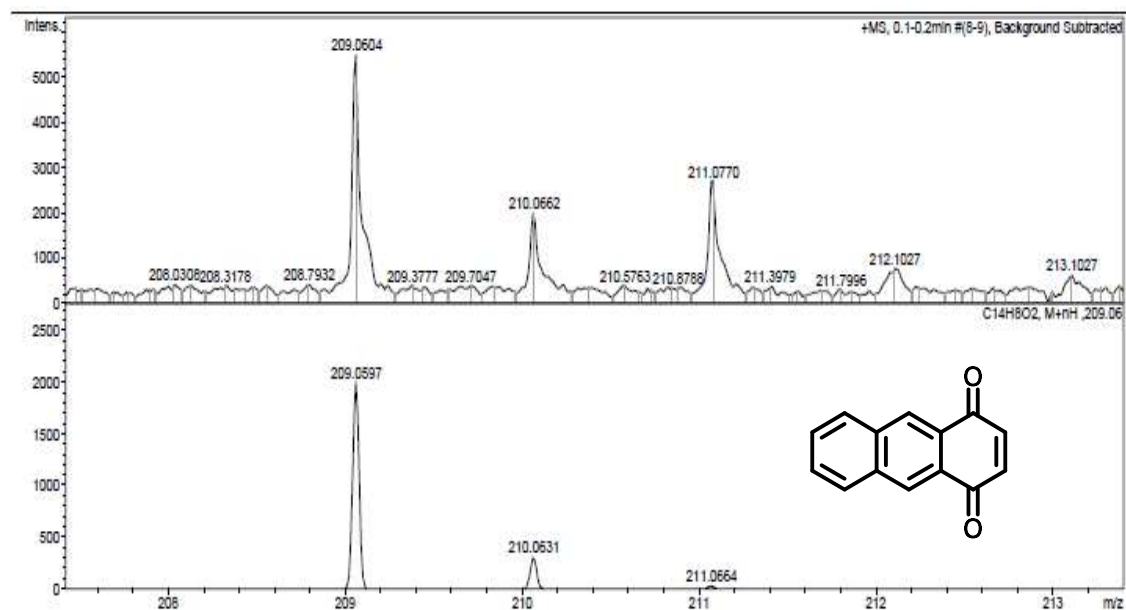


Figure C24. HRMS-ESI (+) of compound 57l.

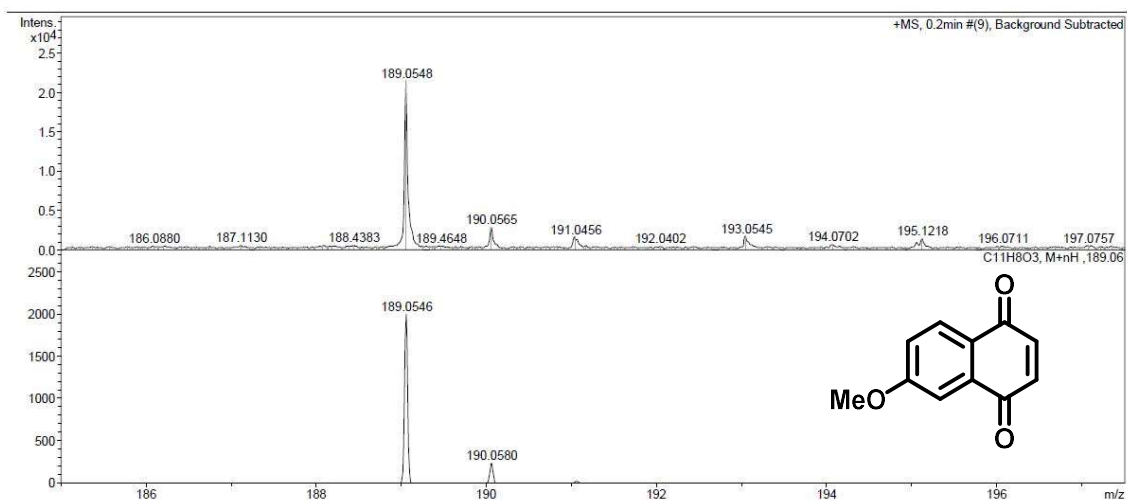


Figure C25. HRMS-ESI (+) of compound 57m.

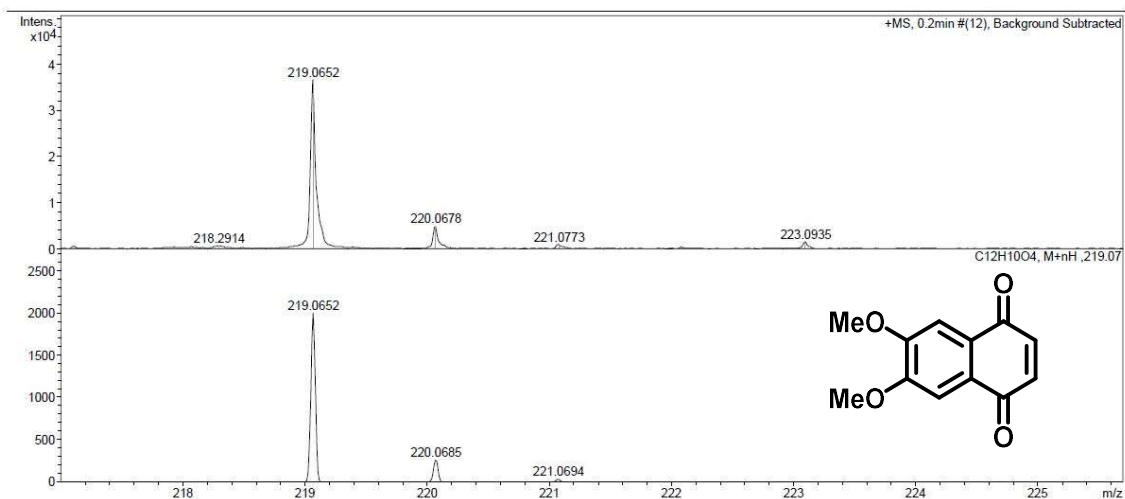


Figure C26. HRMS-ESI (+) of compound 57n.

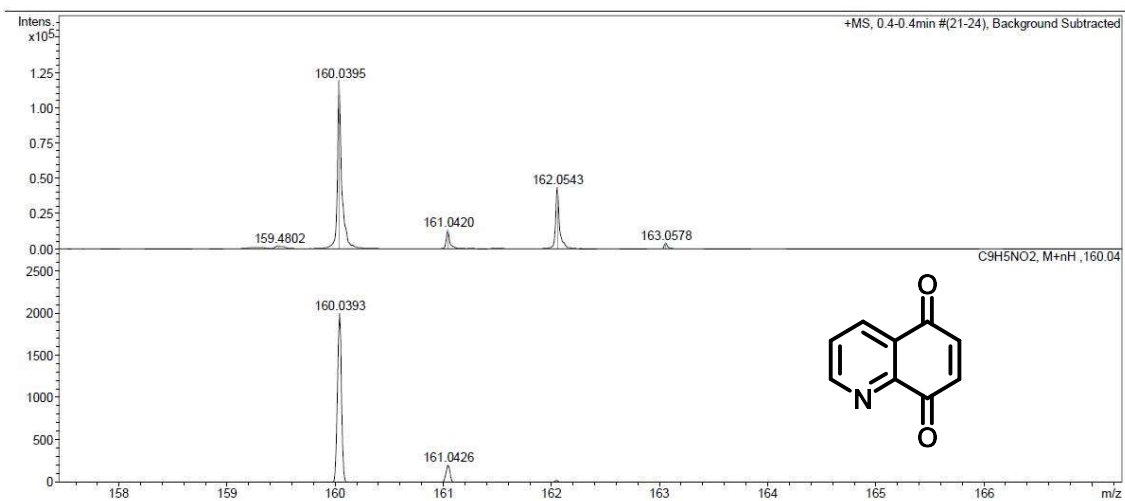


Figure C27. HRMS-ESI (+) of compound 57o.

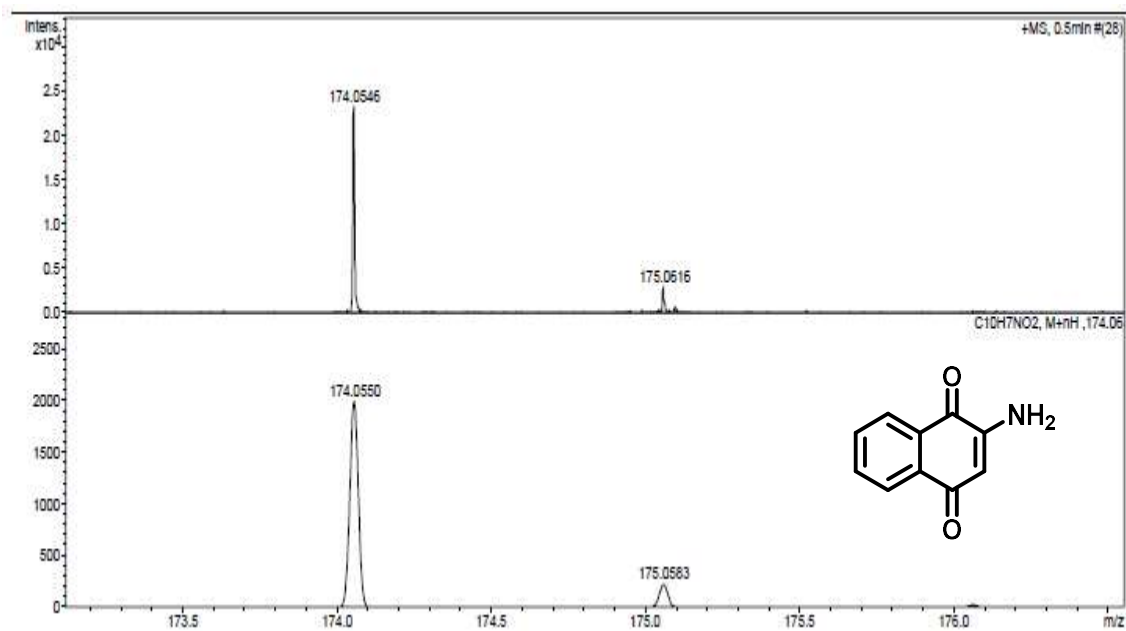


Figure C28. HRMS-ESI (+) of compound 58a.

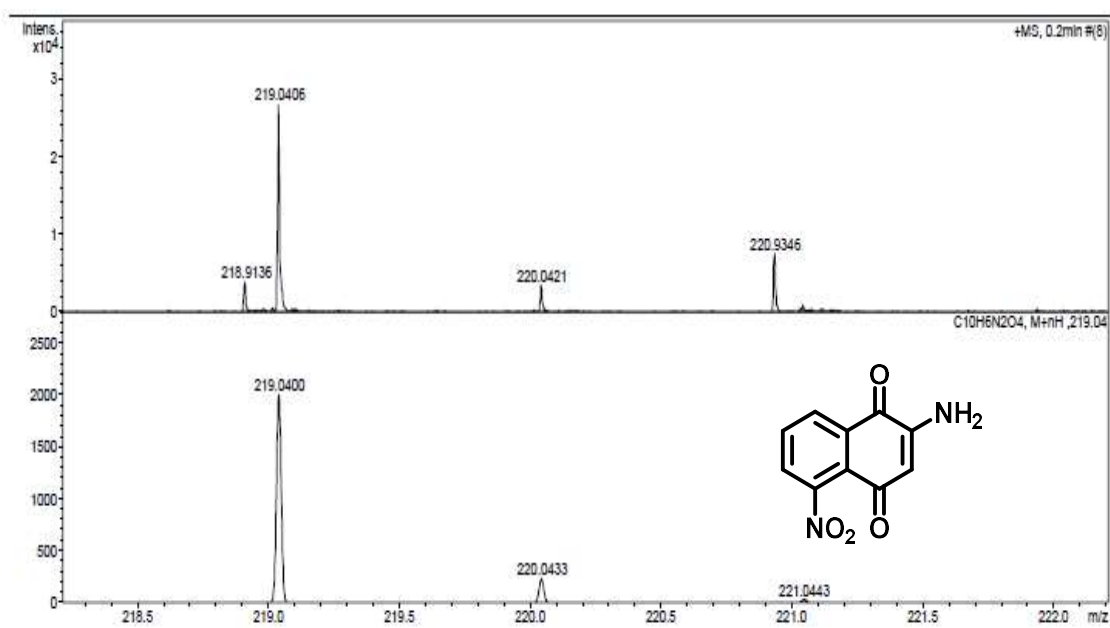


Figure C29. HRMS-ESI (+) of compound 58b.

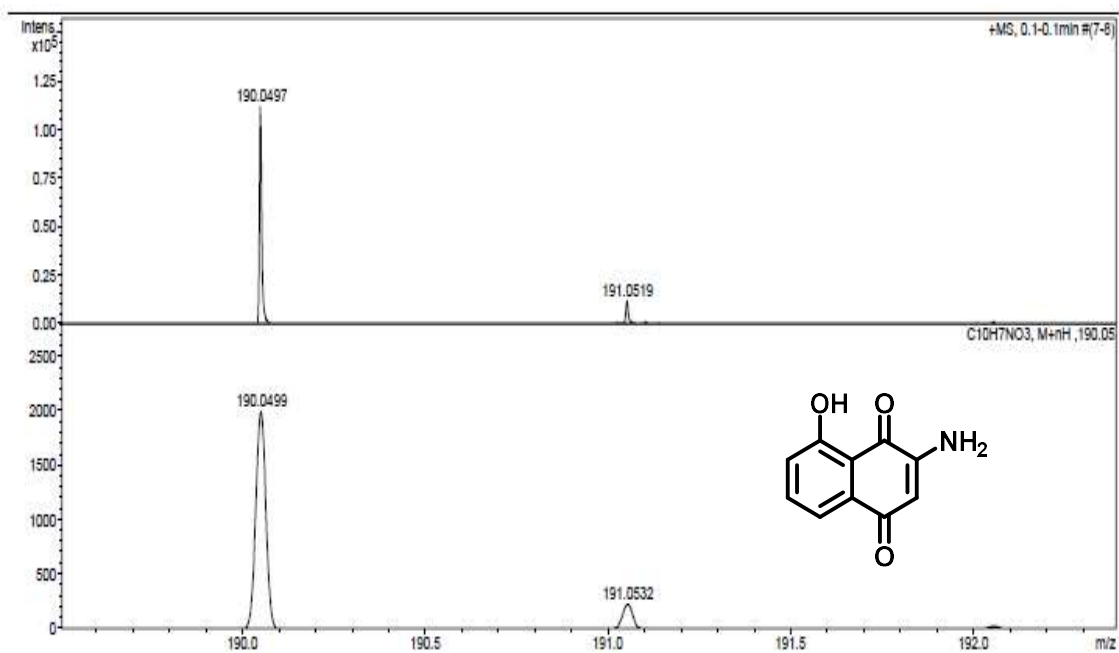


Figure C30. HRMS-ESI (+) of compound 58c.

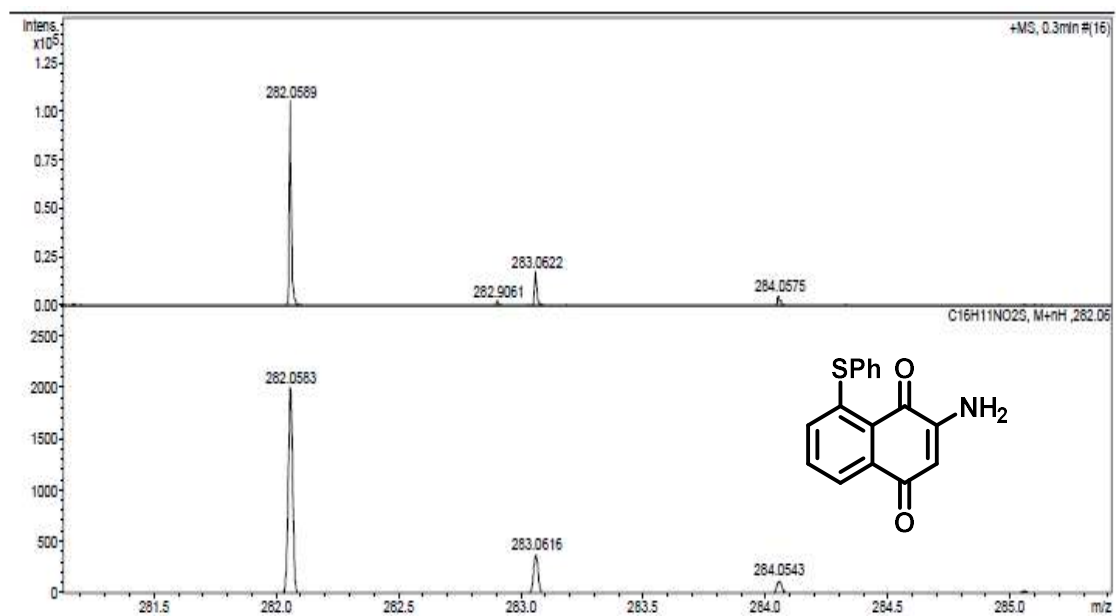


Figure C31. HRMS-ESI (+) of compound 58d.

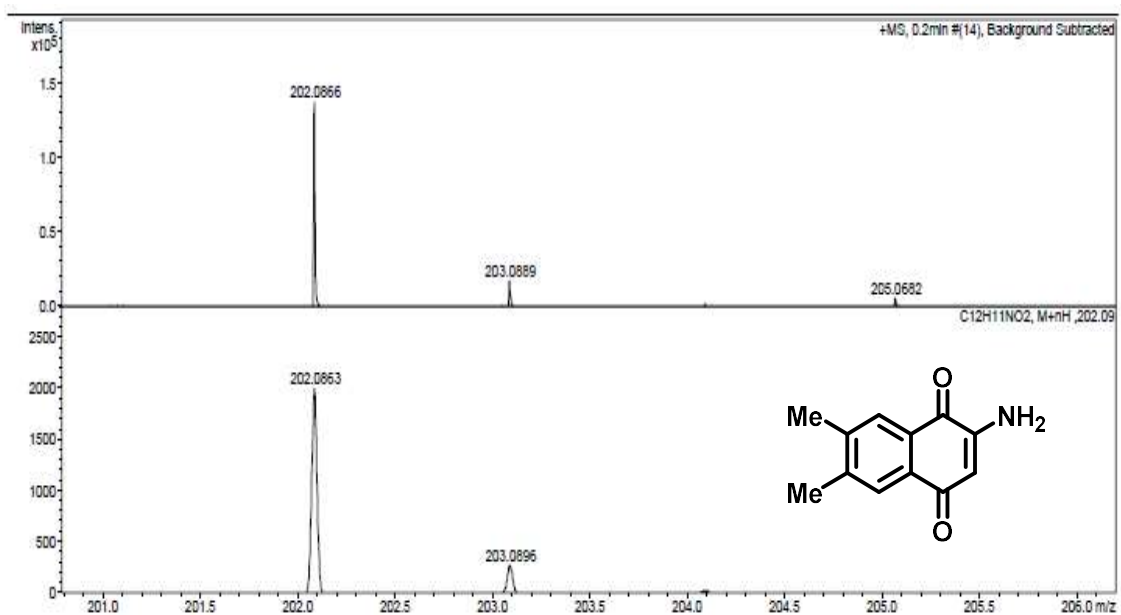


Figure C32. HRMS-ESI (+) of compound 58e.

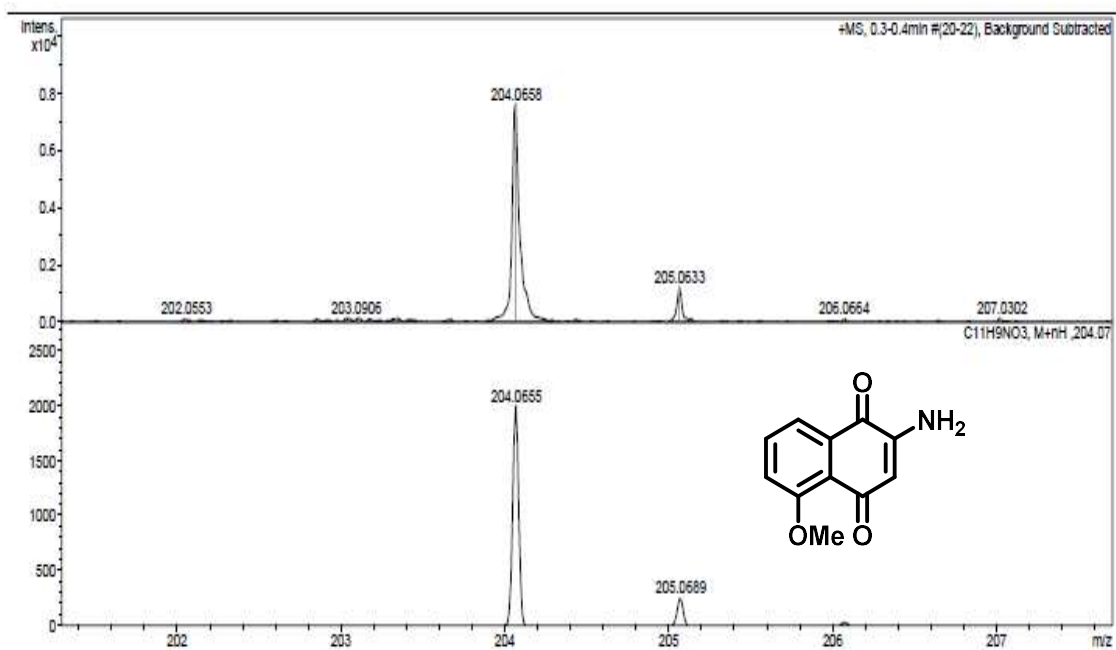


Figure C33. HRMS-ESI (+) of compound 58f.

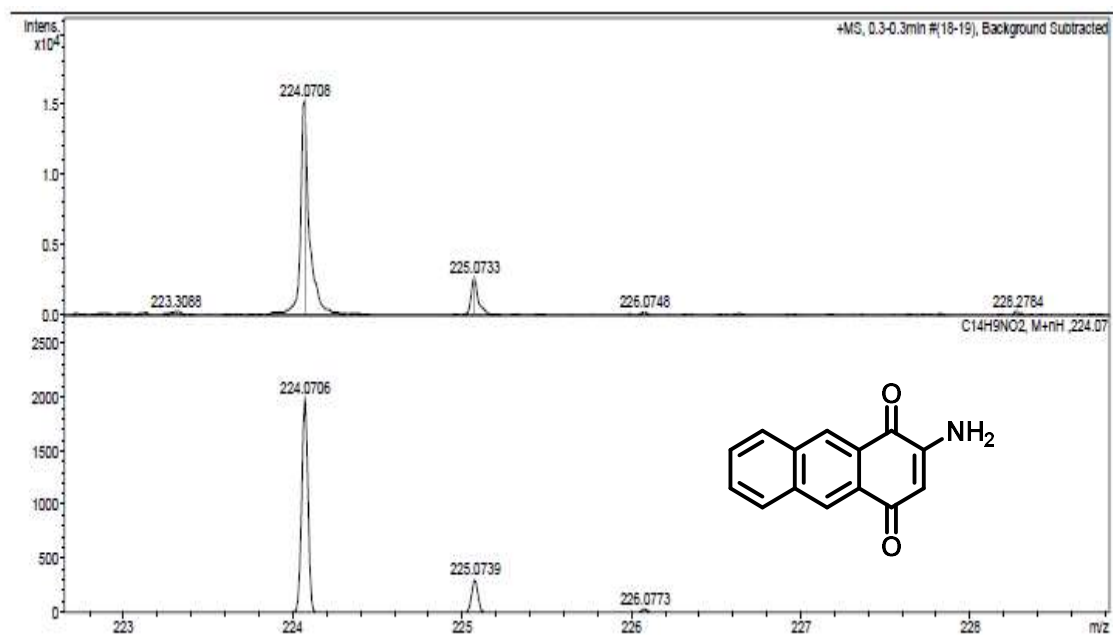


Figure C34. HRMS-ESI (+) of compound 58g.

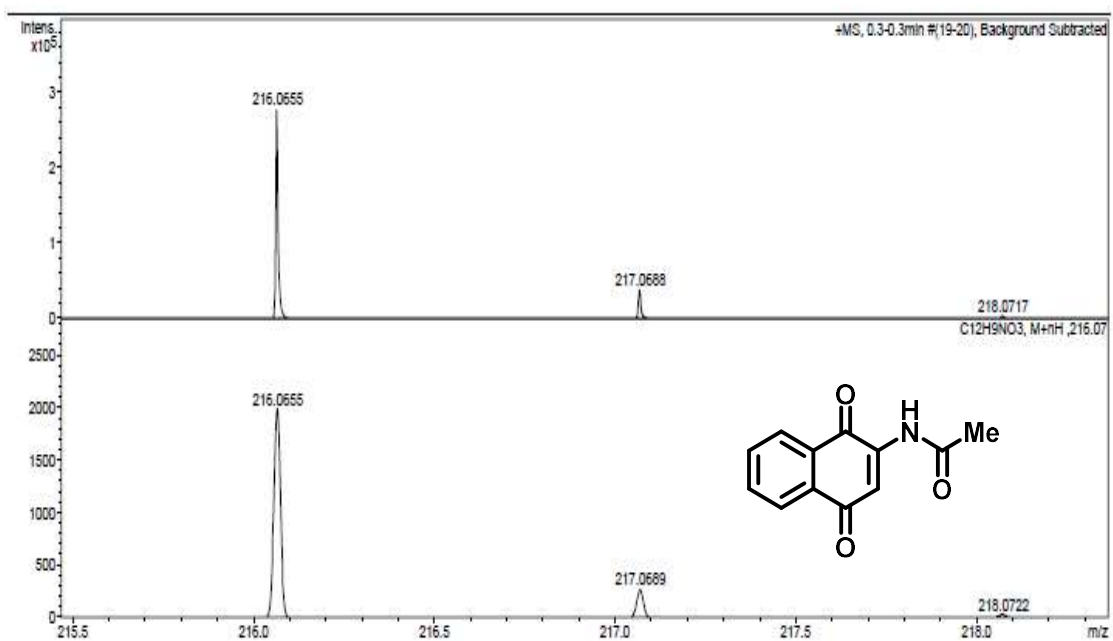


Figure C35. HRMS-ESI (+) of compound 59a.

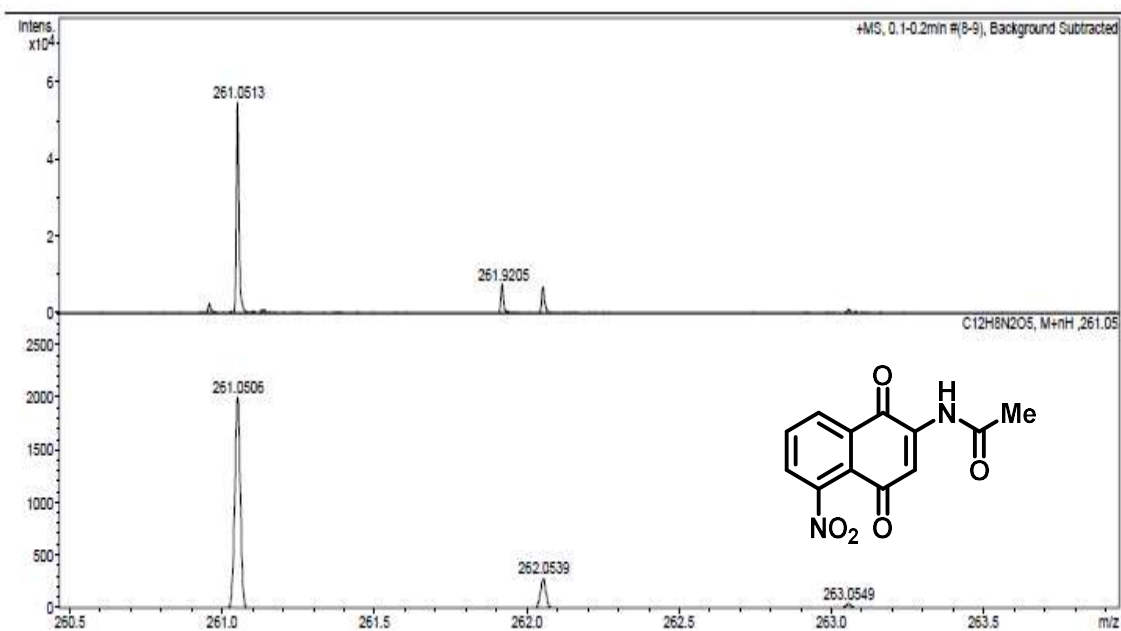


Figure C36. HRMS-ESI (+) of compound **59b**.

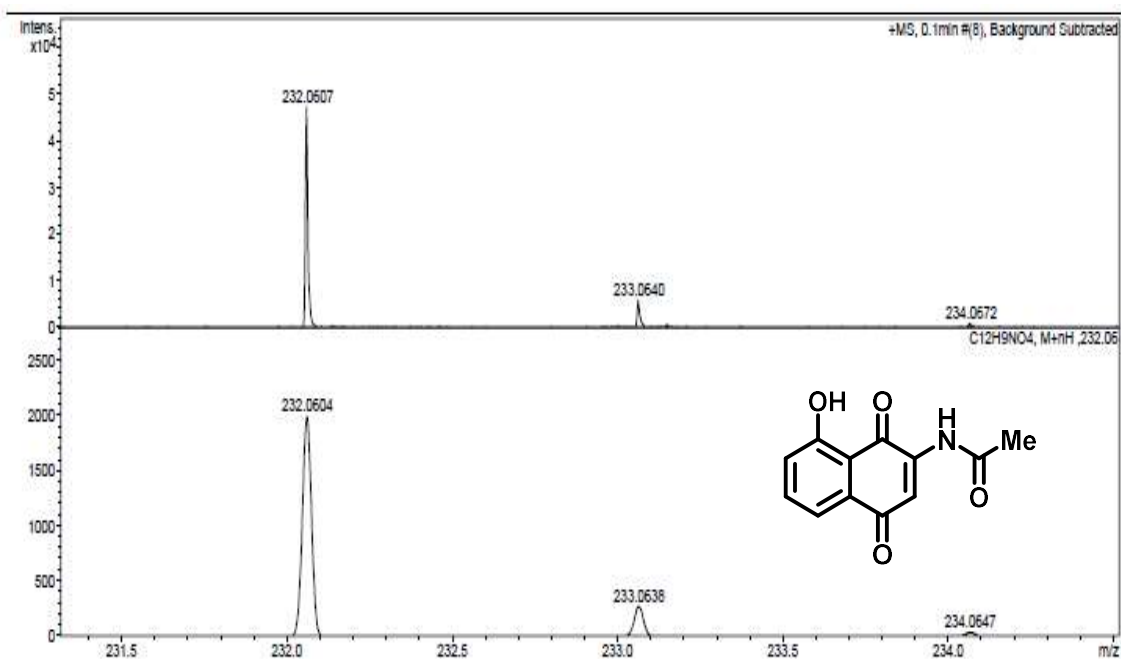


Figure C37. HRMS-ESI (+) of compound **59c**.

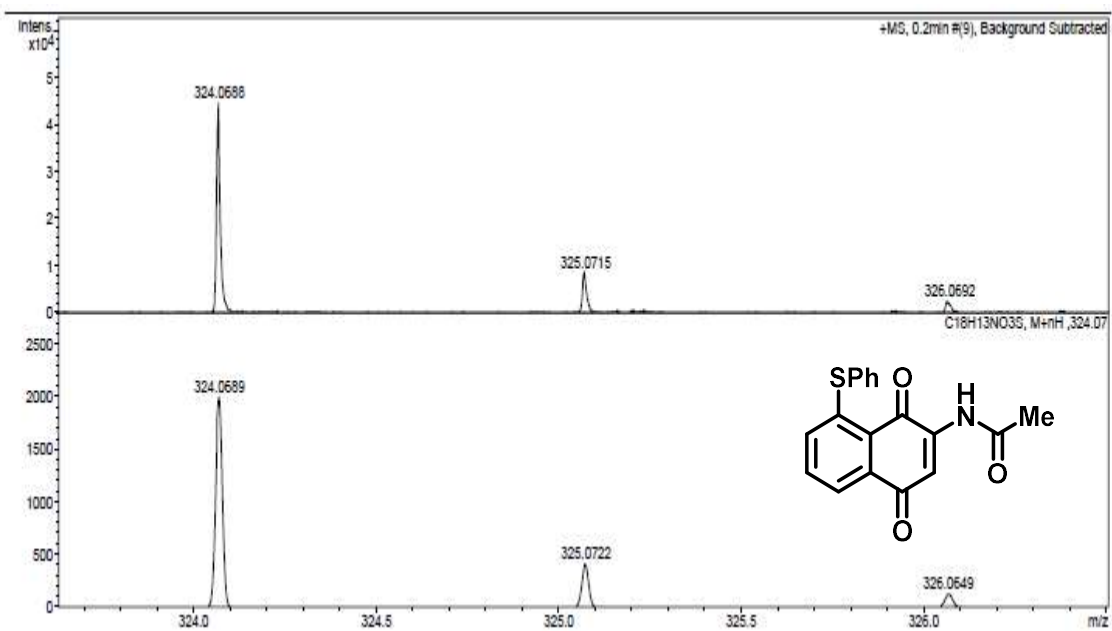


Figure C38. HRMS-ESI (+) of compound 59d.

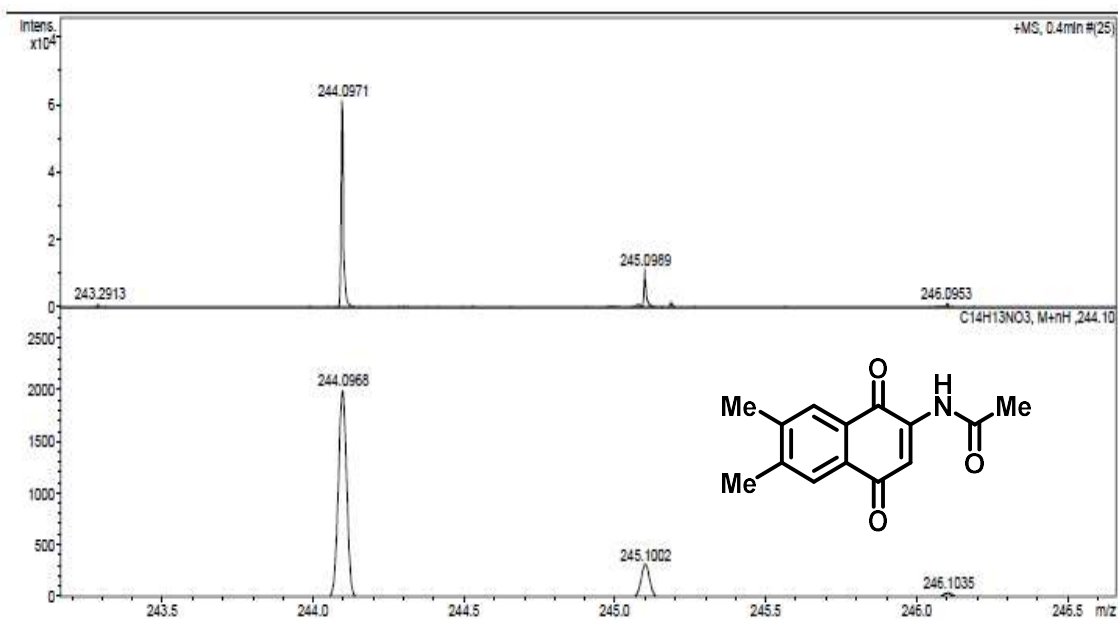


Figure C39. HRMS-ESI (+) of compound 59e.



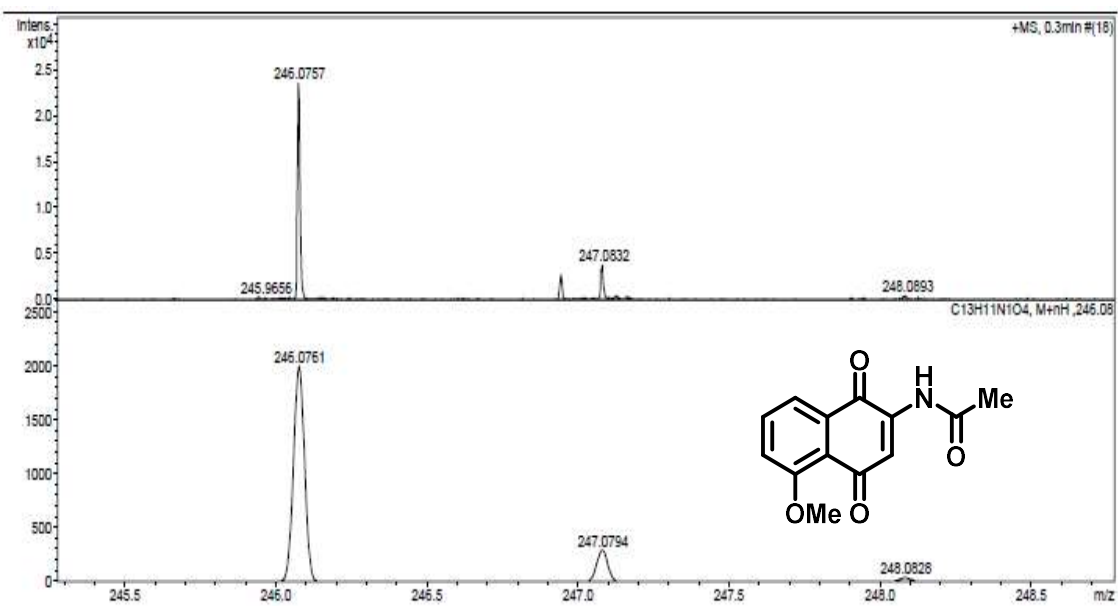


Figure C40. HRMS-ESI (+) of compound 59f.

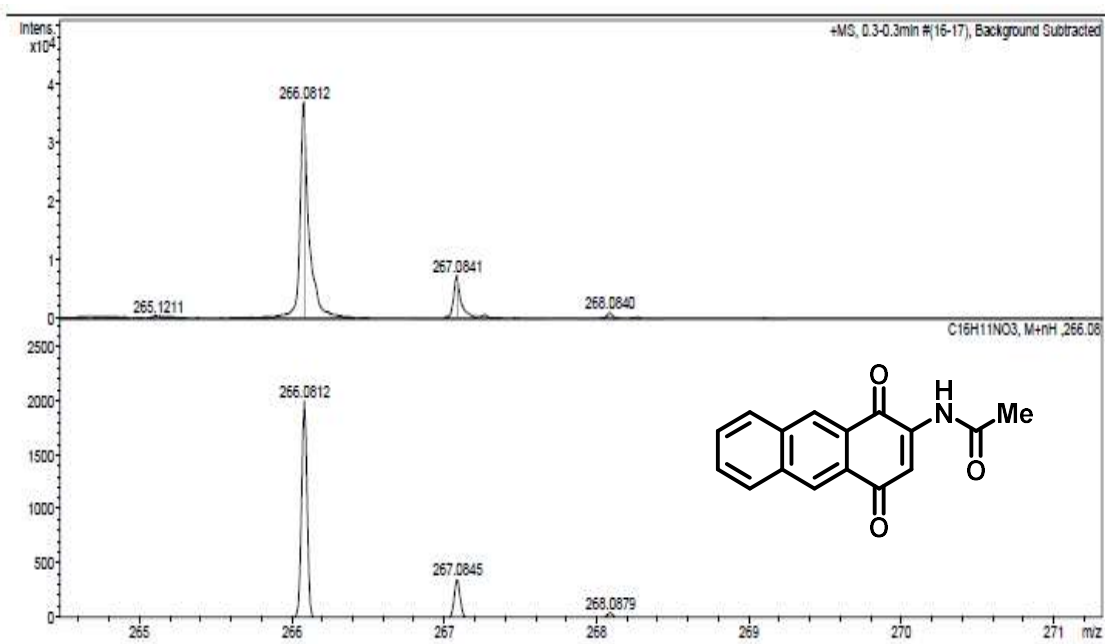


Figure C41. HRMS-ESI (+) of compound 59g.

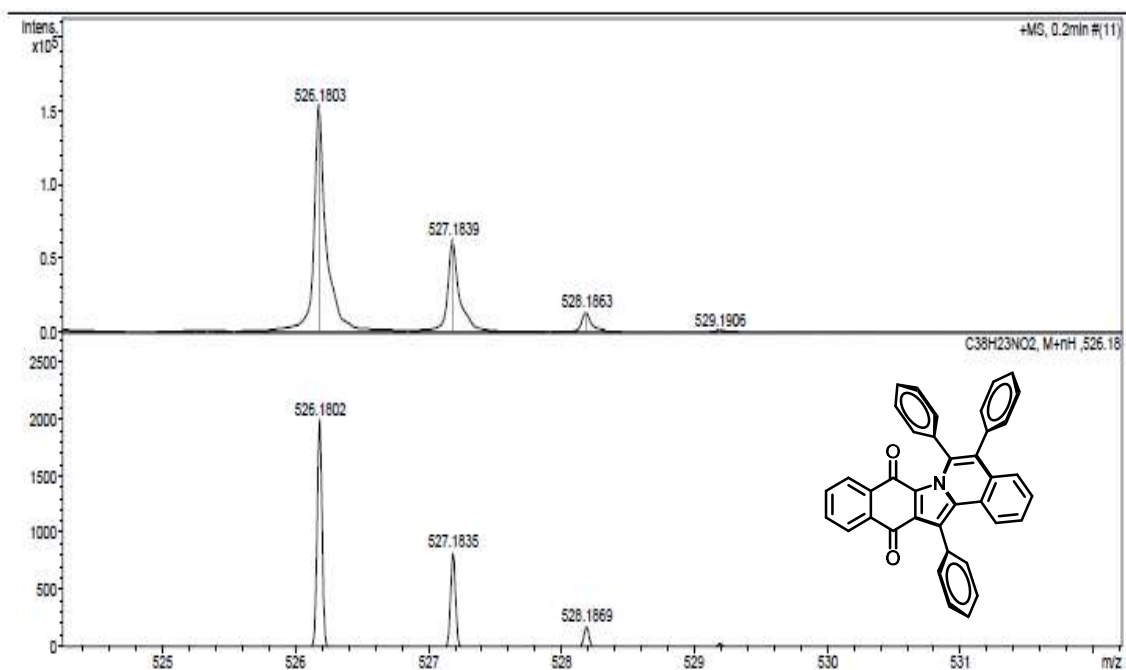


Figure C42. HRMS-ESI (+) of compound 67a.

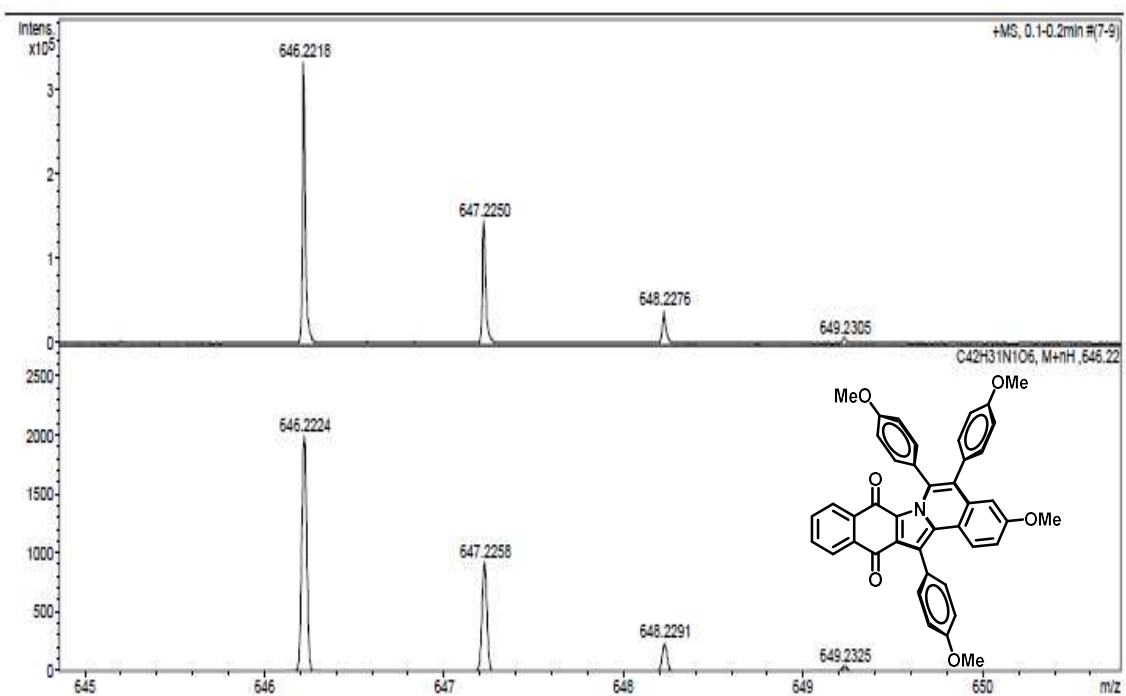


Figure C43. HRMS-ESI (+) of compound 67b.

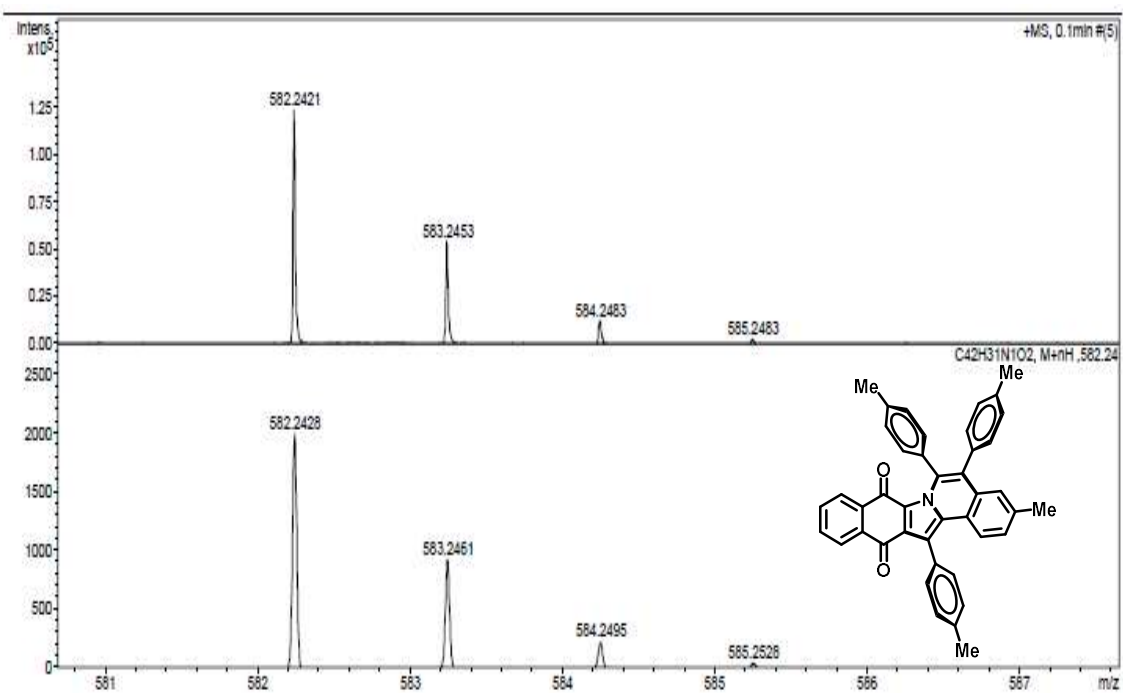


Figure C44. HRMS-ESI (+) of compound 67c.

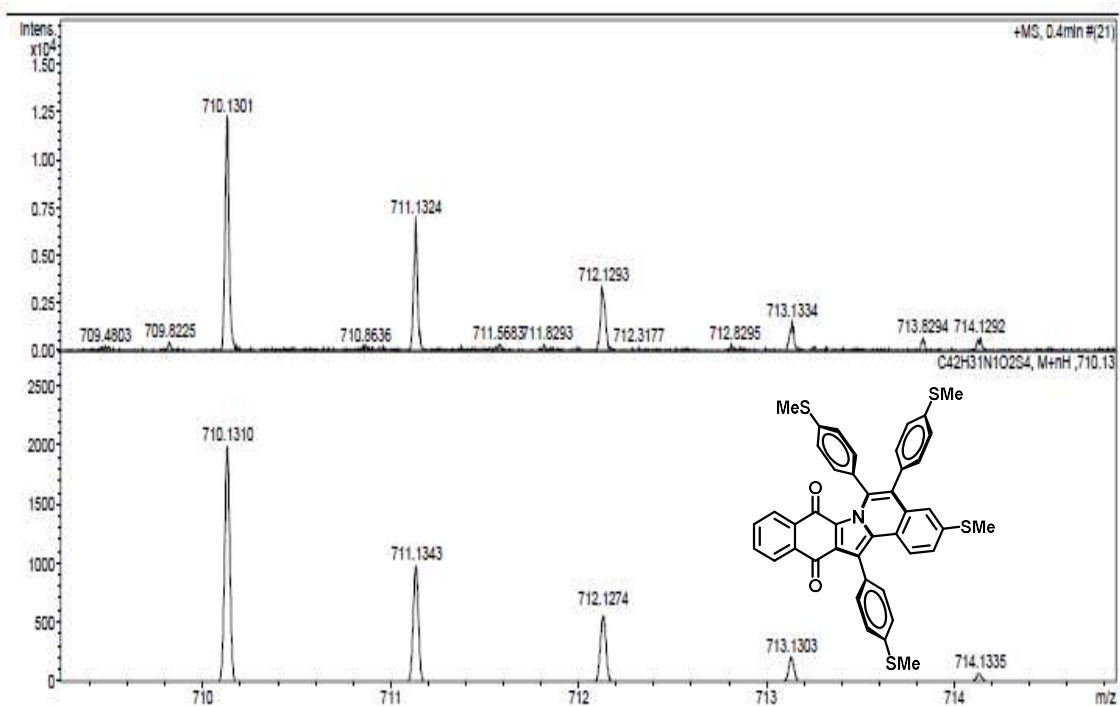


Figure C45. HRMS-ESI (+) of compound 67d.

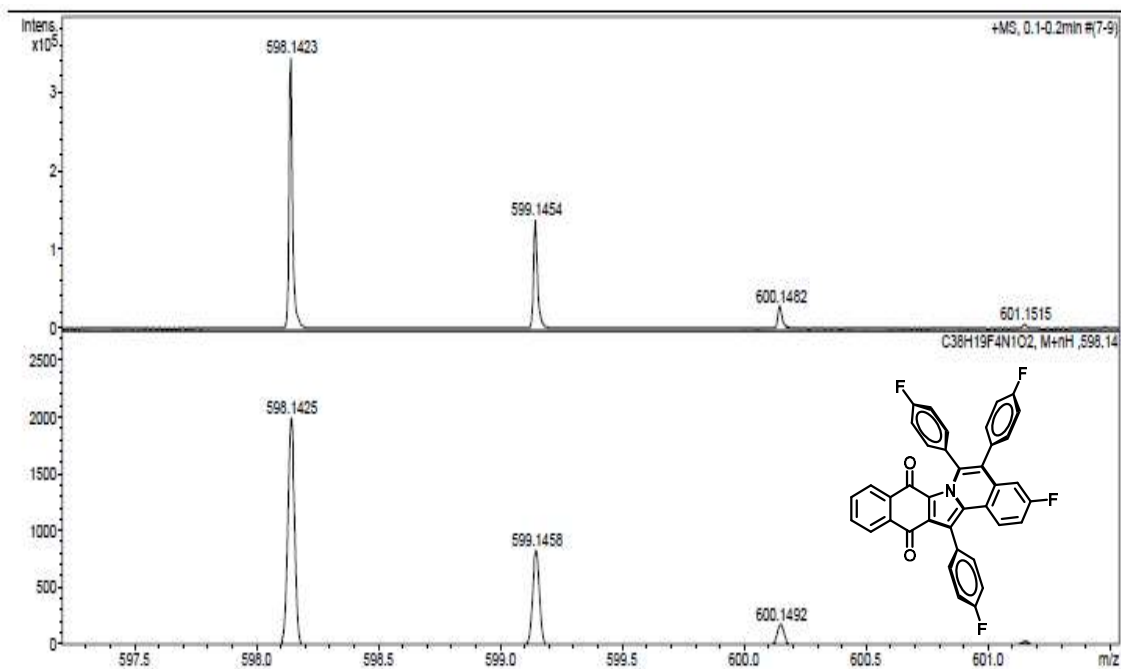


Figure C46. HRMS-ESI (+) of compound 67e.

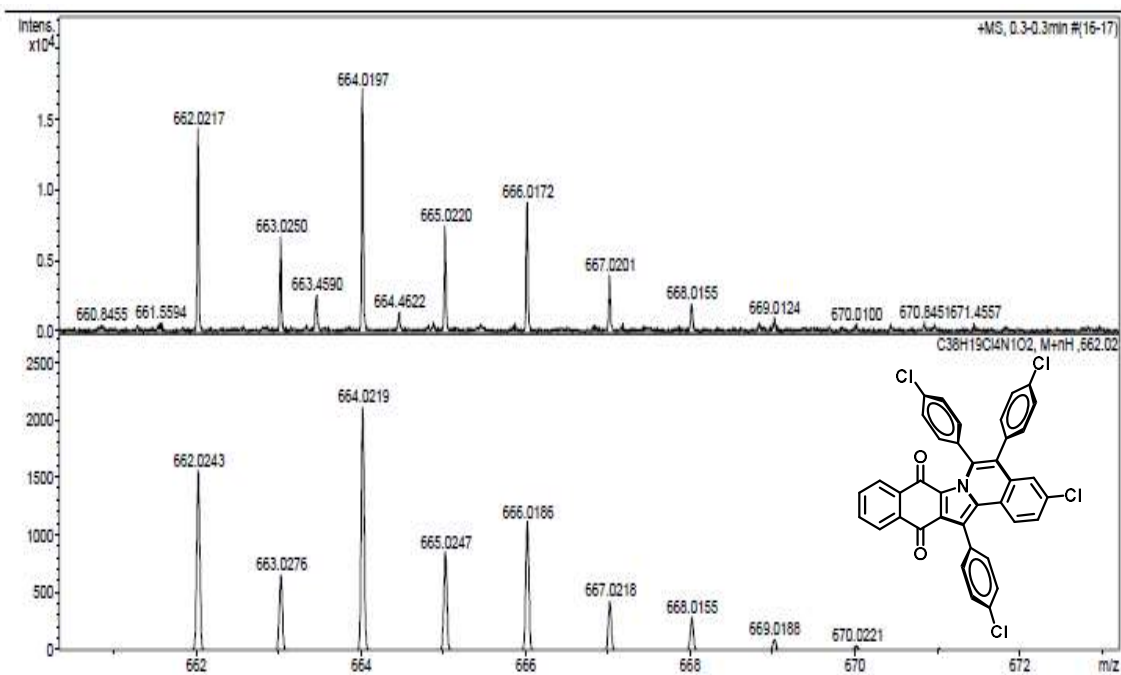


Figure C47. HRMS-ESI (+) of compound 67f.

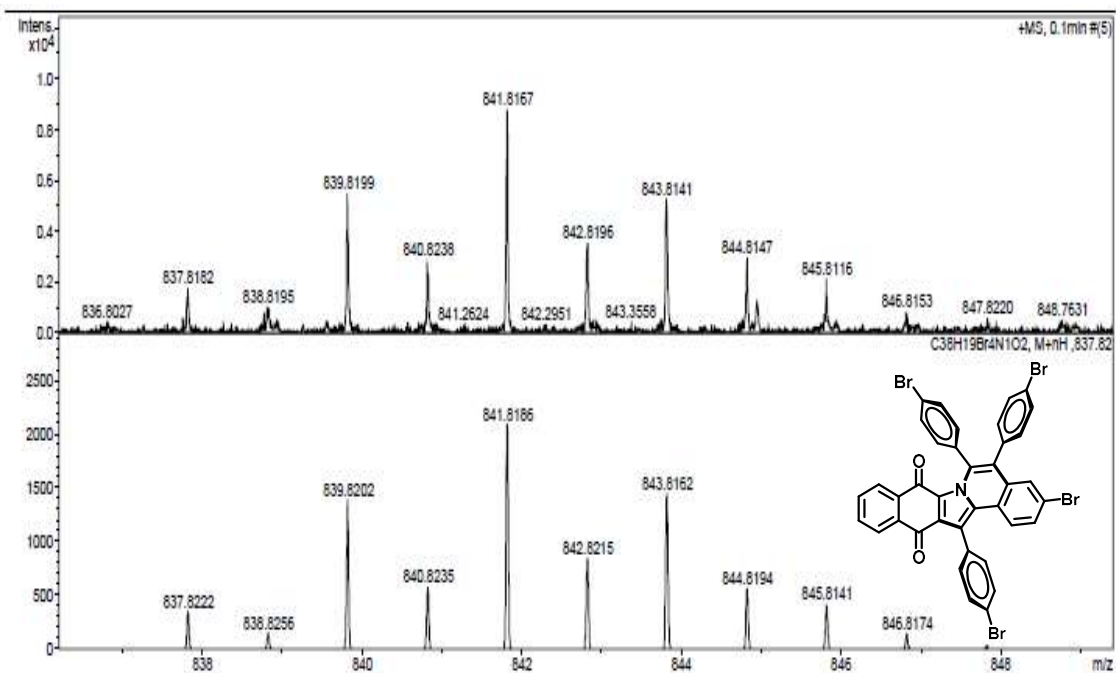


Figure C48. HRMS-ESI (+) of compound 67g.

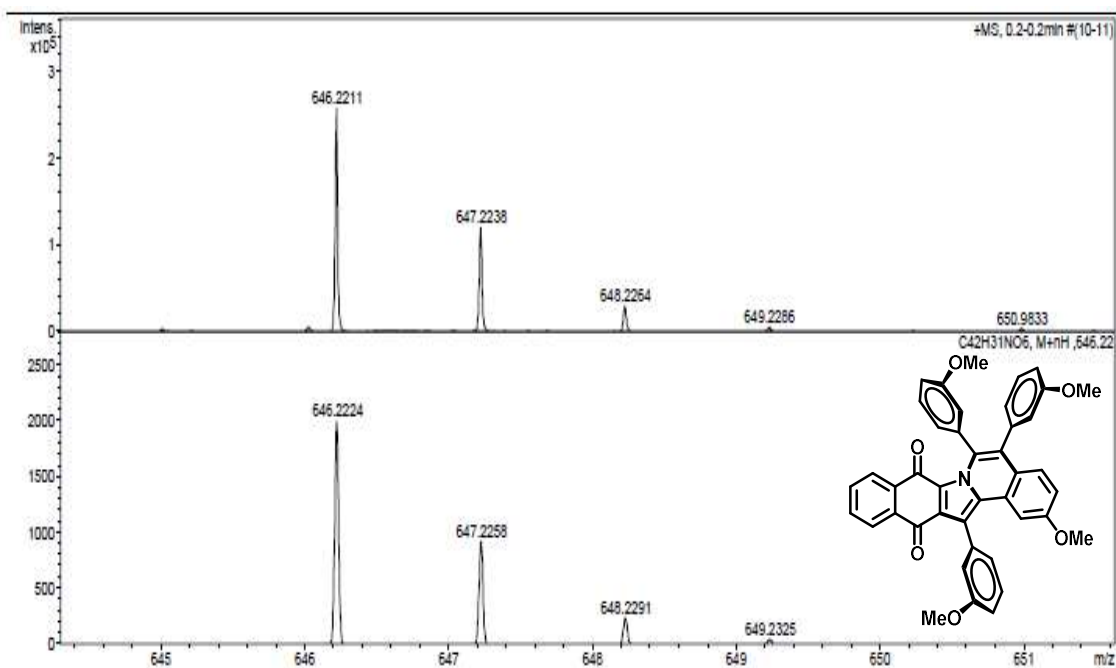


Figure C49. HRMS-ESI (+) of compound 67h.

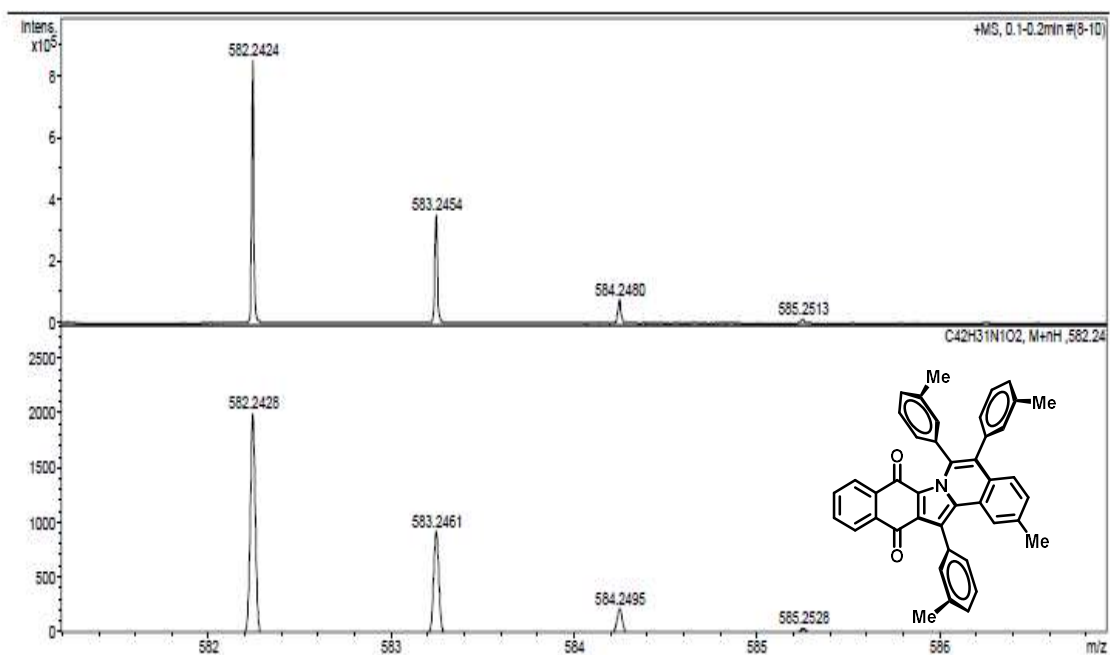


Figure C50. HRMS-ESI (+) of compound 67i.

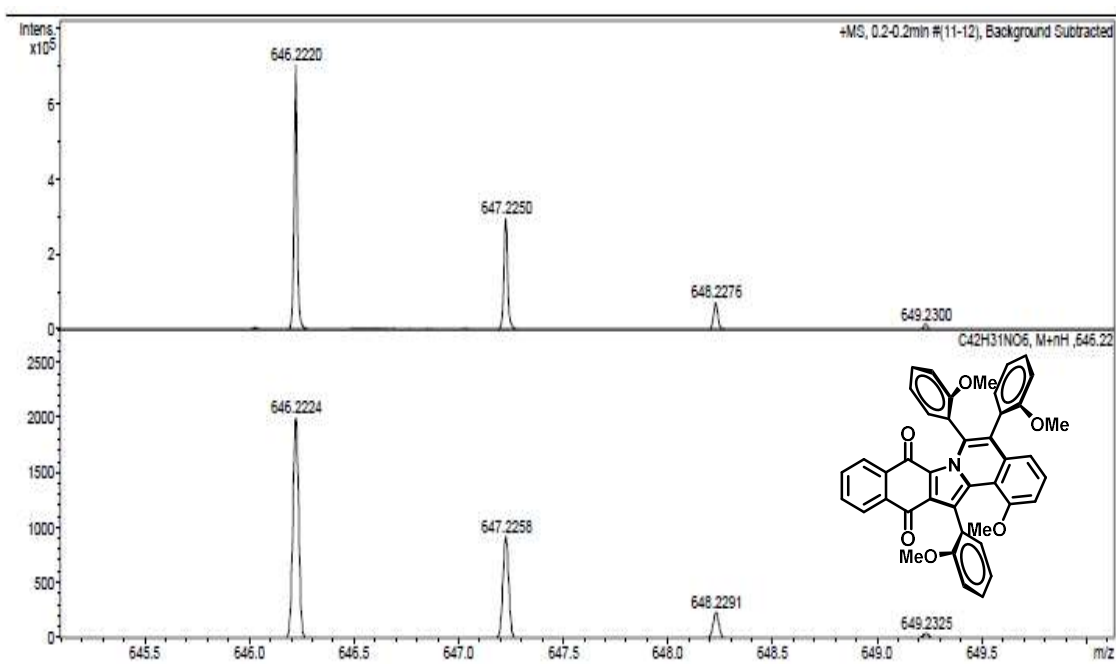


Figure C51. HRMS-ESI (+) of compound 67j.

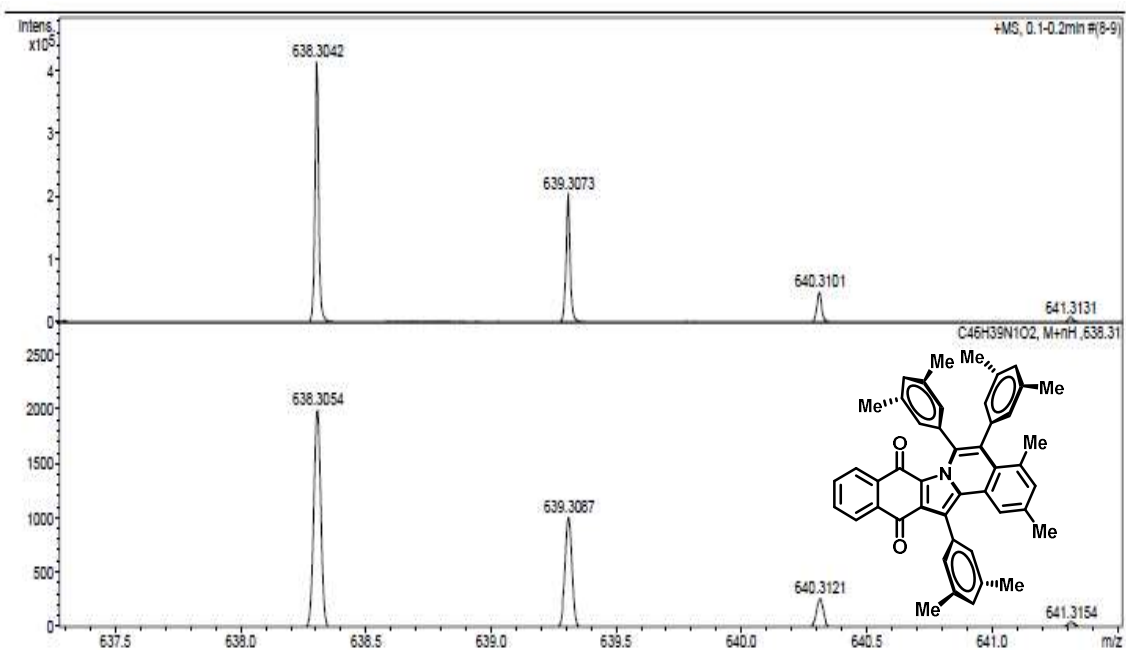


Figure C52. HRMS-ESI (+) of compound 67k.

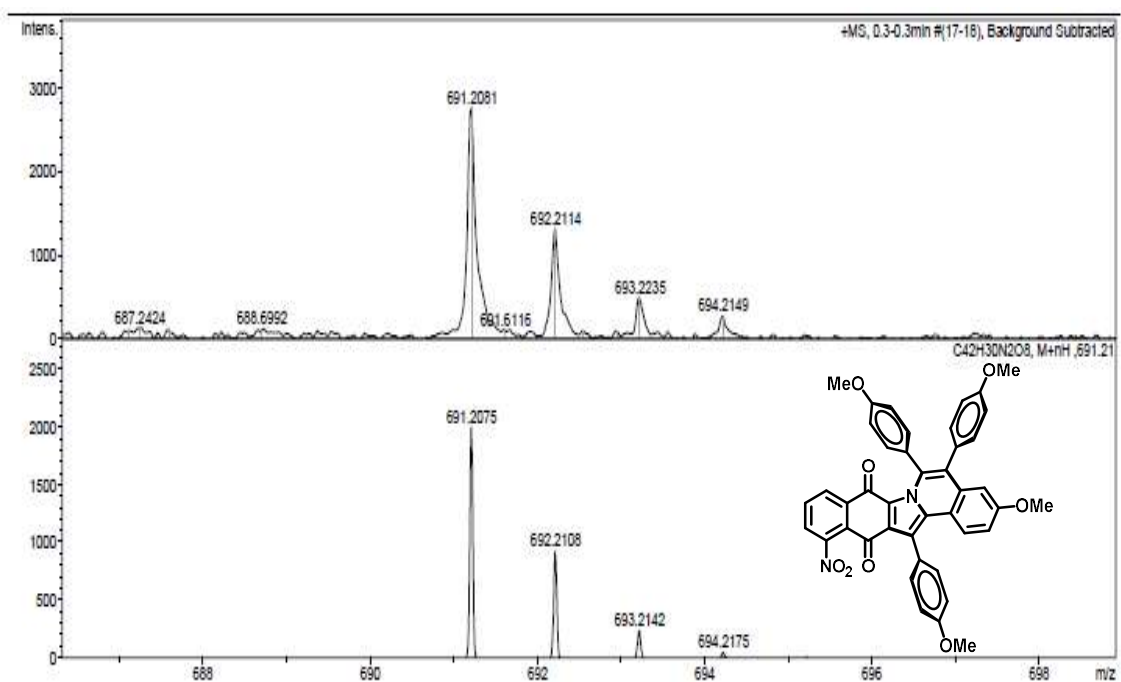


Figure C53. HRMS-ESI (+) of compound 68a.

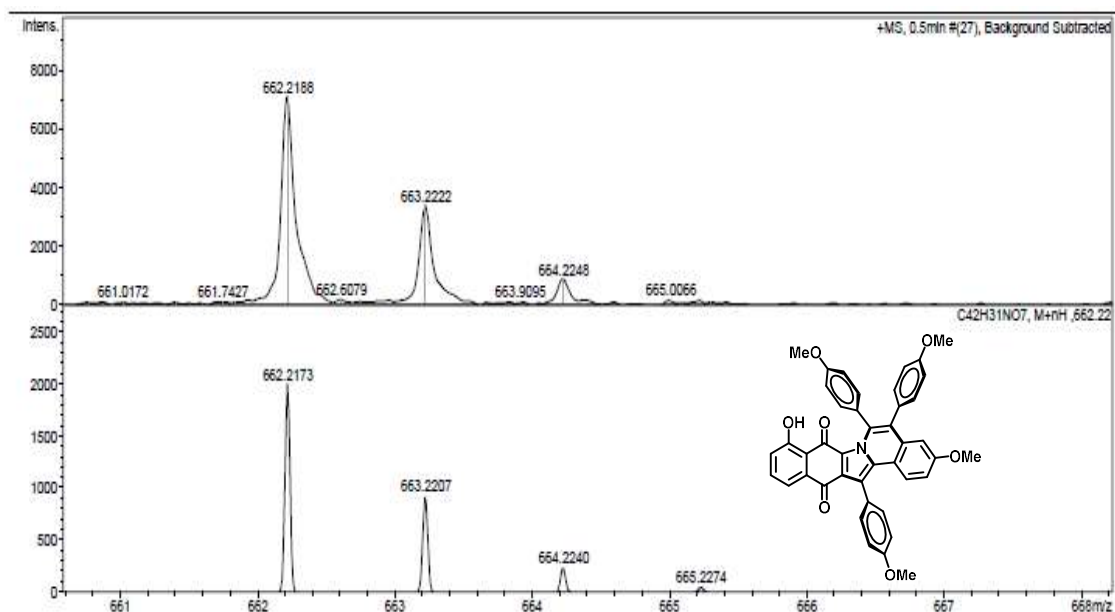


Figure C54. HRMS-ESI (+) of compound 68b.

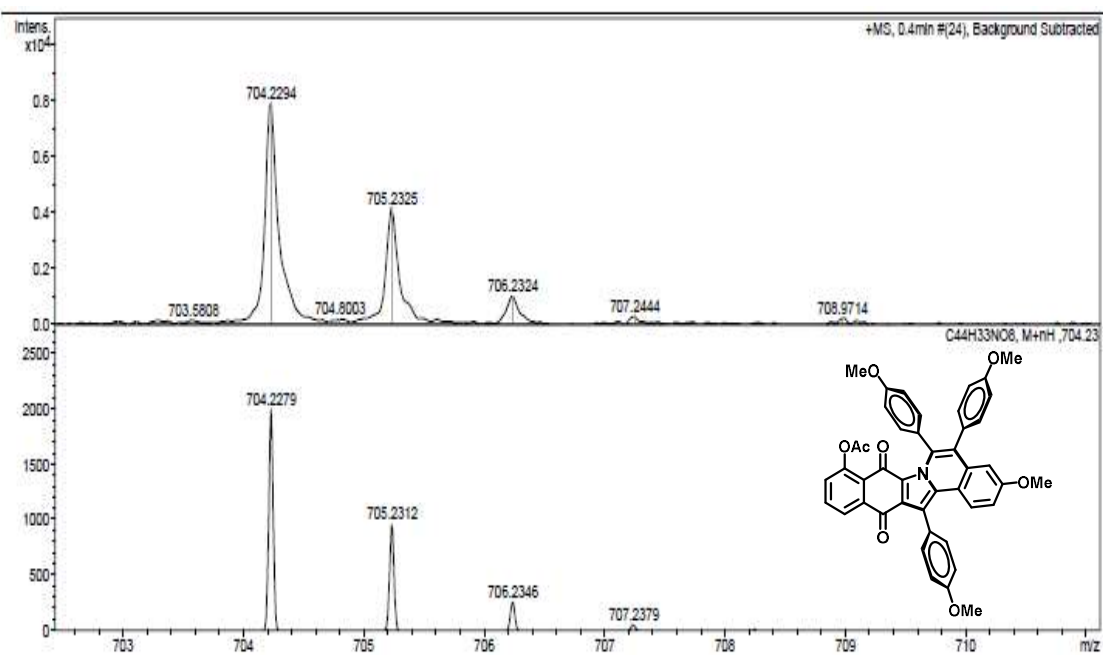


Figure C55. HRMS-ESI (+) of compound 68c.



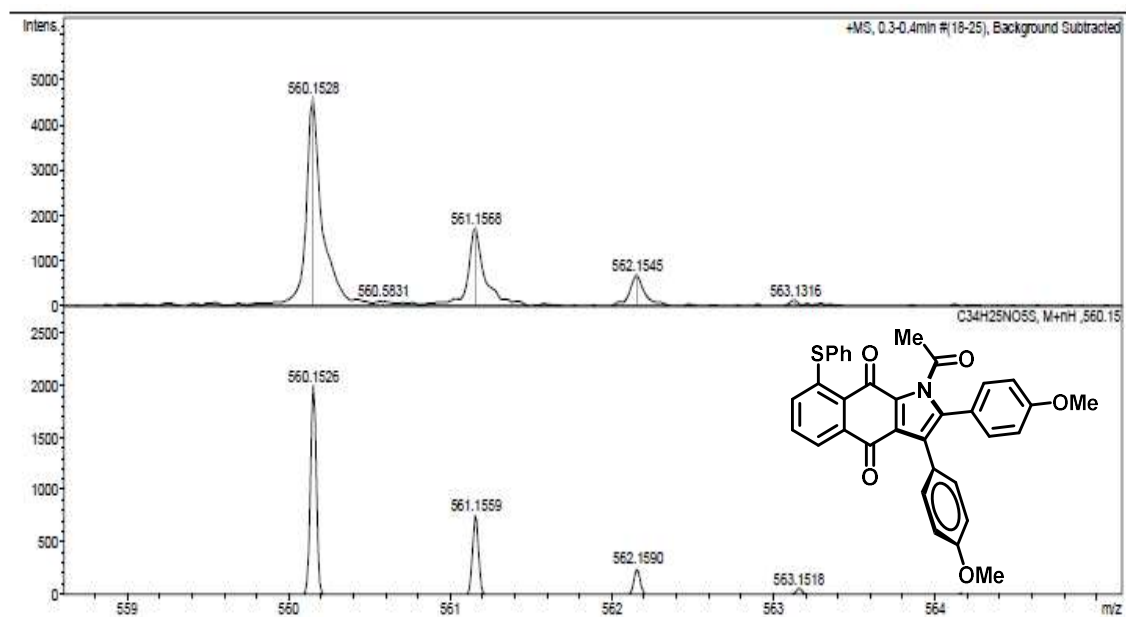


Figure C56. HRMS-ESI (+) of compound 68d.

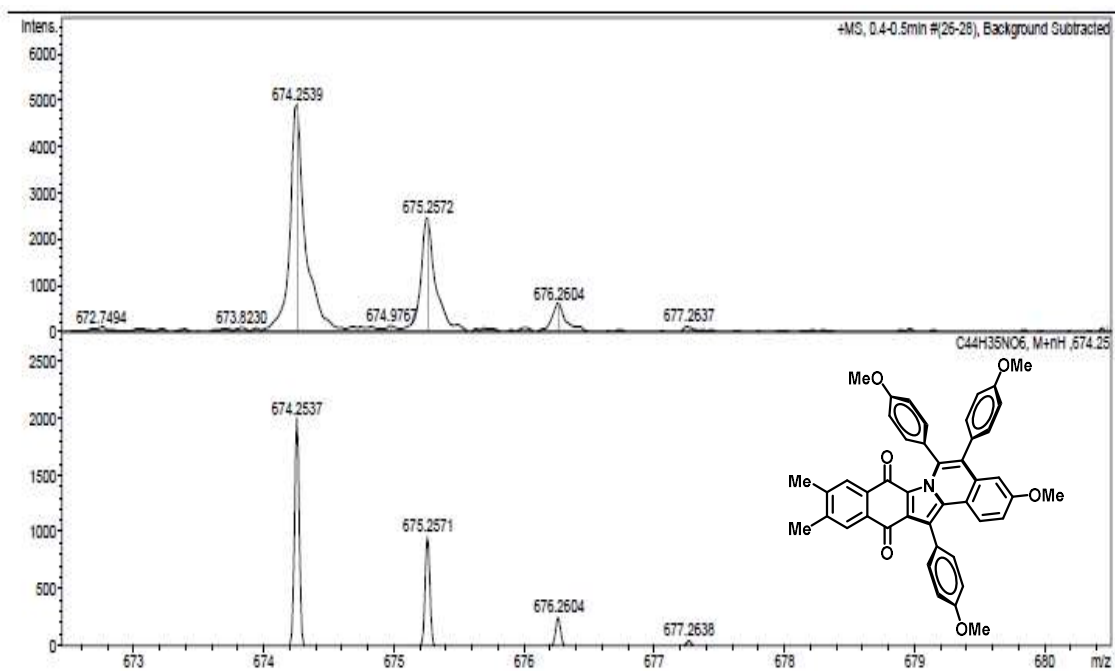


Figure C57. HRMS-ESI (+) of compound 68e.

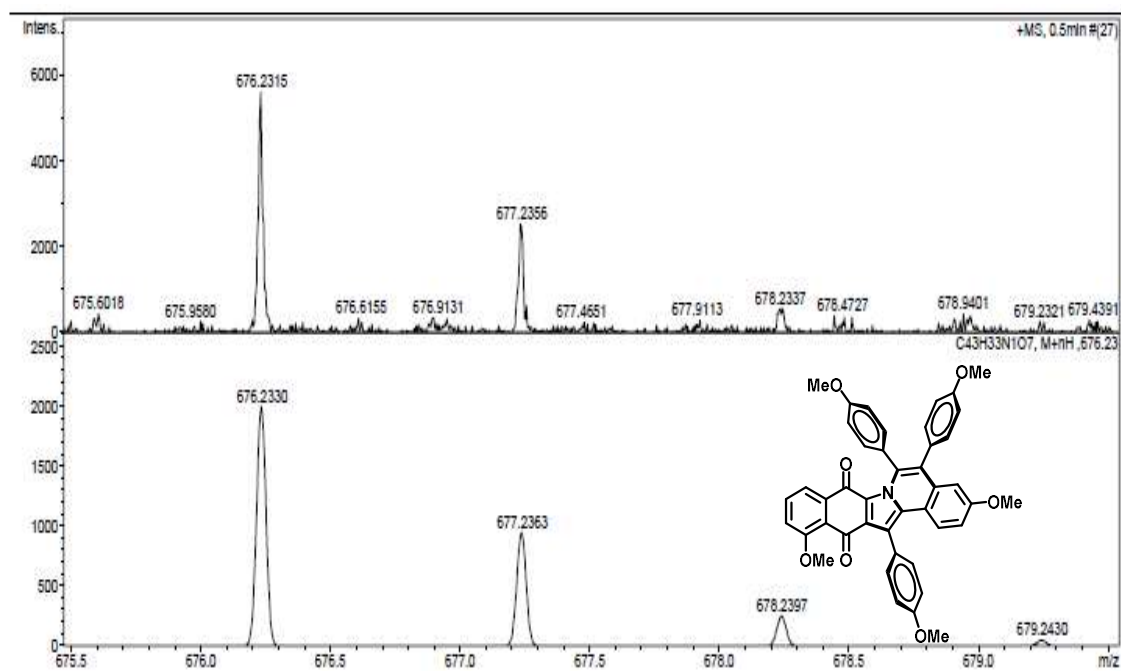


Figure C58. HRMS-ESI (+) of compound 68f.

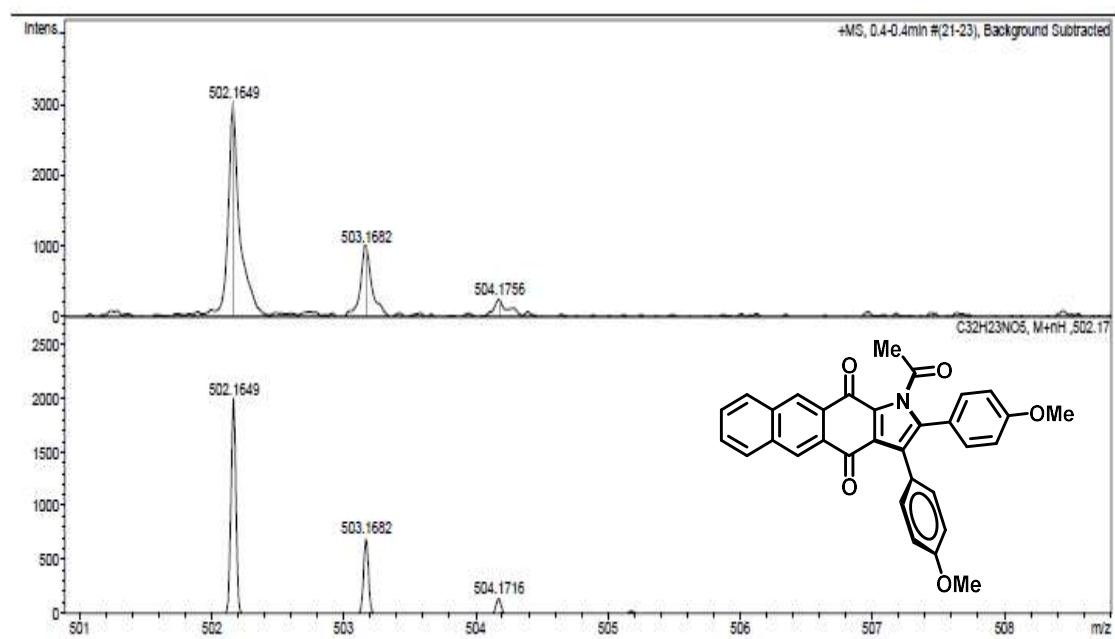


Figure C59. HRMS-ESI (+) of compound 68g.

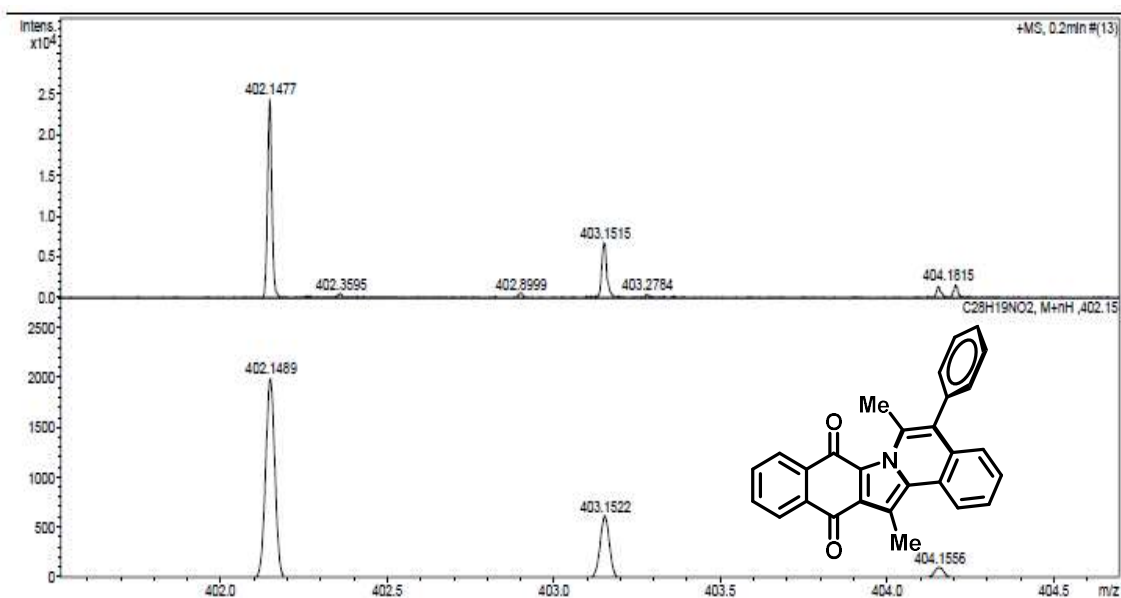


Figure C60. HRMS-ESI (+) of compound 69a.

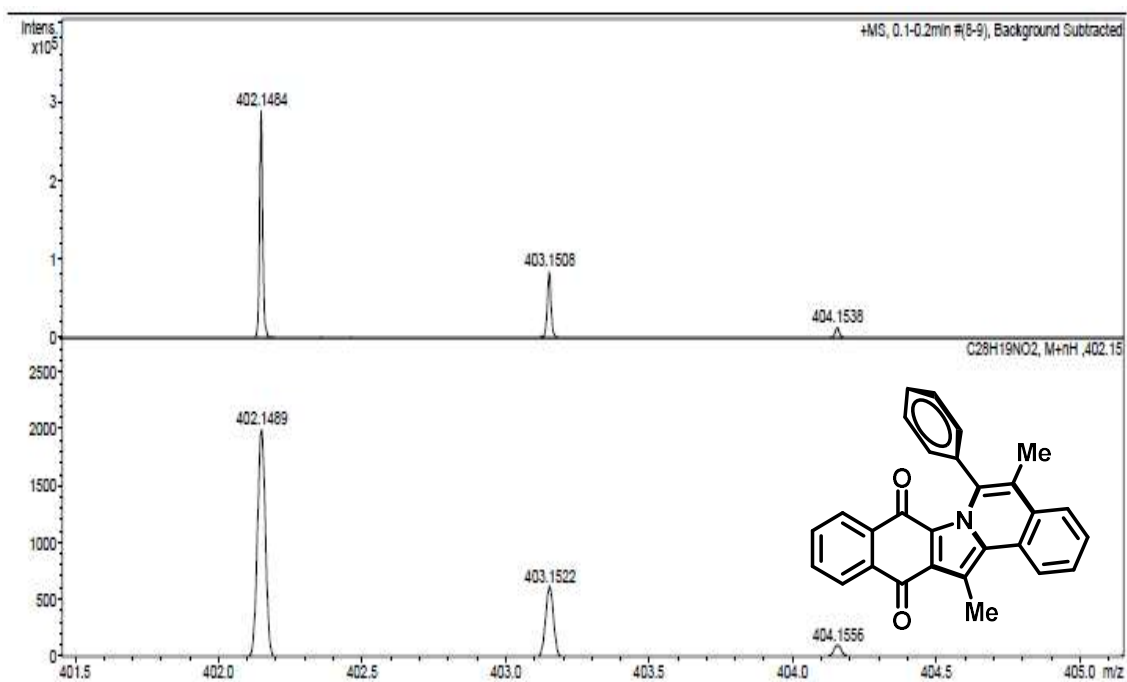


Figure C61. HRMS-ESI (+) of compound 69b.

**Table D1.** Crystallographic data of compound **59b**.

CCDC number	1984912
Identification code	<b>59b</b>
Empirical formula	C <sub>12</sub> H <sub>8</sub> N <sub>2</sub> O <sub>5</sub>
Formula weight	260.20
Temperature/K	100.0
Crystal system	monoclinic
Space group	P2 <sub>1</sub> /c
a/Å	12.9220(17)
b/Å	11.8583(17)
c/Å	7.1494(8)
α/°	90
β/°	96.604(4)
γ/°	90
Volume/Å <sup>3</sup>	1088.3(2)
Z	4
ρ <sub>calc</sub> /cm <sup>3</sup>	1.588
μ/mm <sup>-1</sup>	0.127
F(000)	536.0
Crystal size/mm <sup>3</sup>	0.358 × 0.307 × 0.07
Radiation	MoKα (λ = 0.71073)
2θ range for data collection/°	4.676 to 61.12
Index ranges	-18 ≤ h ≤ 18, -16 ≤ k ≤ 16, -10 ≤ l ≤ 10
Reflections collected	33155
Independent reflections	3312 [R <sub>int</sub> = 0.0311, R <sub>sigma</sub> = 0.0161]
Data/restraints/parameters	3312/0/173
Goodness-of-fit on F <sup>2</sup>	1.059
Final R indexes [I ≥ 2σ (I)]	R <sub>1</sub> = 0.0363, wR <sub>2</sub> = 0.0973
Final R indexes [all data]	R <sub>1</sub> = 0.0414, wR <sub>2</sub> = 0.1013
Largest diff. peak/hole / e Å <sup>-3</sup>	0.44/-0.23

**Table D2.** Crystallographic data of compound **59c**.

CCDC number	1984913
Identification code	<b>59c</b>
Empirical formula	C <sub>12</sub> H <sub>9</sub> NO <sub>4</sub>
Formula weight	231.20
Temperature/K	100.0
Crystal system	monoclinic
Space group	P2 <sub>1</sub> /c
a/Å	10.9162(12)
b/Å	12.8217(12)
c/Å	7.1561(9)
α/°	90
β/°	97.765(4)
γ/°	90
Volume/Å <sup>3</sup>	992.41(19)
Z	4
ρ <sub>calc</sub> /cm <sup>3</sup>	1.547
μ/mm <sup>-1</sup>	0.118
F(000)	480.0
Crystal size/mm <sup>3</sup>	0.472 × 0.348 × 0.108
Radiation	MoKα (λ = 0.71073)
2θ range for data collection/°	4.928 to 63.166
Index ranges	-16 ≤ h ≤ 16, -18 ≤ k ≤ 15, -10 ≤ l ≤ 10
Reflections collected	24191
Independent reflections	3198 [R <sub>int</sub> = 0.0238, R <sub>sigma</sub> = 0.0134]
Data/restraints/parameters	3198/0/162
Goodness-of-fit on F <sup>2</sup>	1.076
Final R indexes [I ≥ 2σ (I)]	R <sub>1</sub> = 0.0389, wR <sub>2</sub> = 0.1118
Final R indexes [all data]	R <sub>1</sub> = 0.0440, wR <sub>2</sub> = 0.1173
Largest diff. peak/hole / e Å <sup>-3</sup>	0.51/-0.21

**Table D3.** Crystallographic data of compound **59d**.

CCDC number	1984914
Identification code	<b>59d</b>
Empirical formula	C <sub>18</sub> H <sub>13</sub> NO <sub>3</sub> S
Formula weight	323.35
Temperature/K	100.0
Crystal system	monoclinic
Space group	P2 <sub>1</sub> /c
a/Å	14.418(2)
b/Å	7.7467(12)
c/Å	13.2774(14)
α/°	90
β/°	105.322(5)
γ/°	90
Volume/Å <sup>3</sup>	1430.2(3)
Z	4
ρ <sub>calc</sub> /cm <sup>3</sup>	1.502
μ/mm <sup>-1</sup>	0.242
F(000)	672.0
Crystal size/mm <sup>3</sup>	0.23 × 0.128 × 0.038
Radiation	MoKα (λ = 0.71073)
2θ range for data collection/°	5.86 to 57.396
Index ranges	-19 ≤ h ≤ 18, -10 ≤ k ≤ 10, -17 ≤ l ≤ 17
Reflections collected	21937
Independent reflections	3683 [R <sub>int</sub> = 0.0324, R <sub>sigma</sub> = 0.0217]
Data/restraints/parameters	3683/0/209
Goodness-of-fit on F <sup>2</sup>	1.041
Final R indexes [I ≥ 2σ (I)]	R <sub>1</sub> = 0.0338, wR <sub>2</sub> = 0.0790
Final R indexes [all data]	R <sub>1</sub> = 0.0407, wR <sub>2</sub> = 0.0836
Largest diff. peak/hole / e Å <sup>-3</sup>	0.42/-0.31

**Table D4.** Crystallographic data of compound **59g**.

CCDC number	1984915
Identification code	<b>59g</b>
Empirical formula	C <sub>16</sub> H <sub>11</sub> NO <sub>3</sub>
Formula weight	265.26
Temperature/K	100.0
Crystal system	monoclinic
Space group	P2 <sub>1</sub>
a/Å	4.8748(11)
b/Å	23.462(5)
c/Å	5.3453(13)
α/°	90
β/°	98.790(7)
γ/°	90
Volume/Å <sup>3</sup>	604.2(2)
Z	2
ρ <sub>calc</sub> /cm <sup>3</sup>	1.458
μ/mm <sup>-1</sup>	0.102
F(000)	276.0
Crystal size/mm <sup>3</sup>	0.365 × 0.242 × 0.028
Radiation	MoKα (λ = 0.71073)
2θ range for data collection/°	6.946 to 55.756
Index ranges	-5 ≤ h ≤ 6, -30 ≤ k ≤ 29, -6 ≤ l ≤ 7
Reflections collected	11653
Independent reflections	2794 [R <sub>int</sub> = 0.0317, R <sub>sigma</sub> = 0.0291]
Data/restraints/parameters	2794/1/185
Goodness-of-fit on F <sup>2</sup>	1.096
Final R indexes [I ≥ 2σ (I)]	R <sub>1</sub> = 0.0409, wR <sub>2</sub> = 0.0929
Final R indexes [all data]	R <sub>1</sub> = 0.0470, wR <sub>2</sub> = 0.0989
Largest diff. peak/hole / e Å <sup>-3</sup>	0.20/-0.20

**Table D5.** Crystallographic data of compound **67a**.

CCDC number	1984922
Identification code	<b>67a</b>
Empirical formula	C <sub>38</sub> H <sub>23</sub> NO <sub>2</sub>
Formula weight	525.57
Temperature/K	99.99
Crystal system	triclinic
Space group	P-1
a/Å	10.6471(12)
b/Å	10.8998(14)
c/Å	12.2801(14)
α/°	68.977(4)
β/°	76.063(4)
γ/°	81.424(5)
Volume/Å <sup>3</sup>	1288.0(3)
Z	2
ρ <sub>calc</sub> /cm <sup>3</sup>	1.355
μ/mm <sup>-1</sup>	0.083
F(000)	548.0
Crystal size/mm <sup>3</sup>	0.2 × 0.18 × 0.04
Radiation	MoKα (λ = 0.71073)
2θ range for data collection/°	4.792 to 54.22
Index ranges	-13 ≤ h ≤ 13, -13 ≤ k ≤ 13, -15 ≤ l ≤ 15
Reflections collected	21455
Independent reflections	5667 [R <sub>int</sub> = 0.0263, R <sub>sigma</sub> = 0.0225]
Data/restraints/parameters	5667/0/370
Goodness-of-fit on F <sup>2</sup>	1.057
Final R indexes [I ≥ 2σ (I)]	R <sub>1</sub> = 0.0402, wR <sub>2</sub> = 0.0986
Final R indexes [all data]	R <sub>1</sub> = 0.0460, wR <sub>2</sub> = 0.1029
Largest diff. peak/hole / e Å <sup>-3</sup>	0.35/-0.22



**Table D6.** Crystallographic data of compound **67b**.

CCDC number	1984923
Identification code	<b>67b</b>
Empirical formula	C <sub>43</sub> Cl <sub>2</sub> H <sub>33</sub> NO <sub>6</sub>
Formula weight	730.60
Temperature/K	100.0
Crystal system	triclinic
Space group	P-1
a/Å	10.601(2)
b/Å	15.824(3)
c/Å	23.190(6)
α/°	77.521(6)
β/°	80.393(7)
γ/°	70.884(5)
Volume/Å <sup>3</sup>	3569.3(14)
Z	4
ρ <sub>calc</sub> /cm <sup>3</sup>	1.360
μ/mm <sup>-1</sup>	0.234
F(000)	1520.0
Crystal size/mm <sup>3</sup>	0.271 × 0.137 × 0.018
Radiation	MoKα (λ = 0.71073)
2θ range for data collection/°	4.64 to 53.004
Index ranges	-13 ≤ h ≤ 13, -19 ≤ k ≤ 19, -29 ≤ l ≤ 28
Reflections collected	93791
Independent reflections	14692 [R <sub>int</sub> = 0.0425, R <sub>sigma</sub> = 0.0272]
Data/restraints/parameters	14692/0/891
Goodness-of-fit on F <sup>2</sup>	1.040
Final R indexes [I ≥ 2σ (I)]	R <sub>1</sub> = 0.0618, wR <sub>2</sub> = 0.1571
Final R indexes [all data]	R <sub>1</sub> = 0.0752, wR <sub>2</sub> = 0.1664
Largest diff. peak/hole / e Å <sup>-3</sup>	1.04/-0.54

**Table D7.** Crystallographic data of compound **67c**.

CCDC number	1984924
Identification code	<b>67c</b>
Empirical formula	C <sub>43</sub> H <sub>33</sub> Cl <sub>2</sub> NO <sub>2</sub>
Formula weight	666.60
Temperature/K	99.99
Crystal system	monoclinic
Space group	P2 <sub>1</sub> /c
a/Å	14.333(3)
b/Å	9.944(2)
c/Å	24.551(4)
α/°	90
β/°	104.753(6)
γ/°	90
Volume/Å <sup>3</sup>	3383.8(12)
Z	4
ρ <sub>calc</sub> /cm <sup>3</sup>	1.308
μ/mm <sup>-1</sup>	0.231
F(000)	1392.0
Crystal size/mm <sup>3</sup>	0.524 × 0.415 × 0.084
Radiation	MoKα (λ = 0.71073)
2θ range for data collection/°	5.042 to 54.31
Index ranges	-18 ≤ h ≤ 18, -12 ≤ k ≤ 11, -31 ≤ l ≤ 31
Reflections collected	36915
Independent reflections	7495 [R <sub>int</sub> = 0.0474, R <sub>sigma</sub> = 0.0339]
Data/restraints/parameters	7495/0/437
Goodness-of-fit on F <sup>2</sup>	1.061
Final R indexes [I ≥ 2σ (I)]	R <sub>1</sub> = 0.0517, wR <sub>2</sub> = 0.1428
Final R indexes [all data]	R <sub>1</sub> = 0.0612, wR <sub>2</sub> = 0.1517
Largest diff. peak/hole / e Å <sup>-3</sup>	0.44/-0.76

**Table D8.** Crystallographic data of compound **67d**.

CCDC number	1984925
Identification code	<b>67d</b>
Empirical formula	C <sub>42</sub> H <sub>31</sub> NO <sub>2</sub> S <sub>4</sub>
Formula weight	709.92
Temperature/K	99.99
Crystal system	triclinic
Space group	P-1
a/Å	10.3354(19)
b/Å	11.577(2)
c/Å	14.604(3)
α/°	72.707(5)
β/°	76.028(5)
γ/°	86.683(6)
Volume/Å <sup>3</sup>	1618.9(5)
Z	2
ρ <sub>calc</sub> /cm <sup>3</sup>	1.456
μ/mm <sup>-1</sup>	0.335
F(000)	740.0
Crystal size/mm <sup>3</sup>	0.206 × 0.122 × 0.018
Radiation	MoKα (λ = 0.71073)
2θ range for data collection/°	5.23 to 61.144
Index ranges	-14 ≤ h ≤ 14, -16 ≤ k ≤ 16, -20 ≤ l ≤ 20
Reflections collected	65509
Independent reflections	9871 [R <sub>int</sub> = 0.0407, R <sub>sigma</sub> = 0.0265]
Data/restraints/parameters	9871/0/446
Goodness-of-fit on F <sup>2</sup>	1.034
Final R indexes [I ≥ 2σ (I)]	R <sub>1</sub> = 0.0464, wR <sub>2</sub> = 0.1198
Final R indexes [all data]	R <sub>1</sub> = 0.0578, wR <sub>2</sub> = 0.1286
Largest diff. peak/hole / e Å <sup>-3</sup>	1.41/-0.56

**Table D9.** Crystallographic data of compound **67e**.

CCDC number	1984926
Identification code	<b>67e</b>
Empirical formula	$C_{77}Cl_2F_8H_{40}N_2O_4$
Formula weight	1280.01
Temperature/K	99.99
Crystal system	monoclinic
Space group	$C2/c$
a/Å	28.713(2)
b/Å	10.6234(12)
c/Å	20.602(2)
$\alpha/^\circ$	90
$\beta/^\circ$	109.635(3)
$\gamma/^\circ$	90
Volume/Å <sup>3</sup>	5918.8(10)
Z	4
$\rho_{\text{calc}}/\text{cm}^3$	1.436
$\mu/\text{mm}^{-1}$	0.192
F(000)	2616.0
Crystal size/mm <sup>3</sup>	$0.33 \times 0.139 \times 0.125$
Radiation	MoK $\alpha$ ( $\lambda = 0.71073$ )
2 $\Theta$ range for data collection/ $^\circ$	4.388 to 59.182
Index ranges	$-39 \leq h \leq 38, -14 \leq k \leq 14, -28 \leq l \leq 28$
Reflections collected	80098
Independent reflections	8316 [ $R_{\text{int}} = 0.0260, R_{\text{sigma}} = 0.0154$ ]
Data/restraints/parameters	8316/0/406
Goodness-of-fit on $F^2$	1.019
Final R indexes [ $I \geq 2\sigma(I)$ ]	$R_1 = 0.0388, wR_2 = 0.0987$
Final R indexes [all data]	$R_1 = 0.0437, wR_2 = 0.1029$
Largest diff. peak/hole / e Å <sup>-3</sup>	0.39/-0.24

**Table D10.** Crystallographic data of compound **67f**.

CCDC number	1984927
Identification code	<b>67f</b>
Empirical formula	C <sub>38</sub> H <sub>19</sub> Cl <sub>4</sub> NO <sub>2</sub>
Formula weight	663.34
Temperature/K	100.0
Crystal system	triclinic
Space group	P-1
a/Å	10.2479(10)
b/Å	11.2804(13)
c/Å	14.5458(17)
α/°	69.233(4)
β/°	74.420(3)
γ/°	85.423(4)
Volume/Å <sup>3</sup>	1514.3(3)
Z	2
ρ <sub>calc</sub> /cm <sup>3</sup>	1.455
μ/mm <sup>-1</sup>	0.429
F(000)	676.0
Crystal size/mm <sup>3</sup>	0.542 × 0.101 × 0.056
Radiation	MoKα (λ = 0.71073)
2θ range for data collection/°	4.026 to 57.432
Index ranges	-13 ≤ h ≤ 13, -15 ≤ k ≤ 15, -19 ≤ l ≤ 19
Reflections collected	74487
Independent reflections	7829 [R <sub>int</sub> = 0.0245, R <sub>sigma</sub> = 0.0129]
Data/restraints/parameters	7829/0/406
Goodness-of-fit on F <sup>2</sup>	1.042
Final R indexes [I ≥ 2σ (I)]	R <sub>1</sub> = 0.0340, wR <sub>2</sub> = 0.0882
Final R indexes [all data]	R <sub>1</sub> = 0.0374, wR <sub>2</sub> = 0.0911
Largest diff. peak/hole / e Å <sup>-3</sup>	0.51/-0.50

**Table D11.** Crystallographic data of compound **67g**.

CCDC number	1984928
Identification code	<b>67g</b>
Empirical formula	C <sub>38</sub> H <sub>19</sub> Br <sub>4</sub> NO <sub>2</sub>
Formula weight	841.18
Temperature/K	100.0
Crystal system	triclinic
Space group	P-1
a/Å	10.3332(7)
b/Å	11.3697(8)
c/Å	14.6296(10)
α/°	69.762(2)
β/°	74.477(2)
γ/°	84.775(2)
Volume/Å <sup>3</sup>	1553.83(19)
Z	2
ρ <sub>calc</sub> /cm <sup>3</sup>	1.798
μ/mm <sup>-1</sup>	5.217
F(000)	820.0
Crystal size/mm <sup>3</sup>	0.248 × 0.17 × 0.056
Radiation	MoKα (λ = 0.71073)
2θ range for data collection/°	5.156 to 57.448
Index ranges	-13 ≤ h ≤ 13, -15 ≤ k ≤ 15, -18 ≤ l ≤ 19
Reflections collected	28402
Independent reflections	7884 [R <sub>int</sub> = 0.0223, R <sub>sigma</sub> = 0.0211]
Data/restraints/parameters	7884/0/406
Goodness-of-fit on F <sup>2</sup>	1.050
Final R indexes [I ≥ 2σ (I)]	R <sub>1</sub> = 0.0228, wR <sub>2</sub> = 0.0518
Final R indexes [all data]	R <sub>1</sub> = 0.0274, wR <sub>2</sub> = 0.0536
Largest diff. peak/hole / e Å <sup>-3</sup>	0.53/-0.72

**Table D12.** Crystallographic data of compound **67k**.

CCDC number	1984929
Identification code	<b>67k</b>
Empirical formula	C <sub>46</sub> H <sub>39</sub> NO <sub>2</sub>
Formula weight	637.78
Temperature/K	100.03
Crystal system	monoclinic
Space group	P2 <sub>1</sub> /c
a/Å	13.528(2)
b/Å	10.2834(18)
c/Å	24.802(4)
α/°	90
β/°	98.510(4)
γ/°	90
Volume/Å <sup>3</sup>	3412.3(10)
Z	4
ρ <sub>calc</sub> /cm <sup>3</sup>	1.241
μ/mm <sup>-1</sup>	0.075
F(000)	1352.0
Crystal size/mm <sup>3</sup>	0.237 × 0.216 × 0.129
Radiation	MoKα (λ = 0.71073)
2θ range for data collection/°	4.826 to 54.316
Index ranges	-17 ≤ h ≤ 17, -13 ≤ k ≤ 13, -31 ≤ l ≤ 31
Reflections collected	55357
Independent reflections	7564 [R <sub>int</sub> = 0.0353, R <sub>sigma</sub> = 0.0204]
Data/restraints/parameters	7564/0/450
Goodness-of-fit on F <sup>2</sup>	1.056
Final R indexes [I ≥ 2σ (I)]	R <sub>1</sub> = 0.0552, wR <sub>2</sub> = 0.1476
Final R indexes [all data]	R <sub>1</sub> = 0.0645, wR <sub>2</sub> = 0.1557
Largest diff. peak/hole / e Å <sup>-3</sup>	0.34/-0.30

**Table D13.** Crystallographic data of compound **68b**.

CCDC number	1984930
Identification code	<b>68b</b>
Empirical formula	C <sub>42</sub> H <sub>31</sub> NO <sub>7</sub>
Formula weight	661.68
Temperature/K	100.0
Crystal system	triclinic
Space group	P-1
a/Å	11.309(4)
b/Å	11.777(5)
c/Å	13.645(6)
α/°	103.821(9)
β/°	100.502(10)
γ/°	104.746(10)
Volume/Å <sup>3</sup>	1648.5(11)
Z	2
ρ <sub>calc</sub> /cm <sup>3</sup>	1.333
μ/mm <sup>-1</sup>	0.091
F(000)	692.0
Crystal size/mm <sup>3</sup>	0.2 × 0.05 × 0.02
Radiation	MoKα (λ = 0.71073)
2θ range for data collection/°	4.318 to 57.618
Index ranges	-13 ≤ h ≤ 15, -15 ≤ k ≤ 15, -18 ≤ l ≤ 18
Reflections collected	76017
Independent reflections	8561 [R <sub>int</sub> = 0.0480, R <sub>sigma</sub> = 0.0281]
Data/restraints/parameters	8561/0/456
Goodness-of-fit on F <sup>2</sup>	1.109
Final R indexes [I ≥ 2σ (I)]	R <sub>1</sub> = 0.0501, wR <sub>2</sub> = 0.1317
Final R indexes [all data]	R <sub>1</sub> = 0.0660, wR <sub>2</sub> = 0.1421
Largest diff. peak/hole / e Å <sup>-3</sup>	0.50/-0.34



**Table D14.** Crystallographic data of compound **68c**.

CCDC number	1984931
Identification code	<b>68c</b>
Empirical formula	C <sub>44.5</sub> ClH <sub>34</sub> NO <sub>8</sub>
Formula weight	746.17
Temperature/K	100.0
Crystal system	triclinic
Space group	P-1
a/Å	10.669(3)
b/Å	13.522(3)
c/Å	13.944(3)
α/°	62.564(5)
β/°	86.480(7)
γ/°	78.919(7)
Volume/Å <sup>3</sup>	1751.3(7)
Z	2
ρ <sub>calc</sub> /cm <sup>3</sup>	1.415
μ/mm <sup>-1</sup>	0.170
F(000)	778.0
Crystal size/mm <sup>3</sup>	0.22 × 0.05 × 0.015
Radiation	MoKα (λ = 0.71073)
2θ range for data collection/°	4.702 to 59.274
Index ranges	-14 ≤ h ≤ 14, -18 ≤ k ≤ 18, -18 ≤ l ≤ 19
Reflections collected	33107
Independent reflections	9674 [R <sub>int</sub> = 0.0409, R <sub>sigma</sub> = 0.0400]
Data/restraints/parameters	9674/0/483
Goodness-of-fit on F <sup>2</sup>	1.081
Final R indexes [I ≥ 2σ (I)]	R <sub>1</sub> = 0.0482, wR <sub>2</sub> = 0.1340
Final R indexes [all data]	R <sub>1</sub> = 0.0648, wR <sub>2</sub> = 0.1471
Largest diff. peak/hole / e Å <sup>-3</sup>	0.46/-0.2

**Table D15.** Crystallographic data of compound **68d**.

CCDC number	1984932
Identification code	<b>68d</b>
Empirical formula	C <sub>34</sub> H <sub>25</sub> NO <sub>5</sub> S
Formula weight	559.61
Temperature/K	100.0
Crystal system	monoclinic
Space group	P2 <sub>1</sub> /c
a/Å	13.7711(14)
b/Å	8.8733(9)
c/Å	22.4265(15)
α/°	90
β/°	99.863(3)
γ/°	90
Volume/Å <sup>3</sup>	2699.9(4)
Z	4
ρ <sub>calc</sub> /cm <sup>3</sup>	1.377
μ/mm <sup>-1</sup>	0.166
F(000)	1168.0
Crystal size/mm <sup>3</sup>	0.31 × 0.18 × 0.04
Radiation	MoKα (λ = 0.71073)
2θ range for data collection/°	4.948 to 57.47
Index ranges	-18 ≤ h ≤ 18, -11 ≤ k ≤ 11, -30 ≤ l ≤ 30
Reflections collected	37062
Independent reflections	6946 [R <sub>int</sub> = 0.0327, R <sub>sigma</sub> = 0.0240]
Data/restraints/parameters	6946/0/373
Goodness-of-fit on F <sup>2</sup>	1.032
Final R indexes [I ≥ 2σ (I)]	R <sub>1</sub> = 0.0358, wR <sub>2</sub> = 0.0871
Final R indexes [all data]	R <sub>1</sub> = 0.0430, wR <sub>2</sub> = 0.0927
Largest diff. peak/hole / e Å <sup>-3</sup>	0.40/-0.31

**Table D16.** Crystallographic data of compound **68g**.

CCDC number	1984933
Identification code	<b>68g</b>
Empirical formula	C <sub>67</sub> H <sub>52</sub> N <sub>2</sub> O <sub>11</sub>
Formula weight	1061.10
Temperature/K	100.0
Crystal system	monoclinic
Space group	P2 <sub>1</sub>
a/Å	6.7461(5)
b/Å	40.606(2)
c/Å	9.6559(7)
α/°	90
β/°	102.191(3)
γ/°	90
Volume/Å <sup>3</sup>	2585.4(3)
Z	2
ρ <sub>calc</sub> /cm <sup>3</sup>	1.363
μ/mm <sup>-1</sup>	0.093
F(000)	1112.0
Crystal size/mm <sup>3</sup>	0.354 × 0.108 × 0.071
Radiation	MoKα (λ = 0.71073)
2θ range for data collection/°	4.43 to 57.372
Index ranges	-9 ≤ h ≤ 9, -54 ≤ k ≤ 54, -13 ≤ l ≤ 13
Reflections collected	83602
Independent reflections	13281 [R <sub>int</sub> = 0.0435, R <sub>sigma</sub> = 0.0299]
Data/restraints/parameters	13281/1/730
Goodness-of-fit on F <sup>2</sup>	1.072
Final R indexes [I ≥ 2σ (I)]	R <sub>1</sub> = 0.0401, wR <sub>2</sub> = 0.0949
Final R indexes [all data]	R <sub>1</sub> = 0.0445, wR <sub>2</sub> = 0.0986
Largest diff. peak/hole / e Å <sup>-3</sup>	0.41/-0.24

**Table D17.** Crystallographic data of compound **69a**.

CCDC number	1984934
Identification code	<b>69a</b>
Empirical formula	C <sub>28</sub> H <sub>19</sub> NO <sub>2</sub>
Formula weight	401.44
Temperature/K	100.0
Crystal system	triclinic
Space group	P-1
a/Å	7.0796(9)
b/Å	11.3528(15)
c/Å	13.3477(19)
α/°	109.767(5)
β/°	103.558(5)
γ/°	98.671(5)
Volume/Å <sup>3</sup>	949.9(2)
Z	2
ρ <sub>calc</sub> /cm <sup>3</sup>	1.404
μ/mm <sup>-1</sup>	0.088
F(000)	420.0
Crystal size/mm <sup>3</sup>	0.229 × 0.198 × 0.119
Radiation	MoKα (λ = 0.71073)
2θ range for data collection/°	6.02 to 61.042
Index ranges	-10 ≤ h ≤ 10, -16 ≤ k ≤ 16, -19 ≤ l ≤ 19
Reflections collected	64069
Independent reflections	5780 [R <sub>int</sub> = 0.0269, R <sub>sigma</sub> = 0.0130]
Data/restraints/parameters	5780/0/282
Goodness-of-fit on F <sup>2</sup>	1.040
Final R indexes [I ≥ 2σ (I)]	R <sub>1</sub> = 0.0380, wR <sub>2</sub> = 0.1059
Final R indexes [all data]	R <sub>1</sub> = 0.0412, wR <sub>2</sub> = 0.1097
Largest diff. peak/hole / e Å <sup>-3</sup>	0.44/-0.22

**Table D18.** Crystallographic data of compound **69b**.

CCDC number	1984935
Identification code	<b>69b</b>
Empirical formula	C <sub>28</sub> H <sub>19</sub> NO <sub>2</sub>
Formula weight	401.44
Temperature/K	99.95
Crystal system	triclinic
Space group	P-1
a/Å	7.2083(8)
b/Å	11.7424(12)
c/Å	12.2281(12)
α/°	75.223(3)
β/°	73.142(3)
γ/°	84.201(4)
Volume/Å <sup>3</sup>	957.37(17)
Z	2
ρ <sub>calc</sub> /cm <sup>3</sup>	1.393
μ/mm <sup>-1</sup>	0.087
F(000)	420.0
Crystal size/mm <sup>3</sup>	0.261 × 0.236 × 0.098
Radiation	MoKα (λ = 0.71073)
2θ range for data collection/°	4.43 to 55.794
Index ranges	-9 ≤ h ≤ 9, -15 ≤ k ≤ 15, -16 ≤ l ≤ 16
Reflections collected	12467
Independent reflections	4469 [R <sub>int</sub> = 0.0230, R <sub>sigma</sub> = 0.0260]
Data/restraints/parameters	4469/0/282
Goodness-of-fit on F <sup>2</sup>	1.057
Final R indexes [I ≥ 2σ (I)]	R <sub>1</sub> = 0.0392, wR <sub>2</sub> = 0.0988
Final R indexes [all data]	R <sub>1</sub> = 0.0441, wR <sub>2</sub> = 0.1044
Largest diff. peak/hole / e Å <sup>-3</sup>	0.35/-0.24